JHR 97: 471–490 (2024)
doi: 10.3897/jhr.97.119871
https://jhr.pensoft.net

RESEARCH ARTICLE

JOURNAL OF Hymenoptera RESEARCH
A peer-reviewed open-access journal
The International Society of Hymenopterists

Description of one new species of *Agriotypus* Curtis, 1832 (Hymenoptera, Ichneumonidae, Agriotypinae) from South Korea

Jin-Kyung Choi[1], Jong-Wook Lee[2], Kazuhiko Konishi[3], Kyong-In Suh[4], Andrew M. R. Bennett[5]

1 *Department of Science Education, Daegu National University of Education, Daegu, 42411, Republic of Korea* **2** *Georim Entomological Institute, Daegu, Republic of Korea* **3** *Ehime University Museum, Matsuyama, 790-8566, Japan* **4** *Division of Animal & Plant Resources Research, Nakdonggang National Institute of Biological Resources, Sangju 37242, Republic of Korea* **5** *Agriculture and Agri-food Canada, Canadian National Collection of Insects, Arachnids and Nematodes, 960 Carling Avenue, Ottawa, Ontario, Canada*

Corresponding author: Jin-Kyung Choi (jkchoi624@dnue.ac.kr)

Academic editor: Tamara Spasojevic | Received 30 January 2024 | Accepted 28 April 2024 | Published 29 May 2024

https://zoobank.org/557D8199-EBFE-46D3-B455-E3CFE3DFB19F

Citation: Choi J-K, Lee J-W, Konishi K, Suh K-I, Bennett AMR (2024) Description of one new species of *Agriotypus* Curtis, 1832 (Hymenoptera, Ichneumonidae, Agriotypinae) from South Korea. Journal of Hymenoptera Research 97: 471–490. https://doi.org/10.3897/jhr.97.119871

Abstract

Two species of the genus *Agriotypus* Curtis, 1832, *A. jilinensis* Chao, 1981 and *A. wangpiensis* **sp. nov.**, are added to the South Korean fauna. In total, four species, *A. gracilis*, *A. jilinensis*, *A. silvestris*, and *A. wangpiensis* **sp. nov.**, have now been found in South Korea. The female of *A. jilinensis* is described for the first time and the species is redescribed based on the first fully eclosed specimens. Photographs of collecting sites, the larva and the adult of *A. wangpiensis* **sp. nov.**, and a key to the South Korean species of *Agriotypus* are provided.

Keywords

Agriotypus wangpiensis sp. nov., *A. jilinensis*, aquatic wasp, DNA barcode, taxonomy, Trichoptera

Introduction

The subfamily Agriotypinae (Hymenoptera: Ichneumonidae) is a small group of aquatic parasitoid wasps which are known to parasitize trichopteran pupae and prepupae in fast-running water but, some species (*A. armatus*) can attack hosts in lakes and

slow-moving rivers (Townes 1969; Bennett 2001). The subfamily is monotypic with *Agriotypus* Curtis as the only recognized genus. Until recently, the genus was comprised of 16 species from the Palaearctic and Oriental Regions (Bennett 2001) however, five species were just reported from China (Tang et al. 2022), thus, a total of 21 species of *Agriotypus* are currently known. In South Korea, two species, *A. gracilis* Waterston and *A. silvestris* Konishi and Aoyagi, were previously recorded and *A. armatus* Curtis was excluded from the South Korean fauna (Kim et al. 2018).

This genus can be easily identified by the following characteristics: a strongly distinct spine on the scutellum; all metasomal sternites fully sclerotized; fused 2nd and 3rd metasomal tergites and sternites. Because of the latter two characteristics, Mason (1971) proposed *Agriotypus* should be given family status in the superfamily Proctotrupoidea. However, all other taxonomists preferred to recognize *Agriotypus* within Ichneumonidae (Short 1952; Townes 1969; Sharkey and Wahl 1992; Bennett 2001). Also, Chao (1992) described the genus *Atopotypus* Chao as a new monotypic Agriotypinae genus, but Bennett (2001) synonymized *Atopotypus* with *Agriotypus* forming *Agriotypus succinctus* (Chao), based on the results of a cladistic analysis of morphological characters of adults and larvae. Bennett (2001) also defined two species groups within *Agriotypus*, the Palaearctic *armatus* species group and the Oriental *himalensis* species group (based on the absence or presence, respectively of longitudinal carinae at the base of the second metasomal tergite). Prior to this study, the *armatus* group included *A. armatus* Curtis, *A. changbaishanus* Chao, *A. gracilis* Waterston, *A. jilinensis* Chao, *A. silvestris* Konishi & Aoyagi and *A. succinctus* (Chao).

In this study, a new species, *A. wangpiensis* sp. nov., and the female of *A. jilinensis* are described, including the larva of *A. wangpiensis* sp. nov. We also provide DNA barcodes and an illustrated identification key to the South Korean species.

Materials and methods

Type specimens of the new species are preserved in the Insect Inquiry Education Institute in Daegu National University of Education (**DNUE-IIEI**, Daegu, Korea), Nakdonggang National Institute of Biological Resources (**NNIBR**, Sangju, Korea), and Ehime University of Matsuyama (**EUM**, Japan). Other examined material is deposited in the Canadian National Collection of Insects, Arachnids and Nematodes (**CNC**, Ottawa, Canada). Specimens used in this study were collected by rearing from trichopteran pupae and prepupae (Figs 2, 3) and Malaise trapping. Most of the images of specimens of the new species were taken using an AxioCam MRc5 camera attached to a stereo microscope (Zeiss SteREO Discovery. V20; Carl Zeiss, Göttingen, Germany), processed using AxioVision SE64 software (Carl Zeiss), and optimized with a Delta imaging system (i-solution, IMT i-Solution Inc. Vancouver, Canada). Some images of the new species were taken using a Leica MC190 HD Camera attached to a Leica M125 Microscope (Leica Microsystems, Germany) and processed using LEICA LAS X software (Leica). The epomia is not visible in Figs 5E, 8D, but we verified that it

extends dorsal to pronotal furrow. This character is very hard to photograph because of two factors: first, the region is highly setose which obscures the epomia and second the area is often in shadow because of the head and mesoscutum. The morphological terminology follows Broad et al (2018), except for the terms for the male genitalia that follow Konishi (2005).

The examined *Agriotypus wangpiensis* sp. nov. specimens for DNA barcoding are deposited in DNUE-IIEI. Genomic DNA from two adult females and five adult males, one pupa, and one larva were extracted using a DNeasy Blood & Tissue Kit (Qiagen, Valencia, California). Each PCR was performed in a 30μl volume consisting of 15μl of premix (*Solg*™ 2× *Taq* PCR Pre-Mix: 0.5× Band Doctor™ with dye, *Taq* DNA polymerase (5U/μl), 10× *Taq* Reaction Buffer (25 mM $MgCl_2$ included), 10 mM each dNTP Mix), 2μl of DNA template, 1μl of each primer as 10 pmol, and 11μl of DNase free water. An approximately 650–700 bp piece of the mitochondrial cytochrome oxidase I(COI) gene was amplified using the primers LCO1490 (5'-GGT CAA CAA ATC ATA AAG ATA TTG G-3') and HCO2198 (5'-TAA ACT TCA GGG TGA CCA AAA AAT CA-3') (Folmer et al. 1994). Polymerase chain reactions were run with an initial predenaturation step at 94 °C for 5 min, followed by 35 cycles of denaturation for 1 min at 94 °C, 1 min of annealing at 50 °C, and 1 min of extension at 72 °C; the last cycle was followed by a final 5 min extension step. The amplified fragments were cleaned and sequenced by BIONEER (Daejeon, South Korea), after which the sequences were edited and aligned. Sequences have been deposited in GenBank under accession numbers OQ981233.1–OQ981241.1. *Agriotypus silvestris* and *A. gracilis* were barcoded with the following modifications to the above protocol. The amplification components were 2μl 2.5 mM dNTPs. 0.2 μl TaKaRa Ex Taq® Hot Start, 2.5 μl 10× Ex Taq buffer, 2 μl 25 mM MgCl2, 1μl of 10 μM primers LCO1490 and HCO2198, 1–4 μlgenomic DNA and water to 25 μl. The amplification protocol was as follows: 95 °C for 1 minute, 35 cycles of 95 °C for 15 s, 49 °C for 15 s, and 72 °C for 45 s, and 72 °C for 4 minutes. The amplified product was viewed on a 2% agarose gel with GelRed, then cleaned with ExoSAP-IT (PE Applied Biosystems, Foster City, CA, USA). Cycle sequencing was completed with the BigDye Terminator v3.1 kit (PE Applied Biosystems, Foster City, CA, USA) in 10 μl reactions. Sequencing was completed at the Agriculture & Agri-Food Canada Ottawa Research and Development Centre Core Sequencing Facility (Ottawa, ON, Canada) on a 3500 xl DNA Genetic Analyzer (PE Applied Biosystems, Foster City, CA, USA). All sequences obtained were assembled and manually edited using Bioedit 7.2.5 (Hall 1999) and finally aligned using ClustalW implemented in MEGA 11 (Tamura et al. 2021). COI sequences were aligned using MEGA 5.2 (Tamura et al. 2011) and Clustal W. A dataset consisting of 25 COI sequences was finally trimmed to 537 bp in length.

We employed two phylogenetic methods: distance-based Neighbor-Joining (NJ) and optimality criterion-based Maximum Likelihood (ML) (Han et al. 2019). A NJ analysis (Saitou and Nei 1987) was performed using MEGA 5.2. Genetic distances were calculated using the Kimura 2-parameter model (Kimura 1980) in MEGA

5.2. The support values for each node were estimated with 1,000 bootstrap replicates (Fig. 9) (Felsenstein 1985).

A ML analysis was performed using the IQ-TREE web server (Trifinopoulos et al. 2016). The best-fit model for the molecular evolution of the COI sequence data was TIM2+F+I (–lnL = 1739.8817) based on the Bayesian information criterion, as determined using ModelFinder (Kalyaanamoorthy et al. 2017). Branch support was evaluated by 1,000 ultrafast bootstrap (UFBoot) replicates (Mihn et al. 2013; Hoang et al. 2017). Also, two species, *Echthrus reluctator* (Linnaeus 1758) (Cryptinae) and *Endasys patulus* (Viereck 1911) (Phygadeuontinae), were included as outgroup taxa for the Maximum Likelihood (ML) analysis (Fig. 10) (Geiger et al. 2016; Hebert et al. 2016; Bennett et al. 2019).

The final tree was visualized using FigTree v1.4.4 (http://tree.bio.ed.ac.uk/software/figtree). The tree is drawn to scale, with branch lengths in the same units as those of the evolutionary distances used to infer the phylogenetic tree. The evolutionary distances were computed using the Kimura 2-parameter method. The evolutionary distance is omitted in the Fig. 10 and shows only bootstrap values above 75%.

Taxonomy

Family Ichneumonidae Latreille, 1802
Subfamily Agriotypinae Haliday,1838

Genus *Agriotypus* Curtis, 1832

Agriotypus Curtis, 1832: 389. Type species: *Agriotypus armatus* Curtis, by original designation.

Crotopus Holmgren, 1858: 353. Type species: *Crotopus abnormis* Holmgren = *armatus* Curtis, by monotypy. Synonymized by Dalla Torre, 1902.

Atopotypus Chao, 1992: 325. Type species: *Atopotypus succintus* Chao, by monotypy. Synonymized by Bennett, 2001.

Key to the species of South Korean *Agriotypus*

1 Females **2**
– Males **5**
2 Face with median vertical ridge. Body color almost entirely reddish brown (Fig. 1A). Propodeum with medial longitudinal carinae nearly parallel (weakly converging posteriorly) (Fig. 1F) ..... ***A. jilinensis***
– Face without median vertical ridge. Body color generally blackish (Fig. 5A). Propodeum with medial longitudinal carinae strongly converging posteriorly (Fig. 5F) **3**

3 Clypeus in anterior view with summit pointed medially (see Fig. 4E in Bennett 2001). Fore wing with hyaline longitudinal bands complete proximal and distal to pterostigma (Fig. 6A).....***A. gracilis***

– Clypeus in anterior view with summit rounded medially (not pointed), (Fig. 5C and see Fig. 1B of Konishi and Aoyagi 1994). Fore wing with hyaline longitudinal bands complete (Fig. 6B) or absent (Fig. 6F, G) proximal and distal to pterostigma.....**4**

4 Basal 1/4 of fourth submarginal cell and third discal cell of fore wing hyaline (arrows in Fig. 6B). Clypeus in lateral view with summit of convexity rounded (see Fig. 1C of Konishi and Aoyagi 1994).....***A. silvestris***

– Basal 1/4 of fourth submarginal cell and third discal cell of fore wing infuscate, without hyaline spot (arrows in Fig. 6F, G). Clypeus in lateral view with summit of convexity angulate (Fig. 5B)..... .....***A. wangpiensis* Choi and Lee, sp. nov.**

5 Face with median vertical ridge. Fore wing with abscissa of vein M between 2rs-m and 2m-cu 0.3–0.9 times as long as 2rs-m. Digitus elongated, but shorter than lamina volsellaris (Fig. 7C).....***A. jilinensis***

– Face without median vertical ridge. Fore wing with abscissa of vein M between 2rs-m and 2m-cu 2.0 times as long as 2rs-m. Digitus strongly elongated, longer than lamina volsellaris (Fig. 7D) **6**

6 Clypeus in anterior view with summit pointed medially (see Fig. 4E, F in Bennett 2001).....***A. gracilis***

– Clypeus in anterior view with summit rounded medially (see Fig. 1E, F of Konishi and Aoyagi 1994) **7**

7 Hypopygium concave in median dorsal margin (see Fig. 5D of Konishi and Aoyagi 1994). Clypeus in lateral view with summit of convexity evenly rounded (not angulate) (see Fig. 1F of Konishi and Aoyagi 1994)..... .....***A. silvestris***

– Hypopygium evenly round in median dorsal margin (Fig. 7B). Clypeus in lateral view with summit of convexity rounded dorsally and angulate ventrally (Fig. 8C).....***A. wangpiensis* Choi and Lee, sp. nov.**

Agriotypus jilinensis Chao, 1981

Figs 1, 6C–D, 7A, C, 8A, B

Agriotypus jilinensis Chao, 1981: 79. Chao & Zhang, 1981, by original description.

Specimens examined. ***Holotype*:** ♂, **China:** Changbaishan Nature Reserve, Jilin Province, 25. vi. 1980 (Y. Zhang) (Fujian Agriculture and Forestry University). **Other material: South Korea:** 1♀, 2.iv.2015, Toegokgyo, Toegok-ri, Yeongok-myeon, Gangneung-si, Gangwon-do (S.W. Jeong) (NNIBR); 1♀, 27.iv–10.v.2003, Jirisan, Hamyang-gun, Samjeong-li, 700 m asl, Malaise trap in a big clearing, 35°20'55"N, 127°38'21"E,

(P. Tripotin) (EUM); 1♀, 11.iv–8.v.2004, Jirisan, Macheon-myeon, Samjeong-li, 700 m asl, Malaise trap on small stream in forest clearing, 36°20.930'N, 127°38.503'E, (P. Tripotin) (EUM); 1♀18♂♂, 8.v–5.vi.2004, Jirisan, Macheon-myeon, Samjeong-li, 700 m asl, Malaise trap on small stream in forest clearing, 36°20.930'N, 127°38.503'E, (P. Tripotin) (EUM); 1♀, 11–18.v.2003, Jirisan, Samcheon-ri, Macheon-myeon, Hamyang-gun, Gyeongsangnam-do, Alt. 700 m, in cleared resinuous forest, (P. Tripotin) (DNUE_IIEI); 2♂♂, 24.iv.1997, Mt. Odae, Pyungchang, Kangwon, yellow pan trap (J.Y. Choi) (EUM); 1♀, 2–26.v.2006, above small stream, Dunjeon-ri, Sangchon-myeon, Yeongdong-gun, Chungcheongbuk-do, Alt. 750 m, 36°04'36"N, 127°50'17"E, (P. Tripotin) (DNUE_IIEI).

Description. Female. Body length 5.6–6.7 mm; fore wing length 4.5–5.2 mm.

Head. Face width (minimum length of inner orbits) 1.1 times as wide as its median height (length between antennal socket and clypeal margin), with a median vertical ridge (see Fig. 4G in Bennett 2001), with dense punctures and hairs except area between lateral ocellus and eye impunctate (Fig. 1B). Antenna with 20–22 flagellomeres, 0.5 times as long as fore wing. Temple behind eyes slightly roundly narrowed in dorsal view. Antennal scrobe deep. POL: OOL = 1:1–1:2. Face with median longitudinal ridge, coarse rugosity and dense pubescence. Area between antennal sockets with a glabrous short longitudinal tubercle. Clypeus in anterior view with apical margin truncate, not pointed; anterior edge in profile moderately convex; summit of convexity in lateral view angulate; shape of angular summit of clypeus in anterior view rounded medially (Fig. 1B). Distance between anterior tentorial pits 1.2–1.3 times as long as length between a tentorial pit and eye. Occipital carina weak, but complete. Malar space 1.4 times as long as basal width of mandible; mandible twisted, lower tooth longer than upper one.

Mesosoma. Pronotum with long and strong epomia extending dorsal of furrow and almost straight. Mesoscutum shiny, anterior 1/2–2/3 of median lobe moderately punctate and setose, the rest of medial lobe and all lateral lobes completely impunctate and lacking setae; notaulus distinct, meeting at around middle (Fig. 1D). Scutellum in dorsal view, long triangle-shaped, 1.6 times as long as its basal width including spine, 0.9–1.1 times as long as propodeum; scutellum with lateral carinae at base, convex medially, tapering toward apex, spine-like apical half, smooth (Fig. 1E); spine 0.5–0.6 times as long as propodeum (distance as long as lateral longitudinal carinae from base to apex); in lateral view roundly curved medially, weakly up-curved (Fig. 8D). Mesopleuron finely punctate and pubescent, with longitudinal groove complete, without longitudinal carina on anterior edge at mid-height; epicnemial carina curving sharply anteriorly to meet anterior edge of mesopleuron and with a vertical extension dorsally; sternaulus present as a weak and wide groove. Metapleuron finely punctate and pubescent Propodeum with lateromedian longitudinal carinae almost parallel; lateral longitudinal carinae straight, complete and parallel to lateromedian longitudinal carinae (Fig. 1F, G).

Wings. Fore wing with 1cu-a distad M&Rs; abscissa of vein M between 2rs-m and 2m-cu 1.0–2.0 times as long as 2rs-m. Hind wing with 6–8 distal hamuli; vein 1/Cu & 1cu-a intercepted by 1/Cu in lower 0.44 Cu (Fig. 1I).

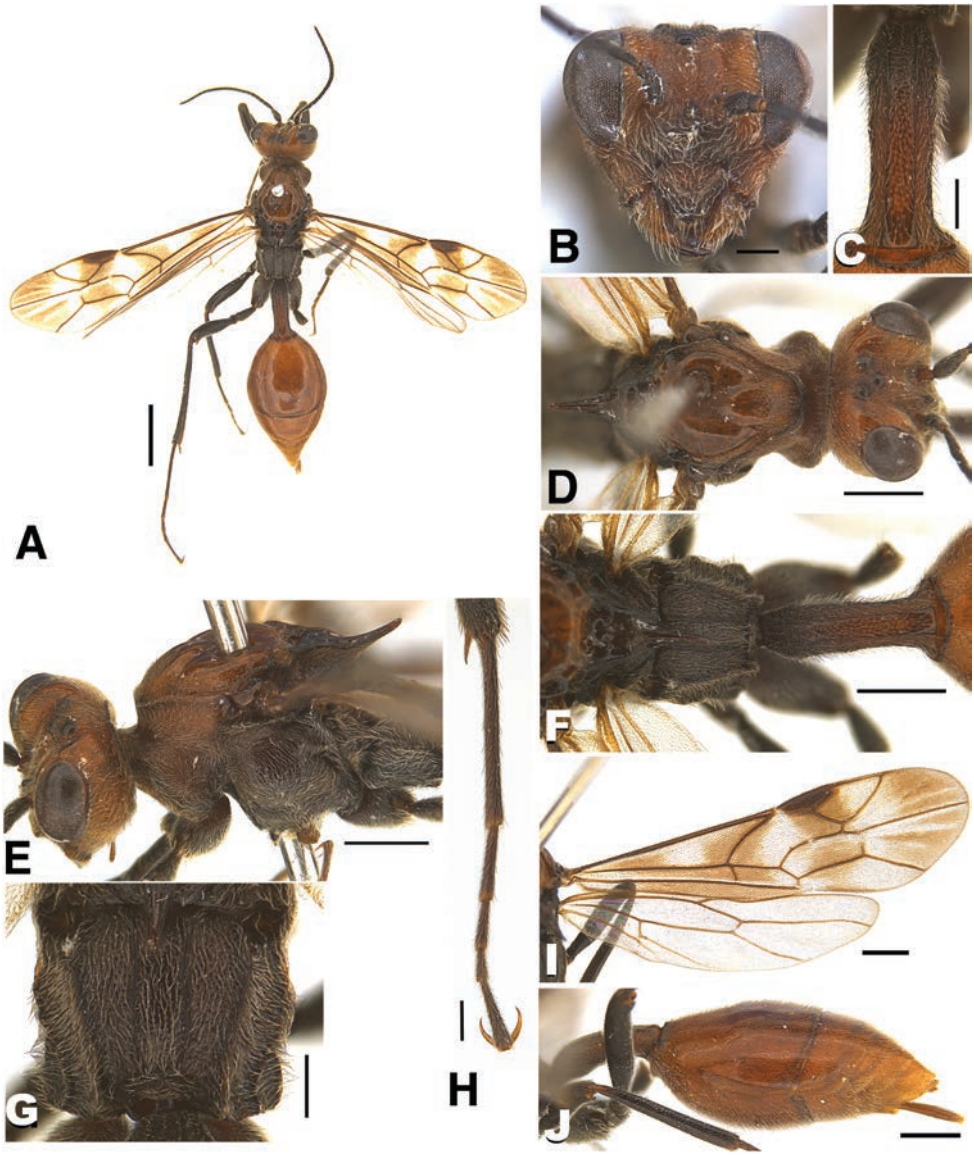

Figure 1. Adult of *A. jilinensis* (female) (non-type) **A** habitus in dorsal view **B** head in frontal view **C** metasomal tergite I in dorsal view **D** head and mesoscutum in dorsal view **E** head and mesosoma in lateral view **F** propodeum and metasomal tergite I in dorsal view **G** propodeum in dorsal view **H** hind tarsomeres and tarsal claw **I** wings **J** metasomal tergites in lateral view. Scale bars: 1 mm (**A**); 0.5 mm (**D, E, F, I, J**); 0.2 mm (**B, C, G, H**).

Metasoma. Metasomal tergite I 3.0–4.2 times as long as its posterior width (Fig. 1C), 1.6 times as long as length of propodeum; metasomal tergite I finely punctulate-reticulate, spiracles situated at anterior 0.20–0.25; lateromedian carinae and dorsolateral carinae complete and strong, reaching to apex. Metasomal tergite II and following

tergites densely punctulate and shiny (Fig. 1J). Metasomal tergite II without dorsal and dorsolateral carinae. Ovipositor sheath 0.6 times as long as length of hind basitarsus.

***Colour*.** Generally reddish brown. Head, pronotum, mesoscutum and metasoma reddish brown. Scutellum and metasomal tergite I dark reddish brown. All legs, mesopleuron and propodeum almost black. Fore wing with fuscous longitudinal bands and with wide hyaline spots occupying middle of basal cell, discosubmarginal cell and distal half of marginal and basal of fourth submarginal cells (Fig. 6C); hind wing hyaline (Fig. 1I).

Male. Agrees with the above-mentioned description of the female, except for the following character states: Body length 5.5–7.4 mm (holotype: 7 mm); fore wing length 4.7–6.0 mm; antenna with 29–34 flagellomeres (holotype: 32 flagellomeres); mesoscutum entirely punctate with setae; spine of scutellum laterally compressed and slightly up-curved or straight (Fig. 8B); abscissa of vein M between 2rs-m and 2cu-m 0.3–0.9 times as long as 2rs-m (Fig. 6D); metasomal tergite I 5.4 times as long as apical width, lateromedian carina incomplete posterior to 0.2 length of segment; body, antenna and legs black; wings hyaline except apical marginal area of fore wing weakly tinged with brown. Male genitalia and hypopygium shown in Fig. 7A, C, with digitus relatively weakly elongated but shorter than half of paramere, somewhat broadened toward apex (Fig. 7C). Apex of paramere almost truncate with corners rounded. Penis valve slightly curved ventrally; basal apodeme of aedeagus striate dorsally.

***Variation*.** The scutellar spine of the male holotype is straight and relatively stout apically compared to some South Korean *A. jilinensis* specimens that are more up-curved and tapered (although some are straight and non-tapered as in Fig. 8B).

Larva. Unknown.

Host. Unidentified Trichoptera.

Distribution. China (Jilin), South Korea (new record).

Region. Eastern Palaearctic.

Remarks. This species has been known previously from only two pharate males (holotype and paratype). Thus, this is the first description of the female and of the wings of the male. (Korean name: Am-bul-eun-bae-mul-beol).

Agriotypus wangpiensis Choi & Lee, sp. nov.

https://zoobank.org/2A235DB3-F5E4-484D-861E-3938B06EC3C6
Figs 2–5, 6E–G, 7B, D, 8C, D

Type materials. ***Holotype*** ♀, **South Korea:** 31.v.2022, Wangpicheon, Uljin-gun, Gyeongsangbuk-do, South Korea (S.J. Kwon), rearing date: 12.vi.2022. Type depository: DNUE-IIEI.

***Paratypes*.** 8 ♀♀, 31.v.2022, Wangpicheon, Uljin-gun, Gyeongsangbuk-do, South Korea (S.J. Kwon), rearing date: 7–17.vi.2022 (DNUE-IIEI, EUM); 2 ♀♀, ditto, (NNIBR-NNIBRIN166268, NIER); 16 ♂♂, Wangpicheon, Uljin-gun, Gyeongsangbuk-do, South Korea (S.J. Kwon), rearing date: 6–15.vi.2022 (DNUE-IIEI, EUM); 2 ♂♂, ditto, (NNIBR-NNIBRIN166269, NIER).

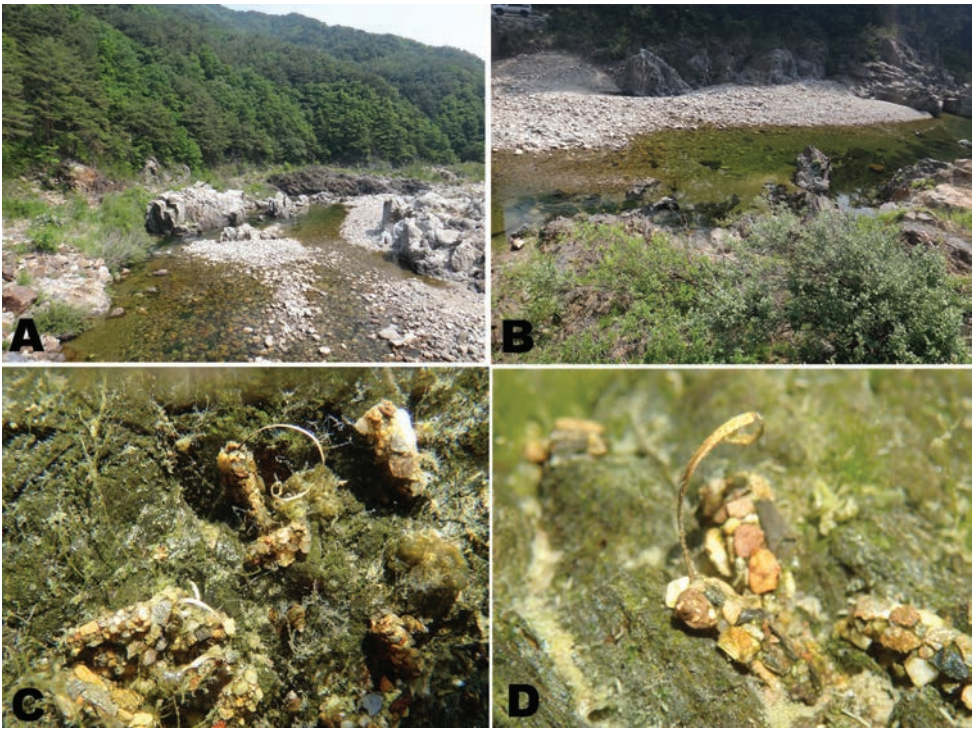

Figure 2. Habitat and collecting sites of *A. wangpiensis* sp. nov. **A** distant view of Wangpicheon stream **B** close range view of Wangpicheon stream **C** parasitized hosts **D** parasitized trichopteran pupae.

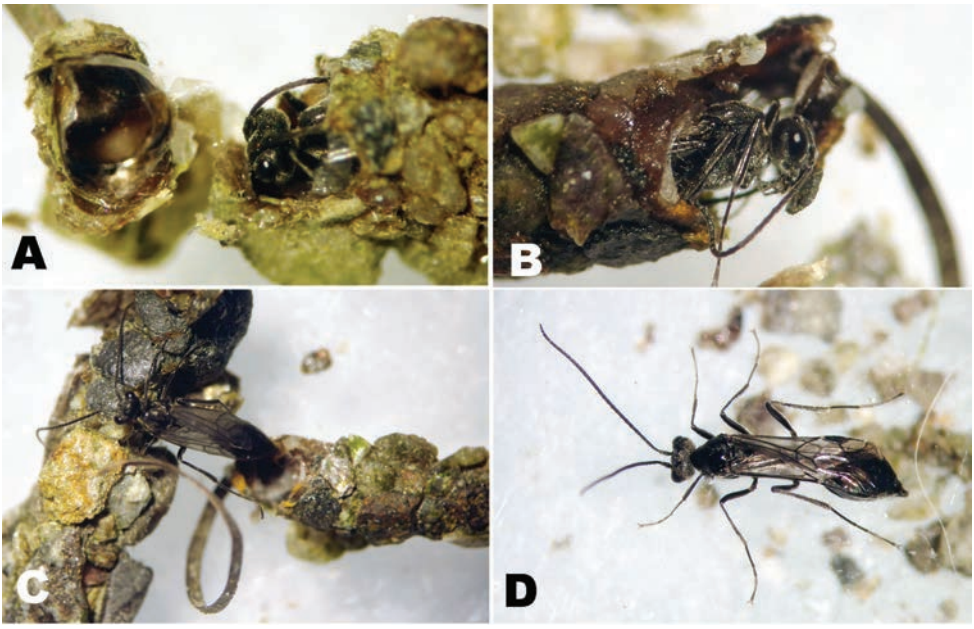

Figure 3. Reared *A. wangpiensis* sp. nov. **A–B** breaking case of trichopteran species **C** exiting trichopteran case **D** male adult following exit from trichopteran case.

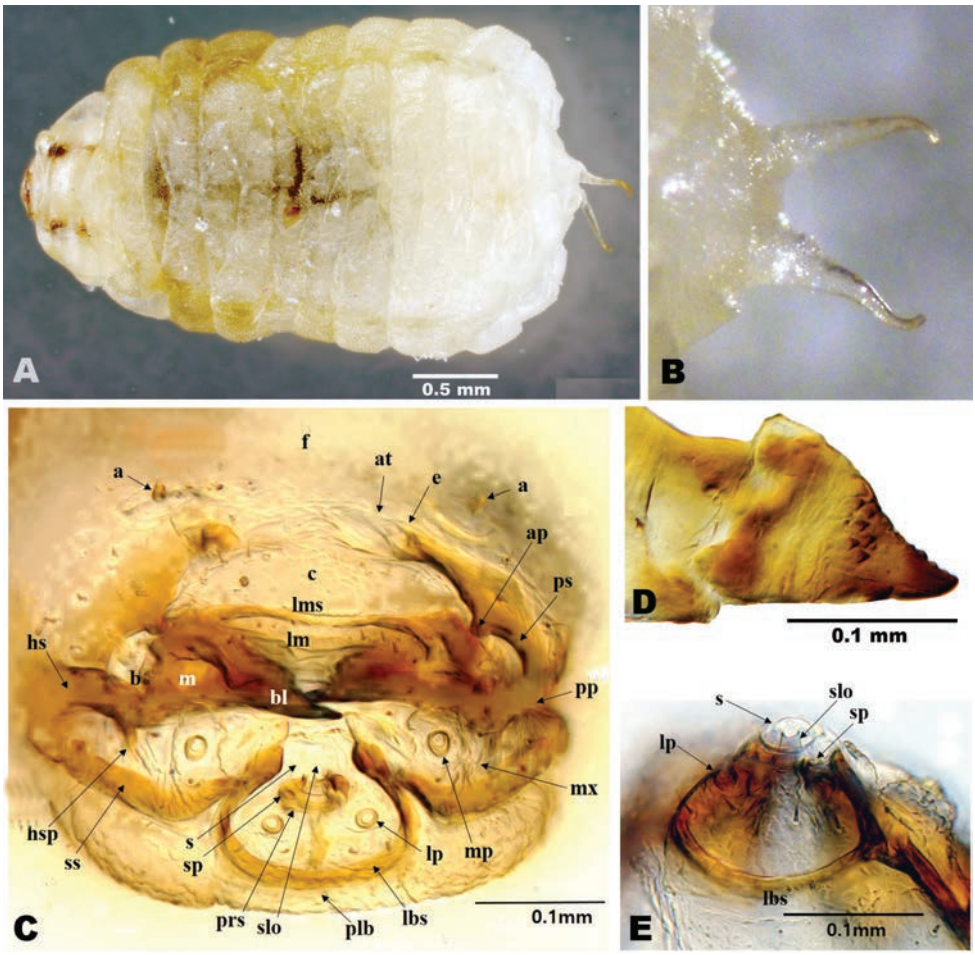

Figure 4. Final larva instar of *A. wangpiensis* sp. nov. **A** whole body of larva in dorsal view **B** caudal filaments **C** head of larva in frontal view **D** mandible of larva **E** salivary orifice (s) and orifice of silk press (slo) in ventral view. [**a**: antenna, **ap**: anterior pleurostomal process, **at**: anterior tentorial pit, **b**; base of mandible, **bl**: blade of mandible, **c:** clypeus, **e:** epistoma, **f:** frons, **hs**: hypostoma, **hsp**: spur of hypostoma, **Ib**: labium, **lbs**: labial sclerite, **1m**: labrum, **lms**: labral sclerite, **lp**: labial palp, **m**: mandible, **mp**: maxillary palp, **mx**: maxilla, **plb**: postlabium, **pp**: posterior pleurostomal process, **prlb**: prelabium, **prs**: prelabial sclerite, **ps**: pleurostoma, **s**: salivary orifice, **slo**: orifice of silk press, **sp**: silk press, **ss**: stipital sclerite].

Diagnosis. Females of *Agriotypus wangpiensis* sp. nov. can be distinguished from all other species for which the female is known by the combination of the following characters: 1) metasomal tergite II lacking dorsal and dorsolateral carinae anteriorly (Fig. 5F) (present in all species of the *A. himalensis* species group); 2) clypeus in lateral view with summit of convexity angulate (Fig. 5B) (rounded in *A. armatus* and *A. silvestris*); 3) clypeus in anterior view with summit of convexity rounded medially (Fig. 5C) (acutely pointed medially in *A. gracilis*); 4) pronotum with a long and strong epomia

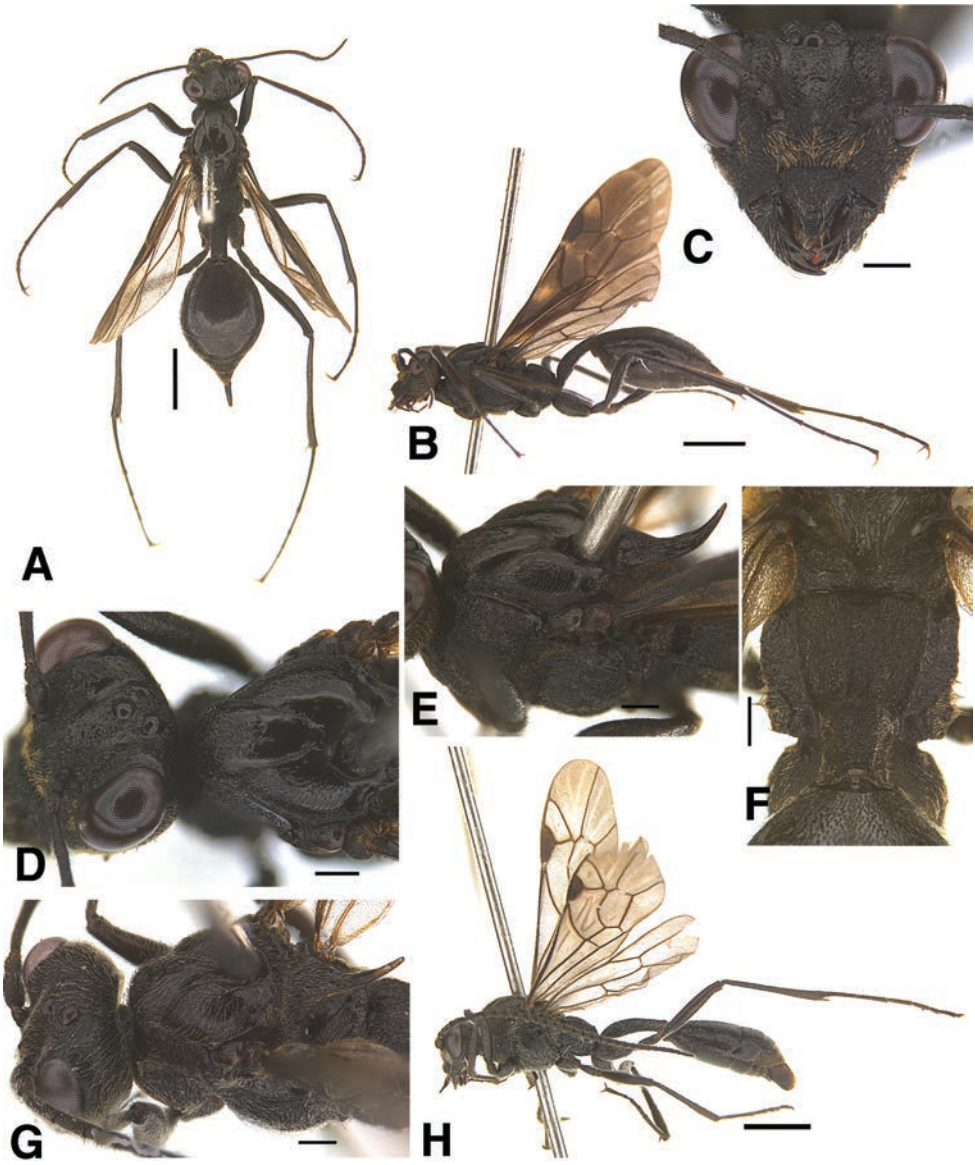

Figure 5. *A. wangpiensis* sp. nov. (Holotype, female **A–F** Paratype, male **G, H**) **A** habitus, dorsal view **B** habitus, lateral view **C** head, frontal view **D** head and mesoscutum, dorsal view **E** mesosoma, lateral view **F** propodeum, dorsal view **G** head and mesoscutum, dorsolateral view **H** habitus, lateral view. Scale bares: 1 mm (**A, B, H**); 0.2 mm (**C–G**).

extending dorsal of pronotal furrow (epomia short in *A. changbaishanus*, not extending dorsal of furrow as in Fig. 5B in Bennett 2001); 5) fore wing lacking complete longitudinal bands proximal and distal to pterostigma, the wing predominantly dark with at most hyaline fascia in basal, discosubmarginal and marginal cells (Fig. 6F, G) (fore

wing with complete longitudinal, hyaline bands proximal and distal to pterostigma in *A. jilinensis* as in Fig. 6C). Note that the female of *A. succinctus* (*A. armatus* group) is not known. In addition, females of several species of the *A. himalensis* species group are unknown, but it is likely they could be distinguished from the new species by character 1 (above). Males of *Agriotypus wangpiensis* sp. nov. can be distinguished from all other species for which the male is known by the combination of characters 1–4 in the female diagnosis as well as the face lacking a medial, vertical ridge (ridge present in *A. jilinensis*). All males of the *A. armatus* group are known.

Description. Female (Adult). Body length 5.0–6.8 mm; fore wing length 4.0–4.9 mm.

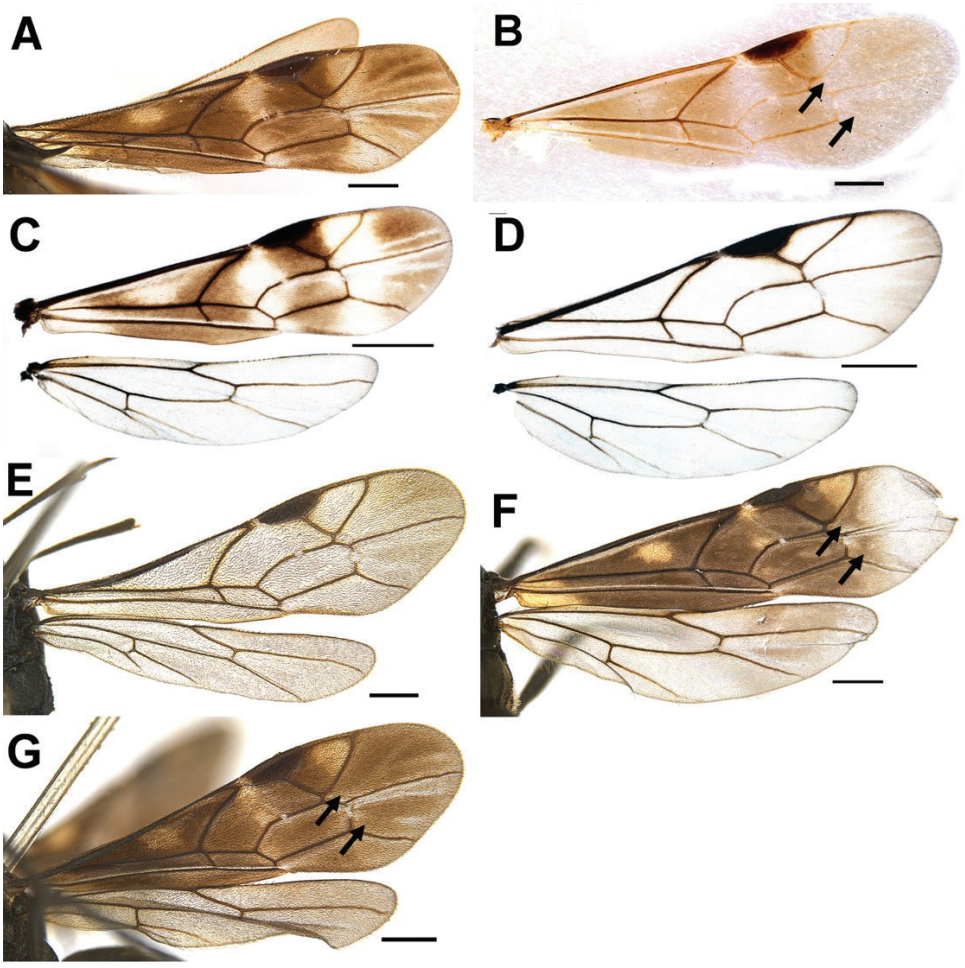

Figure 6. Wings of South Korean *Agriotypus* species (**A–C, F, G** female; **D–E** male) **A** *Agriotypus gracilis* **B** *A. silvestris* **C–D** *A. jilinensis* **E–G** *A. wangpiensis* sp. nov. (**F** = variation in paratype, **G** = holotype). Scale bars: 1 mm (**C, D**); 0.5 mm (**A, B, E–G**).

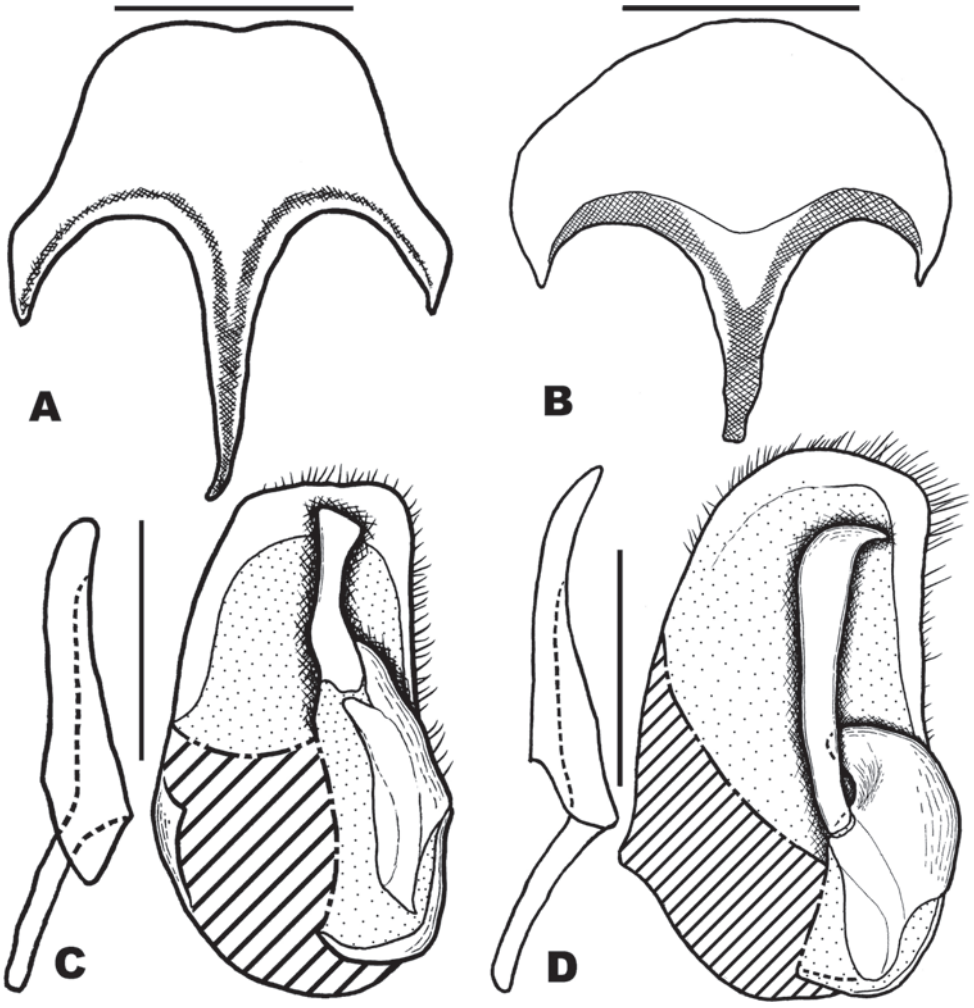

Figure 7. Male genitalia and hypopygium of *Agriotypus jilinensis* (**A, C** non-type) and *A. wangpiensis* sp. nov. (**B, D** paratype) **A** hypopygium, ventral view of *A. jilinensis* **B** hypopygium, ventral view of *A. wangpiensis* sp. nov. **C** genitalia of *A. jilinensis* **D** genitalia of *A. wangpiensis* sp. nov. Scale bar: 0.3 mm.

***Head*.** Head width 1.0 times as wide as its median height (Fig. 5C). Face width (minimum length of inner orbit) 1.57 times as wide as its median height (length between antennal socket and clypeal margin), convex medially, without a median vertical ridge, with coarse rugosity and dense pubescence (Fig. 5C). Antenna with 20 flagellomeres, 0.6 times as long as fore wing. Temple behind eyes roundly narrowed in dorsal view. Transverse diameter of eye 0.9 times as wide as temple in dorsal view. Frons finely densely punctulate-reticulate. Area between antennal sockets lacking a glabrous short longitudinal tubercle. Antennal scrobe deep. POL: OOL = 1: 2. Clypeus in anterior view with apical margin round; anterior edge in profile moderately convex; summit of convexity in lateral view angulate; shape of angular summit of clypeus in anterior view

rounded medially (Fig. 5C). Distance between anterior tentorial pits shorter than length between a tentorial pit and eye; malar space 1.3 times as long as basal width of mandible; mandible twisted, lower tooth longer than upper one. Occipital carina strong.

***Mesosoma*.** Pronotum with long and strong epomia, upper area of pronotum with more than 10 fine carinae dorso-posteriorly. Mesoscutum shiny, anterior half of median lobe and outer side of lateral lobes punctate and setose; notauli distinct, meeting in posterior 0.3 (Fig. 5D, E). Scutellum in dorsal view triangular, 1.8 times as long as its anterior width including spine, 1.25 times as long as length of propodeum; scutellum with lateral carina at base, and spine smooth in lateral view, distinctly upcurved (Figs 5E, 8D). Mesopleuron and metapleuron densely punctate, reticulate and pubescent, with longitudinal groove deep and wide, without longitudinal carina on anterior edge at mid-height; epicnemial carina curving sharply anteriorly to meet anterior edge of mesopleuron and with a vertical extension dorsally. Sternaulus present. Dorsal area of mesopleuron with transverse carinae. Propodeum finely coriaceous-punctate; lateromedian longitudinal and lateral longitudinal carinae weakly convergent posteriorly (Fig. 5F).

Figure 8. Head and mesosoma of *Agriotypus jilinensis* (non-type) (**A, B**) and *A. wangpiensis* sp. nov. paratype (**C, D**) **A** male head, lateral view **B** male mesosoma **C** male head, lateral view (arrow point to ventral angulation of clypeus) **D** male mesosoma. Scale bars: 0.1 mm (**A, C**); 0.2 mm (**B, D**).

***Wings*.** Fore wing with 1cu-a distad of M&Rs; abscissa of vein M between 2rs-m and 2cu-m 2.5–2.7 times as long as 2rs-m. Hind wing with 8 distal hamuli; vein 1/Cu & 1cu-a intercepted by 2/Cu in lower 0.25–0.35 (Fig. 6G).

***Metasoma*.** Metasomal tergite I 3.8 times as long as its apical width, 1.7 times as long as length of propodeum; metasomal tergite I finely punctulate-reticulate, spiracles situated in anterior 0.45, lateromedian and dorsolateral carinae complete and strong, reaching to apex. Metasomal tergite II lacks dorsal and dorsolateral carinae. Ovipositor sheath 0.7 times as long as length of hind basitarsus.

***Colour*.** Almost black. Apical spine of scutellum, posterior metasomal tergites slightly reddish brown. Fore wing generally infuscate, with small hyaline spots occupying middle of basal cell, discosubmarginal cell and marginal cell: hyaline spot of basal cell at basal 0.6 on the basal cell of fore wing, hyaline spots of discosubmarginal cell narrow, distal half of marginal cell with hyaline spot, fourth submarginal cell without hyaline spot (Fig. 6G).

***Variation*.** In some specimens, apical area of fore wing hyaline (Fig. 6F).

Male. Body length 5.0–6.0 mm; fore wing length 4.1–5.1 mm. Antenna with 27–29 flagellomeres. Fore wing with abscissa of vein M between 2rs-m and 2m-cu 2.0 times as long as 2rs-m. Hind wing vein 1/Cu & 1cu-a intercepted by 2/Cu at lower 0.43 (Fig. 6E). Metasomal tergite I 4.1–5.0 times as long as apical width, with incomplete dorsolateral carinae, extending only to 0.35 length of segment; lateromedian carinae of metasomal tergite I incomplete, but extending past spiracles. Fore wing hyaline (Figs 2, 5H, 6E); hind wing hyaline. Otherwise, similar to female. Male genitalia and hypopygium shown in Fig. 7B, D, with digitus relatively strongly elongated, longer than half of paramere, somewhat broadened toward apex, dorso-apical corner rounded and ventro-apical corner produced (Fig. 7D). Apex of paramere slightly convex. Penis valve curved ventrally, apex of penis valve produced, dorso-apical portion with a tooth; basal apodeme of aedeagus striate dorsally.

Last instar larva (Fig. 4). Body length 3.5 mm; body maximum width: 2.0 mm. Cephalic sclerites (Fig. 4D). Hypostoma (hs) wide; stipital sclerite (ss) moderately curved and sclerotized; labial sclerite (lbs) roundly triangular, narrowing dorsally, dorsal part almost 0.5 times as wide as ventral part, moderately sclerotized, except dorsally, with salivary orifice (s) circular (Fig. 4C). Apical part of larva with caudal filaments, paired and curved, apical part of caudal filaments darker (Fig. 4B). Mandible triangular, strongly sclerotized with 6–8 small toothlike projections medially on dorsal edge (Fig. 4D). Body color ivory (Fig. 4A).

Host. *Goera japonica* Banks, 1906 (Trichoptera: Goeridae). (Det. Dr. Kwon). The Wangpicheon River originates from Mt. Geumjangsan (849 m), which straddles Subi-myeon, Yeongyang-gun and Onjeong-myeon, Uljin-gun, GB, and flows into the East Sea through Uljin-gun.

Distribution. South Korea.

Region. Eastern Palaearctic.

Etymology. The species is named after 'Wangpicheon', from the location where the type specimens was collected. (Korean name: Wang-pi-mul-beol).

Molecular data. *COI* barcode sequences (GenBank accession nos. OQ981233.1–OQ981241.1), *Echthrus reluctator* (BOLD GMGMH1512-14) and *Endasys patulus* (BOLD HYCNL036-19; NCBI MK959419) (Figs 9, 10).

Remarks. This new species is similar to *A. silvestris* Konishi & Aoyagi, 1994, but the female can be distinguished from the latter by the profile of the clypeus (convex with angulation but, roundly convex without angulation in *A. silvestris*); the ratio of the lengths of the scutellar spine and the propodeum (scutellar spine length 1.25 times as long as propodeum but only 0.75 times as long as in *A. silvestris*); the colour of the female fore wing (basal areas of fourth submarginal cell and third discal cells of fore wing almost completely dark without hyaline spot (arrows in Fig. 6G) compared to *A. silvestris* that has the basal 1/4 of these cells hyaline (arrows in Fig. 6B)); length of metasomal tergite I of female (3.8 times as long as length of posterior width but 4.6 times as long as posterior width in *A. silvestris*); hypopygium (evenly round median dorsal margin but, emarginate in median dorsal margin in *A. silvestris*).

Agriotypus gracilis Waterston, 1930

Material examined. **Japan:** 1 ♂, 21.iii.2002, Honshu, Aichi, Horai, Shiose (N. Kawase) (DNUE_IIEI); 1 ♀, 21.vi–7.vii.2002, Honshu, Shizuoka, Shimizu (T. Nozaki) (DNUE_IIEI); 1 ♀, 16.xi.2013, Tokyo: Hamura City, Tamagawa River, 35.4507 139.1837, 116 m, reared (S. Shimizu) CNC5245937 (CNC).

Molecular data. *COI* barcode sequences BOLD CNC5245937 (=AIB453 AB2 in Figs 9 and 10).

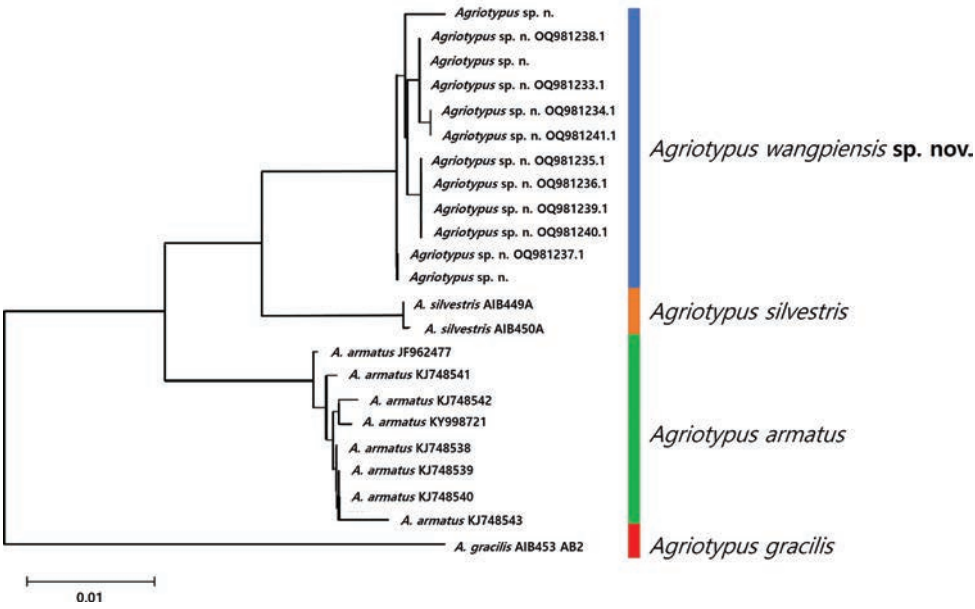

Figure 9. Neighbour-joining tree (NJ) of the successfully DNA barcoded specimens of *Agriotypus*.

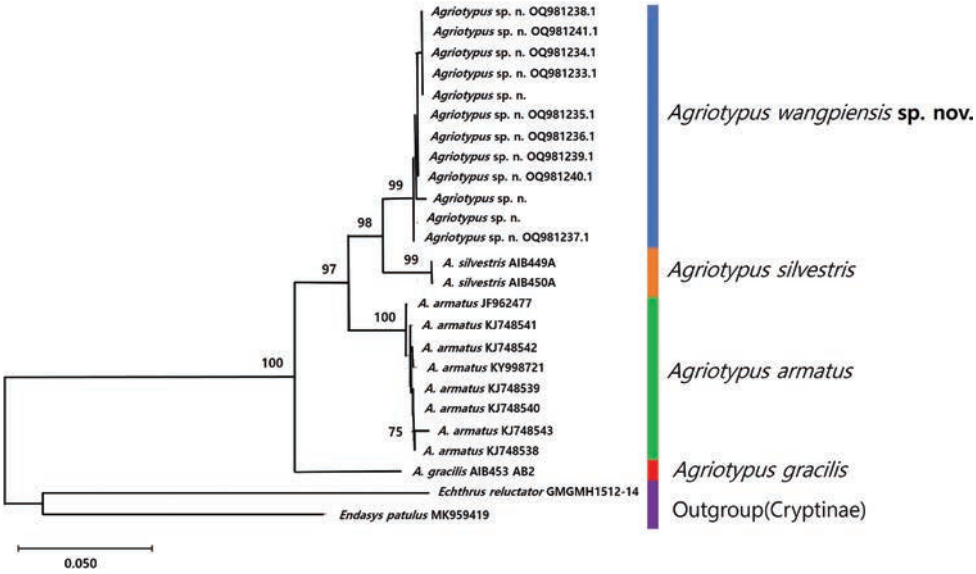

Figure 10. Maximum Likelihood tree (ML) of the successfully DNA barcoded specimens of *Agriotypus*. The bootstrap support for nodes is displayed if higher than 75%.

Agriotypus silvestris Konishi & Aoyagi, 1994

Material examined. Japan: 1 ♀, 11.ix.2006, Hokkaido Oshima, Mori-machi Torisaki river (T. Ito) (DNUE_IIEI); 1 ♂, 1–2.ix.1996, Honshu, Gunma, Matsuida env., 1100 m, yellow pan trap, (L. Masner) CNC5245940 (CNC); 1♂,1♀, 25.viii.1996, Honshu, Iwate, Mt. Hayachine, 750 m, yellow pan trap, (L. Masner & K. Yamagishi) (CNC5245938, CNC5245939) (CNC).

Molecular data. *COI* barcode sequences BOLD CNC5245938 (= AIB449A in Figs 9 and 10), BOLD CNC5245939 (=AIB450A in Figs 9 and 10).

Discussion

The first study on South Korean Agriotypinae by Kim (1963) reported *Agriotypus armatus* from South Korea. However, Konishi and Aoyagi (1994) and Bennett (2001) mentioned that *A. armatus* is very similar to *A. gracilis* but clearly distinguished by the clypeus, mesonotum, metasomal tergite I, host records, and geographical distribution. Kim et al. (2018) excluded the record of *A. armatus* from the South Korean insect fauna based on the literature review and specimen examination. Therefore four species, *A. gracilis*, *A. jilinensis*, *A. silvestris*, and *A. wangpiensis* sp. nov., are now known to be found in South Korea. All of these species belong to the *A. armatus* species group of Bennett (2001) on the basis of the lack of the longitudinal carina at the anterior of metasomal tergite II. Among them, *A. wangpiensis* sp. nov. is a parasitoid of *Goera japonica* Banks, 1906 in Wangpicheon in the northeast of Gyeongsangbuk-do Province.

In the DNA barcode analysis, *Agriotypus gracilis* is highly divergent from the other species (8.5–10% different DNA barcode) and *Agriotypus wangpiensis* sp. nov. is most closely related to *A. silvestris* (Fig. 9). The species status of *A. wangpiensis* sp. nov. is confirmed by both the unique combination of morphological characters (see the species diagnosis) and the molecular analysis that found that the DNA barcode region of the new species is 3.4–3.6% different from *A. silvestris* (Fig. 9). In a ML analysis (Fig. 10), the four species in the genus *Agriotypus* [*Agriotypus wangpiensis* sp. nov., *A. silvestris*, *A. gracilis* and *A. armatus*] clustered as a monophyletic group with strong support (100%). Also, the clustering of all specimens of *A. wangpiensis* sp. nov. together (monophyly of the new species) is supported by the 99% bootstrap score, while the sister relationship of the new species and *A. silvestris* is supported with 98% bootstrap score.

Acknowledgements

We are deeply grateful to Dr. Gavin Broad and an anonymous reviewer for reviewing this manuscript. Reviewers provided constructive criticism that improved this paper. We also thank to Dr. Tamara Spasojevic for acting as associate editor, Dr. Kwon, Soon Jik, Dr. Jeong, Jong-Chul, Mr. P. Tripotin, and Dr. Jeong, Sang Woo for assisting in collecting materials and identification of host. Also, we thank to Amber Bass (Agriculture and Agri-Food Canada) for providing COI sequences of *A. silvestris* and *A. gracilis*. This work was supported by the National Research Foundation of Korea (NRF) grant funded by the Korea government (MSIT) (NRF-2021R1F1A1052395) (Molecular analysis part) and a grant from the Nakdonggang National Institute of Biological Resources (NNIBR), funded by the Ministry of Environment (MOE) of the Republic of Korea (NNIBR202201201).

References

Bennett AMR (2001) Phylogeny of Agriotypinae (Hymenoptera: Ichneumonidae), with comments on the subfamily relationships of the basal Ichneumonidae. Systematic Entomology 26(3): 329–356. https://doi.org/10.1046/j.0307-6970.2001.00155.x

Bennett AMR, Cardinal S, Gauld ID, Wahl DB (2019) Phylogeny of the subfamilies of Ichneumonidae (Hymenoptera). Journal of Hymenoptera Research 71: 1–156. https://doi.org/10.3897/jhr.71.32375

Broad GR, Shaw MR, Fitton MG (2018) Ichneumonid Wasps (Hymenoptera: Ichneumonidae): their Classification and Biology. Natural History Museum 7(12): 418.

Chao HF, Zhang YC (1981) Two new species of *Agriotypus* from Jilin Province (Hymenoptera: Ichneumonoidea, Agriotypidae). [in Chinese with English summary]. Entomotaxonomia 3(2): 79–86.

Chao HF (1992) A new genus and three new species of Agriotypidae from China (Hymenoptera: Ichneumonoidea). Wuyi Science Journal 9: 325–332.

Curtis J (1832) British Entomology; being illustrations and descriptions of the genera of insects found in Great Britain and Ireland 9: 388, 389, 399, 407, 415–418.

Dalla Torre CG de (1902) Catalogus Hymenopterorum. Volumen III. Trigonalidae, Megalyridae, Stephanidae, Ichneumonidae, Agriotypidae, Evaniidae, Pelecinidae. Guilelmi Engelmann. Lipsiae 1901: 1–544. [1902: 545–1141.]

Felsenstein J (1985) Confidence limits on phylog\-enies: an approach using the bootstrap. Evolution 39: 783–791. https://doi.org/10.2307/2408678

Folmer O, Blank M, Hoeh W, Lutz R, Vrijenhoek R (1994) DNA primers for amplification of mitochondrial cytochrome c oxidase subunit I from diverse metazoan invertebrates. Molecular Marine Biology and Biotechnology 3(5): 294–299.

Geiger M, Moriniere J, Hausmann A, Haszprunar G, Wägele W, Hebert P, Rulik B (2016) Testing the Global Malaise Trap Program – How well does the current barcode reference library identify flying insects in Germany. Biodiversity Data Journal 4: e10671. https://doi.org/10.3897/BDJ.4.e10671

Haliday AH (1838) Essay on the classification of parasitic Hymenoptera. Entomological Magazine 5(3): 209–249. [missing p.224–225]

Hall TA (1999) BioEdit: a user-friendly biological sequence alignment editor and analysis program for Windows 95/98/NT. Nucleic Acids Symposium Series 41: 95–98.

Han TM, Kim S-H, Yoon H, Park I, Park HC (2019) Evolutionary history of species of the firefly subgenus Hotaria (Coleoptera, Lampyridae, Luciolinae, Luciola) inferred from DNA barcoding data. Contributions to Zoology 89: 1–19. https://doi.org/10.1163/18759866-20191420

Hebert PDN, Ratnasingham S, Zakharov EV, Telfer AC, Levesque BV, Milton MA, Pedersen S, Jannetta P, deWaard JR (2016) Counting animal species with DNA barcodes: Canadian insects. Philosophical Transactions of the Royal Society 371: 20150333. http://doi.org/10.1098/rstb.2015.0333

Hoang DT, Chernomor O, von Haeseler, A, Minh, BQ, Vinh LS (2017) UFBoot2: improving the ultrafast bootstrap approximation. Molecular Biology and Evolution 35: 518–522. https://doi.org/10.1093/molbev/msx281

Holmgren AE (1858) *Crotopus*, nytt genus ibland Ichneumoniderna. Öfversigt af Kongliga Vetenskaps-Akademiens Förhandlingar 15(1858): 353–354.

Kalyaanamoorthy S, Minh BQ, Wong TKF, von Haeseler A, Jermiin LS (2017) ModelFinder: fast model selection for accurate phylogenetic estimates. Nature Methods 14: 587–589. https://doi.org/10.1038/nmeth.4285

Kim CW (1963) Catalogue of Hymenoptera from Korea. Humanities and Sciences, Natural science, Korea University VI: 243–374.

Kim CJ, Oh SH, Suh KI (2018) Discovery of an Aquatic Wasp, *Agriotypus silvestris* Konishi & Aoyagi (Hymenoptera: Ichneumonidae: Agriotypinae) in South Korea. Korean Journal of Applied Entomology 57(4): 275–278.

Kimura M (1980) A simple method for estimating evolutionary rate of base substitutions through comparative studies of nucleotide sequences.Journal of Molecular Evolution 16: 111–120. https://doi.org/10.1007/BF01731581

Konishi K, Aoyagi M (1994) A new species of the genus *Agriotypus* (Hymenoptera, Ichneumonidae) from Japan. Japanese Journal of Entomology 62(3): 421–431.

Konishi K (2005) A preliminary revision of the subgenus *Netelia* of the genus *Netelia* from Japan (Hymenoptera, Ichneumonidae, Tryphoninae). Insecta Matsumurana 62: 45–121.

Latreille PA (1802) Histoire naturelle, générale et particulière, des Crustacés et des Insectes. Tome troisième. Paris 468 pp. [Ichneumonidae pp. 318–327] https://doi.org/10.5962/bhl.title.15764

Mason WRM (1971) An Indian *Agriotypus* (Hymenoptera: Agriotypidae). Canadian Entomologist 103: 1521–1524. https://doi.org/10.4039/Ent1031521-11

Minh BQ, Nguyen MAT, von Haeseler A (2013) Ultrafast approximation for phylogenetic bootstrap. Molecular Biology and Evolution 30: 1188–1195. https://doi.org/10.1093/molbev/mst024

Saitou N, Nei M (1987) The Neighbor-joining method: a new method for reconstructing phy\-logenetic trees. Molecular Biology and Evolution 4: 406–425.

Sharkey MJ, Wahl DB (1992) Cladistics of the Ichneumonoidea (Hymenoptera). Journal of Hymenoptera Research 1(1): 15–24.

Short JRT (1952) The morphology of the head of larval Hymenoptera with special reference to the head of Ichneumonidae, including a classification of the final instar larvae of the Braconidae. Transactions of the Royal Entomological Society of London 103: 27–84. https://doi.org/10.1111/j.1365-2311.1952.tb02262.x

Tamura K, Peterson D, Peterson N, Stecher G, Nei M, Kumar S (2011) MEGA5: molecular evolutionary genetics analysis using maximum likelihood, evolutionary distance, and maxi\-mum parsimony methods. Molecular Biology and Evolution 28: 2731–2739. https://doi.org/10.1093/molbev/msr121

Tamura K, Stecher G, Kumar S (2021) MEGA11: Molecular Evolutionary Genetics Analysis Version 11. Molecular Biology and Evolution 38: 3022–3027. https://doi.org/10.1093/molbev/msab120

Tang P, He J-h, Chen X-x (2022) Five new species of *Agriotypus* Curtis, 1832 (Hymenoptera, Ichneumonidae, Agriotypinae) from China. Journal of Hymenoptera Research 90: 1–22. https://doi.org/10.3897/jhr.90.79244

Townes HK (1969) The genera of Ichneumonidae, Part 1. Memoirs of the American Entomological Institute. No. 11. 300 pp.

Trifinopoulos J, Nguyen LT, von Haeseler A, Minh BQ (2016) W-IQ-TREE: a fast online phylogenetic tool for maximum likelihood analysis. Nucleic Acids Research 44: W232–W235. https://doi.org/10.1093/nar/gkw256

JHR 97: 491–504 (2024)
doi: 10.3897/jhr.97.121436
https://jhr.pensoft.net

RESEARCH ARTICLE

JOURNAL OF Hymenoptera RESEARCH
A peer-reviewed open-access journal
The International Society of Hymenopterists

A new enigmatic genus of the ichneumonid subfamily Ctenopelmatinae (Hymenoptera, Ichneumonidae) from Thailand

Avunjikkattu P. Ranjith[1], Donald L. J. Quicke[1], Alexey Reshchikov[2], Buntika A. Butcher[1]

1 *Integrative Insect Ecology Research Unit, Department of Biology, Faculty of Science, Chulalongkorn University, Bangkok, Thailand* **2** *Biodiversity and Environmental Change Lab, School of Biological Sciences, University of Hong Kong, Kadoorie Biological Sciences Building, Pokfulam Road, Hong Kong SAR, China*

Corresponding author: Buntika A. Butcher (buntika.a@chula.ac.th)

Academic editor: Tamara Spasojevic | Received 22 February 2024 | Accepted 17 May 2024 | Published 4 June 2024

https://zoobank.org/1B48635F-A630-4A27-A22C-4B6BEA2E1D5B

Citation: Ranjith AP, Quicke DLJ, Reshchikov A, Butcher BA (2024) A new enigmatic genus of the ichneumonid subfamily Ctenopelmatinae (Hymenoptera, Ichneumonidae) from Thailand. Journal of Hymenoptera Research 97: 491–504. https://doi.org/10.3897/jhr.97.121436

Abstract

The Ctenopelmatinae is one of the least explored groups of Ichneumonidae in South East Asia. We describe and illustrate an enigmatic new genus, *Thaictenopelma* Ranjith, Reshchikov & Quicke with the type species, *T. splendida* Ranjith, Reshchikov & Quicke, **sp. nov.**, from a moderately high altitude site in northern Thailand. The new genus shows a unique set of morphological characters that distinguishes it from all other ctenopelmatine genera. The presence of a pair of complete latero-median as well as complete dorso-lateral carinae on the T2 are considered autapomorphic characters of the new genus. Affinities of the new genus within the Ctenopelmatinae are discussed and a note on the taxonomic placement is provided.

Keywords

Malaise trap, new species, parasitoid wasp, South East Asia, taxonomy

Introduction

The ichneumonid subfamily Ctenopelmatinae consists of more than 1,500 species belonging to 113 genera (Yu et al. 2016; Broad et al. 2018; Li et al. 2022; Reshchikov et al. 2022). The subfamily is currently divided into nine tribes (Broad et al. 2018), but

its tribal classification is not stable (Gauld et al. 1997; Bennett et al. 2019) and it has never been recovered as monophyletic in phylogenetic analyses (Quicke et al. 2009; Bennett et al. 2019), possibly being paraphyletic with respect to Mesochorinae, Metopiinae, Oxytorinae and Tatogastrinae (Quicke et al. 2009; Quicke 2015). The most important characters of ctenopelmatines are the presence of an acute dorsal tooth on the apex of the fore tibia and a dorsal, subapical notch on the ovipositor of most species, although it is needle-like and lacking the notch in its egg-larval parasitoid members (most Pionini) (Cameron et al. 2014) as well as in species of some other genera, for example, *Lathrolestes* Förster (Reshchikov et al. 2010). In other respects, ctenopelmatines exhibit a wide spectrum of morphological characters (Townes 1970; Gauld 1984, Gauld et al. 1997). Species of Ctenopelmatinae are koinobiont endoparasitoids of sawfly (Hymenoptera) larvae and exceptionally of Lepidoptera caterpillars (Seyrig 1928; Heath 1961) and Coleoptera larvae (Barron 1994; Broad et al. 2018).

The known Oriental fauna of Ctenopelmatinae comprises 84 species belonging to 29 genera (Yu et al. 2016; Reshchikov et al. 2017a, b, 2022; Reshchikov and van Achterberg 2018; Li et al. 2022). However, since their host sawflies are a predominantly temperate group, it is unsurprising that they are particularly uncommon in tropical regions where they are predominantly restricted to montane areas (Malaise 1945; Gauld 1997; Reshchikov 2015; Reshchikov et al. 2018). The South East Asian fauna is particularly poorly known with the only published records being for *Gilen* Reshchikov & van Achterberg, 2018, *Metopheltes* Uchida, 1932, *Neurogenia* Roman, 1910, *Rhytidaphora* Reshchikov & Quicke, 2022 and *Rhorus* Förster, 1869 (Reshchikov et al. 2017a; Butcher and Quicke 2023), although we have seen specimens of *Scolobates* Gravenhorst, 1829 from Thailand. Of these, both *Gilen* and *Rhytidaphora* were described within the past decade, and the possibility that the recently described Chinese genus, *Unicarinata* Sheng, Li & Sun, 2022 might also occur in the region cannot be neglected.

Here we describe an enigmatic new genus and a species, *Thaictenopelma* Ranjith, Reshchikov & Quicke (type species: *Thaictenopelma splendida* Ranjith, Reshchikov & Quicke sp. nov.) from Doi Pha Hom Pok and Doi Phu Kha National Parks, both located in northern Thailand. In *Thaictenopelma* gen. nov., T2 has a pair of complete latero-median carinae as well as complete dorso-lateral carinae which is a unique combination not present in any other members of the subfamily. The new genus and species are described and comprehensively illustrated photographically, and taxonomic placement of the new genus is discussed.

Methods

All specimens were collected using Malaise traps set up as part of (i) two-year long sampling programme at Doi Phu Kha (2018 and 2022) (ii) from the two year long TIGER sampling programme 2007–2008 across Thailand (for habitat photo see Suppl. material 1), (iii) from Twin Peaks Project, and (iv) Tea Fauna Project (www.teafauna.com) sampling in northern Thailand. In total more than 600 trap months' worth of catches were sorted.

Images were acquired digitally using the Leica M205 C stereomicroscope with a DMC5400 Camera, stacked in LASX (ver. 3.7.4.23463). Images processed later in Adobe Photoshop.

List of repositories

CUMZ Chulalongkorn University Museum of Natural History, Bangkok, Thailand
QSBG Queen Sirikit Botanic Garden, Chiang Mai, Thailand

Morphological terminology follows Broad et al. (2018) and for cuticular sculpture we follow Harris (1979) and is aligned with the Hymenoptera Anatomy Ontology (HAO) (Yoder et al. 2010).

Morphological abbreviations used

F1 antennal flagellomere 1
OD the longest diameter of a posterior lateral ocellus
OOL the shortest distance between a posterior lateral ocellus and a compound eye
POL the shortest distance between the posterior lateral ocelli
S1–7 refers to the metasomal sternites 1–7
T1–T7 refers to the metasomal tergites 1–7

Results

Taxonomy

Thaictenopelma **Ranjith, Reshchikov & Quicke, gen. nov.**
https://zoobank.org/A8B80B96-E702-4500-BDC4-70CE265EDB20
Figs 1–5, see Suppl. material 2

Type species. *Thaictenopelma splendida* Ranjith, Reshchikov & Quicke gen. et sp. nov.

Diagnosis. *Thaictenopelma* gen. nov. can be separated from all other ctenopelmatine genera by its putatively autapomorphic carination pattern of T1 and T2. In particular, the pairs of complete latero-median and dorso-lateral carinae on T2 are completely unknown for the subfamily (Townes 1970). Additionally, the new genus can be distinguished from other ctenopelmatines by a combination of characters viz., the lower tooth of mandible being longer than upper tooth, propodeum with distinct carination, fore wing with rhombic areolet, T2 and T3 with posteriorly diverging groove basally, and T3 with distinct medio-basal protuberances.

Description. Female. ***Head.*** Eyes glabrous (Fig. 1B, C). Clypeus flat separated from face only by series of punctures (clypeal groove indistinct to absent), apical margin slightly concave (Fig. 1B). Mandible bidentate, lower tooth longer than up-

Figure 1. *Thaictenopelma splendida* Ranjith, Reshchikov & Quicke, gen. et sp. nov., holotype, female **A** habitus, lateral view **B** head, anterior view **C** head, antero-lateral view.

per tooth, the former more acute (Fig. 1B, C). Face with a short protuberance between antennal sockets (Fig. 1B). Malar space short, subocular sulcus absent (Figs 1B, C, 2B). Occipital carina complete (Fig. 2A, B, Suppl. material 2), joining with hypostomal carina just above base of mandible (Fig. 2B). Ocellar triangle with broad base, anterior ocellus slightly larger than posterior ocellus (Fig. 2A). Frons anteriorly depressed without median sulcus or carina (Fig. 2A). Terminal antennomere acute (Fig. 1A).

Figure 2. *Thaictenopelma splendida* Ranjith, Reshchikov & Quicke, gen. et sp. nov., holotype, female **A** head, dorsal view **B** head, ventro-lateral view **C** mesosoma, lateral view **D** mesosoma, dorsal view **E** propodeum, dorsal view **F** T1, dorsal view. Abbreviations: dlc, dorso-lateral carina, lmc, latero-median carina.

***Mesosoma*.** Mesosoma longer than high, setose (Fig. 2C). Epomia absent (Fig. 2C). Mesoscutum closely punctate (Fig. 2D). Notauli slightly impressed anteriorly, largely absent posteriorly (Fig. 2D). Mesopleuron closely punctate, smooth medially including speculum (Fig. 2C). Epicnemial carina extending to half height, not joining anterior margin of mesopleuron (Fig. 2C), complete ventrally (see Suppl. material 2). Scuto-scutellar groove smooth, not divided (Fig. 2D). Scutellum slightly bulged in lat-

Figure 3. *Thaictenopelma splendida* Ranjith, Reshchikov & Quicke, gen. et sp. nov., holotype, female **A** metasoma, lateral view **B** T1, lateral view **C** T2–4, dorsal view. Abbreviations: dlc, dorso-lateral carina, lmc, latero-median carina, vlc, ventro-lateral carina.

eral view, lateral scutellar carina present only anteriorly (Fig. 2D). Metanotum closely punctate medially, with irregular wrinkles laterally (Fig. 2E). Metapleuron punctate, setose, submetapleural carina strong forming distinct lobe anteriorly, juxtacoxal carina absent (Fig. 2C). Posterior transverse carina complete ventrally. Propodeum with distinct carinae, area basalis transverse, area superomedia hexagonal, as long as wide, smooth, area externa transverse, closely punctate, area dentipara subtriangular, closely

Figure 4. *Thaictenopelma splendida* Ranjith, Reshchikov & Quicke, gen. et sp. nov., holotype, female **A** apex of fore tibia, lateral view **B** tarsal claw, lateral view **C** wings.

punctate, setose, area petiolaris hexagonal, smooth, setose, area posteroexterna smooth, setose, anterior and posterior transverse carinae present, complete, pleural and lateral longitudinal carinae present, spiracle oval (Fig. 2E).

Wings. Fore wing with rhombic areolet (Fig. 4C). Vein 2r&RS originating from the middle of pterostigma (Fig. 4C). Vein 2m-cu with single, rather wide bulla, joining areolet medially (Fig. 4C). Vein 1cu-a interstitial and declivous (Fig. 4C). Vein CU originating below middle of first subdiscal cell (Fig. 4C). Hind wing with CU&cu-a receiving distal abscissa of CU at middle (Fig. 4C).

Legs. Fore tibia with acute lobe apically, with short spine on dorsal margin (Fig. 4A). Fore and mid coxae smooth, hind coxa punctate (Figs 1A, 3A). Tarsal claw sparsely pectinate to middle (Fig. 4B).

Metasoma. Metasoma coarsely punctate (Figs 2F, 3). T1 setose, transversely, coarsely rugose punctate with dorso-lateral carina (dmc) and latero-median carina (lmc) com-

plete to apex, latero-median carinae with a trace of transverse carina extending laterally at apical 2/3rd, ventro-lateral carina (vlc) present, complete, glymma present basally extending dorsally to join basal depression of tergite (not extending horizontally so that both glymmae are only separated from the dorsal depression by a thin, translucent partition), baso-dorsal depression separated by longitudinal tubercle, posterior margin of T1 convex medially, spiracle located slightly anterior to mid-length (Figs 2F, 3A, B). S1 present in basal ¼th, divided from T1 posteriorly (Fig. 3A, B). T2 coarsely punctate with dorso-lateral and latero-median carinae with a trace of transverse carina extending laterally at apical 2/3rd, pair of posteriorly diverging grooves present baso-laterally, spiracle situated at basal 1/3rd below lateral longitudinal carina, setose posteriorly (Fig. 3A, C). T3 punctate to rugose punctate (less coarse than T2) with posteriorly diverging groove baso-laterally and a pair of protuberances medio-basally, sparsely setose medially and distinctly setose posteriolry (Fig. 3C). T4–7 closely punctate (less coarse than T3) without carinae, setose (Fig. 3A, C). Ovipositor sheath setose (Fig. 3A). Ovipositor with distinct dorsal notch, without dorsal nodus dorso-apically (Fig. 3A, Suppl. material 2).

Etymology. The generic name derived from a combination of '*Thai*' for Thailand and '*Ctenopelma*', type genus of the subfamily Ctenopelmatinae.

Distribution. Thailand.

Species included. The genus is described as monotypic.

Thaictenopelma splendida Ranjith, Reshchikov & Quicke, sp. nov.

https://zoobank.org/290A9FF7-1B38-4EA8-8503-FAE23B475054

Type material. ***Holotype*.** Thailand • ♀, Nan Province, Doi Phu Kha National Park; 19°12.236'N, 101°04.667'E, altitude 1,341 m.a.s.l. 5–6 July 2022, Malaise trap, Worapong Atsawasiramanee leg.; Malaise trap (CUMZ). ***Paratypes*:** Thailand • 2♂, Thailand, Nan province, Pua district, Doi Phu Kha National Park, 19°10.450'N, 101°06.370'E alt. 1677 m, 7–20.ix.2018, Malaise trap, coll. Worapong Atsawasiramanee (CUMZ); 1♀, Chiang Mai Province, Doi Pha Hom Pok National Park, Doi Pha Luang; 20°1.06'N, 99°9.581'E, altitude 1,449 m.a.s.l., 27 Jul. – 3 Aug. 2007, Malaise trap, T2932, Wongchai P. leg.; (QSBG); 1♀ & 1♂; same sampling data but 3–10 Aug. 2007, T2931, Wongchai P. leg. (QSBG); 1♂ same sampling data but 7–14 Oct. 2007, T6209, Wongchai P. leg.; (QSBG).

Description. Female (*holotype*): Body length 8.5 mm, fore wing length 7.8 mm.

***Head*.** Antenna with 42 flagellomeres, all longer than wide, flagellomeres narrowing towards apex, F1 1.5 × as long as F2, F1 & F2 2.4, 1.8 × as long as wide, respectively. Scape approximately as long as maximally wide (Fig. 1B). Head transverse 1.5 × as wide as high in anterior view, 1.8 × as wide as long in dorsal view. Face transverse, flat, distinctly punctate with granulate interspace, setose, 2.0 × as long as wide (Fig. 1B). Inner margin of eyes parallel (Fig. 1B). Clypeus transverse, 3.5 × as long as wide, sepatated from face by distinct suture (Fig. 1B). Malar space 0.4 × as long as basal width of mandible. Lower tooth of mandible 1.6 × as long as upper tooth. Gena 0.6 × as long

as eye in lateral view, 0.7 × as long as transverse diameter of eye in dorsal view. Frons distinctly punctate with granulate interspace, setose (Fig. 2A). OOL 2.1 × OD; OOL 1.9 × POL. Vertex and occiput distinctly punctate with granulate interspaces (Fig. 2A).

Mesosoma. Mesosoma 1.4 × as long as high. Pronotum rugose punctate with indistinct groove laterally, setose (Fig. 2C). Propleuron distinctly punctate, setose (Fig. 2C). Scutellum 0.7 × as long as wide, moderately punctate with smooth interspace, setose (Fig. 2D). Propodeum with area superomedia 1.0 × as long as wide, anterior transverse carina straight laterally, lateral extension of posterior transverse carina distinctly curved (Fig. 2E).

Wings. Pterostigma 3.4 × as long as wide. Fore wing areolet 0.8 × as long as maximum width. Vein 2rs-m 1.5 × as long as 3rs-m.

Legs. Hind femur, tibia and basitarsus 5.4, 5.7, 5.9 × as long as its maximum width, respectively.

Metasoma. T1 1.0 × as long as its maximum width. T2 0.7 × as long as its maximum width. T2 1.1 × as long as T3. T3 0.6 × as long as its maximum width. Ovipositor sheath 0.2 × as long as hind basitarsus.

Coloration. Body mostly black except the following yellow: face and clypeus except medially, mandible except apically, gena postero-basally, frons laterally, pronotum antero- and postero-laterally, mesopleuron posteriorly, scutellum, axilla, metanotum mediobasally and postero-laterally, metapleuron except anterior blackish patch, propodeum except area externa, fore leg, mid coxa, mid femora, mid tibia, mid basitarsus except apically, hind coxa dorsally and baso-ventrally, hind tibia medially, T1 mediobasally, posterior margin of T1, anterior and posterior margin of T2, anterior margin of T3 and ovipositor; the following brown: antenna except medially, hind coxa apico-ventrally, hind trochanter and femur, hind tibia basally and apically, hind basitarsus basal 1/3^{rd,} venation, pterostigma, hind basitarsus apically, hind tarsus 2–3, tarsal claw brown; and the following white: antenna medially, medial tarsomere 4–5, hind basitarsus apical 2/3rd, hind tarsomere 2–5.

Variation. In paratypes from Doi Pha Luang antenna with 39 flagellomeres, occiput more strongly concave, area superomedia with transverse carina more strongly arched posteriorly. Clypeus completely black except apically, metapleuron and anterior part of propodeum black, T2 baso-laterally black.

Male. Same as female except the following characters; Clypeus transverse, 3.2 × as long as wide, clypeal margin protrtuding anteriorly (Fig. 5A). Scape 1.4 × long as its maximum width (Fig. 5A). Face transverse, flat, shallowly punctate with shagreen matt interspace, setose, 1.6 × as long as wide. Malar space 0.3 × as long as basal width of mandible. Lower tooth of mandible 1.8 × as long as upper tooth. T1 1.5 × as long as its maximum width. T2 0.6 × as long as its maximum width (Fig. 5B). Posterior margin of S4 and S6 rounded, of S5 straight (Fig. 5C). Apex of paramere elongate, its margin round (Fig. 5C). Inner margin of ventral side of paramere parallel at base (Fig. 5C). Tip of aedeagus swollen, decurved, its apex rounded. Yellow colored areas relatively larger than in female, those face and clypeus completely, mesopleuron, middle part of T1 between latero-median carina yellow.

Figure 5. *Thaictenopelma splendida* Ranjith, Reshchikov & Quicke, gen. et sp. nov., paratype, male **A** head, anterior view **B** propodeum and T1–3 dorsal view **C** S4–6 and male genitalia ventral view.

Biology. Unknown.

Etymology. The species is named after the magnificent combination of morphological characters which are completely unknown from the members of the subfamily.

Distribution. Thailand.

Discussion

The complete lateral longitudinal cartina of T2 is one of the diagnostic characters used by Townes (1970) to recognise the Ctenopelmatini, although this character state is also present in several species in the genera *Hadrodactylus* Förster, 1869 (Euryproctini) and *Rhorus* (Pionini). However, in members of the Ctenopelmatini, T8 of the female is produced posteromedially between the base of the ovipositor sheath and the cercus whereas in *Thaictenopelma* gen. nov. T8 apical margin is normal. Further, the

carination pattern of T1 and T2 disagrees with a placement in Ctenopelmatini as all carinae (dorso-lateral and latero-median) are extended up to the posterior margins of the tergites. The complete propodeal carination of *Thaictenopelma* gen. nov., including a completely defined area superomedia, is a putatively plesiomorphic character state found in the Pionini Smith & Shenefelt, 1955 (most genera) and Perilissini Thomson, 1883 (*Lathrolestes* Förster, 1869 and *Perilissus* Förster, 1855), and only a few ctenopelmatines (*Austropion* Gauld, 1984, *Hodostates* Förster, 1869, *Glyptorhaestus* Thomson, 1894, *Phaestus* Förster, 1869, *Petilium* Townes, 1970, *Lathrolestes* and *Perilissus*) (Townes 1970; Gauld 1984, Gauld et al. 1997).

The new genus appears most similar to the pionine, *Austropion* from Australia (Gauld 1984), but *Thaictenopelma* gen. nov., which also has the ovipositor with a distinct (albeit shallow) pre-apical dorsal notch (Suppl. material 2), but can be clearly distinguishable from *Austropion* by a combination of following characters; the lower tooth of the mandible longer than the upper tooth (upper tooth longer that lower tooth in *Austropion*), the occipital carina complete (obsolescent in *Austropion*), the fore wing areolet broad basally (petiolate in *Austropion*), T1 with complete dorso-lateral carina (carina absent in apical half in *Austropion*), T2 with a pair of complete latero-median and dorso-lateral carinae (smooth without carinae in *Austropion*), and the ovipositor without an acute dorsal process (with acute dorsal process in *Austropion*). Gauld (1984) placed *Austropion* in the Pionini based on carination but noted that it was rather aberrant. The only other genus tradionally placed in the Pionini with an ovipositor notch is *Hodostates* Foerster, 1869, and based on this character, Cameron et al. (2011) stated that they " ... are confident in rejecting *Hodostates* from Pionini", but the combined molecular and morphological analyses of Quicke et al. (2009) recovered *Hodostates* deeply nested among other Pionini genera and thus it appears that a notched ovipositor is likely to be homoplastic within the subfamily as noted by Cameron et al. (2011).

Thaictenopelma gen. nov. is also similar to the *Priopoda* group of genera (Perilissini) by having the occipital carina joining with hypostomal carina at base of mandible (Fig. 2B, Suppl. material 2). Within *Gilen*, *Neurogenia*, *Priopoda* Holmgren, 1856 and *Lathrolestes*, the new genus is most closely resemble *Gilen* by having T2–3 with a broad subapical transverse impression and T2 lateral longitudinal carina but readily discriminate by lacking produced mid-longitudinal facial projection and having distinct complete latero-median carina of T2.

Due to the presence of rather mixed combination of morphological characters displayed in different tribes (Ctenopelmatini, Perilissini and Pionini) we refrain from assigning the new genus to any of the extant tribes and we prefer to keep it as *incertae sedis* within the Ctenopelmatinae, although on balance it seems most probable that belongs to the Perilissini. Similar conditions have been found in a couple of genera like *Labrossyta* Förster, 1869 and *Hodostates* (Townes 1970). All these strongly point to the need for comprehensive analyses of the tribal classification of the Ctenopelmatinae.

Finally, at the only two known localities, the new species seems either to be very uncommon or not to get collected easily in Malaise traps, since we only found seven individuals from more than 600 Malaise trap months' (>50 years) of sampling.

Acknowledgements

We are grateful to thank Mr. Chatchai Yothawut, Director of Doi Phu Kha National Park, and Mr. Phasin Inkeaw, and Mr Kenneth Rimdahl (Monsoon Tea) for providing facilities, and cooperation during field trips, Prof Michael Sharkey (University of Kentucky) and Dr. Wichai Srisuka (QSBG) for providing samples of TIGER and Twin Peaks projects. APR was supported by a postdoctoral fellowship from the Rachadaphiseksomphot Fund, Graduate School, Chulalongkorn University. DLJQ was supported by a senior postdoctoral fellowship from the Rachadaphiseksomphot Fund, Graduate School, Chulalongkorn University. This research is financially supported by the Thailand Science Research and Innovation Fund Chulalongkorn University and Rachadaphiseksomphot Fund, CU (RU66_008_2300_002) and RSPG Chula to BAB. We thank the section Editor, Drs Andrew Bennett, Filippo Di Giovanni and an anonymous reviewer for the constructive comments and suggestions.

References

Barron JR (1994) The Nearctic species of *Lathrolestes* (Hymenoptera, Ichneumonidae, Ctenopelmatinae). Contributions of the American Entomological Institute. 28(3): 135.

Bennett AMR, Cardinal S, Gauld ID, Wahl DB (2019) Phylogeny of the subfamilies of Ichneumonidae (Hymenoptera). Journal of Hymenoptera Research 71: 1–156. https://doi.org/10.3897/jhr.71.32375

Broad GR, Shaw MR, Fitton MG (2018) Ichneumonid wasps (Hymenoptera: Ichneumonidae): their classification and biology. Handbooks for the Identification of British Insects 7(12): 1–418.

Butcher BA, Quicke DLJ (2023) Parasitoids Wasps of South East Asia. CABI, Wallingford, 440 pp. https://doi.org/10.1079/9781800620605.0000

Cameron MD, Wharton RA (2011) Revision of *Hodostates* (Hymenoptera: Ichneumonidae: Ctenopelmatinae), with a discussion of tribal placement. The Canadian Entomologist 143(2): 136–156. https://doi.org/10.4039/n10-054

Cameron MD, Wharton RA, Restuccia DM (2014) A morphological assessment of the ovipositor in the subfamily Ctenopelmatinae (Hymenoptera: Ichneumonidae) with specific reference to variation in the subapical, dorsal notch and its evolutionary significance. In: Trud Ruskava entomoligicheskava obshtestva [Труды Русского энтомологического общества] 77–90. https://doi.org/10.47640/1605-7678_2014_85_1_77

Gauld ID (1984) An introduction to the Ichneumonidae of Australia. British Museum (Natural History), Publication No. 895, 1–413.

Gauld ID, Wahl D, Bradshaw K, Hanson P, Ward S (1997) The Ichneumonidae of Costa Rica 2. Introduction and keys to species of the smaller subfamilies, Anomaloninae, Ctenopelmatinae, Diplazontinae, Lycorininae, Phrudinae, Tryphoninae (excluding *Netelia*) and Xoridinae, with an appendix on the Rhyssinae. Memoirs of the American Entomological Institute 57: 1–485.

Harris RA (1979) A glossary of surface sculpturing. California Department of Food and Agriculture, Bureau of Entomology, Occasional Paper, No. 28, 1–31.

Heath J (1961) Some parasites of Eriocraniidae (Lep.). Entomologist's Monthly Magazine. 97: 163.

Li T, Sun S-P, Sheng M-L (2022) A new genus and species of Ctenopelmatinae (Hymenoptera, Ichneumonidae) from China. Journal of Hymenoptera Research 92: 199–210. https://doi.org/10.3897/jhr.92.84969

Malaise RE (1945) "Tenthredinoidea" of South-Eastern Asia: with a General Zoogeographical Review. Entomologiska sällskapet 1945: 312.

Quicke DLJ, (2015) The Braconid and Ichneumonid Parasitoid Wasps: Biology, Systematics, Evolution and Ecology. John Wiley & Sons, Chichester, 752 pp. https://doi.org/10.1002/9781118907085

Quicke DLJ, Laurenne NM, Fitton MG, Broad GR (2009) A thousand and one wasps: a 28S rDNA and morphological phylogeny of the Ichneumonidae (Insecta: Hymenoptera) with an investigation into alignment parameter space and elision. Journal of Natural History 43: 1305–1421. https://doi.org/10.1080/00222930902807783

Reshchikov A (2015) The world fauna of the genus *Lathrolestes* (Hymenoptera, Ichneumonidae). Tartu 2015, 247 pp. https://doi.org/10.13140/RG.2.1.3969.4240

Reshchikov A, van Achterberg C (2018) The Unicorn exists! A remarkable new genus and species of Perilissini (Hymenoptera: Ichneumonidae) from South East Asia. Acta Entomologica Musei Nationalis Pragae 58(2): 523–529. https://doi.org/10.2478/aemnp-2018-0041

Reshchikov A, Soper A, Van Driesche R (2010) Review and key to Nearctic *Lathrolestes* Förster (Hymenoptera: Ichneumonidae), with special reference to species attacking leaf mining tenthredinid sawflies in *Betula* Linnaeus (Betulaceae). Zootaxa 2614(2614): 1–17. https://doi.org/10.11646/zootaxa.2614.1.1

Reshchikov A, Choi J-K, Xu Z-F, Pang H (2017a) Two new species of the genus *Rhorus* Förster, 1869 from Thailand (Hymenoptera, Ichneumonidae). Journal of Hymenoptera Research 54: 79–92. https://doi.org/10.3897/jhr.54.11662

Reshchikov A, Xu Z-f, Pang H (2017b) First record of the genus *Lethades* Davis, 1897 from the Oriental region, with description of a new species (Hymenoptera, Ichneumonidae, Ctenopelmatinae). ZooKeys 644: 43–50. https://doi.org/10.3897/zookeys.644.10491

Reshchikov A, Sääksjärvi IE, Pollet M (2018) Review of the New World genus *Nanium* Townes, 1967 (Hymenoptera: Ichneumonidae: Ctenopelmatinae), with two new species from the Neotropical region. European Journal of Taxonomy 459: 1–18. https://doi.org/10.5852/ejt.2018.459

Reshchikov A, Quicke DLJ, Butcher BA (2022) A remarkable new genus and species of Euryproctini (Hymenoptera: Ichneumonidae, Ctenopelmatinae) from Thailand. European Journal of Taxonomy 834: 102–116. https://doi.org/10.5852/ejt.2022.834.1903

Seyrig A (1928) Note sur les Ichneumonides du Museum national d'Histoire naturelle. Bulletin du Muséum National d'Histoire Naturelle, Paris 34: 259–265.

Townes HK (1970) The genera of Ichneumonidae, Part 3. Memoirs of the American Entomological Institute 13: 1–307.

Yoder MJ, Mikó I, Seltmann KC, Bertone MA, Deans AR (2010) A gross anatomy ontology for Hymenoptera. PLOS ONE 5(12): e15991. https://doi.org/10.1371/journal.pone.0015991

Yu DSK, van Achterberg C, Horstmann K (2016) Taxapad 2016, Ichneumonoidea 2015. Database on flash-drive, Nepean, Ontario, Canada.

Supplementary material 1

Type locality of *Thaictenopelma splendida* Ranjith, Reshchikov & Quicke gen. et sp. nov.

Authors: Avunjikkattu P. Ranjith, Donald L. J. Quicke, Alexey Reshchikov, Buntika A. Butcher

Data type: pdf

Link: https://doi.org/10.3897/jhr.97.121436.suppl1

Supplementary material 2

***Thaictenopelma splendida* Ranjith, Reshchikov & Quicke gen. et sp. nov.**

Authors: Avunjikkattu P. Ranjith, Donald L. J. Quicke, Alexey Reshchikov, Buntika A. Butcher

Data type: pdf

Link: https://doi.org/10.3897/jhr.97.121436.suppl2

JHR 97: 505–511 (2024)
doi: 10.3897/jhr.97.123968
https://jhr.pensoft.net

SHORT COMMUNICATION

JOURNAL OF Hymenoptera RESEARCH
A peer-reviewed open-access journal
The International Society of Hymenopterists

Gynandromorph records of *Melissodes trinodis* and *Melissodes communis* (Hymenoptera, Apidae) from North Dakota, USA

Joshua W. Campbell[1*], C. K. Pei[2*], Karen W. Wright[3]

1 *USDA-ARS Pest Management Research Unit, Northern Plains Agricultural Research Laboratory, Sidney, MT, 59270, USA* **2** *University of North Dakota, Earth System Science and Policy, Grand Forks, ND 58201, USA* **3** *Washington State Department of Agriculture, Olympia, WA 98504-2560, USA*

Corresponding author: Joshua W. Campbell (joshua.campbell@usda.gov)

Academic editor: Jack Neff | Received 26 March 2024 | Accepted 12 May 2024 | Published 6 June 2024

https://zoobank.org/707504EB-9077-4B13-9FE5-9F20523B6357

Citation: Campbell JW, Pei CK, Wright KW (2024) Gynandromorph records of *Melissodes trinodis* and *Melissodes communis* (Hymenoptera, Apidae) from North Dakota, USA. Journal of Hymenoptera Research 97: 505–511. https://doi.org/10.3897/jhr.97.123968

Abstract

Bees that express both male and female characteristics are known as gynandromorphs. Here we report and describe two specimens that represent the first documented gynandromorphs of *Melissodes trinodis* Robertson and one specimen of *Melissodes communis* Cresson (Hymenoptera: Apidae) that represents only the second known case. All three specimens were collected in North Dakota, USA and exhibit a mosaic pattern of gynandromorphy.

Keywords

Apoidea, Eucerini, gynandromorph, morphology

Introduction

Gynandromorphs are individuals that are usually genetic chimeras expressing both male and female characteristics and this phenomenon has been found in most insect orders (Pereira et al. 2010; Lightburn et al. 2022). Within bees (Hymenoptera: Apoidea: Anthophila), approximately 140 gynandromorph specimens are described

* These authors contributed equally to this work.

from all bee families (Lightburn et al. 2022). Although documented in over 30 bee genera, gynandromorphy has been reported more frequently in *Andrena* Fabricius (Hymenoptera: Andrenidae) and *Megachile* Latreille (Hymenoptera: Megachilidae) (Michez et al. 2009; Hinojosa-Díaz et al. 2012; Parys et al. 2022).

Gynandromorphy has been documented in many different forms in bees but is most commonly found as mosaics where no clear distribution of male and female characteristics can be discerned (Wcislo et al. 2004). Other less common gynandromorph patterns documented in bees include male and female characteristics separated bilaterally, transversally, and various anterior/posterior separations (Dalla Torre and Friese 1899; Wcislo et al. 2004; Michez et al. 2009).

Although *Melissodes* are one of the more commonly collected apids among researchers in North America, only one known case of gynandromorphy has been documented in the scientific literature (Cockerell 1906). This specimen mentioned by Cockerell (1906), *Melissodes hortivagans* Cockerell (=*M. communis* Cresson), was collected in Fedor, TX and described as a 'partial gynandromorph' with a half yellow (right side) and black (left side) clypeus and labrum. Here we report one individual of *M. communis* and two individuals of *M. trinodis* Robertson from North Dakota, USA exhibiting gynandromorphy. All three individuals exhibited the mosaic pattern described by Michez et al. (2009) or would be partial bilaterals in the system of Dalla Torre and Friese (1899).

Methods

The *M. communis* specimen was collected in a pitfall trap (473 ml Solo cup filled half of the depth with a 50% propylene glycol/water solution) that was active for 7 days (June 10–17, 2021) in the Little Missouri National Grasslands, Billings County, North Dakota (47.30828, -103.45804). Both *M. trinodis* specimens were collected with colored (blue, yellow, and white) pan traps (473 ml pan trap filled with soapy water) that were active for 24 hours. The *M. trinodis* specimens were part of a greater survey effort to sample grassland bee communities in North Dakota (Pei et al. 2022). One gynandromorph was collected in a sampling event on July 26, 2017 from Long Lake National Wildlife Refuge, Burleigh County, North Dakota (48.81845, -100.22222). A second gynandromorph was collected on a July 15, 2018 sampling event in Agnes Marsh Waterfowl Production Area, Grand Forks County, North Dakota (48.08277, -97.72434).

Here, we describe each specimen and provide detailed photographs of the external morphology. For each specimen, the following external morphological measurements were made: total body length (mm), head width (taken from widest part of eyes) (mm), intertegular distance (ITD) (mm), abdominal width (taken from widest part of abdomen) (mm), scape + pedicel length (mm), and flagellum length (mm) (Table 1). All photographs of *M. trinodis* were taken with a Canon EOS 6D Mark II Digital SLR and photographs of *M. communis* with a Leica DMC 4500. The *M. communis* specimen is housed at the USDA Northern Plains Agricultural Research Laboratory native bee collection (Sidney, MT) and the *M. trinodis* specimens are located at North Dakota State University in the School of Natural Resources Sciences (Fargo, ND).

Table 1. Morphological measurements (mm) of total body length, head width, ITD, abdomen width, scape + pedicel length, and flagellum length of *M. communis* and *M. trinodis*. GF= Grand Forks specimen, BC= Burleigh County specimen.

	Melissodes communis	***Melissodes trinodis* (GF)**	***Melissodes trinodis* (BC)**
Total Body Length	11.26	11.49	11.21
Head Width	3.81	3.73	3.86
ITD	2.4	2.91	2.91
Abdomen Width	4.01	4.3	4.5
Scape + Pedicel Length	0.78	0.98	0.95
Flagellum Length	2.91	N/A	2.72

Results

Melissodes communis

This specimen was collected along with 106 other *Melissodes* specimens collected in the same 2021 sampling effort. The specimen exhibits primarily bilateral asymmetric yellow male coloration (right side) and dark female (left side) coloration of clypeus and labrum (Fig. 1A; labrum not visible in photo). Both antennae have 12 segments. Other than the clypeus, labrum and antennae, specimen appears to be male (e.g., legs lacking tibia scopal hair, exhibiting male genitalia) (Fig. 1B–D).

Melissodes trinodis

These specimens were collected along with 1,252 (Burleigh specimen) and 1,126 (Grand Forks specimen) *Melissodes* specimens in the same year sampling effort. Both specimens exhibit bilateral asymmetric male/female (yellow/dark) coloration of clypeus and labrum, with male-associated yellow coloration found on the left side for the Grand Forks specimen and on the right side for the Burleigh specimen (Figs 2A, 3A). All other external characteristics of each specimen appear female (Figs 2B–D, 3B–D). However, the antennae were not present for the specimen from Burleigh County so we cannot ascertain the number of antennal segments. Additionally, one hind tibia is missing from the Grand Forks specimen and, thus, we cannot determine if scopal hairs were present.

Discussion

We describe the first gynandromorphs from *Melissodes trinodis* and the second of *M. communis*. Other than Cockerell (1906), these are the first reports of gynandromorphy from this genus in the scientific literature, and all three specimens appear to follow the mosaic pattern described by Michez et al. (2009). However, *M. communis* and one specimen of *M. trinodis* (specimen from Grand Forks County) display a 'patchiness' of the yellow coloration on their clypeus (see Figs 1A, 2A). This patchiness is also seen on the labrum for *M. trinodis*. Due to the lack

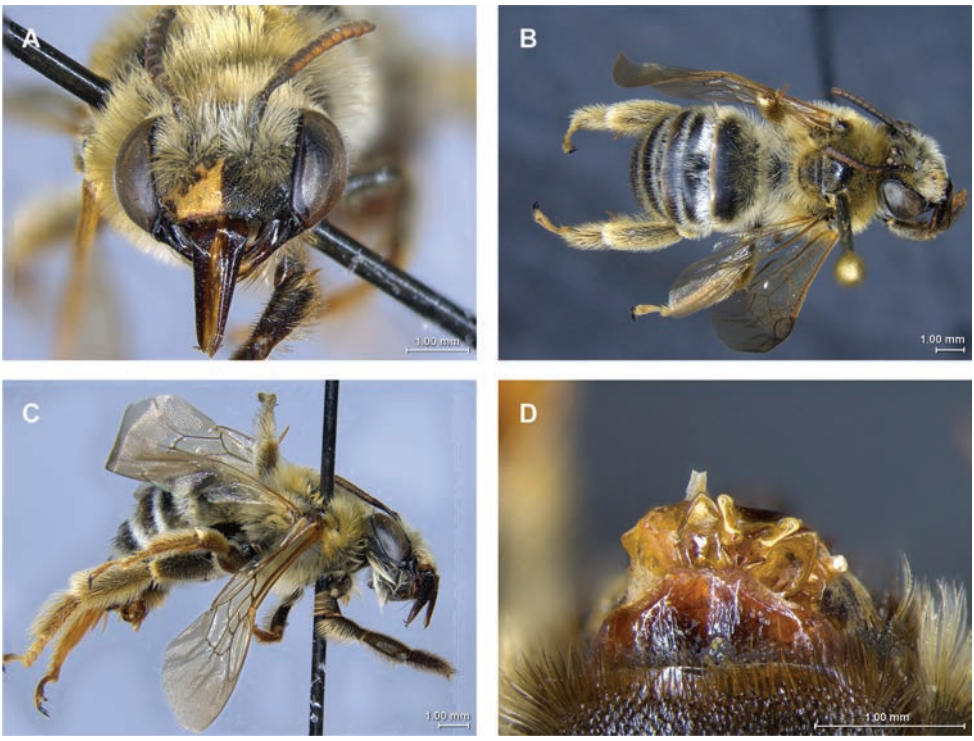

Figure 1. Gynandromorph of *Melissodes communis* collected from Billings County, North Dakota, USA **A** face **B** dorsal view **C** lateral view, and **D** male genitalia (partially exposed).

of sharp morphological distinctions of male and female characters (e.g., clypeus yellow color not uniform), these two specimens could be considered mosaics by Michez et al. (2010) or would be called partial bilaterals in the system of Dalla Torre and Friese (1899).

Both of the bee species in this study are widely distributed in North America, with *M. communis* found throughout the United States, southern Canada and Mexico, whereas *M. trinodis* is primarily found in the eastern half of the United States but can also be found in Canada and Mexico. *Melissodes communis* is polylectic, feeding on multiple pollen sources, whereas *M. trinodis* is primarily considered an Asteraceae specialist and one of the main visitors of flowering cultivated sunflower (Portlas et al. 2018). Jones et al. (2021) was able to observe a gynandromorph bee (*Xenoglossa pruinosa* Say (Hymenoptera: Apidae)) foraging prior to collection, and, thus, was able to glean some behavioral information. Since the specimens described here were collected in passive traps, no behavioral observations could be collected.

Prior to these specimens, only eight other gynandromorphic individuals from tribe Eucerini had been documented, (Cockerell 1906; Jones et al. 2021; Parys et al. 2022), suggesting gynandromorphs may be rare within Eucerini compared to

Figure 2. Gynandromorph of *Melissodes trinodis* collected from Grand Forks County, North Dakota, USA **A** face **B** dorsal view **C** lateral view, and **D** abdomen.

other bee groups. Alternatively, there could be a bias in finding/collecting gynandromorphs from Eucerini or there is a lack of reporting them. In addition to *Melissodes* and *Xenoglossa*, other Eucerini genera in which gynandromorphs have been documented are *Alloscirtetica* Holmberg (Hymenoptera: Apidae) (Urban 1999), *Florilegus* Robertson (Hymenoptera: Apidae) (Parys et al. 2022), and *Tetralonia* Spinola (Hymenoptera: Apidae) (Dalla Torre and Friese 1899). It is unclear why gynandromorphy is uncommon or poorly documented within Eucerini. However, numerous explanations are thought to cause gynandromorphy in bees (or other arthropods) including various developmental mechanisms (Jones et al. 2021), endosymbiotic bacteria (Narita et al. 2010), epigenic causes (Sommaggio et al. 2021), and numerous environmental stressors such as temperature (Drescher and Rothenbuhler 1963) and pollutants (Dantchenko et al. 1995; Olmstead and LeBlanc 2007). The presence of gynandromorphs in wild bee populations is considered rare and the causes unknown and, thus, further research and documentation is widely needed to elucidate the causes of gynandromorphy (Jones et al. 2021; Parys et al. 2022). There has been an increase of documentation of gynandromorphy in wild bees in recent literature (Jones et al. 2021), but whether this is an upsurge of interest by the scientific community to document this occurrence or an increase in a causation of this phenomenon remains unknown.

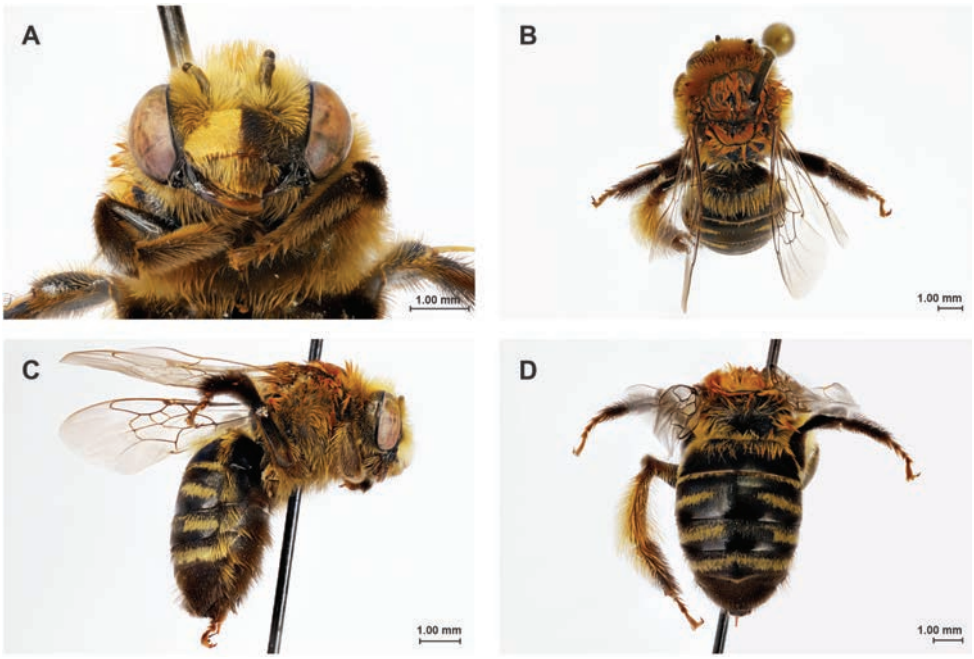

Figure 3. Gynandromorph of *Melissodes trinodis* collected from Burleigh County, North Dakota, USA **A** face **B** dorsal view **C** lateral view, and **D** abdomen.

Acknowledgments

We thank Fraser Watson and Niall Horton for pitfall collection and Cody Meservy for providing photographs and morphological measurements and Alex Morphew for specimen processing. We thank Carissa Wonkka funding the creeping juniper project resulting in the *M. communis* specimen. We would also like to thank those associated with the NDSU Statewide Pollinator Survey project for providing the *M. trinodis* specimens.

References

Cockerell TDA (1906) XLVI.—Descriptions and records of bees.—X. Journal of Natural History 17(100): 359–369. https://www.tandfonline.com/doi/abs/10.1080/00222930608562537

Dalla Torre KW, Friese H (1899) Die hermaphroditen und gynandromorphen Hymenopteren (The hermaphrodite and gynandromorphic Hymenoptera). Ber. Naturwiss-Mediz. Ver. Innsbruck 24: 1–96.

Dantchenko A, Emmel TC, Sourakov A (1995) Nuclear pollution and gynandromorphic butterflies in Southern Russia. Holarctic Lepidoptera 2(2): 77–79. https://journals.flvc.org/holarctic/article/view/90381

Drescher W, Rothenbuhler WC (1963) Gynandromorph production by egg chilling: cytological mechanisms in honey bees. Journal of Heredity 54(5): 194–201. https://doi.org/10.1093/oxfordjournals.jhered.a107247

Hinojosa-Díaz IA, Gonzalez VH, Ayala R, Mérida J, Sagot P, Engel MS (2012) New orchid and leaf-cutter bee gynandromorphs, with an updated review (Hymenoptera, Apoidea). Zoosystematics and Evolution 88: 205–214. https://doi.org/10.1002/zoos.201200017

Jones LJ, Kilpatrick SK, López-Uribe MM (2021) Gynandromorph of the squash bee *Eucera* (*Peponapis*) *pruinosa* (Hymenoptera: Apidae: Eucerini) from an agricultural field in western Pennsylvania, USA. Journal of Melittology 100: 1–10. https://journals.ku.edu/melittology/article/view/13744

Lightburn K, van Acker R, Raine N (2022) The first gynandromorph record of the North American bee *Hylaeus modestus* (Hymenoptera: Colletidae). The Journal of the Entomological Society of Ontario 153: jeso2022003.

Michez D, Rasmont P, Terzo M, Vereecken NJ (2009) A synthesis of gynandromorphy among wild bees (Hymenoptera: Apoidea), with an annotated description of several new cases. Annales de la Société Entomologique de France 45: 365–375. https://doi.org/10.1080/00379271.2009.10697621

Narita S, Pereira RAS, Kjellberg F, Kageyama D (2010) Gynandromorphs and intersexes: potential to understand the mechanism of sex determination in arthropods. Terrestrial Arthropod Reviews 3(1): 63–96. https://doi.org/10.1163/187498310X496190

Olmstead AW, LeBlanc GA (2007) The environmental-endocrine basis of gynandromorphism (intersex) in a crustacean. International Journal of Biological Sciences *3*(2): 77–84. 10.7150/ijbs.3.77

Parys KA, Davis KA, James ST, Davis JB, Tyler H, Griswold T (2022) First report of a gynandromorph of *Florilegus condignus* (Cresson, 1878) (Hymenoptera, Apidae), with notes on phenology and abundance. Journal of Hymenoptera Research 89: 233–244. https://doi.org/10.3897/jhr.89.75857

Pei CK, Hovick TJ, Duquette CA, Limb RF, Harmon JP, Geaumont BA (2022) Two common bee-sampling methods reflect different assemblages of the bee (Hymenoptera: Apoidea) community in mixed-grass prairie systems and are dependent on surrounding floral resource availability. Journal of Insect Conservation 26(1): 69–83. https://doi.org/10.1007/s10841-021-00362-3

Pereira R, Narita S, Kageyama D, Kjellberg F (2010) Gynandromorphs and intersexes: potential to understand the mechanism of sex determination in arthropods. Terrestrial Arthropod Reviews 3(1): 63–96. https://doi.org/10.1163/187498310X496190

Portlas ZM, Tetlie JR, Prischmann-Voldseth D, Hulke BS, Prasifka JR (2018) Variation in floret size explains differences in wild bee visitation to cultivated sunflowers. Plant Genetic Resources 16(6): 498–503. https://doi.org/10.1017/S1479262118000072

Sommaggio D, Fusco G, Uliana M, Minelli A (2021) Possible epigenetic origin of a recurrent gynandromorph pattern in *Megachile* wild bees. Insects 12(5): 437. https://doi.org/10.3390/insects12050437

Urban D (1999) Ginandromorfia em *Alloscirtetica brethesi* (Gynandromorph of *Alloscirtetica brethesi*) (Joergensen) (Hymenoptera, Anthophoridae). Revista Brasileira de Zoologia 16: 171–173. https://doi.org/10.1590/S0101-81751999000500008

Wcislo WT, Gonzalez VH, Arneson L (2004) A review of deviant phenotypes in bees in relation to brood parasitism, and a gynandromorph of *Megalopta genalis* (Hymenoptera: Halictidae). Journal of Natural History 38(11): 1443–1457. https://doi.org/10.1080/0022293031000155322

JHR 97: 513–530 (2024)
doi: 10.3897/jhr.97.125408
https://jhr.pensoft.net

RESEARCH ARTICLE

JOURNAL OF Hymenoptera RESEARCH
A peer-reviewed open-access journal
The International Society of Hymenopterists

New records of bees (Hymenoptera, Apoidea) from Morocco

Ahlam Sentil[1], Paolo Rosa[1], Clément Tourbez[1], Achik Dorchin[1], Petr Bogusch[2], Denis Michez[1]

1 *Laboratory of Zoology, University of Mons, Research Institute for Biosciences, Mons, Belgium* **2** *Department of Biology, University of Hradec Kralove, Faculty of Science, Hradec Králové, Czech Republic*

Corresponding author: Sentil Ahlam (ahlam.sentil@umons.ac.be)

Academic editor: Jack Neff | Received 15 April 2024 | Accepted 7 May 2024 | Published 14 June 2024

https://zoobank.org/E43691B1-31C6-4BAF-BF62-510C22230E9C

Citation: Sentil A, Rosa P, Tourbez C, Dorchin A, Bogusch P, Michez D (2024) New records of bees (Hymenoptera, Apoidea) from Morocco. Journal of Hymenoptera Research 97: 513–530. https://doi.org/10.3897/jhr.97.125408

Abstract

Morocco is considered to be one of the main diversity hotspots of bees in the Mediterranean basin. However, this fauna remains largely understudied in both urban and natural eco-systems. Bee monitoring primarily conducted during 2023 in an urban area (i.e. Safi) has unveiled three new bee species for Morocco: *Lithurgus tibialis*, *Tetralonia* aff. *lanzarotensis* and *Coelioxys ruficauda* as well as records of 28 new bee species for the region Marrakech Safi. This work provides descriptions of the spatial distribution, the diagnostic characters, and host plants of these three species. We also take the opportunity to highlight the quality of urban areas as habitats for bees and the importance of implementating bee-friendly management practices to preserve bee species.

Keywords

Bee conservation, cemetery, city, management practices, Mediterranean, new species

Introduction

Morocco has a unique geographical position, situated at a crossroads of two biogeographical regions (i.e. the Afrotropic and the Palaearctic). This country is characterized by a wide topographic gradient, from the Atlantic and Mediterranean coasts to the

summit of the Atlas Mountains, and different climate types, from Mediterranean in the north to arid desert in the south, leading to a wide range of habitats (e.g. sclerophyllous forest, alpine meadows, coastal cliffs, shrubs, semideserts). From this habitat diversity derives the diverse Moroccan flora (Rankou et al. 2013), which in turn provides key ecosystem services.

The economic value of insect pollination in Morocco is up to $1.23 billion, representing 8.5% of the total value of agricultural gross domestic product (Sabbahi 2022) and 25% of the total value of agricultural production in North Africa (Gallai et al. 2009). The main non-bee pollinators recorded in the country are butterflies with 136 species (Verovnik et al. 2018) and hoverflies with 150 species (Sahib et al. 2020). In comparison, the Moroccan bee fauna impressively includes 962 bee species, which are classified in six bee families and 68 genera (Lhomme et al. 2020). This figure is comparable to that of other Mediterranean countries, such as Greece (1186), Spain (1166), and Italy (1051) (Reverté et al. 2023), collectively demonstrating the vast Mediterranean bee fauna (Orr et al. 2021).

Many bee species have already been recorded since the first check list of Lhomme et al. (2020), and other have been newly described (Wood et al. 2020, 2021; Wood 2023a, Wood 2023b) or await future description, and these will be ultimately added to the national list of Moroccan bees. The monitoring of Moroccan bees is spatially uneven, with a focus on agro-ecosystems (El Abdouni et al. 2022) and touristic areas (e.g. Michez et al. 2007). Further inventory studies are required to document the species diversity of Moroccan bees, especially in natural and urban areas.

As a first step to fill this gap, this work reports three species newly recorded for Morocco, which were discovered during faunal surveys in a coastal urban area in the middle of the country (city of Safi) and a botanical garden (Meknes). For each species, we provide information on spatial distribution, diagnosis, records of host plants and illustrations. Finaly, we highlight the importance of urban areas as a refuge for bees in a Mediterranean country.

Methods

Study area

All the bees were collected in Morocco at Safi (latitude: 32.2439 to 32.3418, longitude: -9.2069 to -9.2445), except two specimens, which were collected in Meknes (33.84079, -5.47737). Safi is a small city located on the Atlantic coast of western Morocco, while Meknes is situated in northern Morocco. Both towns are characterized by a Mediterranean climate with hot, dry summers and mild, wet winters. Bees were collected between February and October 2023 along roadsides, at cemeteries, and in vacant lots in Safi (Fig. 1), and in the botanical garden of the National School of Agriculture (ENAM) in Meknes, located 20 km south-east from the city.

Figure 1. Illustrations of the sites that were surveyed within Safi, Morocco **A** cemetery **B** roadside borders **C** vacant lots.

Bee identification

All bees were identified to the genus level following keys adapted from Michez et al. (2019), then sent to expert taxonomists for specific identification. Van der Zanden (1986), Al-Shahat and Hossni (2020), and available reference collections were used for morphological identification of the newly recorded species. The following abbreviations were used in the diagnosis: S = metasomal sterna and T = metasomal terga.

Bee pictures

The pictures of the new bee species were taken with an Olympus OMD E-M1 Mark II camera, using the Olympus Zuiko 60 mm objective and a Marumi lens for general habitus and a Mitutoyo plan achromatic lens LWD 5×. Images were stacked with the Helicon software and then enhanced with Adobe Photoshop CS6.

Pollen preparation and identification

Pollen host plants of the species newly recorded from Morocco were identified by examining pollen loads removed from female specimens under a microscope. *Coelioxys*, which is a parasitic (cuckoo) bee and *Lithurgus*, which comprised only males, were excluded from the pollen analysis, because they do not collect pollen. The pollen preparation followed the protocol described by Wood and Roberts (2017). Pollen load sizes were visually estimated relative to the bee size, ranging from a full load (1) to a

one-fourth load (0.25). Pollen grains were extracted from the scopa of females and deposited onto a microscope slide using an entomological pin. The pollen was then placed in a drop of water to separate aggregates. After gentle heating to allow evaporation, pollen grains were dried using a cube of fuchsin jelly added and melted to seal the slide with a coverslip. Pollen grains were finally identified to the subfamily level using author's personal experience and pollen picture databases (PalDat 2024).

Results

Bee species records

We collected a total of 1,624 bees, belonging to 27 genera and 102 identified bee species (Suppl. material 1). *Eucera* represented 27% of the total abundance, followed by *Andrena* (12%), *Tetralonia* (11%), *Osmia* (9%) and *Nomada* (9%) (Table 1). The most species-rich genera were *Andrena* (20 species), *Eucera* (10 species), *Osmia* (9 species) and *Anthophora* (8 species) (Table 1). Twenty eight percent of the species collected in Safi

Table 1. A summary of the list of genera collected in this study. The bee species richness (i.e., number of distinct bee species per genus) and abundance (i.e., the number of bee individuals collected per genus) are indicated.

Family	Genus	Bee species richness	Bee abundance
Andrenidae	*Andrena*	20	148
Apidae	*Eucera*	10	347
Apidae	*Anthophora*	8	64
Apidae	*Nomada*	7	109
Apidae	*Thyreus*	4	5
Apidae	*Amegilla*	3	23
Apidae	*Ammobates*	2	13
Apidae	*Ceratina*	2	9
Apidae	*Tetralonia*	2	136
Colletidae	*Colletes*	2	3
Colletidae	*Hylaeus*	1	12
Halictidae	*Lasioglossum*	5	19
Halictidae	*Halictus*	2	22
Halictidae	*Nomioides*	2	39
Halictidae	*Seladonia*	2	23
Halictidae	*Nomiapis*	1	3
Halictidae	*Rophites*	1	3
Halictidae	*Sphecodes*	1	9
Megachilidae	*Osmia*	9	119
Megachilidae	*Megachile*	7	61
Megachilidae	*Hoplitis*	4	32
Megachilidae	*Rhodanthidium*	2	15
Megachilidae	*Anthidium*	1	4
Megachilidae	*Chelostoma*	1	4
Megachilidae	*Coelioxys*	1	20
Megachilidae	*Lithurgus*	1	2
Megachilidae	*Stelis*	1	1

(i.e., 28 bee species) are new records for the region Marrakech Safi (Suppl. material 1) and *Tetralonia* aff. *lanzarotensis* and *Coelioxys ruficauda* are new species for the country. The two specimens collected in Meknes represent males of *Lithurgus tibialis*, marking its first recorded occurrence in Morocco.

New species for Morocco

Lithurgus tibialis Morawitz, 1875

Material examined. Morocco. 2♂; Meknes; 33.8405, -5.4775; 22 Jul. 2023; A. Sentil leg.; sweep net.

Diagnosis. The male of *Lithurgus tibialis* is distinguished from other Palaearctic *Lithurgus* species by its smaller size, 8–9 mm, while other species measure over 11 mm (Fig. 2A, B). Furthermore, it is easily identified by its swollen femur III, its curved tibia III, and the presence of a strong spine between the two spurs of tibia III (Fig. 2C), the size of which reaches or exceeds the thickness of the metabasitarsus III (Van der Zanden 1986; Al-Shahat and Hossni 2020). The female of *Lithurgus tibialis* is distinguished from all other *Lithurgus* species in the Palaearctic region by its size, 8–10 mm, while other species measure over 12 mm, associated with its white-coloured scopa (Van der Zanden 1986; Al-Shahat and Hossni 2020).

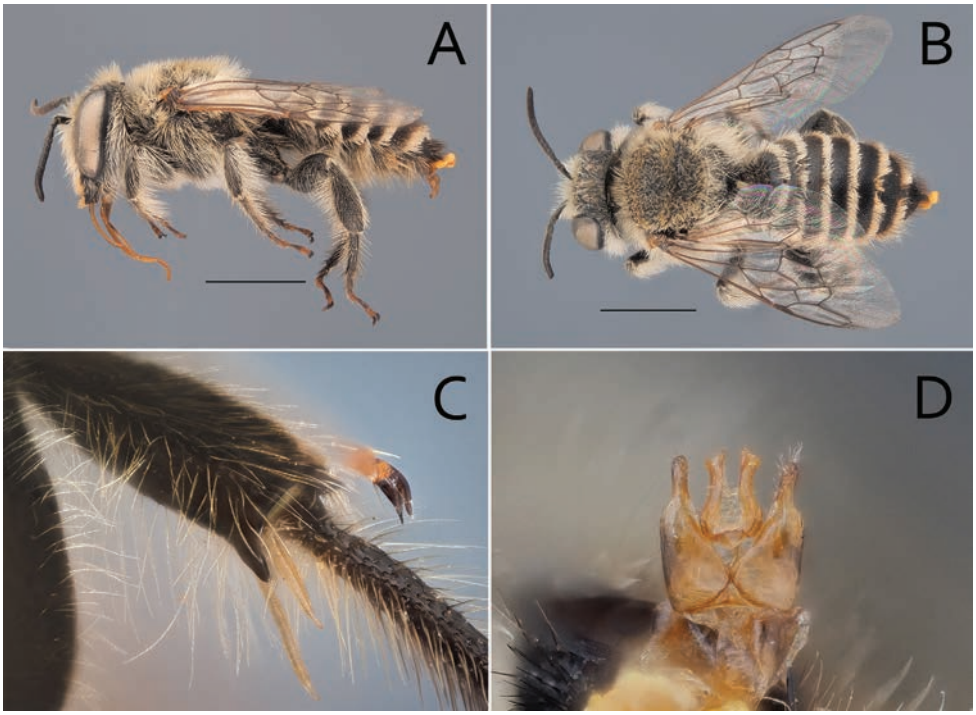

Figure 2. *Lithurgus tibialis*, male **A** lateral view **B** dorsal view **C** the spine in between metatibial spurs **D** genitalia.

Distribution. The distribution of *Lithurgus tibialis* spans from Southern Europe, Northern Africa, and the Middle East to Southern and Central Asia. In Europe, it has been reported in Cyprus, Greece, Italy, Portugal, Spain, Malta and Turkey (Van der Zanden 1986; Reverté et al. 2023). Its range extends into the Middle East, with records in Iran, Israel, Jordan, Syria, and the United Arab Emirates (Al-Shahat and Hossni 2020). This species also inhabits the Caucasus and Southern to Central Asia, as it has been documented in Afghanistan, Azerbaijan, India, Pakistan, Southern Russia, Tajikistan, Turkmenistan, and Uzbekistan (Fateryga et al. 2018; Maharramov et al. 2023). In Northern Africa, it is found in Algeria (Cros 1939) and Egypt (Al-Shahat and Hossni 2020). A previous citation for *Lithurgus tibialis* was given in a list of bee species pollinating a single crop in Morocco, without any further information (El Abdouni et al. 2022). The mentioned specimen was no longer available for this study.

Floral preferences. The females of *Lithurgus tibialis* appear to be oligolectic, primarily foraging on the Euphorbiaceae *Chrozophora tinctoria* (Christophe Praz, personal observation), while males may collect nectar from other species such as *Mentha* spp., on which the Moroccan specimens were collected.

Tetralonia aff. *lanzarotensis* Tkalců, 1993

Material examined. Morocco. 8♂, 1♀; Safi; 32.2587, -9.2386; 09 Apr. 2023; A. Sentil leg.; sweep net • 1♂; Safi; 32.2587, -9.2386; 15 Apr. 2023; A. Sentil leg.; sweep net • 3♂, 3♀; Safi; 32.2731, -9.2335; 21 Apr. 2023; A. Sentil leg.; sweep net • 3♂, 1♀; Safi; 32.3356, -9.2166; 23 Apr. 2023; A. Sentil leg.; sweep net • 15♂, 2♀; Safi; 32.2686, -9.2323; 25 Apr. 2023; A. Sentil leg.; sweep net • 1♀; Safi; 32.2625, -9.226617; 01 May 2023; A. Sentil leg.; sweep net • 2♂; Safi; 32.2587, -9.2386; 02 Jul. 2023; A. Sentil leg.; sweep net • 1♂, 6♀; Safi; 32.2735, -9.2334; 11 Jul. 2023; A. Sentil leg.; sweep net • 2♀; Safi; 32.2735, -9.2334; 15 Jul. 2023; A. Sentil leg.; sweep net.

Diagnosis. The species belongs to the *ruficornis*-group (Tkalců 1979) based on the metasomal hair pattern and structure, which comprises basal tomentum, and the marginal zones of T2–4 that largely exposed (Fig. 3B); the strongly branched scopal hairs (Fig. 3A); the lack of ventral mesosomal brush of unbranched thickened hairs of females; the shape of the medial longitudinal groove of S6, and the ventral tubercule of hind femur of males. Within the group, females of *Tetralonia lanzarotensis* can be diagnosed based on the short metasomal basal tomentum that does not reach the marginal zones of T3 and not (Lanzarote) or barely (Morocco) reach that of T4 medially; it differentiates from most other species, except *T. fulvescens* Giraud, by the black, immaculate face, and can be differentiated from that latter species by the lighter, ferruginous to reddish ventral side of flagellar segments 2–12 (Fig. 4A, B) (although some southern distributed specimens of *T. fulvescens* have lighter flagellar segments, and the diagnosability of this characteristic is not determined), and by the slightly smaller body size of about 9 mm (compared to mostly above 10 mm in *T. fulvescens*). The males are similar to females in their body size, 8.5–9 mm, short basal tomentum on T2–4 (Fig. 3D),

Figure 3. *Tetralonia* aff. *lanzarotensis*, female, from Morocco **A** lateral view **B** dorsal view. *Tetralonia* aff. *lanzarotensis*, male, from Morocco **C** lateral view **D** dorsal view.

and light flagellar segments ventrally; the ventral tubercule of hind femur is blunt and giving rise to dense, stiff sclerotised hairs. These characteristics, and to a lesser extent, also the widely emarginated lateral process of S7 (Fig. 4C), are most closely resembling *T. julliani* (Pérez), from which they can be easily differentiated by the elbowed gonostylus as seen in lateral view, with the apex produced medially, L-shaped as seen in dorsal view (compared to more gently curved and apically straight in *T. julliani* and in *T. fulvescens*). The genital complex of the male, which is usually diagnostic in the Eucerini, is nearly identical in specimens from the type locality in Lanzarote and in males from continental populations in Morocco (Fig. 4D). However, both the females and males clearly differ in the sculpture (and color) of the metasomal tergites (Fig. 3B, D), having sparser punctures apicomedially on the marginal zones and wider and translucent apical impunctate margins in specimens from Lanzarote as compared to those of the continent. The males from Lanzarote also have conspicuously shorter antennae. While such differences are generally considered sufficiently diagnostic at the species level, additional study that includes molecular evidence would be useful to determine species concepts with confidence.

Distribution. As far as it is known to us, the species has previously been recorded only from the island of Lanzarote in the Canary Islands (Reverté et al. 2023). It is first

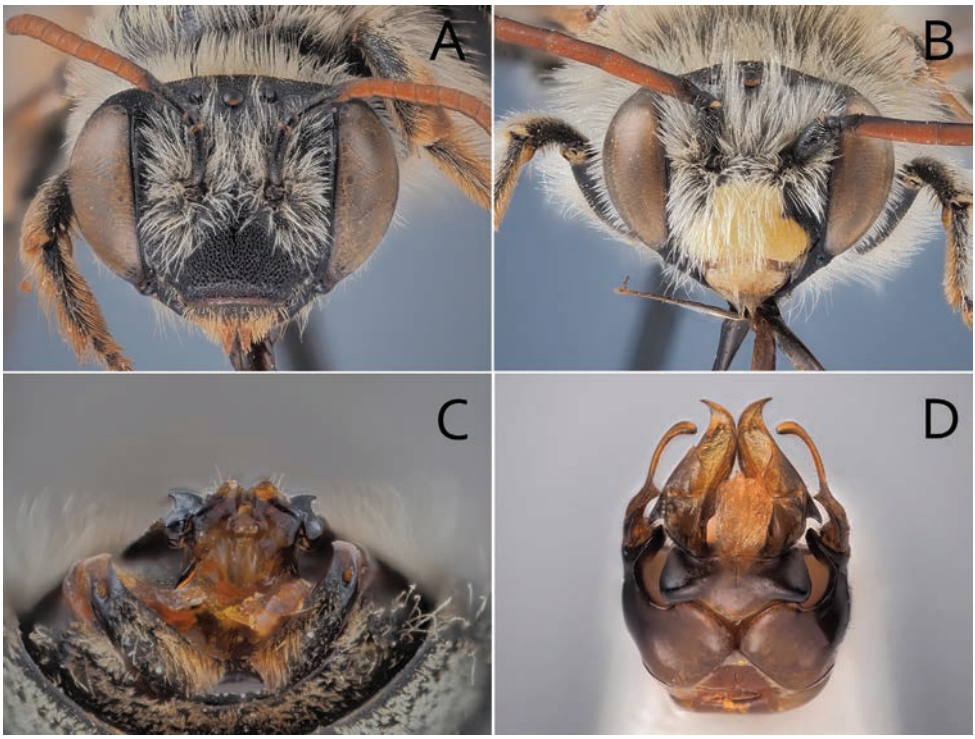

Figure 4. *Tetralonia* aff. *lanzarotensis*, female, from Morocco **A** frontal view. *Tetralonia* aff. *lanzarotensis*, male, from Morocco **B** frontal view **C** metasomal sterna 6 **D** genital capsule.

reported in this work from several localities in Morocco based on specimens from Safi and Tamri near Agadir on the Atlantic coast, and a single specimen examined from Ait Ibourk near Ouarzazate.

Floral preferences. Analyses of pollen removed from the scopa of ten female specimens from Safi, show that the species is associated exclusively with Asteraceae. More specifically eight females collected a pure sample of pollen of the subfamily *Asteroidea*, only one specimen collected a significant amount of pollen of *Carduoidea* (thistles), and another specimen collected a negligible amount of *Cichorioidea*.

Coelioxys ruficauda Lepeletier, 1841

Material examined. Morocco. 12♂; Safi; 32.2587, -9.2386; 09 Apr. 2023; A. Sentil leg.; sweep net • 1♂; Safi; 32.2587, -9.2386; 15 Apr. 2023; A. Sentil leg.; sweep net • 1♀; Safi; 32.2731, -9.2335; 21 Apr. 2023; A. Sentil leg.; sweep net • 1♂; Safi; 32.3356, -9.2166; 23 Apr. 2024; sweep net • 1♂; Safi; 32.2686, -9.2323; 25 Apr 2023; A. Sentil leg.; sweep net • 1♀; Safi; 32.2625, -9.2266; 30 Apr. 2023; A Sentil leg.; sweep net • 1♀; Safi; 32.2625, -9.2266; 01 May 2023; A. Sentil leg.; sweep net.

Diagnosis. The species belongs to the subgenus *Allocoelioxys*, which comprises usually smaller species with scale-like hair on the body (Fig. 5A–D). This species has snow-white hairs on the body and short last metasomal segments. Very often and especially in populations from North Africa, the bees display reddish pattern, especially on the last metasomal segments, parts of legs, flagellum and mandible. The portion of reddish colouration is smaller than in other related species, except *Coelioxys echinatus* (Warncke 1992). Both sexes have unbroken whitish apical bands on T1–T5, while the band on male T5 is wider than in the other species.

The male has unbroken whitish bands of scale-like hair on the metasoma (Fig. 5D) and the S4 is without emargination. The T2 has a transverse carina, which can differ this species from *C. afer*, in which this carina is absent (Fig. 5D). Medial teeth on T6 are reduced and the whole S6 is much more narrowed than in other related species (Fig. 6B). The female can be recognized by its slightly elongate last tergum and sternum of reddish colour (Fig. 6A). The apex of S6 is triangular-shaped and bears reddish hairs, and is considered typical for this species (Fig. 6A).

The last metasomal segments are much narrower than those of all related species and the distance between apical tooth-like processes on last tergum and sternum is very small, much smaller than in all other similar species (Fig. 6B).

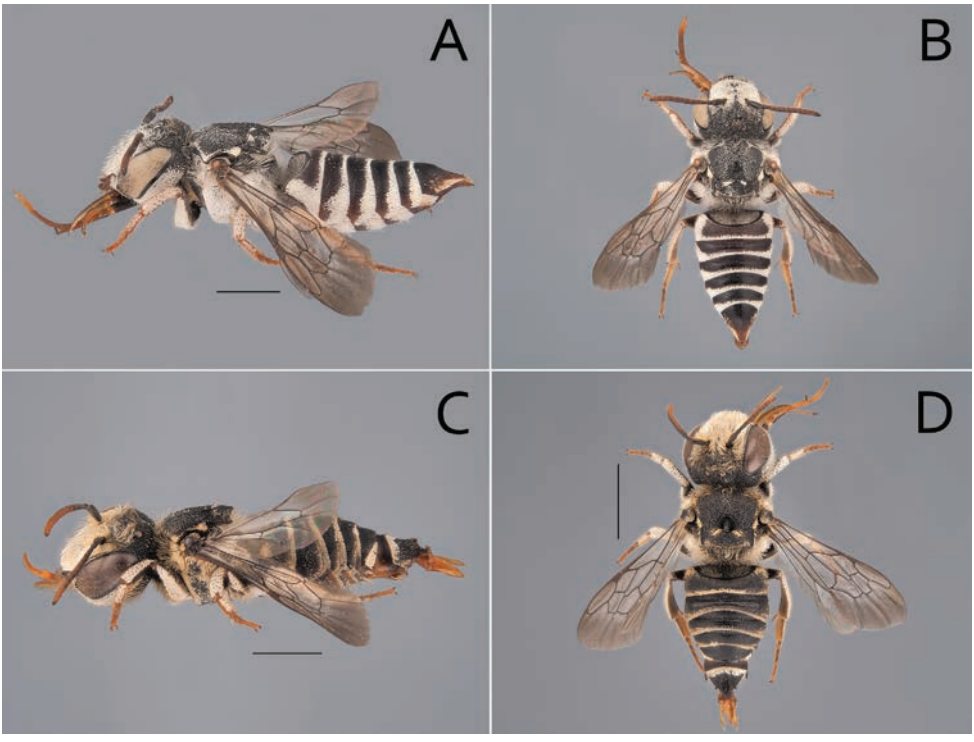

Figure 5. *Coelioxys ruficauda*, female **A** lateral view **B** dorsal view. *Coelioxys ruficauda*, male **C** lateral view **D** dorsal view.

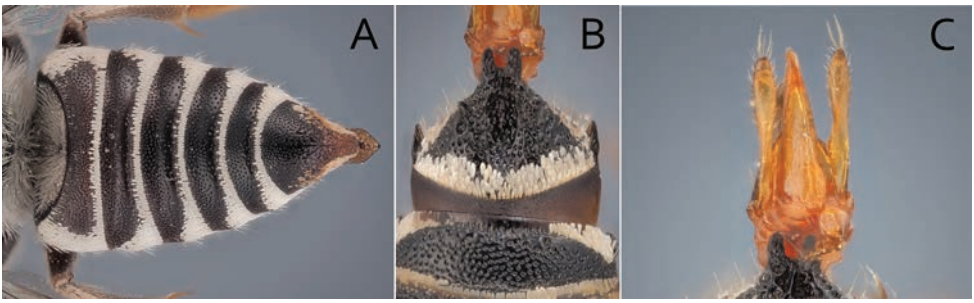

Figure 6. *Coelioxys ruficauda*, female **A** last metasomal terga, dorsal view. *Coelioxys ruficauda*, male **B** last metasomal terga, dorsal view **C** genitalia, dorsal view.

Distribution. The species is known from southern and Central Europe, Middle East and North Africa (Warncke 1992), with the northern distribution border going through the Czech Republic (Reverté et al. 2023). In Europe, most records are known from the South-West (South of France, Spain and Portugal) (Baldock et al. 2018). It occurs mainly in dry habitats with a high proportion of salt in the ground and it is everywhere considered to be a rare species.

Host. This species is a cuckoo bee and therefore does not collect pollen. *Megachile deceptoria* (P. Bogusch, personal observation) is its main host species in Central Europe. Both sexes feed on nectar of various plants, usually of the family Asteraceae (*e.g.*, genera *Centaurea*, *Cirsium*, and *Inula*).

Further information. Warncke (1992) found out that this species was for a long time recorded under the junior synonym *Coelioxys obtusa* Pérez, 1884.

Discussion

Despite the considerable works conducted over the last years in Morocco (Lhomme et al. 2020; Wood et al. 2020; Wood 2023a, Wood 2023b), significant knowledge gaps on bee diversity and ecology still persist. Opportunistic monitoring in a small urban area and a botanical garden, revealed three new species for Morocco, 28 new bee species for the region Marrakech Safi and a new species for science (*Anthophora ahlamae*, Rasmont and Wood (2024)). The three new records were expected, considering their occurrence in neighboring countries. This highlights the potential faunistic influence from Europe, Northern Africa, and regional endemism (Patiny and Michez 2007).

Our results highlight the extent to which the Moroccan bee fauna remains poorly documented. Research initiatives and national monitoring programs on bee diversity, distribution, behavior and ecology are lacking. The status and trends of Moroccan bee populations are entirely unknown. Further investigations and substantial taxonomic changes are needed for their taxonomy and classification. Without a consistent taxonomic framework and clearer insight into national bee diversity and distribution,

advanced research on the Moroccan bee fauna (e.g. population trends, national red list, factors of decline) may be hindered and future conservation actions may fail to support bees. Despite the high economic value of crop pollination and the crucial role bees play in ecosystem functioning (Klein et al. 2007; Ollerton et al. 2011; Sabbahi 2022), which have led to numerous inventories and research on bee conservation in agricultural and natural landscapes (Christmann et al. 2017, 2021; Hamroud et al. 2021; Sentil et al. 2021; Sentil et al. 2022a, Sentil et al. 2022b; Bencharki et al. 2022; El Abdouni et al. 2022), the bee fauna in urban areas remains largely unexplored.

Urban areas can also drive bee decline (Oke et al. 2021). Urbanization refers to the growth and the expansion of cities, which lead to the removal of natural habitats or the fragmentation of continuous habitats (Gu et al. 2021). It is generally considered to be one of the most important factors driving pollinator decline (IPBES 2019a, 2019b) and one of the most inhospitable environments for bees (Oke et al. 2021). However, some factors, such as floral resource availability, green spaces and undisturbed sites can offer favorable microhabitats for bees (Hall et al. 2017), at least for some functional groups of bees (Fauviau et al. 2022). In Safi, the tolerance of wild flowering plants in vacant lots and field borders, along with the presence of semi-natural habitats (e.g., in cemeteries), has led to the observation of more than one-tenth of the Moroccan bee species fauna, despite the low sampling effort. The importance of urban areas as a refuge for wild bee communities has been demonstrated in many publications; for instance, one-third of the bee fauna of France has been recorded in Lyon (Fortel et al. 2014) and half of the German bee species in Berlin (Saure 1996). Cities should promote pollinators for two reasons: (1) biodiversity protection and (2) pollination service provision. The expansion of urban areas worldwide is leading to significant losses in natural habitats (Wenzel et al. 2020). Thus, supporting bees that are losing their native habitats requires the incorporation of bee conservation plans in urban planning and agendas (Nilon et al. 2017). Moreover, cities with favorable bee habitats (e.g., cemeteries, roadside verges, parks), could act as refuges and corridors for bees (Fig. 7), and thus improve bee diversity in nearby simplified landscapes through spillover effect (Goulson et al. 2010). Additionally, bees ensure the pollination of native and ornamental plants, which in turn provide habitats and resources for other organisms, including insects, birds, and mammals. Also, high levels of biodiversity are required to boost urban ecosystem resilience in the face of climate change (Engström et al. 2020). Therefore, it is necessary to establish and maintain bee-friendly habitats in urban areas to promote and sustain diverse bee communities.

To date, no conservation strategies or initiatives have been developed to protect bees in Moroccan cities. The current knowledge of citizens about bees and the valuable services they provide is low and insufficient to catalyze the policy makers to implement conservation actions. These factors, combined with some management practices such as mowing, herbicide application and livestock grazing aggravate the pressures that bees are encountering in cities.

Nevertheless, bee conservation in Moroccan cities is still possible. A first step would be the transfer of knowledge on bees, and their ecological and economic

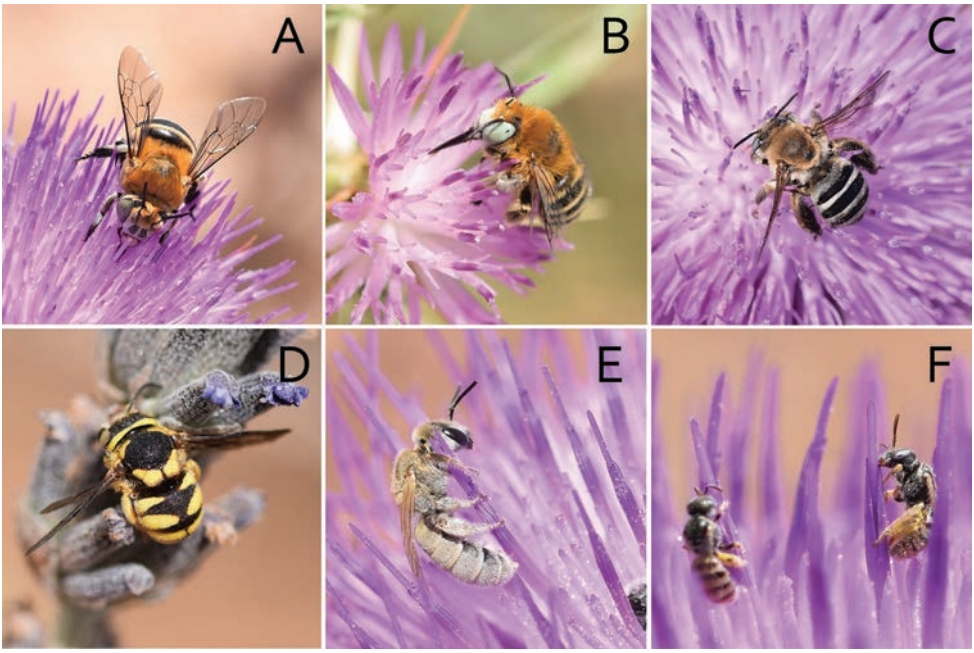

Figure 7. photos of some wild bee species observed during insect survey on wild flowering plants **A** *Amegilla quadrifaciata* **B** *Anthophora* sp. **C** *Eucera dentata* **D** *Anthidium strigatum* **E** *Seladonia* sp. **F** *Nomioides* sp.

importance to policy makers and urban planners. Second, adjust the urban management practices to promote bee-friendly environments, for instance: (i) delaying the mowing of roadside vegetation and/or reducing the mowing frequency (Chaudron et al. 2016; Wastian et al. 2016). Consider mowing the strip of vegetation immediately adjacent to roadsides, leaving the remainder of the row vegetation and the bee populations it supports intact. (ii) Prohibiting the use of herbicides in cities. For example, cemeteries provide suitable nesting sites and forage sources for bees (McCune et al. 2020; Macinnis et al. 2023). However, the urban cleaning service applies annually herbicides during spring to eliminate wild flowering plants. Alternatively, instead of eradicating all the wild plant fauna, we propose to at least preserve the existing wild flowering strips around cemeteries.

Conclusion

Despite the considerable efforts made to explore the Moroccan fauna, significant knowledge gaps persist regarding bee diversity and ecology. National monitoring programs and research initiatives on bee diversity, biogeography and ecology are imperatives for tailoring effective conservation actions. While urbanization poses threats to

bees, it can still provide suitable habitats that promote bee communities. Transferring knowledge to city planners and preventing harmful practices can mitigate pressures on urban bee populations and ensure their preservation.

Acknowledgements

We warmly thank Jakub Straka, Andreas Müller, Romain Le Divelec, Thomas James Wood, Pierre Rasmont, Simone Flaminio, Max Kasparek and Christophe Praz for bee identification. We would like to thank Abderrahim El Karmy and Isaad Es-Sayeh for their help with fieldwork.

This research was supported by the Federation Wallonia – Brussels (FNRS) and the Institute for bioscience, Belgium.

References

Al-Shahat AM, Hossni MT (2020) Taxonomic revision of genus *Lithurgus* (Hymenoptera: Megachilidae) of Egypt with a new record. Egyptian Academic Journal of Biological Sciences 13: 215–227. https://doi.org/10.21608/eajbsa.2020.90870

Baldock DW, Wood TJ, Smit JT (2018) The bees of Portugal (Hymenoptera: Apoidea: Anthophila). Entomofauna Supplement 22: 1–164.

Bencharki Y, Christmann S, Lhomme P, Ihsane O, Sentil A, El Abdouni I, Hamroud L, Rasmont P, Michez D (2022) "Farming with Alternative Pollinators" approach supports diverse and abundant pollinator community in melon fields in a semi-arid landscape. Renewable Agriculture and Food Systems: 1–34. https://doi.org/10.1017/S1742170522000394

Chaudron C, Chauvel B, Isselin-Nondedeu F (2016) Effects of late mowing on plant species richness and seed rain in road verges and adjacent arable fields. Agriculture, Ecosystems and Environment 232: 218–226. https://doi.org/10.1016/j.agee.2016.03.047

Christmann S, Bencharki Y, Anougmar S, Rasmont P, Smaili MC, Tsivelikas A, Aw-Hassan A (2021) Farming with Alternative Pollinators benefits pollinators, natural enemies, and yields, and offers transformative change to agriculture. Scientific Reports 11: 18206. https://doi.org/10.1038/s41598-021-97695-5

Christmann S, Aw-Hassan A, Rajabov T, Khamraev AS, Tsivelikas A (2017) Farming with alternative pollinators increases yields and incomes of cucumber and sour cherry. Agronomy for Sustainable Development 37: 24. https://doi.org/10.1007/s13593-017-0433-y

Cros A (1939) Considérations générales sur le Genre *Lithurgus* Latreille et Biologie du *Lithurgus tibialis*. Bulletin de la Société Fouad d'Entomologie 22: 37–57.

El Abdouni I, Lhomme P, Christmann S, Dorchin A, Sentil A, Pauly A, Hamroud L, Ihsane O, Reverté S, Patiny S, Wood TJ, Bencharki Y, Rasmont P, Michez D (2022) Diversity and Relative abundance of insect pollinators in Moroccan agroecosystems. Frontiers in Ecology and Evolution 10: 1–11. https://doi.org/10.3389/fevo.2022.866581

El Abdouni I, Lhomme P, Hamroud L, Wood T, Christmann S, Rasmont P, Michez D (2021) Comparative ecology of two specialist bees: *Dasypoda visnaga* Rossi, 1790 and *Dasypoda maura* Pérez, 1895 (Hymenoptera, Melittidae). Journal of Hymenoptera Research 81: 109–126. https://doi.org/10.3897/jhr.81.60528

Engström G, Gren Å, Li CZ, Krishnamurthy CKB (2020) Valuing biodiversity and resilience: an application to pollinator diversity in the Stockholm region. Spatial Economic Analysis 15(3): 238–261. https://doi.org/10.1080/17421772.2020.1784988

Fateryga AV, Proshchalykin MY, Astafurova YV, Popov IB (2018) New records of megachilid bees (Hymenoptera, Megachilidae) from the North Caucasus and neighbouring regions of Russia. Entomological Review 98: 1165–1174. https://doi.org/10.1134/S0013873818090026

Fauviau A, Baude M, Bazin N, Fiordaliso W, Fisogni A, Fortel L, Garrigue J, Geslin B, Goulnik J, Guilbaud L, Hautekèete N, Heiniger C, Kuhlmann M, Lambert O, Langlois D, Le Féon V, Lopez Vaamonde C, Maillet G, Massol F, Michel N, Michelot-Antalik A, Michez D, Mouret H, Piquot Y, Potts SG, Roberts S, Ropars L, Schurr L, Van Reeth C, Villalta I, Zaninotto V, Dajoz I, Henry M (2022) A large-scale dataset reveals taxonomic and functional specificities of wild bee communities in urban habitats of Western Europe. Scientific Reports 12: 1–15. https://doi.org/10.1038/s41598-022-21512-w

Fortel L, Henry M, Guilbaud L, Guirao AL, Kuhlmann M, Mouret H, Rollin O, Vaissière BE (2014) Decreasing abundance, increasing diversity and changing structure of the wild bee community (Hymenoptera: Anthophila) along an urbanization gradient. PLOS ONE 9(8): e104679. https://doi.org/10.1371/journal.pone.0104679

Gallai N, Salles JM, Settele J, Vaissière BE (2009) Economic valuation of the vulnerability of world agriculture confronted with pollinator decline. Ecological Economics 68: 810–821. https://doi.org/10.1016/j.ecolecon.2008.06.014

Goulson D, Lepais O, O'Connor S, Osborne JL, Sanderson RA, Cussans J, Goffe L, Darvill B (2010) Effects of land use at a landscape scale on bumblebee nest density and survival. Journal of Applied Ecology 47: 1207–1215. https://doi.org/10.1111/j.1365-2664.2010.01872.x

Gu D, Andreev K, Dupre ME (2021) Major Trends in Population Growth Around the World. China CDC Weekly 3: 604–613. https://doi.org/10.46234/ccdcw2021.160

Hall DM, Camilo GR, Tonietto RK, Ollerton J, Ahrné K, Arduser M, Ascher JS, Baldock KCR, Fowler R, Frankie G, Goulson D, Gunnarsson B, Hanley ME, Jackson JI, Langellotto G, Lowenstein D, Minor ES, Philpott SM, Potts SG, Sirohi MH, Spevak EM, Stone GN, Threlfall CG (2017) The city as a refuge for insect pollinators. Conservation Biology 31: 24–29. https://doi.org/10.1111/cobi.12840

Hamroud L, Lhomme P, Christmann S, Sentil A, Michez D, Rasmont P (2022) Conserving wild bees for crop pollination: efficiency of bee hotels in Moroccan cherry orchards (*Prunus avium*). Journal of Apicultural Research62: 1123–1131. https://doi.org/10.1080/00218839.2022.2046528

IPBES [Intergovernmental Science-Policy Platform on Biodiversity and Ecosystem Services](2019a) Global Assessment Report on Biodiversity and Ecosystem Services of the

Intergovernmental Science-Policy Platform on Biodiversity and Ecosystem Services. IPBES secretariat, Bonn.

IPBES [Intergovernmental Science-Policy Platform on Biodiversity and Ecosystem Services] (2019b) Summary for policymakers of the global assessment report on biodiversity and ecosystem services of the Intergovernmental Science-Policy Platform on Biodiversity and Ecosystem Services. Díaz S, Settele J, Brondizio ES, Ngo HT, Guèze J, et al. (Eds). IPBES secretariat, Bonn, 53 pp.

Klein AM, Vaissière BE, Cane JH, Steffan-Dewenter I, Cunningham SA, Kremen C, Tscharntke T (2007) Importance of pollinators in changing landscapes for world crops. Proceedings of the Royal Society B: Biological Sciences 274: 303–313. https://doi.org/10.1098/rspb.2006.3721

Lhomme P, Michez D, Christmann S, Scheuchl E, El Abdouni I, Hamroud L, Ihsane O, Sentil A, Smaili MC, Schwarz M, Dathe HH, Straka J, Pauly A, Schmid-Egger C, Patiny S, Terzo M, Muller A, Praz C, Risch S, Kasparek M, Kuhlmann M, Wood TJ, Bogusch P, Ascher JS, Rasmont P (2020) The wild bees (Hymenoptera: Apoidea) of Morocco. Zootaxa 4892: 1–159. https://doi.org/10.11646/zootaxa.4892.1.1

Macinnis G, Normandin E, Ziter CD (2023) Decline in wild bee species richness associated with honey bee (*Apis mellifera* L.) abundance in an urban ecosystem. PeerJ 11: e14699. https://doi.org/10.7717/peerj.14699

Maharramov MM, Fateryga AV, Proshchalykin MY (2023) New records of megachilid bees (Hymenoptera: Megachilidae) from the Nakhchivan Autonomous Republic of Azerbaijan. Far Eastern Entomologist 472: 18–24. https://doi.org/10.25221/fee.472.2

McCune F, Normandin É, Mazerolle MJ, Fournier V (2020) Response of wild bee communities to beekeeping, urbanization, and flower availability. Urban Ecosystems 23: 39–54. https://doi.org/10.1007/s11252-019-00909-y

Michez D, Rasmont P, Terzo M, Vereecken NJ (2019) Bees of Europe. NAP Editions.

Michez D, Else GR, Roberts SPM (2007) Biogeography, floral choices and redescription of *Promelitta alboclypeata* (Friese 1900) (Hymenoptera: Apoidea: Melittidae). African Entomology 15: 197–203. https://doi.org/10.4001/1021-3589-15.1.197

Nilon CH, Aronson MFJ, Cilliers SS, Dobbs C, Frazee LJ, Goddard MA, O'Neill KM, Roberts D, Stander EK, Werner P, Winter M, Yocom KP (2017) Planning for the future of urban biodiversity: A global review of city-scale initiatives. BioScience 67: 332–342. https://doi.org/10.1093/biosci/bix012

Oke C, Bekessy SA, Frantzeskaki N, Bush J, Fitzsimons JA, Garrard GE, Grenfell M, Harrison L, Hartigan M, Callow D, Cotter B, Gawler S (2021) Cities should respond to the biodiversity extinction crisis. npj Urban Sustainability 1: 11. https://doi.org/10.1038/s42949-020-00010-w

Ollerton J, Winfree R, Tarrant S (2011) How many flowering plants are pollinated by animals? Oikos 120: 321–326. https://doi.org/10.1111/j.1600-0706.2010.18644.x

Orr MC, Hughes AC, Chesters D, Pickering J, Zhu CD, Ascher JS (2021) Global patterns and drivers of bee distribution. Current Biology 31: 451–458. https://doi.org/10.1016/j.cub.2020.10.053

PalDat (2024) PalDat: Palynological Database. https://www.paldat.org/ [Accessed on 09.04.2024]

Patiny S, Michez D (2007) Biogeography of bees (Hymenoptera, Apoidea) in Sahara and the Arabian deserts. Insect Systematics and Evolution 38: 19–34. https://doi.org/10.1163/187631207788784012

Rankou H, Culham A, Jury SL, Christenhusz MJM (2013) The endemic flora of Morocco. Phytotaxa 78: 1. https://doi.org/10.11646/phytotaxa.78.1.1

Reverté S, Miličić M, Ačanski J, Andrić A, Aracil A, Aubert M, Balzan MV, Bartomeus I, Bogusch P, Bosch J, Budrys E, Cantú-Salazar L, Castro S, Cornalba M, Demeter I, Devalez J, Dorchin A, Dufrêne E, Đorđević A, Fisler L, Fitzpatrick Ú, Flaminio S, Földesi R, Gaspar H, Genoud D, Geslin B, Ghisbain G, Gilbert F, Gogala A, Grković A, Heimburg H, Herrera-Mesías F, Jacobs M, Janković Milosavljević M, Janssen K, Jensen JK, Ješovnik A, Józan Z, Karlis G, Kasparek M, Kovács-Hostyánszki A, Kuhlmann M, Le Divelec R, Leclercq N, Likov L, Litman J, Ljubomirov T, Madsen HB, Marshall L, Mazánek L, Milić D, Mignot M, Mudri-Stojnić S, Müller A, Nedeljković Z, Nikolić P, Ødegaard F, Patiny S, Paukkunen J, Pennards G, Pérez-Bañón C, Perrard A, Petanidou T, Pettersson LB, Popov G, Popov S, Praz C, Prokhorov A, Quaranta M, Radchenko VG, Radenković S, Rasmont P, Rasmussen C, Reemer M, Ricarte A, Risch S, Roberts SPM, Rojo S, Ropars L, Rosa P, Ruiz C, Sentil A, Shparyk V, Smit J, Sommaggio D, Soon V, Ssymank A, Ståhls G, Stavrinides M, Straka J, Tarlap P, Terzo M, Tomozii B, Tot T, van der Ent LJ, van Steenis J, van Steenis W, Varnava AI, Vereecken NJ, Veselić S, Vesnić A, Weigand A, Wisniowski B, Wood TJ, Zimmermann D, Michez D, Vujić A (2023) National records of 3000 European bee and hoverfly species: A contribution to pollinator conservation. Insect Conservation and Diversity 16: 758–775. https://doi.org/10.1111/icad.12680

Rasmont P, Wood TJ (2024) An enigmatic anthophorine bee from the south of France revealed as a new species: *Anthophora* (*Paramegilla*) *ahlamae* n. sp. (Hymenoptera: Apidae). Annales de La Société Entomologique de France (N.S.) 1–15. https://doi.org/10.1080/00379271.2024.2325688

Sabbahi R (2022) Economic value of insect pollination of major crops in Morocco. International Journal of Tropical Insect Science 42: 1275–1284. https://doi.org/10.1007/s42690-021-00645-x

Sahib S, Driauach O, Belqat B (2020) New data on the hoverflies of Morocco (Diptera, Syrphidae) with faunistic and bibliographical inventories. ZooKeys 971: 59–103. https://doi.org/10.3897/zookeys.971.49416

Saure C (1996) Urban habitats for bees: the example of the city of Berlin. The conservation of bees. Academic Press, New York.

Sentil A, Reverté S, Lhomme P, Bencharki Y, Rasmont P, Christmann S, Michez D (2022b) Wild vegetation and 'farming with alternative pollinators' approach support pollinator diversity in farmland. Journal of Applied Entomology 146: 1155–1168. https://doi.org/10.1111/jen.13060

Sentil A, Wood TJ, Lhomme P, Hamroud L, El Abdouni I, Ihsane O, Bencharki Y, Rasmont P, Christmann S, Michez D (2022a) Impact of the "Farming With Alternative Pollinators"

approach on crop pollinator pollen diet. Frontiers in Ecology and Evolution 10: 1–12. https://doi.org/10.3389/fevo.2022.824474

Sentil A, Lhomme P, Michez D, Reverté S, Rasmont P, Christmann S (2021) "Farming with Alternative Pollinators" approach increases pollinator abundance and diversity in faba bean fields. Journal of Insect Conservation 26: 401–414. https://doi.org/10.1007/s10841-021-00351-6

Tkalců B (1979) Revision der europäischen Vertreter der Artengruppe von *Tetralonia ruficornis* (Fabricius)(Hymenoptera, Apoidea). Časopis Moravského Muzea. Vědy Přírodní 64: 127–152.

Van der Zanden G (1986) Die paläarktischen Arten der Gattung *Lithurgus* Latreille, 1825 (Hymenoptera, Apoidea, Megachilidae). Mitteilungen aus dem Museum für Naturkunde in Berlin 62: 53–59. https://doi.org/10.1002/mmnz.19860620105

Verovnik R, Beretta S, Rowlings M (2018) Contribution to the knowledge of the spring butterfly fauna of the southern anti-atlas region, Morocco (Lepidoptera: Papilionoidea). SHILAP Revista de lepidopterologia 46: 81–90. https://doi.org/10.57065/shilap.839

Warncke K (1992) Die westpaläarktischen Arten der Bienengattung *Coelioxys* Latr. (Hymenoptera, Apidae, Megachilidae). Bericht der Naturforschenden Gesellschaft Augsburg 196: 31–77.

Wastian L, Unterweger PA, Betz O (2016) Influence of the reduction of urban lawn mowing on wild bee diversity (Hymenoptera, Apoidea). Journal of Hymenoptera Research 49: 51–63. https://doi.org/10.3897/JHR.49.7929

Wenzel A, Grass I, Belavadi VV, Tscharntke T (2020) How urbanization is driving pollinator diversity and pollination – A systematic review. Biological Conservation 241: 108321. https://doi.org/10.1016/j.biocon.2019.108321

Wood TJ (2023b) Revisions to the *Andrena* fauna of north-western Africa with a focus on Morocco (Hymenoptera: Andrenidae). European Journal of Taxonomy 916: 1–85. https://doi.org/10.5852/ejt.2023.916.2381

Wood TJ (2023a) Bee species newly recorded for the Moroccan fauna, including two new species of *Ammobatoides* and *Thyreus* (Hymenoptera: Anthophila). Annales de la Société entomologique de France 59: 177–203. https://doi.org/10.1080/00379271.2023.2215216

Wood TJ, Ghisbain G, Michez D, Praz CJ (2021) Revisions to the faunas of *Andrena* of the Iberian Peninsula and Morocco with the descriptions of four new species (Hymenoptera: Andrenidae). European Journal of Taxonomy 758: 147–193. https://doi.org/10.5852/ejt.2021.758.1431

Wood TJ, Michez D, Cejas D, Lhomme P, Rasmont P (2020) An update and revision of the *Andrena* fauna of Morocco (Hymenoptera, apoidea, Andrenidae) with the description of eleven new north African species. ZooKeys 974: 31–92. https://doi.org/10.3897/zookeys.974.54794

Wood TJ, Roberts SPM (2017) An assessment of historical and contemporary diet breadth in polylectic *Andrena* bee species. Biological Conservation 215: 72–80. https://doi.org/10.1016/j.biocon.2017.09.009

Supplementary material 1

List of bee species collected during the course of the study

Authors: Ahlam Sentil, Paolo Rosa, Clément Tourbez, Achik Dorchin, Petr Bogusch, Denis Michez

Data type: xlsx

Explanation note: The table summarizes the list of bee species collected during the course of the study. The bee species abundance (the number of bee individuals collected per genus) are indicated. The bee species newly recorded in the region Marrakech Safi are written in bold and highlighted in green.

Link: https://doi.org/10.3897/jhr.97.125408.suppl1

JHR 97: 531–539 (2024)
doi: 10.3897/jhr.97.123966
https://jhr.pensoft.net

RESEARCH ARTICLE

JOURNAL OF Hymenoptera RESEARCH
A peer-reviewed open-access journal
The International Society of Hymenopterists

Distribution of the sand wasp *Bicyrtes variegatus* (Oliver, 1789) (Hymenoptera, Crabronidae) in the Galápagos Islands, with notes on its ecology

Andrea C. Román[1,2], Patricio Picón-Rentería[2,3], Charlotte E. Causton[1], Lenyn Betancourt-Cargua[1], Catherine Frey[3], Henri W. Herrera[3]

1 *Charles Darwin Research Station, Charles Darwin Foundation, Santa Cruz, Galápagos, Ecuador* **2** *Universidad Nacional de Colombia, Instituto de Ciencias Naturales, Laboratorio de Sistemática y Biología Comparada de Insectos, Bogotá, Colombia* **3** *Entomology Museum, Facultad de Recursos Naturales. Escuela Superior Politécnica de Chimborazo. Panamericana sur Km 1½, Riobamba, Ecuador*

Corresponding author: Andrea C. Román (andrea.carvajal@fcdarwin.org.ec)

Academic editor: Christopher K. Starr | Received 25 March 2024 | Accepted 1 July 2024 | Published 10 July 2024

https://zoobank.org/83299778-E57B-490E-A1DF-82C17CC11D99

Citation: Román AC, Picón-Rentería P, Causton CE, Betancourt-Cargua L, Frey C, Herrera HW (2024) Distribution of the sand wasp *Bicyrtes variegatus* (Oliver, 1789) (Hymenoptera, Crabronidae) in the Galápagos Islands, with notes on its ecology. Journal of Hymenoptera Research 97: 531–539. https://doi.org/10.3897/jhr.97.123966

Abstract

Very little is known about the sand wasp, *Bicyrtes variegatus*, in the Galápagos archipelago. In this study, we compiled information from surveys, museum collections and the literature to better understand its distribution and ecology. We found records of *B. variegatus* on seven islands with the earliest known record from 1964, from San Cristóbal Island. Wasps have been collected in the littoral, arid, transition and humid vegetation zones and have been reported visiting endemic, native, cryptogenic, and introduced plants. Sun dances and a tight cluster of wasps, similar in form to what others have called "mating balls", were observed in the hot season.

Keywords

Bembicinae, flower visitors, mating, sand wasp

Introduction

Despite the biological importance of the Galápagos archipelago, there are still groups of insects about which little is known (Causton et al. 2006). Recently, researchers have increased efforts to study the Hymenoptera of the Galápagos Islands, resulting in the discovery of new taxa as well as new locality records for species that were already registered (Fernández et al. 2018; Herrera et al. 2024). One of these is the sand wasp *Bicyrtes variegatus* (Oliver, 1789) (Crabronidae). Species of this genus are recognized by the scarlike middle ocellus, papal formula (6–4), and lateral projections of the propodeum (Bohart 1996). Of the 27 described species, 16 are found in South America, eight in North America, and the remaining species in Panama (Bohart and Menke 1976).

Species from this genus are solitary wasps, feeding mainly on Hemiptera of the families Alydidae, Coreidae, Cydnidae, Lygaeidae, Pentatomidae, Pyrrhocoridae, Reduviidae, Rhopalidae, and Scutelleridae, as well as Diptera (Eberhard 1974; Evans and O'Neill 2007). Evans and O'Neill (2007) identified three methods of provisioning nests (mass, delayed, and progressive), depending on the timing and duration of provisioning a cell, and found that the number of cells per nest ranges from one to five, with 3–24 prey in a cell. These authors also report nesting-site fidelity, in which wasps remain in the same place each year. Males display a variety of strategies for attracting mates including "sun dances".

Bicyrtes variegatus is easily recognized by the yellow band across the anterior part of the scutellum (Bohart 1996) and has been reported from Texas to Argentina (Bohart and Menke 1976; Genise 1979; Amarante 2002; Buys and Trad 2021). Nesting aggregations have also been reported from Santa Cruz Island in the Galápagos (Larsson 1992). Throughout its range, this species is mainly found in coastal habitats, with observations of females digging nests on the beach (Evans 1976). *B. variegatus* is considered a mass provisioner, laying an egg on the prey that it places inside a cell in the ground nest and then closing the cell. This behavior has been associated with prey scarcity or poor weather conditions rather than with a particular habitat condition (Evans and O'Neill 2007). Once the larva matures, a cocoon is made and pupation is initiated. The cocoon was described by Buys and Trad (2021) as an ovoid and granulose structure with a length of 9–10 mm. *B. variegatus* is reported to build nests in the same area each year, with only the males seeking mates (Evans 1974; Evans and O'Neill 2007).

Very little is known about *B. variegatus* in the Galápagos Islands. In this study, we compiled information from surveys, museum collections, and literature to better understand the distribution and ecology of this species in the archipelago.

Methods

We reviewed specimens deposited in the Invertebrate Collection of the Charles Darwin Research Station (ICCDRS) up to August 2023 and specimens from the California Academy of Science (CAS) online database (Monarch 2023). John Heraty kindly

provided information on specimens at the University of California, Riverside (UCRC) and the Canadian Museum of Nature (CMNC), collected during the Peck expeditions (Peck, 2001). The ecological information on the labels or in the databases (e.g., interaction with plants) was also extracted. In addition, we conducted a search of the literature. Lastly, we checked material collected in the project "Study of invasive species and diversity of terrestrial invertebrates in the Galápagos Islands" within the framework of the ESPOCH agreement with the Charles Darwin Foundation". In this, a structured method was used (Longino and Colwell 1997) to inventory Hymenoptera archipelago-wide in 2018, 2019, and 2021. Sampling was carried out in the littoral, dry, transition, and humid zones (Jackson 1993; Tye and Francisco-Ortega 2011) on the islands of Española, Fernandina, Floreana, Genovesa, Isabela (Alcedo, Darwin, and Sierra Negra volcanoes), Marchena, Pinta, San Cristóbal, Santa Cruz, and Santiago using three methods: i) Malaise traps (three traps per zone separated by a minimum of 50 m along the altitudinal transect and set out for eight days), ii) yellow trays (three trays per zone separated by a minimum of 5 m and placed around each Malaise trap for three days), and iii) sweep-net collections (four runs of 50 double passes and free capture in each zone).

Results and discussion

Distribution

The earliest record of *B. variegatus* that we found was from 1964 collected by R. L. Usinger on San Cristóbal Island and deposited at CAS. To date, *B. variegatus* has been reported from islands currently inhabited by humans (Floreana, Isabela, San Cristóbal and Santa Cruz), inhabited by humans in the past (Santiago; Lundh 2001), and from uninhabited islands (Española and Fernandina). In the material we examined we found records of *B. variegatus* from the littoral, arid, and transition vegetation zones (Tye and Francisco-Ortega 2011), but notably also from the more humid areas (e.g. Bellavista on Santa Cruz Island and Cerro Pajas on Floreana Island). The highest elevations it was recorded at was 400 m.a.s.l. NE of Cabo Hammond on Fernandina Island and 335 m.a.s.l. at Cerro Pajas on Floreana Island (Fig. 1). Collection localities include: Española: Gardner Bay; Fernandina: NE of Cabo Hammond; Floreana: Cerro Pajas, Finca Cruz, Mina de Granillo Negro, Playa Negra, Post Office Bay; Isabela: Bosque de los Niños and Puerto Villamil; San Cristóbal: Camino a las Negritas, Camino a Tijeras, El Chino, Puerto Baquerizo Moreno, Puerto Chino; Santa Cruz: Bellavista, Charles Darwin Research Station (CDRS), Mina Granillo Negro, Playa el Garrapatero, Tortuga Bay. In addition to these records, *B. variegatus*, incorrectly named *Bycertis*, is reported in the literature from Santiago (Traveset et al. 2013) at a site later identified as Puerto Egas (H.W.H.). No specimens were collected in the archipelago-wide surveys conducted by ESPOCH between 2018 and 2021, which included setting out traps in the littoral-arid zones, the preferred habitat of these wasps.

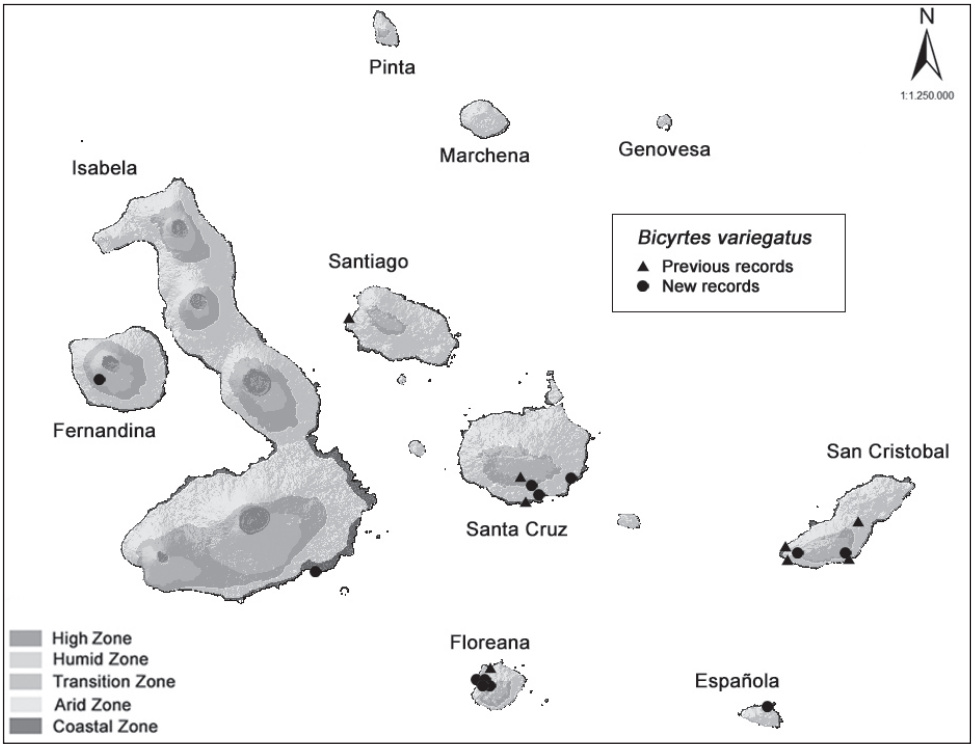

Figure 1. Distribution of *Bicyrtes variegatus* in the Galápagos archipelago.

How *B. variegatus* reached the archipelago is unknown. Little information is available in the literature about how *B. variegatus* can disperse over long distances, including how it has dispersed to new islands (e.g. Bohart and Menke 1976). It is possible that it arrived in the Galápagos in sand and soil imported for the construction of military posts during World War II (US 1947; Peck et al. 1998). These wasps are known to build their nests in sandy material (Evans and O'Neill 2007) and have been found in sand used in construction (Eberhard 1974). The cocoons of *B. variegatus* are made of soil particles bound together with silk, and the prepupae of some *Bicyrtes* species can remain dormant for extended periods (Martins et al. 1998; Buys and Trad 2021).

Interaction with plants and mating behavior

Bicyrtes are known to visit flowering plants in other parts of the world (Porter 1980; Freitas et al. 2001). Plants are visited to obtain carbohydrates, but are also used for hunting prey and resting (Martins et al. 1998; Evans and O'Neill 2007). In the Galápagos, multiple studies have documented Hymenoptera associated with plants (e.g. McMullen 1986, 1993; Linsley and Usinger 1966; Peck et al. 1998), but did not report *Bicyrtes* visiting flowers. However, *Bicyrtes* sp. was recorded in the literature

(Boada 2005; Traveset et al. 2013; Hervías-Parejo et al. 2018), or on labels, visiting the following plants: *Bidens pilosa* (cryptogenic), *Croton scouleri* (endemic), *Galactia striata* (native), *Heliotropium angiospermum* (native), *Lantana camara* (introduced), *Mollugo flavescens* (endemic), *Scalesia cordata* (endemic), *Scalesia gordilloi* (endemic), *Vachellia rorudiana* (native), *Vallesia glabra* (native), *Varronia leucophlyctis* (endemic), and *Waltheria ovata* (native).

Other than plant visits, little is known about the behavior of *B. variegatus* in Galápagos. In February 2022, we observed hundreds of *Bicyrtes* wasps flying near Garrapatero beach on Santa Cruz Island. The wasps were close to the sand and formed aggregations akin to mass swarms. These are aggregations of males in the sites where virgin females emerge (Evans and O'Neill 2007). Such "sun dances" have been documented as a mating strategy of sand wasps (Bembicinae) (O'Neill 2008). We also saw a tight cluster of wasps similar in form to what others have called "mating balls" (Evans and O'Neill 2007), although we did not observe mating (Fig. 2). This behavior was only observed in February during the hot rainy season. In the following months, only a few individuals were observed flying over the ground surface.

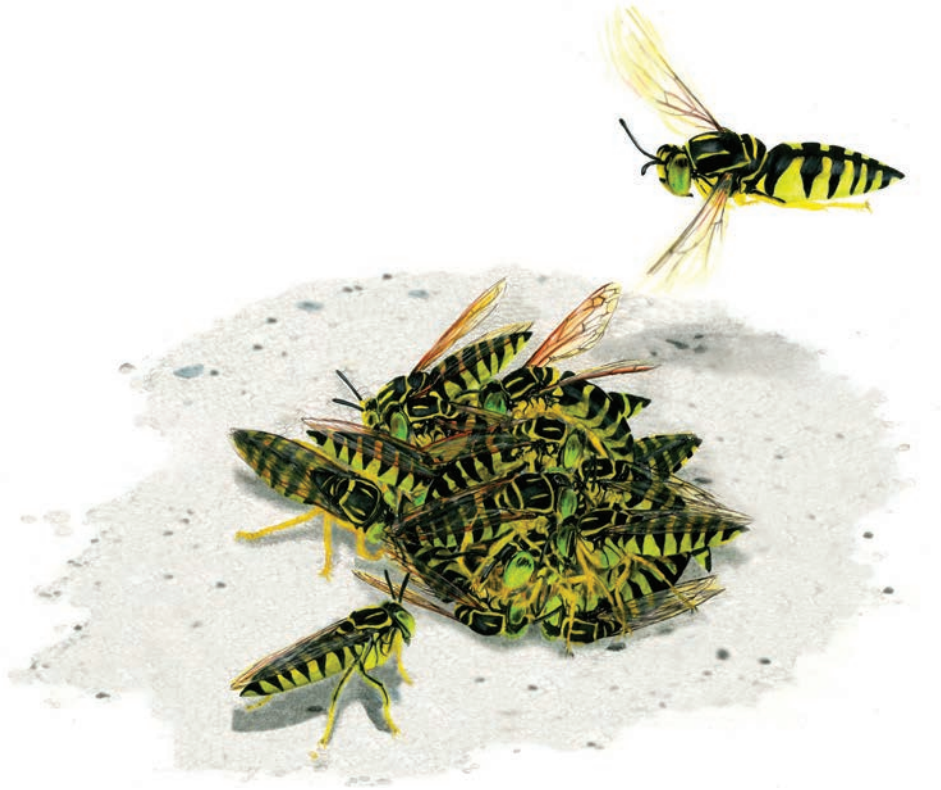

Figure 2. "Mating ball" of *Bicyrtes variegatus* on the sand. Credit for illustration: José Falcón Reibán.

Material examined

Ecuador, Galápagos – **Española** • 3♂♂, 5♀♀; Gardner Bay; 1.35111°S, 89.662222°W; 0–20 m; 27 Apr. 1991; J. Heraty leg.; arid zone; swp; H91-006; UCRC: UCRCENT00467383-00467390 – **Fernandina** • 1♂; 10 Km N[orth]e[ast] Cabo Hammond; 0.419166°S, 91.581111°W; 400 m; 9 May. 1991; J. Heraty leg.; transition [zone]; H91-027; UCRC: UCRCENT00467381 – **Floreana** • 1; Mina de Granillo Negro; 1.281212°S, 90.467887°W; 169 m; 8 May. 2019; A. Acurio, L. Betancourt leg.; ICCDRS 42756 • 1; 3Km E[ast] Playa Negra; 120 m; 21–28 Mar.1989; S. Peck and B.J. Sinclair leg.; Malaise trap; (89–140); ICCDRS 48230 • 1; Post Office Bay; 30 Abr. 1983; Y. Lubin Leg.; ICCDRS 54389 • 1; Between beach & lagoon, E. end Post Office Bay; 1.235389°S, 90.451361°W; 14 Feb. 1967; Ira L. Wiggins leg.; CASENT 8556863 • 2 ♀♀; Cerro Pajas; 1.293611°S, 90.457222°W; 335 m; 27 Mar.-22 Apr. 1996; S. Peck leg.; Forest edge; Malaise; 96–54; CMNC: UCRCENT00467399, 00467400 • 2♀♀; Finca Cruz; 130 m, 16–22 Apr. 1996; S. Peck leg.; arid zone forest; Malaise; 96–107; CMNC: UCRCENT00467396, 00467397 • 6♀♀; Finca Cruz; 130 m; 27 Mar.-16 Apr 1996; S. Peck leg.; arid zone forest; Malaise; 96–58; CMNC: UCRCENT00467392-00467395 – **Isabela** • 1; P[uer]to Villamil; 7 Mar. 1989; B.J. Sinclair leg.; littoral; sweeping sand beach; ICCDRS 48225 • 1; Bosque de Niños; 20 Mar. 1995; P. Delgado leg; Licking on *Scalesia cordata*; 11:51; ICCDRS 48223 – **San Cristóbal** • 1; Camino a las Negritas; 31 Mar. 2002; R. Boada leg.; *S. gordilloi* (leaves); ICCDRS 48221 • 1; Camino a las Negritas, 31 Mar. 2002; R. Boada leg.; *S. gordilloi* (flowers); ICCDRS 48228 • 1; [Puerto] Baquerizo; 10 m; 11–23 Feb. 1989; S. Peck leg.; Malaise trap; (89-47); ICCDRS 48224 • 1; El Chino, Z[one] Agrícola; 13 Apr. 2003; P. Lincango, A. Mieles leg.; Manual collection (Beach); ICCDRS 48226 • 1; P[uer]to Baquerizo [Moreno]; 12 Feb. 2007; M. Flores leg.; Manual collection (in the car); ICCDRS 48227 • 1; Puerto Chino; 26 Feb. 2011; M. Noguera leg.; Manual collection; on *Lantana camara*; #SC-544; ICCDRS 54393 • 1; Camino a Tijeras; 2 Mar. 2010; R. Castro, S. Chamorro leg.; Manual collection; on *Croton scouleri*; ICCDRS 54390 • 3; Progresso (trail to); 0.846271°S, 89.441822°W; 23 Feb. 1964; R.L. Usinger leg.; CASENT 8556860, 8556861, 8556862 – **Santa Cruz** • 1; C[harles] D[arwin] R[esearch] S[tation]; 5 Mar. 1996; C. Blanton leg.; ICCDRS 48222 • 1; Charles Darwin Research Station; 13 Feb. 2007; A. Muth leg.; Malaise; ICCDRS 48229 • 1; Bellavista; 0.6989167°S, 90.3207222°W; 199 m; 12 Feb. 2020; C.R. Gil Jaramillo leg.; Entomological net; ICCDRS 46547 • 1; Mina Granillo [Negro]; 8 May. 2011; S. Chamorro leg.; Manual collection; on *Bidens pilosa*; ICCDRS 54391 • 1; Tortuga Bay; 23 Feb. 2010; S. Chamorro leg.; Manual collection; on *Waltheria ovata*; ICCDRS 54392 • 2; Playa el Garrapatero; 16 Mar. 2022; A. Mieles Leg; Entomological net; ICCDRS 53891, 53892.

Author contributions

Conceptualization: ACR, PPR. Data curation and formal analysis: ACR, PPR, LBC. Supervision: HWH, CEC. Writing – original draft: ACR, PPR, CEC. Writing – review and editing: ACR, CEC, PPR, LBC, CF, HWH.

Acknowledgments

The Galápagos National Park Directorate (DPNG) and the Ministry of Environment (MAATE), provided the permits for the annual operation of the Galápagos Natural History Collections (N°MAATE-MCMEVS-2023-075) under which this project was conducted. The Study of invasive species and diversity of terrestrial invertebrates in the Galápagos Islands within the framework of the Escuela Superior Politécnica de Chimborazo (ESPOCH) and Charles Darwin Foundation (CDF) agreement was conducted with permits from DPNG: PC-43-18, PC-44-19, PC-43-20, PC-39-21. We thank John Heraty for providing us with new island records and observations on the manuscript and Kevin O´Neill for his insightful comments, which improved the manuscript. We also thank Alejandro Mieles for collecting the specimens from the Garrapatero beach and José Falcón Reibán for the illustration of the "mating ball" of *Bicyrtes variegatus*. Funding support for the ICCDRS collection comes from Gordon and Betty Moore Foundation, Lindblad Expeditions -National Geographic, and Ecoaventura. This publication is contribution number 2627 of the Charles Darwin Foundation for the Galápagos Islands, and number 009 under the agreement ESPOCH-CDF.

Open Access funding enabled by the project "Study of invasive species and diversity of terrestrial invertebrates in the Galápagos Islands", within the framework of the agreement between the Escuela Superior Politécnica de Chimborazo and the Charles Darwin Foundation.

References

Amarante STP (2002) A synonymic catalog of the Neotropical Crabronidae and Sphecidae (Hymenoptera: Apoidea). Arquivos de Zoologia 37: 1–139. https://doi.org/10.11606/issn.2176-7793.v37i1p1-139

Boada R (2005) Insects associated with endangered plants in the Galápagos Islands, Ecuador. Entomotropica 20: 77–88.

Bohart RM (1996) A review of the genus *Bicyrtes* (Hymenoptera: Sphecidae, Nyssoninae, Bembicini). Insecta Mundi 19: 139–152. https://doi.org/10.1525/9780520309548

Bohart RM, Menke AS (1976) Sphecid Wasps of the World: A Generic Revision. University of California Press, Berkley, 1–695. https://doi.org/10.1525/9780520309548

Buys SC, Trad BM (2021) Morfología del capullo de *Bicyrtes variegatus* (Oliver, 1789) (Hymenoptera: Crabronidae), con notas sobre el hábitat y las interacciones biológicas. Revista Chilena de Entomología 47: 205–209. https://doi.org/10.35249/rche.47.2.21.05

Causton CE, Peck SB, Sinclair BJ, Roque-Albelo L, Hodgson CJ, Landry B (2006) Alien insects: threats and implications for conservation of Galápagos Islands. Annals of the Entomological Society of America 99: 121–143. https://doi.org/10.1603/0013-8746(2006)099[0121:AITAIF]2.0.CO;2

Eberhard W (1974) Insectos y hongos que atacan a la chinche del cacao, *Antiteuchus tripterus*. Revista de la Facultad Nacional de Agronomía Medellín 29: 65–72.

Evans HE (1974) Digger wasps as colonizers of new habitat (Hymenoptera: Aculeata). Journal of the New York Entomological Society 82: 259–267.

Evans HE (1976) Bembicini of Baja California Sur: Notes on nests, prey, and distribution. Pan-Pacific Entomologist 52: 314–320.

Evans HE, O'Neill KM (2007) The Sand Wasps: Natural History and Behavior. Harvard University Press, Cambridge, 1–340. https://doi.org/10.4159/9780674036611

Fernández F, Sarmiento CE, Herrera HW (2018) First record of the Sclerogibbidae (Hymenoptera) from the Gálapagos Islands, Ecuador. Pan-Pacific Entomologist 94: 27–31. https://doi.org/10.3956/2018-94.1.27

Freitas L, Bernardello G, Galetto L, Paoli AA (2001) Nectaries and reproductive biology of *Croton sarcopetalus* (Euphorbiaceae). Botanical Journal of the Linnean Society 136: 267–277. https://doi.org/10.1111/j.1095-8339.2001.tb00572.x

Genise JF (1979) Comportamiento de nidificación de *Bicyrtes variegata* y *B. discisa* (Hymenoptera. Sphecidae). Revista de la Sociedad Entomológica Argentina 38: 123–126.

Herrera HW, Tocora MC, Fiorentino G, Causton CE, Dekoninck W, Hendrickx F (2024) The ants of the Galápagos Islands (Hymenoptera, Formicidae): a historical overview, checklist, and identification key. ZooKeys 1191: 151–213. https://doi.org/10.3897/zookeys.1191.107324

Hervías-Parejo S, Traveset A (2018) Pollination effectiveness of opportunistic Galápagos birds compared to that of insects: from fruit set to seedling emergence. American Journal of Botany 105: 1142–1153. https://doi.org/10.1002/ajb2.1122

Jackson MH (1993) Gálapagos, a Natural History. University of Calgary Press, Calgary, 1–315.

Larsson FK (1992) Research News. Sphecos 23. https://naturalhistory.si.edu/sites/default/files/media/file/sphecos23-dec-1991.pdf

Linsley EG, Usinger RL (1966) Insects of the Gálapagos islands. Proceedings of the California Academy of Sciences 33: 113–196.

Longino JR Colwell RK (1997) Biodiversity assessment using structured inventory: capturing the ant fauna of a tropical rainforest. Ecological Applications 7: 1263–1277. https://doi.org/10.2307/2641213

Lundh JP (2001) The Gálapagos: A brief history. https://whalesite.org/galapagos/2001%20-%20Lundh%20-%20Galapagos%20a%20Brief%20History%20new.htm

Martins RP, Soares LA, Yanega D (1998) The nesting behavior and dynamics of *Bicyrtes angulata* (F. Smith) with a comparison to other species in the genus (Hymenoptera: Sphecidae). Journal of Hymenoptera Research 7: 165–177.

McMullen CK (1986) Observations on insect visitors to flowering plants on Isla Santa Cruz, Part II. Butterflies, moths, ants, hover flies and stilt bugs. Noticias de Galápagos 43: 21–23.

McMullen CK (1993) Flower-visiting insects of the Gálapagos Islands. Pan-Pacific Entomologist 69: 95–106.

Monarch (2023) Entomology collection website. https://monarch.calacademy.org/collections/harvestparams.php

O'Neill, KM (2008) Apoid wasps (Hymenoptera: Apoidea: Spheciformes). In: Capinera JL (Ed.) Encyclopedia of Entomology. Springer, Dordrecht, 230–239. https://doi.org/10.1007/978-1-4020-6359-6_10300

Peck SB (2001) Smaller orders of insects of the Galápagos Islands, Ecuador: evolution, ecology, and diversity. NRC Research Press, Ottawa, 1–278.

Peck SB, Heraty J, Landry B, Sinclair BJ (1998) Introduced insect fauna of an oceanic archipelago: The Galápagos Islands, Ecuador. American Entomologist 44: 218–237. https://doi.org/10.1093/ae/44.4.218

Porter CC (1980) *Bicyrtes* Lepeletier (Hymenoptera: Sphecidae) in the Lower Rio Grande Valley of Texas and in Northeast Mexico. Florida Entomologist 63: 281–285. http://doi.org/10.2307/3494623

Traveset A, Heleno R, Chamorro S, Vargas P, McMullen CK, Castro-Urgal R, Nogales M, Herrera HW, Olesen JM (2013) Invaders of pollination networks in the Galápagos Islands: emergence of novel communities. Proceedings of the Royal Society B: Biological Sciences 280(1758): 20123040. http://doi.org/10.1098/rspb.2012.3040

Tye A, Francisco-Ortega J (2011) Origins and evolution of Galápagos endemic vascular plants. In: Bramwell D, Caujapé-Castells J (Eds) The Biology of Island Floras. Cambridge University Press, Cambridge, 89–153. https://doi.org/10.1017/CBO9780511844270.006

United States (1947) Building the Navy's bases in World War II; history of the Bureau of Yards and Docks and the Civil Engineer Corps, 1940–1946. https://www.history.navy.mil/research/library/online-reading-room/title-list-alphabetically/b/building-the-navys-bases/building-the-navys-bases-vol-2.html#1-18

JHR 97: 541–544 (2024)
doi: 10.3897/jhr.97.123853
https://jhr.pensoft.net

SHORT COMMUNICATION

JOURNAL OF Hymenoptera RESEARCH
A peer-reviewed open-access journal
The International Society of Hymenopterists

Use of a novel nesting material by the spider wasp *Dipogon variegatus* (Hymenoptera, Pompilidae)

Sergio Albacete[1,2], Gonzalo Sancho[1,2], Jordi Bosch[2]

1 *Universitat Autònoma de Barcelona, 08193 Bellaterra, Spain* **2** *Centre for Ecological Research and Forestry Applications (CREAF), 08193 Bellaterra, Spain*

Corresponding author: Sergio Albacete (s.albacete@creaf.uab.cat)

Academic editor: Christopher K. Starr | Received 24 March 2024 | Accepted 20 May 2024 | Published 24 July 2024

https://zoobank.org/4E0C2EBF-229F-4294-881E-659A972E360B

Citation: Albacete S, Sancho G, Bosch J (2024) Use of a novel nesting material by the spider wasp *Dipogon variegatus* (Hymenoptera, Pompilidae). Journal of Hymenoptera Research 97: 541–544. https://doi.org/10.3897/jhr.97.123853

Abstract

A female spider wasp *Dipogon variegatus* was filmed stealing fragments of pollen-nectar provision from a solitary bee (*Osmia cornuta*) nest and using them for the construction of her nest. The female wasp applied the sticky fragments of the pollen-nectar provision to the outer surface of her closing nest plug, thus gluing together pieces of debris filling the nesting cavity. Previous descriptions of *D. variegatus* nests indicate that females of this species usually use spider silk to provide cohesion to the nest plug. Our observations provide an example of behavioural plasticity and innovation in the use of nesting materials. We describe the structure of the nest and the sequence of emergence of the progeny.

Keywords

Behavioural plasticity, nesting biology, *Osmia*, solitary bee

Most bees and wasps in the superfamilies Apoidea, Pompiloidea and Vespoidea are solitary and build nests in which they deposit food provisions for their progeny. Many of these species excavate their nests (usually underground), but some use a variety of pre-established cavities (O'Neill 2001; Danforth et al. 2019). Cavity-nesters typically incorporate external materials such as mud, pebbles, and various sorts of plant matter, including resin, pubescence, leaf cuttings and masticated leaf, to delimit cells and close their nests. The nesting materials used are species-specific. Most species use a single type of material, but some use a combination (Stephen et al. 1969; Iwata 1976). Notably among the latter

are *Dipogon* and other related genera of spider wasps (Pompilidae), which use a combination of materials of mineral, plant, and animal origin (Krombein 1967; Shimizu and Ishikawa 2002). Here we describe a nest of the spider wasp *Dipogon variegatus* (Linnaeus, 1758) and report on the collection and use of a novel nesting material by this species.

In May 2020 we observed a *D. variegatus* female nesting at a nesting station for mason bees (*Osmia* spp.) in Santa Caterina, Parc del Montgrí (Girona, NE Spain). The nesting station contained four nesting wooden blocks. Each block had 25 drilled holes into which paper straws (15 cm long, 8 mm diameter) were inserted. At the time of the observations, several *Osmia cornuta* (Latreille 1805) females were nesting in the wooden blocks. Like other solitary bees, *O. cornuta* stock their nests with provisions of pollen mixed with nectar.

On 5 May, we observed a *D. variegatus* female, entering an active *O. cornuta* nest and coming out with small pieces of provision between her mandibles (https://youtu.be/umbqd9v9n-s). The wasp female then walked to her nesting cavity and applied the stolen piece of provision to the plug of her nest (Fig. 1). This sequence of events was repeated at least 3 times.

On 7 May, the paper straw containing the *D. variegatus* nest was taken to the laboratory and on 17 May we analysed its contents. The spider provisions had completely been consumed and the wasp larvae had already spun their cocoons.

The nest occupied most of the length of the paper tube and had a loose structure, without clearly-defined cell partitions. It contained six cocoons longitudinally or obliquely arranged along the inner third of the paper straw (Fig. 2). The rest of the nest was filled with loose debris, including clumps of soil, pebbles, fragments of leafs and twigs, male pine cones and snail feces. The fragments of *O. cornuta* pollen-nectar provision were only found on the outer surface of the closing plug (Figs 1, 2).

Cocoons were 0.8–1 cm long and 2–3 mm wide and had two distinct layers. The inner layer consisted of a non-translucent whitish matrix with a shiny inner surface. The outer layer was a mesh of silk strands with debris attached to them (Fig. 3). We placed the cocoons individually in small plastic containers and kept them outdoors in a shaded area. Four adults emerged over a period of 4 days (a male from cocoon 5 on the

Figure 1. Plug of *Dipogon variegatus* nest (top left) plastered with pieces of orange-coloured pollen-nectar provision stolen from an *Osmia cornuta* nest. The two mud plugs at the bottom are *O. cornuta* nests.

Figure 2. *Dipogon variegatus* nest. The blue arrows indicate the location of the six cocoons, partially hidden by the debris. The red arrow indicates the fragments of the orange-coloured *Osmia cornuta* provision.

Figure 3. Close-up of the six cocoons after partial removal of the debris.

4th of June, two females from cocoons 1 and 3 on the 6th June, and a male from cocoon 6 on the 7th June). On July 15th we dissected the two remaining cocoons. Cocoon 2 contained a dead prepupa and cocoon 4 a dead male pupa.

Species of *Dipogon* and related genera are known to use a wide variety of materials to build their nests (Krombein 1967), including parts of dead insects and even entire ant corpses (Staab et al. 2014). To our knowledge, however, this is the first report of a solitary wasp using pollen as a nesting material. *D. variegatus* is known to use spider silk to bind together the debris filling its nest, especially at the entrance (Junco and Reyes 1951; Day 1988). The nest we examined had no traces of spider silk. The female we observed used a completely different kind of sticky material, the pollen-nectar provision from a solitary bee nest, to provide cohesion to the various fragments of debris conforming the nest plug. The nesting station created a situation in which a large number of uncapped active solitary bee nests were available in close vicinity of the wasp's nest. This scenario probably facilitated the encounter and use of pollen-nectar provisions by the *D. variegatus* female.

The use of novel nesting materials, sometimes of anthropic origin, has long been documented in birds and has been interpreted as a behavioural innovation in response to a new environmental situation (Hansell 2000). Although not so frequently, this phenomenon has also been reported in solitary wasps and bees. A potter wasp *Symmorphus murarius* (Linnaeus) female was found to cover the external surface of her mud nest plug with flakes of dry paint (Westrich 2020), and various leafcutting bee species, *Megachile* spp., have been reported to use plastic cuttings to line their nests (MacIvor and Moore 2013; Allasino et al. 2019; Wilson et al. 2020; Quintos-Andrade et al. 2021). Our study

provides another example of the capacity of solitary bees and wasps to modify an a priori well-established behaviour whenever the need and/or the opportunity arise.

We thank C. Schmid-Egger for kindly confirming the identification of the spider wasp. This study was supported by the Spanish MCINN project RTI2018-098399-B-I00.

References

Allasino ML, Marrero HJ, Dorado J, Torretta JP (2019) Scientific note: first global report of a bee nest built only with plastic. Apidologie 50: 230–233. https://doi.org/10.1007/s13592-019-00635-6

Danforth BN, Minckley RL, Neff JL, Fawcett F (2019) The Solitary Bees: Biology, Evolution, Conservation. Princeton University Press, Princeton, 472 pp. https://doi.org/10.1515/9780691189321

Day MC (1988) Spider wasps. Hymenoptera: Pompilidae. Royal Entomological Society of London, London. Handbooks for the Identification of British Insects 6, Part 4: 1–60.

Hansell MH (2000) Bird nests and construction behaviour. Cambridge University Press, Cambridge, 280 pp. https://doi.org/10.1017/CBO9781139106788

Iwata K (1976) Evolution of Instinct. Comparative Ethology of Hymenoptera. Amerind Publish, New Delhi, 535 pp.

Krombein KV (1967) Trap-nesting wasps and bees: life histories, nests, and associates. Smithsonian Institution Press, Washington DC, 570 pp. https://doi.org/10.5962/bhl.title.46295

MacIvor JS, Moore AE (2013) Bees collect polyurethane and polyethylene plastics as novel nest materials. Ecosphere 4(12): 1–6. https://doi.org/10.1890/ES13-00308.1

O'Neill KM (2001) Solitary Wasps: Natural History and Behavior. Cornell University Press, Ithaca, New York, 424 pp. https://doi.org/10.7591/9781501737367

Quintos-Andrade G, Torres F, Vivyan P (2021) Observación de *Megachile saulcyi* (Guérin-Méneville, 1844) (Hymenoptera: Megachilidae) utilizando plástico para la construcción de nidos en Chile. Revista Chilena de Entomología 47(2): 201–204. https://doi.org/10.35249/rche.47.2.21.04

Shimizu A, Ishikawa R (2002) Taxonomic studies on the Pompilidae occurring in Japan north of the Ryukyus: genus *Dipogon*, subgenus *Deuteragenia* (Hymenoptera) (Part 1). Entomological Science 5(2): 219–235.

Staab M, Ohl M, Zhu CD, Klein AM (2014) A unique nest-protection strategy in a new species of spider wasp. PLOS ONE 9(7): e101592. https://doi.org/10.1371/journal.pone.0101592

Stephen WP, Bohart GE, Torchio PF (1969) The biology and external morphology of bees. Agricultural Experiment Station, Oregon State University, Corvallis, 140 pp.

Westrich P (2020) Die Faltenwespe *Symmorphus murarius* (Linnaeus 1758) als Urheber blauer Nestverschlüsse (Hymenoptera: Vespidae). Eucera 14: 31–34.

Wilson JS, Jones SI, McCleve S, Carril OM (2020) Evidence of leaf-cutter bees using plastic flagging as nesting material. Matters 6(10): 1–3.

JHR 97: 545–589 (2024)
doi: 10.3897/jhr.97.127702
https://jhr.pensoft.net

RESEARCH ARTICLE

JOURNAL OF Hymenoptera RESEARCH
A peer-reviewed open-access journal
The International Society of Hymenopterists

The genus *Acerocephala* and observations of the life history of *Acerocephala hanuuanamu* sp. nov. (Hymenoptera, Cerocephalidae) and its bark beetle host on the island of O‘ahu, Hawai‘i

David N. Honsberger[1], Maya Honsberger[1], J. Hau‘oli Lorenzo-Elarco[2,3], Mark G. Wright[1]

1 *Department of Plant and Environmental Protection Sciences, University of Hawai‘i at Mānoa, 3050 Maile Way #310, Honolulu, HI 96822, USA* **2** *Ka Haka ‘Ula o Ke‘elikōlani, College of Hawaiian Language, University of Hawai‘i at Hilo, 200 W. Kāwili St., Hilo, HI 96720, Honolulu, USA* **3** *Honolulu Community College, 874 Dillingham Blvd., Honolulu, HI 96817, USA*

Corresponding author: David N. Honsberger (dnh8@hawaii.edu)

Academic editor: Ankita Gupta | Received 20 May 2024 | Accepted 10 July 2024 | Published 24 July 2024

https://zoobank.org/A94BB011-E39F-4B21-BB18-B2AF4D8AA2D1

Citation: Honsberger DN, Honsberger M, Lorenzo-Elarco JH, Wright MG (2024) The genus *Acerocephala* and observations of the life history of *Acerocephala hanuuanamu* sp. nov. (Hymenoptera, Cerocephalidae) and its bark beetle host on the island of O‘ahu, Hawai‘i. Journal of Hymenoptera Research 97: 545–589. https://doi.org/10.3897/jhr.97.127702

Abstract

The behavior of *Acerocephala hanuuanamu* **sp. nov.** found parasitizing *Cryphalus brasiliensis* under the surface of wood in *Ficus microcarpa* trees on the island of O‘ahu in Hawai‘i is deduced from observations in naturally occuring branches, and from direct observation using specially designed “phloem sandwich” observation chambers which consist of tree bark peeled through the phloem layer from freshly cut branches and sandwiched between a sheet of aluminum and a sheet of plexiglass. *Cryphalus brasiliensis* beetles, found living in large numbers in the phloem tissues in *F. microcarpa* trees, were collected and placed into these chambers. They tunneled into the wood and reproduced, producing an active colony of all life stages. *Acerocephala hanuuanamu* wasps were then placed into the system and their behavior observed. Typical behavior, aspects of which were recorded in video and still images, was as follows. A female *A. hanuuanamu* enters the tunnels of the bark beetles. She digs through the debris in the tunnels in a search for larvae and pupae. *Cryphalus brasiliensis* prepupae construct a hard pupal chamber around themselves before they pupate, and upon encountering a larva in the tunnels or the exterior of a pupal chamber with a pupa inside, she adeptly turns around in the tunnel to sting it, either inserting her ovipositor directly into the larva or by laboriously pushing it through the hard shell of the pupal chamber.

When finished stinging, she withdraws her ovipositor slowly and carefully, often extracting tissue from the beetle immature as a sheath around her ovipositor. This structure remains projecting from the larva or pupa, and then the wasp turns around and host feeds through this structure, in the case of a pupa at a substantial distance through the wall of the pupal chamber. Oviposition occurs on larval stages and pupal stages. The egg hatches and the larva develops as an ectoparasitoid on the beetle. When finished feeding, it detaches and pupates in the tunnel. Mating behavior is also described. In addition to *C. brasiliensis* in *F. microcarpa*, *A. hanuuanamu* was also observed attacking C*ryphalus mangiferae* in mango (*Mangifera indica*) branches. *Acerocephala ihulena* **sp. nov.** was also found on Oʻahu parasitizing *Eidophelus pacificus* in hau (*Hibiscus tiliaceus*) branches, and is described. The genus *Acerocephala* is revised given the perspective resulting from these two new species and aspects of functional morphology observed in the behavioral studies, *Acerocephala indica* **comb. nov.** is transferred to the genus, and a key to the genus is provided.

Keywords
Cerocephalinae, cryptoparasitoids, functional morphology, observation chamber, parasitoids

Introduction

The behavior and life history of insects that live inside wood or other plant parts can be difficult to observe. Mechanically opening up the plant material usually results in disrupting many of its inhabitants and their scattering, and it can be difficult to deduce their behavior prior to disruption. Simply placing the arthropods themselves or opened plant parts in a container for observation alters the environment substantially, and it can be unreliable to connect observed behavior in such circumstances with natural behavior. In this study we report observations of the behavior of a new species of cryptoparasitic wasp in tunnels constructed by its host beetles in an observation chamber as a semi-realistic representation of the environment in which we have found this species naturally.

This study is far from the only attempt at documenting the behavior of bark beetles and their natural enemies in concealed habitats. There is a history of making observation systems similar to the one constructed and used in this study, called "phloem sandwiches," which are variations on the idea of compressing natural wood or artificial diet between two hard sheets, at least one of which is clear to permit observation of its inhabitants (Beanlands 1966; Gouger et al. 1975; Nagel and Fitzgerald 1975; Kinn and Miller 1981; Salom et al. 1986; Grosman et al. 1992; Taylor et al. 1992; Aflitto et al. 2014; Sharma et al. 2016; Vega et al. 2017). These methods create an environment where wood boring beetles are able to construct their own tunnels and behavior within the tunnels can be observed. The environment in such systems is, however, still somewhat manipulated and not totally consistent with systems encountered in nature. In recent years, observations of wood boring insects in truly natural situations have also been successfully attempted. Alba-Alejandre et al. (2018) used a series of micro-CT scans to track the lives of coffee berry borer beetles, *Hypothenemus hampei* (Ferrari, 1867), inside coffee berries. Rezende et al. (2019) also used x-ray radiographs to track the movements of a thrips species thought to attack the coffee berry borer inside coffee

berries. These methods produced clear records of the biology and behavior of these insects, but only in static images.

This study focuses on *A. hanuuanamu* sp. nov. (Hymenoptera: Cerocephalidae) found attacking *Cryphalus brasiliensis* Schedl, 1976 (Coleoptera: Curculionidae: Scolytinae) on *Ficus microcarpa* L.f. trees on the island of Oʻahu in Hawaiʻi. In this study we reared *C. brasiliensis* in phloem sandwiches until overlapping generations composed of all life stages were present, then introduced the wasps and studied and recorded their behavior.

The discovery of this and another species results in perspective that allows for a revision of the genus *Acerocephala* Gahan. Cerocephalinae was first described by Gahan (1946) as a subfamily of Pteromalidae, *Acerocephala* described as part of this subfamily and two species included, *A. atroviolacea* and *A. aenigma*. The subfamily was later revised by Hedqvist (1969). Bouček (1988) added a third species to *Acerocephala*, *A. pacifica*, but stated that it was of uncertain generic identity, appearing substantially different from the other two previously described species which are morphologically very close. Cerocephalinae was then raised to the family level, as Cerocephalidae, by Burks et al. (2022). A key to genera of Cerocephalidae is provided by Bläser et al. (2015). All Cerocephalidae with known biological information are parasitoids of beetles in cryptic habitats (Bouček 1988).

Methods

Species descriptions

Specimens collected from wood and other plant parts were examined and photographed using a Leica MZ16 stereomicroscope or Macropod Pro imaging system. Specimens were also dissected, examined, and photographed using an Olympus CX31 compound microscope. Terminology relating to morphological characters follows Gibson (1997).

Morphometrics were measured as shown in Fig. 1, morphometrics of the head all measured in full face view or in lateral view, whichever was less obstructed by the antennae, except hea.l which was measured in lateral view. Acronyms in Fig. 1 and descriptions of the measurements, following Klimmek and Baur (2018), are as follows:

vac.l Full length of head; longitudinal line even with posterior of vertex to anterolateral corner of face (excludes mandibles).

vol.l Vertex-ocular line; longitudinal line even with posterior of vertex to even with top of compound eye.

vey.l Length of vertex to bottom of eye; longitudinal line even with vertex to even with bottom of compound eye.

vsc.l Length of vertex to scrobes; longitudinal line even with vertex to even with top of scrobal depression.

vto.l Length of vertex to toruli; longitudinal line even with vertex to even with center of toruli

eye.h Height of eye; posterior margin to anterior margin of compound eye.

mdb.l Length of mandible; straight line distance between protruding lateral corner at base of mandible and tip of mandible.

hea.b Breadth of head; maximum width of head including eyes

eye.d Eye distance; minimum distance between compound eyes on front of face

hac.d Width of head at anterolateral corner; distance between anterolateral corners of face.

msp.l Malar space; anterior margin of compound eye to anterolateral corner of face

wot.l Width of ocellar triangle; distance between outer margins of posterior ocelli.

pol.l Posterior ocellar line; shortest distance between inner margins of posterior ocelli.

ool.l Ocellar-ocular line; shortest distance from margin of posterior ocellus to margin of compound eye.

fcc.l Length of facial concavity; length of mesal line from even with anteriolateral corners of face to anterior of declivitous region comprising front of face, at posterior margin of projected clypeus.

cly.l Length of clypeal projection; length from anterior reach of clypeal projection to its base at the declivitous region at front of face.

hea.l Thickness of head; in lateral view, thickest part of head perpendicular to general plane of face and ventral surface of the head, typically at the level of the compound eyes for the species described.

prn.l Length of pronotum; base of pronotum on dorsomedian line to occipital foramen.

prn.b Breadth of pronotum; maximum width of pronotum measured in dorsal view.

msc.b Breadth of mesoscutum; width of mesoscutum just anterior of tegulae, measured in dorsal view.

tsa.l Length of transscutal articulation; in dorsal view, distance between intersections of transscutal articulation and axillar carina.

tsm.l Medial region of transscutal articulation; distance between where scutoscutellar lines join with transscutal articulation.

sct.l Length of scutellum; along median line, transscutal articulation to apex of scutellum and frenum.

mtn.l Length of metanotum; in dorsal view, distance along median line from apex of frenum to apex of metanotum.

ppd.l Length of propodeal disk; in dorsal view, distance along median line from metanotum to even with apex of propodeum.

pps.d Width of propodeal disk; in dorsal view, distance between propodeal spiracles.

gso.l Length of gaster excluding ovipositor; apex of petiole to apex of metasoma not including ovipositor or ovipositor sheaths.

ovi.l Length of ovipositor; apex of metasoma not including ovipositor or ovipositor sheaths, to apex of ovipositor or ovipositor sheaths.

Body length was obtained by adding the length of the head from the anterolatertal corner of the face to the occipital foramen, the occipital foramen to the anterior of the tegula, the anterior of the tegula to the petiole, and the petiole to the apex of the abdomen.

Morphometric measurements are reported in Suppl. materials 1, 2.

Repositories

Specimens are deposited in the following museums:

UHIM University of Hawai'i Insect Museum, Honolulu, Hawai'i, USA
BPBM Bernice Pauahi Bishop Museum, Honolulu, Hawai'i, USA
NMNH Smithsonian National Museum of Natural History, Washington DC, USA

"Phloem sandwich" observation chambers

(Fig. 10c, d)

An apparatus was constructed for the purpose of observing the parasitoids and their hosts in an environment resembling the below-bark environment in which they naturally occur (Fig. 10c, d). These observation chambers, a variation on the idea of a "phloem sandwich," consist of thin sheets of host wood; bark peeled from a branch through the phloem or cambium layer, sandwiched between a plexiglass sheet and an aluminum sheet. Adult *C. brasiliensis* were introduced to the wood through holes in the plexiglass, and if the conditions were appropriate, they would then tunnel into the wood and lay eggs. When the resulting larvae were at a stage suitable for parasitization, and as the colony developed further, *A. hanuuanamu* sp. nov. adults were introduced into the environment and their behavior was observed. The *C. brasiliensis* beetles this wasp uses as a host live typically in the thin layer of wood straddling the cambium, so a two-dimensional representation of their environment such as used here is likely a reasonably accurate representation of their actual habitat. Videos of behavior were recorded using a Dino-Lite Edge Digital Microscope and photos were taken using either the same Dino-Lite Edge or a Canon DLSR camera with a macro lens.

Construction of observation chambers and initiation of beetle colonies within them

The "phloem sandwich" style observation chambers used in this study are shown in Fig. 10c–f. The bottom layer of the sandwich is a 9.0 cm square of 1/16 inch (approximately 1.6 mm) sheet aluminum. Above it is a spacer made from a 9.0 cm square of 1/16 inch sheet aluminum with a rectangular hole 5.1 × 6.3 cm cut out of the middle. The top of the sandwich is a 9.0 cm square sheet of plexiglass. Holes were drilled at each corner through all three sheets, and 1/4 inch (approximately 6.35 mm) bolts were used to clamp the sheets together with a piece of host wood in the middle. Two additional small holes were drilled through the plexiglass to introduce beetles to the

chamber. This thickness of aluminum was chosen for the separator layer because it is slightly larger than the width of the *C. brasiliensis* beetles, which assured that beetles could move through the apparatus. Because the beetles were most interested in the phloem and cambium layer facing the plexiglass, they tended to make their tunnels up against the plexiglass and the full width of the tunnels were usually visible through it.

Using a knife and a chisel, *F. microcarpa* bark was carefully peeled off a branch down to the xylem layer. Branches with bark just slightly thicker than the 1/16 inch separator were chosen so the wood would be compressed tightly between the top and bottom of the sandwich, accounting for slight shrinkage when drying. The resulting sheets of bark were cut into pieces approximately 4.3 cm by 5.5 cm so that when placed in the aluminum forms there would be space for the beetles to travel around the perimeter. The freshly peeled bark was clamped between two ¾ inch × 5 ½ inch (1.9 cm × 14 cm) cedar boards with small holes drilled in them for airflow and left to dry for a few days. The wood, still clamped between the two cedar boards, was then autoclaved. This process is similar to steam bending wood, and as such, the bark would maintain its flat shape when the boards were unclamped and the wood was removed. The aluminum, nuts, bolts, and washers were also autoclaved, and the plexiglass was soaked and cleaned with a 70% ethanol solution before assembly. The parts were assembled quickly under a laminar flow hood to limit contamination. Parafilm or hot glue was used to seal any imperfections in the edges of the sandwich.

The correct stage of decay and water content of the wood is important for the beetles. The wood had been left to age and dry for a few days when clamped between the cedar boards, and was then reinfused with water during the autoclave treatment. After the boxes were assembled, the beetles were entered into them through the two small holes in the plexiglass sheets and then the holes were covered with tape. The beetles would often remain outside the wood for some time. The two larger holes in the aluminum on the bottom side of the boxes were initially left uncovered, resulting in gradual drying of the wood. Beetles entering the wood was assumed to indicate that the water content and age of the wood was appropriate for them, and when this was observed, tape was stuck over the holes to prevent further drying. If the wood seemed to get too dry, the tape was removed and a few drops of water added into the holes to absorb into the wood. Using these methods, approximately 10 separate colonies were produced. The apparatus was illuminated for observation using natural sunlight or fiber optic gooseneck microscope lights powered by a halogen lamp.

Observation in naturally infested wood

Ficus microcarpa branches containing bark beetles were observed in place by peeling off bark from branches still attached to the tree, or by cutting branches and dissecting them. To facilitate locating wood at a desired stage of decay, fresh branches were also cut, suspended off the tree, and later dissected. All such observations were taken from wood on a large *F. microcarpa* tree located in an unmaintained area of the campus of the University of Hawai'i at Mānoa at (21.2954°N, 157.8145°W, 15 m) (Fig. 10a),

or from other trees in the immediate vicinity. Additional host records were found by dissecting wood from a variety of tree species and locations as a part of a larger survey of bark beetle natural enemies on Oʻahu.

Results

Acerocephala Gahan, 1946

Redescription. Head subrectangular in face view, somewhat thin and elongate in side view, flattened dorsoventrally and not globose (vac.l/hea.l approximately 1.7 or greater). Anterolateral corner of head a distinct angle, sides of face either progressively widening to this corner or mildly curved mesally to reach it. Mandibles long and arcing (mdb.l/hea.b approximately 0.5 or greater), placed widely on face, their lateral corners at or nearly at anterolateral corners of face. Anterior of face a concave arc; clypeus, which has its base near the ventral side of this arc, may be visible in dorsal view projecting into the space between the mandibles. Compound eyes placed nearer back of head than front, so that vey.l/vac.l ≤ 0.5. Antennae inserted well anterior of compound eye, funicle with 5 or 6 segments in female. Scrobes deep and extend posteriorly well behind toruli. Scrobes separated by interantennal ridge that extends well behind the toruli to join with the upper face, the ridge flattened or mildly curved dorsally and protruding or not from plane of the face.

Forewing with or without callus on parastigma, but the callus, if present, without a tuft of setae. Wing membrane with slightly rippled texture and without setae on its surface; stigmal vein short, postmarginal vein short if present. Males of some species may be wingless.

Diagnosis and differential diagnosis. This genus can be distinguished within Cerocephalidae by the combination of elongate rectangular, thin head shape (vac.l/hea.l ≥ 1.7); anterolateral corner of face a distinct angle, and with long mandibles placed with their outer edges near the anterolateral corner of the face; antennae inserted distinctly anterior of compound eye; forewing without a tuft of thick setae on callus on the parastigma, or lacking a callus, and without setae extending from its membrane; clypeus may project into space between mandibles from near ventral side of arc that comprises the anterior of the face, dorsal plane of head lacking a distinct anterior projection into space between mandibles.

Within Cerocephalidae, this genus appears closest to *Choetospilisca* (Fig. 9), *Paralaesthia*, and *Muesbeckisia*. It can be distinguished from *Choetospilisca* by the elongate rectangular shape of the head in dorsal view and long arcing mandibles extending from just inside the anterolateral corner of face; and broad interantennal ridge joining to the plane of the upper face. (*Choetospilisca* with head more globose in side view; face broadly tapers anteriorly, and thick but shorter mandibles extending from well inside the lateral edge). The overall shape of the face is similar to *Paralaesthia*, but it can be

distinguished by the lack of a tuft of thick setae on the callus of the parastigma; at most a small projection of the clypeus into the space between the mandibles, which has its base on the ventral side of the arc that comprises the front of the face; scrobal grooves posterior to toruli deep and separated by a large, broad interantennal ridge connecting to the upper face; lack of a mesal groove on the upper face; funicle segments slightly nodose-bead like or transverse (*Paralaesthia* with thick setae emerging from the callus; lower face anteriorly extended into a large triangular region between the mandibles, its base extending from the dorsal plane of the face; a mesal groove running the length of the upper face; scrobes shallow and not extended greatly posterior to toruli, interantennal ridge small and similarly not of much consequence posterior to toruli; funicle segments elongate cylindrical). It can be distinguished from *Muesebeckisia* by the more elongate head shape and location of antennal insertion well below the anterior margin of the eyes, and broad interantennal ridge. (*Muesbeckisia* with head globose, eye reaching the anterior half of the face, and antennal insertion above anterior margin of eye).

Acerocephala indica comb. nov.

Choetospilisca indica Saraswat & Mukerjee, 1975

Remark. This species was only known from the holotype (female), slide mounted, from Yercaud, in the Eastern Ghats of Tamil Nadu, India. What appears to be the same species was found in the NMNH collection, a female and male point mounted with this collection data: "PUERTO RICO // Santa Isabel // 21-VIII-1991 // S. Medina-Gand //// ex mango // branch dying // of fire //// #91-9140 // Acerocephala // n. sp. // det. // E. Grissell 1991" (female) and "PUERTO RICO // Santa Isabel // 21-VIII-1991 // S. Medina-Gand //// ex mango // branch dying // of fire" (male). See Fig. 6 for photos, and key for distinguishing characters.

Acerocephala hanuuanamu Honsberger & Lorenzo-Elarco, sp. nov.

https://zoobank.org/9AD9CC44-408F-4BE6-AEF1-73F5C5626856
Figs 1–3, 10a

Diagnosis. Females of this species can be distinguished from other known *Acerocephala* by the antenna with the first four funicular segments transverse and of similar size and shape, followed by a larger and subcircular fifth segment and the clava; interantennal ridge flush with face, not elevated in lateral view, and only slightly widened anteriorly; scrobes reaching more than half the length of the head; submarginal and marginal veins of forewing join smoothly with no callus; clypeus, to its apex, fills the space between the mandibles when mandibles are closed. Males are similar to females in characters of the head with the exception of the antennae, so can be distinguished from other known species by these characters as well.

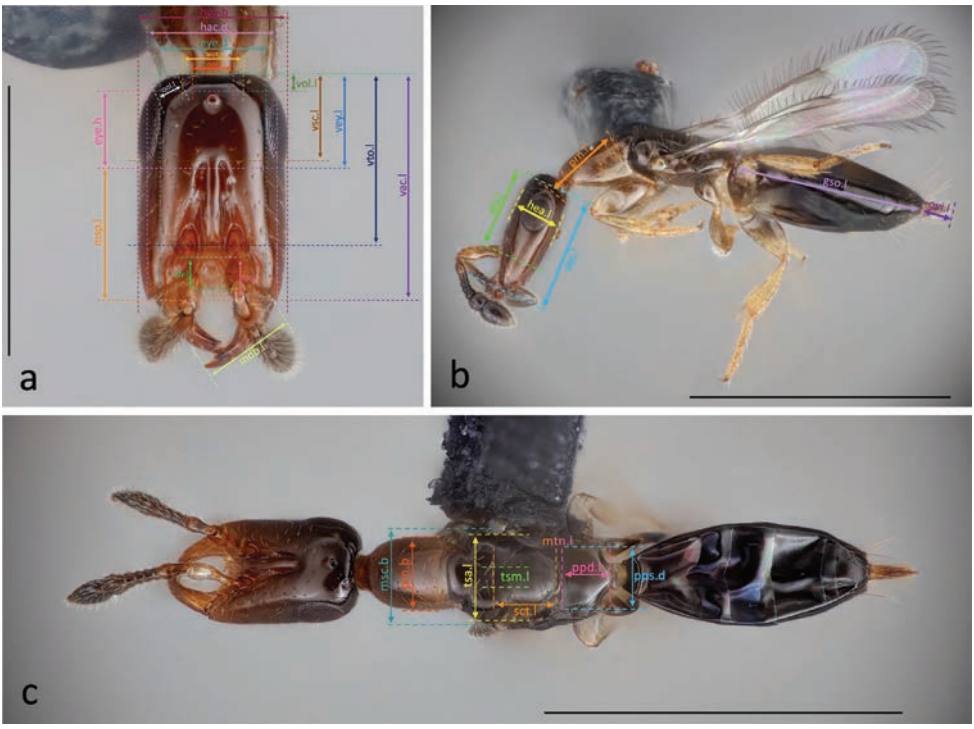

Figure 1. *Acerocephala hanuuanamu* sp. nov. (paratypes) showing morphometric measurements. Acronyms explained in text. Scale bars: 1 mm (**b, c**); 500 μm (**a**).

Differential diagnosis. Females are easily distinguished from *A. atroviolacea*, *A. aenigma*, and *A. pacifica* by the first four funicular segments much smaller and shorter than the fifth; overall gracility of the head and body; interantennal ridge not elevated from the face in lateral view (*A. atroviolacea*, *A. aenigma*, and *A. pacifica* with fifth funicular segment of similar size to preceding segments; body and head thicker and more robust; interantennal ridge elevated from the face in lateral view); and from *A. atroviolacea* and *A. aenigma* by lack of callus on the forewing (*A. atroviolacea* and *A. aenigma* with callus present).

A. hanuuanamu is closest to *A. ihulena* sp. nov. and *A. indica*. Females can be distinguished from *A. ihulena* and *A. indica* by interantennal ridge not elevated from the face in lateral view; first four funicular segments of similar size and distinctly smaller than the fifth; ovipositor sheaths only slightly exerted, extending less than 1/3 the length of the gaster; scutoscutellar grooves foveolate and meeting the transscutal articulation lateral of medial line (*A. ihulena* and *A. indica* with interantennal ridge elevated from the face in lateral view; fourth funicular segment slightly but distinctly larger than the first three; ovipositor sheaths distinctly exerted from the gaster, near half its length, dark brown at the apex and lighter near the base; scutoscutellar grooves a subcircular sulcus that reach the transscutal articulation mesally).

Description. Female (Figs 1, 2a–d, 3a–c, e–j, 10a; morphometric measurements in Suppl. material 1). ***Length*****:** Variable, depending on size of host. On *C. brasiliensis* individuals range from 1.18–2.31 mm (Holotype 1.96 mm), the largest individual collected was 2.50 mm from *C. mangiferae*, a slightly larger beetle.

Coloration**:** Head brown; slightly lighter anteriorly in lower face, basal part of mandibles, and scape and pedicel. Mesosoma brown, prothorax and apex of propodeum often somewhat lighter. Petiole yellow. Gaster dark brown except basoventrally where it is light brown, and the ovipositor sheaths which are light brown. Legs yellow-brown, pro- and metacoxae somewhat lighter in color than their respective tibiae.

Head**:** Head subrectangular in full face view; more or less parallel sided, subtly widest across eyes, of nearly equal width at about half its length, and tapers very slightly to the anterolateral corner. Anterior of head, excluding the mandibles and projected clypeus, a strongly concave arc. Clypeus projected medially, subrectangular with slightly rounded base and longer than wide, to its apex occupies all the lateral space between the mandibles when mandibles are closed. Interantennal ridge flush with the face lateral of scrobes, not elevated dorsally from the face in lateral view; its anterior half, to about even with where the scrobes narrow, laterally carinate, dorsally smooth and slightly convex between the carinae; posterior to this non-carinate, more narrowly and evenly rounded, along the median line joining smoothly with the upper face. Lateral margins of scrobal depression just above the toruli extend approximately half the width of the face, lateral margins distinctly taper and at about half the length of the interantennal ridge where its carina ends; anterior of this the lateral margins are lightly carinate and the depressions deeper; posterior to this with rounded margins and the depressions become progressively narrower and shallow before they join with the upper face. Mandibles long and curved with three apical teeth; dorsal and middle tooth of a similar conical shape but with a deep groove between them, middle tooth projecting slightly more than dorsal tooth, ventral tooth projecting about twice this much relative to the middle tooth. Bottom of toruli adjacent to the dorsoventrally inclined arc that comprises the anterior of the face. Occipital carina just posterior to posterior ocelli, subcircular. Dorsal side of the face with smooth and shiny texture and with sparse setae, the setae increase slightly in length and density anteriorly, more densely placed short setae around the occipital carina. Ventral side of head generally flat with some longer setae posteriorly, median suture extends longitudinally from the mouthparts to the occipital carina, basal area near the suture indented slightly for about 2/5 the length of the head, the cuticle in this indent with reticulate texture, cuticle on ventral side of face otherwise smooth and shiny.

Antennal flagellum composed of 5 funicular segments and a subconical clava. First four funicular segments transverse cylindrical and of similar size and shape, 5th funicular segment subspherical and larger than the first four, clava is approximately 1.4 times as long as the first four flagellar segments, rounded subconical. All antennal segments with thin setae projecting at approximately 45 degrees, the first four funicular

Figure 2. *Acerocephala hanuuanamu* sp. nov. holotype ♀ (**a–d**) and allotype ♂ (**e–h**) **a, e** side view **b, f** head **c, g** anterior view of head showing mandibles **d, h** dorsal view. Scale bars: 1 mm (**a, d, e, h**); 250 μm (**b, c, f, g**).

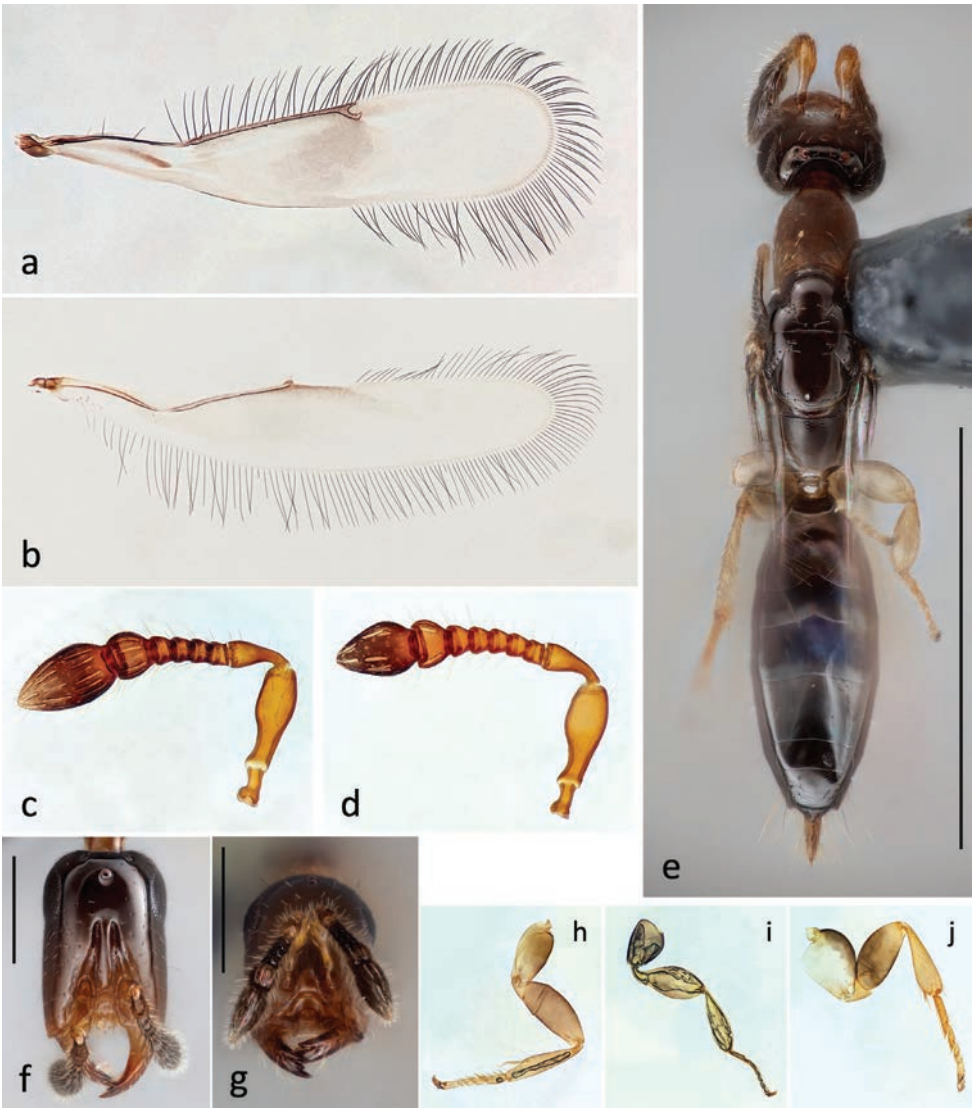

Figure 3. *Acerocephala hanuuanamu* sp. nov. **a** forewing ♀ **b** hindwing ♀ **c** antenna ♀ **d** antenna ♂ **e** dorsal view ♀ (paratype) **f** head ♀ (paratype) **g** anterior view of head showing mandibles ♀ (paratype) **h** foreleg ♀ **i** midleg ♀ **j** hindleg ♀. Scale bars: 1 mm (**e**); 250 μm (**f, g**).

segments with a single whorl of setae of length slightly less than the width of the segments, setae becoming progressively shorter towards the apex of the antenna. The 5th funicular segment with MPS and the clava with three whorls of MPS; the first four flagellar segments lack MPS. Mean length/mean width (Ratio) of antennal segments, length and width measured relative to length of F1 (n = 12): Scape 6.0/2.3 (2.7) ; Pedicel 3.4/1.7 (2.0) ; F1 1.0/1.5 (0.7) ; F2 0.9/1.5 (0.6) ; F3 1.0/1.6 (0.6) ; F4 1.1/1.8 (0.6) ; F5 2.5/3.0 (0.8) ; Clava 6.5/4.1 (1.6).

***Mesosoma*:** Long prothorax articulates with mesothorax, rotating from in line with the rest of the mesosoma to approximately 110 degrees. A light longitudinal carina present laterally on pronotal neck, pronotum otherwise smooth, lacking a transverse pronotal carina. Pronotal neck and collar smooth, collar with scattered mesal pointing setae except on its dorsal surface near the medial line where there are no setae. In dorsal view, pronotum very slightly widest near its middle, but at its widest distinctly narrower than the mesonotum. Transscutal articulation deep and well defined, straight until the lateral section where the sclerites incline vertically. Notauli and scutoscutellar suture both foveolate and visible relative to the otherwise smooth and shiny mesonotum, marked by punctures and a mild sulcus, setae on either side of the sutures, the notauli deepening anteriorly and giving the mesonotum a shouldered appearance. Lateral of the median line, notaulus and scutoscutellar suture meet the transscutal articulation at approximately a 45 degree angle and at approximately the same point, so the medial lobe of the mesoscutum and the scutellum run up against each other for a distance (see morphometric measurements). In dorsal view, scutoscutellar sutures are fairly straight until they meet the transscutal articulation, notauli are mildly curved. Posterior margin of scutellum evenly convex. Mesonotum smooth and glassy, free of setae except on either side of the notauli and on either side of the scutoscutellar suture, a few scattered setae on the axillae, and near posterior margin of the scutellum. Metanotum visible behind scutellum. Propodeum slightly wrinkled at its anterior margin and on the callus anterior of the spiracle, otherwise smooth and glassy, flat longitudinally and lightly rounded transversely. Propodeal spiracle slightly recessed in a small depression, paraspiracular sulcus a very slight and smoothly rounded depression continuing from the spiracular depression posteromedially and gradually fading. Sides of the propodeum slightly tapering posteriorly until above attachment of the rear coxae, where they abruptly taper to about 60 degrees from the anteroventral line, then curve to be slightly more longitudinally oriented toward their apex at the nucha, top of petiolar insertion flush with dorsal surface of propodeum. Setae near the lateral margins of propodeum: on callus anterior of the spiracle, on lateral margin where callus meets the metapleuron, and just above where the propodeum accommodates the hind coxal foramen. Mesopleuron with light reticulate texture, mesepisternum with setae.

***Wings*:** Forewing: Length of marginal vein approximately 1.15 × length of submarginal vein. Short postmarginal vein extends to approximately even with the stigma or somewhat less. Stigmal vein projects from marginal vein at slightly less than 45 degrees and has a slight curve apically. Three dorsal setae on marginal vein, basal one small and inconspicuous. Marginal setae begin at the base of marginal vein and continue around apex of wing with approximately consistent length to trailing edge approximately even with stigmal vein, just apical of retinaculum. Parastigma not swollen, submarginal and marginal veins joining smoothly and unperturbed with no swollen area or change in pigmentation; lacking any sign of a tuft of setae on the parastigma. Membrane subhyaline with slightly rippled texture and without setae; basally to end of venation lightly infuscated, the area near and posterior to stigma most shaded.

Hindwing: Venation with a concavity at approximately half the distance from the base to the hamuli, venation hyaline at the culmination of this concavity; anterior

margin of wing membrane extends more or less straight in this region so at the apex of the concavity the venation reaches nearly ½ the distance to the posterior of the wing membrane. Venation ends at the hamuli but the very anterior of the membrane in line with venation remains somewhat pigmented beyond the hamuli, to approximately 2/3 the length of the wing. Marginal setae present from the end of this pigmented region around to base of trailing edge of wing, longest around trailing edge where they are approximately ¾ the maximum width of the wing.

***Legs*:** Fore and rear coxae globose, subequal in size and shape though the fore coxa hides somewhat under the pronotum. Femora also globose, slightly larger than their respective coxae in the front and mid, legs, subequal in the back leg. Tibiae of similar length to their respective femora, also globose apically, but narrower basally. In all legs, first tarsal segment longest, 2nd through 4th segments sequentially decrease in length; 5th segment not including the claw intermediate between 1st and 2nd in front and middle legs, subequal to 2nd in back legs. Protibial spur deviates from straight with a jog of shape similar to a logistic function, its base set back on the tibia and extending just past base of first tarsal segment, tibia beneath the spur with protibial comb. Midleg and back leg with narrower, straight protibial spur extending from near the apex of the segment. Fore and midleg with the two basal tarsi of each leg spinose, spines fading on the apical segments; hindleg with spines smaller except for those at the apex of the tarsal segments. Tibiae with narrow setae and no additional spines, except for the very apex of the back leg.

***Metasoma*:** Petiole somewhat globose-vase shaped, the widest point marked by one or two lateral setae on a small knob; somewhat flat dorsally, overall of subequal length and width. First and second gastral segments emarginate medially, subsequent segments with straight posterior margin. Gaster in living individuals expands and contracts during feeding, use of the ovipositor, and movement; therefore the following applies to dried individuals. 1st and 4th gastral tergites longest, 3rd slightly shorter, 2nd substantially shorter than 3rd; 5th very short; 6th subequal in length to 2nd. Gaster not heavily sclerotized, shrivels slightly on drying. Gaster with few, small setae on first five segments, 6th with many setae, some short, some longer than the exserted ovipositor sheath, but rarely reaching past it due to their angle. Ovipositor sheaths also setose, and are slightly exserted; ovipositor thin and needle-like.

Male (Figs 2e–h, 3d; morphometric measurements in Suppl. material 1). ***Length*:** Typically, but not always, smaller than females developing in the same colony of hosts. As with the female, size depends on the size of the host, but the smallest individuals are nearly always male. Very variable, from 0.83–1.65 mm (allotype 1.60 mm).

Similar to female except: Wingless. Antennae with 6 funicular segments, similar to that of female except that the four similarly shaped basal flagellar segments in the female are five in the male, the sixth larger and subcircular; clava with two whorls of MPS. Mean length/mean width (Ratio) of antennal segments, length and width measured relative to length of F1 (n = 7): Scape 6.5/2.4 (2.7) ; Pedicel 3.7/1.8 (2.1) ; F1 1.0/1.4 (0.7) ; F2 1.1/1.5 (0.8) ; F3 1.1/1.6 (0.7) ; F4 1.2/1.8 (0.7) ; F5 1.4/2.1 (0.7) ; F6 2.1/2.9 (0.7); Clava 5.3/3.7 (1.5). Ocelli absent and compound eye smaller than in female, morphometrics of face otherwise similar, mandibles similar. Posterior region

of pronotum tapers slightly to fit around the narrower medial lobe of the mesoscutum. Notauli nearly meet on the medial line at the transscutal articulation, scutoscutellar suture meets transscutal articulation lateral to this, similar to the female. Pro- and mesoscutum smaller than in female, scutellum much shorter than in female, metanotum behind it appears in dorsal view nearly straight with nearly parallel anterior and posterior margins. Femora, tibiae, and tarsal segments somewhat stouter than in female, but their relative lengths remain similar. Posterior margin of propodeal disk with scattered setae. Gaster shorter, apically truncated-looking in dry specimens.

Materials examined. ***Holotype*** (Fig. 2a–d): ♀; Hawaiian Islands, Oʻahu, Mānoa; 21.2946°N, 157.8136°W; 2.viii.2022; below bark of *Ficus microcarpa* branch (deposited in UHIM).

Allotype (Fig. 2e–h): ♂; Hawaiian Islands, Oʻahu, Mānoa; 21.2946°N, 157.8136°W; 2.viii.2022; below bark of *Ficus microcarpa* branch (UHIM).

***Paratypes*:** 65♀, 54♂. Hawaiian Islands, Oʻahu, Mānoa; 21.2946°N, 157.8136°W; 2.viii.2022; below bark of *Ficus microcarpa* branches; 57♀, 52♂ (19♀, 18♂ UHIM; 19♀, 17♂ BPBM; 19♀, 18♂ NMNH) • Hawaiian Islands, Oʻahu, Mānoa; 21.3060°N, 157.8092°W; 15.xii.2020; below bark of *Artocarpus altilis* branch; 2 adult ♀ and 1 pupa glued to point (UHIM) • Hawaiian Islands, Oʻahu, Mānoa; 21.5604°N, 157.8765°W; 31.i.2020; below bark of *Mangifera indica* branches; 3♀, 1♂ (1♀, 1♂ UHIM; 1♀ BPBM; 1♀ NMNH) • Hawaiian Islands, Oʻahu, Mānoa; 21.2954°N, 157.8145°W; 27.vii.2018; below bark of *Ficus microcarpa* branches; 3♀, 1♂ (1♀, 1♂ UHIM; 1♀ BPBM; 1♀ NMNH).

Other materials examined. Hawaiian Islands, Oʻahu, Mānoa; 21.2952°N, 157.8141°W; 3.xii.2020; below bark of *Trema orientalis* branch; wasp ex tunnels inhabited by the beetle; 1 ♀ and 1 *C. brasiliensis* adult glued to point (UHIM).

Etymology. The species name is Hawaiian, hanuʻuanamū (lit., flowing between caves of the insect). This species constructs a feeding tube to host-feed through the walls of the pupation chamber constructed by its host. Hanuʻu represents the continuous action of ebb, flow, and exchange of fluid through the connection bridging the cavern (ana) and the wasp, and ana mū recognize the system of tunnels and caverns constructed by the host insect (mū), reminiscent of lava chambers.

Known distribution. This species is known from the island of Oʻahu in Hawaiʻi, where it is likely adventive.

Known hosts. *Cryphalus* spp., including *C. brasiliensis* and *C. mangiferae*.

Acerocephala ihulena Honsberger & Lorenzo-Elarco, sp. nov.

https://zoobank.org/4C02F85F-8AA5-4847-95F6-01C3C4235F5A
Figs 4, 5

Diagnosis. Females of this species can be distinguished from other known *Acerocephala* by the antenna with the first three funicular segments transverse and of similar size and shape, the fourth segment slightly but distinctly larger, the fifth larger and subcircular;

internantennal ridge elongate-oval in dorsal view, elevated from face in lateral view; submarginal and marginal veins of forewing join smoothly with no callus; clypeus projected between the mandibles subrectangular and apically mildly bidentate; ovipositor sheaths exerted from gaster, approximately half its length, apically dark brown and basally lighter.

Differential diagnosis. Females are easily distinguished from *A. atroviolacea*, *A. aenigma*, and *A. pacifica* by the first four funicular segments transverse and much smaller and shorter than the fifth; the overall gracility of the head and body; and the elongate-oval shape of the interantennal ridge (*A. atroviolacea*, *A. aenigma*, and *A. pacifica* with fifth funicular segment of similar size to preceding segments; body and head thicker and more robust; interantennal ridge in dorsal view triangular or wedge shaped); and from *A. atroviolacea* and *A. aenigma* by lack of callus on the forewing (*A. atroviolacea* and *A. aenigma* with callus present).

Females can be distinguished from *A. hanuuanamu* by the fourth funicular segment slightly but distinctly larger than the first three; interantennal ridge elevated from the plane of the face; ovipositor exerted from the gaster approximately half its length, dark brown apically and lighter basally; scutoscutellar lines sulcate and form a consistent arc to meet the transscutal articulation along the mesal line (*A. hanuuanamu* with the fourth funicular segment indistinctly larger than the first three; interantennal ridge flush with the face lateral of the scrobes; ovipositor only slightly exerted from the gaster; scutoscutellar lines foveolate and meet the transscutal articulation lateral of the mesal line).

Females can be distinguished from *A. indica* by the shape of the interantennal ridge, in *A. ihulena* elongate-oval and reminiscent of the nose of a proboscis monkey (*A. indica* with interantennal ridge blunt wedge-like, widening posteriorly with somewhat straight margins); by the anterior of the face excluding the clypeus distinctly concave in *A. indica* (nearly straight between the anterolatral corners of the face in *A. ihulena*); and by the stigmal vein of the forewing, *A. ihulena* with the stigmal vein very short, only incompletely separating the stigma from the marginal/postmarginal veins (*A. indica* with stigmal vein short, but a distinct vein-like constriction between the marginal/postmarginal vein and the stigma).

Description. Female (Figs 4a–d, 5a–g; morphometric measurements in Suppl. material 2). ***Length*:** Can be expected to vary depending on the size of the host; the 7 individuals collected range from 1.52–1.84 mm (Holotype 1.80 mm).

***Coloration*:** Head brown, slightly lighter anteriorly in lower face, basal part of mandibles, and scape. Mesosoma orange, prothorax somewhat lighter. Gaster dark brown, slightly lighter basally, and ovipositor sheaths yellow in their basal 2/3 and brown apically. Legs yellow, pro- and metacoxae sometimes nearly translucent.

***Head*:** Head subrectangular in full face view; more or less parallel sided, but subtly widest across eyes, of nearly equal width at about three quarters its length, and tapers slightly to the anterolateral corner; vertex between posterior ocelli nearly straight, broadly rounded laterally to eyes. Anterior of head excluding mandibles and projected clypeus a mildly concave arc. Clypeus projected medially, somewhat square in shape and mildly bidentate, occupies about half the lateral space between the mandibles when mandibles are closed. Interantennal ridge widest at about half its length, shape elongate-

Figure 4. *Acerocephala ihulena* sp. nov. holotype ♀ (**a–d**) and allotype ♂ (**e–h**) **a, e** side view **b, f** head **c, g** anterior view of head showing mandibles **d, h** dorsal view. Scale bars: 1 mm (**a, d**); 500 μm (**e, h**); 250 μm (**b, c, f, g**).

oval, similar to that of a proboscis monkey; carinate laterally, medially between the carinae slightly convexely rounded with light longitudinal striations; slightly elevated from the level of the face lateral of scrobes, in lateral view of head extends tangential to curve of face at its thickest point disregarding the interantennal ridge, and continues

Figure 5. *Acerocephala ihulena* sp. nov. **a** head (paratype ♀) **b** antenna (♀) **c** side view (paratype ♀) **d** forewing (♀) **e** hindwing (♀) **f** dorsal view (paratype ♀) **g** anterior view of head showing mandibles (paratype ♀) **h** head (paratype ♂) **i** anterior view of head showing mandibles (paratype ♂) **j** dorsal view (paratype ♂). Scale bars: 1 mm (**c, f**); 250 μm (**a, g–j**).

straight more or less parallel with ventral profile of the head, giving the head approximately equal thickness over its length while the face lateral of scrobes thins towards the mandibles. Interantennal ridge begins a gradual descent to the mouthparts posterior to the toruli, and at about even with middle of the toruli, somewhat abruptly curves downward, to connect with the projection of the clypeus, at an approximate 60 degree angle to the overall plane of its dorsal surface. Lateral margins of scrobal depression a consistent arc, narrowing posteriorly, and slightly carinate; scrobes decrease in depth posteriorly. Mandibles long and curved with three apical teeth; dorsal and middle tooth of a similar conical shape but with a deep groove between them, middle tooth projecting only very slightly more than dorsal tooth, ventral tooth joined to middle tooth more closely and projecting a short way beyond it. Occipital carina just posterior to posterior ocelli, subcircular. Texture smooth and shiny with sparse setae, on the dorsal

side setae concentrated on the gena anterior of the compound eyes and on the face just above the scrobes, a few longer setae dorsally around the occipital carina, ventral side of head posterior of the indented region also with longer setae. Bottom of toruli adjacent to the dorsoventrally inclined arc that comprises the anterior of the face. Ventral side of head generally flat, median suture extends longitudinally from the mouthparts to the occipital carina, basal area near the suture indented slightly for about 2/5 the length of the head, cuticle posterior of this indent of rougher texture than cuticle within it.

Antennal flagellum composed of 5 funicular segments and a subconical clava. First three funicular segments transverse cylindrical, progressively becoming subtly conical, and of similar size, 4th is slightly rounded and slightly but distinctly larger than first three, 5th is subspherical and larger than the 4th; clava is approximately 1.4 times as long as the first four flagellar segments together, rounded subconical. All antennal segments with thin setae projecting at approximately 45 degrees, first four funicular segments each with a single whorl of longer setae of length subequal to the width of the segments, setae becoming progressively shorter towards apex of antenna. 5th funicular segment and claval segments with MPS, clava with 3 whorls of MPS, first four flagellar segments lacking MPS. Mean length/mean width (Ratio) of antennal segments, length and width measured relative to length of F1 (n = 7): Scape 6.8/1.7 (4.0); Pedicel 2.9/1.4 (2.0); F1 1.0/1.2 (0.8); F2 0.9/1.2 (0.7); F3 1.0/1.4 (0.7); F4 1.3/1.8 (0.7); F5 2.1/2.6 (0.8); Clava 5.8/3.2 (1.8).

***Mesosoma*:** Long prothorax articulates with mesothorax. A light longitudinal carina present laterally on pronotal neck, pronotum otherwise smooth, neck distinct from collar but lacking transverse pronotal carina. Pronotal neck with light transversely ridged texture, and collar smooth; collar with scattered mesal pointing setae except on its dorsal surface near the median line where there are no setae; one or two longer setae on its ventral side, of similar length to those on the ventral side of the head. Pronotum distinctly widest at its middle, but at its widest distinctly narrower than mesonotum in dorsal view, at its maximum width a little less than 3/4 the width of mesoscutum not including the tegulae. Transscutal articulation straight, inclines to vertical at its lateral edges. Notauli and scutoscutellar suture both well defined sulci; mesoscutum and scutellum lacking setae medially, a few setae present near the notauli, scutoscutellar suture, and transcutal articulation. On each side of the median line, notaulus curves to meet the transscutal articulation in the vicinity of 60 degrees, and scutoscutellar suture arcs to meet the transscutal articulation along the medial line, so medial lobe of mesoscutum runs up against transscutal articulation but scutellum is separated from it by the axillae except at its middle point (see morphometric measurements). Posterior margin of scutellum evenly convex. Mesonotum smooth and glassy, free of setae except on either side of the notauli and on either side of the scutoscutellar suture, a few scattered setae on the axillae and near the posterior margin of the scutellum. Metanotum visible behind scutellum. Propodeum slightly wrinkled at its anterior margin but otherwise smooth and glassy, flat longitudinally and lightly rounded transversely. Propodeal spiracle slightly recessed in a small depression. Sides of propodeum slightly tapering posteriorly until above the attachment of the rear coxae, where its dorsal margin bends to

run nearly transversely except for at the nucha which is bumped out posteriorly, top of petiolar insertion flush with disk of propodeum. Setae near lateral margins of the propodeum: on callus anterior of the spiracle, and on lateral margin where the callus meets the metapleuron. Mesopleuron with light reticulate texture, mesepisternum with setae.

***Wings*:** Forewing: Length of marginal vein approximately 1.1 × length of submarginal vein. Stigmal vein very short, hardly separating stigma from marginal vein, postmarginal vein also very short or absent, appearing together with stigmal vein as a slightly thickened apex of the marginal vein. Marginal vein without dorsal setae. Marginal setae begin at base of marginal vein and continue around apex of the wing with approximately consistent length to trailing edge approximately even with stigmal vein, just apical of the retinaculum. Parastigma not swollen, submarginal and marginal veins joining smoothly and unperturbed with no swollen area or change in pigmentation; lack of any sign of a tuft of setae on the parastigma. Membrane subhyaline with a slightly rippled texture and without setae.

Hindwing: Venation with a concavity at approximately half the distance from the base to the hamuli; anterior margin of wing membrane extends more or less straight in this region so at the apex of the concavity the venation reaches nearly ½ the distance to the posterior of the wing membrane. Venation ends at hamuli but the very anterior of the membrane in line with venation remains somewhat pigmented beyond the hamuli, to approximately 2/3 the length of the wing. Marginal setae present from the end of this pigmented region around to the base of the trailing edge of the wing, longest around trailing edge and posterior margin where they are approximately 3/4 the maximum width of the wing.

***Legs*:** Fore and rear coxae globose, rear coxa larger than fore coxa, mid coxa smallest. Femora also globose, slightly larger than their respective coxae in front and mid legs, of similar size but more elongate in back legs. Tibiae of similar length to their respective femora, also globose apically, but narrower basally. In all legs, first tarsal segment longest, 2nd through 4th segments sequentially decrease in length; 5th segment not including the claw subequal to 1st in front legs, subequal to the 2nd in mid and back legs. Protibial spur deviates from straight with a jog of shape similar to a logistic function, its base set back on tibia and extending near middle of the first tarsal segment, tibia beneath spur with a protibial comb.

***Metasoma*:** Petiole somewhat narrower medially than basally or apically, one or two lateral setae on a small knob near its middle; overall somewhat longer than wide. In dried individuals, 1st gastral tergite longest; 4th tergite a little more than half the length of 1st; 2nd and 3rd subequal and about half the 4th; 5th very short; 6th a little shorter than 4th. Gaster not heavily sclerotized, shrivels slightly on drying. Gaster with few, small setae on first five segments, 6th with many setae, some short, some longer and reaching about half the length of the exerted ovipositor sheaths. Dried individuals have hypopygium distinct. Ovipositor sheaths substantially exserted from apex of gaster, setae basally present on only ventral side, medially and apically present; longest setae at about half its length, reaching approximately the apex of the sheaths; ovipositor thin and needle-like.

Male (Figs 4e–h, 5h–j; morphometric measurements in Suppl. material 2). ***Length*.** Only two individuals collected, allotype 1.14 mm, paratype 0.85 mm.

Similar to female except: Wingless. Antennae with 6 funicular segments, basal four segments of relatively consistent size, fourth through sixth increasing in size; clava with two whorls of MPS. Mean length/mean width (Ratio) of antennal segments, length and width measured relative to length of F1 (n = 2): Scape 9.1/2.7 (3.4) ; Pedicel 4.3/2.3 (1.9) ; F1 1.0/1.8 (0.6) ; F2 1.2/1.9 (0.6) ; F3 1.1/1.9 (0.6) ; F4 1.4/2.1 (0.7) ; F5 2.1/3.2 (0.7) ; F6 2.9/4.1 (0.7); Clava 6.9/4.7 (1.4). Ocelli absent and compound eye smaller than in female, face very subtly widest about even with middle of scrobes, morphometrics of face otherwise similar, mandibles similar. Body size relative to head size smaller than in female. Posterior region of pronotum tapers slightly to fit around the narrower medial lobe of the mesoscutum. Notauli meet on medial line anterior of transscutal articulation, scutoscutellar suture meets transscutal articulation lateral to this. Pro- and mesoscutum smaller than in female, scutellum much shorter than in female, metanotum behind it appears in dorsal view with nearly straight posterior margin but partially covered by the scutellum medially. Femora, tibiae, and tarsal segments somewhat stouter than in female, but their relative lengths remain similar. Posterior margin of propodeal disk with scattered setae. Gaster shorter, truncated-looking apically in dry specimens.

Materials examined. ***Holotype*** (Fig. 4a–d): ♀; Hawaiian Islands, Oʻahu, Mānoa; 21.5571°N, 157.8783°W; 24.vii.2018; ex *Hibiscus tiliaceus* branches (deposited in UHIM).

Allotype (Fig. 4e–h): ♂; Hawaiian Islands, Oʻahu, Mānoa; 21.5571°N, 157.8783°W; 11.xii.2019; pupating next to *Eidophelus pacificus* dessicated larva in *E. pacificus* tunnel in *H. tiliaceus* branch (deposited in UHIM).

***Paratypes*:** 12♀, 1♂. Hawaiian Islands, Oʻahu, Mānoa; 21.5571°N, 157.8783°W; 24.vii.2018; ex *Hibiscus tiliaceus* branches; 7♀ point mounted, 1♀ slide mounted (2 point mounted, 1 slide mounted UHIM; 2 BPBM; 3 NMNH) • Hawaiian Islands, Oʻahu, Mānoa; 21.5571°N, 157.8783°W; 17.x.2018; ex *Hibiscus tiliaceus* branches; 2♀ point mounted (1 BPBM; 1 NMNH) • Hawaiian Islands, Oʻahu, Mānoa; 21.5571°N, 157.8783°W; 2.xii.2019; ectoparasitoid on *E. pacificus* larva found under bark of *H. tiliaceus* branch; 1♀ (BPBM) • Hawaiian Islands, Oʻahu, Mānoa; 21.5571°N, 157.8783°W; 11.xii.2019; pupating next to *Eidophelus pacificus* dessicated larva in *E. pacificus* tunnel in *H. tiliaceus* branch; 1♂ (NMNH) • labeled "Tapatapao // Upolu, Samoa // vii-13-40 //// 1000' //// Beating dead branches //// EC Zimmerman Collector"; 1♀ (BPBM).

Etymology. The species name is Hawaiian (lit., yellow nose). The nose-like interantennal ridge appears to be a good distinguishing character in the genus. In this species the interantennal ridge is distinguished from that in other *Acerocephala* by its elongate-oval shape with carinate edges and light longitudinal striations, reminiscent of a banana cut in half longitudinally. Ihulena is a play on ihu (nose) and iholena, a short and rounded variety of banana brought by Polynesian ocean voyagers and grown in Hawaiʻi.

Known distribution. This species is known from the island of Oʻahu in Hawaiʻi, and the island of Upolu in Sāmoa. It is likely adventive in Hawaiʻi.

Known hosts. Found developing as an ectoparasitoid of an *Eidophelus pacificus* (Schedl, 1941) (Coleoptera: Scolytinae) larva in tunnels under the bark of a *Hibiscus tiliaceus* L. log in Kahana Bay, Oʻahu, 21.5571°N, 157.8783°W, 15 m (Fig. 17b, c). Also found pupating next to dessicated larvae of *E. pacificus* in otherwise uninhabited larval feeding tunnels in the same logs (Fig. 17a, b).

Key to world known *Acerocephala* spp. females

(See Figs 1–8 for photos)

1 Callus on parastigma of forewing; antennal funicle 6-segmented; mandibles 4-dentate **2**

– Submarginal vein of forewing joins smoothly to marginal vein without a callus or especially thickened region; antennal funicle 5-segmented (males may be 6-segmented); mandibles 3-dentate **3**

2 Interantennal ridge truncate anteriorly, in side view abruptly becomes vertical relative to the plane of the face; scrobal grooves reach to approximately even with the middle of the compound eyes ..... ***A. atroviolacea*** (Fig. 8a–e)

– Interantennal ridge rounded anteriorly, in side view gently sloped as it nears the clypeus; scrobal grooves reach to approximately even with the anterior margin of the compound eyes ..... ***A. aenigma*** (Fig. 8f–h)

3 First two antennal funicle segments distinctly longer than wide; head widest at eyes and at anterolateral corner, head below eyes progressively widens to the anterolateral corner ..... ***A. pacifica*** (Fig. 7)

– At least first 3 funicle segments distinctly shorter and compressed relative to distal funicle segments, subequal length and width or transverse; head widest across eyes and at about half its length, tapers slightly as it approaches the anterolateral corner **4**

4 First four funicle segments of similar shape and size, much smaller and compressed compared to the fifth which is more round; scrobes reach past half the length of the face; interantennal ridge not elevated, flush with face lateral of scrobes; ovipositor sheaths only slightly exerted from apex of gaster, less than 1/3 the length of the gaster; scutoscutallar grooves meet the transscutal articulation lateral of the median line, so the scutellum runs up against the mesoscutum for a short distance ..... ***A. hanuuanamu*** (Figs 1–3, 10a)

– First three funicle segments small and compressed, the fourth and fifth distinctly progressively larger and more rounded; interantennal ridge slightly elevated relative to the face lateral of the scrobes; ovipositor sheaths distinctly exerted from apex of gaster, nearly half or more its length; scutoscullar grooves arc to meet the transscutal articulation along its midpoint, so the scutellum is only directly next to the mesoscutum at this midpoint, and is separated from it laterally by the axillae..... **5**

5 Internantennal ridge elongate-oval shape, narrowed anteriorly and posteriorly relative to its middle; anterior of the face between the anterolateral corners

excluding the projected clypeus nearly straight; stigmal vein very short, so the stigma is nearly contiguous with the marginal/postmarginal veins though it may narrow somewhat between them .....***A. ihulena*** (Figs 4, 5)

– Interantennal ridge blunt-wedge shaped, progressively widening posteriorly with somewhat straight margins; anterior of the face between the anterolateral corners excluding the clypeus distinctly concave; stigmal vein somewhat longer, distinctly separating the stigma from the marginal/postmarginal vein .....***A. indica*** (Fig. 6)

Note: Males are only known for *A. hanuuanamu*, *A. ihulena*, *A. indica*, and *A. aenigma*, so males of other species must be found before distinguishing characters are determined with certainty. Males of *A. hanuuanamu*, *A. ihulena*, *A. indica*, and *A. aenigma* are, however, very similar to females in characters of the head with the exception of the antennae in all four species, and the smaller eye and lack of ocelli associated with aptery in *A. hanuuanamu*, *A. ihulena*, and *A. indica*; the overall shape of the head and the interantennal ridge very similar between the sexes. If this pattern holds for other species, males may likely be identified using these same characters of the head as well, listed in the key. Males are wingless in *A. hanuuanamu*, *A. ihulena*, and *A. indica*, and winged similar to the females in *A. aenigma*, so wings and the associated development of the mesosoma, along with characters of the gaster associated with their sex, may be expected to differ.

Behavior of *C. brasiliensis* and *A. hanuuanamu* in phloem sandwiches

Cryphalus brasiliensis **beetle galleries in** ***F. microcarpa*** **wood**

Some of the *C. brasiliensis* beetles placed in the phloem sandwiches bored into the wood and excavated somewhat irregular subovate chambers, much wider than the entry tunnel, in which they laid their eggs (as in Fig. 12a, see also Fig. 11b for the corresponding stage of development in natural wood). Adult beetles were observed to actively clean the inside of these chambers by pushing debris out of the entrance to the tunnel with their elytral declivity. Larvae hatching from their eggs chewed tunnels around the perimeter of the chamber and then progressed generally along the grain of the wood, often moving as a whole in somewhat of a comb pattern but with staggered progress. On one occasion, an adult beetle was observed using its head and prothorax to vigorously and repeatedly push a newly emerged larva, the behavior continuing for a minute or two. The purpose of this behavior was unclear to us, but two possibilities may be (1) an attempt to assist the larva in starting its own feeding tunnel off the main gallery, or (2) a transfer of symbiotic organisms to the larva. If the view boxes were suddenly exposed to high levels of light, adults were observed to become somewhat agitated and occasionally cannibalize their eggs. We did not observe any clear differences in the behavior of immature beetles when exposed to different levels of light.

Moving through the beetle galleries
(Video 1 (https://vimeo.com/717186840))

Female *A. hanuuanamu* entered wood in the phloem sandwiches through holes drilled by the beetles. After entering the tunnels, adult beetles with eggs or larvae deeper in their tunnels were observed to actively attempt to block the wasp from progressing past them deeper into the tunnel. A beetle did so by sharply moving its posterior to block attempts

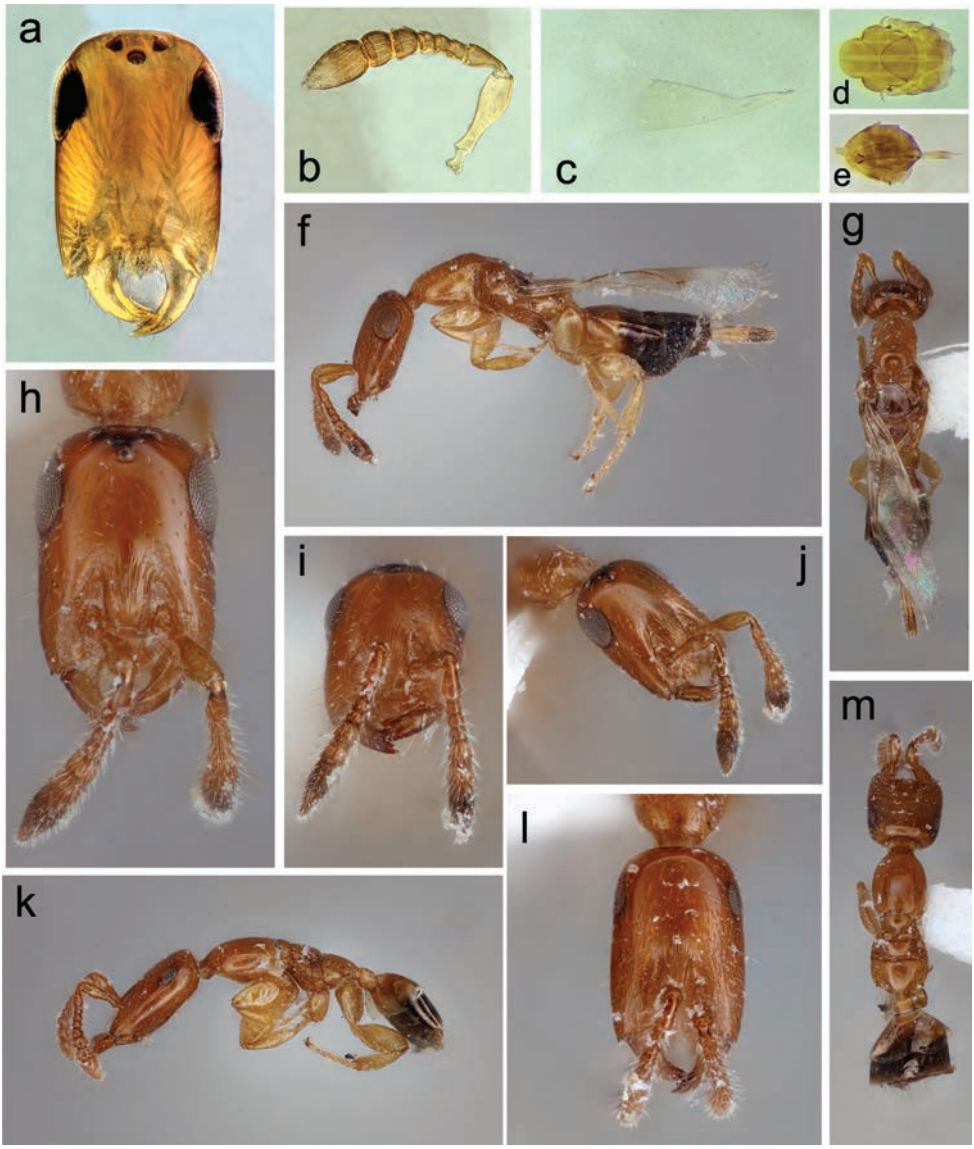

Figure 6. *Acerocephala indica*. Holotype ♀ (**a–e**); non-type ♀ (**f–j**); non-type ♂ (**k–m**) **a, h, l** head **b** antenna **c** forewing **d** mesosoma (dorsal view) **e** gaster **f, k** side view **g, m** dorsal view **i** anterior view of head showing mandibles **j** head.

by the wasp to go around. Wasps were observed to grab the elytral declivity or posterior of the abdomen of beetles with their mandibles when attempting to pass them, though this was not observed to actually help them progress past the bark beetle. Physically encountering an adult beetle in an open area, either in a spacious gallery or outside wood, not in the confined space of a tunnel, resulted in the wasp quickly moving away. Such avoidance behavior was potentially for good reason, as when wasps and beetles were placed together in a confined space such as a tube, it was not uncommon to see wasps missing their entire gaster which, though this was never actually observed, was presumably bitten off by the beetles.

The beginnings of some tunnels bored by the larvae were very narrow due to the small size of the larvae in their early development, though small larvae were also observed to sometimes work in small groups of two or three larvae that would move through the wood side by side and create a wider tunnel (e.g. Fig. 12c and the two larvae on the right side in Fig. 12a). Though *A. hanuuanamu* adults vary substantially in size depending on size of the host on which they develop, even some of the smallest female wasps were not able to fit through these smaller larval tunnels. As time progressed, more space opened up as beetle larvae and adults developed and created

Figure 7. *Acerocephala pacifica*. Holotype ♀ (**a–c**) and paratype ♀ (**d–g**) **a, g** side view **b, d** dorsal view **c, e** head **f** view of head showing mandibles. All photos taken by Lisha Jasper and Jeremy Frank at BPBM.

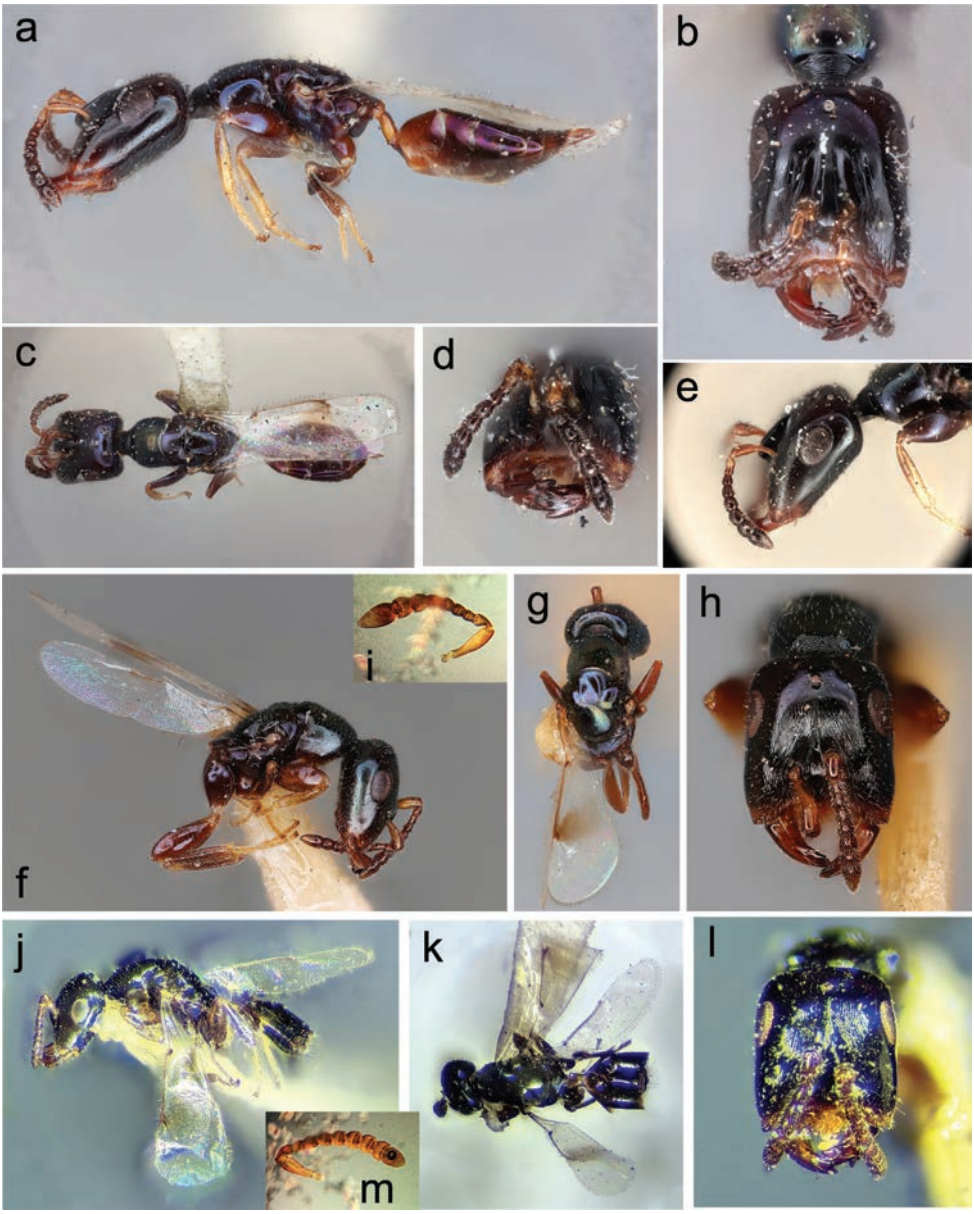

Figure 8. *Acerocephala atroviolacea* and *Acerocephala aenigma*. *Acerocephala atroviolacea* paratype ♀ (**a–e**); *A. aenigma* holotype ♀ (**f–h**) (photos from NMNH database); *A. aenigma* allotype ♂ (**j–l**) **a, f, j** side view **b, h, l** head **c, g, k** dorsal view **d** anterior view of head showing mandibles **e** side view of head showing antenna **i** *A. aenigma* antenna (paratype ♀) **m** *A. aenigma* antenna (paratype ♂).

tunnels in the wood, and individual, isolated tunnels formed a network of intersecting tunnels. Observations in both naturally infested wood (see Fig. 11d, e) and the phloem sandwiches (see Fig. 10d) showed that this dynamic would progress until eventually almost all the inner bark had been consumed and the outer bark was only loosely at-

Figure 9. *Choetospilisca tabida* holotype ♀ (**a–e**) and allotype ♂ (**f–i**) **a, f** side view **b, i** dorsal view **c** antenna **d, g** head **e, h** anterior view of head showing mandibles.

tached to the xylem layer. In a developed tunnel network such as this with a population of host beetles, *A. hanuuanamu* adults were able to move around with much more ease, encounter more potential hosts and fewer one-way tunnels blocked by adult beetles, and seemed to have the most success.

Such tunnel systems often contained frass and debris from the beetles' excavation, sometimes packed somewhat densely, and the wasps would dig through it in pursuit of hosts. *Acerocephala hanuuanamu* has remarkably large mandibles, for which one use was to facilitate this digging behavior. Females progressed through debris-filled tunnels by grabbing a chunk of debris with the mandibles, wrestling it loose, and then passing it within reach of the front legs. Then using all her legs in sequence she would quickly roll it back behind her abdomen in a running motion. In this way, the wasp was able to travel through the tunnels in a way reminiscent of a bubble in a tube of liquid: surrounded on all sides and moving material around its margins to progress through.

Acerocephala hanuuanamu females having entered a tunnel seemed to be able to sense the approximate location of potential host larvae they could not directly see, shown by apparent deliberate motion in its direction, though the sensory mechanisms involved were not clear.

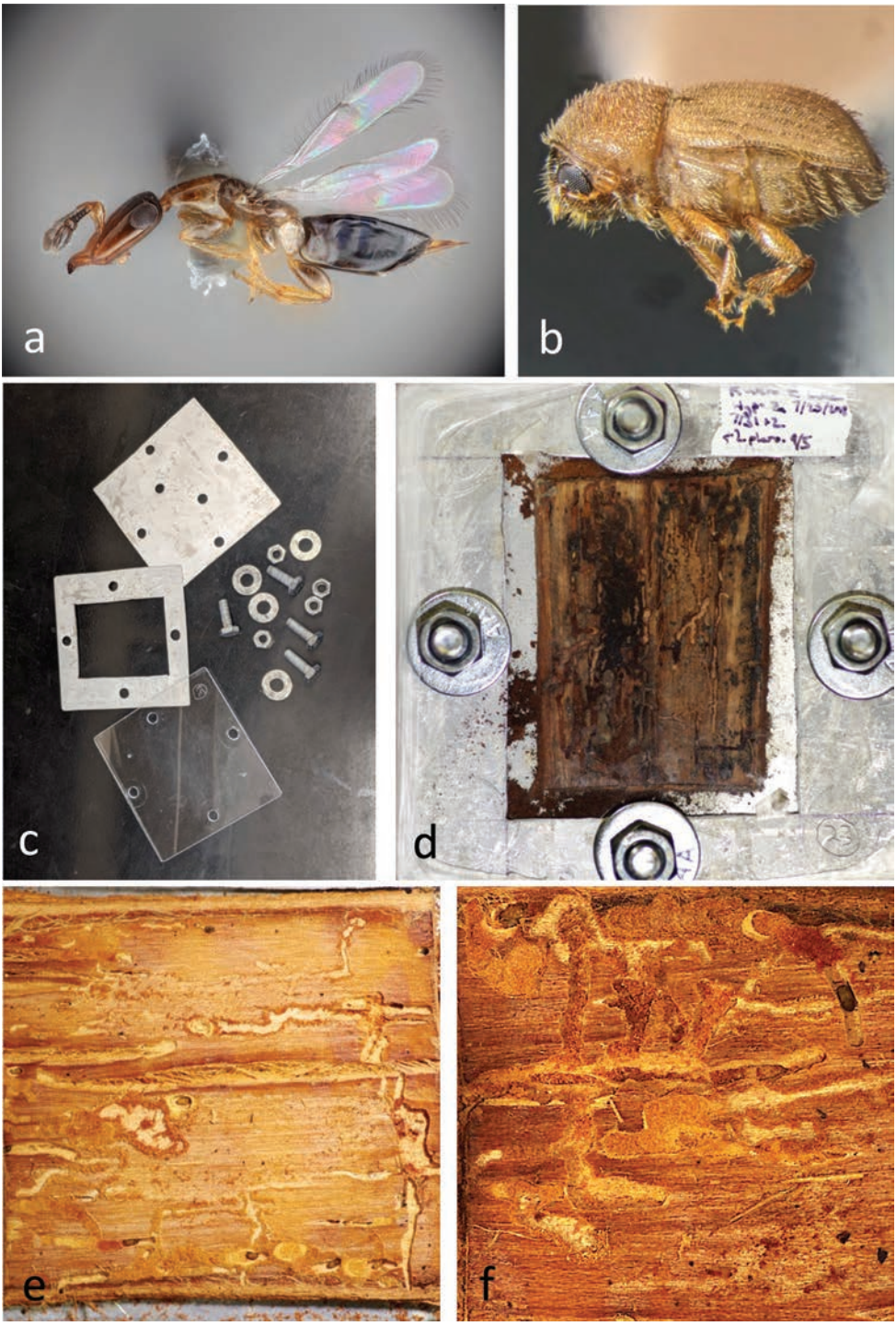

Figure 10. *Acerocephala hanuuanamu*, *Cryphalus brasiliensis*, and the phloem sandwiches **a** *A. hanuuanamu* ♀ **b** *C. brasiliensis* ♀ **c** parts of phloem sandwich style observation chamber **d** phloem sandwich with colonies of *C. brasiliensis* in *F. microcarpa* wood **e, f** closeups of additional phloem sandwiches.

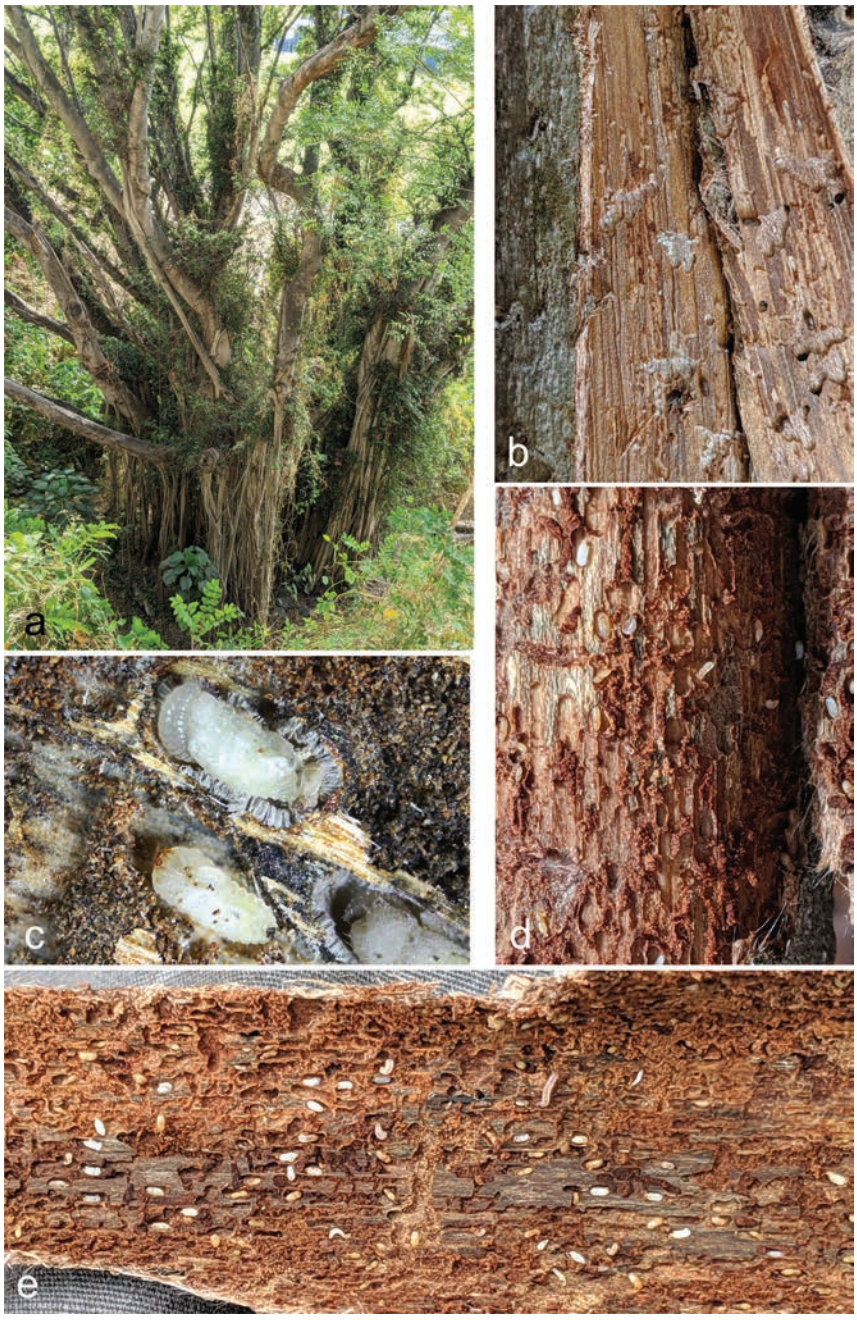

Figure 11. *Ficus microcarpa* wood where observations of behavior in a natural system were made. Photographs of wood are from naturally infested branches taken after peeling off the bark **a** the *F. microcarpa* tree from which most branches were collected and observations were made, in an unmaintained area of the University of Hawai'i at Mānoa **b** wood in an early stage of colonization by *C. brasiliensis* beetles **c** three *C. brasiliensis* beetle immatures, each parasitized by a feeding *A. hanuuanamu* larva **d** *Ficus microcarpa* branch with bark peeled off, showing *C. brasiliensis* tunnel systems and beetles, and *A. hanuuanamu* larvae, prepupae, and pupae **e** same as (**d**) except the bark layer of the branch.

Turning around
(Fig. 13; Videos 1 (https://vimeo.com/717186840), 2 (https://vimeo.com/716967741))

One amazing feat of agility accomplished by *A. hanuuanamu* with regularity is their ability to turn around in the tight confines of a tunnel, often not much wider than the wasp itself. The wasp first articulates its neck to face its head down, then bends its prothorax down, and in doing so slides its head under the rest of the as-of-yet unmoved posterior parts of its mesosoma. Bending its body along its points of articulation and pushing on its own body with its legs while doubled over to assist its progress, the prothorax is followed by the rest of the mesosoma and finally by the flexible gaster, ending with the wasp being in more or less the same location but facing the opposite direction. This maneuver is carried out very fluidly and quickly, and usually takes less than a few seconds, but sometimes longer if the wasp appears not to have a strong purpose for its movement. The fluidity in this snake-like maneuver is in part made possible by the head, the prothorax, and the rest of the mesosoma all being subequal in length, and the ability of the prothorax to articulate with the rest of the mesosoma. A similarly long,

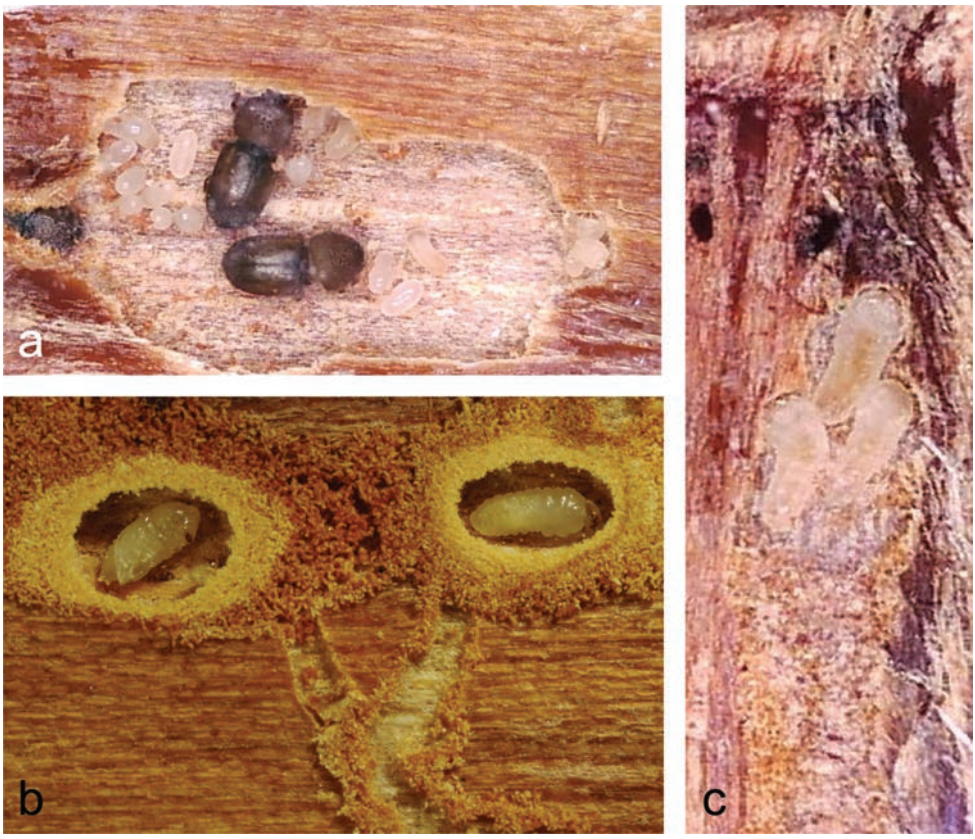

Figure 12. *Cryphalus brasiliensis* in phloem sandwiches **a** *C. brasiliensis* adults in a gallery with eggs and newly hatched larvae feeding and creating tunnels on the margins of the gallery **b** *C. brasiliensis* pupa and prepupa in hard pupal chambers they constructed **c** *C. brasiliensis* larvae feeding and moving through wood.

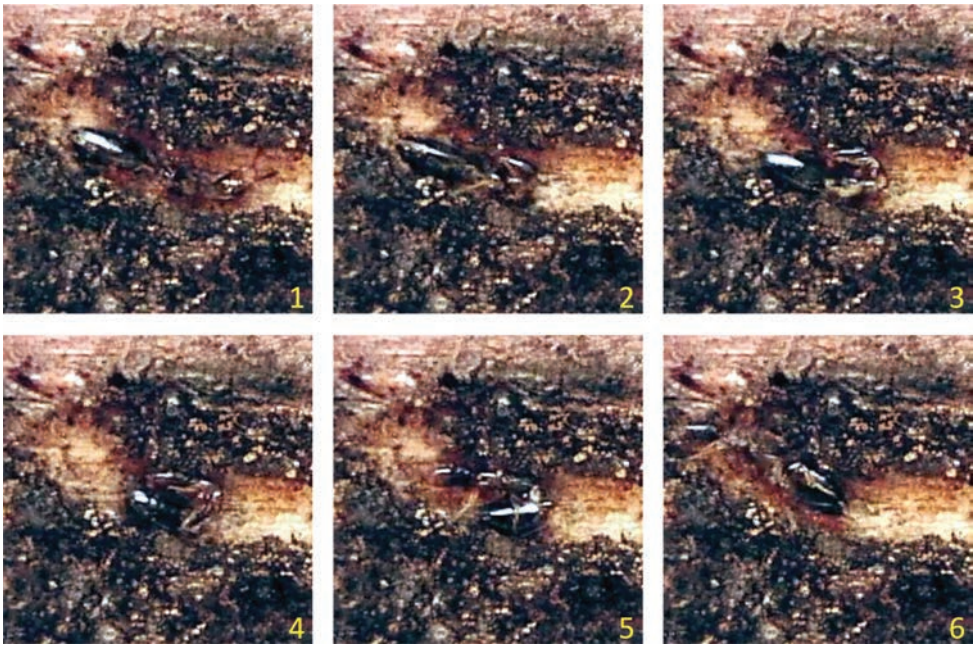

Figure 13. *Acerocephala hanuuanamu* turning around in *C. brasiliensis* tunnels in a phloem sandwich: sequence showing this agile maneuver frequently used to reverse orientation in the tunnels.

articulating prothorax is a character found in other unrelated taxa, such as much of the Bethylidae, which also typically attack their hosts in concealed environments. The agility in a tunnel system or tight space that this trait confers could potentially be what has resulted in this convergence.

Parasitism and host feeding on larvae in tunnels and construction of a feeding tube

(Figs 14–16; Videos 1 (https://vimeo.com/717186840), 2 (https://vimeo.com/716967741))

When a host larva was encountered in the tunnels, the *A. hanuuanamu* female would antennate upon it. Special attention was seemingly placed on the frass and debris around the larva, suggesting that this is a cue for host location, host acceptance, or both. Once a host was identified, the wasp would then turn around using the previously described turning maneuver and back up in the direction of the larva, moving its body backward in pulses and extending its ovipositor. Sometimes the wasp would contact the larva with its ovipositor, but other times it would not, and turn around to reexamine the larva with its antennae. The wasp seemed very cautious when encountering the larva, especially when backing up into it, presumably because of the danger presented by its mandibles. If the ovipositor made contact with the larva, the wasp would fully extend it into the body of the larva (Fig. 14a). The wasp would typically remain with its ovipositor inside the larva for approximately 15 minutes. During this time, the larva would gradually cease motion, the wasp apparently having injected it with a paralytic venom.

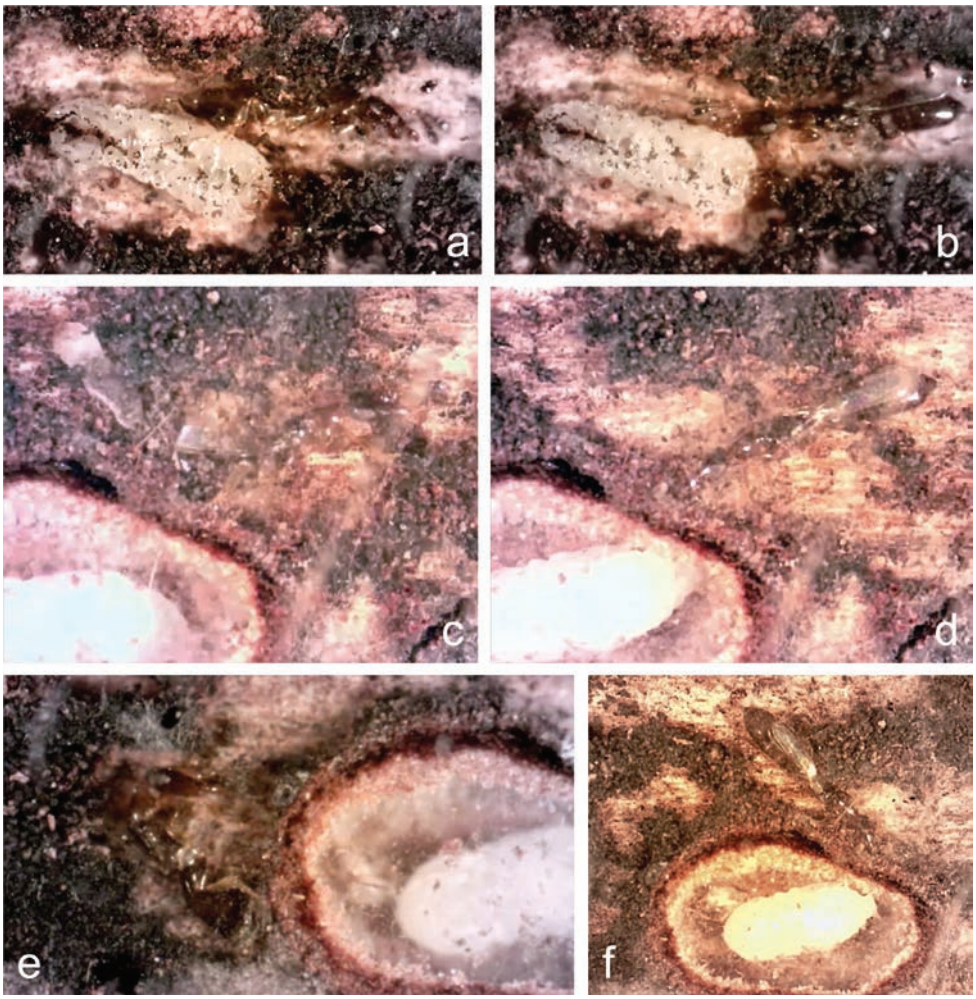

Figure 14. *Acerocephala hanuuanamu* stinging *C. brasiliensis* and host feeding in phloem sandwiches **a** stinging a *C. brasiliensis* larva. The ovipositor is visible extending nearly the length of the wasp's gaster within the larva **b** subsequent host feeding on the same larva as in (**a**), on the same spot where it stung the larva **c** stinging a *C. brasiliensis* pupa through its hard pupal chamber after excavating the loose debris outside the chamber. The ovipositor is visible in the empty space between the chamber wall and the pupa **d** subsequent to stinging the pupa in (**c**), host feeding through the wall of the pupal chamber. Part of the feeding tube is marginally visible protruding from the pupa as a small bump between the pupa and the interior of the chamber wall, on the part of the pupa most proximal to the mouth of the wasp **e** probing with the ovipositor to find the pupa inside the chamber. The ovipositor is visible extending towards the pupa within the chamber. This attempt by the wasp was unsuccessful due to the position of the pupa within the chamber **f** an additional subsequent feeding event by the same wasp on the same pupa. The gaster is distended and the liquid periodically excreted by the wasp as it feeds is visible just past the end of the wasp's gaster.

When finally removing its ovipositor from the larva, the wasp would do so slowly and carefully. In a few observed instances as it withdrew from the larva, tissue from inside the body of the larva was visibly pulled out as a sheath around the ovipositor.

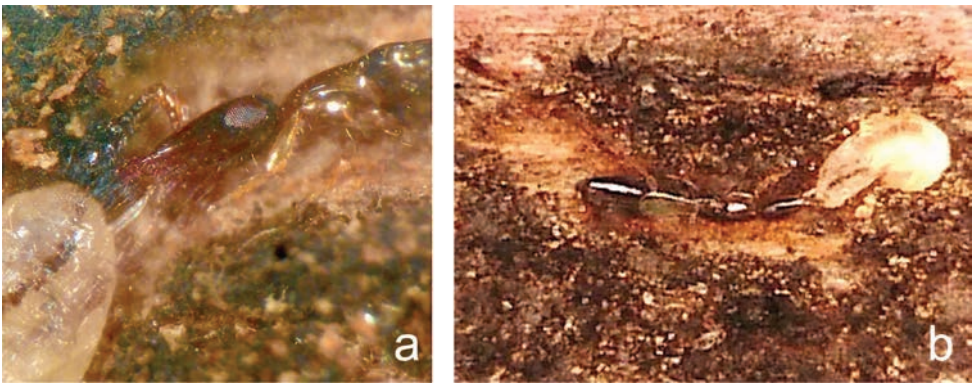

Figure 15. Feeding tube constructed by *Acerocephala hanuuanamu* after stinging, in phloem sandwiches **a** close-up of a tube constructed on a larva as the wasp host feeds **b** tube is visible extending from the posterior end of the larva near the wasp's mouth. Such tubes constructed for feeding through the hard shell of the pupal chamber are also marginally visible in Fig. 14d, f.

This sheath would remain projecting from the larva after the wasp had extracted its ovipositor. The wasp would then turn around in the tunnel and put its mouthparts on that projection, and host feed on the larva through it, evidently having produced a drinking straw (Fig. 15). On occasions when construction of such a straw was not observed, the wasp would still put its mouthparts precisely on the place where it had stung the larva. The wasp would remain in this position, host feeding typically for about 15 minutes. The wasp's body would be still but its mouthparts could be seen moving slightly, and it would periodically expel a clear liquid from its abdomen (Fig. 14b). This liquid is likely to be excess fluid excreted for the purpose of concentrating nutrients from the host within the body of the wasp. Eventually the wasp would stop feeding and would then often turn around again, sting the larva for a similar amount of time as it had initially, and then feed again. This process was often observed to be repeated three or four times on the same larva. Stinging was always observed to result in death of the beetle immature. The wasp would most often leave the larva without laying an egg, and sometimes it would eventually lay an egg on the same larva upon which it had host-fed.

Feeding and oviposition through a pupal chamber
(Video 2 (https://vimeo.com/716967741))

Cryphalus brasiliensis prepupae were observed to build a hard pupal shell around themselves made from bonded tunnel debris before they pupated (Fig. 12b). Upon approaching a pupal chamber, wasps were clearly able to sense the presence of a host and were stimulated to excavate the loose material in the vicinity of the pupal chamber and dig into the hard pupal shell as far as possible. This process of excavating appeared to be very laborious and was observed to last over an hour on occasion. Due to the toughness of the wall, which seemed to increase in strength near its inner boundary, the wasps were not

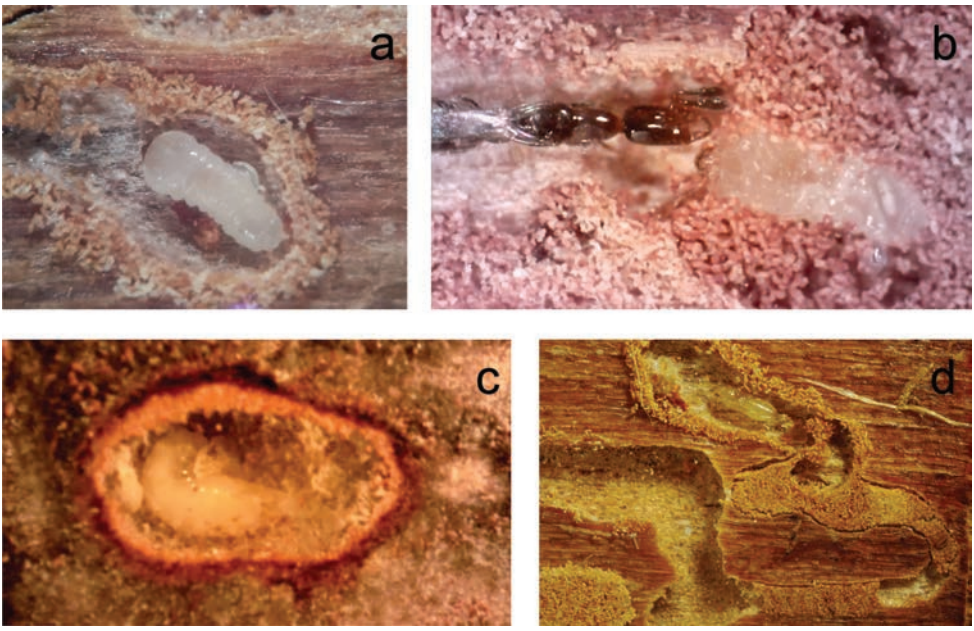

Figure 16. Development of *A. hanuuanamu* on *C. brasiliensis* in phloem sandwiches **a** small *A. hanuuanamu* larva on a *C. brasiliensis* larva **b** *A. hanuuanamu* female remaining motionless near a developing larva on its *C. brasiliensis* host for a long period of time as if guarding it **c** *A. hanuuanamu* larva inside a *C. brasiliensis* pupal chamber having consumed all the hemolymph of its host. This is the same pupal chamber as pictured in Fig. 14c–f, the wasp having oviposited on the pupa subsequent to stinging and host feeding on it multiple times **d** *A. hanuuanamu* pupa inside *C. brasiliensis* tunnels.

observed to break all the way through the shell to the pupa or prepupa inside. After progressing as far as it deemed practical, the wasp would stop digging, turn around, place its back legs on the wall of the pupal shell with its gaster pointing towards the inside of the chamber, extend its ovipositor, and use its body to push its ovipositor through the shell. This was a lengthy process. After pushing and pushing, the ovipositor would finally break through to the other side (Fig. 14c). The wasp would then flex the ovipositor, probing the space in an attempt to contact the larva or pupa inside. Great flexibility and control over its ovipositor was observed (Fig. 14e; Video 2 (https://vimeo.com/716967741)). If able to contact and penetrate the pupa or prepupa inside, it would sting it for about 15 minutes, and then eventually remove its ovipositor, slowly and carefully as it did when stinging a larva, simultaneously pulling the pupa or prepupa into contact with the wall of the chamber. The wasp would then turn around and put its mouthparts on the exact place where it had drilled through the pupal chamber. Physically separated from the pupa by the wall of the pupal chamber, it would then begin feeding, again through a tube it had made (Fig. 14d, f). This was observed multiple times. That it was actually feeding successfully was clear: its abdomen would progressively distend and periodically excrete clear liquid, and the pupa would noticeably progressively shrink in size. A feed-

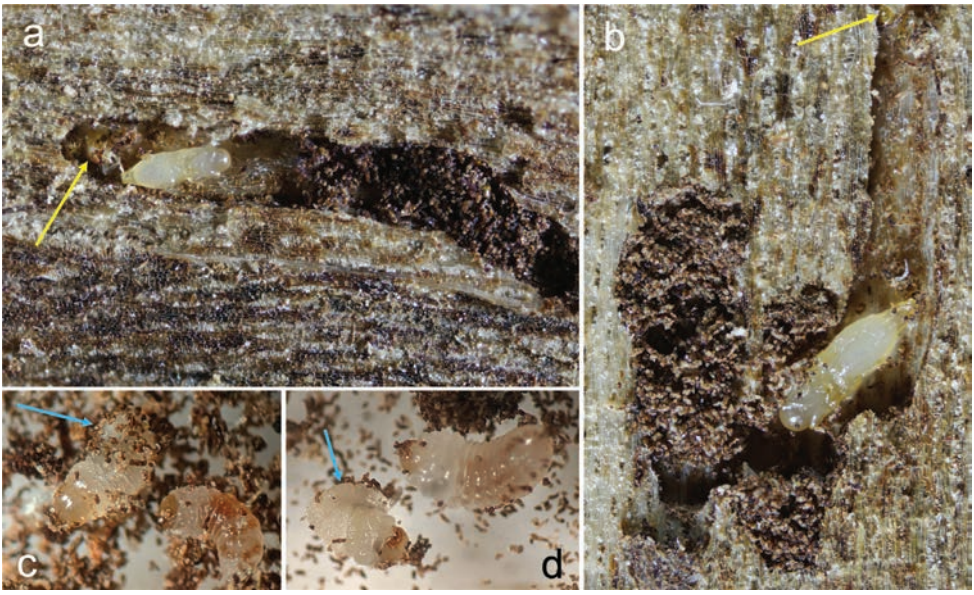

Figure 17. *Acerocephala ihulena* development. Photos are from naturally infested wood taken after peeling off bark **a** *A. ihulena* male (paratype) pupa in an *E. pacificus* tunnel under the bark of *H. tiliaceus* wood, having developed on the desiccated *E. pacificus* larva next to it (indicated by yellow arrow) **b** *A. ihulena* female (paratype) pupa found in the same branches, also having developed on the now desiccated *E. pacificus* larva (indicated by yellow arrow) **c, d** *E. pacificus* larvae from tunnels under the bark of *H. tiliaceus*, with larval *A. ihulena* males developing as ectoparasitoids (parasitoid larvae indicated by blue arrows).

ing straw was never observed directly due to its position within the material, but it was clearly utilizing one as it was feeding from a distance through the wall. Occasionally a small bump was observed on the pupa or prepupa where it was in contact with the wall (Fig. 14d, f), presumably comprising the proximal part of the feeding tube. Wasps were observed repeating this drilling and feeding behavior multiple times on the same pupa before oviposition, the egg having also passed through its ovipositor and the narrow hole it had drilled through the wall of the pupal chamber.

Oviposition and development

An egg was never directly observed coming out of the ovipositor but was often later observed on a larva or pupa, often the same one on which a wasp had previously host fed. The surface of the eggs appears to be adhesive, and eggs were either stuck directly to the larva or pupa, or were placed in the tunnel adjacent to it. A wasp larva emerging from the egg would attach to the beetle larva or pupa (Fig. 16a, b), and over the next 2 or 3 days the wasp larva would suck the hemolymph out of the beetle larva or pupa, transferring more or less all of it to its own body, leaving the shriveled cuticle of its host (Fig. 16c). It would then detach and later pupate (Fig. 16d, Video 3 (https://

vimeo.com/717187250)). The adult wasp would thus emerge in the tunnel or pupal chamber. Interestingly, though this was never observed in action, emergent adult wasps seemed to be able to make their way out from the inside of the beetle pupal chambers.

Mating
(Video 4 (https://vimeo.com/717187205))

A female and male were observed on two occasions to encounter each other and mate. Upon encounter, the wasps slowed their pace and touched antennae to antennae, maintaining that position for a few seconds. The female seemed to relax and the male moved onto the dorsal part of her abdomen, and then curled his abdomen around the female's abdomen to copulate. The act of copulation took in the vicinity of one minute. The wasps then remained near each other, the male often contacting the body of the female with the antennae, the female remaining calm and slow. This sequence of events, including both copulation that appeared successful and attempts that did not seem mechanically successful, were repeated multiple times until the female moved away.

Both times mating was observed, it was outside the piece of wood in the open area of the observation chamber. This should not necessarily be taken to imply that mating takes place external to the wood in nature, though. The place it occurred both times was in frass/debris piles pushed out by the beetles during construction and maintenance of their tunnels. Mating was likely observed there because the chance of males and females encountering each other in the region outside the tunnels was high given that it was a somewhat open space and there were often wasps present in that region.

Observation in naturally infested wood

In *F. microcarpa*
(Fig. 11)

Cryphalus brasiliensis beetles seem to be some of the first colonizers of the environment below the surface of *F. microcarpa* wood at the location studied on O'ahu (Fig. 11a). They drill through the bark and form tunnels straddling the phloem and xylem layers of the wood, but can also be found entirely in the phloem layer on branches with thicker bark. For healthy wood cut from the tree in the studied environment, initial colonization of wood typically happens 3–5 weeks after it is separated from the tree. As multiple generations of beetle adults and larvae feed and tunnel through the wood, the tunnels become increasingly dense, often forming networks covering nearly the whole phloem layer underneath the bark. The beetles then begin to leave the branch at around this stage, and the bark often begins to separate from the rest of the branch, the phloem layer having largely been removed by the beetles. In sections of branches still connected to the tree that seemed to have been somewhat abruptly cut off from the vascular system of the tree, *C. brasiliensis* beetles were present in large numbers throughout the phloem layer for a period of time similar to those in the cut branches.

They were also found to infest older branches at the junction between the dead section and where sap was still flowing. In these, it was difficult to tell whether the beetles were overcoming the immune defenses of the tree in that area and contributing to death of the wood progressively down the branch, or only progressing to the point where the wood had already stopped sap flow for other reasons.

Where there were reproducing *C. brasiliensis* in these trees, it was common to find both female and male *A. hanuuanamu* traveling in their tunnels, especially where there was a high density of *C. brasiliensis* larvae and pupae. In fact, in branches both disconnected from the tree and still attached to the tree, it was rare to find *C. brasiliensis* without at least females of these wasps also present. This suggests that the female wasps are efficient at locating wood newly infested by *C. brasiliensis*, and likely that they can do so by flying. The ectoparasitic larvae and pupae of *A. hanuuanamu*, reared to confirm their identity, were often found in the tunnels and pupal chambers built by *C. brasiliensis* beetles. Parasitoid larvae were found developing on both early and late instar larvae, which was reflected in the great size variation found in both female and male *A. hanuuanamu*. Parasitized larger larvae seemed to be substantially more common, which implies a preference for larger larvae given that these wasps are idiobionts. The parasitism rate seemed very high in some places; many pupal chambers or larval tunnels ending with parasitized beetle immatures or wasp prepupae or pupae (Fig. 11d, e). Two other ectoparasitoids were observed also parasitizing the *C. brasiliensis* beetles. These were an *Ecphylus* sp. (Braconidae) that oviposits into larvae and pupae through the bark, whose pupae could be distinguished morphologically or by the pupal cocoon they build when they pupate, and *Cerocephala dinoderi* Gahan, 1925, which was much more rare than *A. hanuuanamu* or the *Ecphylus* sp., and whose ectoparasitic larvae were observed feeding on *C. brasiliensis* larvae. The cerambycid *Pterolophia bigibbera* (Newman, 1842) was also common in this wood, and was parasitized by *Rhaconotus vagrans* (Bridwell, 1920) (Braconidae), *Sclerodermus immigrans* Bridwell, 1918 (Bethylidae), and *Allobethylus ewa* (Bridwell, 1920) (Bethylidae).

Additional hosts of *Acerocephala hanuuanamu*

In addition to *C. brasiliensis* in *F. microcarpa*, *A. hanuuanamu* was also found parasitizing *Cryphalus mangiferae* Stebbing, 1914 in mango branches (*Mangifera indica* L.) in the area of Kahana Bay on Oʻahu island (21.5604°N, 157.8765°W), and a *Cryphalus* sp. in breadfruit (*Artocarpus altilis* (Parkinson) Fosberg) branches in Mānoa Valley on Oʻahu island (21.2954°N, 157.8145°W). Identities were confirmed by rearing of parasitoid larvae, and when bark beetle larvae could be clearly associated with the adult beetles in the tunnels. *Acerocephala hanuuanamu* was also found emerging from breadfruit fruits with *Cryphalus negrosensis* Browne, 1979, which presents another putative host because the beetle was in high numbers and the only scolytid emerging from the fruits, though this was not confirmed through observation and rearing of parasitized beetles. Adults were also found with *C. brasiliensis* in *Trema orientalis* (L.) Blume branches in Mānoa Valley (21.2952°N, 157.8141°W).

Discussion

Aspects of the behavior of *Acerocephala hanuuanamu*

Some aspects of the behavior of *A. hanuuanamu*, as viewed in the phloem sandwiches, were remarkable. Adult *C. brasiliensis* were observed to actively attempt to block the wasps from passing them in the tunnels. *Acerocephala hanuuanamu* were observed to move through tunnels packed with debris by removing chunks in their direction of travel with their large mandibles and using their legs to pass the material posterior to their bodies. They fluidly and adeptly turned around in narrow tunnels, demonstrating the morphological advantage of a long articulating prothorax also found convergently in other unrelated lineages of cryptoparasitoids such as bethylids. Stinging and host feeding behavior was observed, including, possibly most remarkably, the use of the ovipositor to construct a feeding tube that allowed the wasps to host feed at a distance on pupae through the hard shell of a pupal chamber.

Implications about taxonomic position of the new species given functional aspects of morphology

Especially in taxa where there are few known species, morphological characters of phylogenetic significance are not always immediately clearly differentiated from characters variable within the taxa, nor are meaningful groupings of species into clades. The species here are close to previously described *Acerocephala* species but also differ somewhat, and thus their placement within existing genera, or if a new genus should be constructed, is not immediately obvious. In the original description of *Acerocephala*, Gahan (1946) described the genus consisting of *A. aenigma* and *A. atroviolacea* (in part by a 4-dentate mandible, forewing with callus on the parastigma but lacking a tuft of setae on the callus, long mandibles, and a 6-segmented antennal funicle in females), and considered *Acerocephala* close to the monotypic *Paralaesthia*, sharing a similarly elongate subrectangular head, but distinguished it by the mandible teeth, callus of the forewing lacking setae, and lack of a mesal groove extending the length of the frons. Hedqvist (1969) described the monotypic *Muesebeckisia* as also close to *Acerocephala*, distinguishing it by the mandible teeth and lack of callus on the forewing. Use of the keys provided by Hedqvist (1969) and Bläser et al. (2015) would guide both of the species described here to *Choetospilisca* (Fig. 9) given the number and shape of the antennal funicle segments, and lack of a setose callus on the forewing. Bouček (1988) grouped *A. pacifica* from Australia in with the two previously described *Acerocephala* from the Americas, identifying differences from these species in the antennae, shape and placement of features on the head, callus on the forewing, and characters of the meso- and metasoma, but it was not determined necessary to describe a new genus for it. The family Cerocephalidae as a whole is thought to generally be cryptoparasitic on wood boring insects concealed within the wood. The only known host association previously reported within these putatively related genera is *A. atroviolacea*, which is thought to parasitize a scolytid in

pine cones. The two species described here are similarly parasitoids of scolytids, these in the phloem layer under tree bark and potentially also in fruits. Here, observed aspects of functional morphology and behavior, in combination with the spectrum of habitats among tunnel systems of scolytids and other wood-borers, are used to propose hypotheses about traits that may be conserved and traits that may vary among closely related species. These hypotheses are then used to explain the present revision of the genus.

In observations of the behavior of *A. hanuuanamu* two functions of the antennae were of particular note. 1. When the wasp presses its mouthparts against a substrate as it searches for the spot through which to host feed, whether the opening of a feeding tube passing through the wall of a pupal chamber, or on the cuticle of a larva, it uses the antennae to gently probe the area around and between its mandibles and projection of the clypeus to sense where to place its mouthparts to feed (Videos 1 (https://vimeo.com/717186840), 2 (https://vimeo.com/716967741)). 2. In excavating a path through the debris-filled tunnel systems, the antennal club was placed at the apex of the mandibles to inform the manipulation of the debris using the mandibles, and possibly also to sense promising directions of travel for host searching inferred from chemical characteristics of the debris particles (Video 1 (https://vimeo.com/717186840)). Additionally, when debris was picked up by the mandibles, the antennae rested on top of the particle as if further sensing its characteristics. Antennae can, in general, be predicted to be most mobile, with the least amount of movement of the scape and pedicel resulting in greatest movement of the terminal antennal segments, when the scape is positioned approximately perpendicular to the plane of the face and the pedicel is bent at 90 degrees. In *A. hanuuanamu* the antennal segments are of such length that, when in this position, the club of the antenna reaches near the apex of the mandibles. Therefore, the length of the antennae coincides with their observed function in sensing the vicinity of the mouthparts to inform host feeding and excavation of debris.

Other than as a mechanism to hold the mandibles and move debris being held by the mandibles, the head was not observed to be directly used in digging in *A. hanuuanamu*; that is, it was not used to push material or as a wedge to open up space. The thinness and gracility of the head was observed to be important for the action of turning around within the tight opening excavated by the wasp. If the head were thicker, the tunnel would have to be larger to accommodate its size underneath the mesosoma, and would make turning around in the tight space more difficult.

There is substantial diversity in debris particle size, density, and tunnel geometry among bark beetles and other wood borers; for example, the converging feeding chambers produced by *Ips typographus* (Linnaeus, 1758), clean linear tunnels typical of Xyleborini, and debris-filled linear tunnels produced by cerambycid larvae. In the *C. brasisilensis* tunnel systems observed in this study, the debris is of relatively small particle size. In generations subsequent to the initial colonizers, the tunnel system develops into a network of tunnels that have grown together to form a two-dimensional expanse of debris that the parasitoid must dig its way through to pursue hosts. *Cryphalus brasiliensis* pupae also construct hard chambers that are difficult to penetrate. The previously discussed aspects of morphology of *A. hanuuanamu* were observed to be useful for navigating the specifics

of this host-habitat system: the length of the antennae appeared useful in informing host feeding, debris manipulation, and travel through the tunnels using the mandibles and legs; and the thin head and long articulating prothorax was useful for turning around in the tight spaces opened up during its travel through the debris.

In other species that exist in different host-habitats below the surface of wood, the methods of passing through the tunnel systems to find their hosts may be different, and this would likely be reflected in morphological differences. *Acerocephala pacifica*, *A. atroviolacea* and *A. aenigma* have longer antennae and more stout heads. What follows is speculative, but longer antennae could be useful in more open tunnel systems not as packed with debris as in *C. brasiliensis* tunnels, as longer antennae would be able to sense a larger area around the wasp to inform its direction of movement in the dark tunnels. The stouter head could be used as a wedge to open a path for movement through tunnel debris less dense than that found in *C. brasiliensis* tunnels, and the protruding interantennal ridge would protect the antennae while doing so. In the species with longer antennae, *A. atroviolacea*, *A. aenigma*, and *A. pacifica*, when the scape is folded back into the scrobes, the antenna reach just about the apex of the mandibles, possibly allowing for sensing and manipulation of debris by the mandibles concurrent with the utilization of the head as a wedge. In *C. brasiliensis* tunnels, longer antennae or a larger head would be of little use, and likely a hinderance, because the density of the debris would typically prevent a wide area for exploration by long antennae, and the size of the debris is small enough that it is manipulable using the mandibles; use of the head as a wedge would presumably only cause the particles to jam and would not effectively open a path for movement. For *A. hanuuanamu* in *C. brasiliensis* tunnels, searching for a host appears to be a tactile process of digging through small particles in a direction informed by chemical cues in the particles. In linear tunnel systems, in contrast, there is no option for direction of travel except forward or backwards through the tunnel, and thus less directional decision making needs to happen. This, combined with debris of larger grain size, or less debris, would make longer antennae and a stouter head possibly more useful for exploring more open space and moving through tunnels that contain debris some of which is too large to be picked up using the mandibles.

Therefore, parasitism of hosts that are related but differ in characteristics of their tunnels such as tunnel geometry, frass/debris size, and other aspects of host biology such as the creation of a hard pupal chamber in *C. brasiliensis*, may incur heavy selection on characters such as length of antennae, head size, size and protrusion of the interantennal ridge, and to some extent size of mandibles. These characters, while they should not be disregarded, should be used with some caution in making phylogenetic implications above the level of species. Other characters not observed to be as functionally relevant based on subtle habitat differences may be better clues to higher taxonomic relationships. Here are some considerations:

1. The antennae of *A. hanuuanamu*, *A. ihulena*, and *A. indica* have the basal three or four funicular segments much shorter than those of *A. pacifica*, *A. atroviolacea*, and *A. aenigma*. Interestingly, the basal funicular segments of *A. pacifica*, and to some ex-

tent also *A. aenigma* and *A. atroviolacea*, may be viewed as a nodose version of those in *A. hanuuanamu*, *A. ihulena*, and *A. indica*, the terminal portion of the segments of similar shape; that is, if the neck of the first segments were much shortened and the segments otherwise remained the same, antennae of the species with elongate antennae would appear similar to those with the compressed funicle segments. It is plausible that this variation could be in evolutionary response to their function in debris manipulation and host feeding described above, where the optimal length of the antennae depends on characteristics of the host-habitat system such as grain size, grain density, tunnel geometry, and the logistics of host feeding given the existence of pupal chambers or lack thereof. *A. hanuuanamu* and *A. ihulena* are the species for which we know host-habitat environments. The characteristics of the *C. brasiliensis* system in *F. microcarpa*, and *E. pacificus* in *H. tiliaceus* wood, are similar expanses of small grain-size debris in tunnels having grown together. These could be predicted to be best manipulated and traversed using the mandibles in combination with shortened antennae.

The number of flagellar segments has been used in keys to cerocephalid genera (Hedqvist 1969; Bläser et al. 2015) and also appears to be different in the overall more robust *A. atroviolacea* and *A. aenigma* (females 6-segmented) as compared to *A. hanuuanamu*, *A. ihulena*, *A. indica*, and *A. pacifica* (females 5-segmented). Slide mounted antennae of *A. hanuuanamu*, *A. ihulena*, *A. indica*, and *A. aenigma* females were examined, and the clava of *A. hanuuanamu*, *A. ihulena*, and *A. indica* were found to have three distinct whorls of MPS (Figs 3c, 5b, 6b), suggesting that they are formed from 3 fused segments, giving the total number of ancestral flagellar segments at 8. The clava of female *A. aenigma* appeared to be composed of two fused segments based on the distribution of MPS (Fig. 8i), thus also giving a total number of flagellar segments at 8. Therefore the number of ancestral segments appears to be conserved among all the species, the difference being that one of these segments is in the clava of *A. hanuuanamu*, *A. ihulena*, and *A. indica* while separate from the clava in *A. aenigma*. Males of *A. hanuuanamu*, *A. ihulena*, and *A. indica* also have a 6-segmented funicle and a clava that appears to be composed of 2 segments based on the whorls of MPS (Figs 3d, 6k), and thus the same original number of funicle segments as in the female. *A. aenigma* males had one more segment, with 6 funicular segments and a clava formed from two clearly distinct segments, the apical one with two whorls of MPS (Fig. 8m). Overall, the number of antennal segments therefore does not give a good indication that at least *A. aenigma* is phylogenetically distant from the species with one fewer funicular segment, and because of the overall similarity between *A. aenigma* and *A. atroviolacea*, the same can be said for the group as a whole.

Therefore, length of the antennae given the morphology of the funicular segments and that length is putatively under strong selection for the host-habitat environment, and number of funicular segments, does not appear to clearly separate the species into distinct higher taxa.

2. While the overall shape of the head in full face view is similar among the species, there are differences in head thickness. These are largely a result of the elevation of the interantennal ridge and overall robustness of the head, which may be subject

to selection as in the above discussion, based on host environment. *A. atroviolacea* and *A. aenigma*, and to some extent, *A. pacifica*, are more robust wasps with a greatly protruding interantennal ridge. These are also the species with longer antennae. These characters together would be consistent with the putative adaptation to manipulating larger grain-size debris in less densely packed tunnel systems, possibly using the head as a wedge. The elevation of the interantennal ridge occurs over a gradient among species, some being more lifted (*A. atroviolacea*, *A. aenigma*, *A. pacifica*), *A. hanuuanamu* flush with the face lateral of the scrobes, *A. ihulena* and *A. indica* intermediate. These characters of the shape of the head are thus used with caution to distinguish clades above the level of the species.

3. As discussed by Bouček (1988), the petiole is substantially longer in *A. aenigma* and *A. atroviolacea* than it is in *A. pacifica*. The other species now known have petiole similarly shorter. The shape of the petiole is, however, somewhat conserved. It is thus likely of little phylogenetic significance above the species level.

4. Males of *A. hanuuanamu*, *A. ihulena*, and *A. indica* are wingless and have smaller body size, while males of *A. aenigma* are fully winged and sized similar to the females (males of *A. pacifica* and *A. atroviolacea* are unknown). In the agaonid subfamily Sycophaginae, aptery in males is known to be variable among and sometimes within genera likely dependent on life history strategies including brood size and likelihood of being able to mate without leaving the plant material (Cruaud et al. 2011). Given that such variability in life history is likely also within *Acerocephala*, possibly partially dependent on density and tunneling strategies of hosts (e.g. *A. hanuuanamu* found along with its hosts often in high density and in interconnected tunnel systems, and with apterous males), male aptery and body size relative to the female does not provide a clear reason to split the genus.

5. An exception to the above considerations that give little reason to divide this genus is the presence or absence of a callus on the parastigma of the forewing. A callus is present in *A. atroviolacea* and *A. aenigma*, but absent in *A. hanuuanamu*, *A. ihulena*, *A. pacifica*, and *A. indica*. Characteristics of the callus or lack of a callus appear to be good generic characters within Cerocephalidae. While only *A. atroviolacea* and *A. aenigma* have a defined callus, some very subtle variation among individuals was observed in *A. hanuuanamu* as to a slight thickening of the parastigma in some individuals. *A. pacifica* in other characters seems intermediate between the more robust *A. atroviolacea* and *A. aenigma* and the other species, but lacks a callus. Therefore, presence or absence of a callus does not seem to clearly separate the species, especially when other characters are considered as well.

Thus while there are differences among species in the genus, some of which may suggest grouping into clades, all seem to best be placed in *Acerocephala*, the differences appearing not at the level for which we view a new genus to be necessary. *A. atroviolacea* and *A. aenigma* are both larger wasps and overall appear closely related, and are the only two with a callus. In general, characters of the species included in the putatively related genera *Choetospilisca*, *Paralaesthia*, and *Muesbeckisia* are distinctly

different and fall well outside such a range of variation between the species placed here in *Acerocephala*. Collection of more species, of which there are undoubtedly many in the world-–cryptoparasitoids within wood are typically little known–will likely illuminate these considerations better.

Acknowledgements

We are thankful for the presence of unmaintained and unmanicured areas on and near the campus of UH Mānoa where many of these wasps were collected and observations were made. We thank Lisha Jasper, Keith Arakaki, and Jeremy Frank of Bishop Museum for providing access and assistance in collections and photographing specimens, and Cecilia Escobar and Michael Gates of the National Museum of Natural History for access to collections and loaning of specimens. We also thank our coworkers and lab mates Conrad Gillett, Ali Miarkiani, Michelle Au, Abdullah Ali, Mitchell Logan, Robert Sakuda, Maisha Lucas, Shannon Wilson, Vanessa Goodman, and Laura Doucet for their assistance and for creating an enjoyable and productive working environment. We acknowledge that this research took place on the mokupuni (island) of Oʻahu in the ahupuaʻa (land division) of Waikīkī and Kapālama in the moku (district) of Kona, and Kahana in the moku of Koʻolauloa, the ancestral and traditional land of Native Hawaiian people. We are very grateful to HDoA and Hatch project HAW09041-H, administered by CTAHR, for their funding.

References

Alba-Alejandre I, Alba-Tercedor J, Vega FE (2018) Observing the devastating coffee berry borer (*Hypothenemus hampei*) inside the coffee berry using micro-computed tomography. Scientific Reports 8: 17033. https://doi.org/10.1038/s41598-018-35324-4

Aflitto NC, Hofstetter RW, McGuire R, Dunn DD, Potter KA (2014) Technique for studying arthropod and microbial communities within tree tissues. Journal of Visualized Experiments 93: e50793. https://doi.org/10.3791/50793

Beanlands GE (1966) A laboratory-rearing method for observing adult bark beetles and their developing brood. The Canadian Entomologist 98: 412–414. https://doi.org/10.4039/Ent98412-4

Bläser M, Krogmann L, Peters RS (2015) Two new fossil genera and species of Cerocphalinae (Hymenoptera, Chalcidoidea, Pteromalidae), including the first record from the Eocene. ZooKeys 545: 89–100. https://doi.org/10.3897/zookeys.545.6470

Burks R, Mitroiu MD, Fusu L, Heraty JM, Janšta P, Heydon S, Dale-Skey Papilloud N, Peters RS, Tselikh EV, Woolley JB, van Noort S, Baur H, Cruaud A, Darling C, Haas M, Hanson P, Krogmann L, Rasplus JY (2022) From hell's heart I stab at thee! A determined approach towards a monophyletic Pteromalidae and reclassification of Chalcidoidea. Journal of Hymenoptera Research 94: 13–88. https://doi.org/10.3897/jhr.94.94263

Cruaud A, Zahab-Jabbour R, Genson G, Kjellberg F, Kobmoo N, van Noort S, Da-Rong Y, Yan-Qiong P, Ubaidillah R, Hanson PE, Santos-Mattos O, Farache FHA, Pereira RAS, Kerdelhué C, Rasplus JY (2011) Phylogeny and evolution of life-history strategies in the Sycophaginae non-pollinating fig wasps (Hymenoptera, Chalcidoidea). BMC Evolutionary Biology 11: 178. https://doi.org/10.1186/1471-2148-11-178

Gahan AB (1946) Review of some chalcidoid genera related to *Cerocephala* Westwood. Proceedings of the United States National Museum 96: 349–378. https://doi.org/10.5479/si.00963801.96-3203.349

Gibson GAP (1997) Morphology and Terminology. In: Gibson GAP, Huber JT, Woolley JB (Eds) Annotated Keys to the Genera of Nearctic Chalcidoidea (Hymenoptera). NRC Research Press, Ottawa, 16–44.

Gouger RJ, Yearian WC, Wilkinson RC (1975) Feeding and reproductive behavior of *Ips avulsus*. The Florida Entomologist 58(4): 221–229. https://doi.org/10.2307/3493679

Grosman DM, Salom SM, Payne TL (1992) Laboratory study of conspecific avoidance by host colonizing *Dendroctonus frontalis* Zimm. (Coleoptera: Scolytidae). Journal of Insect Behavior 5: 263–271. https://doi.org/10.1007/BF01049293

Hedqvist KJ (1969) Notes on Cerocephalini with descriptions of new genera and species (Hymenoptera: Chalcidoidea: Pteromalidae). Proceedings of the Entomological Society of Washington 71: 449–467. https://biostor.org/reference/71494

Kinn DN, Miller MC (1981) A phloem sandwich unit for observing bark beetles, associated predators, and parasites. Southern Forest Experiment Station Research Note SO-269: 1–3. https://doi.org/10.2737/SO-RN-269

Kirkendall LR, Biedermann PHW, Jordal BH (2015) Evolution and diversity of bark and ambrosia beetles. In: Vega FE, Hofstetter RW (Eds) Bark beetles: biology and ecology of native and invasive species. 1st ed. Academic Press, London, 85–156. https://doi.org/10.1016/B978-0-12-417156-5.00003-4

Klimmek F, Baur H (2018) An interactive key to Central European species of the *Pteromalus albipennis* species group and other species of the genus (Hymenoptera: Chalcidoidea: Pteromalidae), with the description of a new species. Biodiversity Data Journal 6: e27722. https://doi.org/10.3897/BDJ.6.e27722

Nagel WP, Fitzgerald TD (1975) *Medetera aldrichii* larval feeding behavior and prey consumption (Dipt.: Dolichopodidae). Entomophaga 20(1): 121–127. https://doi.org/10.1007/BF02373458

Rezende MQ, Pantoja G, Coffler T, Cardoso IM, Janssen A, Venzon M (2019) *Inga* spp. mediated coffee berry borer predation by an omnivorous thrips. International Entomophagous Insects Conference 6, Perugia (Italy), 9–13 September 2019.

Salom SM, Stephen FM, Thompson LC (1986) Development of *Hylobius pales* (Herbst) immatures in two types of phloem media. Journal of Entomological Science 21(1): 43–51. https://doi.org/10.18474/0749-8004-21.1.43

Sharma T, Dedes J, Macquarrie CJK (2016) A modified technique for rearing wood boring insects permits visualization of larval development. Journal of the Entomological Society of Ontario 147: 7–14. https://journal.lib.uoguelph.ca/index.php/eso/article/view/3863

Taylor AD, Hayes JL, Roton L, Moser JC (1992) A phloem sandwich allowing attack and colonization by bark beetles (Coleoptera: Scolytidae) and associates. Journal of Entomological Science 27(4): 311–316. https://doi.org/10.18474/0749-8004-27.4.311

Vega FE, Infante F, Johnson AJ (2015) The genus *Hypothenemus*, with emphasis on *H. hampei*, the coffee berry borer. In: Vega FE, Hofstetter RW (Eds) Bark beetles: biology and ecology of native and invasive species. 1st ed. Academic Press, London, 427–494. https://doi.org/10.1016/B978-0-12-417156-5.00011-3

Vega FE, Simpkins A, Rodríguez-Soto MM, Infante F, Biedermann PHW (2017) Artificial diet sandwich reveals subsocial behaviour in the coffee berry borer *Hypothenemus hampei* (Coleoptera: Curculionidae: Scolytinae). Journal of Applied Entomology 141: 470–476. https://doi.org/10.1111/jen.12362

Supplementary material 1

***Acerocephala hanuuanamu* sp. nov. morphometric measurements**

Authors: David N. Honsberger, Maya Honsberger, J. Hau'oli Lorenzo-Elarco, Mark G. Wright

Data type: csv

Link: https://doi.org/10.3897/jhr.97.127702.suppl1

Supplementary material 2

***Acerocephala ihulena* sp. nov. morphometric measurements**

Authors: David N. Honsberger, Maya Honsberger, J. Hau'oli Lorenzo-Elarco, Mark G. Wright

Data type: csv

Link: https://doi.org/10.3897/jhr.97.127702.suppl2

JHR 97: 591–620 (2024)
doi: 10.3897/jhr.97.127112
https://jhr.pensoft.net

RESEARCH ARTICLE

JOURNAL OF Hymenoptera RESEARCH
A peer-reviewed open-access journal
The International Society of Hymenopterists

Telenomus Haliday (Hymenoptera, Scelionidae) parasitizing Pentatomidae (Hemiptera) in the Palearctic region

Francesco Tortorici[1], Bianca Orrù[1], Alexander V. Timokhov[2], Alexandre Bout[3], Marie-Claude Bon[4], Luciana Tavella[1], Elijah J. Talamas[5]

1 *Dipartimento di Scienze Agrarie, Forestali e Alimentari (DISAFA), University of Torino, largo P. Braccini 2, 10095 Grugliasco (TO), Italy* **2** *Department of Entomology, Lomonosov Moscow State University, 119234 Moscow, Russia* **3** *INRAE, UMR 1355 Institut Sophia Agrobiotech, CNRS 7254, Université Côté d'Azur, 400 route des Chappes, BP 167, 06903 Sophia Antipolis, France* **4** *European Biological Control Laboratory, Montpellier, France* **5** *Florida Department of Agriculture and Consumer Services, Gainesville, USA*

Corresponding author: Francesco Tortorici (francesco.tortorici@unito.it)

Academic editor: Zachary Lahey | Received 8 May 2024 | Accepted 3 July 2024 | Published 13 August 2024

https://zoobank.org/5F640AA2-13CD-4A58-AAD5-ED89D519F6BC

Citation: Tortorici F, Orrù B, Timokhov AV, Bout A, Bon M-C, Tavella L, Talamas EJ (2024) *Telenomus* Haliday (Hymenoptera, Scelionidae) parasitizing Pentatomidae (Hemiptera) in the Palearctic region. Journal of Hymenoptera Research 97: 591–620. https://doi.org/10.3897/jhr.97.127112

Abstract

In recent years, the collection of eggs of stink bugs (Pentatomidae) has intensified because of the attention given to egg parasitoids in classical biological control strategies against *Halyomorpha halys* (Stål) in Europe. Several specimens belonging to the genus *Telenomus* Haliday emerged from field-collected pentatomid eggs. Taxonomic knowledge to date has not been sufficient to enable the research community to identify these specimens to species level. Three species of scelionid wasps (Scelionidae) associated with Pentatomidae, *Telenomus gifuensis* Ashmead, *Telenomus truncatus* (Nees von Esenbeck) and *Telenomus turesis* Walker, have been characterized on a morphological basis. A *COI* barcode analysis confirmed the genetic distance between the latter two species. An identification key to the three *Telenomus* species occurring in the Palearctic region associated with stink bugs is provided. *Telenomus heydeni* Mayr is here considered conspecific with *Telenomus truncatus* (Nees von Esenbeck).

Keywords

Biological control, DNA barcoding, identification key, Platygastroidea, species description, taxonomy

Introduction

The subfamily Telenominae (Hymenoptera, Scelionidae), particularly the genera *Trissolcus* Ashmead and *Telenomus* Haliday, have been studied, in part, because of their potential as biological control agents (BCAs) of economically important pests. Species of *Trissolcus* parasitize eggs of stink bugs (Pentatomoidea), particularly Pentatomidae and Scutelleridae, and a few are phoretic on leaf-footed bugs (Coreidae) (Kozlov and Kononova 1983; Johnson 1984a, 1984b, 1987, 1991; Yan et al. 2022). Species of *Telenomus* share these hosts, but also attack a wider range of Heteroptera, as well as Auchenorrhyncha, Lepidoptera, Diptera and Neuroptera (Bin and Johnson 1982; Johnson and Bin 1982; Kozlov and Kononova 1983; Johnson 1984b).

Telenomus is by far the largest genus in the subfamily and includes a considerable number of species that cannot be reliably identified. This taxonomic challenge has its roots in the diversity and size of the genus, and in what Meier et al. (2022) termed the "superficial description impediment". Descriptions for Palearctic taxa, particularly from the early years of European insect taxonomy, are woefully insufficient for species-level identification. Despite these inauspicious beginnings, there have been notable advancements in the classification of telenomine wasps. Kozlov (1967, 1968), Kozlov and Kononova (1983), and Kononova (2014) treated Palearctic species; Johnson (1981) dealt with Nearctic *Telenomus* with keys to identify the species of the *nigricornis* group (Johnson 1981), and *podisi* and *phymatae* groups (Johnson 1984b). After this, the world fauna was catalogued by Johnson (1992). The *podisi* species group, which parasitizes the eggs of Pentatomidae and Scutelleridae, was defined by Johnson (1984b) and includes the species treated here.

The taxonomy of *Telenomus* in the western Palearctic received little attention in the 21st century until the arrival of the brown marmorated stink bug, *Halyomorpha halys* (Stål) (Hemiptera, Pentatomidae). The pestiferous nature of this stink bug and the potential risk of dispersal to other countries (Zhu et al. 2012) has led several institutions to deepen the knowledge on biological control strategies (Gariepy et al. 2014b; Maistrello et al. 2017; Bosco et al. 2018; Leskey and Nielsen 2018; Moore et al. 2019). In Integrated Pest Management (IPM) programs, much attention has been given to the ability of BCAs to counter the pest population, and, in the specific case of stink bugs, first to native and then exotic egg parasitoids. To study the diversity of egg parasitoids and their impact on native pentatomid species, egg mass survey programs have been performed in several countries in different habitats (e.g., forests, orchards, urban parks) (Koppel et al. 2009; Dieckhoff et al. 2017; Jones et al. 2017; Moonga et al. 2018; Sabbatini Peverieri et al. 2019; Holthouse et al. 2020; Andreadis et al. 2021; Moraglio et al. 2021b; Japoshvili et al. 2022; Ozdemir et al. 2022). These investigations have expanded knowledge of the distribution and biology of parasitoids attacking stink bugs throughout the western Palearctic and have made significant progress in advancing the species-level taxonomy of Telenominae (Matsuo et al. 2014; Talamas et al. 2015, 2017; Tortorici et al. 2019; Moraglio et al. 2021a).

Trissolcus japonicus (Ashmead) and *Tr. mitsukurii* (Ashmead) (Hymenoptera, Scelionidae) have been shown in Europe to be the most promising BCAs of *H. halys* in terms of habitat suitability (Yonow et al. 2021; Tortorici et al. 2023), exploitation efficiency, and parasitoid impact (Giovannini et al. 2022). These species were quickly recognized because the Palearctic fauna of *Trissolcus* has been well-characterized using morphology, molecular data, and mating experiments to resolve cryptic species (Talamas et al. 2017; Tortorici et al. 2019; Ranjbar et al. 2021). However, the same is not true for *Telenomus*, despite that some species are widespread and are known to attack stink bug eggs.

In Europe, some authors have reported *Te. chloropus* (Thomson) from their surveys (Haye et al. 2015; Roversi et al. 2017) and numerous studies of biological attributes have also used this name (Orr et al. 1985a, b; Orr 1988; Bulezza 1996; Açikgöz and Gözüaçik 2021), but most *Telenomus* species reared from large-scale surveys of stink bug egg parasitism have been indicated as "*Telenomus* spp." (Abram et al. 2017; Moraglio et al. 2020; Bout et al. 2021; Rot et al. 2021; Zapponi et al. 2021; Ozdemir et al. 2022; Ricupero et al. 2022). This reflects the challenge of species-level identification for *Telenomus* and clearly points to the need for better diagnostic tools. Here, we make progress in meeting this need by providing taxonomic treatments of two Palearctic species in the *Te. podisi* group, *Te. truncatus* (Nees von Esenbeck) and *Te. turesis* Walker, which attack stink bugs in the families Pentatomidae and Scutelleridae (Javahery 1968; Voegelé 1969; Kozlov and Kononova 1983; Johnson 1984b; Graham 1988a) and an overview of *Telenomus* species found to parasitize eggs of pentatomids and scutellerids in Europe. *Telenomus gifuensis* Ashmead has been reported as a parasitoid of pentatomids in the eastern Palearctic region. To our knowledge, this species has not been reported from the western Palearctic, but we included it in our identification key because the limits of its distribution are not known and there may be regions where it overlaps with the distributions of *Te. truncatus* and *Te. turesis*.

Our work includes examination of historical type specimens, some of which are nearly 200 years old, which is essential for resolving long-standing ambiguity. An updated morphological diagnosis section provides previously unexplored or unused character systems, and we provide simplified descriptions that focus on diagnostic characters. As other Old-World species of the *Te. podisi* group are treated taxonomically, these descriptions are likely to expand to include characters used for the species group more broadly. We complement our analysis with molecular data that is helpful for establishing which characters are prone to interspecific variation and which are diagnostically stable. For the analyzed species, we provide host associations and biological observations.

Synopsis of Palearctic species in the *Te. podisi* group

The earliest species, described by Nees von Esenbeck (1834), were *Te. truncatus* and *Te. linnei*, originally placed in the genus *Teleas* Latreille. Shortly thereafter, *Te. turesis* was described by Walker (1836). Thomson (1861) described *Te. chloropus* (as *Phanurus*). Mayr described *Te. heydeni* (1879) and *Te. sokolowi* (1897). Mayr (1879) considered *Teleas Zetterstedtii* Ratzeburg to be conspecific with *Te. truncatus* based on a non-type specimen that was

identified by Ratzeburg and was reported to emerge from eggs of *Calliteara pudibunda* Linnaeus (Lepidoptera, Erebidae). Ashmead described *Te. gifuensis* (1904) followed by Nixon's species, *Te. tischleri* (1939). Kozlov (1963) considered *Te. mayri* Sokolov a junior synonym of *Te. sokolowi* Mayr and, subsequently, the same author (1967) considered *Te. sokolowi*, *Te. gifuensis* and *Te. tischleri* to be conspecific with *Te. chloropus*. Javahery (1968) provided the most detailed descriptions of *Te. sokolowi* and *Te. truncatus*. Graham (1988a) designated the lectotype of the latter species. Johnson (1984b) analyzed primary types and considered *Te. gifuensis* to be a valid species and removed its synonymy. Mineo (2010) treated *Te. chloropus* and *Te. turesis* as conspecific, with Walker's species name having priority.

Materials and methods

Reared specimens

Telenomus specimens were reared from naturally laid egg masses (Pentatomidae and Scutelleridae) collected in different sites in Piedmont, Italy, from 2019 to 2022 during surveys to investigate the egg parasitoid populations of native and exotic bugs. Each egg mass was isolated in a plastic Petri dish (6 cm diameter) and reared in a climate-controlled chamber at 24 ± 1 °C, 65 ± 5% r.h., and L16:D8 photoperiod. All egg masses were examined under a stereomicroscope and identified to the species or family level according to Derjanschi and Péricart (2005), Péricart (2010), Ribes and Pagola-Carte (2013). The eggs were visually inspected daily and emerging bug nymphs or parasitoid adults were examined. Parasitoids were stored in 99% ethanol until species identification, as described below. Additional specimens of *Telenomus* were collected on November 26, 2022, in Liguria, Italy, hidden in leaf mines of *Phyllonorycter viburni* (Kumata) (Lepidoptera, Gracillariidae).

Telenomus specimens were also reared from egg masses of *Palomena prasina* (Linnaeus) (Hemiptera, Pentatomidae) or collected by sweeping in their natural habitats in Moscow Province, Russia, in 2016 for a cytogenetic study (Gokhman and Timokhov 2020). Each egg mass was isolated in plastic tubes (5 cm^3) and reared in a thermostatic chamber at 24 ± 1 °C. Female parasitoids (both *Te. truncatus* and *Te. turesis*) were then individually transferred to egg masses of a lab host, *Graphosoma lineatum* Linnaeus (Hemiptera, Pentatomidae), for oviposition. To obtain a proper immature stage of wasps for the cytogenetic study, parasitized host eggs were incubated under thermostatic conditions for a few days (Gokhman and Timokhov 2020).

Morphological analysis

A Wild M5 steromicroscope with 15× oculars and a spotlight were used for biometric diagnosis. Slides were mounted with Eukitt mounting medium (Merck Life Science, Milan, Italy) and examined under a Leitz Dialux 20 EB compound microscope. Male genitalia were prepared by following the protocol of Polaszek and Kimani (1990). Terminology for surface sculpture and morphological terminology follows

Harris (1979), Johnson (1984b), Mikó et al. (2007), and Talamas et al. (2017). The morphological identification was performed independently from keys and once the morphometric analysis of characters was complete and confirmed by molecular analysis, species names were assigned by comparison to primary types.

Imaging

Images of primary type specimens were taken with a Macropod imaging system using 10× and 20× Mitutoyo objective lenses (Mitutoyo Corporation, Kawasaki, Japan) and rendered with Helicon Focus (HeliconSoft Limit., Kharkiv, Ukraine). Photographs of non-type specimens were taken using a Canon 90D camera (Canon Inc., Tokyo, Japan) equipped with an extension tube; 5×, 10×, 20×, and 50× LWD microscope lenses mounted on a macro-rail and illuminated with two speedlight flashes. The frames were merged with Zerene Stacker (PMax algorithm, Zerene Systems LLC, Richland, WA, USA).

The ultrastructures of non-type specimens were examined under a Jeol JSM-6380 scanning electron microscope (SEM) after critical point drying (Hitachi HCP-2) of the specimens and sputter coating with gold (Giko JSM-6380).

Molecular analysis

DNA extraction, amplification, and sequencing were performed at multiple institutions. At the Florida State Collection of Arthropods (FSCA) and the European Biological Control Laboratory (EBCL), this was performed as in Talamas et al. (2021). Cytochrome Oxidase subunit I (*COI*) sequences from French specimens (INRAE UMR ISA) were obtained as in Bout et al. (2021). At the Dipartimento di Scienze Agrarie, Forestali e Alimentari laboratory (DISAFA) of the University of Torino, a non-destructive Chelex DNA extraction method was performed and adapted according to Kaartinen et al. (2010). DNA was extracted from insects by dipping samples in 50 µl of 5% Chelex with 5 µl of 20 mg/ml proteinase K at 37 °C for at least 18 h. The specimens were boiled at 95 °C for 5 min to inactivate proteinase K and then used as templates for PCR. The insects were then removed from the Chelex, washed in 70% ethanol and later mounted on card points. The barcode region of the mitochondrial *COI* was amplified using the universal Folmer primer LCO1490 (5'-GGTCAACAAATCATAAAGATATTGG-3') (Folmer et al. 1994) and the primer HCOout (5'-CCAGGTAAAATTAAAATATAAACTTC-3') (Carpenter 1999). PCR amplifications were performed on a C1000 Touch™ Thermal Cycler (Bio-Rad, CA, USA) in 25 µl volume containing: 2.5 µl of 10 X Buffer and 10 mM dNTPs, 1.25 µl of $MgCl_2$, 0.3 µl of Taq Polymerase, 0.1 µl of 100 µM forward and reverse primer, 16.25 µl of sterile water, and 2 µl of DNA template. Thermocycling conditions were: 95 °C for 15 min, followed by 34 cycles of 95 °C for 30 s, 50 °C for 45 s, and 72 °C for 1 min. After a final extension at 72 °C for 5 min, reactions were held at 4 °C. For the nested PCR, 2 µl of the first PCR was used a template using the reverse primer HCO2189 (5'-TAAACTTCAGGGTGACCAAAAAATCA-3') and the forward

primer LCO1490, using the same PCR cycling program described above. The fragment size at the end of nested PCR was 700 bp. PCR products were examined by electrophoresis on a 1% agarose gel. Positive samples were purified using a commercial kit (QIAquick PCR Purification Kit, Qiagen, Hilden, Germany), and sequenced by a commercial service (Eurofins Genomics, Germany).

The sequences were compared with the GenBank database using the Basic Local Alignment Search Tool (http://www.ncbi.nlm.nih.gov/BLASTn). All sequences obtained from this study are deposited in GenBank or BOLD (Ratnasingham and Hebert 2007), and all residual DNAs are achieved at DISAFA, FSCA, INRAE UMR ISA or EBCL. Sequences were used to query GenBank (Altschul et al. 1990) and BOLD for similar sequences, which were downloaded from both databases. The *COI* barcodes of *Trissolcus belenus* (Walker) (MN603806) and of *Tr. semistriatus* (Nees von Esenbeck) (MN603800) (Tortorici et al. 2019) were selected as outgroups for the Maximum Likelihood analysis. All sequences were aligned using MUSCLE with default setting as implemented in MegaX (Kumar et al. 2018), and a phylogenetic tree was created by using the Maximum Likelihood method and Tamura-Nei model (Tamura and Nei 1993). Initial tree(s) for the heuristic search were obtained automatically by applying Neighbor-Joining and BioNJ algorithms to a matrix of pairwise distances estimated using the Tamura-Nei model, and then selecting the topology with superior log likelihood value. The resulting phylogenetic tree was exported and redrawn in the Interactive Tree of Life (iTOL) v5 (Letunic and Bork 2021).

Geographic records of specimens used for molecular and morphological analysis were retrieved from GPS latitude and longitude coordinates and from available data on the GenBank and BOLD dataset as obtained above. A distribution map was created using QGIS.org (2023).

Collections

DISAFA	Dipartimento di Scienze Agrarie, Forestali e Alimentari, University of Torino, Torino, Italy
FSCA	Florida State Collection of Arthropods, Gainesville, United States
INRAE	INRAE UMR Institut Sophia Agrobiotech, Sophia-Antipolis, France
MZLU	Lund Museum of Zoology, Lund University, Lund, Sweden
NHMW	Naturhistorisches Museum Wien, Vienna, Austria
NMINH	National Museum of Ireland - Natural History, Dublin, Ireland
OUMNH	Oxford University Museum of Natural History, Oxford, United Kingdom
ZIN	Zoological Institute, St. Petersburg, Russia
ZMMU	Zoological Museum, Lomonosov Moscow State University, Moscow, Russia

The data for the examined specimens were uploaded onto the BOLD platform (www.barcodinglife.org), and the list of material examined was generated as a supplementary spreadsheet file (Suppl. material 4).

Results and discussion

Taxonomy

Two species were detected in our surveys, *Te. truncatus* and *Te. turesis*, which we identified by comparison to type material (Table 1). Doğanlar (2001) simply described morphological characters of *Te. chloropus*. According to Kozlov and Kononova (1983), the sculpture of the posterior margin of mesoscutum was not clear, and this character is considerably variable in the specimens examined by us. The color of the femora weakly matches with the types of both species, but this is difficult to assess because the types are very old. The description of the shape of A2–A4 of males of both species corresponds with our opinion. The most accurate description for the two species was made by Javahery (1968).

Table 1. Links to images of primary type specimens.

Images of primary type	Original combination	Valid name
https://zenodo.org/record/7846207	*Teleas truncatus* Nees von Esenbeck	*Telenomus truncatus* (Nees von Esenbeck)
https://zenodo.org/record/7622511	*Teleas Linnei* Nees von Esenbeck	*Telenomus truncatus* (Nees von Esenbeck)
https://zenodo.org/record/7846277	*Telenomus Turesis* Walker	*Telenomus turesis* Walker
https://www.flickr.com/photos/127240649@N08/50121706058/in/photostream/	*Phanurus chloropus* Thomson	*Telenomus turesis* Walker
https://zenodo.org/record/7442921	*Telenomus heydeni* Mayr	*Telenomus truncatus* (Nees von Esenbeck)
https://zenodo.org/record/7443068	*Telenomus Sokolowi* Mayr	*Telenomus turesis* Walker

According to Graham (1988a), the most detailed description of *Te. chloropus* was provided by Johnson (1984). Graham, referring to the postocellar furrows behind the lateral ocelli, reported by Johnson (1984), wrote that there are at least two "European forms" of this character: the form, described as *Te. sokolovi* by Javahery (1968) with short, weak postocellar furrows extending inward behind the lateral ocelli, and the form erroneously described as *Te. truncatus* Nees by Javahery (1968) with long, marked postocellar furrows extending inward behind the lateral ocelli. Graham associated the character of eyes densely covered with moderately long hairs and eyes sparsely covered with short hairs, with the two forms, respectively. The two forms described by Graham concur respectively with our concepts of *Te. turesis* and *Te. truncatus*.

The present study reports a similar composition of hosts for *Te. truncatus* and *Te. turesis* as reported by previous authors (Javahery 1968; Kozlov 1968; Samin et al. 2010) but with some new records (Table 2). Some other dubious records from Coleoptera eggs are reported for both species (Kieffer 1926; Samin et al. 2010).

Table 2. Host associations. "X" indicates an association recorded during the present study.

	Stink bugs species	***Telenomus turesis***	***Te. truncatus***
Pentatomidae	*Acrosternum* sp.	X	
	Aelia acuminata (L.)	(Kozlov 1968)	
	Aelia furcula Fieber	(Kozlov 1968)	
	Aelia rostrata Boheman	(Kozlov 1968), X	
	Arma custos (F.)	X	
	Carpocoris sp.	X	X
	Carpocoris fuscispinus (Boheman)	(Kozlov 1968)	
	Dolycoris baccarum (L.)	(Kozlov 1968; Samin et al. 2010), X	X
	Graphosoma lineatum (L.)	(Kozlov 1968)	X
	Halyomorpha halys (Stål)	X	X
	Holcostethus strictus (F.)	X	
	Palomena prasina (L.)	(Kozlov 1968), X	(Kozlov 1968), X
	Palomena viridissima (Poda)	(Kozlov 1968)	(Kozlov 1968)
	Picromerus bidens (L.)	(Javahery 1968)	(Javahery 1968)
	Piezodorus lituratus (F.)	(Javahery 1968), X	(Javahery 1968), X
	Rhaphigaster nebulosa (Poda)		(Kozlov 1968), X
Scutelleridae	*Eurygaster austriaca* (Schrank)	(Kozlov 1968)	
	Eurygaster integriceps Puton	(Javahery 1968; Kozlov 1968; Samin et al. 2010)	(Javahery 1968)
	Eurygaster maura (L.)	(Kozlov 1968), X	
	Eurygaster testudinaria (Geoffroy)	(Samin et al. 2010)	

Diagnosis

We identified specimens of *Te. truncatus* and *Te. turesis* based on characters in the following species treatments:

***Telenomus truncatus* (Nees von Esenbeck)**
Figs 1–4, 8A, C, E, 9A, C, E

Teleas truncatus Nees von Esenbeck, 1834: 289 (original description); Graham 1988b: 28 (type information); Graham 1988a: 86 (lectotype designation).

Teleas Linnei Nees von Esenbeck, 1834: 288 (original description); Mayr 1879: 707 (synonym of *Telenomus truncatus* (Nees von Esenbeck)); Graham 1988b: 28 (type information); Johnson 1992: 617 (type information).

Teleas Zetterstedtii Ratzeburg 1844: 185 (original description); Mayr 1879: 707 (synonym of *Telenomus truncatus* (Nees von Esenbeck)).

Telenomus truncatus (Nees von Esenbeck): Mayr 1879: 700, 702, 707 (description, generic transfer, synonymy, keyed); Kieffer 1926: 25, 26, 31(description, keyed); Javahery 1968: 431 (description, keyed); Szabó 1978: 219, 222 (description, neotype designation, keyed); Johnson 1984b: 41 (taxonomic status, neotype information); Johnson 1992: 617 (cataloged, type information); Mineo 2012: 61 (placed in *turesis* group).

Telenomus Heydeni Mayr, 1879: 702, 706 (original description, keyed). syn. nov.

Telenomus Giraudi Kieffer, 1906: 163 (original description).
Prophanurus Giraudi Kieffer: Kieffer 1912: 46, 58 (description, generic transfer).
Prophanurus Heydeni (Mayr): Kieffer 1912: 59 (description, generic transfer).
Prophanurus Truncatus (Nees von Esenbeck): Kieffer 1912: 47, 58 (description, generic transfer).
Telenomus giraudi Kieffer: Kieffer 1926: 25, 26, 31 (description, keyed); Szabó 1978: 221 (junior synonym of *Telenomus heydeni* Mayr).
Telenomus heydeni Mayr: Kieffer 1926: 26, 36 (description, keyed); Kozlov 1967: 360, 364, 372 (description, lectotype designation); Kozlov 1968: 216 (description, keyed); Voegelé 1969: 148 (keyed); Mineo 1977: 84 (description of preimaginal stages); Kozlov 1978: 638, 644 (keyed); Szabó 1978: 219, 221 (description, lectotype designation, keyed); Johnson 1992: 591 (cataloged, type information); Petrov 1994: 276 (keyed); Mineo 2012: 61 (placed in *turesis* group); Timokhov 2019: 55 (cataloged); Gokhman and Timokhov 2020: 216 (karyotype).
Telenomus (*Telenomus*) *heydeni* Mayr: Kozlov and Kononova 1983: 140, 164 (description, subgeneric assignment, keyed); Kononova 2014: 141, 144 (description, keyed).
Teleas linnei Nees von Esenbeck: Graham 1988a: 88 (lectotype designation).

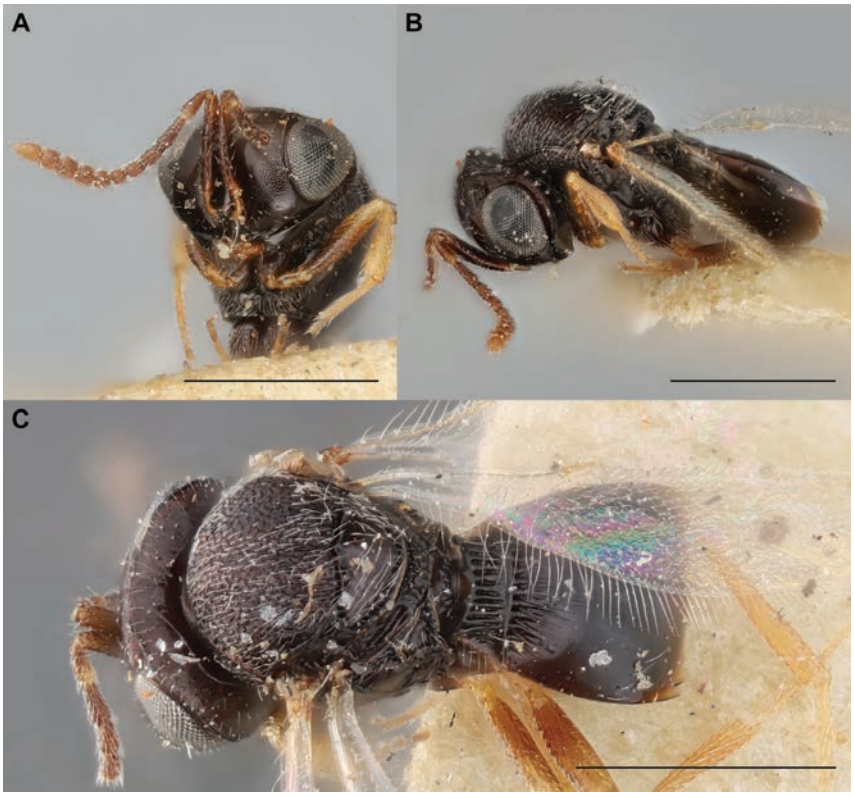

Figure 1. *Telenomus truncatus*. Female lectotype (OXUM 0011): head in frontal view (**A**); habitus in lateral view (**B**); habitus in dorsal view (**C**). Scale bars: 0.5 mm.

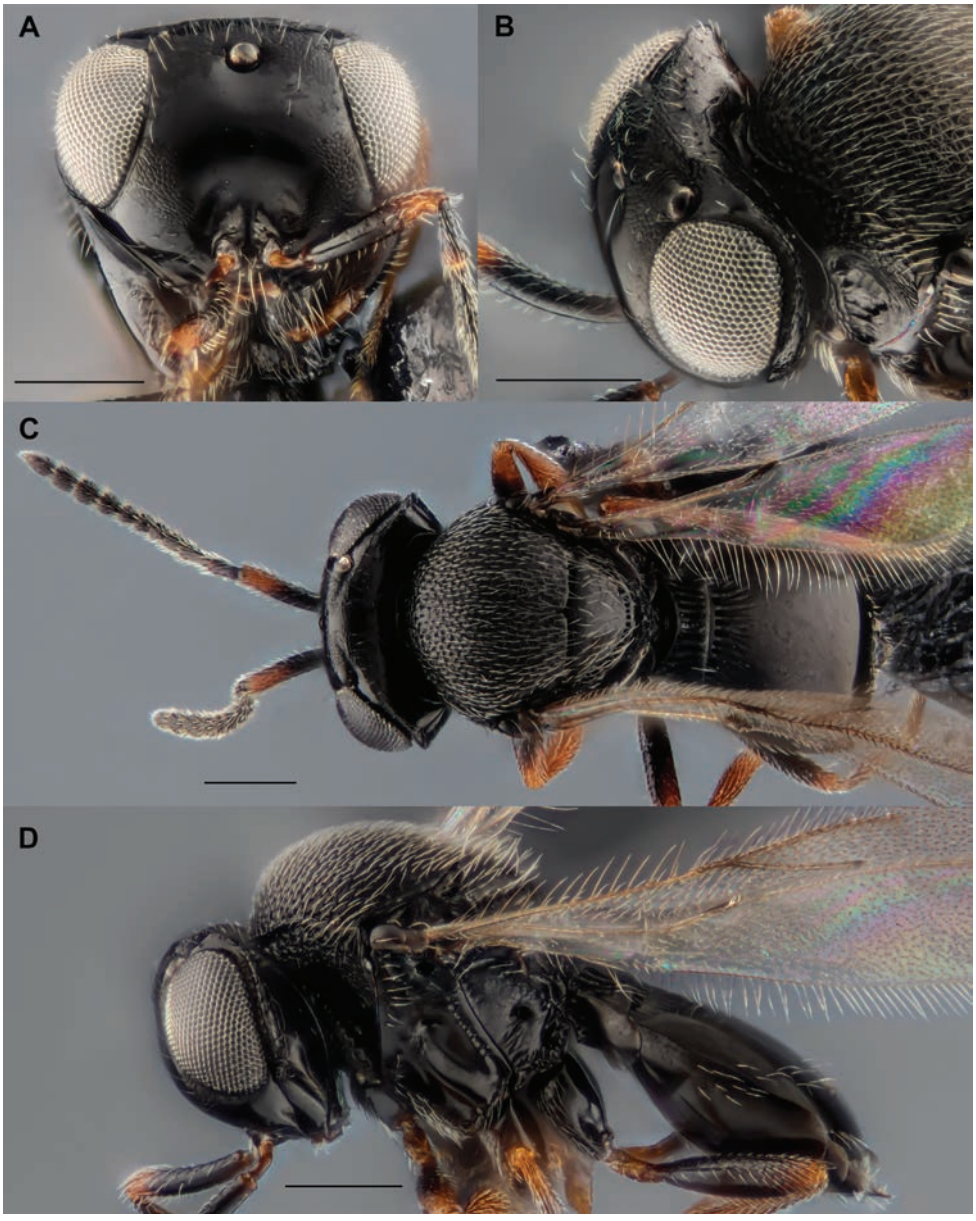

Figure 2. *Telenomus truncatus*. Female (DISAFA-FT HYM-0519): head in frontal view (**A**); head in dorso-lateral view (**B**); habitus in dorsal view (**C**); habitus in lateral view (**D**). Scale bars: 0.2 mm.

Diagnostic characters. Female. ***Head*****:** compound eye with sparse and short setation throughout (Figs 1A, 2B, 3B, 4A, 8C); vertex shallowly and evenly granulate (Figs 1C, 2B, 3B, 4A, 8C); occipital carina complete (Fig. 8A); hyperoccipital carina present directly behind the lateral ocellus, carina sharp and well defined, sculpture smooth along

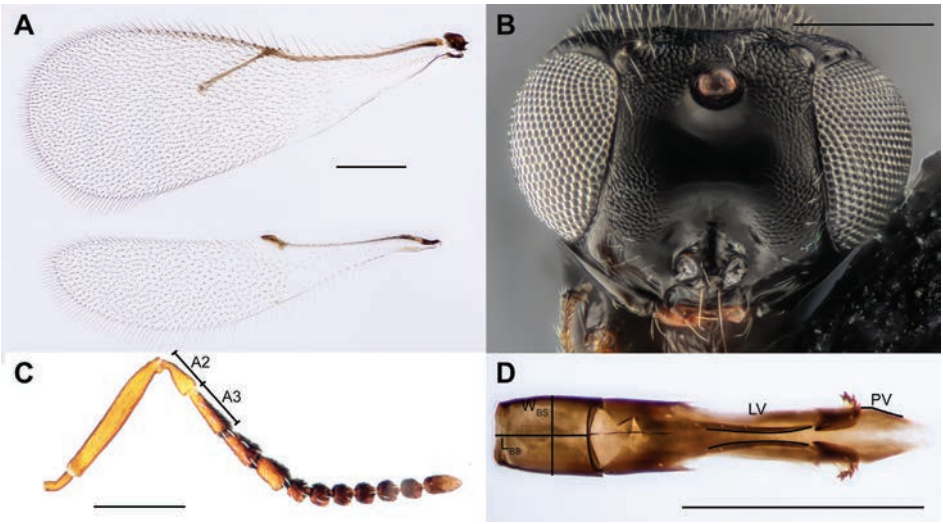

Figure 3. *Telenomus truncatus*. Female (DISAFA-FT HYM-0650): fore and hind wings (**A**). Male (DISAFA-FT HYM-0516): head in frontal view (**B**); antenna (**C**); genitalia (**D**). Scale bars: 0.2 mm.

posterior margin of carina (Fig. 8C); outer orbital furrow wide (2–2.5 times as wide as an ommatidium) (Fig. 8C); clypeal sensillum present above the line connecting the medial and lateral clypeal setae (Fig. 8E).

***Mesosoma*:** mesoscutal humeral sulcus (mshs) present as a smooth furrow (Figs 1B, 2D, 9A); metapleural carina in antero-dorsal area of metapleuron (pdms, between metapleural arm and propodeal spiracle) complete, distinct and strong (Fig. 9A); surface of the furrow between metanotal trough and metascutellar arm (msn) usually crenulate (Fig. 9A); mesoscutum longitudinally strigose posteriorly (Fig. 9C); median mesoscutal sulcus present in largest specimens, barely visible in smaller ones. Fore wing postmarginal (pm) and stigmal (st) veins length ratio: pm:st = 1.9:1 (n=20) (Fig. 3A). Hind femora dark brown with yellowish tips (Fig. 2C, D).

***Metasoma*:** first metasomal tergite with one or rarely two pairs of sublateral setae (ss) (Figs 1C, 2C, 9E).

Male. *Head*: antennal length ratio A3:A2 = 1.2:1 (n=20), antennomeres A6–A11 bead-like, subequal (Fig. 3C). Genitalia: basal ring ratio: Length: Width = 6:5; minimum distance between inner margin of laminae volsellares: narrow (laminae volsellares lyre-shaped); external margin of penis valve more intensely sclerotized curved and distally converging (Fig. 3D). Hind femora yellow to pale brown. Other morphological characters as in female.

From the analysis of the lectotype of *Te. heydeni* (NHMW-HYM#0005387), the combination of morphological characters (Fig. 4) coincides with the characters of the lectotype of *Te. truncatus* (OXUM 0011), and the length ratio between the A3 and A2 antennomeres (Fig. 4A) matches with that of the male of *Te. truncatus* (Fig. 3C). Therefore, *Te. heydeni* is here considered a junior synonym of *Te. truncatus*.

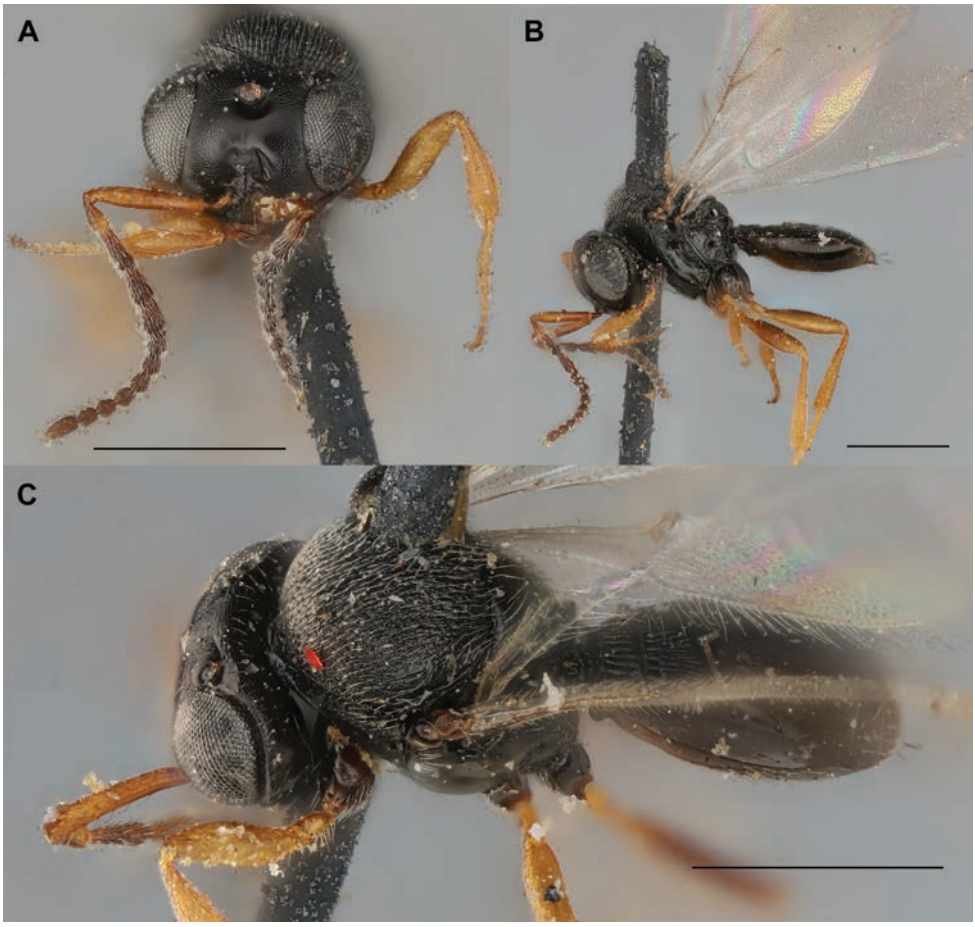

Figure 4. *Telenomus heydeni*. Male lectotype (NHMW-HYM#0005387): head in frontal view (**A**); habitus in lateral view (**B**); habitus in dorso-lateral view (**C**). Scale bars: 0.5 mm.

Biological information. Host species associated: Table 2. The specimen DISAFA-FT HYM-0657 - OQ466097 was found overwintering in November in *Viburnum* leaf mines created by *P. viburni*; the specimens AVT001908 and AVT001909 were found already dead in egg-mass of *Lymantria monacha* (Linnaeus) (Lepidoptera, Erebidae), presumably after wintering.

DNA barcoding. Barcode sequences were obtained from 49 specimens of *Te. truncatus*. Pairwise distance values within species are shown in Suppl. material 3. The genetic distances between the insects identified as the same species were between 0.000 and 0.074 (mean 0.013 +/- 0.003). The analysis of *COI* sequences discovered that *Te. truncatus* includes the specimen OL631282, previously identified as *Telenomus* sp. (Ricupero et al., 2022) (Suppl. material 1).

Distribution. Suppl. material 2

Material examined. Suppl. material 4.

***Telenomus turesis* Walker**
Figs 5–7, 8B, D, F, 9B, D, F

Telenomus Turesis Walker, 1836: 353 (original description).
Phanurus chloropus Thomson, 1861: 173 (original description).
Telenomus turesis Walker: Mayr 1879: 699, 705 (description, keyed). Fergusson 1984: 232 (lectotype designation); Mineo et al. 2010: 116 (synonymy, type information, new distribution record for Ireland); Johnson 1992: 617 (cataloged, type information); Timokhov 2019: 55 (cataloged); Gokhman and Timokhov 2020: 216 (karyotype).
Telenomus Sokolowi Mayr, 1897: 442 (original description); Johnson 1992: 579 (type information).
Telenomus Mayri Sokolov, 1904: 29 (original description).
Aphanurus Turesis (Walker): Kieffer 1912: 75 (description, generic transfer).
Prophanurus Sokolowi (Mayr): Kieffer 1912: 53, 60 (description, generic transfer)
Microphanurus turesis (Walker): Kieffer 1926: 92, 98 (description, generic transfer, keyed).
Telenomus chloropus (Thomson): Kieffer 1926: 25, 29 (description, keyed); Kozlov 1967: 361, 364, 371 (lectotype designation, keyed); Kozlov 1968: 216, 217 (description, keyed); Boldaruyev 1969: 161, 170 (description, keyed); Voegelé 1969: 148 (keyed); Kozlov 1978: 638, 643 (keyed); Johnson 1984b: 39, 65 (description, keyed); Graham 1988a: 86 (taxonomic status); Johnson 1992: 579 (cataloged, type information); Petrov 1994: 276 (keyed); Doğanlar 2001: 112 (description); O'Connor and Mineo 2009: 106 (distribution); Mineo et al. 2010: 116 (junior synonym of *Telenomus turesis* Walker, possible type information).
Telenomus sokolowi Mayr: Kieffer 1926: 25, 26, 34 (description, keyed).
Telenomus tischleri Nixon, 1939: 129 (original description); Kozlov 1967: 364 (junior synonym of *Telenomus chloropus* (Thomson)); Johnson 1992: 580 (type information).
Telenomus sokolovi Mayr: Meier 1940: 79, 80 (description, keyed); Rjachovskij 1959: 82 (keyed); Kozlov 1963: 295 (synonymy); Viktorov 1967: 91 (keyed); Kozlov 1967: 361, 364 (lectotype designation, junior synonym of *Telenomus chloropus* (Thomson)); Javahery 1968: 431, 434 (description, keyed).
Telenomus mayri Sokolov: Kozlov 1963: 295, 296 (junior synonoym of *Telenomus sokolovi* Mayr).
Trissolcus turesis (Walker): Fergusson 1978: 120 (generic transfer).
Telenomus (*Telenomus*) *chloropus* (Thomson): Kozlov and Kononova 1983: 140, 161 (keyed, description, subgeneric assignment); Kononova 1995: 100 (keyed); Kononova and Proshchalykin 2012: 135 (cataloged); Kononova 2014: 141, 142 (description, keyed).

Diagnostic characters. Female. ***Head*****:** dense setation on compound eyes (Figs 6A, 7B, 8D); granulate sculpture on the vertex (Figs 5C, 6B, 8D); occipital carina incomplete (Fig. 8B); hyperoccipital carina directly behind the lateral ocelli weakly indicated (almost absent in smaller specimens) (Figs 5C, 6B, 8D); outer orbital furrow narrow, (1–1.5 times as wide as an ommatidium) (Fig. 8D); clypeal sensillum present below the line connecting the medial and lateral clypeal setae (Fig. 8F).

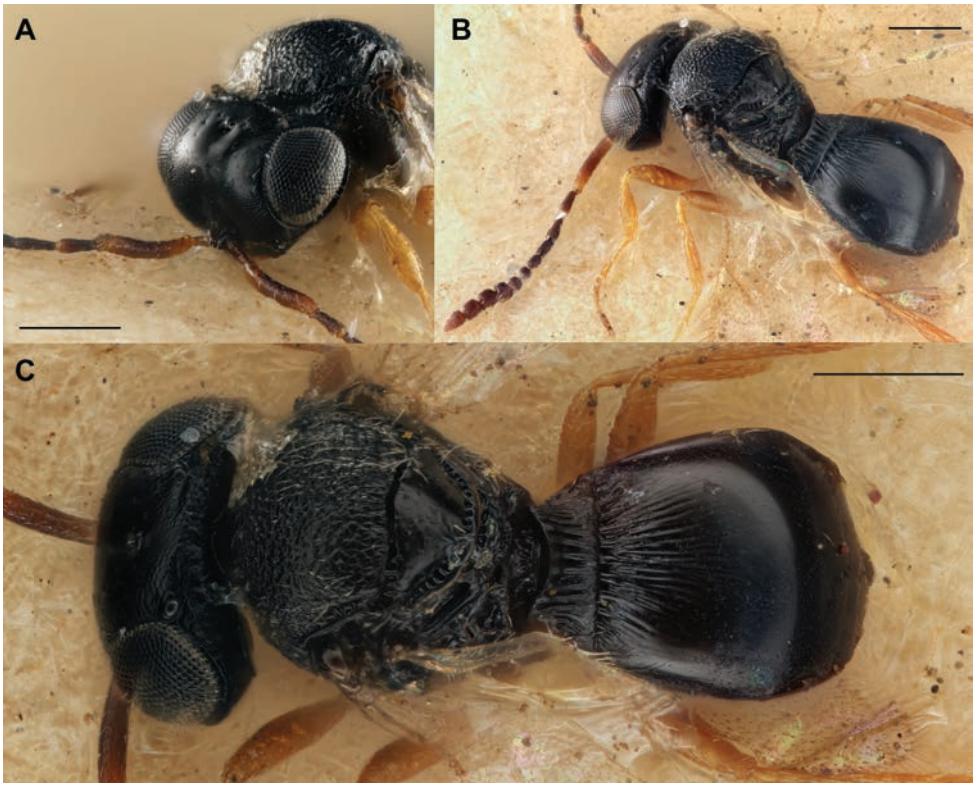

Figure 5. *Telenomus turesis*. Female lectotype (NMINH:2018:11:54): head in latero-frontal view (**A**); habitus in dorso-lateral view (**B**); habitus in dorsal view (**C**). Scale bars: 0.2 mm.

***Mesosoma*:** mesoscutal humeral sulcus (mshs) indicated by cells (Figs 6B, 9B); metapleural carinain antero-dorsal area of metapleuron (pdms, between metapleural arm and propodeal spiracle) incomplete, irregular (Fig. 9B); surface of the furrow between metanotal trough and metascutellar arm (mns) smooth (Fig. 9B); macrosculpture of mesoscutum imbricate (Fig. 9D). Fore wing postmarginal (pm) and stigmal (st) veins length ratio: pm:st = 1.9:1 (n=20) (Fig. 7A). Hind femora yellow to pale brown (Figs 5C, 6D).

***Metasoma*:** first metasomal tergite with one or rarely two pairs of sublateral setae (ss) (Figs 6C, D, 9F).

Male. Antennal length ratio A3:A2 = 2:1 (n=20), antennomeres A6–A11 elongate, uniform in length (Fig. 7C). Genitalia: basal ring (BS) ratio: Length:Width = 7:4; minimum distance between inner margin of laminae volsellares (LV): wide; external margin of penis valve (PV) more intensely sclerotized and parallel rods (Fig. 7D). Other morphological characters as in female.

Biological information. Host species associated: Table 2. Three specimens (DISAFA-FT HYM-0667, HYM-0666 - OQ466110, and HYM-0662 - OQ466105) were found overwintering in November in the mines of *P. viburni* in *Viburnum* leaves.

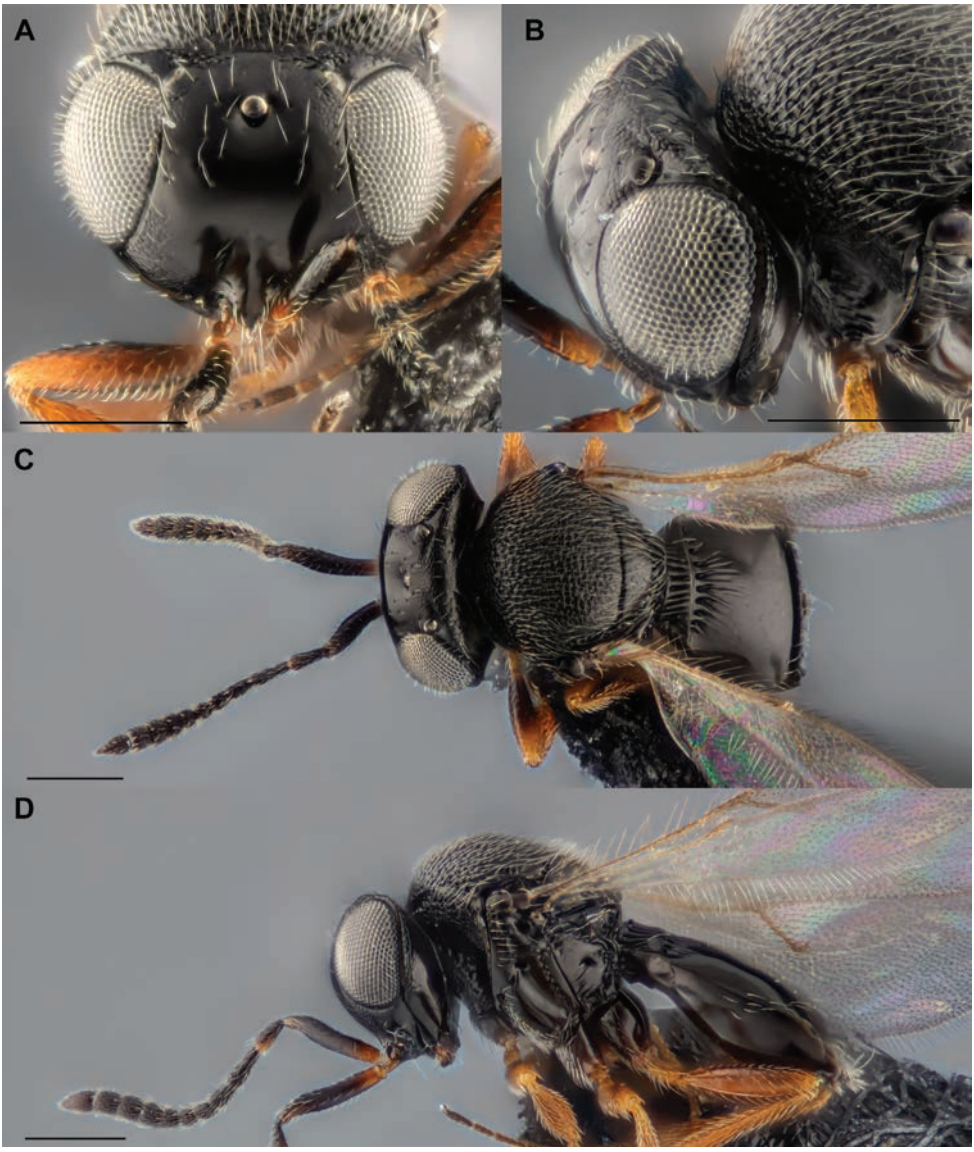

Figure 6. *Telenomus turesis*. Female (DISAFA-FT HYM-0536): head in frontal view (**A**); head in dorsolateral view (**B**); habitus in dorsal view (**C**); habitus in lateral view (**D**). Scale bars: 0.2 mm.

DNA barcoding. Barcode sequences were obtained from 46 specimens of *Te. turesis*. Pairwise distance values within species are shown in Suppl. material 3. The genetic distances between the insects identified as the same species were between 0.000 and 0.096 (mean 0.015 +/- 0.004).

The analysis of *COI* sequences discovered that *Te. turesis* includes samples KY843528 (Ashfaq et al. 2022); the specimens BIOUG55155-D12, BIOUG16220-G06,

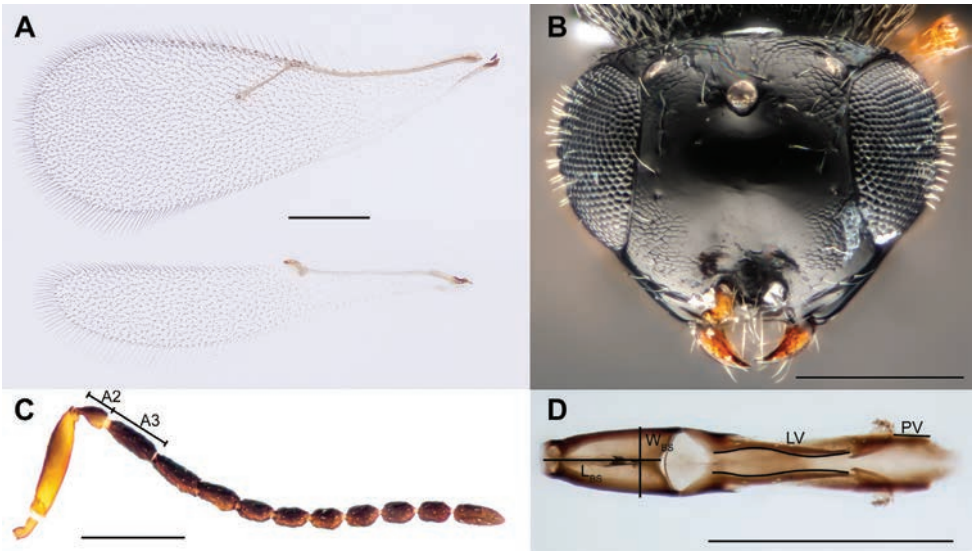

Figure 7. *Telenomus turesis*. Female (DISAFA-FT HYM-0625): fore and hind wings (**A**). Male (DISAFA-FT HYM-0532): head in frontal view (**B**); antenna (**C**); genitalia (**D**). Scale bars: 0.2 mm.

BIOUG15112-C08, BIOUG36831-G01, BIOUG27850-E03, and KF303516 (Gariepy et al. 2014a), previously identified as *Te. chloropus*, and the sample OK562072 (Ozdemir et al. 2022) (Suppl. material 1).

Distribution. Suppl. material 2.

Material examined. Suppl. material 4.

Telenomus gifuensis Ashmead

Fig. 1A–C

Diagnosis. The distance between the inner margin of the compound eyes is smaller than the width of the compound eyes in frontal view (Fig. 10A), and the presence of two sublateral setae on the first tergite (Fig. 10B) separate this species from *Te. truncatus* (figs 1–45), and *Te. turesis* (Figs 5–7). In addition, *Te. gifuensis* can be distinguished from *Te. turesis* by the presence of a median mesoscutal line (mml) on the posterior margin of the mesoscutum (Fig. 10C). Mahmoud and Lim (2008) reported this species as a solitary parasitoid of *D. baccarum*, *Piezodorus hybneri* (Gmelin), *Riptortus clavatus* (Thunberg), and *Nezara antennata* Scott. We also add *Piezodorus rubrofasciatus* (Fabricius) to the list of species as a new associated host (specimen AVT002233). Apart from this last record from Korea and the original description from Japan (Ashmead 1904), there are no further reports outside of the eastern Palearctic region.

Material examined. Suppl. material 4.

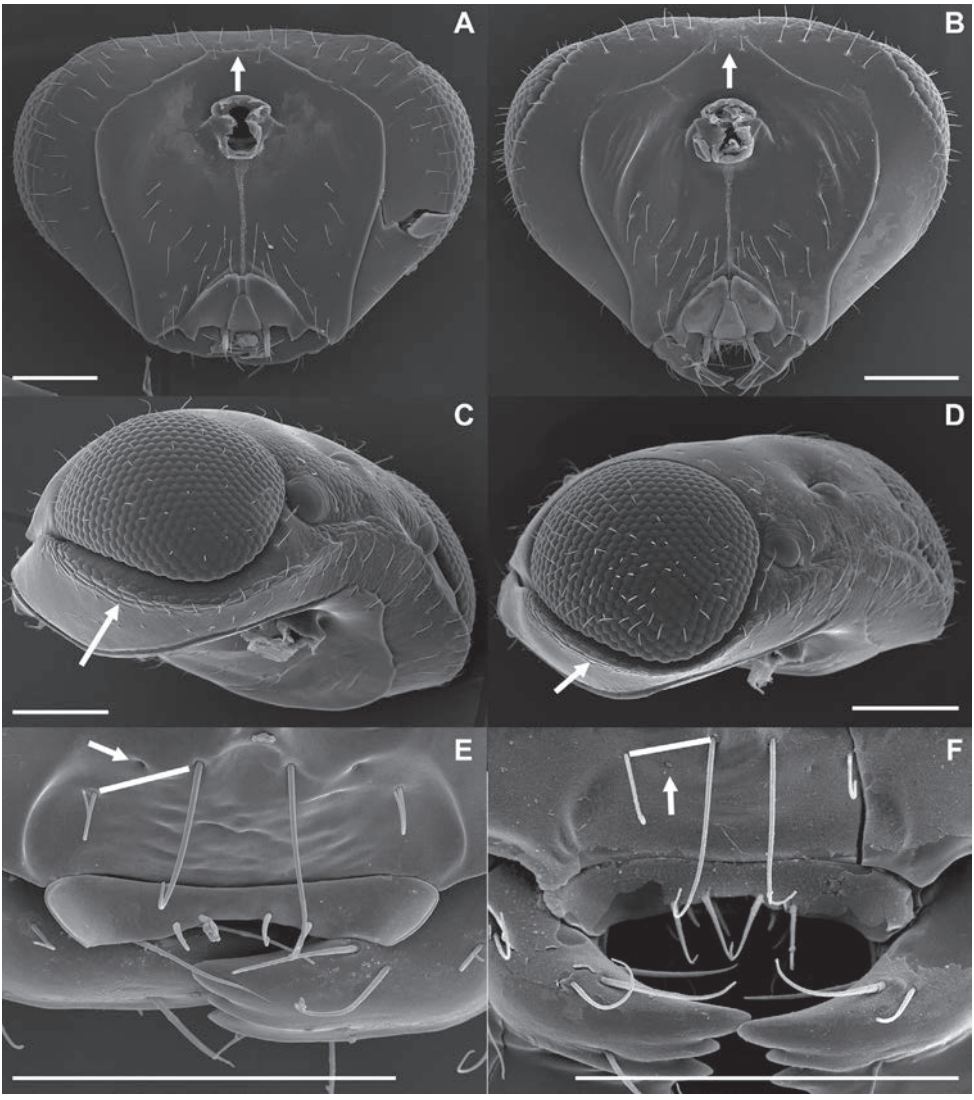

Figure 8. Head in posterior view: *Telenomus truncatus* (**A**) and *Te. turesis* (**B**); head in dorso-lateral view: *Te. truncatus* (**C**) and *Te. turesis* (**D**); clypeus: *Te. truncatus* (**E**) and *Te. turesis* (**F**). Scale bars: 0.1 mm.

Key to species

1 Metasomal tergite 1 with two pairs of sublateral setae (Fig. 10B); frons narrow, minimum distance between inner margin of compound eyes less than eye width in frontal view (Fig. 10A) ..... ***Telenomus gifuensis* Ashmead**

– Metasomal tergite 1 with one pair of sublateral setae (Fig. 9E, F); frons wide, minimum distance between inner margin of compound eyes more than eye width in frontal view (Figs 2A, 3B, 6A, 7B) **2**

2 Female **3**
– Male **4**
3 Compound eyes with sparse, short setation throughout (Figs 1A, 2B, 3B, 4A, 8C); hyperoccipital carina present directly posterior to the lateral ocellus; hyperoccipital carina sharp and smooth anteriorly, and sculpture on the surface behind the vertex smooth (Figs 2B, 8C); median and posterior femora dark brown with yellowish tips (Fig. 2D) ..... ***Telenomus truncatus*** **(Nees von Esenbeck)**
– Compound eyes with dense setation throughout (Figs 6A, 7B, 8D); hyperoccipital carina present directly posterior to the lateral ocellus but weakly sharp, and sculpture on the surface behind the vertex imbricate (Figs 5C, 6B, 8D); median and posterior femora yellow to pale brown (Figs 5C, 6D)..... ***Telenomus turesis*** **Walker**
4 Compound eyes with sparse and short setation throughout (Fig. 4B); antennal length ratio A3:A2 = 1.2:1 (Fig. 3C)... ***Telenomus truncatus*** **(Nees von Esenbeck)**
– Compound eyes with dense setation throughout (Fig. 7B); antennal length ratio A3:A2 = 2:1 (Fig. 7C) ..... ***Telenomus turesis*** **Walker**

Molecular analysis

The analysis involved 105 nucleotide sequences. All positions with less than 95% site coverage were eliminated, i.e., fewer than 5% alignment gaps, missing data, and ambiguous bases were allowed at any position (partial deletion option). There was a total of 492 positions in the final dataset. Barcode sequences were obtained from 95 *Telenomus* specimens (Suppl. material 1) from the Palearctic Region. They were compared with eight sequences of specimens from the Nearctic Region identified as *Te. cristatus* Johnson (n: 4), *Te. persimilis* Ashmead (n: 3), and *Te. sanctivincenti* Ashmead (n: 1). The mean pairwise distances between the samples identified as the same species were much lower than those observed between the samples identified as different species (Suppl. material 3), as expected. The average of the pairwise evolutionary divergence (ED) between Palearctic and Nearctic *Telenomus* is 0.418 +/- 0.6671 (respectively, n: 95 and n: 8, 1000 replicates). The ED average in the two Palearctic species is 0.431 +/- 1.106 (*Te. truncatus* n: 49 and *Te. turesis* n: 46, 1000 replicates). The Blast search showed that the sequences of *Te. truncatus* have a 99.67% sequence identity with the GenBank sequence from *Telenomus* sp. (accession no. OL631282). The sequences from *Te. turesis* showed a 99.58% identity with a *Te. turesis* GenBank sequence (accession no. KY843528), a 99.38% identity with the GenBank and BOLD sequences from *Te. chloropus* (accession no. KF303516, BIOUG55155-D12, BIOUG16220-G06, BIOUG15112-C08, BIOUG36831-G01, BIOUG27850-E03), and a 99.84% identity with a *Te. turesis* GenBank sequence (accession no. OK562072). The ED average between sequences is 0.013 +/- 0.0028 (n. 49, 1000 replicates) within *Te. truncatus* and 0.241 +/- 0.0015 (n: 46, 1000 replicates) within *Te. turesis* (Suppl. material 3). The presence of different haplotypes in each species (Suppl. material 1) suggests that it may be necessary to sequence multiple molecular markers to investigate the different clades for both species.

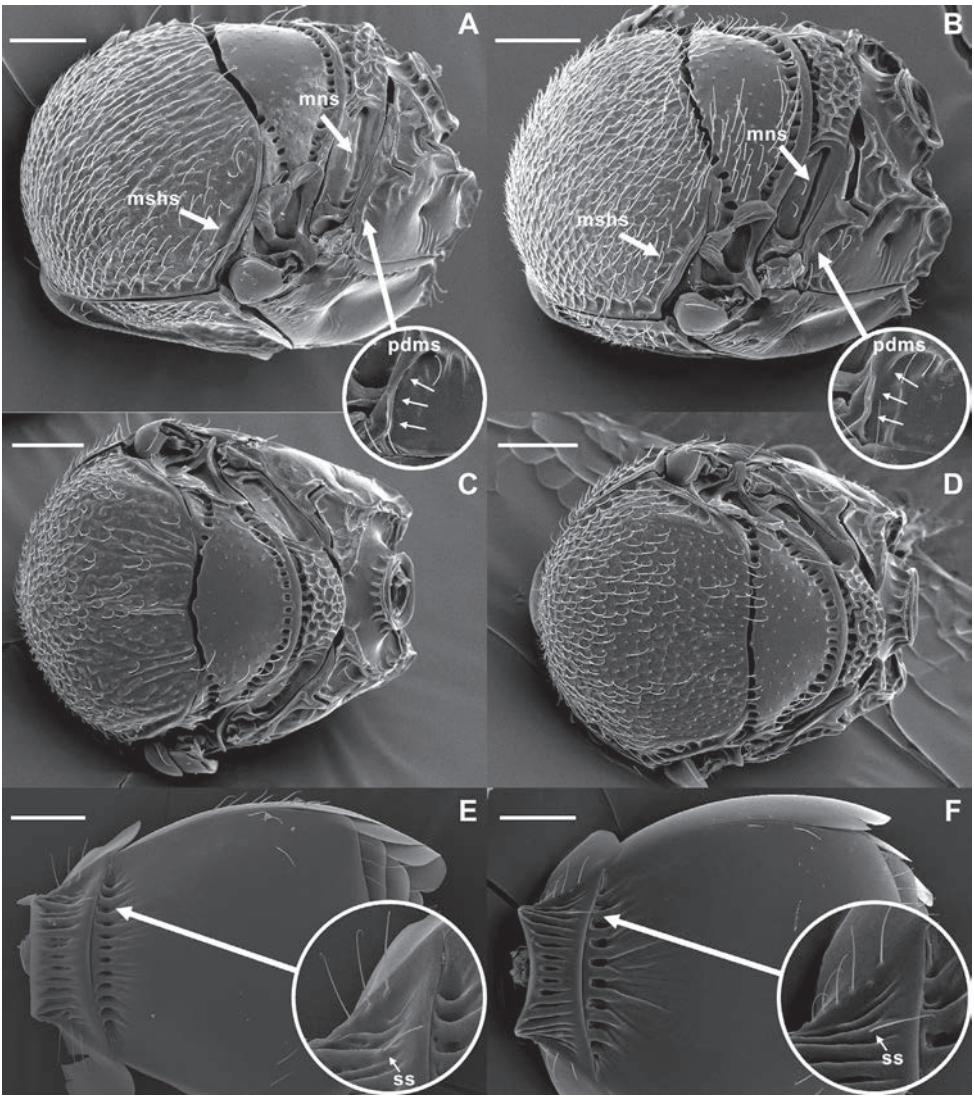

Figure 9. Thorax in dorso-lateral view: *Telenomus truncatus* (**A**) and *Te. turesis* (**B**); thorax in dorsal view: *Te. truncatus* (**C**) and *Te. turesis* (**D**); abdomen in dorsal view (ss: sublateral setae): *Te. truncatus* (**E**) and *Te. turesis* (**F**). Scale bars: 0.1 mm.

Conclusion

In recent years, researchers have limited the identification of *Telenomus* to genus level or grouped all of the specimens, referring only to *Te. chloropus* when they emerged from eggs of pentatomids in western Palearctic region. Despite the setbacks of these misidentifications, the taxonomy of Palearctic species of *Telenomus* associated with stink bugs has advanced, and we here provide a more solid foundation for continued

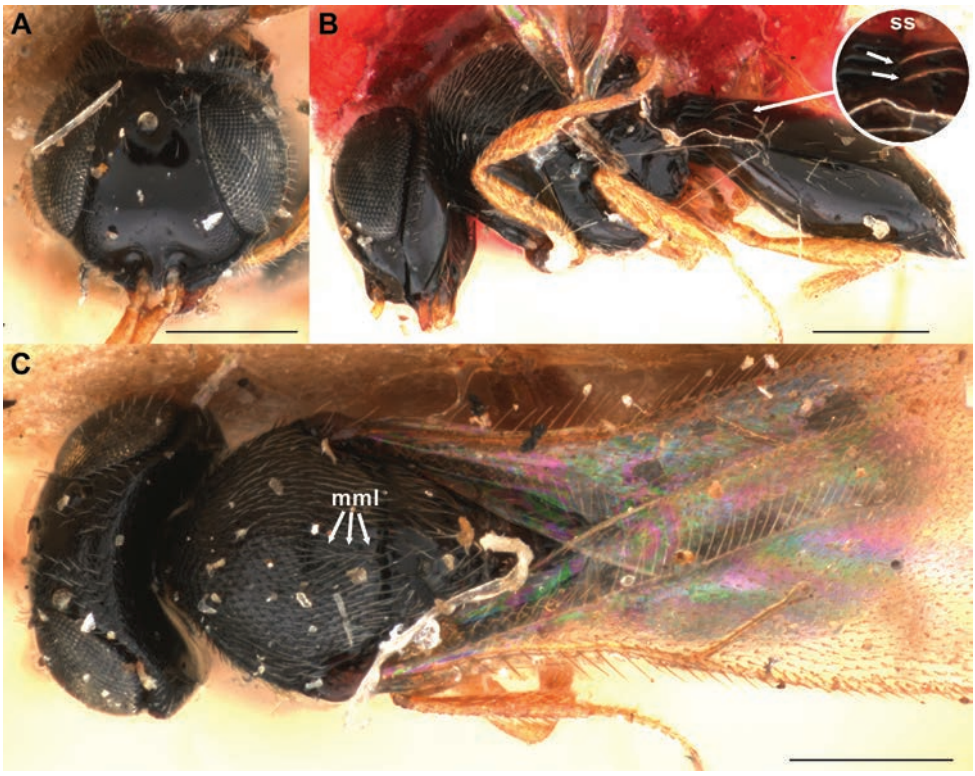

Figure 10. *Telenomus gifuensis*. Female paralectotype (USNMENT01109267): head in frontal view (**A**); female lectotype (USNMENT01109265): habitus in lateral view (**B**); female paralectotype (USNMENT01109266): habitus in dorsal view (**C**). Scale bars: 0.2 mm.

research. For the first time, the West Palearctic species of the *Te. podisi* species group associated with the Pentatomidae can be reliably identified, with diagnostic tools based on multiple lines of evidence. The logical next test of our species concepts would be interbreeding studies, as were performed for cryptic species of the genus *Trissolcus* (Matsuo et al. 2014; Tortorici et al. 2019; Moraglio et al. 2021a). The identification of European *Telenomus* species that attack stink bugs also provides new prospects for a detailed study of their biology, which may lead to improved pest management. Furthermore, identification of the wasps from new localities and hosts will expand the distributional and biological knowledge that is available from specimens in collections.

Acknowledgements

This study was carried out within the Agritech National Research Center and received funding from the European Union Next-GenerationEU (PIANO NAZIONALE DI RIPRESA E RESILIENZA (PNRR) – MISSIONE 4 COMPONENTE 2, INVESTIMENTO 1.4 – D.D. 1032 17/06/2022, CN00000022). This manuscript reflects

only the authors' views and opinions; neither the European Union nor the European Commission can be considered responsible for them. Elijah Talamas was supported by the Florida Department of Agriculture and Consumer Services, Division of Plant Industry. Some of the sequence data were produced by Matthew R. Moore, Cheryl G. Roberts and Lynn A. Combee at the Molecular Diagnostics Laboratory (FDACS/DPI). We are very thankful to the colleagues from the Interdepartmental Laboratory of Electron Microscopy (Faculty of Biology, Lomonosov Moscow State University) for the provided facilities and help during electron microscopic studies.

We are also grateful to Silvia Teresa Moraglio, Paolo Navone, and Sara Scovero for collecting specimens used in our analyses.

References

Abram PK, Hoelmer KA, Acebes-Doria AL, Andrews H, Beers EH, Bergh JC, Bessin R, Biddinger D, Botch P, Buffington ML, Cornelius ML, Costi E, Delfosse ES, Dieckhoff C, Dobson R, Donais Z, Grieshop M, Hamilton G, Haye T, Hedstrom C, Herlihy MV, Hoddle MS, Hooks CRR, Jentsch PJ, Joshi NK, Kuhar TP, Lara JR, Lee JC, Legrand A, Leskey TC, Lowenstein D, Maistrello L, Mathews CR, Milnes JM, Morrison WR, Nielsen AL, Ogburn EC, Pickett CH, Poley K, Pote J, Radl J, Shrewsbury PM, Talamas EJ, Tavella L, Walgenbach JF, Waterworth R, Weber DC, Welty C, Wiman NG (2017) Indigenous arthropod natural enemies of the invasive brown marmorated stink bug in North America and Europe. Journal of Pest Science 90: 1009–1020. https://doi.org/10.1007/s10340-017-0891-7

Açikgöz M, Gözüaçik C (2021) Studies on egg parasitoid, *Trissolcus* (Hymenoptera: Scelionidae) species of sunn pest *Eurygaster* spp. in cereal planting areas: iğdır, ağrı and van provinces, Turkey. Türkiye Tarımsal Araştırmalar Dergisi 8: 345–351. https://doi.org/10.19159/tutad.998869

Altschul SF, Gish W, Miller W, Myers EW, Lipman DJ (1990) Basic local alignment search tool. Journal of Molecular Biology 215: 403–410. https://doi.org/10.1016/S0022-2836(05)80360-2

Andreadis SS, Gogolashvili NE, Fifis GT, Navrozidis EI, Thomidis T (2021) First Report of Native Parasitoids of *Halyomorpha halys* (Hemiptera: Pentatomidae) in Greece. Insects 12: 984. https://doi.org/10.3390/insects12110984

Ashfaq M, Khan AM, Rasool A, Akhtar S, Nazir N, Ahmed N, Manzoor F, Sones J, Perez K, Sarwar G, Khan AA, Akhter M, Saeed S, Sultana R, Tahir HM, Rafi MA, Iftikhar R, Naseem MT, Masood M, Tufail M, Kumar S, Afzal S, McKeown J, Samejo AA, Khaliq I, D'Souza ML, Mansoor S, Hebert PDN (2022) A DNA barcode survey of insect biodiversity in Pakistan. PeerJ 10: e13267. https://doi.org/10.7717/peerj.13267

Ashmead WH (1904) Descriptions of new Hymenoptera from Japan — I. Journal of the New York Entomological Society 12: 65–84. https://doi.org/10.5281/zenodo.23555

Bin F, Johnson NF (1982) Potential of Telenominae in biocontrol with egg parasitoids (Hym., Scelionidae). Colloques de l'INRA (France) 9: 175–287.

Boldaruyev VO (1969) [Egg parasites of the subfamily Telenominae (Hymenoptera, Scelionidae), reared from the eggs of harmful insects]. Trudy Buryatskogo Instituta Estestvennykh Nauk

Buryatskii Filial Siirskogo Otdeleniya Akademii Nauk SSSR 7: 156–171. https://doi.org/10.5281/zenodo.23600

Bosco L, Moraglio ST, Tavella L (2018) *Halyomorpha halys*, a serious threat for hazelnut in newly invaded areas. Journal of Pest Science 91: 661–670. https://doi.org/10.1007/S10340-017-0937-X

Bout A, Tortorici F, Hamidi R, Warot S, Tavella L, Thomas M (2021) First detection of the adventive egg parasitoid of *Halyomorpha halys* (Stål) (Hemiptera: Pentatomidae) *Trissolcus mitsukurii* (Ashmead) (Hymenoptera: Scelionidae) in France. Insects 12: 761. https://doi.org/10.3390/insects12090761

Buleza VV (1996) Interspecific competition between *Trissolcus grandis* and *Telenomus chloropus* (Hymenoptera, Scelionidae). Zoologicheskiĭ Zhurnal 75: 1174–1181.

Carpenter JM (1999) Towards simultaneous analysis of morphological and molecular data in Hymenoptera. Zoologica Scripta 28: 251–260. https://doi.org/10.1046/j.1463-6409.1999.00009.x

Derjanschi V, Péricart J (2005) 1 Faune de France 90: Hèmiptères Pentatomoidea euro-méditerranéens. Fèdération Francaise des sociétés de Sciences Naturelles, Paris, 494 pp.

Dieckhoff C, Tatman KM, Hoelmer KA (2017) Natural biological control of *Halyomorpha halys* by native egg parasitoids: a multi-year survey in northern Delaware. Journal of Pest Science 90: 1143–1158. https://doi.org/10.1007/S10340-017-0868-6

Doğanlar M (2001) Egg parasitoids of *Rhaphigaster nebulosa* (Poda) (Heteroptera; Pentatomidae) with description of a new species of *Trissolcus* Ashmead (Hymenoptera: Scelionidae). Turkish Journal of Entomology 25: 109–114. https://www.acarindex.com/pdfs/822874

Fergusson NDM (1978) Proctotrupoidea and Ceraphonoidea. In: Fitton MG et al. (Eds) A check list of British insects by George Sidney Kloct and the late Walter Douglas Hincks, 2nd edn. (completely revised). Part 4: Handbooks Ident. Brit. Ins. 11(4). 159 pp. Hymenoptera, 110–126.

Fergusson NDM (1984) The type-specimens and identity of the British species of *Trissolcus* Ashmead (Hym., Proctotrupoidea, Scelionidae). Entomologists Monthly Magazine 120: 229–232. https://doi.org/10.5281/zenodo.24004

Folmer O, Black M, Hoeh W, Lutz R, Vrijenhoek R (1994) DNA primers for amplification of mitochondrial cytochrome c oxidase subunit I from diverse metazoan invertebrates. Molecular Marine Biology and Biotechnology 3: 294–299.

Gariepy TD, Haye T, Zhang J (2014a) A molecular diagnostic tool for the preliminary assessment of host-parasitoid associations in biological control programmes for a new invasive pest. Molecular Ecology 23: 3912–3924. https://doi.org/10.1111/MEC.12515

Gariepy TD, Fraser H, Scott-Dupree CD (2014b) Brown marmorated stink bug (Hemiptera: Pentatomidae) in Canada: recent establishment, occurrence, and pest status in southern Ontario. The Canadian Entomologist 146: 579–582. https://doi.org/10.4039/TCE.2014.4

Giovannini L, Sabbatini Peverieri G, Marianelli L, Rondoni G, Conti E, Roversi PF (2022) Physiological host range of *Trissolcus mitsukurii*, a candidate biological control agent of *Halyomorpha halys* in Europe. Journal of Pest Science 95: 605–618. https://doi.org/10.1007/s10340-021-01415-x

Gokhman VE, Timokhov AV (2020) Karyotypes of four species of the genus *Telenomus* Haliday, 1833 (Hymenoptera: Scelionidae). Russian Entomological Journal 29: 214–217. https://doi.org/10.15298/rusentj.29.2.17

Graham MWR de V (1988a) Madeira insects: additions to the list of parasitic Hymenoptera, with some comments on problems of conservation. Boletim do Museu Municipal do Funchal 40: 75–92. https://doi.org/10.5281/zenodo.24128

Graham MWR de V (1988b) The remains of Nees von Esenbeck's collection of Hymenoptera in the University Museum, Oxford. Entomologists Monthly Magazine 124: 19–35. https://doi.org/10.5281/zenodo.23986

Harris RA (1979) A glossary of surface sculpturing. Occasional Papers in Entomology, State of California Department of Food and Agriculture Division of Plant Industry Laboratory Services 28: 1–31. https://doi.org/10.5281/zenodo.26215

Haye T, Fischer S, Zhang JP, Gariepy TD (2015) Can native egg parasitoids adopt the invasive brown marmorated stink bug, *Halyomorpha halys* (Heteroptera: Pentatomidae), in Europe? Journal of Pest Science 88: 693–705. https://doi.org/10.1007/S10340-015-0671-1

Holthouse MC, Schumm ZR, Talamas EJ, Spears LR, Alston DG (2020) Surveys in northern Utah for egg parasitoids of *Halyomorpha halys* (Stål) (Hemiptera: Pentatomidae) detect *Trissolcus japonicus* (Ashmead) (Hymenoptera: Scelionidae). Biodiversity Data Journal 8: e53363. https://doi.org/10.3897/BDJ.8.E53363

Japoshvili G, Arabuli T, Salakaia M, Tskaruashvili Z, Kirkitadze G, Talamas E (2022) Surveys for *Halyomorpha halys* (Stål) (Hemiptera: Pentatomidae) and its biocontrol potential by parasitic wasps in the Republic of Georgia (Sakartvelo). Phytoparasitica 50: 127–137. https://doi.org/10.1007/S12600-021-00949-1

Javahery M (1968) The egg parasite complex of British Pentatomoidea (Hemiptera): Taxonomy of Telenominae (Hymenoptera: Scelionidae). Transactions of the Royal Entomological Society of London 120: 417–436. https://doi.org/10.1111/j.1365-2311.1968.tb00345.x

Johnson NF (1981) The New World species of the *Telenomus nigricornis* group (Hymenoptera: Scelionidae). Annals of the Entomological Society of America: 73–78. https://doi.org/10.1093/aesa/74.1.73

Johnson NF (1984a) Revision of the Nearctic species of the *Trissolcus flavipes* group (Hymenoptera: Scelionidae). Proceedings of the Entomological Society of Washington 86: 797–807. https://doi.org/10.5281/zenodo.24227

Johnson NF (1984b) Systematics of Nearctic *Telenomus*: classification and revisions of the *podisi* and *phymatae* species groups (Hymenoptera: Scelionidae). Bulletin of the Ohio Biological Survey 6: 1–113. https://doi.org/10.5281/zenodo.23887

Johnson NF (1987) Systematics of New World *Trissolcus*, a genus of pentatomid egg-parasites (Hymenoptera: Scelionidae): Neotropical species of the *flavipes* group. Journal of Natural History 21: 285–304. https://doi.org/10.1080/00222938700771021

Johnson NF (1991) Revision of Australasian *Trissolcus* species (Hymenoptera: Scelionidae). Invertebrate Systematics 5: 211–239. https://doi.org/10.1071/IT9910211

Johnson NF (1992) Catalog of world Proctotrupoidea excluding Platygastridae. Memoirs of the American Entomological Institute 51: 1–825. https://doi.org/10.5281/zenodo.23657

Johnson NF, Bin F (1982) Species of *Telenomus* (Hym., Scelionidae), parasitoids of stalked eggs of Neuroptera (Chrysopidae and Berothidae). Redia 65: 189–206. https://doi.org/10.5281/zenodo.24019

Jones AL, Jennings DE, Hooks CRR, Shrewsbury PM (2017) Field surveys of egg mortality and indigenous egg parasitoids of the brown marmorated stink bug, *Halyomorpha halys*, in

ornamental nurseries in the mid-Atlantic region of the USA. Journal of Pest Science 90: 1159–1168. https://doi.org/10.1007/S10340-017-0890-8

Kaartinen R, Stone GN, Hearn J, Lohse K, Roslin T (2010) Revealing secret liaisons: DNA barcoding changes our understanding of food webs. Ecological Entomology 35: 623–638. https://doi.org/10.1111/J.1365-2311.2010.01224.X

Kieffer JJ (1906) Description de quelques nouveaux serphides. Bulletin de la Société d'Histoire Naturelle de Metz 25: 1–7. https://doi.org/10.5281/zenodo.23783

Kieffer JJ (1912) Proctotrypidae (3e partie). Species des Hyménoptères d'Europe et d'Algérie 11: 1–160. https://doi.org/10.3406/lsoc.1980.1236

Kieffer JJ (1926) Scelionidae. Das Tierreich. Walter de Gruytcr & Co., Berlin, 885 pp.

Kononova SV (1995) [25. Fam. Scelionidae]. In: Lehr PA (Ed.) Key to insects of Russian Far East in six volume. vol. 4. Neuropteroidea, Mecoptera, Hymenoptera. Part 2. Hymenoptera, pp. 600. Dal'nauka, Vladivostok, 57–121.

Kononova SV (2014) [Telenominae of the Palaearctics (Hymenoptera, Scelionidae). Subfamily Telenominae]. Naukova Dumka, Kiev, 487 pp.

Kononova SV, Proshchalykin MYu (2012) Family Scelionidae. In: Annotated catalog of the insects of Russian Far East. Vol.1. Hymenoptera, pp. 636. Leley, A.S., Dal'nauka, Vladivostok, 131–138.

Koppel AL, Herbert DA, Kuhar TP, Kamminga K (2009) Survey of stink bug (Hemiptera: Pentatomidae) egg parasitoids in wheat, soybean, and vegetable crops in Southeast Virginia. Environmental Entomology 38: 375–379. https://doi.org/10.1603/022.038.0209

Kozlov MA (1963) [New synonyms of species of the genus *Asolcus* Nak., *Gryon* Hal. and *Telenomus* Hal. (Hymenoptera, Scelionidae), egg parasites of *Eurygaster integriceps* Put.]. Zoologicheskii Zhurnal 42: 294–296. https://doi.org/10.5281/zenodo.23970

Kozlov MA (1967) Palearctic species of egg parasites of the genus *Telenomus* Haliday (Hymenoptera, Scelionidae, Telenominae). Entomologicheskoye Obozreniye 46: 361–378. https://doi.org/10.5281/zenodo.23962

Kozlov MA (1968) Telenomines (Hymenoptera, Scelionidae, Telenominae) of the Caucasus - egg parasites of the sunn pest (*Eurygaster integriceps* Put.) and other grain bugs. Trudy Vsesoyuznogo Entomologicheskogo Obshchestva 52: 188–223. https://doi.org/10.5281/zenodo.24000

Kozlov MA (1978) Superfamily Proctotrupoidea]. In: [Determination of insects of the European portion of the USSR. Vol. 3, part 2. , 538–664.

Kozlov MA, Kononova SV (1983) Telenominae of the fauna of the USSR. Nauka, Leningrad, 336 pp.

Kumar S, Stecher G, Li M, Knyaz C, Tamura K (2018) MEGA X: Molecular Evolutionary Genetics Analysis across Computing Platforms. Molecular Biology and Evolution 35: 1547–1549. https://doi.org/10.1093/molbev/msy096

Leskey TC, Nielsen AL (2018) Impact of the invasive brown marmorated stink bug in North America and Europe: history, biology, ecology, and management. Annual Review of Entomology 63: 599–618. https://doi.org/10.1146/ANNUREV-ENTO-020117-043226

Letunic I, Bork P (2021) Interactive Tree Of Life (iTOL) v5: an online tool for phylogenetic tree display and annotation. Nucleic Acids Research 49: W293–W296. https://doi.org/10.1093/NAR/GKAB301

Mahmoud AMA, Lim UT (2008) Host discrimination and interspecific competition of *Trissolcus nigripedius* and *Telenomus gifuensis* (Hymenoptera: Scelionidae), sympatric parasitoids of *Dolycoris baccarum* (Heteroptera: Pentatomidae). Biological Control 45: 337–343. https://doi.org/10.1016/j.biocontrol.2008.01.019

Maistrello L, Vaccari G, Caruso S, Costi E, Bortolini S, Macavei L, Foca G, Ulrici A, Bortolotti PP, Nannini R, Casoli L, Fornaciari M, Mazzoli GL, Dioli P (2017) Monitoring of the invasive *Halyomorpha halys*, a new key pest of fruit orchards in northern Italy. Journal of Pest Science 90: 1231–1244. https://doi.org/10.1007/S10340-017-0896-2

Matsuo K, Hirose Y, Johnson NF (2014) A taxonomic issue of two species of *Trissolcus* (Hymenoptera: Platygastridae) parasitic on eggs of the brown-winged green bug, *Plautia stali* (Hemiptera: Pentatomidae): resurrection of *T. plautiae*, a cryptic species of *T. japonicus*. Applied Entomology and Zoology 49: 385–394. https://doi.org/10.1007/s13355-014-0260-4

Mayr G (1879) Ueber die Schlupfwespengattung *Telenomus*. Verhandlungen der Zoologisch-Botanischen Gesellschaft in Wien 29: 697–714. https://doi.org/10.5281/zenodo.23967

Mayr G (1897) *Telenomus Sokolowi*, sp.n. Trudy Russkogo Entomologicheskogo Obshchestva 30: 442–443. https://mbd-db.osu.edu/hol/publications/122e94c4-c8a7-4326-8a5d-80c42f9c1894?filters[filter_options][]=bd2b44d7-bbfd-4247-9b30-2227ea68ae4a

Meier NF (1940) Parasites reared in the USSR in 1938-1939 from eggs of the corn-bug (Eurygaster integriceps Osch.). Vestnik Zashchita Rastenii 3: 79–82. https://doi.org/10.5281/zenodo.23987

Meier R, Blaimer BB, Buenaventura E, Hartop E, von Rintelen T, Srivathsan A, Yeo D (2022) A re-analysis of the data in Sharkey et al.'s (2021) minimalist revision reveals that BINs do not deserve names, but BOLD Systems needs a stronger commitment to open science. Cladistics 38: 264–275. https://doi.org/10.1111/CLA.12489

Mikó I, Vilhelmsen L, Johnson NF, Masner L, Pénzes Z (2007) Skeletomusculature of Scelionidae (Hymenoptera: Platygastroidea): head and mesosoma. Zootaxa 1571: 1–78. https://doi.org/10.11646/zootaxa.1571.1.1

Mineo G (1977) Studi morfo-biologici comparativi sugli stadi preimmaginali degli scelionidi (Hym. Proctotrupoidea). II. Su alcune specie del genere *Gryon* Haliday e *Telenomus heydeni* Mayr. Bollettino dell'Istituto di Entomologia Agraria e dell'Osservatorio di Fitopatologia di Palermo 10: 81–94. https://doi.org/10.5281/zenodo.23971

Mineo G (2012) On the Palaearctic species of *Telenomus* Haliday of the *brachialis* and *turesis* groups (Hym. Platygastroidea: Scelionidae Telenominae). Frustula Entomologica 33: 51–69.

Mineo G, O'Connor JP, Ashe P (2010) Records of Irish scelionid wasps (Hymenoptera: Platygastroidea, Scelionidae) including notes on the genus *Verrucosicephalia* Szabò. Irish Naturalists' Journal Ltd. 31: 113–117. https://www.jstor.org/stable/41419118

Moonga MN, Kamminga K, Davis JA (2018) Status of stink bug (Hemiptera: Pentatomidae) egg parasitoids in soybeans in Louisiana. Environmental Entomology 47: 1459–1464. https://doi.org/10.1093/EE/NVY154

Moore L, Tirello P, Scaccini D, Toews MD, Duso C, Pozzebon A (2019) Characterizing damage potential of the brown marmorated stink bug in cherry orchards in Italy. Entomologia Generalis 39: 271–283. https://doi.org/10.1127/entomologia/2019/0799

Moraglio ST, Tortorici F, Visentin S, Pansa MG, Tavella L (2021a) *Trissolcus kozlovi* in North Italy: host specificity and augmentative releases against *Halyomorpha halys* in hazelnut orchards. Insects 12: 464. https://doi.org/10.3390/insects12050464

Moraglio ST, Tortorici F, Giromini D, Pansa MG, Visentin S, Tavella L (2021b) Field collection of egg parasitoids of Pentatomidae and Scutelleridae in Northwest Italy and their efficacy in parasitizing *Halyomorpha halys* under laboratory conditions. Entomologia Experimentalis et Applicata 169: 52–63. https://doi.org/10.1111/EEA.12966

Moraglio ST, Tortorici F, Pansa MG, Castelli G, Pontini M, Scovero S, Visentin S, Tavella L (2020) A 3-year survey on parasitism of *Halyomorpha halys* by egg parasitoids in northern Italy. Journal of Pest Science 93: 183–194. https://doi.org/10.1007/s10340-019-01136-2

Nees von Esenbeck CGD (1834) 2 Hymenopterorum ichneumonibus affinium monographiae, genera Europaea et species illustrantes. J.G. Cottae, Stuttgartiae. https://doi.org/10.5962/bhl.title.26555

Nixon GEJ (1939) Parasites of hemipterous grain-pests in Europe (Hymenoptera: Proctotrupoidea). Arbeiten über Morphologische und Taxonomische Entomologie aus Berlin-Dahlem 6: 129–136. https://doi.org/10.5281/zenodo.23913

O'Connor JP, Mineo G (2009) *Telenomus chloropus* (Thomson) new to Ireland and second Irish records of *T. nitidulus* (Thomson) and *Trissolcus flavipes* (Thomson) (Hym., Scelionidae). Entomologists Monthly Magazine 145: 106.

Orr DB, Boethel DJ, Jones WA (1985a) Development and emergence of *Telenomus chloropus* and *Trissolcus basalis* (Hymenoptera: Scelionidae) at various temperatures and relative humidities. Annals of the Entomological Society of America 78: 615–619. https://doi.org/10.1093/aesa/78.5.615

Orr DB, Boethel DJ, Jones WA (1985b) Biology of *Telenomus chloropus* (Hymenoptera: Scelionidae) from eggs of *Nezara viridula* (Hemiptera: Pentatomidae) reared on resistant and susceptible soybean genotypes. The Canadian Entomologist 117: 1137–1142. https://doi.org/10.4039/Ent1171137-9

Orr DB (1988) Scelionid wasps as biological control agets: a review. Florida Entomologist 71: 506–528. https://doi.org/10.2307/3495011

Ozdemir IO, Tuncer C, Tortorici F, Ozer G (2022) Egg parasitoids of green shield bug, *Palomena prasina* L. (Hemiptera: Pentatomidae) in hazelnut orchards of Turkey. Biocontrol Science and Technology: 1–15. https://doi.org/10.1080/09583157.2022.2158308

Péricart J (2010) 3 Faune de France 93: Hèmiptères Pentatomoidea euro-méditerranéens. Fèdération Francaise des sociétés de Sciences Naturelles, Paris, 291 pp.

Petrov S (1994) [Contribution to the knowledge of genus *Telenomus* Haliday (Scelionidae, Proctotrupoidea, Hymenoptera)]. Vissh Selskostopanski Institut "Vasil Kolvarv" Nauchni Trudove 39: 275–278.

Polaszek A, Kimani SW (1990) *Telenomus* species (Hymenopetra: Scelionidae) attacking eggs of pyralid pests (Lepidoptera) in Africa: a review and guide to identification. Bulletin of Entomological Research 80: 57–71. https://doi.org/10.1017/S0007485300045922

QGIS.org (2023) QGIS Geographic Information System. Open Source Geospatial Foundation Project. http://qgis.org

Ranjbar F, Amin Jalali M, Ziaaddini M, Gholamalizade Z, Talamas EJ (2021) Stink bug egg parasitoids (Hymenoptera, Scelionidae) associated with pistachio in Iran and description of a new species: *Trissolcus darreh* Talamas. Journal of Hymenoptera Research 87: 291–308. https://doi.org/10.3897/JHR.87.72838

Ratnasingham S, Hebert PDN (2007) bold: The Barcode of Life Data System (http://www.barcodinglife.org). Molecular Ecology Notes 7: 355–364. https://doi.org/10.1111/J.1471-8286.2007.01678.X

Ratzeburg JTC (1844) Die Ichneumonen der Forstinsecten in forstlicher und entomologischer Beziehung. Nicolaischen Buchhandlung, Berlin, 224 pp. https://doi.org/10.5962/bhl.title.11094

Ribes J, Pagola-Carte S (2013) 2 Faune de France 96: Hèmiptères Pentatomoidea euro-méditerranéens. Fèdération Francaise des sociétés de Sciences Naturelles, Paris, 394 pp.

Ricupero M, Cammarata S, Gugliuzzo A, Biondi A, Zappalà L, Siscaro G (2022) The parasitic complex of *Halyomorpha halys* : preliminary data on adaptation of native egg parasitoids to the invasive host. Acta Horticulturae 1354: 215–222. https://doi.org/10.17660/ActaHortic.2022.1354.28

Rjachovskij VV (1959) Egg parasites of the sunn pest in the Ukrainian SSR. Ukrainskii Nauchno-Issledovatel'skii Institut Zashchity Rastenii 8: 76–88. https://doi.org/10.5281/zenodo.23969

Rot M, Maistrello L, Costi E, Bernardinelli I, Malossini G, Benvenuto L, Trdan S (2021) Native and non-native egg parasitoids associated with brown marmorated stink bug (*Halyomorpha halys* [Stål, 1855]; Hemiptera: Pentatomidae) in western Slovenia. Insects 12: 505. https://doi.org/10.3390/insects12060505

Roversi PF, Binazzi F, Marianelli L, Costi E, Maistrello L, Sabbatini Peverieri G (2017) Searching for native egg-parasitoids of the invasive alien species *Halyomorpha halys* Stål (Heteroptera Pentatomidae) in Southern Europe. Redia 99: 63. https://dx.doi.org/10.19263/REDIA-99.16.01

Sabbatini Peverieri G, Mitroiu MD, Bon MC, Balusu R, Benvenuto L, Bernardinelli I, Fadamiro H, Falagiarda M, Fusu L, Grove E, Haye T, Hoelmer K, Lemke E, Malossini G, Marianelli L, Moore MR, Pozzebon A, Roversi PF, Scaccini D, Shrewsbury P, Tillman G, Tirello P, Waterworth R, Talamas EJ (2019) Surveys of stink bug egg parasitism in Asia, Europe and North America, morphological taxonomy, and molecular analysis reveal the Holarctic distribution of *Acroclisoides sinicus* (Huang & Liao) (Hymenoptera, Pteromalidae). Journal of Hymenoptera Research 74: 123–151. https://doi.org/10.3897/JHR.74.46701

Samin N, Shojai M, Asgari S, Ghahari H, Koçak E (2010) Sunn pest (*Eurygaster integriceps* PUTON, Hemiptera: Scutelleridae) and its scelionid (Hymenoptera: Scelionidae) and tachinid (Diptera: Tachinidae) parasitoids in Iran. Linzer Biologische Beiträge 42: 1421–1435.

Sokolov NN (1904) The striated bug (*Aelia furcula* Fieb.). Trudy Byuro po Entomologii 4: 26–30.

Szabó JB (1978) Neue und wenig bekannte *Telenomus* Haliday, 1833 Arten aus dem Karpatenbecken (Hymenoptera: Scelionidae). Folia Entomologica Hungarica 31: 219–236. https://doi.org/10.5281/zenodo.24009

Talamas EJ, Johnson NF, Buffington ML (2015) Key to Nearctic species of *Trissolcus* Ashmead (Hymenoptera, Scelionidae), natural enemies of native and invasive stink bugs (Hemiptera, Pentatomidae). Journal of Hymenoptera Research 43: 45–110. https://doi.org/10.3897/JHR.43.8560

Talamas EJ, Buffington ML, Hoelmer KA (2017) Revision of Palearctic *Trissolcus* Ashmead (Hymenoptera, Scelionidae). Journal of Hymenoptera Research 56: 3. https://doi.org/10.3897/JHR.56.10158

Talamas EJ, Bremer JS, Moore MR, Bon MC, Lahey Z, Roberts CG, Combee LA, McGathey N, van Noort S, Timokhov AV, Hougardy E, Hogg B (2021) A maximalist approach to the systematics of a biological control agent: *Gryon aetherium* Talamas, sp. nov. (Hymenoptera, Scelionidae). Journal of Hymenoptera Research 87: 323–480. https://doi.org/10.3897/JHR.87.72842

Tamura K, Nei M (1993) Estimation of the number of nucleotide substitutions in the control region of mitochondrial DNA in humans and chimpanzees. Molecular Biology and Evolution 10: 512–526. https://doi.org/10.1093/oxfordjournals.molbev.a040023

Thomson CG (1861) Sverges Proctotruper. Tribus IX. Telenomini. Tribus X. Dryinini. Öfversigt af Kongliga Vetenskaps-Akadamiens Förhandlingar 17: 169–181. https://doi.org/10.5281/zenodo.23879

Timokhov AV (2019) Superfamily Platygastroidea. In: Annotated catalog of the Hymenoptera of Russia. Belokobylskij SA, Samartsev KG, Il'inskaya AS, Proceedings of the Zoological Institute Russian Academy of Sciences. Suppement 8. Zoological Institute RAS (St. Petersburg), 42–57.

Tortorici F, Talamas EJ, Moraglio ST, Pansa MG, Asadi-Farfar M, Tavella L, Caleca V (2019) A morphological, biological and molecular approach reveals four cryptic species of *Trissolcus* Ashmead (Hymenoptera, Scelionidae), egg parasitoids of Pentatomidae (Hemiptera). Journal of Hymenoptera Research 93: 153–200. https://doi.org/10.3897/JHR.73.39052

Tortorici F, Bombi P, Loru L, Mele A, Moraglio ST, Scaccini D, Pozzebon A, Pantaleoni RA, Tavella L (2023) *Halyomorpha halys* and its egg parasitoids *Trissolcus japonicus* and *T. mitsukurii*: the geographic dimension of the interaction. NeoBiota 85: 197–221. https://doi.org/10.3897/neobiota.85.102501

Viktorov GA (1967) Problems in insect population dynamics with reference to the sunn pest. Nauka, Moscow, 271 pp.

Voegelé J (1969) Les hyménoptères parasites oophages des *Aelia*. Al Awamia 31: 137–323.

Walker F (1836) On the species of *Platygaster*, &c. Entomological Magazine 3: 217–274. https://doi.org/10.5281/zenodo.24083

Yan C-J, Talamas E, Lahey Z, Chen H-Y (2022) *Protelenomus* Kieffer is a derived lineage of *Trissolcus* Ashmead (Hymenoptera, Scelionidae), with comments on the evolution of phoresy in Scelionidae. Journal of Hymenoptera Research 94: 121–137. https://doi.org/10.3897/jhr.94.95961

Yonow T, Kriticos DJ, Ota N, Avila GA, Hoelmer KA, Chen H, Caron V (2021) Modelling the potential geographic distribution of two *Trissolcus* species for the brown marmorated stink bug, *Halyomorpha halys*. Insects 12: 491. https://doi.org/10.3390/insects12060491

Zapponi L, Tortorici F, Anfora G, Bardella S, Bariselli M, Benvenuto L, Bernardinelli I, Butturini A, Caruso S, Colla R, Costi E, Culatti P, Di Bella E, Falagiarda M, Giovannini L, Haye

T, Maistrello L, Malossini G, Marazzi C, Marianelli L, Mele A, Michelon L, Moraglio ST, Pozzebon A, Preti M, Salvetti M, Scaccini D, Schmidt S, Szalatnay D, Roversi PF, Tavella L, Tommasini MG, Vaccari G, Zandigiacomo P, Sabbatini Peverieri G (2021) Assessing the distribution of exotic egg parasitoids of *Halyomorpha halys* in Europe with a large-scale monitoring program. Insects 12: 316. https://doi.org/10.3390/insects12040316

Zhu GP, Bu W, Gao Y, Liu G (2012) Potential geographic distribution of brown marmorated stink bug invasion (*Halyomorpha halys*). PLoS ONE 7(2): e31246. https://doi.org/10.1371/journal.pone.0031246

Supplementary material 1

Phylogeny reconstruction of COI of *Telenomus truncatus* and *Te. turesis*

Authors: Francesco Tortorici

Data type: tif

Explanation note: The tree of life was inferred by using the Maximum Likelihood method and Tamura-Nei model with an interior branch test and 1000 bootstrap replications. The percentage of trees in which the associated taxa clustered together is shown next to the branches. This analysis involved 97 nucleotide sequences. There was a total of 492 positions in the final dataset. Star (*) indicates sequences mined from online datasets.

Link: https://doi.org/10.3897/jhr.97.127112.suppl1

Supplementary material 2

Distribution map

Authors: Francesco Tortorici

Data type: tif

Explanation note: Distribution map indicating the points for *Telenomus truncatus* (blue spots) and for *Te. turesis* (red spots) retrieved from material examined and from BOLD barcodes.

Link: https://doi.org/10.3897/jhr.97.127112.suppl2

Supplementary material 3

Estimates of Evolutionary Divergence between Sequences

Authors: Francesco Tortorici

Data type: xlsx

Explanation note: The number of base substitutions per site from between sequences are shown. Analyses were conducted using the Maximum Composite Likelihood model (Tamura and Kumar 2004). The rate variation among sites was modeled with a gamma distribution (shape parameter = 1). This analysis involved 105 nucleotide sequences. All ambiguous positions were removed for each sequence pair (pairwise deletion option). There were a total of 861 positions in the final dataset. Evolutionary analyses were conducted in MEGA X (Kumar et al. 2018). Kumar S., Stecher G., Li M., Knyaz C., and Tamura K. (2018). MEGA X: Molecular Evolutionary Genetics Analysis across computing platforms. Molecular Biology and Evolution 35: 1547–1549. Tamura K., Nei M., and Kumar S. (2004). Prospects for inferring very large phylogenies by using the neighbor-joining method. Proceedings of the National Academy of Sciences (USA) 101:11030–11035.

Link: https://doi.org/10.3897/jhr.97.127112.suppl3

Supplementary material 4

List of the specimens examined

Authors: Francesco Tortorici, Bianca Orrù, Alexander V. Timokhov, Alexandre Bout, Marie-Claude Bon, Luciana Tavella, Elijah J. Talamas

Data type: xlsx

Explanation note: Images and sequence data for species of *Telenomus* that are classified in the podisi species group (sensu Johnson 1984).

Link: https://doi.org/10.3897/jhr.97.127112.suppl4

JHR 97: 621–698 (2024)
doi: 10.3897/jhr.97.131350
https://jhr.pensoft.net

RESEARCH ARTICLE

JOURNAL OF Hymenoptera RESEARCH
A peer-reviewed open-access journal
The International Society of Hymenopterists

Integrative characterisation of the Northwestern European species of *Anacharis* Dalman, 1823 (Hymenoptera, Cynipoidea, Figitidae) with the description of three new species

Jonathan Vogel[1], Mattias Forshage[2], Saskia B. Bartsch[1], Anne Ankermann[1], Christoph Mayer[1], Pia von Falkenhausen[1], Vera Rduch[1], Björn Müller[1], Christoph Braun[1], Hans-Joachim Krammer[1], Ralph S. Peters[1]

1 *Leibniz Institute for the Analysis of Biodiversity Change, Museum Koenig Bonn, Adenauerallee 127, 53113 Bonn, North Rhine-Westphalia, Germany* **2** *Swedish Museum of Natural History, Department of Zoology, P.O. Box 50007, 104 05 Stockholm, Stockholms län, Sweden*

Corresponding author: Jonathan Vogel (j.vogel@leibniz-lib.de, jvogel.hym@gmail.com)

Academic editor: Miles Zhang | Received 5 July 2024 | Accepted 24 July 2024 | Published 29 August 2024

https://zoobank.org/EA190992-B01B-4F1B-A362-A4549C725580

Citation: Vogel J, Forshage M, Bartsch SB, Ankermann A, Mayer C, von Falkenhausen P, Rduch V, Müller B, Braun C, Krammer H-J, Peters RS (2024) Integrative characterisation of the Northwestern European species of *Anacharis* Dalman, 1823 (Hymenoptera, Cynipoidea, Figitidae) with the description of three new species. Journal of Hymenoptera Research 97: 621–698. https://doi.org/10.3897/jhr.97.131350

Abstract

The genus *Anacharis* Dalman, 1823 comprises parasitoid wasps that target early instars of brown lacewing larvae (Neuroptera: Hemerobiidae). So far, five species were recognised from the Western Palaearctic region, of which four are reported from Northwestern Europe.

In this study, we address the Northwestern European species diversity of the genus with an extended integrative taxonomy toolkit. A total of 700 specimens were examined for their external morphology, including the relevant type specimens. For 354 specimens, we obtained CO1 barcode sequences and applied three molecular species delimitation methods. All DNA barcode data are made publicly available via the German Barcode of Life (GBOL) and Barcode of Life Data system (BOLD) database. In addition, we examined images of Wing Interference Patterns (WIPs), examined the male genitalia and performed multivariate morphometric analyses.

The analyses revealed two clusters which we describe as the *immunis* and *eucharioides* species groups based on differences in DNA barcode, external morphology, WIPs and size of the male genitalia. Furthermore, we complement the diagnosis of the genus *Anacharis* and describe three new species,

Anacharis martinae Vogel, Forshage & Peters, **sp. nov.**, *Anacharis maxima* Vogel, Forshage & Peters, **sp. nov**. and *Anacharis minima* Vogel, Forshage & Peters, **sp. nov.** Finally, we synonymise *A. fergussoni* Mata-Casanova & Pujade-Villar, 2018, **syn. nov.** with *A. euchariodes* (Dalman, 1818), and we reinstate *A. ensifer* Walker, 1835, **stat. rev.**, *A. typica* Walker, 1835, **stat. rev.** and *A. petiolata* Zetterstedt, 1838, **stat. rev.** as valid species. In total, we recognise nine Northwestern European species to which we provide an identification key.

The species of *Anacharis* are morphologically very variable. Morphometric analyses alone did not provide information sufficient to delimit species, neither did analyses of WIPs and male genitalia, with few notable exceptions. Analyses of molecular sequence data proved crucially helpful to reliably delimit species and to find morphological diagnostic characters in a reverse taxonomy approach. For delimiting species groups, all included analyses proved helpful, and we show that exploring an extended integrative taxonomy toolkit can be beneficial for a comprehensive characterisation of species. We acknowledge that a complete overview of species distributions, and characterisation of ecological niches & host records is still required to deeply understand the genus as a whole, yet our results already allow broad access to and inclusion of *Anacharis* species in downstream biodiversity research.

Keywords
CO1 barcoding, integrative taxonomy, male genitalia, morphometrics, Western Palaearctic, WIPs

Introduction

Anacharis Dalman, 1823 (Figitidae: Anacharitinae) is a genus of parasitoid wasps that target early instar larvae of brown lacewings (Neuroptera: Hemerobiidae) as hosts. Specimens of the genus *Anacharis* can be quite common in Malaise trap or sweep net samples and are clearly the most common representatives of Anacharitinae in the Western Palaearctic region. They are typically found on or near vegetation in various habitats (herbs, shrubs, canopy of deciduous and coniferous trees) in which their hosts occur (Walker 1835; Handlirsch 1886; Aspöck et al. 1980; Miller and Lambdin 1985; Cave and Miller 1987; label data, own experience).

Until recently, only two species were recognised as valid for the Western Palaearctic region: *A. euchariodes* (Dalman, 1818) and *A. immunis* Walker, 1835, with a large number of names regarded as junior-synonyms of either of the two (Fergusson 1986). In 2018, the Palaearctic (and Indomalayan) species were revised, leading to a more detailed picture of the studied region's fauna (Mata-Casanova et al. 2018). Three new species, *A. belizini* Mata-Casanova & Pujade-Villar, 2018, *A. fergussoni* Mata-Casanova & Pujade-Villar, 2018 and *A. norvegica* Mata-Casanova & Pujade-Villar, 2018 were described and the already known species re-described. All treated taxa were integrated in a new dichotomous key that was based on previously unrecognised diagnostic characters. With this addition to the taxonomic knowledge of Western Palaearctic species, the total number of species in Western Palaearctic *Anacharis* was raised to five (*A. immunis*, *A. norvegica*, *A. euchariodes*, *A. fergussoni*, *A. parapsidalis*), of which four (all except *A. parapsidalis*) occur in Northwestern Europe. In addition, Mata-Casanova et al. (2018) treated two species, *A. antennata* and *A. belizini*, from the Indomalayan region. The revision was based on morphological data only.

In this study, we re-target the Northwestern European fauna of *Anacharis* by examining several hundred specimens, including relevant type specimens. For the first time for this genus we analyse CO1 barcode data in addition to examination of external morphology, and also include analyses of wing interference patterns, examination of dissected male genitalia and multivariate morphometrics. We aimed to characterise the species present in the study region but also to explore an extended integrative taxonomy toolkit in this challenging parasitoid wasp taxon, following the principle of a unified species concept as described by De Queiroz (2007).

We generated high quality DNA barcode data in the framework of the GBOL III: Dark Taxa project (Awad et al. 2020; Hausmann et al. 2020). The sequences and the respective metadata of the specimens are made publicly available at the GBOL (https://data.bolgermany.de/ergebnisse/results) and BOLD reference database (boldsystems.org). We applied automated species delimitation methods, namely ASAP (Puillandre et al. 2021), multirate PTP (Kapli et al. 2017), and objective clustering by using species identifier (Meier et al. 2006) on the barcode data and used the results as taxonomic orientation in a reversed taxonomy approach (Markmann and Tautz 2005). This allowed us to draw informed conclusions about species limits and connect these integratively composed species hypotheses with historical names by comparing our voucher specimens to type specimens.

The first character we explored in addition to morphological examination and analyses of DNA barcodes, are Wing Interference Patterns (WIPs), which are a property of insect wings. Especially wings of smaller insects show a remarkable array of colourful patterns on their wing membranes if the lighting conditions are right. The differences in colour and extent of each pattern is largely determined by the thickness and texture of the wings. Shevtsova and Hansson (2011) investigated WIPs for their potential in species delimitation within the genus *Achrysocharoides* Girault, 1913 (Chalcidoidea: Eulophidae), and the patterns were shown to be consistent within species. In the past decade, taxonomic studies of different parasitoid wasp taxa occasionally included WIPs in their species treatments (e.g. Buffington and Condon 2013; Buffington and Forshage 2014; Moser et al. 2023), while other studies highlighted their use for species delimitation in combination with machine-based analyses (Hosseini et al. 2019; Cannet et al. 2022, 2023; Jin et al. 2023). In Cynipoidea, the WIPs were shown to exhibit phylogenetically conserved patterns and their use for species delimitation was proposed for *Ganaspidium* Weld, 1952 (Figitidae) and *Andricus* Hartig, 1840 (Cynipidae) but never tested (Buffington and Sandler 2011). Here, we present the first larger-scale analysis of WIPs in Cynipoidea.

Little is known about the function of WIPs and their role might vary from group to group. They are hypothesised to be used for communication with conspecifics in, for example, courtship and mating of *Drosophila* Fallén, 1823 (Katayama et al. 2014; Hawkes et al. 2019) and *Pteromalus cassotis* Howard, 1889 (Shevtsova et al. 2011), and for signalling habitat occupation in fig wasps (Shevtsova et al. 2011).

The second character complex we explored here is the morphology of male genitalia. In recent years, the analysis of male genitalia of parasitoid wasps went through a renais-

sance. Studies made progress in describing genitalia morphology, facilitating comparison between various lineages, for example, Ceraphronoidea and Ichneumonoidea (Mikó et al. 2013; Dal Pos et al. 2023) and identifying homologous structures to the more complex ancestral apparatus of the Symphyta (Schulmeister et al. 2002). The male genitalia of parasitoid wasp taxa have been used as diagnostic character complexes in parasitoid wasp taxonomy, for example in Ceraphronoidea (Mikó et al. 2013; Trietsch et al. 2018; Salden and Peters 2023), Chalcidoidea: Trichogrammatidae (Hayat 2009; Polaszek et al. 2022) and Ichneumonoidea: Braconidae: Agathidinae (Žikić et al. 2011). The male genitalia of the superfamily Cynipoidea (e.g. Ronquist and Nordlander 1989; Fontal-Cazalla et al. 2002) are less complex than those of Ceraphronoidea (e.g. Salden and Peters 2023) and Symphyta (e.g. Schulmeister et al. 2002). The morphology of the male genitalia was used in a cladistic analysis of the figitid subfamily Eucoilinae (Fontal-Cazalla et al. 2002). However, the potential of male genitalia for species or species group delimitation in Cynipoidea has not been evaluated yet and is explored here for the first time.

As a third line of enquiry, we explored multivariate analyses of morphometric characters. Morphometric characters and ratios are routinely applied by taxonomists to complement species' diagnoses and descriptions (e.g. van Achterberg and Shaw 2016; Mata-Casanova et al. 2018). Further, multivariate morphometric analysis can be used to extract the character ratios with the most diagnostic value and proved therefore invaluable to characterise species (e.g. Baur 2015; Janšta et al. 2020). Here, we apply multivariate morphometric analyses following Baur and Leuenberger (2011) for delimitation of species and species groups in *Anacharis*.

With this study we contribute to a clearer picture of the diversity of the Northwestern European *Anacharis* species, their intraspecific morphological variability, and show the potential of still relatively unexplored character traits for their use in alpha-taxonomical studies. Moreover, we refine the diagnosis of the genus and diagnose two species groups. The results of this work convey the release of the currently most comprehensive and taxonomically evaluated CO1 DNA barcode sequence dataset of *Anacharis* worldwide.

Material and methods

Institutional abbreviations

CNC	Canadian National Collection of Insects, Arachnids and Nematodes, Ottawa, Canada
MGAB	Muzeul Național de Istorie Naturală Grigore Antipa, Bucharest, Romania
MHNG	Muséum d'Histoire Naturelle, Genève, Switzerland
MZLU	Zoological Museum Lund, Sweden
NHMUK	Natural History Museum, London, United Kingdom
NHRS	Naturhistoriska riksmuseet, Stockholm, Sweden
NMBE	Naturhistorisches Museum Bern, Switzerland

SDEI	Senckenberg Deutsches Entomologisches Institut, Müncheberg, Germany
ZFMK	Leibniz Institute for the Analysis of Biodiversity Change, Museum Koenig Bonn, Germany
ZMHB	Museum für Naturkunde, Berlin, Germany
ZMUC	University of Copenhagen, Zoological Museum, Copenhagen, Denmark
ZSM	Zoologische Staatssammlung München, Germany

Specimens and identification

In total, we acquired 394 fresh ethanol-preserved specimens in the course of the German Barcode of Life project (GBOL III: Dark Taxa) (see Suppl. material 1 for details). In addition, we examined 306 dry-mounted specimens from museum collections. For preparation, mounting and examination, a Leica M205 C stereomicroscope was used. We tentatively identified the specimens following Mata-Casanova et al. (2018) and identified the sexes by the presence of the female ovipositor or male genitalia in cases they were exerted. When they were retracted or obscured because of other reasons, we counted the number of antennomeres (13 in ♀, 14 in ♂). Additionally, the sexes were differentiated by the shape of the 7st metasomal sternite (7st) and tergite (7tg) as follows: The 7st of the female (hypopygium) is keel-shaped and has a longitudinal line of setae directly lateral to the ventral edge on each side. It is laterally overlapping the 7tg, which is dorsally more or less straight so that 6tg seamlessly transitions into 7tg in lateral view. The 7st of the male is ventrally flattened with a setal patch covering the surface. It is not overlapping the 7tg, which is distinctly sloping posteriorly. In consequence the male metasoma appears more "loaf-shaped" with a straight ventral delimitation and an almost even posteroventral angle with a sharp posterior slope; and the female metasoma appears more lens-shaped with a convex ventral side and posteriorly a somewhat sharp angle. Also, the female metasoma is relatively larger, and the petiole is distinctly shorter than in males of the same species. Beyond these characters, males and females of *Anacharis* look remarkably similar and can be treated together in diagnoses and descriptions.

We cite the label information of the historical type specimens verbatim in congruence with the Example 1 of the Darwin Core term "verbatimLabel" (i.e. citing one label per line, with personal interpretations of ambiguous label contents in square brackets, see https://dwc.tdwg.org/examples/verbatimLabel for details). All other specimens are cited as recommended by the journal's author guidelines and separated into 1. type material, 1.1 primary type specimen(s), 1.2 secondary type specimen(s) and 2. other material, 2.1 DNA barcode vouchers, 2.2 Material without DNA Barcode.

All specimens are deposited at the ZFMK if not indicated otherwise. The specimen database, using Darwin Core terms, is attached as Suppl. material 1.

For the vertical distribution of each species we only accounted for the specimens where either elevation, coordinates or both were given on the labels and are likely biased when extreme statements are made. Especially those statements about lowland preference are affected due to the Swiss specimens that usually lack this information.

Terminology

The terminology used herein follows Ronquist and Nordlander (1989) for external morphological terms and Harris (1979) for surface sculpture terms.

One character is newly defined here:

posteroventral hypocoxal furrow = The posteroventral groove of the mesopleuron that is located just before the insertion of the mid coxa (e.g. Fig. 17B).

Imaging

For imaging of the specimens, we used a Canon EOS 7D® camera mounted on a P-51 Cam-Lift (Dun, Inc.). For lighting, we used a bidirectional flashlight arrangement set to medium intensity for habitus- and maximum intensity for detail-shots. We placed a sandwich paper-coated acrylic glass tube (ca. 6 cm diameter) around the specimen for light diffusion. The aperture was set as high as possible without underexposing the specimen. The image series were evaluated in ADOBE LIGHTROOM® v.5.6 and stacked with HELICON FOCUS® v.8.2.2.

For the SEM imaging, we mounted the heads of two specimens (*Anacharis petiolata*: ZFMK-HYM-00039676 and *Aegilips* sp.: ZFMK-HYM-00039677) on specimen holder stubs for gold coating with a Cressington Sputtercoater 108auto. The SEM images were then generated using a Zeiss Sigma 300VP system with the settings shown in Fig. 4A–D respectively. After the imaging, we mounted the gilded heads to the side of the cardboard of the corresponding specimens.

DNA sequencing and molecular species delimitation

We performed non-destructive full-body DNA extractions from our specimens at the Center for Molecular Biodiversity Research (ZMB) at the ZFMK. The mtDNA barcode region of the CO1 gene was amplified by using the LCO1490-JJ forward and HCO2198-JJ reverse primer (Astrin and Stüben 2008) and the PCR protocol as described in Jafari et al. (2023). The sequences of both reads were assembled to a consensus sequence in GENEIOUS Prime v.2022.1.1 (Biomatters Ltd.). We kept and used those sequences for downstream analyses if they fulfilled the GBOL gold standard (i.e. consensus sequences have 1. ≥ 500 base pairs sequence length, 2. a high quality bin assignment, and 3. ≤ 1% disagreements and ambiguities, see Jafari et al. 2023 for more details). In addition to our own sequences (tagged with "ZFMK-TIS-..."), we accessed 71 *Anacharis* spp. CO1 sequences from BOLD (Ratnasingham and Hebert 2007), which were at least 500 bp long. They originate from Germany (65), Belarus (3), and Norway (3). We aligned the sequences using the built-in MUSCLE alignment algorithm with a maximum of 8 iterations (Edgar 2004) in GENEIOUS. The herein produced DNA barcode sequences can be accessed via bolgermany.de (German Barcode of Life Consortium 2011) and on boldsystems.org. Respective BOLD-IDs of all

sequences we used can be found in Suppl. material 1 for the specimens that were studied morphologically as well and Suppl. material 2 for the sequences that we accessed via BOLD and did not study the morphology of the respective specimens.

Using IQ-TREE v2.2.2.6 (Minh et al. 2020), we reconstructed a maximum likelihood tree and calculated ultrafast bootstrap support with 1000 replicates (Hoang et al. 2018) without further specifications. For species delimitation, the ASAP species delimitation algorithm (via https://bioinfo.mnhn.fr/abi/public/asap/, default settings, accessed 26th February 2024; Puillandre et al. 2021) and the Clustering function of Species Identifier v.1.6.2 (Meier et al. 2006) set to a 3% threshold (hereafter referenced as SpID) was applied to our alignment and multirate PTP (hereafter referenced as mPTP, Kapli et al. 2017) via a web server (https://mptp.h-its.org/#/tree, 26th February 2024) was applied to the tree file that was previously rooted with an outgroup sequence (*Aegilips* sp., BOLD-ID: CNKLH2372-15) in Figtree v1.4.4 (Andrew Rambaut, available at http://tree.bio.ed.ac.uk/software/figtree/). Fig. 1 was then composed in INKSCAPE v.1.3 (Inkscape project) by combining the final tree and the species delimitation results.

For the molecular characterisation of species (see species treatments), we analysed the distance matrix from the alignment provided in GENEIOUS to extract maximum intraspecific distances and minimum interspecific distances, stating the name of the closest species in parentheses. The consensus sequence was generated by aligning the sequences of each species separately in GENEIOUS. For the molecular characterisation we only used the sequences of those specimens that we also studied morphologically, i.e. excluding the sequences downloaded from BOLD.

WIPs analysis

We performed all steps of a WIP preparation and imaging protocol for small ethanol-preserved insect (wasp) specimens (DOI: dx.doi.org/10.17504/protocols.io.bp2l6xyy1lqe/v1) published along with this manuscript. In short, the protocol covers instructions for the following steps:

Section 1 - Slide preparation
: Descriptions of how to dissect the wings, get fore and hind wing centrally positioned on a microscopic slide for better standardisation and prepare the slide for long term storage in a natural history collection.

Section 2 - Imaging
: Information on the camera system we used, the settings and how the raw images of the WIPs were acquired.

Section 3 - Image processing
: All steps to manually adjust the image values to make the WIPs stand out (cf. Fig. 2) and to automatically remove the background, left-align and position the fore and hind wing in standardised angles to each other to make the series of images utilisable for, e.g. machine learning applications.

In this study, we applied the following specifications to the protocol:

We used an Olympus SZX12 for a first batch of 179 preparations and a Leica M205 C for stereo microscope for a second batch of 37 preparations.

The first 179 wing dissections were done prior to DNA lysis and the wings were kept in ethanol tubes until further processing.

As background for imaging the WIPs, we used a cardboard painted with "ultrablack" Musou black from KOYO Orient Japan Co., Ltd., which absorbs up to 99.4% of light (according to the manufacturer).

The steps of section 3 (image processing) were followed only for the WIPs images shown in Fig. 2. Re-sizing the images to put them to scale was not necessary as the magnification during photography and the resulting resolution was the same for the entire series. For all other images, the raw images were used to compare WIPs within and between the species by eye.

By publishing the protocol for wing preparation and WIPs imaging from ethanol-preserved (small) insect specimens, we tried to provide standardisation for the necessary steps, specifically to a) produce standardised, artifact-free and high-quality WIP images, b) secure long-term-storage of the specimens, c) make the prepared wings re-traceable to the specimens they have been taken from, d) secure reproducibility of the imaging even decades after preparation (i.e. easy cleaning of the wing specimens prior to imaging), and to e) allow reproduction of the protocol with minimal financial resources. In all these aspects, there is undeniably room for improvement, yet we deliberately published the protocol on protocols.io. All interested parties are thereby invited to contribute to an optimised protocol. This will allow integration of WIPs in further applications such as advanced statistical or machine learning methods aiming at automated species identification.

Male genitalia

We dissected the genitalia of 21 male specimens. The first 15 genitalia were extracted from metasomas that were dissected prior to the DNA lysis. The remaining six were extracted post-lysis without dissecting the entire metasoma. The genitalia were removed from the metasomas by fixating the metasomas with forceps and scooping out the genital with a minuten pin mounted on a skewer. In most cases, the apical half of the metasoma needed to be cut off as squeezing it did not let the genital capsule extrude. In those cases, we disintegrated the gaster to lay bare the genital. The "remaining" fragments of the gaster were discarded.

We used a Zeiss Axio Imager.Z2m. to produce multi-focus images that were later stacked with Helicon Focus v.8.2.2 (Helicon Soft Ltd.). For the genitalia shown in Fig. 3, the backgrounds of the stack images were removed in GNU image manipulation program v.2.10.34 (GIMP development team, available at www.gimp.org). The genital width and length were determined using these images.

Morphometrics

Of a total of 115 specimens, consisting of 68 males and 47 females, we measured 48 external morphological characters. The selection of characters is mainly based on the measurements implemented in Mata-Casanova et al. (2018). The characters measured are listed in Table 1.

For the measurements, a calibrated scale ocular on a Leica M205 C stereomicroscope was used. Of those specimens that lacked wings due to the preparation of WIPs images, the wing length & marginal cell dimensions were measured on the WIPs images digitally using GIMP. As many male metasomas were dissected and/or destroyed prior to the measurements, no metasomal measurements for those specimens could be obtained, except the petiole length in most cases. The complete raw data is attached in Suppl. material 3.

We applied the imputation function of the mice R package (Buuren and Groothuis-Oudshoorn 2011) to account for missing data. For the multivariate morphometric analyses, the measurements of the metasoma, except the petiole length, the antennal measurements, and the male genitalia measurements were excluded (see characters marked with asterisk in Table 1). As 51 of the 68 male gasters could not be measured due to the destruction of the gaster during the extraction of the male genitalia, the resulting gap in the data was too large to be reliably imputed. We excluded the antennal and male genitalia measurements because the deviating number of segments between males (14) and females (13) complicated the downstream analysis and the male genitalia measurements due to both sex-specificity and relatively few measured individuals (21 of 68 males), causing a gap too large to be reliably imputed. The imputed dataset is supplied in Suppl. material 4.

We applied multivariate morphometric analysis based on Baur and Leuenberger (2011, 2020) and Baur et al. (2015) and performed principal component analysis (PCA), linear discriminant analysis (lda) and allometry analyses using R 4.3.3 and the R scripts provided by Baur and Leuenberger (2020).

Results

Molecular analyses

We obtained the CO1 barcode sequences of 354 out of 394 specimens (90% success rate). 348 sequences had the full 658 bp DNA barcode length, 6 had shorter sequences with a minimum length of 645 bp.

The numbers of species suggested by the automated species delimitation approaches ranges from seven (spID with 97% similarity threshold and mPTP) to nine (ASAP) (Fig. 1). Only few incongruencies with morphological data are

apparent (Fig. 1); these are presented and discussed in the integrative species treatments below.

Two species groups are apparent from the analyses of the DNA barcode data (see also taxonomic section), with a minimum distance of 16%.

Table 1. Characters marked with asterisk were excluded from the morphometric analyses..

Character	Orientation	Description
Head length	Lateral	Distance from below the toruli in a right angle to the vertical head axis until the posterior edge of the head
Head width	Frontal and dorsal	Longest distance between the outer delimitation of the eyes.
Head height	Frontal	Distance from ventral clypeal margin to top of ocellar triangle
Malar space length	Frontal	Shortest distance between most dorsal corner of mandibular base to the eye
Eye height	Frontal	Longest distance between ventral margin of eye and the eye dorsally
Eye-to-eye distance	Frontal	= transfacial line in Mata-Casanova et al. (2018) = Shortest distance between eyes
Torulus diameter	Frontal	Diameter of an individual torulus, either left or right
Toruli distance	Frontal	Shortest distance between the toruli
Torulus eye distance	Frontal	Shortest distance between torulus and eye, left or right
Post ocellar line (POL)	Dorsal	Shortest distance between margins of median ocellus and lateral ocellus, either left or right
Ocular ocellar line (OOL)	Dorsal	Shortests distance between margins of lateral ocellus, left or right, and eye
Lateral ocellar line (LOL)	Dorsal	Shortest distance between margins of lateral ocelli
Ocellar Diameter (OD)	Dorsal	Diameter of the median ocellus
Antenna length*	Lateral or dorsal, depending on the positioning of the antenna	Distance from basal margin of scape to the apex of the last antennomere, measured on left or right antenna; in some cases calculated from the sum of the individual segments, as the antennae were too strongly bent
Antennomere length*	Lateral or dorsal, depending on the positioning of the antenna, scape always measured in lateral view	Distance from the basal margin of an antennomere to its apex, measured medially on left or right antenna
Length of mesosoma	Lateral	Distance between most anterior point of pronotum to the most posterior point of the nucha
Mesoscutum length	Dorsal	Longest distance between anterior and posterior margin of the mesoscutum
Mesoscutum width	Dorsal	Longest distance between the lateral margins of the mesoscutum
Mesoscutellum length	Dorsal	Longest median distance from anterior to posterior margin of the mesoscutellum
Fore wing marginal cell length	Dorsal	Distance between transversal section of front wing vein R1 and the intersection of R1 and Rs
Fore wing marginal cell width	Dorsal	Shortest distance between intersection of vein r and Rs and the marginal section of vein R1
Hind coxa length	Lateral	Longest distance between basal annular girdle and apical margin of the metacoxa
Length of metasoma*	Lateral	Longest distance between posterior margin of nucha and posterior margin of the 7th metasomal sternite
Petiole length	Lateral	Distance between anterior constriction of petiole to anterior margin of the 2nd metasomal tergite
Metasomal tergite 2 length*	Lateral	Longest median distance between anterior and posterior margin of the tergite
Metasomal tergite 2 length*	Dorsal	Longest median distance between anterior and posterior margin of the tergite
Metasomal tergite 3 length*	Lateral	Longest median distance between anterior and posterior margin of the tergite
Metasomal tergite 3 length*	Dorsal	Longest median distance between anterior and posterior margin of the tergite
Metasomal tergite 4 length*	Lateral	Longest median distance between anterior and posterior margin of the tergite
Metasomal tergite 4 length*	Dorsal	Longest median distance between anterior and posterior margin of the tergite
Male genital length*	Ventral	Median distance between the anterior parameral plate and the apex of the aedeagus
Male genital aedeagus width*	Ventral	Longest distance between lateral margins of the vertical penis valves

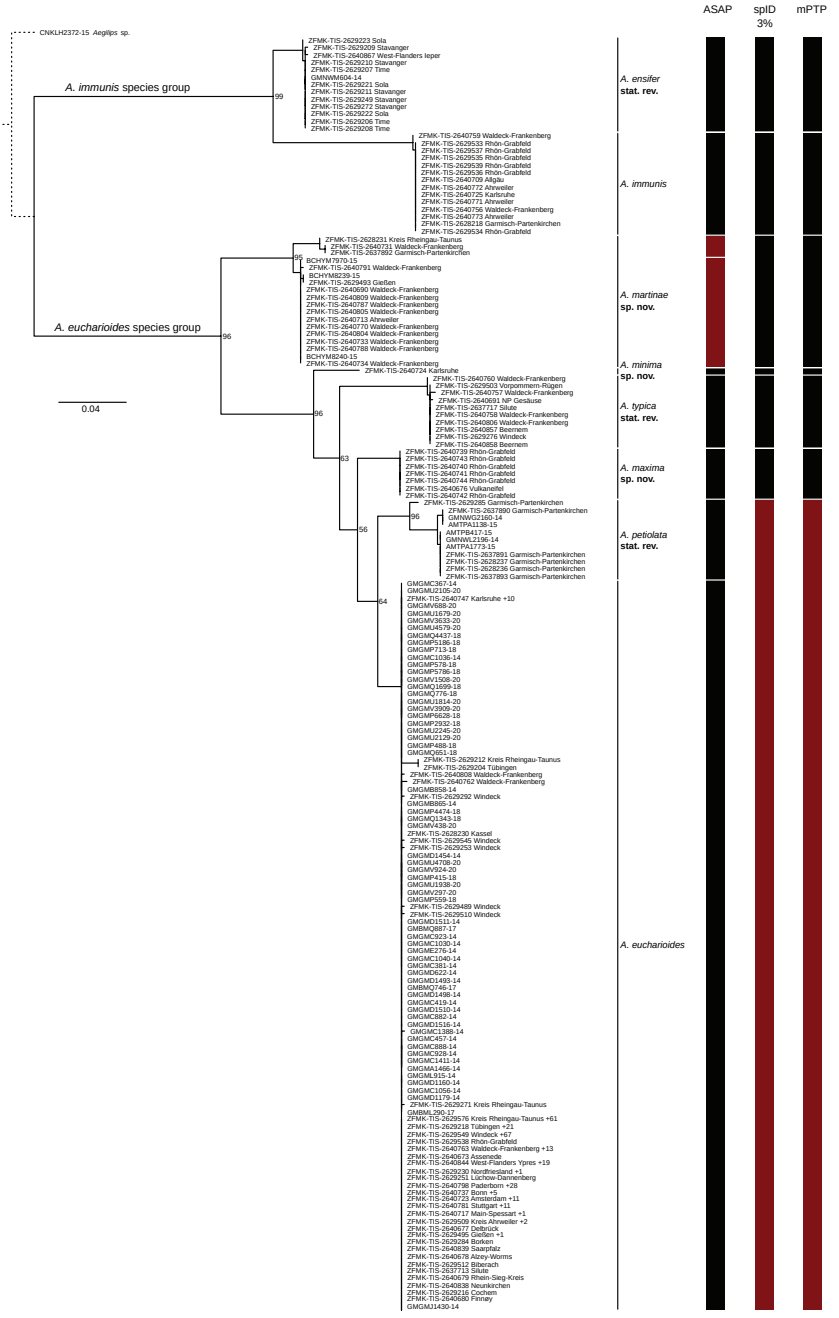

Figure 1. Maximum likelihood tree based on DNA barcode data, constructed with IQ Tree. The results of the species delimitation analyses are summarised on the right. Black boxes indicate congruence with our morphological examinations, while the red boxes highlight disagreements. Species and species groups are named according to the results of our integrative taxonomy approach (see corresponding treatments). The dotted line is connecting the outgroup, *Aegilips* sp., to the remaining tree and is not to scale. Identical sequences from the same sites are combined in respective tip labels and are indicated with a (+ n). Ultrafast-bootstrap support is shown on the nodes.

WIPs

In total, we prepared 186 images of WIPs (145 *A. eucharioides*, 14 *A. norvegica*, 9 *A. martinae*, 7 *A. immunis*, 6 *A. typica*, 4 *A. maxima*, 1 *A. petiolata*). We could not obtain any image for *A. minima*.

The WIPs exhibit the following general characteristics. The basal and marginal cell of the fore wing is largely pattern-free. The radial area (defined by wing margin, vein Rs, and the non-sclerotised vein M) has an absent to faint pattern of straight to curved purple bands that does not reach the wing apex. How close the band-pattern extends towards the wing apex varies slightly between species. The patterns on the median area (defined by the wing margin and the non-sclerotised veins Rs+M, M, Cu_1 and Cu_{1a}) vary inter- and intraspecifically.

The basal cell of the hind wing is pattern-free. The radial, medial and cubital areas are fused to an apical area (defined by vein R1, Rs&1r-m, its shortest distance to the wing's hind margin and the wing margin). The pattern of the apical area consists of a

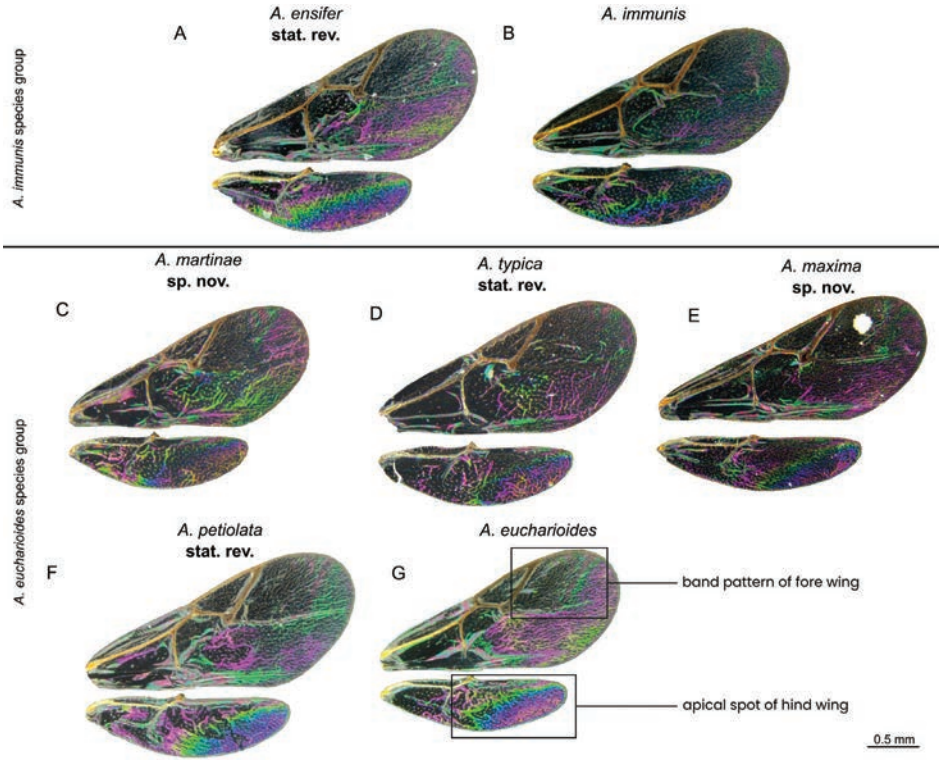

Figure 2. Fore and hind wings of different species of *Anacharis* showing the WIPs **A** *A. ensifer* stat. rev. male (ZFMK-TIS-2629206) **B** *A. immunis* male (ZFMK-TIS-2629539) **C** *A. martinae* sp. nov. female holotype (ZFMK-TIS-2640787) **D** *A. typica* stat. rev. female (ZFMK-TIS-2640857) **E** *A. maxima* sp. nov. male paratype (ZFMK-TIS-2640676) **F** *A. petiolata* stat. rev. female (ZFMK-TIS-2629285) **G** *A. eucharioides* male (ZFMK-TIS-2629201).

spot that is situated at the apex of the wings which is surrounded by colour that does not follow an intraspecifically consistent pattern. The spot is running along the hind margin of the wing to an extent that varies between species groups. The dimensions, i.e. how much of the apical area is filled with the apical spot, partly varies between species (see descriptions of *A. martinae* sp. nov. and *A. maxima* sp. nov.). The basiocubital area (defined by the shortest distance of Rs&1r-m to the wing's hind margin, M+Cu1 and the wing margin) is often pattern-free or shows variable patterns.

Male genitalia

The male genitalia of 21 specimens, representing all species except *A. petiolata* and *A. minima*, were dissected and measured. The post-DNA-lysis genitalia (Fig. 3C–E) turned out more transparent than the non-lysed genitalia (Fig. 3A, B, F). This greatly enhanced the visibility of the sclerotised structures and setae and eliminates the need for an extra maceration step.

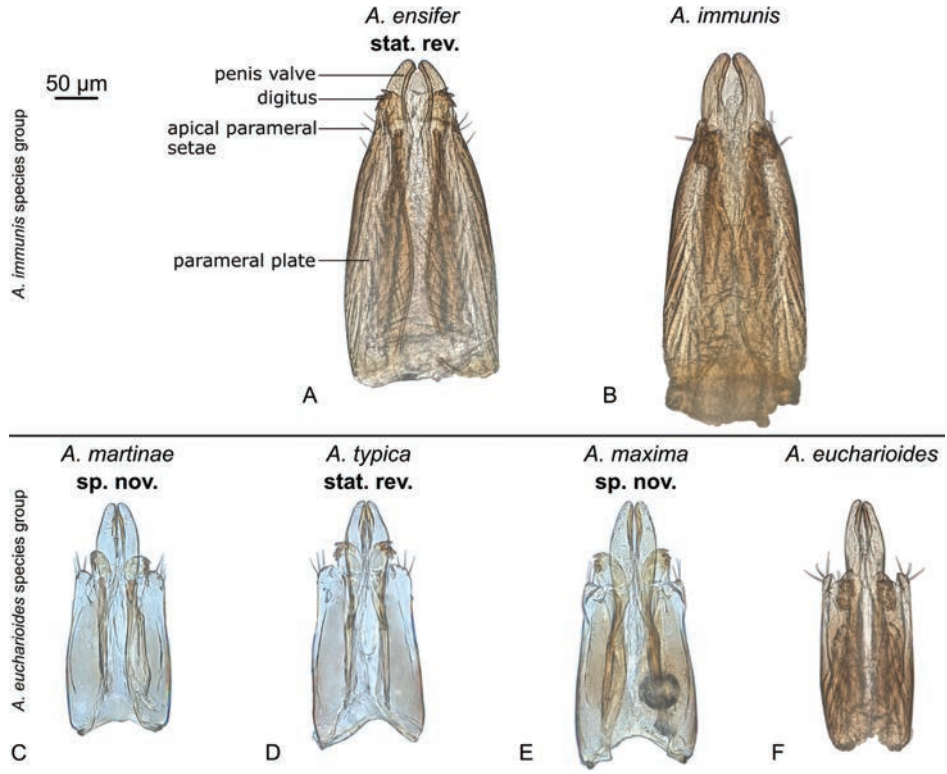

Figure 3. Comparison of *Anacharis* male genitalia in ventral view **A** *A. ensifer* stat. rev. (ZFMK-TIS-2629209) **B** *A. immunis* (ZFMK-TIS-2629539) **C** *A. martinae* sp. nov. male paratype (ZFMK-TIS-2640733) **D** *A. typica* stat. rev. (ZFMK-TIS-2640757) **E** *A. maxima* sp. nov., male paratype (ZFMK-TIS-2640741) **F** *A. eucharioides* (ZFMK-TIS-2629243) **A, B, F** were dissected prior to DNA lysis **C, D, E** after lysis.

The overall shape of the genitalia of *Anacharis* is very similar between species (Fig. 3). The genitalia are elongate with clearly protruding penis valves. The digiti are protruding beyond the parameres when stretched out and not protruding when bent. The digiti have two to four apical spines each. Note that due to the often concealed positioning of the digiti, our attempts to determine the absolute number of spines remained inconclusive for most genitalia. The apex of the parameral plate usually has three setae with differences in their respective positions (see diagnoses of the species groups).

The genitalia are 243–423 μm in length, with a distinct difference between the species groups (see treatment section below). We observe consistent species-specific traits in *A. eucharioides* (Fig. 3F) and *A. maxima* sp. nov. (Fig. 3E).

Multivariate morphometrics

On species group-level, the morphometric analyses almost fully separate two groups in a PCA (Fig. 5 left), and provide two extracted ratios that fully separate the two groups (Fig. 5 right). These results and ratios are used and discussed in the taxonomic treatment of the two species groups below.

On species-level, restricted to the *eucharioides* species group, all species overlap in a PCA when included in the same analyses (Fig. 7). To make interspecific differences better visible and to potentially extract delimitating ratios, we performed pairwise species-level PCA and ratio extractor analyses. Results of three analyses are shown in Fig. 8, representing different levels of separation between species. First, the PCA of *A. eucharioides* against the remaining species of the *eucharidoides* group shows wide overlap and no ratios that can reliably separate the species (Fig. 8A). Second, the PCA of *A. martinae* sp. nov. against the remaining species of the *eucharioides* species groups shows partial overlap and ratios that can separate at least most of the specimens of the two groups (Fig. 8B). Finally, the PCA of *A. maxima* sp. nov. against the remaining species of the *eucharioides* species group shows almost full separation of the species, and the ratio extractor provided two ratios which in combination can fully separate *A. maxima* sp. nov. from all other species (Fig. 8C). The results of the PCA and ratio extractor are used and discussed in the diagnoses and remarks of the species treatments below.

The PCA and ratio extractor results of the addional species-level analyses as well as the results of the allometry tests of all species group- and species-level comparisions are given in Suppl. material 5.

Taxonomic section

Anacharis **Dalman, 1823**

Anacharis Dalman, 1823 - Type species: *Cynips eucharioides* Dalman, 1818.

Megapelmus Hartig, 1840 - Type species: *Megapelmus spheciformis* Hartig, 1840 (= *Anacharis euchariodes* (Dalman, 1818)).

Synapsis Förster, 1869 - Type species: *Synapsis aquisgranensis* Förster, 1869 (= *Anacharis immunis* Walker, 1835), homonymous with beetle genus *Synapsis* Bates, 1868.

Prosynapsis Dalla Torre & Kieffer, 1910 - Type species: *Prosynapsis aquisgranensis* (Förster, 1869) (= *Anacharis immunis* Walker, 1835) - replacement name for *Synapsis* Förster, 1869, due to the aforementioned homonymy.

Diagnosis. The genus *Anacharis* is characterised by an elongate, smooth petiole (sometimes with some vague longitudinal striae, but never sculptured as in *Aegilips* Walker, 1835 and *Xyalaspis* Hartig, 1843). The mesoscutellum does not overhang the propodeum (as sometimes in *Aegilips* and always in *Xyalaspis*). The mesoscutellum is posteriorly rounded, never extended apically (usually pointed in *Aegilips*, pointed or extended into a spine in *Xyalaspis*). The mesoscutellum always possesses a posterior carina that separates the mesoscutellum into a dorsal and posterior surface (circumscutellar carina absent, indistinct or present in *Aegilips* and *Xyalaspis*). The circumscutellar carina is sometimes posteriorly flanged upwards, appearing tooth-like in lateral view (never flanged upwards in *Aegilips* and *Xyalaspis*, if carina is present). The mesopleural line is exhibited as a rugose and/or striate furrow, often extending from the anterior to close to the posterior margin of the mesopleuron (mesopleural sculpture in *Aegilips* and *Xyalaspis* not concentrated in any sort of furrow but equally spread out along anterior margin, sometimes reduced to the anterior half of mesopleuron or totally absent). The metasoma is apically pointed, especially in females (metasoma apically ending more abruptly in *Aegilips* and *Xyalaspis*). The occiput is either smooth, striolate, or striate (smooth in *Aegilips* and *Xyalaspis*). The upper face has a usually shallow to sometimes more distinct median dent (Fig. 4C, usually absent in *Aegilips* and *Xyalaspis* Fig. 4D).

Etymology and grammatical gender. Derived from Greek "Ana (ἀνά, up, back, against, above, across, throughout, again, counter)" and "charis (Χάρις, grace, beauty, favour, loveliness)". Dalman describes *Anacharis* as looking similar to eucharitids (Dalman 1823) and arguably wanted to emphasise them as at least a "counterbeauty" to the eucharitids.

The grammatical gender of *Anacharis* is female (as used in Westwood 1833 and discussed in Reinhard 1860).

Remarks. The most recent diagnoses of the genus are presented in van Noort et al. (2015) and Mata-Casanova et al. (2016). The differential diagnosis presented here is a complemented version of the previous diagnoses. It aims to characterise the genus in the Western Palaearctic fauna by differentiating it against *Aegilips* and *Xyalaspis*, which are the only other anacharitine genera known from the Western Palaearctic. The added characters have not been evaluated as to their diagnostic value for the anacharitine fauna outside the Western Palaearctic.

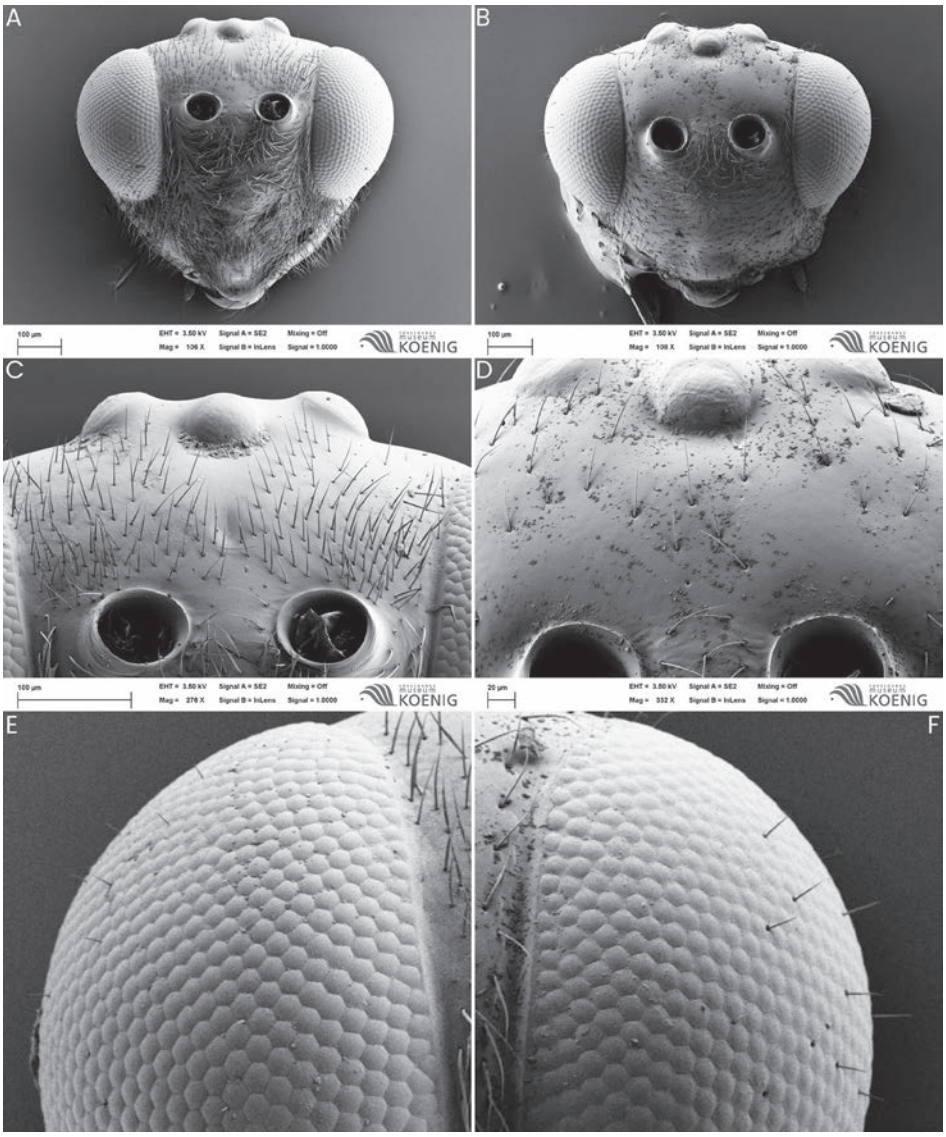

Figure 4. SEM images of the heads of *Anacharis typica*: ZFMK-HYM-00039676 (left: **A, C, E**) and *Aegilips* sp.: ZFMK-HYM-00039677 (right: **B, D, F**) with the specifications used for the SEM imaging shown at the bottom of each image (**A–D**) **A, B** overview of the head in frontal view **C, D** Upper face, frontal, showing the median dent typical for *Anacharis* (**C**) and its absence in *Aegilips* sp. (**D**) **E, F** the compound eyes with scattered setae (cropped images from **A** and **B** respectively).

The species groups

The presence of two groups within *Anacharis* is corroborated by all methods applied here, i.e. the molecular analysis (Fig. 1), differences in WIPs (Fig. 2), differences in male genitalia proportions (Fig. 3) and the multivariate morphometric analysis (Fig. 5).

The description of two species groups is well-suited to classify the Western Palaearctic fauna. Species from outside this region are currently not considered and species groups and their diagnoses might need revision after treatment of the *Anacharis* world fauna. For example, the placement of the Nearctic *A. melanoneura* into one of the species groups might be problematic, as females of the species are reported to have placodeal sensillae starting at flagellomere two (Mata-Casanova et al. 2018), while they start at flagellomere one (*euchariodes* group) or three (*immunis* group) in the Western Palaearctic species.

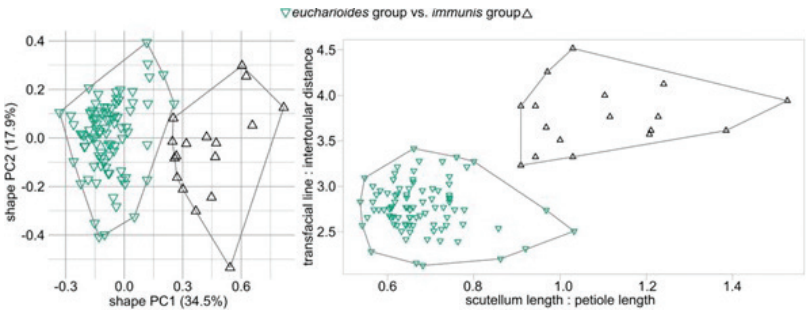

Figure 5. Results of morphometric analyses of the *euchariodes* species group against the *immunis* species group shape PCA shows almost full separation between species groups (Fig. 5 left) lda-ratio extractor suggests two ratios to fully separate the two species groups, which are included in the diagnoses of the respective groups groups (Fig. 5 right).

immunis species group

Diagnosis. The genal carina is at a right angle to the vertical axis of the face in facial view (Figs 9C, 11C). The coriaceous texture of the malar area is meeting the eye only on its ventral margin. The occiput is smooth (Fig. 18A). The placodeal sensilla in the female antenna are starting at the fourth flagellomere. The eye-to-eye distance is 3.2 to 4.5 times longer than the intertorular distance (Figs 5 right, 9C, 11C). The notauli are weak, fading to absence anteriorly, inside without transversal carinae (Figs 9D, 11D). The mesopleural line is posteriorly fading and points to the posterior margin submedially (Figs 9B, 11B). The nuchal collar is slim and is either dorsomedially confluent with the median carina of the propodeum or it is dorsally bilobed, but never projecting dorsomedially (Fig. 6A, B). The inner side of the hind coxa has an equally distributed pubescence on its entire length (Fig. 11B). The mesoscutellum is 0.9–1.5 times longer than the petiole (Figs 5 right, 9A, 11A). In the WIPs, the apical spot of the hind wing is not restricted to the apical area but distinctly extending into the basiocubital area (Fig. 2A, B). The genitalia of the *immunis* species group are 374–423 (mean 401) µm long (Fig. 3A, B). The male genitalia have one of the apical parameral setae situated sub-apically.

Species included. *Anacharis ensifer* Walker, 1835, stat. rev., *A. immunis* Walker, 1835 and *A. norvegica* Mata-Casanova & Pujade-Villar, 2018.

Remarks. Previously, the species of *Anacharis* were grouped by their petiole length relative to the hind coxa length. Fergusson (1986), for example, separates his *A. immunis* and *A. eucharioides* by stating that the former has a petiole that is shorter than the hind coxa and the latter having it longer than the hind coxa. Mata-Casanova et al. (2018) changed the state of the species *A. immunis* and *A. norvegica* (i.e. what we call the *immunis* species group) to "petiole as long as hind coxa". We found the ratio of the petiole length to the metacoxa length to be quite variable inter- and intraspecifically. The morphometric analysis revealed that instead the ratio of mesoscutellum length and petiole length is better suited to characterise the species groups (Fig. 5B). In addition to the relative petiole length, we propose a manifold of mainly qualitative characters that can be used more reliably to separate the two species groups.

The multivariate morphometrics on species group- level resulted in the addition of two diagnostic characters that are – in particular when combined – suited to separate specimens from either species group. Accordingly, the addition of morphometric analyses proved useful for separating *Anacharis* specimens on species group- level.

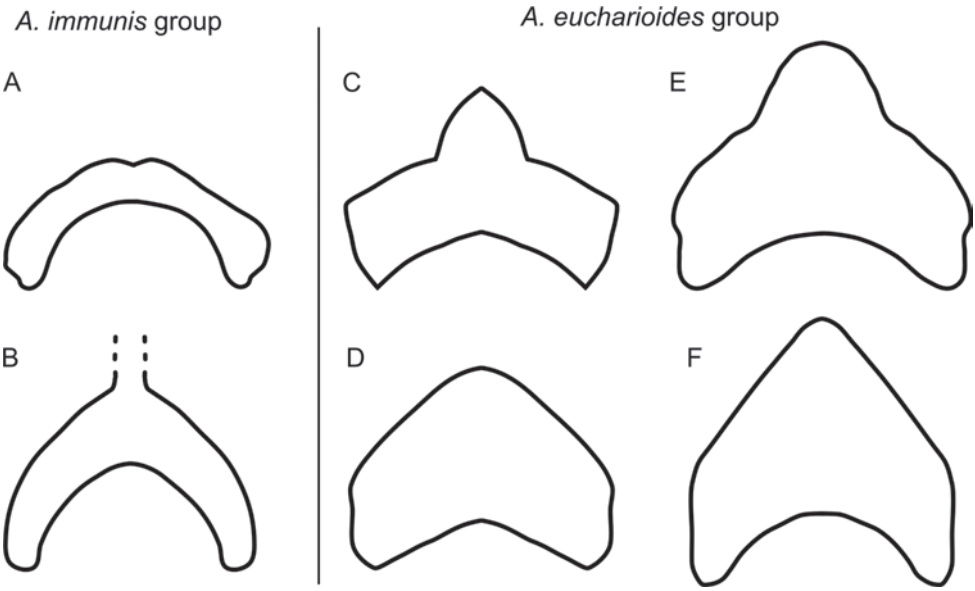

Figure 6. Variation of the nuchal collar within the two species groups **A** bilobed **B** confluent with median carina of propodeum **C** dorsomedial narrow tooth (as typical but not exclusive for *A. martinae* sp. nov.) **D** broad projection **E** blunt tooth **F** broad and high projection.

eucharioides species group

Diagnosis. The genal carina within the *eucharioides* species group is not at a right angle to the vertical axis of the face in facial view (e.g. Fig. 10C). The coriaceous texture of the malar area is meeting the eye along its ventral and inner margin. The occiput has at least some noticeable transversal striolation to striation laterally to medially (Fig. 18B).

The placodeal sensilla in the female antenna are starting at the first flagellomere. The eye-to-eye distance is 2.1–3.4 times longer than the intertorular distance (Fig. 5 right, e.g. Fig. 10C). The notauli are weak and smooth (Fig. 14D) to strong and with distinct transversal carinae inside, never fading anteriorly (e.g. Fig. 10D). The mesopleural line is not distinctly fading posteriorly (except in *A. petiolata* & *A. typica*), and abruptly sloping towards posteroventral hypocoxal furrow in posterior quarter (e.g. Fig. 14B). The nuchal collar is broader and has a broad or narrow dorsomedial projection or tooth, which is not confluent with the median carina of the propodeum (Fig. 6C–F). The inner side of the hind coxa has no continuous pubescence along its entire length; it has some few setae dorsally or is entirely glabrous and has a patch of pubescence ventrally. The mesoscutellum is 0.5–1 times longer than the petiole (Fig. 5 right, e.g. Fig. 10A). In the WIPs, the apical spot of the hind wing is restricted to the apical area (Fig. 2C–G). The genitalia of the *euchariodes* species group are 243–331 (mean 278) µm long (Fig. 3C–F). The male genitalia have all of the three apical parameral setae situated distinctly apically.

Species included. *A. euchariodes* (Dalman, 1818), *A. martinae* sp.nov., *A. maxima* sp. nov., *A. minima* sp. nov., *A. petiolata* (Zetterstedt, 1838), stat. rev. & *A. typica* Walker, 1835, stat. rev.

Remarks. For a discussion of the relationship between the two species groups, see remarks under *immunis* species groups.

The PCA of the *euchariodes* species group (Fig. 7) including all species shows wide overlap, i.e. that it is not possible to discriminate the species on single morphometric ratios alone. It indicates that species are quite variable morphometrically. In addition, the low values of variation explained by PC1 and PC2 indicate that all species are relatively similar morphometrically. In summary, the results shown in Fig. 7 indicate that diagnosing species in the *euchariodes* species group must largely rely on qualitative characters, and an integration of the species delimitation results from analysis of molecular sequence data.

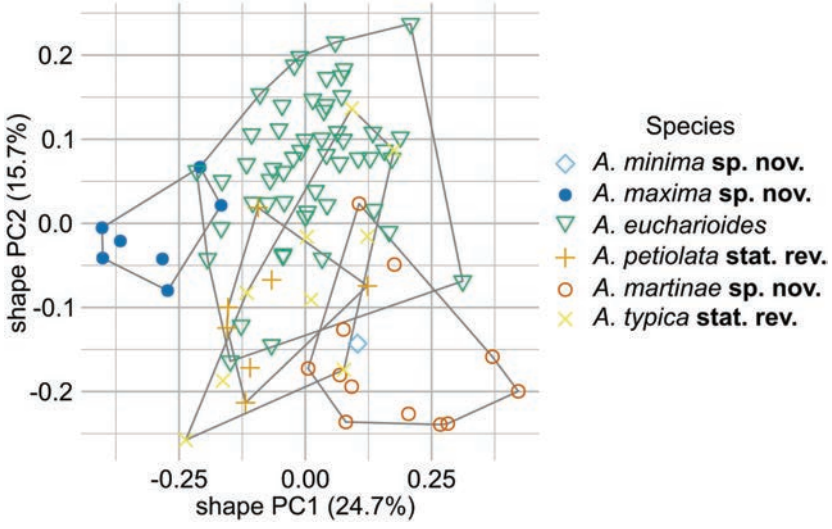

Figure 7. PCA of all species of the euchariodes species group.

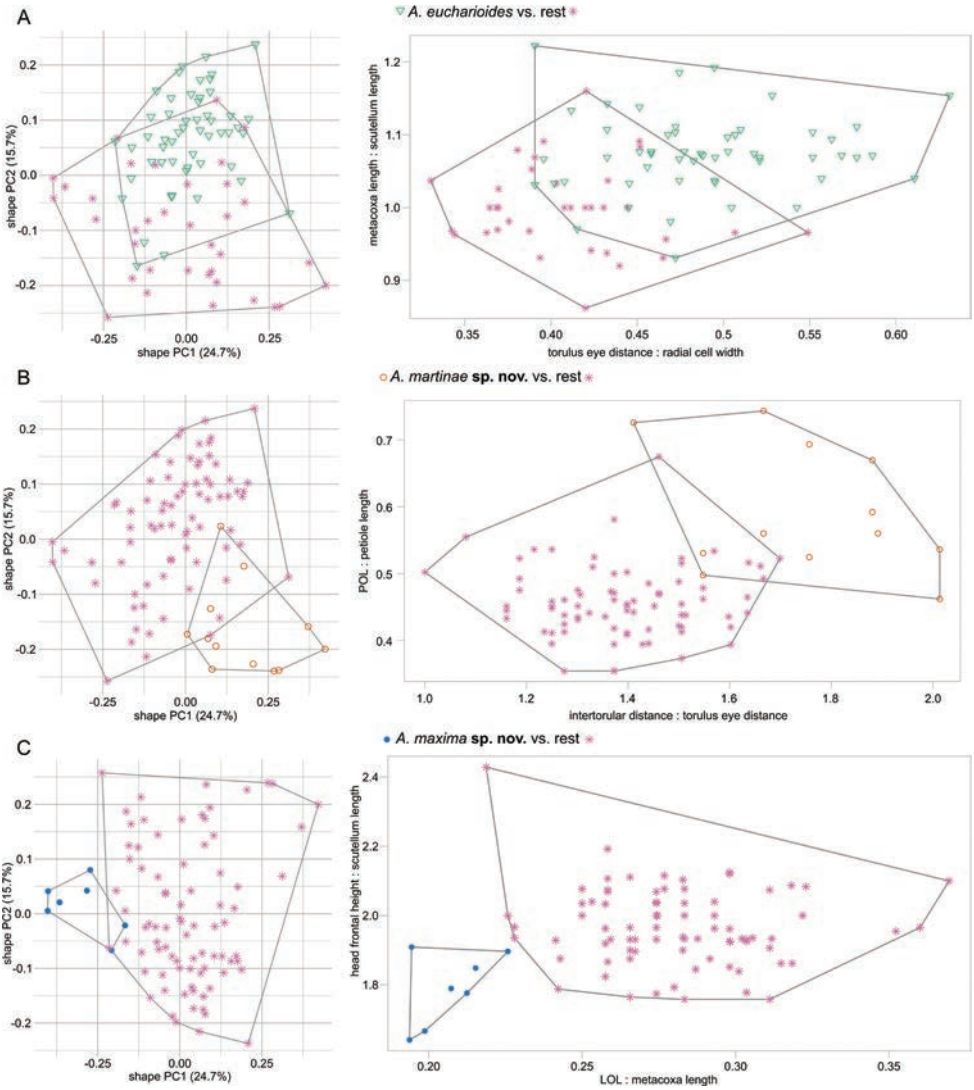

Figure 8. The PCA plot (left) and lda extractor plot (right) of **A** *A. euchariodes* against the rest of the *euchariodes* species group **B** *A. martinae* sp. nov. against the rest of the *euchariodes* species group **C** *A. maxima* sp. nov. against the rest of the *euchariodes* species group.

Anacharis ensifer Walker, 1835, stat. rev.

Figs 2A, 3A, 9A–E

Anacharis ensifer Walker, 1835: 522 - lectotype (NHMUK) ♀, photographs examined.
Megapelmus rufiventris Hartig, 1841: 358 (removed from synonymy with *A. immunis*) - lectotype (ZSM) ♀, photographs examined.

Diagnosis (n=13). Belongs to the *immunis* species group. Similar to *A. norvegica* in generally having a largely sculptured mesoscutellum (largely smooth in *A. immunis*) (Fig.

9D). Different from *A. norvegica* by having its mesoscutellum covered with reticulate-foveate sculpture resulting in larger foveae (smaller foveae on mesoscutellum in *A. norvegica*) (Fig. 9D). The circumscutellar carina is distinct and usually flanged upwards and appears in lateral view like a posterodorsal tooth (circumscutellar carina not flanged and less distinct in *A. norvegica*, not appearing like a tooth) (Fig. 9B). The mesopleural line is dorsally well-defined in its anterior half (dorsal margin in anterior half diffused by rugose sculpture of mesopleuron in *A. norvegica*) (Fig. 9B). The mesoscutum lacks, or has just a few, wrinkles and has no distinct anteroadmedian signa (in *A. norvegica*, wrinkles on mesoscutum strong, amplifying the visibility of anteroadmedian signa) (Fig. 9D).

CO1 barcode. n=12. Maximum intraspecific distance = 0.5%. Minimum distance to closest species (*A. immunis*) = 7.8%. CO1 barcode consensus sequence:

AATTTTATACTTTATTTTAGGAATCTGGTCAGCAATATTAGGATCAAGACTTAGTATAATTATTCGAATAGAATTAGGCACCCCATCTCAATTAATCAGAAATGACCAAATTTACAATTCAATTGTAACAGCTCATGCATTTATTATAATTTTTTTTTATAGTTATACCTATTATAGTCGGAGGATTTGGAAATTACCTAATTCCATTAATACTCCTATCCCCAGATATAGCTTTCCCACGATTAAATAATATAAGATTTTGATTTCTAATCCCCTCTTTAATTTTAATAGCTTCAAGATTATTTATTGATCAAGGAGCAGGAACCGGATGAACAGTATATCCCCCTTTATCTTCATTAACAGGTCACTCAGGGATTGCAGTAGACATAACAATTTACTCTCTTCATTTAAGAGGAATTTCTTCAATTTTAGGCTCAATTAATTTTATTAGAACAATTTTAAATATACGAATCAATAAAGTATCAATAGATAAAATTACCCTATTTACATGATCAATTTTTTTAACTACAATTCTATTACTTTTATCATTACCCGTCCTAGCAGGAGGGATCACTATACTTTTATTTGACCGAAACTTAAATACCTCCTTTTTCGATCCCATAGGAGGAGGAGACCCAATTTTATATCAACATTTATTT

Type material.

Lectotype of *Anacharis ensifer* Walker, 1835, designated by Fergusson (1986)

F Walker Coll. 81–86

LECTO-TYPE

B.M. 1981 . Under A. ensifer

LECTOTYPE of A. ensifer Walker det. N.D.M.Fergusson, 1981

B.M. TYPE HYM 7. 161

[QR-code] NHMUK010640456

[for images, see https://data.nhm.ac.uk/dataset/56e711e6-c847-4f99-915a-6894bb5c5dea/resource/05ff2255-c38a-40c9-b657-4ccb55ab2feb/record/10638964]

Lectotype of *Anacharis rufiventris* Hartig, 1841, designated by Fergusson (1986)

LECTO-TYPE

Megapelmus n. sp. ? [handwritten, probably by Hartig himself]

rufiventris. [handwritten, probably by Hartig himself]

LECTOTYPE of Megapelmus rufiventris Hartig det. N.D.M.Fergusson 1982

Anacharis immunis det. N.D.M.Fergusson 1982

Other material examined. DNA barcode vouchers. Belgium • 1 ♀; West Flanders, Ypres, De Triangel, Urban park (bushes); 50.8418°N, 2.8838°E; ca 20 m a.s.l.; 2–23 Jul. 2022; Verheyde, Fons leg.; Malaise trap; ZFMK-TIS-2640867.

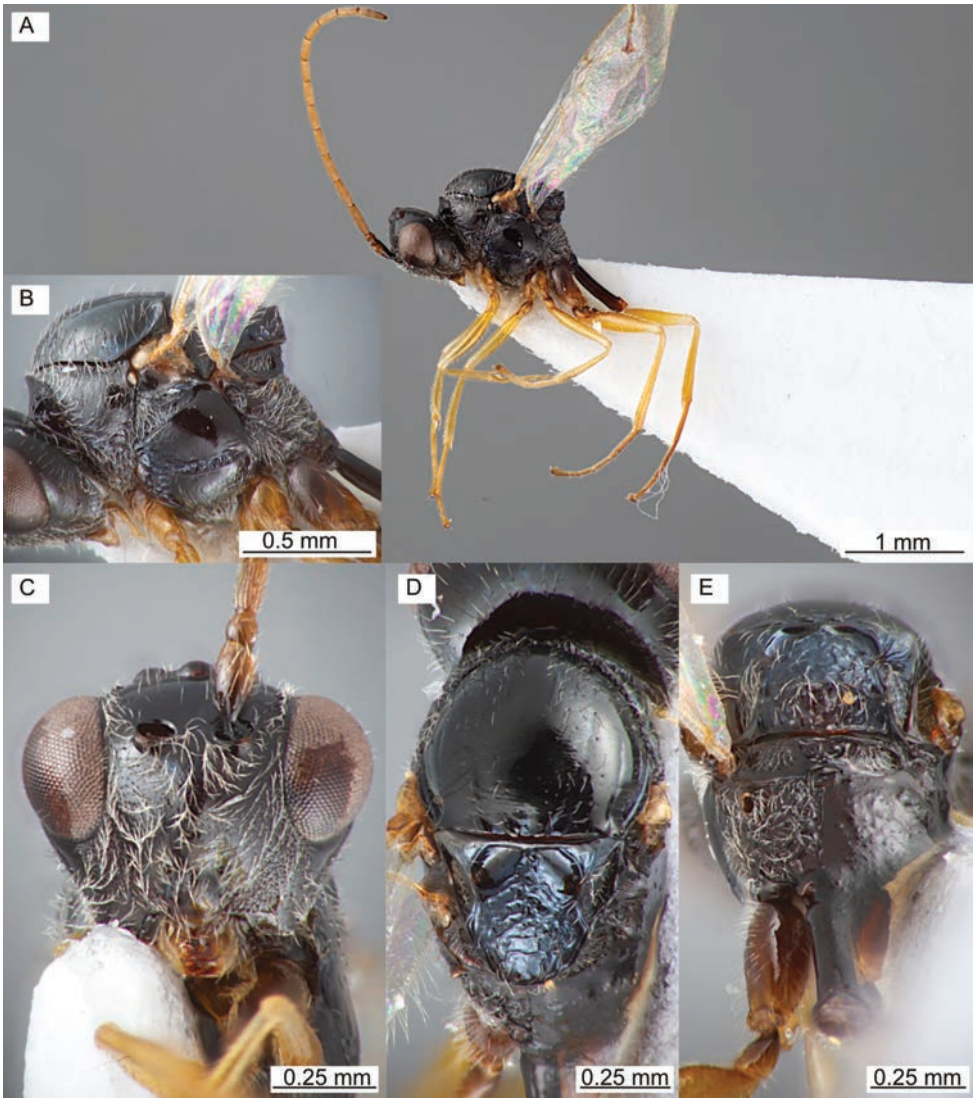

Figure 9. *Anacharis ensifer*, male (ZFMK-TIS-2629206) **A** habitus **B** mesosoma lateral **C** face **D** mesosoma dorsal **E** mesosoma posterior view.

Norway • 2 ♂♂; Rogaland Ytre, Sola, Indraberget; 58.9124°N, 5.6628°E; ca 20 m a.s.l.; 24 Aug.-6 Sep. 2020; Leendertse, Arjen leg.; Malaise trap; ZFMK-TIS-2629222, ZFMK-TIS-2629223. • 1 ♂; same collection data as for preceding; 20 Sep.-5 Oct. 2020; ZFMK-TIS-2629221. • 1 ♀, 3 ♂♂; Rogaland Ytre, Stavanger, Byhaugen; 58.9731°N, 5.6988°E; ca 50 m a.s.l.; 6–29 Aug. 2020; Birkeland, Jarl leg.; Malaise trap; female - ZFMK-TIS-2629272; males - ZFMK-TIS-2629209, ZFMK-TIS-2629210, ZFMK-TIS-2629211. • 1 ♀; same collection data as for preceding; 25 Sep.-31 Oct. 2020; ZFMK-TIS-2629249. • 3 ♂♂; Rogaland Ytre, Time, Mossige;

58.69°N, 5.7239°E; ca 60 m a.s.l.; 17 Sep.-11 Oct. 2020; Mjøs, Alf Tore leg.; Malaise trap; ZFMK-TIS-2629206, ZFMK-TIS-2629207, ZFMK-TIS-2629208.

Material without DNA barcode. Belgium • 3 ♂♂; Walloon Brabant, Ottignies; 16–23 Jul. 1983; Paul Dessart leg.; Malaise trap; JV_Prel_0047 (RBINS), JV_Prel_0048 (RBINS), JV_Prel_0049 (RBINS). • 1 ♀; West Flanders, Ypres, De Triangel, Urban park (pool vegetation); 50.8427°N, 2.884°E; ca 20 m a.s.l.; 18 Jun.-2 Jul. 2022; Fons Verheyde leg.; Malaise trap; ZFMK-TIS-2640864.

Denmark • 1 ♂; Eastern Jutland, Alminde hule, 20 km S of Vejle; 30 May 1982; Torkhild Munk leg.; NHRS-HEVA 000023120 (NHRS). • 1 ♂; Eastern Jutland, Klattrup, 10 km S of Velje, Bygade, on compost heap; 28–29 Jul. 1982; Torkhild Munk leg.; NHRS-HEVA 000023118 (NHRS). • 1 ♀; Eastern Jutland, Nørreskov, 10 km E of Kording; 31 Jul. 1984; Torkhild Munk leg.; NHRS-HEVA 000023119 (NHRS).

Germany • 2 ♀♀; Bavaria, near Schwandorf; 49.3042°N, 12.1184°E; ca 360 m a.s.l.; Ernst Klimsa leg.; specimen in coll MF. • 1 ♂; Brandenburg, Potsdam-Mittelmark, Kleinmachnow; 22 Jun. 1925; S. Bollow leg.; JV_Prel_0042 (SDEI). • 1 ♀; North Rhine-Westphalia, Rhein-Sieg-Kreis, Schladern near Windeck, Sieg river, right river bank; 50.8°N, 7.585°E; ca 130 m a.s.l.; 4–11 Jul. 2017; ZFMK et al. leg.; Malaise trap; ZFMK-TIS-2629278.

The Netherlands • 1 ♀; Gelderland, Nijmegen, Gelderse poort; 23 Aug. 2022; R. Lexmond leg.; Malaise trap; JV_Prel_0050 (RBINS).

Norway • 2 ♀♀; Akershus, Baerum, Ostøya; 10 Jun.-1 Jul. 1984; Fred Midtgaard leg.; NHRS-HEVA 000023124 (NHRS), NHRS-HEVA 000023125 (NHRS). • 1 ♀; Norvegia alpina (“Nv alp”); [1832]; Carl Henning Boheman leg.; NHRS-HEVA 000023123 (NHRS). • 2 ♀♀; Rogaland Ytre, Stavanger, Byhaugen; 58.9731°N, 5.6988°E; ca 50 m a.s.l.; 6–29 Aug. 2020; Jarl Birkeland leg.; Malaise trap; ZFMK-TIS-2629273, ZFMK-TIS-2629274. • 1 ♂; same collection data as for preceding 25 Sep.-31 Oct. 2020; ZFMK-TIS-2629205.

Sweden • 1 ♀; Gotska sandön, Lilla lövskogen; 6 Aug. 1952; Anton Jansson leg.; NHRS-HEVA 000023126 (NHRS). • 3 ♂♂; Öland, Ås, Ottenbylund, glade in deciduous grove; 56.2194°N, 16.4224°E; ca 10 m a.s.l.; 24 Jul.-1 Aug. 2003; Swedish Malaise Trap Project (Swedish Museum of Natural History) leg.; Malaise trap; NHRS-HEVA 000023139 (NHRS), NHRS-HEVA 000023140 (NHRS), NHRS-HEVA 000023141 (NHRS). • 1 ♂; Öland, Kastlösa; 26 Jun. 1952; Karl-Johan Hedqvist leg.; NHRS-HEVA 000023138 (NHRS). • 1 ♂; Öland, Torslunda, Gamla skogsby, Diversitetsängen, rich transitional meadow with shrubs near nemoral forest; 56.6167°N, 16.5076°E; ca 40 m a.s.l.; 17 Jul.-7 Aug. 2003; Swedish Malaise Trap Project (Swedish Museum of Natural History) leg.; Malaise trap; NHRS-HEVA 000023142 (NHRS). • 2 ♂♂; Östergötland, Omberg, Stocklycke, meadow in Tilia-dominated forest; 58.3075°N, 14.631°E; ca 130 m a.s.l.; 22 Jul.-5 Aug. 2003; Swedish Malaise Trap Project (Swedish Museum of Natural History) leg.; Malaise trap; NHRS-HEVA 000023143 (NHRS), NHRS-HEVA 000023144 (NHRS). • 3 ♀♀, 1 ♂; Småland; [18xx]; Carl Henning Boheman leg.; females - NHRS-HEVA 000023127 (NHRS), NHRS-HEVA 000023128 (NHRS), NHRS-HEVA 000023129 (NHRS);

male - NHRS-HEVA 000023130 (NHRS). • 1 ♀, 1 ♂; Södermanland, Ludgo s:n, Tovetorp fieldstation; 58.9478°N, 17.1485°E; ca 50 m a.s.l.; 6 Aug. 2012; Mattias Forshage leg.; sweep net; female - NHRS-HEVA 000023131 (NHRS); male - NHRS-HEVA 000023132 (NHRS). • 1 ♀; Södermanland, Trosa kommun, Hunga södergård 1, agricultural backyard, heavily eutrophicated, in tall grass near stable manure pile; 58.9207°N, 17.5212°E; ca 20 m a.s.l.; 9–19 Aug. 2004; Swedish Malaise Trap Project (Swedish Museum of Natural History) leg.; Malaise trap; NHRS-HEVA 000023133 (NHRS). • 1 ♀; Uppland, Håbo kommun, Biskops-Arnö, northern beach, elm grove; 59.6721°N, 17.5009°E; ca 10 m a.s.l.; 20 May-20 Jun. 2005; Swedish Malaise Trap Project (Swedish Museum of Natural History) leg.; Malaise trap; NHRS-HEVA 000023136 (NHRS). • 1 ♀; Uppland, Uppsala kommun, Ekdalen, herb-rich open oak forest; 59.9715°N, 18.355°E; ca 40 m a.s.l.; 21 Jul.-4 Aug. 2003; Swedish Malaise Trap Project (Swedish Museum of Natural History) leg.; Malaise trap; NHRS-HEVA 000023135 (NHRS). • 1 ♀; same collection data as for preceding 23 Aug.-6 Sep. 2004; NHRS-HEVA 000023134 (NHRS). • 1 ♂; Uppland, Vallentuna, forest; 19 Jul. 1959; Karl-Johan Hedqvist leg.; sweep net; NHRS-HEVA 000023137 (NHRS).

Switzerland • 1 ♀; Genève, La Louton; 12 Aug. 1960; André Comellini leg.; specimen at MHNG. • 1 ♀; Neuchâtel, Auvernier; 2 Aug. 1960; Jacques de Beaumont leg.; specimen at MHNG. • 1 ♀; same collection data as for preceding 5 Aug. 1959; specimen at MHNG. • 1 ♂; same collection data as for preceding 8 Aug. 1957; specimen at MHNG. • 1 ♂; same collection data as for preceding 18 Aug. 1986; specimen at MHNG. • 1 ♀; same collection data as for preceding 26 Aug. 1956; specimen at MHNG. • 1 ♀; same collection data as for preceding 28 Aug. 1956; specimen at MHNG. • 1 ♂; same collection data as for preceding 31 Aug. 1956; specimen at MHNG. • 1 ♂; Vaud, Bussigny; 26 Jul. 1958; Jacques de Beaumont leg.; specimen at MHNG. • 1 ♂; Vaud, Lutry Aug. 1956; Jacques Aubert leg.; specimen at MHNG. • 1 ♀; Vaud, Pampigny; 19 Jun. 1960; Jacques de Beaumont leg.; specimen at MHNG.

Biology. Summer species, flying mainly from May to October, peak in August. Collected mainly in deciduous forest and in open nemoral habitats.

Distribution. Verified by morphological examination: Belgium, Denmark, Germany, The Netherlands, Norway, Sweden, Switzerland, United Kingdom (locus typicus: England, near London or Windsor forest).

No DNA barcode matches with publicly available sequences from other countries.

Lowland species, occurring in elevations below 400 m a.s.l.

Remarks. We remove *A. ensifer* from the synonymy with *A. immunis* that was established by Fergusson (1986).

Walker's original name *Anacharis ensifer* was changed into *A. ensifera* by Reinhard (1860). While Thomson (1862) maintained 'ensifer', most authors from Cameron (1890) on followed Reinhard's emendation. However, 'ensifer' can be a noun as well as an adjective (and Walker's intentions are not clear in the description), but Reinhard's emendation for gender agreement purposes makes sense only if it is an adjective. §31.2.2 in the zoological code (ICZN 1999) clearly states that in such ambiguous

cases it is to be treated as a noun, thus the original spelling is retained and the gender ending remains unchanged.

Almost all specimens of *A. ensifer* show an intermediate stage of sculpturing of the mesoscutellum between *A. immunis* (largely smooth) and *A. norvegica* Mata-Casanova & Pujade-Villar, 2018 (finely foveate on both dorsal and posterior surface of the mesoscutellum), with the exception of ZFMK-TIS-2629272, which has a largely smooth mesoscutellum like in *A. immunis* but clusters within *A. ensifer* by its CO1 barcode sequence.

Anacharis ensifer falls within the diagnosis of *A. immunis* in Mata-Casanova et al. (2018) and thus the two host records and all distributional data given therein must be re-evaluated considering the existence of two species behind *A. immunis* sensu Mata-Casanova et al. (2018).

Works prior to Fergusson (1986) describe *A. ensifer* largely based on colouration, but always state a smooth mesoscutellum (e.g. Reinhard 1860 & von Dalla-Torre and Kieffer 1910), which is not in line with our findings. Historical literature records therefore require critical evaluation, too.

***Anacharis eucharioides* (Dalman, 1818)**

Figs 2G, 3F, 10A–E

Cynips eucharioides Dalman, 1818: 78 - type lost.
Anacharis tinctus Walker, 1835: 520 - lectotype (NHMUK) ♀, synonymised in Fergusson (1968), photographs examined.
Megapelmus spheciformis Hartig, 1840: 202 (removed from synonymy with *A. typica*) - lectotype (ZSM) ♂, first synonymised in Reinhard (1860), examined.
Anacharis fergussoni Mata-Casanova & Pujade-Villar, 2018: 16 syn. nov. - holotype (CNC) ♀, photographs examined.
Anacharis eucharoides auct., common misspelling.

Diagnosis (n=290). Most common species within the *eucharioides* species group. Medium sized body (2.7–3.4, mean 3.1 mm, similar to *A. typica*, *A. petiolata* & *A. martinae*). Differing from *A. typica* and *A. petiolata* by having a mesoscutellum with a median carina present, which is typically interrupted centrally by reticulation (largely smooth and even in *A. petiolata* and *A. typica*) (Fig. 10D). Differing from *A. martinae* by having the lateromedial area of the pronotum smooth to rugose (Fig. 10B, with longitudinal carinae that are a continuation of the ventral carinae in *A. martinae*). Unique in usually having the mesoscutum glabrous to more sparsely pubescent than the rest of the mesoscutum (Fig. 10D, more evenly pubescent in all other species). The male genitalia of *A. eucharioides* (Fig. 3F) are unique in not being significantly widened basally or medially, i.e. being more parallel-sided (basally or medially widened in all other species Fig. 3C–E).

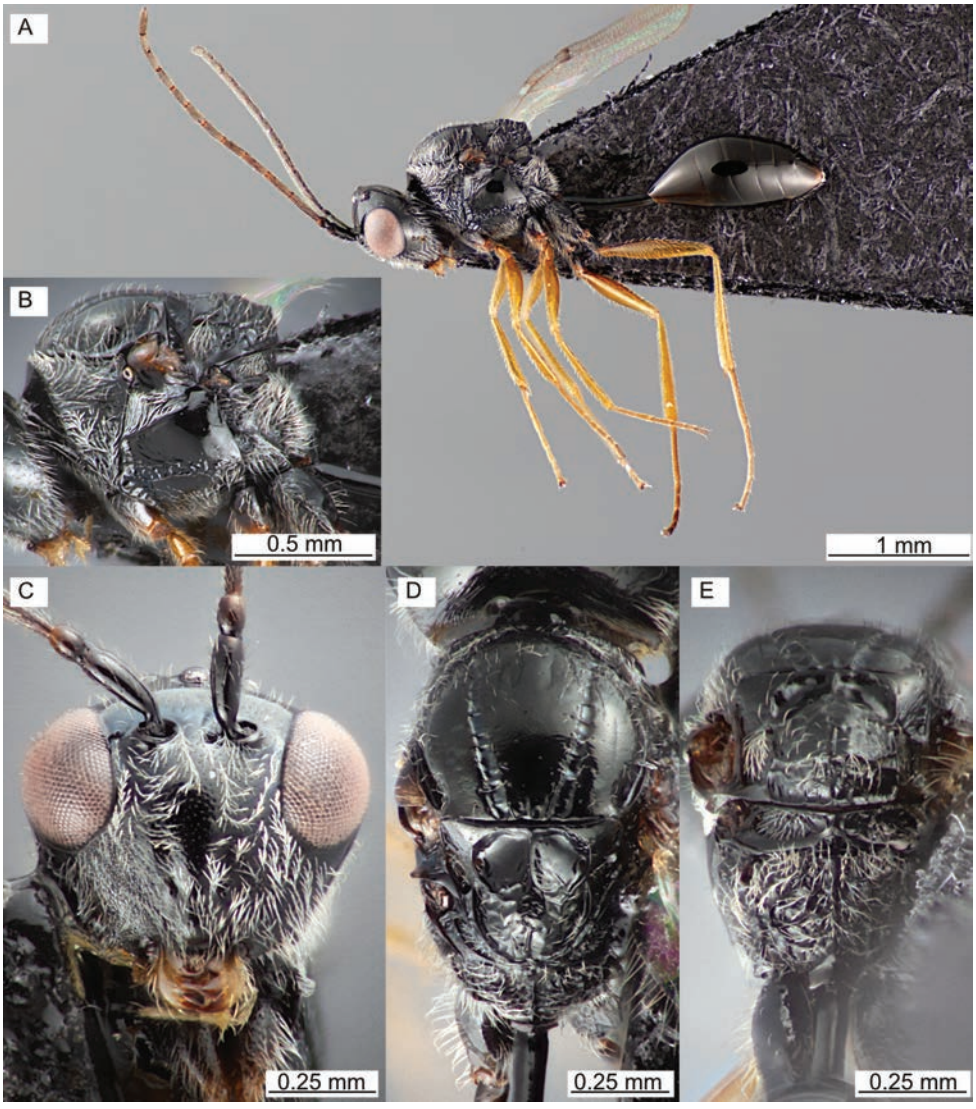

Figure 10. *Anacharis euchariodes*, female (ZFMK-TIS-2640762) **A** habitus **B** mesosoma lateral **C** face **D** mesosoma dorsal **E** mesosoma posterior view

CO1 barcode. n=289. Maximum intraspecific distance = 2.5%. Minimum distance to closest species (*A. petiolata*) = 2.9%. CO1 barcode consensus sequence:

AATTTTATACTTTATTTTAGGTATTTGATCTGGAATAATAGGAT-
CAAGATTAAGAATAATTATTCGAATAGAATTAGGAACCCCATCTCAAT-
TAATCATAAATGATCAAATTTATAATTCAATTGTAACTGCTCATGCATT-
TATTATAATTTTCTTTATAGTTATACCTATTATAGTTGGAGGATTTGG-
GAATTATTTAGTACCTTTAATATTAATTTCTCCTGATATAGCTTTTC-
CACGATTAAATAATTTAAGATTTTGATTTTTAATCCCTTCCTTATTTT-

TAATAACAATTAATTTATTTATTGATCAAGGAGCAGGAACAGGATGAACT-
GTTTACCCTCCATTATCCTCCCTAACAGGTCATCCATCTATATCAGTA-
GATTTAGTTATTTACTCATTACATTTAAGTGGAATTTCATCAATTCTTG-
GATCAATTAATTTTATTGTAACCATTTTAAATATACGAATAACTTCTA-
TATCTATAGACAAAATTTCATTATTTATTTGATCTATTTTTCTAACTA-
CAATTTTACTATTATTATCTTTACCCGTACTAGCAGGAGGATTAACGA-
TACTATTATTTGATCGAAATTTAAATACATCTTTTTTTGACCCCACAG-
GAGGAGGAGACCCTATTCTTTATCAACATTTATTT

Type material.

Lectotype of *Anacharis tinctus* Walker, 1835, designated by Fergusson (1986)

81 86 [on backside of mounting board]

Type

B.M.1981 . Under tincta

LECTO-TYPE

LECTOTYPE Anacharis tincta Walker det. N.D.M.Fergusson, 1981

B.M. TYPE HYM 7.162

[QR code] NHMUK 012858912

[for images, see https://data.nhm.ac.uk/dataset/56e711e6-c847-4f99-915a-6894bb5c5dea/resource/05ff2255-c38a-40c9-b657-4ccb55ab2feb/record/10470209]

Lectotype of *Megapelmus spheciformis* Hartig, 1840, designated by Weld (1952)

Weld 1931

Megapelmus spheciformis [handwritten, probably by Hartig himself]

LECTOTYPE of MEGAPELMUS spheciformis det. N.D.M.Fergusson, 1982

Anacharis eucharoides Dal. det. N.D.M.Fergusson, 1982

Anacharis eucharioides (Dalman, 1818) ♂ Det. Jonathan Vogel 2024

Holotype of *Anacharis fergussoni* Mata-Casanova & Pujade-Villar, 2018

Germany • 1 ♀; Rhineland Palatinate, Mainz-Bingen, Ingelheim am Rhein, orchard; 1–30 Sep. 1968; I. Sreffan leg.; Malaise trap.

[for images, see https://www.cnc.agr.gc.ca/taxonomy/Specimen.php?id=3274133]

Other material examined. DNA barcode vouchers. Belgium • 1 ♀; East Flanders, Assenede, Isabellepolder, Agricultural land with Partridge mix; 51.266°N, 3.71°E; ca 0 m a.s.l.; 12–19 Jun. 2019; UGent leg.; yellow pan trap; ZFMK-TIS-2640673. • 2 ♂♂; West Flanders, Ypres, De Triangel, Urban park (bushes); 50.8418°N, 2.8838°E; ca 20 m a.s.l.; 30 Apr.-14 May 2022; Verheyde, Fons leg.; Malaise trap; ZFMK-TIS-2640843, ZFMK-TIS-2640844. • 3 ♀♀, 9 ♂♂; same collection data as for preceding 14–28 May 2022; females - ZFMK-TIS-2640845, ZFMK-TIS-2640846, ZFMK-TIS-2640847, ZFMK-TIS-2640859, ZFMK-TIS-2640860, ZFMK-TIS-2640861; males - ZFMK-TIS-2640848, ZFMK-TIS-2640849, ZFMK-TIS-2640850, ZFMK-TIS-2640851, ZFMK-TIS-2640852, ZFMK-TIS-2640853, ZFMK-TIS-2640854, ZFMK-TIS-2640855, ZFMK-TIS-2640856, ZFMK-TIS-2640862, ZFMK-TIS-2640863. • 1 ♂; same collection data as for preceding 2–23 Jul. 2022; ZFMK-TIS-2640868. • 3 ♀♀, 2 ♂♂; West Flanders, Ypres, De Triangel, Urban park (pool vegetation); 50.8427°N, 2.884°E; ca 20 m a.s.l.; 14–28 May 2022; Verheyde, Fons

leg.; Malaise trap; females - ZFMK-TIS-2640859, ZFMK-TIS-2640860, ZFMK-TIS-2640861; males - ZFMK-TIS-2640862, ZFMK-TIS-2640863.

Germany • 1 ♂; Baden-Württemberg, Biberach, Altheim; 48.1399°N, 9.4491°E; ca 540 m a.s.l.; 6–19 Aug. 2013; Schmalfuß, H. leg.; Malaise trap; ZFMK-TIS-2629512. • 2 ♀♀, 8 ♂♂; Baden-Württemberg, Karlsruhe, Malsch, Hansjakobstraße, garden; 48.8835°N, 8.3197°E; ca 120 m a.s.l.; 26 Apr.-10 May 2020; Dieter Doczkal leg.; Malaise trap; females - ZFMK-TIS-2640753, ZFMK-TIS-2640754; males -ZFMK-TIS-2640745, ZFMK-TIS-2640746, ZFMK-TIS-2640747, ZFMK-TIS-2640748, ZFMK-TIS-2640749, ZFMK-TIS-2640750, ZFMK-TIS-2640751, ZFMK-TIS-2640752. • 1 ♂; same collection data as for preceding 25 Oct.-8 Nov. 2020; ZFMK-TIS-2640726. • 11 ♀♀, 1 ♂; Baden-Württemberg, Stuttgart, Espan; 49.6167°N, 9.2667°E; ca 280 m a.s.l.; 28 Jul.-28 Aug. 2014; Woog, F. leg.; females - ZFMK-TIS-2640775, ZFMK-TIS-2640776, ZFMK-TIS-2640777, ZFMK-TIS-2640778, ZFMK-TIS-2640779, ZFMK-TIS-2640780, ZFMK-TIS-2640781, ZFMK-TIS-2640782, ZFMK-TIS-2640783, ZFMK-TIS-2640784, ZFMK-TIS-2640785; male - ZFMK-TIS-2640786. • 1 ♀, 10 ♂♂; Baden-Württemberg, Tübingen, Hirschau, Oberes Tal, orchard; 48.505°N, 8.993°E; ca 390 m a.s.l.; 29 Apr.-13 May 2014; Kothe, T., Engelhardt, M., Bartsch, D. leg.; Malaise trap; female - ZFMK-TIS-2629263; males - ZFMK-TIS-2629200, ZFMK-TIS-2629201, ZFMK-TIS-2629202, ZFMK-TIS-2629203, ZFMK-TIS-2629204, ZFMK-TIS-2629218, ZFMK-TIS-2629540, ZFMK-TIS-2629541, ZFMK-TIS-2629542, ZFMK-TIS-2640774. • 1 ♂; Baden-Württemberg, Tübingen, Hirschau, Oberes Tal, orchard; 48.505°N, 8.9935°E; ca 370 m a.s.l.; 23 May-6 Jun. 2014; Kothe, T., Engelhardt, M., Bartsch, D. leg.; Malaise trap; ZFMK-TIS-2628235. • 3 ♀♀; Baden-Württemberg, Tübingen, Hirschau, Wiesenweingärten; 48.5043°N, 8.9956°E; ca 380 m a.s.l.; 17–31 Jul. 2014; Kothe, T., Engeldhardt, M., König, C. leg.; Malaise trap; ZFMK-TIS-2629238, ZFMK-TIS-2629267, ZFMK-TIS-2629268. • 1 ♀; Baden-Württemberg, Tübingen, Steinenberg; 48.5306°N, 9.0312°E; ca 470 m a.s.l.; 31 Jul.-14 Aug. 2014; Kothe, T., Engeldhardt, M., König, C. leg.; Malaise trap; ZFMK-TIS-2629237. • 4 ♀♀; Baden-Württemberg, Tübingen, Steinenberg; 48.5313°N, 9.03°E; ca 490 m a.s.l.; 4–17 Jul. 2014; Kothe, T., Engelhardt, M., König, Ch. leg.; ZFMK-TIS-2629504, ZFMK-TIS-2629505, ZFMK-TIS-2629506, ZFMK-TIS-2629507. • 1 ♀, 1 ♂; Baden-Württemberg, Tübingen, Steinenbergturm; 48.531°N, 9.03°E; ca 490 m a.s.l.; 14–29 Aug. 2014; Kothe, T., Engeldhardt, M., König, C. leg.; Malaise trap; female - ZFMK-TIS-2629236; male - ZFMK-TIS-2629219. • 1 ♂; Baden-Württemberg, Tübingen, Wurmlingen, Gengental, orchard; 48.5131°N, 8.9923°E; ca 370 m a.s.l.; 13–23 May 2014; Kothe, T., Engeldhardt, M., König, C. leg.; Malaise trap; ZFMK-TIS-2640681. • 1 ♀, 1 ♂; Bavaria, Main-Spessart, Lohr, Nat. res. Romberg, pasture woodland; 49.9864°N, 9.5896°E; ca 190 m a.s.l.; 9 Jun.-6 Jul. 2018; Dieter Doczkal leg.; Malaise trap; female - ZFMK-TIS-2640717; male - ZFMK-TIS-2640716. • 1 ♂; Bavaria, Rhön-Grabfeld, Fladungen, Nat. res. Schwarzes Moor, Karpatenbirkenwald; 50.5117°N, 10.071°E; ca 780 m a.s.l.; 26 Jun.-18 Jul. 2017; Dieter Doczkal leg.; Malaise trap; ZFMK-TIS-2629538. • 2 ♀♀; Hesse, Gießen, Nat. res. Holzwäldchen bei

Gleiberg; 50.605°N, 8.6316°E; ca 190 m a.s.l.; 14 Jun. 2021; GBOL III leg.; sweep net; ZFMK-TIS-2629494, ZFMK-TIS-2629495. • 1 ♀; Hesse, Kassel, Nat. res., „Fuldaschleuse Wolfsanger“, meadow along Fulda river with Salix and Phragmites; 51.329°N, 9.5565°E; ca 130 m a.s.l.; 13–27 Oct. 2020; GBOL III leg.; sweep net; Loc. 1; ZFMK-TIS-2628230. • 3 ♀♀; Hesse, Rheingau-Taunus, Lorch am Rhein, above Nollig castle; 50.0491°N, 7.7978°E; ca 240 m a.s.l.; 27 May-7 Jun. 2013; Niehuis, Oliver leg.; Malaise trap; MF 1; ZFMK-TIS-2629498, ZFMK-TIS-2629499, ZFMK-TIS-2629500. • 1 ♀, 1 ♂; same collection data as for preceding 17–25 Jun. 2015; MF 4; female - ZFMK-TIS-2629248; male - ZFMK-TIS-2629214. • 8 ♂♂; same collection data as for preceding 15–21 Jul. 2013; MF 1; ZFMK-TIS-2629227, ZFMK-TIS-2629240, ZFMK-TIS-2629241, ZFMK-TIS-2629521, ZFMK-TIS-2629522, ZFMK-TIS-2629523, ZFMK-TIS-2629524, ZFMK-TIS-2629525. • 20 ♂♂; same collection data as for preceding 21–27 Jul. 2013; ZFMK-TIS-2629225, ZFMK-TIS-2629226, ZFMK-TIS-2629553, ZFMK-TIS-2629554, ZFMK-TIS-2629555, ZFMK-TIS-2629556, ZFMK-TIS-2629557, ZFMK-TIS-2629558, ZFMK-TIS-2629559, ZFMK-TIS-2629560, ZFMK-TIS-2629576, ZFMK-TIS-2629577, ZFMK-TIS-2640820, ZFMK-TIS-2640821, ZFMK-TIS-2640822, ZFMK-TIS-2640823, ZFMK-TIS-2640824, ZFMK-TIS-2640825, ZFMK-TIS-2640826, ZFMK-TIS-2640827. • 1 ♀; Hesse, Rheingau-Taunus, Lorch am Rhein, above Nollig castle; 50.0495°N, 7.7966°E; ca 250 m a.s.l.; 12–17 Jun. 2015; Niehuis, Oliver leg.; Malaise trap; MF 3; ZFMK-TIS-2629252. • 3 ♂♂; same collection data as for preceding 17–25 Jun. 2015; ZFMK-TIS-2628232, ZFMK-TIS-2629212, ZFMK-TIS-2629213. • 1 ♀; Hesse, Rheingau-Taunus, Lorch am Rhein, above Nollig castle; 50.0498°N, 7.7974°E; ca 260 m a.s.l.; 27 May-7 Jun. 2013; Niehuis, Oliver leg.; Malaise trap; MF 2; ZFMK-TIS-2629266. • 2 ♀♀; same collection data as for preceding 7–15 Jun. 2013; ZFMK-TIS-2628233, ZFMK-TIS-2629250. • 5 ♀♀; same collection data as for preceding 15–23 Jun. 2013; ZFMK-TIS-2629269, ZFMK-TIS-2629270, ZFMK-TIS-2629271, ZFMK-TIS-2629501, ZFMK-TIS-2629502. • 7 ♂♂; same collection data as for preceding 15–21 Jul. 2013; ZFMK-TIS-2629513, ZFMK-TIS-2629515, ZFMK-TIS-2629550, ZFMK-TIS-2629551, ZFMK-TIS-2629552, ZFMK-TIS-2640710, ZFMK-TIS-2640711. • 12 ♂♂; same collection data as for preceding 21–27 Jul. 2013; ZFMK-TIS-2629243, ZFMK-TIS-2629244, ZFMK-TIS-2629245, ZFMK-TIS-2629246, ZFMK-TIS-2629496, ZFMK-TIS-2629497, ZFMK-TIS-2629527, ZFMK-TIS-2629528, ZFMK-TIS-2629529, ZFMK-TIS-2629530, ZFMK-TIS-2629531, ZFMK-TIS-2629532. • 1 ♀, 1 ♂; Hesse, Waldeck-Frankenberg, National park Kellerwald-Edersee, Banfehaus, old floodplain of the Banfe; 51.167°N, 8.9749°E; ca 270 m a.s.l.; 22 Jul.-5 Aug. 2021; GBOL III leg.; Malaise trap (Krefeld version); female - ZFMK-TIS-2640790; male - ZFMK-TIS-2640792. • 2 ♀♀; Hesse, Waldeck-Frankenberg, National park Kellerwald-Edersee, Maierwiesen; 51.1555°N, 9.0015°E; ca 370 m a.s.l.; 22 Jun.-8 Jul. 2021; GBOL III leg.; Malaise trap (Krefeld version); ZFMK-TIS-2640807, ZFMK-TIS-2640808. • 9 ♀♀, 1 ♂; Hesse, Waldeck-Frankenberg, NP Kellerwald-Edersee, „Banfe-Haus“; 51.167°N, 8.9749°E; ca 270 m a.s.l.; 7–21 Jul.

2022; GBOL III leg.; Malaise trap; females - ZFMK-TIS-2640761, ZFMK-TIS-2640762, ZFMK-TIS-2640763, ZFMK-TIS-2640764, ZFMK-TIS-2640765, ZFMK-TIS-2640766, ZFMK-TIS-2640767, ZFMK-TIS-2640768, ZFMK-TIS-2640769; male - ZFMK-TIS-2640755. • 1 ♀; Hesse, Waldeck-Frankenberg, NP Kellerwald-Edersee, „Kleiner Mehlberg“; 51.2105°N, 9.042°E; ca 360 m a.s.l.; 30 Sep.-14 Oct. 2021; GBOL III leg.; Malaise trap; ZFMK-TIS-2640610. • 1 ♂; Hesse, Waldeck-Frankenberg, NP Kellerwald-Edersee, „Maierwiesen“; 51.1555°N, 9.0015°E; ca 370 m a.s.l.; 8–22 Jul. 2021; GBOL III leg.; Malaise trap; ZFMK-TIS-2640732. • 1 ♀; Lower Saxony, Lüchow-Dannenberg, Pevestorf, Deichvorland & Deich; 53.0636°N, 11.4742°E; ca 20 m a.s.l.; 6–10 Aug. 2013; Krogmann, Lars leg.; Malaise trap; ZFMK-TIS-2629251. • 1 ♀, 3 ♂♂; North Rhine-Westphalia, Bonn, Garden of Museum Koenig, Various habitats; 50.7215°N, 7.1137°E; ca 70 m a.s.l.; 4 Jul. 2022; Schwingeler, Josefine, Jonathan Vogel leg.; sweep net; female - ZFMK-TIS-2640738; males - ZFMK-TIS-2640735, ZFMK-TIS-2640736, ZFMK-TIS-2640737. • 2 ♀♀; North Rhine-Westphalia, Bonn, Museum Koenig, garden; 50.7214°N, 7.1139°E; ca 70 m a.s.l.; 4 Oct. 2022; Salden, Tobias leg.; sweep net; ZFMK-TIS-2635303, ZFMK-TIS-2635304. • 1 ♀; North Rhine-Westphalia, Borken, Borken, spinach field with flower strip; 51.8078°N, 6.8324°E; ca 60 m a.s.l.; 2–9 Aug. 2016; Schwarz et al. leg.; Malaise trap; ZFMK-TIS-2629284. • 1 ♂; North Rhine-Westphalia, Delbrück, Delbrück, Nat. res. „Steinhorster Becken“; 51.8217°N, 8.542°E; ca 90 m a.s.l.; 22 Jul.-5 Aug. 2021; GBOL III leg.; Malaise trap; ZFMK-TIS-2640677. • 1 ♀; North Rhine-Westphalia, Paderborn, Delbrück, Nat. res. „Erdgarten-Lauerwiesen“, alder carr surrounded by wet meadows, ponds, muddy, geese; 51.7989°N, 8.6582°E; ca 110 m a.s.l.; 31 Aug.-14 Sep. 2021; GBOL III leg.; Malaise trap; ZFMK-TIS-2640674. • 1 ♀; North Rhine-Westphalia, Paderborn, Delbrück, Nat. res. „Steinhorster Becken“; 51.82°N, 8.5409°E; ca 90 m a.s.l.; 19 Aug.-2 Sep. 2021; GBOL III leg.; Malaise trap; ZFMK-TIS-2640692. • 1 ♀, 1 ♂; same collection data as for preceding 2–16 Sep. 2021; female - ZFMK-TIS-2640715; male - ZFMK-TIS-2640714. • 1 ♀, 4 ♂♂; same collection data as for preceding 16–30 Sep. 2021; female - ZFMK-TIS-2640803; males - ZFMK-TIS-2640799, ZFMK-TIS-2640800, ZFMK-TIS-2640801, ZFMK-TIS-2640802. • 9 ♂♂; same collection data as for preceding 30 Sep.-14 Oct. 2021; ZFMK-TIS-2640810, ZFMK-TIS-2640811, ZFMK-TIS-2640812, ZFMK-TIS-2640813, ZFMK-TIS-2640814, ZFMK-TIS-2640815, ZFMK-TIS-2640816, ZFMK-TIS-2640817, ZFMK-TIS-2640818. • 1 ♀; North Rhine-Westphalia, Paderborn, Delbrück, Nat. res. „Steinhorster Becken“; 51.8252°N, 8.5359°E; ca 90 m a.s.l.; 19 Aug.-2 Sep. 2021; GBOL III leg.; Malaise trap; ZFMK-TIS-2640693. • 6 ♂♂; same collection data as for preceding 2–16 Sep. 2021; ZFMK-TIS-2640793, ZFMK-TIS-2640794, ZFMK-TIS-2640795, ZFMK-TIS-2640796, ZFMK-TIS-2640797, ZFMK-TIS-2640798. • 4 ♂♂; same collection data as for preceding 16–30 Sep. 2021; ZFMK-TIS-2640727, ZFMK-TIS-2640728, ZFMK-TIS-2640729, ZFMK-TIS-2640730. • 1 ♀; North Rhine-Westphalia, Rhein-Sieg-Kreis, Oberdrees, Buschfeld; 50.6371°N, 6.9157°E; ca 160 m a.s.l.; 28 May-6 Jun. 2021; GBOL III leg.; Malaise trap; ZFMK-TIS-2640679. • 1 ♀; North Rhine-Westphalia, Rhein-Sieg-Kre-

is, Schladern near Windeck, Sieg river, right river bank; 50.8°N, 7.585°E; ca 130 m a.s.l.; 30 May-6 Jun. 2017; ZFMK et al. leg.; Malaise trap; ZFMK-TIS-2628234. • 1 ♀; same collection data as for preceding 6–13 Jun. 2017; ZFMK-TIS-2629239. • 1 ♀; same collection data as for preceding 13–20 Jun. 2017; ZFMK-TIS-2629262. • 4 ♀♀; same collection data as for preceding 20–27 Jun. 2017; ZFMK-TIS-2629279, ZFMK-TIS-2629280, ZFMK-TIS-2629281, ZFMK-TIS-2629282. • 2 ♀♀; same collection data as for preceding 27 Jun.-4 Jul. 2017; ZFMK-TIS-2629260, ZFMK-TIS-2629261. • 3 ♀♀; same collection data as for preceding 4–11 Jul. 2017; ZFMK-TIS-2629264, ZFMK-TIS-2629275, ZFMK-TIS-2629277. • 10 ♀♀, 23 ♂♂; same collection data as for preceding 18–25 Jul. 2017; females - ZFMK-TIS-2629290, ZFMK-TIS-2629292, ZFMK-TIS-2629487, ZFMK-TIS-2629488, ZFMK-TIS-2629489, ZFMK-TIS-2629490, ZFMK-TIS-2629508, ZFMK-TIS-2629561, ZFMK-TIS-2629562, ZFMK-TIS-2629563; males - ZFMK-TIS-2629217, ZFMK-TIS-2629247, ZFMK-TIS-2629265, ZFMK-TIS-2629286, ZFMK-TIS-2629287, ZFMK-TIS-2629288, ZFMK-TIS-2629291, ZFMK-TIS-2629293, ZFMK-TIS-2629294, ZFMK-TIS-2629486, ZFMK-TIS-2629492, ZFMK-TIS-2629510, ZFMK-TIS-2629511, ZFMK-TIS-2629518, ZFMK-TIS-2629519, ZFMK-TIS-2629520, ZFMK-TIS-2629564, ZFMK-TIS-2629565, ZFMK-TIS-2629566, ZFMK-TIS-2629567, ZFMK-TIS-2629569, ZFMK-TIS-2629570, ZFMK-TIS-2629571. • 7 ♀♀, 19 ♂♂; same collection data as for preceding 1–8 Aug. 2017; females - ZFMK-TIS-2629253, ZFMK-TIS-2629254, ZFMK-TIS-2629255, ZFMK-TIS-2629256, ZFMK-TIS-2629257, ZFMK-TIS-2629258, ZFMK-TIS-2629259; males - ZFMK-TIS-2629215, ZFMK-TIS-2629224, ZFMK-TIS-2629228, ZFMK-TIS-2629231, ZFMK-TIS-2629232, ZFMK-TIS-2629233, ZFMK-TIS-2629234, ZFMK-TIS-2629235, ZFMK-TIS-2629543, ZFMK-TIS-2629544, ZFMK-TIS-2629545, ZFMK-TIS-2629546, ZFMK-TIS-2629547, ZFMK-TIS-2629548, ZFMK-TIS-2629549, ZFMK-TIS-2629572, ZFMK-TIS-2629573, ZFMK-TIS-2629574, ZFMK-TIS-2629575. • 2 ♂♂; same collection data as for preceding 15–30 Aug. 2017; ZFMK-TIS-2629220, ZFMK-TIS-2640675. • 1 ♂; Rhineland-Palatinate, Ahrweiler, Niederzissen, Bausenberg; 50.4679°N, 7.2223°E; ca 330 m a.s.l.; 12–27 Jul. 2022; Jaume-Schinkel, Santiago leg.; Gressit Malaise trap; ZFMK-TIS-2640672. • 1 ♀, 1 ♂; Rhineland-Palatinate, Ahrweiler, Niederzissen, Bausenberg, dry grassland; 50.4647°N, 7.2222°E; ca 320 m a.s.l.; 14–20 Jul. 2017; ZFMK et al. leg.; Malaise trap; MF 5; female - ZFMK-TIS-2629509; male - ZFMK-TIS-2629516. • 1 ♀; Rhineland-Palatinate, Alzey-Worms, Wine fields north of Monsheim, shrub islands between wine fields, mostly poplars; 49.6406°N, 8.2137°E; ca 150 m a.s.l.; 5–24 Aug. 2021; Gilgenbach, Carolin leg.; Malaise trap; ZFMK-TIS-2640678. • 1 ♂; Rhineland-Palatinate, Cochem, Nat. res. Brauselay; 50.1421°N, 7.1881°E; ca 120 m a.s.l.; 29 May 2020; DINA leg.; Malaise trap; ZFMK-TIS-2629216 (EVK). • 1 ♀; Saarland, Neunkirchen, Schiffweiler, Landsweiler-Reden, Höfertal; 50.0767°N, 7.3283°E; ca 370 m a.s.l.; 18 Jun. 2022; AK Diptera leg.; sweep net; ZFMK-TIS-2640838. • 1 ♂; Saarland, Saarpfalz, Gersheim; 49.31°N, 8.1683°E; ca 140 m a.s.l.; 19 Jun. 2022; AK Diptera leg.; sweep net; ZFMK-TIS-2640839. • 2 ♂♂;

Schleswig-Holstein, Nordfriesland, Nat. res. Luetjenholmer Heidedünen; 54.6963°N, 9.0643°E; ca 0 m a.s.l.; 29 May 2020; DINA leg.; Malaise trap; ZFMK-TIS-2629229 (EVK), ZFMK-TIS-2629230 (EVK).

Lithuania • 1 ♀; Silute distr., Sysa, Sysa, control plot; 55.3127°N, 21.4049°E; ca 0 m a.s.l.; 15–25 Jul. 2020; Petrasiunas, Andrius leg.; Malaise trap; ZFMK-TIS-2637713.

The Netherlands • 1 ♂; Noord-Holland, Amsterdam, Vondelpark; 52.3581°N, 4.8681°E; ca 0 m a.s.l.; 3–12 Jun. 2019; Taxon Expeditions Team leg.; Malaise trap; ZFMK-TIS-2640687. • 2 ♀♀, 1 ♂; same collection data as for preceding 12–15 Jun. 2019; females - ZFMK-TIS-2640718, ZFMK-TIS-2640719; male - ZFMK-TIS-2640720. • 1 ♂; same collection data as for preceding 21–25 Jun. 2019; ZFMK-TIS-2640689. • 1 ♀; same collection data as for preceding 19–27 Jul. 2019. • 2 ♀♀, 1 ♂; same collection data as for preceding 7 Aug. 2019; females - ZFMK-TIS-2640721, ZFMK-TIS-2640722; male - ZFMK-TIS-2640723. • 2 ♂♂; Noord-Holland, Amsterdam, Vondelpark, Urban park; 52.356°N, 4.861°E; ca 0 m a.s.l.; 19–27 Jul. 2019; Taxon Expeditions (M. Schilthuizen) leg.; Malaise trap; ZFMK-TIS-2640841, ZFMK-TIS-2640842. • 1 ♀; same collection data as for preceding 2019; ZFMK-TIS-2640840.

Norway • 1 ♂; Rogaland Ytre, Finnøy, Nordre Vignes; 59.1679°N, 5.7883°E; ca 10 m a.s.l.; 22 Sep.-1 Nov. 2020; Tengesdal, Gaute leg.; Malaise trap; ZFMK-TIS-2640680.

Material without DNA barcode. Belgium • 1 ♂; Walloon Brabant, Ottignies; 3–10 Sep. 1983; Paul Dessart leg.; Malaise trap; JV_Prel_0057 (RBINS). • 1 ♀, 1 ♂; Walloon Region, Luik, Wanze, Antheit (Corphalie); 50.5363°N, 5.2515°E; ca 110 m a.s.l.; 14–28 Jul. 1989; R. Detry leg.; Malaise trap; ZFMK-HYM-00039669, JV_Prel_0044 (RBINS). • 1 ♂; same collection data as for preceding 28 Jul.-11 Aug. 1989; JV_Prel_0054 (RBINS). • 1 ♀, 1 ♂; West Flanders, Oostkamp, Private garden; 51.168°N, 3.276°E; ca 0 m a.s.l.; 16–30 Aug. 2020; Arnout Zwaenepoel leg.; Malaise trap; female - ZFMK-TIS-2640697; male - ZFMK-TIS-2640696. • 1 ♂; West Flanders, Snellegem, Vloethembos; 9 Jun. 1983; P. Grootaert leg.; hand caught; JV_Prel_0059 (RBINS). • 1 ♀; West Flanders, Ypres, De Triangel, Urban park (bushes); 50.8418°N, 2.8838°E; ca 20 m a.s.l.; 28 May-18 Jun. 2022; Fons Verheyde leg.; Malaise trap; JV_Prel_0058 (RBINS). • 1 ♀; same collection data as for preceding 20 Aug.-3 Sep. 2022; JV_Prel_0053 (RBINS). • 1 ♀; same collection data as for preceding 17 Sep.-1 Oct. 2022; JV_Prel_0055 (RBINS). • 15 ♀♀, 8 ♂♂; West Flanders, Ypres, De Triangel, Urban park (pool vegetation); 50.8427°N, 2.884°E; ca 20 m a.s.l.; 6–20 Aug. 2022; Fons Verheyde leg.; Malaise trap; females - JV_Prel_0111 (RBINS), JV_Prel_0112 (RBINS), JV_Prel_0113 (RBINS), JV_Prel_0114 (RBINS), JV_Prel_0115 (RBINS), JV_Prel_0116 (RBINS), JV_Prel_0117 (RBINS), JV_Prel_0118 (RBINS), JV_Prel_0119 (RBINS), JV_Prel_0120 (RBINS), JV_Prel_0121 (RBINS), JV_Prel_0122 (RBINS), JV_Prel_0123 (RBINS), JV_Prel_0124 (RBINS), JV_Prel_0125 (RBINS); males - JV_Prel_0103 (RBINS, JV_Prel_0104 (RBINS), JV_Prel_0105 (RBINS), JV_Prel_0106 (RBINS), JV_Prel_0107 (RBINS), JV_Prel_0108 (RBINS), JV_Prel_0109 (RBINS), JV_Prel_0110 (RBINS). • 8 ♀♀, 10 ♂♂; same collection data as for preceding 20 Aug.-

3 Sep. 2022; females -JV_Prel_0095 (RBINS), JV_Prel_0096 (RBINS), JV_Prel_0097 (RBINS), JV_Prel_0098 (RBINS), JV_Prel_0099 (RBINS), JV_Prel_0100 (RBINS), JV_Prel_0101 (RBINS), JV_Prel_0102 (RBINS); males - JV_Prel_0085 (RBINS), JV_Prel_0086 (RBINS), JV_Prel_0087 (RBINS), JV_Prel_0088 (RBINS), JV_Prel_0089 (RBINS), JV_Prel_0090 (RBINS), JV_Prel_0091 (RBINS), JV_Prel_0092 (RBINS), JV_Prel_0093 (RBINS), JV_Prel_0094 (RBINS). • 5 ♀♀, 9 ♂♂; same collection data as for preceding 3–17 Sep. 2022; females - JV_Prel_0068 (RBINS), JV_Prel_0069 (RBINS), JV_Prel_0070 (RBINS), JV_Prel_0071 (RBINS), JV_Prel_0072 (RBINS); males - JV_Prel_0061 (RBINS), JV_Prel_0062 (RBINS), JV_Prel_0063 (RBINS), JV_Prel_0064 (RBINS), JV_Prel_0065 (RBINS), JV_Prel_0066 (RBINS), JV_Prel_0067 (RBINS), ZFMK-HYM-00039673, ZFMK-HYM-00039672.

Denmark • 4 ♂♂; Southern Jutland, Rømø; 24 Sep. 2000; Torkhild Munk leg.; NHRS-HEVA 000023146 (NHRS), NHRS-HEVA 000023147 (NHRS), NHRS-HEVA 000023148 (NHRS), NHRS-HEVA 000023149 (NHRS). • 1 ♀; Western Jutland, Baldersbaek, plantation; 12 Jul. 1993; Torkhild Munk leg.; NHRS-HEVA 000023150 (NHRS).

Germany • 1 ♀; Baden-Württemberg, Karlsruhe, Malsch, Luderbusch, south faced slope; 48.9131°N, 8.3325°E; ca 120 m a.s.l.; 26 Jul.-2 Aug. 2020; Dieter Doczkal | K. Grabow leg.; Malaise trap; ZFMK-TIS-2640695. • 1 ♂; Bavaria, Allgäu, Balderschwang, Leiterberg; 47.4858°N, 10.0899°E; ca 1290 m a.s.l.; 4–21 Sep. 2017; Dieter Doczkal | Johannes Voith leg.; Malaise trap; ZFMK-TIS-2640708. • 1 ♀; Berlin, Berlin, Chausseestraße 109, ruderal area; 29 Jun.-5 Jul. 2009; A. Wiesener | V. Richter | F. Koch leg.; MfN URI: 57384a (ZHMB). • 1 ♀; Hesse, Gießen, Botanical garden; 50.5859°N, 8.678°E; ca 170 m a.s.l.; 18 Jun. 2021; GBOL III leg.; sweep net; ZFMK-TIS-2629491. • 1 ♂; Hesse, Rheingau-Taunus, Lorch am Rhein, oberhalb der Burg Nollig; 50.0491°N, 7.7978°E; ca 240 m a.s.l.; 21–27 Jul. 2013; Oliver Niehuis leg.; Malaise trap; ZFMK-TIS-2629579. • 1 ♂; Hesse, Rheingau-Taunus, Lorch am Rhein, oberhalb der Burg Nollig; 50.0498°N, 7.7974°E; ca 260 m a.s.l.; 15–21 Jul. 2013; Oliver Niehuis leg.; Malaise trap; ZFMK-TIS-2629514. • 2 ♂♂; same collection data as for preceding 21–27 Jul. 2013; ZFMK-TIS-2629242, ZFMK-TIS-2629526. • 5 ♂♂; Hesse, Werra-Meißner-Kreis, Großalmerode, Private garden, Siedlerweg, semi-abandoned garden with wet spot, ivy hedge and salix; 51.2591°N, 9.7871°E; ca 380 m a.s.l.; 12–20 Jul. 2022; Jonathan Vogel leg.; Malaise trap; ZFMK-TIS-2640700, ZFMK-TIS-2640701, ZFMK-TIS-2640702, ZFMK-TIS-2640703, ZFMK-TIS-2640705. • 2 ♀♀; North Rhine-Westphalia, Bonn, ZFMK garden, lawn and bushes; 50.7218°N, 7.1132°E; ca 70 m a.s.l.; 30 Aug. 2022; AG Hymenoptera leg.; sweep net; ZFMK-TIS-2640698, ZFMK-TIS-2640699. • 1 ♀; same collection data as for preceding 1 Sep. 2022; ZFMK-HYM-00039670. • 1 ♀; North Rhine-Westphalia, Rhein-Sieg-Kreis, Alfter, Mirbachstrasse; 50.7307°N, 7.0142°E; ca 90 m a.s.l.; 22 Jul. 2021; GBOL III leg.; sweep net; ZFMK-TIS-2629298. • 1 ♀; North Rhine-Westphalia, Rhein-Sieg-Kreis, Schladern near Windeck, Sieg river, right river bank; 50.8°N, 7.585°E; ca 130 m a.s.l.; 20–27 Jun. 2017; ZFMK et al. leg.; Malaise trap; ZFMK-TIS-2629283. • 1 ♀, 2 ♂♂; same collection data as for preced-

ing 18–25 Jul. 2017; female - ZFMK-TIS-2629289; males - ZFMK-TIS-2629485, ZFMK-TIS-2629568. • 2 ♂♂; Rhineland-Palatinate, Ahrweiler, Niederzissen, Bausenberg, slope of volcanic mountain, mixed broad-leaved forest; 50.4679°N, 7.2223°E; ca 330 m a.s.l.; 12–27 Jul. 2022; Santiago Jaume Schinkel leg.; Gressitt Malaise trap; ZFMK-HYM-00039687, ZFMK-HYM-00039688. • 1 ♂; Rhineland-Palatinate, Ahrweiler, Niederzissen, Bausenberg, upper part of volcanic mountain, next to oak tree; 50.4672°N, 7.2212°E; ca 310 m a.s.l.; 12–27 Jul. 2022; Santiago Jaume Schinkel leg.; Gressitt Malaise trap; ZFMK-HYM-00039671. • 1 ♂; Saxony, Leipzig, surroundings of Naunhof; 28 Jul. 1957; Michalk leg.; JV_Prel_0046 (SDEI).

The Netherlands • 1 ♀; Gelderland, Beek-Ubbergen, Goudenregenstraat, garden; 51.8268°N, 5.9332°E; ca 10 m a.s.l.; 1 Oct. 2023; Jochem Kühnen leg.; hand caught; ZFMK-HYM-00039657. • 1 ♂; Gelderland, Nijmegen, Gelderse poort; 10 May 2022; R. Lexmond leg.; Malaise trap; JV_Prel_0043 (RBINS). • 1 ♀, 7 ♂♂; same collection data as for preceding 20 Jul. 2022; female - JV_Prel_0077 (RBINS); males - JV_Prel_0078 (RBINS), JV_Prel_0079 (RBINS), JV_Prel_0080 (RBINS), JV_Prel_0081 (RBINS), JV_Prel_0082 (RBINS), JV_Prel_0083 (RBINS), JV_Prel_0084 (RBINS). • 1 ♀; same collection data as for preceding 23 Aug. 2022; JV_Prel_0060 (RBINS).

Portugal • 1 ♂; Madeira, Funchal, Curral das Romeiros; ca 550 m a.s.l.; 8 Feb. 1991; Martti Koponen leg.; specimen in coll. Koponen.

Sweden • 1 ♂; Dalarna, Rättvik, Glostjärn; 20 May-30 Jun. 1977; Tord Tjeder leg.; NHRS-HEVA 000023151 (NHRS). • 1 ♀; Hälsingland, Älgesjön; 62.16°N, 16.212°E; ca 300 m a.s.l.; 17 May-15 Jun. 2002; Erik Sahlin leg.; window trap; Tömn 1, specimen in coll MF. • 1 ♂; Närke; 10 Aug. 1953; Anton Jansson leg.; NHRS-HEVA 000023153 (NHRS). • 1 ♂; Närke, Oset; 8 Aug. 1941; Anton Jansson leg.; NHRS-HEVA 000023152 (NHRS). • 1 ♂; Öland, Kastlösa; 26 Jun. 1962; Karl-Johan Hedqvist leg.; NHRS-HEVA 000023175 (NHRS). • 1 ♀; Öland, Mörbylånga kommun, Skogsby, Ecological research station, lawn in garden with sandy soil; 56.6283°N, 16.4918°E; ca 30 m a.s.l.; 29 Aug.-11 Sep. 2008; Swedish Malaise Trap Project (Swedish Museum of Natural History) leg.; Malaise trap; NHRS-HEVA 000023174 (NHRS). • 1 ♂; Östergötland, S:t Anna, Svensmarö, Sanningholmen; 7 Aug. 1976; Gustaf Wängsjö leg.; NHRS-HEVA 000023176 (NHRS). • 1 ♂; Scania, Kristianstads kommun, Trunelän, Degeberga, Grazed meadow at alder stand along stream; 55.7746°N, 14.2156°E; ca 80 m a.s.l.; 1–13 Aug. 2019; Swedish Insect Inventory Programme (SIIP), Station Linné leg.; Malaise trap; NHRS-HEVA 000023155 (NHRS). • 1 ♂; Scania, Malmö kommun, Klagshamn, Limhamns kalkbrott, Limestone quarry; 55.5694°N, 12.9267°E; ca -50 m a.s.l.; 4–12 Jun. 2018; Swedish Insect Inventory Programme (SIIP), Station Linné leg.; Malaise trap; NHRS-HEVA 000023154 (NHRS). • 2 ♂♂; Södermanland, Trosa kommun, Hunga södergård 1, agricultural backyard, heavily eutrophicated, in tall grass near stable manure pile; 58.9207°N, 17.5212°E; ca 20 m a.s.l.; 16 May-13 Jun. 2004; Swedish Malaise Trap Project (Swedish Museum of Natural History) leg.; Malaise trap; NHRS-HEVA 000023156 (NHRS), NHRS-HEVA 000023157 (NHRS). • 4 ♀♀, 3 ♂♂; same collection data as for preceding 9–19 Aug. 2004; females - NHRS-HEVA 000023158 (NHRS), NHRS-HEVA 000023160

(NHRS), NHRS-HEVA 000023161 (NHRS), NHRS-HEVA 000023164 (NHRS); males - NHRS-HEVA 000023159 (NHRS), NHRS-HEVA 000023162 (NHRS), NHRS-HEVA 000023163 (NHRS). • 1 ♂; Södermanland, Väsbyön; 11 Aug. 1950; Anton Jansson leg.; NHRS-HEVA 000023165 (NHRS). • 1 ♀; Uppland, Almunge, Harparbol; 20 Jun. 1948; Olov Lundblad leg.; NHRS-HEVA 000023169 (NHRS). • 1 ♀, 1 ♂; Uppland, Älvkarleby, Båtfors, flood-regiment oldgrowth birch edge of pine forest; 60.4607°N, 17.3178°E; ca 40 m a.s.l.; 14 Jun.-4 Jul. 2005; Swedish Malaise Trap Project (Swedish Museum of Natural History) leg.; Malaise trap; female - NHRS-HEVA 000023167 (NHRS); male - NHRS-HEVA 000023166 (NHRS). • 1 ♂; Uppland, Håbo kommun, Biskops-Arnö, elm grove; 59.6721°N, 17.5009°E; ca 10 m a.s.l.; 27 Aug.-10 Sep. 2004; Swedish Malaise Trap Project (Swedish Museum of Natural History) leg.; Malaise trap; NHRS-HEVA 000023168 (NHRS). • 1 ♀; Uppland, Uppsala, Vårdsätra skog, forest; 7–28 Oct. 2002; Fredrik Ronquist leg.; Malaise trap; specimen in coll MF. • 2 ♂♂; Västerbotten, Hällnäs; 22 Aug. 1961; Karl-Johan Hedqvist leg.; NHRS-HEVA 000023170 (NHRS), NHRS-HEVA 000023171 (NHRS). • 1 ♀; Västergötland, South of Alingsås; 29 Jul. 1998; Torkhild Munk leg.; NHRS-HEVA 000023172 (NHRS). • 1 ♀; Västmanland, Sala kommun, Västerfärnebo, Nötmyran (Östermyran), birch stand in moist haymaking meadow; 59.942°N, 16.3095°E; ca 70 m a.s.l.; 18 Aug.-1 Sep. 2003; Swedish Malaise Trap Project (Swedish Museum of Natural History) leg.; Malaise trap; NHRS-HEVA 000023173 (NHRS).

Switzerland • 1 ♀; Neuchâtel, Montmollin; 1 Aug. 1966; Jacques de Beaumont leg.; specimen at MHNG. • 2 ♂♂; same collection data as for preceding 3 Aug. 1957; specimens at MHNG. • 1 ♂; same collection data as for preceding 17 Aug. 1962; specimen at MHNG. • 1 ♂; same collection data as for preceding 19 Aug. 1957; specimen at MHNG. • 2 ♂♂; same collection data as for preceding 31 Aug. 1956; specimens at MHNG. • 1 ♂; same collection data as for preceding 29 Sep. 1956; specimen at MHNG. • 1 ♀; St. Gallen, Pfäfers; 9 Sep. 1992; F. Amiet leg.; specimen at NMBE. • 1 ♀; Valais, Visperterminen; ca 1550 m a.s.l.; 4 Aug. 1996; Gerhard Bächli | Bernhard Merz leg.; specimen at NMBE. • 1 ♂; Vaud, Ferreyres; 8 Sep. 1964; Jacques de Beaumont leg.; specimens at MHNG. • 1 ♀; Vaud, Lausanne, Vidy; 9 Sep. 1948; Jacques Aubert leg.; specimens at MHNG. • 1 ♀; Vaud, Lutry; 18 Jun. 1954; Jacques Aubert leg.; specimens at MHNG. • 1 ♂; Vaud, Rougemont; ca 1000 m a.s.l.; 14 Jun. 1963; Claude Besuchet leg.; specimens at MHNG.

Biology. Summer species, flying mainly from May to October, peak in July. Collected in all kinds of habitats: deciduous and coniferous forests, gardens, parks and orchards, agricultural fields, pastures and meadows, ruderal land, ponds and marshes

Distribution. Verified by morphological examination: Belgium, Denmark, Germany (locus typicus of *A. spheciformis*; locus typicus of *A. fergussoni*: Ingelheim am Rhein), Lithuania, The Netherlands, Norway, Portugal, Sweden (locus typicus of *A. eucharioides*: Västergötland), Switzerland, United Kingdom (locus typicus of *A. tincta*: unclear, either near London, Isle of Wight or Machynlleth (North Wales)).

CO1 barcode sequence matches: Belarus (e.g. GMBMQ746-17) and Canada (e.g. BBHYJ932-10).

Lowland species, usually occurring in elevations below 500 m a.s.l., rarely collected in higher altitudes, most specimens between 0–100 m a.s.l.

Remarks. *A. eucharioides* is both the most commonly collected and the most morphologically heterogeneous species within the genus *Anacharis*. Specimens often exhibit slight metallic sheen on their mesoscutum and head that is more notable in ethanol-stored specimens but sometimes retains on dried specimens.

The type of *A. eucharioides* is reportedly lost (Fergusson 1986, Mata-Casanova et al. 2018), which we confirm herein by having searched the collection of the NHRS in addition to previous efforts at other possible depositories (NHMUK, MZLU). In the current situation with several new species, we disagree with Fergusson's statement, that "…there is no confusion about the identity of this species" and that "a neotype is not required" (Fergusson 1986) and rather stress the necessity to designate a neotype from the broader type locality at Västergötland. However, as we were not able to acquire a fresh specimen suitable for DNA sequencing from the type locality, we withhold taking action until a more suitable occasion.

The lectotype of *A. tincta* is glued to its ventral side on cardboard, face down, the wings also glued to the board. It is overall intact, except the terminal four segments of the left antenna, which are detached from the rest to the specimen but still present on the cardboard. Also, the left fore tarsomeres are detached, the second tarsomere is missing, the rest is glued on the card. Both wings and legs obscure the lateral mesosoma on both sides. We here confirm the synonymy with *A. eucharioides*.

The lectotype of *A. spheciformis* (Hartig, 1840) was designated by Weld (1952), who reported the syntype series to consist of 12 specimens. Interestingly, Fergusson (1986) reports only one specimen under the name *A. spheciformis* from the Hartig collection, meaning that 11 syntypes might be lost. Fergusson additionally states the sex of the lectotype to be female, while the specimen is clearly a male. The species was treated as a synonym of *A. typica* by Dalla-Torre and Kieffer (1910) and Weld (1952), as established by Reinhard (1860), but the lectotype has a clearly sculptured mesoscutellum, which makes it distinct from *A. typica*. We agree with the latest treatments of *A. spheciformis* as synonym of *A. eucharioides* (Fergusson 1986; Mata-Casanova et al. 2018) but as we consider *A. typica* a valid species, we formally move it from synonymy with *A. typica* to *A. eucharioides*.

A. fergussoni is diagnosed against *A. parapsidalis* and *A. melanoneura* in Mata-Casanova et al. (2018). The reason why it is not considered similar to *A. eucharioides* by the authors is likely due to the distinction they make based on the parascutal sulcus (present in *A. fergussoni*, absent in *A. eucharioides*), as used in their key (couplet 3). As we found this character to be very variable within *A. eucharioides*, this is not sufficient for discrimination. The character states used to diagnose *A. fergussoni* against *A. parapsidalis* and *A. melanoneura* given by Mata-Casanova et al. (2018) match with the re-description of *A. eucharioides* by Mata-Casanova et al. (2018) and our observations. The morphometric values given for *A. fergussoni* fall into the range of *A. eucharioides* as diagnosed herein (Table 2), except the head width:length and the petiole length:metacoxa length which exhibit unusual high values in the description of *A. fergussoni*. However, the former is only 0.1 off of the range of *A. eucharioides*, and might well fall into the error range, and

the latter (relative petiole length) seems erroneous in the description ("about 2.0 times as long as metacoxa" Mata-Casanova et al. 2018), as we measure a value of 1.4 on the images of the holotype, which falls well into the range of what we measured for *A. eucharioides* and is even close to the mean (1.0–1.7, mean 1.5). In terms of qualitative characters, the centrally sparsely pubescent to glabrous median lobe of the mesoscutum, the well-foveated notauli, the median carina of the mesoscutellum that is medially morphing into reticulate sculpture and the smooth to rugose lateromedial area of pronotum are typical for *A. eucharioides*. Based on this re-evaluation of possible morphometric differences and the similarity in qualitative characters between the specimens examined herein and the holotype of *A. fergussoni* we synonymise *A. fergussoni* with *A. eucharioides*.

We want to note that images of the holotype, kindly provided to kindly provided to us by the team at CNC, do not correspond to all the SEM images in Mata-Casanova et al. (2018, Fig. 4A–C). Fig. 4A clearly shows the holotype before the right wings were removed, as does fig. 4B though the image is vertically flipped, but fig. 4C shows a different antennal position and must be a different specimen.

Here, we demonstrate that, given the morphometric variability within *A. eucharioides* and the whole *eucharioides* species group, morphometric characters/analyses cannot reliably separate this species from the others (Fig. 8A). Our diagnosis rather relies on qualitative characters and species delimitation has been crucially informed by the results from analysis of molecular sequence data, which show a distinct cluster/putative species with small intraspecific variability based on almost 300 specimens from various localities. Without this reverse taxonomy approach included, finding and defining species limits within the *eucharioides* species group, and especially of *A. eucharioides* would have been difficult if not impossible.

Additional distribution records are listed in Mata-Casanova et al. (2018) for Andorra, France, Romania, Spain, Slovakia and Hungary. Since our circumscription of *A. eucharioides* is narrower than that of Mata-Casanova et al. (2018), we cannot confirm the presence of the species in these countries (specimens listed as *A. eucharioides* could also belong to *A. typica* or *A. petiolata*) but it is likely present in these regions, too.

Table 2. Comparison of morphometric values between **A** *A. fergussoni* in the description of Mata-Casanova et al. (2018), **B** measurements taken from images of the holotype of *A. fergussoni*, **C** *A. eucharioides* in the redescription of Mata-Casanova et al. (2018), and **D** our measured values for *A. eucharioides* (n = 58).

Entities measured	Head dorsal width: length	Head frontal width: height	Malar sulcus length: eye height	Eye-to-eyee dist.: eye height	mesoscutum width:length	mesoscutellum_l mesoscutum_l	Radial cell length: width	Petiole length: metacoxa length
A *A. fergussoni* in description (Mata-Casanova et al. 2018)	2.4	1.3	0.7	1.1	1.2	0.6	2.7	2
B *A. fergussoni* holotype, measured herein		1.2	0.6	1.0	1.2	0.8		1.4
C *A. eucharioides* in redescription (Mata-Casanova et al. 2018)	2	1.3	0.6	1	1.2	0.8	2.6	>1
D *A. eucharioides* range, measured herein	1.8–2.3	1.0–1.3	0.6–0.8	1.0–1.1	1.0–1.2	0.6–0.8	2.4–3.3	1.0–1.7

***Anacharis immunis* Walker, 1835**
Figs 2B, 3B, 11A–E

Anacharis immunis Walker, 1835: 521 - lectotype (NHMUK) ♂, syn. by Fergusson (1968), photographs examined.
Anacharis staegeri Dahlbom, 1842: 4 - lectotype (MZLU) ♀, syn. by Dalla Torre (1893), photographs examined.
Synapsis aquisgranensis Förster, 1869: 361 - Holotype (ZMHB) ♂, syn. by Kierych (1984), not examined.

Diagnosis (n = 14). Belongs to the *immunis* species group. *Anacharis immunis* can be distinguished from *A. ensifer* and *A. norvegica* by having a largely smooth and even dorsal surface of the mesoscutellum, especially centrally (reticulate-foveate in *A. ensifer* and *A. norvegica*) (Fig. 11D). The fore and mid coxae are usually as dark as the hind coxa (usually distinctly paler than the hind coxa in *A. ensifer*).

CO1 barcode. n = 14. Maximum intraspecific distance = 0.2%. Minimum distance to closest species (*A. ensifer*) = 7.8%. CO1 barcode consensus sequence:
AATTTTATACTTTATTATAGGAATCTGATCAGCAATATTAG-
GATCAAGACTTAGTATAATTATCCGAATAGAATTAGGGACTCCAT-
CACAATTAATTAGAAATGAACAAATTTACAATTCAATTGTAACCGCA-
CATGCATTTATCATAATTTTTTTTATAGTTATACCTATTATAGTAG-
GAGGATTTGGAAATTACCTAATCCCATTAATACTTTTATCTCCAGA-
TATAGCTTTTCCACGATTAAATAATATAAGATTTTGATTTTTAATTCC-
CTCTTTAGCTTTAATATCTTCTAGTTTATTTATTGATCAAGGGGCAG-
GAACAGGATGAACAATTTACCCTCCTTTATCTTCATTAACAG-
GACACTCAGGAATTGCAGTAGATATAACAATCTACTCCCTTCATTTAA-
GAGGAATTTCTTCAATTTTAGGATCAATTAATTTTATCAGAACAATTT-
TAAACATACGAATTAATAAAGTATCAATAGATAAAATTACTCTATTTA-
GATGATCAATCTTTTTAACTACAATTTTATTACTTCTATCATTACCT-
GTGCTTGCAGGAGGAATTACTATACTTTTATTTGACCGAAACTTAAA-
CACCTCCTTTTTCGACCCCATAGGGGGAGGAGACCCAATCTTATAT-
CAACATTTATTT

Type material.

Lectotype of *A. immunis* Walker, 1835:

Type
immunis, Walk. [handwritten, probably by Walker himself]
In coll under immunis
LECTOTYPE
B.M. TYPE HYM 7. 160
LECTOTYPE of A. immunis Walker det. N.D.M.Fergusson, 1981
[QR code] NHMUK010640455
[for images, see https://data.nhm.ac.uk/dataset/56e711e6-c847-4f99-915a-6894bb5c5dea/resource/05ff2255-c38a-40c9-b657-4ccb55ab2feb/record/10638963]

Lectotype of *A. staegeri* Dahlbom, 1842:
♀
LECTOTYPE
LECTOTYPE of Anacharis staegeri Dahlm det. N.D.M.Fergusson, 1983
1983 366
MZLU 00215544
MZLU Type no. 6511:1
[for images, see https://www.flickr.com/photos/tags/mzlutype06511]

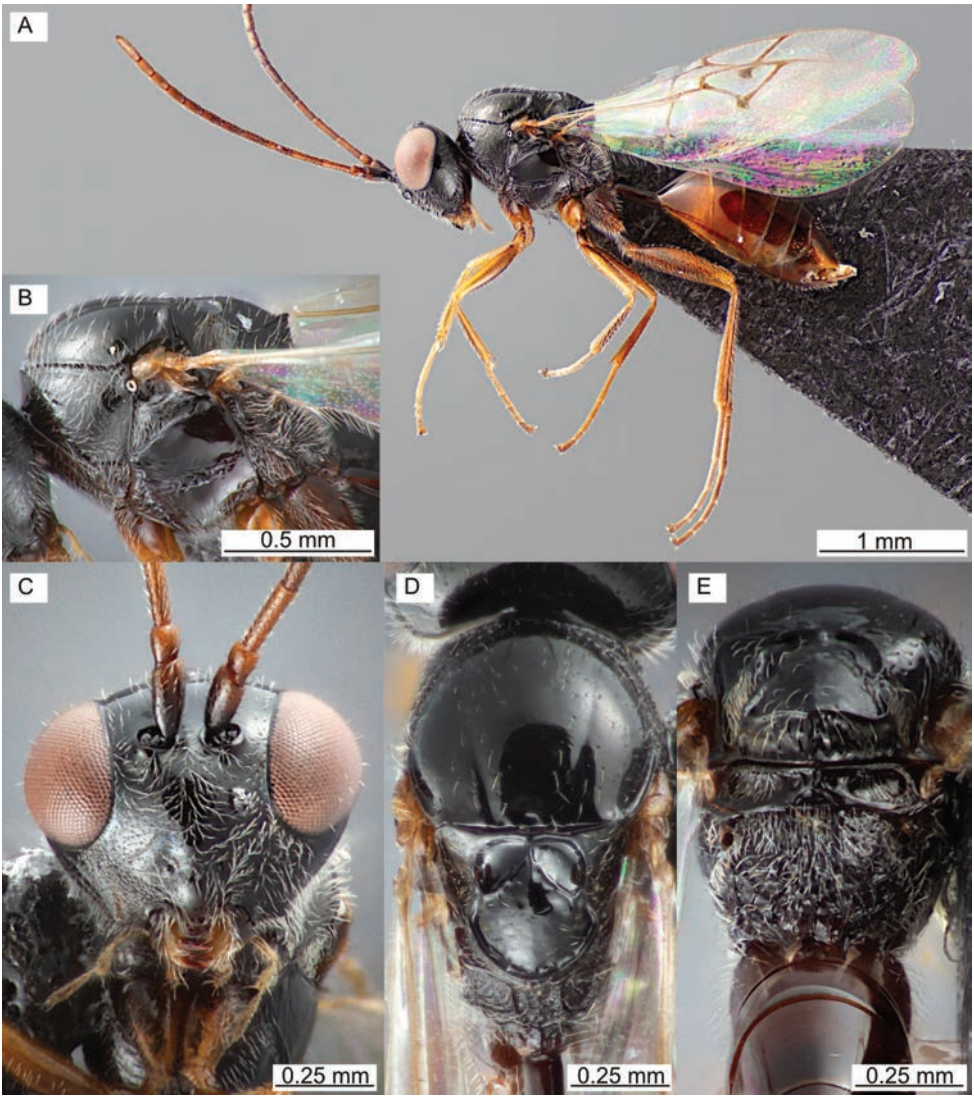

Figure 11. *Anacharis immunis*, female (ZFMK-TIS-2640709) **A** habitus **B** mesosoma lateral **C** face **D** mesosoma dorsal **E** mesosoma posterior view.

Other material examined. DNA barcode vouchers. Germany • 1 ♀; Baden-Württemberg, Karlsruhe, Malsch, Hansjakobstraße, garden; 48.8835°N, 8.3197°E; ca 120 m a.s.l.; 25 Oct.-8 Nov. 2020; Dieter Doczkal leg.; Malaise trap; ZFMK-TIS-2640725. • 1 ♀; Bavaria, Allgäu, Balderschwang, Leiterberg; 47.4858°N, 10.0899°E; ca 1290 m a.s.l.; 4–21 Sep. 2017; Doczkal, Dieter, Voith, J. leg.; Malaise trap; ZFMK-TIS-2640709. • 1 ♀; Bavaria, Garmisch-Partenkirchen, Zugspitze, mountain; 47.4068°N, 11.008°E; ca 2010 m a.s.l.; 20 Jun.-5 Jul. 2018; Doczkal, D., Voith, J. leg.; Malaise trap; ZFMK-TIS-2628218. • 6 ♂♂; Bavaria, Rhön-Grabfeld, Fladungen, Nat. res. Schwarzes Moor, Karpatenbirkenwald; 50.5117°N, 10.071°E; ca 780 m a.s.l.; 26 Jun.-18 Jul. 2017; Dieter Doczkal leg.; Malaise trap; ZFMK-TIS-2629533, ZFMK-TIS-2629534, ZFMK-TIS-2629535, ZFMK-TIS-2629536, ZFMK-TIS-2629537, ZFMK-TIS-2629539. • 2 ♂♂; Hesse, Waldeck-Frankenberg, NP Kellerwald-Edersee, „Banfe-Haus“; 51.167°N, 8.9749°E; ca 270 m a.s.l.; 7–21 Jul. 2022; GBOL III leg.; Malaise trap; ZFMK-TIS-2640756, ZFMK-TIS-2640759. • 3 ♂♂; Rhineland-Palatinate, Ahrweiler, Niederzissen, Bausenberg, upper part of volcanic mountain, next to oak tree; 50.4672°N, 7.2212°E; ca 310 m a.s.l.; 12–27 Jul. 2022; Jaume-Schinkel, Santiago leg.; Gressit Malaise trap; ZFMK-TIS-2640771, ZFMK-TIS-2640772, ZFMK-TIS-2640773.

Material without DNA barcode. Belgium • 1 ♂; Walloon Brabant, Ottignies; 9–16 Jul. 1983; Paul Dessart leg.; Malaise trap; JV_Prel_0073 (RBINS). • 1 ♀; same collection data as for preceding 24 Sep.-1 Oct. 1983; JV_Prel_0051 (RBINS). • 1 ♀; Walloon Region, Luik, Wanze, Antheit (Corphalie); 50.5363°N, 5.2515°E; ca 110 m a.s.l.; 16–30 May 1989; R. Detry leg.; Blue pan trap; JV_Prel_0056 (RBINS).

Denmark • 1 ♂; Eastern Jutland, Fugslev; 56.2667°N, 10.7167°E; ca 20 m a.s.l.; 1999; Torkhild Munk leg.; NHRS-HEVA 000023102 (NHRS). • 4 ♂♂; Eastern Jutland, Hjelm; 3–5 Aug. 1992; Torkhild Munk leg.; NHRS-HEVA 000023104 (NHRS), NHRS-HEVA 000023104 (NHRS), NHRS-HEVA 000023104 (NHRS), NHRS-HEVA 000023105 (NHRS). • 1 ♂; Eastern Jutland, Rugård, Sønderskov; 56.2667°N, 10.8167°E; ca 30 m a.s.l.; 20 Jul. 1996; Torkhild Munk leg.; NHRS-HEVA 000023103 (NHRS). • 1 ♀, 1 ♂; Northwestern Jutland, Torup, klitplantage; 56.9667°N, 8.4°E; ca 20 m a.s.l.; 27 Jul. 1989; Torkhild Munk leg.; female - NHRS-HEVA 000023106 (NHRS); male - NHRS-HEVA 000023101 (NHRS).

Germany • 1 ♀; Bavaria, Garmisch-Partenkirchen, Zugspitze, mountain; 47.4053°N, 11.0091°E; ca 1980 m a.s.l.; 2–13 Aug. 2018; Dieter Doczkal | Johannes Voith leg.; Malaise trap; ZFMK-HYM-00039683. • 3 ♂♂; Rhineland-Palatinate, Ahrweiler, Niederzissen, Bausenberg, slope of volcanic mountain, mixed broad-leaved forest; 50.4679°N, 7.2223°E; ca 330 m a.s.l.; 12–27 Jul. 2022; Santiago Jaume Schinkel leg.; Gressitt Malaise trap; ZFMK-HYM-00039684, ZFMK-HYM-00039685, ZFMK-HYM-00039686. • 18 ♂♂; Rhineland-Palatinate, Ahrweiler, Niederzissen, Bausenberg, upper part of volcanic mountain, next to oak tree; 50.4672°N, 7.2212°E; ca 310 m a.s.l.; 12–27 Jul. 2022; Santiago Jaume Schinkel leg.; Gressitt Malaise trap; ZFMK-HYM-00039689, ZFMK-HYM-00039690, ZFMK-HYM-00039691, ZFMK-HYM-00039692, ZFMK-HYM-00039693, ZFMK-HYM-00039694,

ZFMK-HYM-00039695, ZFMK-HYM-00039696, ZFMK-HYM-00039697, ZFMK-HYM-00039698, ZFMK-HYM-00039699, ZFMK-HYM-00039700, ZFMK-HYM-00039701, ZFMK-HYM-00039702, ZFMK-HYM-00039703, ZFMK-HYM-00039704, ZFMK-HYM-00039705.

Sweden • 1 ♀; Närke, Örebro, Adolfsberg; 19 Sep. 1953; Anton Jansson leg.; NHRS-HEVA 000023107 (NHRS). • 1 ♀; Öland, Ekerums strand, dry meadow with mixed trees; 31 Jul. 1977; Sven Johansson leg.; NHRS-HEVA 000023115 (NHRS). • 1 ♂; Östergötland, S:t Anna, Svensmarö, Sanningsholmen; 11 Aug. 1976; Gustav Wängsjö leg.; NHRS-HEVA 000023117 (NHRS). • 1 ♂; Östergötland, Tjärholm; 5 Jul. 1976; Gustav Wängsjö leg.; NHRS-HEVA 000023116 (NHRS). • 1 ♂; Scania, Kristianstads kommun, Trunelän, Degeberga, Grazed meadow at alder stand along stream; 55.7746°N, 14.2156°E; ca 80 m a.s.l.; 16–26 Sep. 2018; Swedish Insect Inventory Programme (SIIP), Station Linné leg.; Malaise trap; NHRS-HEVA 000023109 (NHRS). • 1 ♂; Scania, Kristianstads kommun, Trunelän, Degeberga, Grazed meadow at alder stand along stream; 55.7746°N, 14.2156°E; ca 80 m a.s.l.; 31 May-9 Jun. 2019; Swedish Insect Inventory Programme (SIIP), Station Linné leg.; Malaise trap; NHRS-HEVA 000023108 (NHRS). • 1 ♂; Scania, Kvistofta; 1 Aug. 1949; Anton Jansson leg.; NHRS-HEVA 000023110 (NHRS). • 1 ♀; Småland, Bäckebo, Grytsjön, moist haymaking meadow at birch-spruce forest edge; 56.9314°N, 16.0855°E; ca 80 m a.s.l.; 12 Jul.-18 Aug. 2005; Swedish Malaise Trap Project (Swedish Museum of Natural History) leg.; NHRS-HEVA 000023113 (NHRS). • 2 ♀♀; Småland; [19th cent.]; Carl Henning Boheman leg.; NHRS-HEVA 000023111 (NHRS), NHRS-HEVA 000023112 (NHRS). • 1 ♀; Södermanland, Åva; 20 Sep. 1953; Tor-Erik Leiler leg.; NHRS-HEVA 000023114 (NHRS).

Switzerland • 1 ♂; Neuchâtel, Auvernier; 1 Aug. 1953; Jacques de Beaumont leg.; specimen at MHNG. • 1 ♂; same collection data as for preceding 10 Aug. 1957; specimen at MHNG. • 1 ♀; same collection data as for preceding 15 Aug. 1956; specimen at MHNG. • 1 ♀; same collection data as for preceding 25 Aug. 1966; specimen at MHNG. • 1 ♂; Neuchâtel, La Tourne; 26 Aug. 1960; Jacques de Beaumont leg.; specimen at MHNG. • 1 ♂; Neuchâtel, Montmollin; 14 Aug. 1957; Jacques de Beaumont leg.; specimen at MHNG. • 1 ♀; Valais, Mayens de Sion Aug. 1957; Jean-Louis Nicod leg.; specimen at MHNG. • 1 ♀; Vaud, Jorat; 29 Jun. 1960; Jacques de Beaumont leg.; specimen at MHNG. • 1 ♀; Vaud, Vidy; 28 Sep. 1953; Jacques de Beaumont leg.; specimen at MHNG.

Biology. Summer species, flying mainly from July to September, peak in July. No clear habitat preference but in Sweden and Denmark often collected in open sandy pine forest.

Distribution. Verified by morphological examination: Belgium, Denmark, Germany (locus typicus of *A. aquisgranensis*: Aachen and *Megapelmus rufiventris* Hartig, 1841), Sweden (locus typicus of *A. staegeri*), Switzerland, United Kingdom (locus typicus of *A. immunis*: near London).

No DNA barcode matches with publicly available sequences from other countries.

Mainly collected in lowlands below 400 m a.s.l., occasionally found in higher altitudes at 700–900 m a.s.l. and rarely even higher.

Remarks. *Anacharis aquisgranensis* was described by Förster (1869) because of its holotype having the mesoscutum fused with the mesoscutellum. He even erected the monotypic genus *Synapsis* (later replaced by *Prosynapsis* Dalla Torre & Kieffer, 1910, due to homonymy) based on that state. Kierych (1984) considered the fusion as an aberrant state and synonymised *Prosynapsis* under *Anacharis* and *A. aquisgranensis* under *A. immunis*. We have not seen such a character state, but it seems rather aberrant if real, and we see no reason to question Kierych's judgment until further.

The distribution records of *A. immunis* reported by Mata-Casanova et al. (2018) require re-evaluation as *A. immunis* sensu Mata-Casanova et al. (2018) also includes *A. ensifer* (see remarks there).

Anacharis martinae Vogel, Forshage & Peters, sp. nov.

https://zoobank.orgD30ADE83-C297-4381-AEA7-FAA4AB2376C5
Figs 2F, 3C, 12A–E

Diagnosis (n = 18). Belongs to the *euchariodes* species group. Medium sized species (2.6–3.3, mean 2.9 mm, similar to *A. euchariodes*, *A. petiolata* and *A. typica*). Different from *A. petiolata* and *A. typica* in having a centrally carinate mesoscutellum (Fig. 12D, centrally smooth in *A. petiolata* and *A. typica*). Different from *A. euchariodes* by having oblique carinae on the lateromedial area of the pronotum (Fig. 12B). This character is shared with *A. belizini*, which is an Indomalayan species described from Thailand. *Anacharis martinae* differs from *A. belizini* by having a larger glabrous area on the clypeus medioventrally (largely pubescent in *A. belizini*) (Fig. 12C) and a brown to dark-brown metasoma (black in *A. belizini*) (Fig. 12A). WIPs: The band pattern of the fore wings reaching along about half the length of the non-sclerotised vein M (Fig. 2C, reaching along at least 2/3 the length of the non-sclerotised vein M in all other species, including those of the *immunis* species group). The apical spot of the hind wing fills almost the entire apical area (Fig. 2C, filling about half the apical area in other species of the *euchariodes* species group).

Description. Both sexes. ***Size*.** Body: ♀ 2.6–3.2 (3.2) mm, ♂ 2.3–2.9 mm. Antennae: ♀ 1.7–2.3 (2.1) mm, ♂ 2–2.3 mm. Fore wing: 2.1–2.8 (2.5) mm

***Colour*.** Body black to reddish-brown (Fig. 12A); base of scape usually (Fig. 12A, C), head always (Fig. 12A, C), base of mandibles usually (Fig. 12C), mesosoma usually (Fig. 12A, B, D, E), coxa to a varying degree (Fig. 12A), hind-trochanter usually basally, and petiole usually black (Fig. 12A); scape usally apically (Fig. 12C), rest of antennae (Fig. 12A), tegulae (Fig. 12B, D) and metasoma brown (Fig. 12A); mandibles & palps (Fig. 12C) and rest of legs (Fig. 12A) testaceous.

***Head*.** Roundish-trapezoid in frontal view, genae gently kinked, in an angle <90° to the vertical axis of the face (Fig. 12C); lower face with thick silvery hairs, densely punctured (Fig. 12C); clypeal margin bilobed, somewhat flanged upwards, clypeus otherwise convex, medioventrally smooth, otherwise punctate (Fig. 12C); malar area with coriaceous texture, reaching from ventral eye margin along entire stretch of mandibular

base (Fig. 18B), anteroventral corner of mandibular base sometimes smooth; genae smooth around eye, with increasingly dense punctation and regular setae towards the hind margin; upper face with somewhat thinner setae, punctured, with usually shallow median dent; space between toruli sometimes transversally striolate, intertorular distance:torulus to eye distance 1.4–2.0(1.9); eyes with scattered setae, extent varying (Fig. 12C); POL:OOL:LOL:OD 2.4–2.8(2.6):1.2–2.1(1.3):1–1.4(1.2):1, POL:petiole length 0.45–0.75(0.59); vertex pubescent between lateral ocellus and compound eye, small glabrous area anterior of median ocellus reaching until median dent of upper face; head in dorsal view 1.9–2.5 (2.3) times wider than long, laterally longer than medially; vertex and occiput sometimes with shallow and smooth median furrow, occiput with transverse striae (Fig. 12D), interrupted medially by furrow if present.

Antennae. ♀ formula:

1.9–2.3(2.1):1:2.1–2.8(2.5):1.6–2.1(2.0):1.4–2(1.8):1.3–1.9(1.8):1.3–1.7(1.6):1.3–1.6(1.6):1.3–1.7(1.5):1.3–1.6(1.4):1.1–1.5(1.4):1.1–1.5(1.4):2.1–2.5(2.3)

♂ formula:

1.6–2.7:1:2–2.9:1.6–2.5:1.4–2.3:1.3–2:1.3–1.9:1.3–2.1:1.3–2:1.3–2:1.1–2:1.1–2:1.3–2

Mesosoma. Mesosoma 1.3–1.4(1.4) times longer than high (Fig. 12B); pronotal plate variable in sculpture, usually smooth with some few radial carinae; pronotum laterally setose, with longitudinal carinae along entire stretch reaching the posterior margin (Fig. 12B), sometimes somewhat branching; mesopleuron without coriaceous texture, rugulose anteroventrally, setose anteroventrally and along ventral margin, otherwise glabrous (Fig. 12B); mesopleural line merging with posteroventral hypocoxal furrow, ventral margin somewhat continuous, dorsally marked by influent striae (Fig. 12B); mesopleural triangle separated from mesopleuron by carina that fades before reaching the posterior subalar pit, posterodorsally smooth and shiny; axillulae well delimited (Fig. 12B), inside setose and longitudinally striate; mesoscutum 1.0–1.2 (1.1) times wider than long and 1.3–1.5(1.4) times longer than the mesoscutellum (Fig. 12D); notauli distinct, sometimes deep, with weak or strong transversal carination inside that is less dense than in *A. eucharioides*, usually surrounded by weak to strong wrinkles (Fig. 12D); median lobe of mesoscutum setose, gradually weakening towards posterior end (Fig. 12D), lateral lobes denser setose along outer margins than along inner margins; mesoscutellar foveae sometimes each delimited by a circumfoveal carina (Fig. 12D), which is sometimes not fusing with median carina; median carina sometimes extending over entire dorsal surface of mesoscutellum (Fig. 12D), sometimes interrupted, rarely completely absent, usually accompanied by lateral carinae that are less distinct but are not prone to disappear among general reticulate inside (as in *A. eucharioides*); posterior surface of mesoscutellum medially broadly raised (Fig. 12E), evenly setose, with one, two or more (sub-)median longitudinal carinae (Fig.

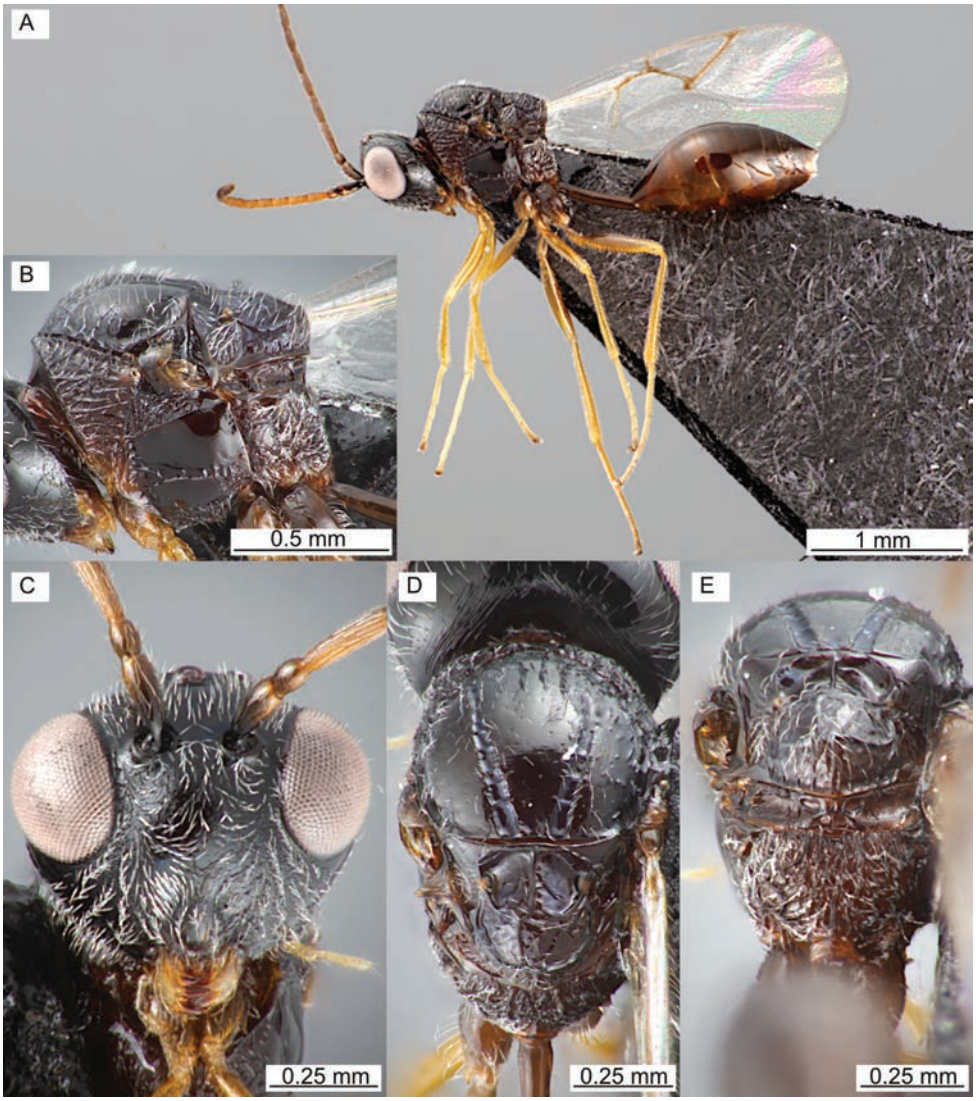

Figure 12. *Anacharis martinae* sp. nov., holotype, female (ZFMK-TIS-2640787) **A** lateral habitus **B** mesosoma lateral **C** face frontal **D** mesoscutum and mesoscutellum dorsal **E** mesosoma posterior view.

12E), rarely branching, laterally smooth to reticulate; dorsal axillular area laterally rugose to striate (Fig. 12D–E); sculpture of propodeum variable; nuchal collar usually with a narrow tooth dorsomedially (Figs 6C, 12E).

Wings. Marginal cell of fore wing 2.5–2.8 (2.6) times longer than wide (Fig. 2C). WIPs (Fig. 2C): Purple band pattern of fore wing reaching along about half the length of vein M. Apical spot of hind wing large, filling almost entire apical area.

Metasoma. 0.9–1.2 (1.2) times longer than rest of body (Fig. 12A); gaster 2.1–2.4 (2.4) times longer than petiole (Fig. 12A); petiole 1.0–1.6 (1.4) times longer than

hind coxa (Fig. 12A); metasomal tergite 2 (T2) with 0–4 (2) lateral setae on each side, with irregular punctures, T3-4 with narrow bands of punctures, dorsally usually interrupted, T5 with broad band of punctures, decreasing in width on T6-7, T7 with few setae along the band and more setae in posterior half than in the anterior half.

***Male genitalia*.** Parameral plate submedially widened, basoventral margin rounded, without tooth.

Males. Flagellomeres dorsoventrally bicoloured yellow-dark brown, gaster shorter than in females. T7 in males almost entirely punctured except medially, long setae across surface, except on smooth area.

Variation. The specimens from the Bavarian Forest National Park (BC-ZSM-HYM-27596-F10 & BC-ZSM-HYM-27596-F09) are in colouration similar to the holotype (Fig. 12), but more distinct, i.e. the head is distinctly darker than the rest of the body. They are also smaller than the average. ZFMK-TIS-2640713 has a strong sculpture on its pronotal plate, whilst other specimens are rather smooth and of weaker sculpture. ZFMK-TIS-2640791 has a completely smooth dorsal surface of the mesoscutellum but fits otherwise well within the species morphologically.

CO1 barcode. n=18. Maximum intraspecific distance = 2.3%. Minimum distance to closest species (*A. eucharioides*) = 7.9%. CO1 barcode consensus sequence:

AATTTTATACTTTATTTTAGGTATTTGATCAGGAATAATAGGATCAAGATTAAGAATAATTATTCGAATAGAATTAGGAACCCCATCTCAATTAATCATAAATGATCAAATTTATAACTCAATTGTAACTGCTCATGCATTTATTATAATTTTTTTTTATAGTAATACCAATTATAGTAGGAGGATTTGGAAATTATCTGGTTCCTCTAATACTAATTTCTCCTGATATAGCCTTCCCACGATTAAATAATTTAAGATTTTGATTTTTAATCCCATCCCTATTTTTAATAACAATAAATTTATTTATTGATCAAGGAGCTGGTACAGGATGAACTGTATACCCTCCACTATCCTCCTTAACGGGTCATCCATCAATATCAGTAGATTTAGTTATTTATTCTCTTCATTTAAGAGGAATTTCTTCAATTCTTGGTTCAATTAATTTTATTGTAACAATTTTAAATATACGAATAAACTCAATAACAATAGATAAAATTTCATTATTCATTTGATCTATTTTTTTTAACAACTATTTTACTATTATTATCATTACCTGTATTAGCTGGAGGTTTAACAATATTACTTTTTGATCGAAACTTAAATACATCATTTTTTGATCCTACAGGAGGAGGAGACCCAATTTTATATCAACATTTATTT

Type material. ***Holotype*.** Germany • ♀; Hesse, Waldeck-Frankenberg, National park Kellerwald-Edersee, Banfehaus, old floodplain of the Banfe; 51.167°N, 8.9749°E; ca 270 m a.s.l.; 22 Jul.-5 Aug. 2021; GBOL III leg.; Malaise trap (Krefeld version); ZFMK-TIS-2640787.

***Paratypes*.** Germany • 2 ♂♂; same collection data as for holotype; ZFMK-TIS-2640788, ZFMK-TIS-2640791. • 1 ♂; Bavaria, Bavarian Forest National Park; 48.937°N, 13.42°E; ca 830 m a.s.l.; 1 Jun. 2013; BC-ZSM-HYM-27764-H01 (ZSM). • 1 ♀, 1 ♂; Bavaria, Bavarian Forest National Park; 49.099°N, 13.233°E; ca 710 m a.s.l.; 1 Jun. 2013; female - BC-ZSM-HYM-27596-F10 (ZSM); male - BC-ZSM-HYM-27596-F09 (ZSM). • 1 ♂; Bavaria, Garmisch-Partenkirchen, Zugspitze, mountain; 47.4062°N, 11.0095°E; ca 1970 m a.s.l.; 20 Jun.-5 Jul. 2018; Doczkal, D., Voith,

J. leg.; Malaise trap; ZFMK-TIS-2637892 (NHMUK). • 1 ♂; Hesse, Gießen, Hohberg, Großen-Buseck; 50.6196°N, 8.7844°E; ca 300 m a.s.l.; 17 Jun. 2021; GBOL III leg.; sweep net; ZFMK-TIS-2629493. • 1 ♂; Hesse, Rheingau-Taunus, Lorch am Rhein, above Nollig castle; 50.0495°N, 7.7966°E; ca 250 m a.s.l.; 17–25 Jun. 2015; Niehuis, Oliver leg.; Malaise trap; MF 3; ZFMK-TIS-2628231. • 1 ♀, 2 ♂♂; Hesse, Waldeck-Frankenberg, National park Kellerwald-Edersee, Maierwiesen; 51.1555°N, 9.0015°E; ca 370 m a.s.l.; 22 Jun.-8 Jul. 2021; GBOL III leg.; Malaise trap (Krefeld version); female - ZFMK-TIS-2640809 (NHRS); males - ZFMK-TIS-2640804, ZFMK-TIS-2640805 (NHRS). • 1 ♀; Hesse, Waldeck-Frankenberg, NP Kellerwald-Edersee, „Banfe-Haus"; 51.167°N, 8.9749°E; ca 270 m a.s.l.; 7–21 Jul. 2022; GBOL III leg.; Malaise trap; ZFMK-TIS-2640770. • 1 ♀; Hesse, Waldeck-Frankenberg, NP Kellerwald-Edersee, „Große Küche"; 51.1564°N, 8.9879°E; ca 320 m a.s.l.; 19 Aug.-2 Sep. 2021; GBOL III leg.; Malaise trap; ZFMK-TIS-2640690 (NHMUK). • 1 ♀, 2 ♂♂; Hesse, Waldeck-Frankenberg, NP Kellerwald-Edersee, „Maierwiesen"; 51.1555°N, 9.0015°E; ca 370 m a.s.l.; 8–22 Jul. 2021; GBOL III leg.; Malaise trap; female - ZFMK-TIS-2640734 (SMNS); males - ZFMK-TIS-2640731, ZFMK-TIS-2640733 (SMNS). • 1 ♀; Rhineland-Palatinate, Ahrweiler, Niederzissen, Bausenberg, upper part of volcanic mountain, next to oak tree; 50.4672°N, 7.2212°E; ca 310 m a.s.l.; 26 May-12 Jun. 2022; Jaume-Schinkel, Santiago leg.; Gressit Malaise trap; ZFMK-TIS-2640713.

Other material examined. Without DNA barcode. Belgium • 1 ♀; Walloon Region, Namur, Nismes; 50.0744°N, 4.5556°E; ca 220 m a.s.l.; 10 Jul. 2022; W. Declercq leg.; Light trap; ZFMK-HYM-00039668 (RBINS). • 1 ♀; Walloon Region, Tellin, Ri d'Howisse; 50.1113°N, 5.2531°E; ca 260 m a.s.l.; 18 Jul. 2022; W. Declercq leg.; Light trap; ZFMK-HYM-00039667 (RBINS).

France • 1 ♂; Bitche; 7 Aug. 1979; Henk J. Vlug leg.; sweep net; specimen in coll MF.

Sweden • 1 ♂; Hälsingland, Skog sn, Noran; 5 Aug. 1949; Olov Lundblad leg.; NHRS-HEVA 000023178 (NHRS). • 1 ♂; Scania, Ystad kommun, Sandhammaren, Järahusen, oak shrub forest on coastal sand dunes; 55.4038°N, 14.1999°E; ca 10 m a.s.l.; 22 May-15 Jul. 2005; Swedish Malaise Trap Project (Swedish Museum of Natural History) leg.; Malaise trap; NHRS-HEVA 000023179 (NHRS).

Switzerland • 1 ♂; Neuchâtel, Auvernier; 8 Aug. 1957; Jacques de Beaumont leg.; specimen at MHNG. • 1 ♀; same collection data as for preceding 15 Aug. 1956; specimen at MHNG.

Biology. Summer species, flying mainly from June to September, peak in July. No clear preferences in terms of habitat.

Distribution. Belgium, France, Germany (locus typicus: Kellerwald-Edersee National Park, Banfehaus), Sweden, Switzerland.

No DNA barcode matches with publicly available sequences from other countries.

Mainly collected in lowlands below 400 m a.s.l., occasionally found in higher altitudes at 700–900 m a.s.l. and rarely even higher.

Etymology. Named after the first author's wife, Martina Vogel.

Remarks. In the molecular analysis, *A. martinae* is split into two clades by ASAP. The gap between the two clusters is 2.3% and cannot be attributed to poor quality sequences. As ASAP is the only analysis to split this cluster by that gap and we cannot find morphological evidence for a split into two species, we regard this result as an oversplit.

The diagnosis against *A. belizini* is based on the description and the accompanying SEM images of the holotype in Mata-Casanova et al. (2018). There, *A. belizini* is described as having a smooth occiput. In the SEM images, however, we can see occipital striolation or striation, which would match with the diagnosis of the *euchariodes* species group. In Mata-Casanova et al. (2018), *A. belizini* is said to be most similar to *A. antennata*, while we think that *A. antennata* is much closer morphologically to *A. petiolata*/*typica* based on the SEM images provided, showing the interrupted mesopleural line, the smooth mesoscutellum and the smooth to rugose lateromedial area of the pronotum.

On the SEM images of *A. belizini*, the pronotal plate is significantly laterally projecting in dorsal view (Fig. 3. C. in Mata-Casanova et al. (2018) vs. Fig. 12D). This is not the case in *A. martinae*, and shape of the pronotal plate could be another diagnostic feature to separate *A. belizini* and *A. martinae*. Additionally, the parascutal sulcus seems very strongly impressed and carinate in *A. belizini*, much more so than in any of our specimens of *A. martinae* (Fig. 12B). As we discussed in the treatment of *A. euchariodes*, the parascutal sulcus is very variable and cannot be used as a diagnostic character. If such extremes as present in *A. belizini* are consistent or not is currently impossible to evaluate because there is only a single specimen (the holotype) known for *A. belizini*.

The morphometric analysis (Fig. 8B) revealed overlap with the remaining species of the *euchariodes* species group. However, the morphospace overlaps only partially, which allows us to make statements of inclusive and exclusive ranges in the two ratios extracted as separating species best. The intertorular distance:torulus to eye distance (Fig. 8B, right) ranges from 1.4 to 2.0, but no other species than *A. martinae* has a ratio of higher than 1.7, making >1.7 to 2.0 the exclusive *A. martinae* range. For POL:petiole length, a ratio of >0.7 is exclusive for *A. martinae*, but any ratio below could be other species. While we included the ratios in the description of the species, we refrained from including them in the diagnosis. This partial separation between *A. martinae* and the remaining species in the morphometric analyses again highlights the morphometric variability of the species in *Anacharis* (see also remarks on *A. euchariodes*) but also points towards the potential power of morphometric analyses which will prove helpful in delimitation of another species (*A. maxima*, see below).

***Anacharis maxima* Vogel, Forshage & Peters, sp. nov.**
https://zoobank.org/94B47FEC-2AE0-42C4-92E9-0B82C143488C
Figs 2G, 3F, 13A–E

Diagnosis (n = 6, all males). Belongs to the *euchariodes* species group. Large species (3.5–4.0, mean 3.8 mm, unique in Northwestern European fauna). Similar to

A. euchariodes by having the lateromedial area of the pronotum smooth to rugose (Fig. 13B, smooth in *A. minima*, *A. petiolata* and *A. typica*, longitudinal carinae in *A. martinae*). Differing from all other Northwestern European species by its large size (other species usually not larger than 3.5 mm), its mesoscutellar sculpture having oblique to transversal carinae only in the anterior half between the mesoscutellar foveae (Fig. 13D, smooth to entirely carinate or differently oriented carinae in other Northwestern European species) and having a LOL:metacoxa ratio of < 0.225 combined with a head frontal height:mesoscutellum length ratio of ≤ 1.9 (Fig. 8C right, LOL:metacoxa ratio usually > 0.225, if around 0.225, then head frontal height:mesoscutellum length ratio >1.9 in other Northwestern European species). In the Western Palaearctic fauna, *A. maxima* is most similar to *A. parapsidalis*, mainly due to its size. *Anacharis parapsidalis* was not reported from Northwestern Europe but from Japan and Romania (Mata-Casanova et al. 2018). *Anacharis maxima* differs from *A. parapsidalis* in its mesoscutellar sculpture (Fig. 13D, mesoscutellum reticulate-carinate all over mesoscutellum in *A. parapsidalis*), the lateromedial area of the pronotum is smooth to rugose (Fig. 13B, reticulate-carinate in *A. parapsidalis*), the mesopleural line not reaching the posteroventral hypocoxal furrow (Fig. 13B) (reaching it in *A. parapsidalis*) and the presence of punctures on the metasomal tergites (absent in *A. parapsidalis*).

Description. Male. ***Size.*** Large; body: 3.5–4.0 (3.9) mm; antennae: 2.7–3.4 (3.1) mm; fore wing: 2.5–3.3 (3.3) mm

Colour. Body black (Fig. 13A); scape, head, mesosoma, and metasoma entirely black (Fig. 13); pedicel largely black (Fig. 13C), flagellomeres bicoloured dorsoventrally (Fig. 13A); mid and hind coxa, as well as hind femur largely (Fig. 13A), fore coxa partially black (Fig. 13A, B) and hind tarsomeres darkened (Fig. 13A), otherwise yellow (Fig. 13A); mandibles basally and apically darkened, otherwise yellow (Fig. 13C); palps pale yellow (Fig. 13C).

Head. Trapezoid in frontal view, genae abruptly kinked, meeting mandibular base in an angle < 90° (Fig. 13C); lower face with thick silvery hairs (Fig. 13C), punctate; clypeal margin usually slightly bilobed, clypeus with central convex area, medially to medioventrally smooth (Fig. 13C), otherwise punctate-rugulose; malar area coriaceous, reaching from ventral eye margin along entire stretch of mandibular base (Fig. 18B), anteroventral corner of mandibular base sometimes smooth; genae smooth around eye, with increasingly dense punctation and regular setae towards the hind margin (Fig. 13B); upper face setose, punctured, with usually noticeable, sometimes shallow median dent; space between toruli smooth (Fig. 13C); eyes with few scattered setae (Fig. 13C); vertex setose; POL:OOL:LOL:OD 2.2:1.3:0.8:1 (2.3:1.3:0.8:1), glabrous along OOL and anterior to median ocellus; head in dorsal view 2.0 times wider than long, laterally longer than medially; vertex and occiput usually with shallow median furrow, occiput broadly yet finely striate to striolate (Fig. 13D), not interrupted by median furrow.

Antennae. ♂ formula:

2.1-2.4(2.2):1:2.6-2.7(2.7):2.3-2.4(2.4):2.2-2.3(2.2):2-2.1(2.1):2-2.1(2):1.9-2.1(1.9):1.9-2(1.9):1.8-2(1.9):1.8-1.9(1.8):1.7-1.9(1.8):1.7-1.8(1.7):2-2.6(2.5)

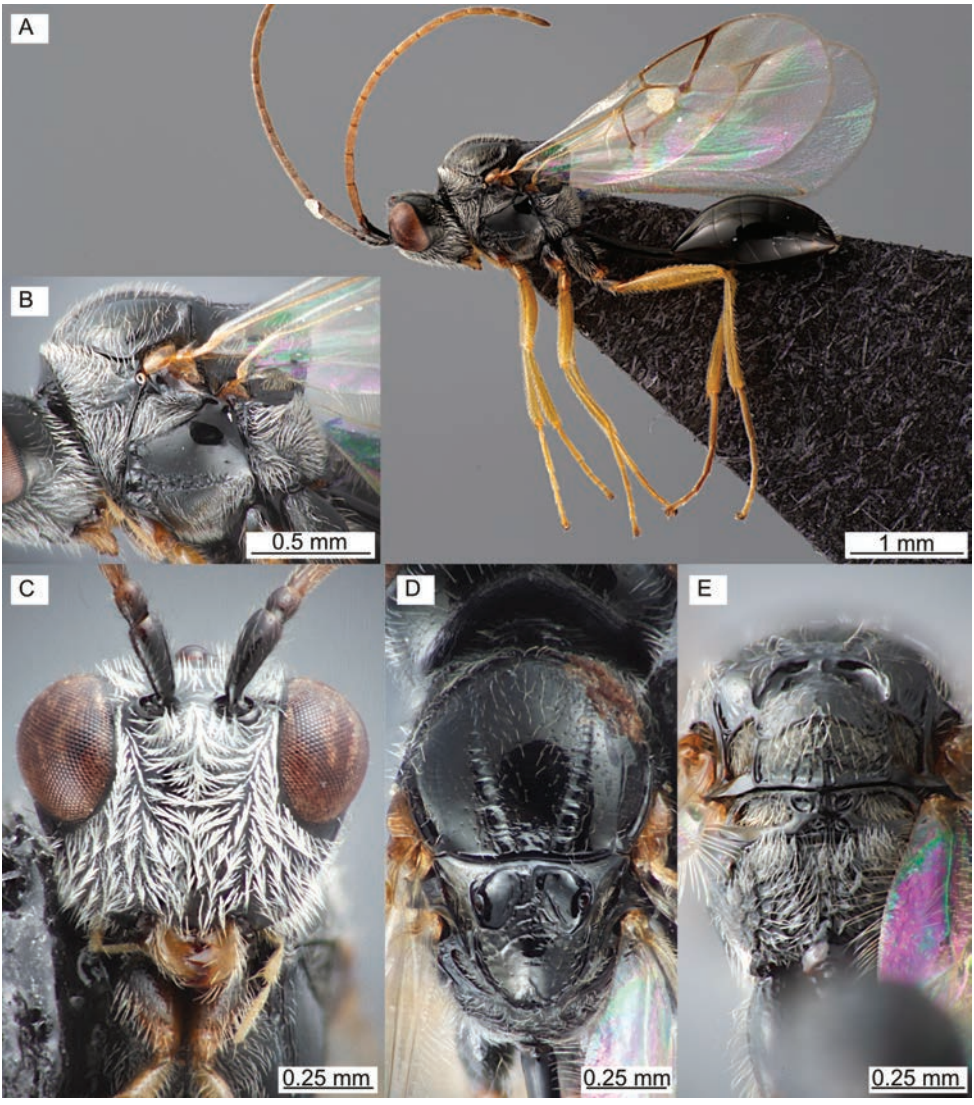

Figure 13. *Anacharis maxima* sp. nov., holotype, male (ZFMK-TIS-2640744) **A** lateral habitus **B** mesosoma lateral **C** face frontal **D** mesosoma dorsal **E** mesosoma posterior view.

***Mesosoma*.** Mesosoma 1.3 times longer than high (Fig. 13B); pronotal plate centrally smooth, laterally coriaceous with a few carinae radiating from the centre, setose centrally and laterally, otherwise glabrous; pronotum laterally with dense silvery setae (Fig. 13B), with longitudinal carinae along anterior margin, reaching hind margin in ventral region, lateromedial area slightly rugose, without regular carinae (Fig. 13B); mesopleuron sometimes coriaceous dorsally and ventrally of mesopleural line, otherwise smooth (Fig. 13B), scrobiculate along anteroventral margin (Fig. 13B), reaching into venter; mesopleuron setose along ventral margin,

otherwise glabrous (Fig. 13B); mesopleural line separated from posteroventral hypocoxal furrow (Fig. 13B), ventral margin somewhat continuous, dorsally marked by few to some influent striae (Fig. 13B); mesopleural triangle separated from mesopleuron by carina that fades before reaching the posterior subalar pit (Fig. 13B), posterodorsally smooth and shiny (Fig. 13B); axillulae well delimited (Fig. 13E), inside setose and longitudinally striolate; mesoscutum 1.1 times wider than long and 1.3–1.4 (1.3) times longer than the mesoscutellum (Fig. 13D); notauli deep and distinct, with strong transversal carinae inside (Fig. 13D), without (Fig. 13D) or with fine wrinkles along them; median lobe of mesoscutum setose (Fig. 13D), sometimes somewhat coriaceous, then lateral lobes also coriaceous, but less than median lobe; mesoscutellar foveae usually well delimited posteriorly by circumfoveal carinae (Fig. 13D), fusing with median carina or not (Fig. 13D); median carina starting to branch obliquely to transversally before reaching posterior end of foveae (Fig. 13D), circumscutellar carina raised posteriorly (Fig. 13D, E), appearing like a posterodorsal tooth on the mesoscutellum in lateral view; posterior surface of mesoscutellum medially broadly raised, evenly setose, ventrally scrobiculate, surface reticulate-striate (Fig. 13E); dorsal axillular area striate on posterolateral margin, otherwise smooth (Fig. 13D, E); nuchal collar broadly projecting dorsally, point rounded (Figs 6F, 13E); fore trochanter, mid coxa and hind coxa with conspiciously long setae (Fig. 13A).

Wings. Marginal cell of fore wing 2.6–2.9 (2.6) times longer than wide (Fig. 2E); WIPs (Fig. 2E): apical spot of hind wing narrow, covering less than half of the apical area.

Metasoma. 1.3 times longer than rest of body (Fig. 13A); gaster twice as long as petiole (Fig. 13A); petiole 1.3–1.5 (1.5) times longer than hind coxa (Fig. 13A); metasomal tergite 2 (T2) with two setae dorsolaterally on each side along weak band of punctures; T3 and T4 with narrow bands of punctures, T5 and T6 with broad bands of punctures; T7 medially without punctures, otherwise filled with punctures with long setae dorsally.

Male genitalia. Parameral plate basally widened, ventrally with basal tooth-like projections pointing inwards (Fig. 3E).

Female. Unknown.

CO1 barcode. n=7. Maximum intraspecific distance: 0%. Minimum distance to closest species (*A. eucharioides*): 3.9%. CO1 barcode consensus sequence:

TATTTTATACTTTATTTTAGGTATTTGATCTGGAATAATAGGAT-
CAAGATTAAGAATAATTATTCGAATAGAATTAGGGACCCCATCC-
CAATTAATTATAAATGATCAAATTTATAATTCAATTGTAACTGCA-
CATGCATTTATTATAATTTTCTTTATAGTTATACCTATCATAGTAG-
GAGGATTTGGAAATTATTTAGTACCTTTAATATTAATTTCTCCTGA-
TATAGCTTTCCCTCGATTAAATAATTTAAGATTTTGATTTTTAATC-
CCTTCCTTATTTTTAATAACAATTAATTTATTTATTGATCAAGGGA-
CAGGAACAGGATGAACTGTTTATCCCCCATTATCATCCATCACAG-
GTCATCCATCTATATCAGTAGATTTAGTTATTTACTCATTACATTTAA-

GTGGAATTTCTTCAATTCTTGGATCAATTAATTTTATTGTAACCATTT-
TAAATATACGAATAATCTCCATATCTATAGACAAAGTCTCATTATT-
TATTTGATCTATTTTTTTAACTACAATTTTACTATTATTATCTTTACC-
CGTACTAGCAGGAGGATTAACTATACTATTATTTGATCGAAATTTAAA-
TACATCTTTTTTTTGACCCTACAGGAGGAGGAGACCCTATTCTTTAT-
CAACACTTATTT

Type material. ***Holotype*.** Germany • ♂; Bavaria, Rhön-Grabfeld, Hausen, Eisgraben, basalt depot at forest margin; 50.5026°N, 10.0895°E; ca 740 m a.s.l.; 12–23 Jul. 2018; Dieter Doczkal leg.; Malaise trap; ZFMK-TIS-2640744.

***Paratypes*.** Germany • 5 ♂♂; Same collection data as for holotype; ZFMK-TIS-2640739, ZFMK-TIS-2640740 (ZSM), ZFMK-TIS-2640741 (SMNS), ZFMK-TIS-2640742 (NHMUK), ZFMK-TIS-2640743 (NHRS). • 1 ♂; Rhineland-Palatinate, Vulkaneifel, Jünkerath, private garden, wet meadow, right next to ditch; 50.3343°N, 6.595°E; ca 450 m a.s.l.; 6–8 Aug. 2021; Jonathan Vogel leg.; Malaise trap; ZFMK-TIS-2640676.

Other material examined. Without DNA barcode. Sweden • 1 ♂; Uppland, Norrtälje, Singö; 15 Jul. 1962; Karl-Johan Hedqvist leg.; NHRS-HEVA 000023177 (NHRS).

Switzerland • 1 ♂; Vaud, Aigle, Solalex; 4 Aug. 1954; Jacques Aubert leg.; specimen at MHNG.

Biology. Summer species, flying from July to August, peak in July. No clear preferences in terms of habitat.

Distribution. Germany (locus typicus: Bavaria, Rhön-Grabfeld, Hausen, Eisgraben), Sweden, Switzerland.

No DNA barcode matches with publicly available sequences from other countries.

Probably preferring higher altitudes, as all specimens were collected at 400 to 800 m a.s.l.

Etymology. From the latin word "maximus", meaning the greatest, referring to the tall size of the species.

Remarks. *A. maxima* is not frequently collected, though with six specimens caught from one collection event at one site, it seems like it can be locally relatively abundant. The diagnosis against *A. parapsidalis* is based on comparisons with the SEM images and the redescription (Mata-Casanova et al. 2018) as no specimen of *A. parapsidalis* was available to us.

The morphometric analysis revealed only little overlap of *A. maxima* with the other species within the *eucharioides* species group (Fig. 8C left). The lda extractor provided two ratios, which – separately – can almost and – in combination – fully separate *A. maxima* from the remaining species (Fig. 7, Fig. 8C right). We included these ratios into the diagnosis of *A. maxima*. For this species, the morphometric analyses proved helpful in finding diagnostic characters. Note that this was not the case in *A. eucharioides*, and only partially in *A. martinae* (see above), highlighting both the morphometric variability and overall similarity of the *Anacharis* species and the power and applicability of multivariate morphometrics.

***Anacharis minima* Vogel, Forshage & Peters, sp. nov.**
https://zoobank.org/22711BED-98BF-4795-A81E-B709E12667E1
Fig. 14A–E

Diagnosis (n = 1). Belongs to the *euchariodes* species group. Small species (2.4 mm). Similar to *A. petiolata* and *A. typica* by having a centrally smooth mesoscutellum (centrally carinate in *A. euchariodes*, *A. martinae* and *A. maxima*). The small body size and the narrow coriaceous texture of the malar space that extends only around the dorsal corner of the mandibular base (Fig. 19A) is unique in the Palaearctic fauna (coriaceous texture of malar space extending along entire length of mandibular base in all other species).

Description. Female. ***Size*.** Small; body: ♀ 2.4 mm. Antennae: ♀ 1.6 mm. Fore wing: 1.9 mm

***Colour*.** Body black (Fig. 14A); scape, head, mesosoma, coxa, petiole black (Fig. 14); mandibles (Fig. 14C), palps (Fig. 14B), rest of legs (hind tarsi darker) (Fig. 14A) yellow; pedicel and flagellomeres (Fig. 14A), tegulae (Fig. 14B, D), and gaster (Fig. 14A) dark brown.

***Head*.** Roundish triangular in frontal view, genae not abruptly kinked (Fig. 14C); lower face setose (Fig. 14C), with punctures; clypeal margin margin bilobed and flanged, clypeus smooth; coriaceous texture of malar area narrow, coriaceous texture of the malar space narrow, extending only around the dorsal corner of the mandibular base (Fig. 19A); genae smooth around eye, with increasingly dense punctation and regular setae towards the hind margin (Fig. 14A); upper face sparsely setose and very few punctures, centrally with shallow dent (Fig. 14C); space between toruli smooth; eyes with scattered setal stubs (Fig. 14C); ocellar triangle with wide base, ocelli small, POL:OOL:LOL:OD = 3.1:1.7:1.4:1.0; setose between lateral ocellus and eye, small glabrous area in front of median ocellus not reaching median dent of upper face; head in dorsal view 1.8 times wider than long, laterally longer than medially; vertex and occiput with smooth shallow median furrow, occiput with medially interrupted striolation (Fig. 14D).

***Antennae*.** ♀ formula:

1.9:1.0:2.1:1.4:1.4:1.4:1.4:1.4:1.3:1.2:1.2:1.2:1.1:2.1

***Mesosoma*.** Mesosoma 1.3 times longer than high (Fig. 14B); pronotal plate coriaceous, with some few radial carinae; pronotum laterally setose (Fig. 14B), with only few carinae ventrally and along anterior margin (Fig. 14B), posterodorsal area smooth and even (Fig. 14B); mesopleuron without distinct coriaceous sculpture, scrobiculate along anterior margin (Fig. 14B), setose along ventral margin, otherwise glabrous (Fig. 14B); mesopleural line meeting posteroventral hypocoxal furrow with its ventral margin only, ventral margin somewhat continuous, dorsally marked by influent striae (Fig. 14B); mesopleural triangle separated from mesopleuron by carina that fades before reaching the posterior subalar pit, setae mostly in anterior two-thirds; axillulae well delimited, inside setose and longitudinally rugose-carinate; mesoscutum 1.1 times

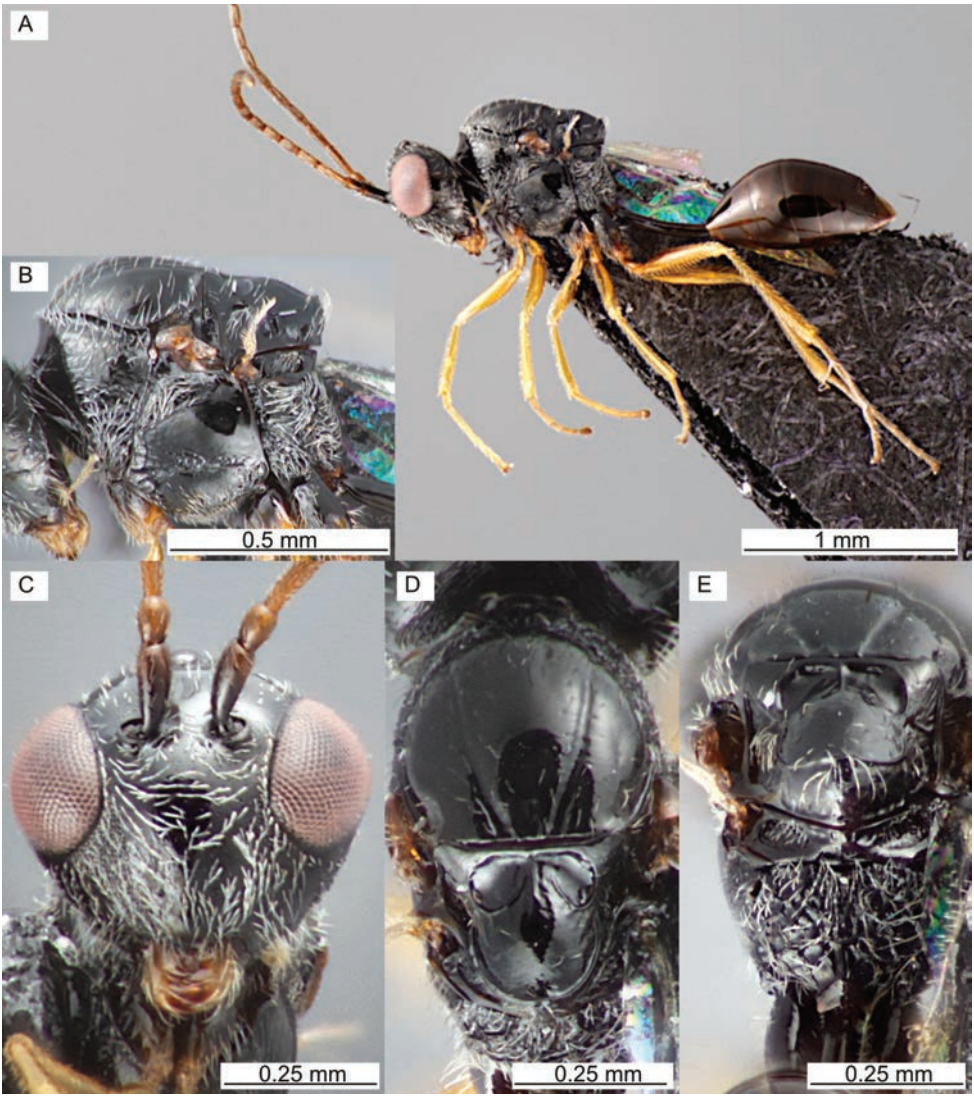

Figure 14. *Anacharis minima* sp. nov., holotype, female (ZFMK-TIS-2640724) **A** lateral habitus **B** mesosoma lateral **C** face frontal **D** mesosoma dorsal **E** mesosoma posterior view.

wider than long and 1.4 times longer than the mesoscutellum (Fig. 14D); notauli complete, inside not carinate, wrinkles weak to absent (Fig. 14D); lateral and median lobes of mesoscutum centrally glabrous, otherwise setose, increasingly so towards margins (Fig. 14D); mesoscutellar foveae closed, with circumfoveal carina delimiting each fovea (Fig. 14D), not touching the median carina (Fig. 14D); mesoscutellum smooth on dorsal and posterior surface (Fig. 14D), posterior surface medially distinctly raised (Fig. 14D), laterally smooth (Fig. 14D); ventral half of dorsal axillular area rugose (Fig. 14E); propodeal area defined by carinae (Fig. 14E), inside carinate-rugose, median

carina present ventrally (Fig. 14E); nuchal collar broadly extending posteriorly, tip rounded (Figs 6D, 14E).

***Wings*.** Marginal cell of fore wing 2.6 times longer than wide.

***Metasoma*.** 1.2 times longer than rest of body (Fig. 14A); gaster 2.3 times longer than petiole (Fig. 14A); petiole 1.5 times longer than hind coxa Fig. 14A); metasomal tergite 2 (T2) and T3 with weak line of punctures dorsally, T4 with scattered band of punctures, T5-6 with narrow band, T7 with medially weaker band, laterally with few setae.

Male. Unknown

CO1 barcode. n=1. Maximum intraspecific distance = not applicable. Minimum distance to closest species (*A. euchariodes*) = 5.6%. CO1 barcode consensus sequence:

AATTTTATACTTTATTTTAGGTATTTGATCCGGAATAATAGGTTCAA-
GATTAAGAATAATTATTCGAATAGAACTAGGAACCCCATCTCAAT-
TAATCATAAATGATCAAATTTATAATTCAATTGTAACCGCACATGCCTT-
TATTATAATTTTTTTTATAGTTATACCCATTATAGTAGGAGGATTTG-
GAAATTATTTAGTGCCTTTAATATTAATCTCTCCTGATATAGCTTTCC-
CACGATTAAATAATTTAAGATTTTGATTTTTAATCCCTTCCCTATTTT-
TAATAACAATTAACTTATTTATTGATCAAGGAGCAGGGACAGGATGAACT-
GTATACCCACCATTATCATCCCTCACAGGTCATCCATCTATATCAGTA-
GATTTAGTTATTTATTCACTACATTTAAGAGGTATCTCATCAATTCTTG-
GATCAATTAATTTTATTGTAACCATTTTAAATATACGAATAAACTCTG-
TATCTATAGACAAAATTTCATTATTTATTTGATCTATCTTTTTAACTA-
CAATTTTACTATTATTATCTTTACCTGTATTAGCAGGAGGATTAACTA-
TATTATTATTTGATCGAAATTTAAATACATCTTTTTTTGACCCTACAG-
GAGGGGGAGACCCAATTCTTTATCAACACTTATTT

Type material. ***Holotype*.** Germany • ♀; Baden-Württemberg, Karlsruhe, Malsch, Hansjakobstraße, garden; 48.8835°N, 8.3197°E; ca 120 m a.s.l.; 25 Oct.-8 Nov. 2020; Dieter Doczkal leg.; Malaise trap; ZFMK-TIS-2640724.

Biology. The holotype was collected in autumn (between October and November) in a garden.

Distribution. Germany (locus typicus: Karlsruhe, Malsch).

No DNA barcode matches with publicly available sequences from other countries.

Holotype collected from ca. 120 m a.s.l.

Etymology. From the latin word for "the smallest", referring to its distinct small body size.

Remarks. While *A. minima* is molecularly clearly distinct from other species, the morphology overlaps in many aspects with other species that show a smooth mesoscutellum. It is the name-giving small size that seems to hold the most diagnostic value but there is no way to say for sure which characters are morphologically diagnostic for *A. minima* based on a single specimen. Some specimens, which we currently classify as *A. typica* (NHRS-HEVA 000023181 and a specimen from MHNG) show similarities to the holotype of *A. minima*, but they deviate in size and sculpture to regard them as not conspecific. The morphological diagnosis is in need of extension by studying further material of which the barcode matches that of *A. minima*.

Anacharis norvegica Mata-Casanova & Pujade-Villar, 2018

Diagnosis (n = 1). Belongs to the *A. immunis* species group. Similar to *A. ensifer* in generally having a largely sculptured mesoscutellum (largely smooth in *A. immunis*). Different to *A. ensifer* by having its mesoscutellum covered with reticulate-foveate sculpture resulting in smaller foveae (larger foveae in *A. ensifer*). The circumscutellar carina is less distinct and not flanged upwards posteriorly (usually distinctly flanged upwards, appearing in lateral view like a posterodorsal tooth in *A. ensifer* and *A. immunis*). The dorsal margin of the mesopleural line is diffused by rugose sculpture of mesopleuron in its anterior half (dorsally well-defined mesopleural line in its anterior half in *A. ensifer* and *A. immunis*). Wrinkles on mesoscutum, especially in anteromedian area, strong, making the anteroadmedian signa distinct (less to no wrinkles and thereby less notable anteroadmedian signa in *A. ensifer* and *A. immunis*).

Other material examined. Material without DNA barcode. Sweden • 1 ♀; Torne lappmark, Kiruna, Abisko Nationalpark, dry sparse alpine downy birch forest; 68.3539°N, 18.7822°E; ca 410 m a.s.l.; 21 Jul.-7 Aug. 2003; Swedish Malaise Trap Project (Swedish Museum of Natural History) leg.; Malaise trap; NHRS-HEVA 000023145 (NHRS).

Biology. Summer species, type series collected in July and August, as was the specimen studied here. Probably preferring boreal habitats.

Distribution. Norway (locus typicus: Oppdal), Sweden.

Collected in higher elevations from 400 (specimen studied here) to 900 m a.s.l. (type series).

Remarks. Despite not having had a fresh specimen at hand for sequencing, we regard this species as different from *A. ensifer* due to the clear differences in sculpture of the mesoscutum, mesoscutellum and mesopleuron.

The species was described from one locality in central Norway (Oppdal) (Mata-Casanova et al. 2018) and we found only one additional specimen from Abisko national park (Sweden) within the older dry-mounted specimens originating from all over Sweden (coll. NHRS) and Switzerland (coll. MHNG & NMBE). Our diagnosis was made as an amendment to the diagnosis by Mata-Casanova et al. (2018), considering the single specimen we had at hand as well as the data and illustrations given in Mata-Casanova et al. (2018). The fresh samples that we had access to were mainly collected in Germany and Belgium, with a few additions from Southern Norway. As we did not find more specimens of that species, we deem it possible that its distribution is limited to boreal habitats in the scandic mountains.

Anacharis petiolata (Zetterstedt, 1838), stat. rev.

Figs 2C, 15A–E

Cynips petiolata Zetterstedt, 1838:409 - lectotype (MZLU) ♀, photographs examined.
Anacharis gracilipes Ionescu, 1969:75 syn. nov. (removed from synonymy with *A. eucharioides*) - holotype (MGAB) ♀, examined.

Diagnosis (n = 9). Belongs to the *eucharioides* species group. Medium sized species (3.0–3.4, mean 3.2 mm, similar to *A. eucharioides*, *A. martinae* and *A. typica*). Differing from *A. eucharioides* and *A. martinae* by having a centrally smooth mesoscutellum (Fig. 15D, E, centrally carinate in *A. eucharioides* and *A. martinae*) and a smooth lateromedial area of the pronotum (Fig. 15B, rugose to obliquely carinate in *A. eucharioides* and *A. martinae*). Differs from *A. typica* mainly by having the hind coxa less distinctly bicoloured, weak paling is notable apically (Fig. 15A, distinctly bicoloured with distinct paling in hind coxa in *A. typica*). The hind trochanter in *A. petiolata* is similarly dark as the hind coxa (similar pattern of paling as hind coxa or pale as hind femur in *A. typica*). Additional to morphological differences, based on the limited material at hand, *A. petiolata* seems to be exclusively collected in boreal or montane environments from above 1,000 meters above sea level (whilst *A. typica* is collected from temperate environments below 700 meters above sea level).

CO1 barcode. n=9. Maximum intraspecific distance: 2.2%. Minimum distance to closest species (*A. eucharioides*): 3.2%. CO1 barcode consensus sequence:

AATTTTATACTTTATTTTAGGTATTTGATCAGGAATAATAGGATCAAGATTAAGAATAATTATTCGAATAGAGTTAGGTACCCCATCTCAATTAATTATAAATGATCAAATTTATAATTCAATTGTAACTGCACATGCATTTATCATAATTTTCTTTATAGTTATACCTATCATAGTAGGAGGATTTGGAAATTATTTAGTACCTTTAATATTAATCTCTCCTGATATAGCTTTCCCACGATTAAATAATTTAAGATTTTGATTTGCAATCCCTTCCTTATTTTTAATAACAATTAATTTATTTATCGACCAAGGAGCAGGAACAGGATGAACTGTTTATCCTCCATTATCCTCTCTAACAGGTCACCCATCTATATCAGTAGATTTAGTTATTTATTCATTACATTTAAGTGGAATCTCTTCAATTCTTGGATCAATTAATTTTATTGTTACCATTTTAAATATACGAATAAATTCTATATTTATAGACAAAATTTCATTATTTATTTGATCTATTTTTCTAACTACAATTTTACTATTATTATCTTTACCCGTACTAGCAGGAGGATTAACTATACTATTATTTGATCGAAATTTAAATACATCTTTTTTTGACCCCACAGGAGGGGGAGACCCAATCCTTTATCAACATTTATTT

Type material.

Lectotype of *Cynips petiolata* Zetterstedt, 1838

LECTO-TYPE
C. petiola ta ♀.
1982 855
LECTOTYPE Cynips petiolata Zett det. N.D.M.Fergusson, 1982
Anacharis eucharoides (Dal.) det. N.D.M.Fergusson, 1982
MZLU 00207341
MZLU Type no. 7814:1
[for images, see https://www.flickr.com/photos/tags/mzlutype07814]

Holotype of *Anacharis gracilipes* Ionescu 1969

Anacharis gracilipes n. sp. ♀ Holotip
26.7.956 Rarău,
GAL 0340/9

Anacharis eucharoides ♀ (Dalman, 1823) JP-V 2012 det
HOLOTYPUS, Anacharis gracilipes Ionescu, 1969, MGAB
[Fig. 16E]

Other material examined. DNA barcode vouchers. Germany • 1 ♀; Bavaria, Allgäu, Oberstdorf, Oytal, Schochen, alpine meadow; 47.392°N, 10.37°E; ca 1930 m a.s.l.; 6 Aug. 2014; BC-ZSM-HYM-24109-D01 (ZSM). • 1 ♀; same collection data as for preceding; 4 Sep. 2014; BC-ZSM-HYM-24073-F03 (ZSM). • 1 ♀; Bavaria, Allgäu, Oberstdorf, Schochen, south faced ridge; 47.394°N, 10.369°E; ca

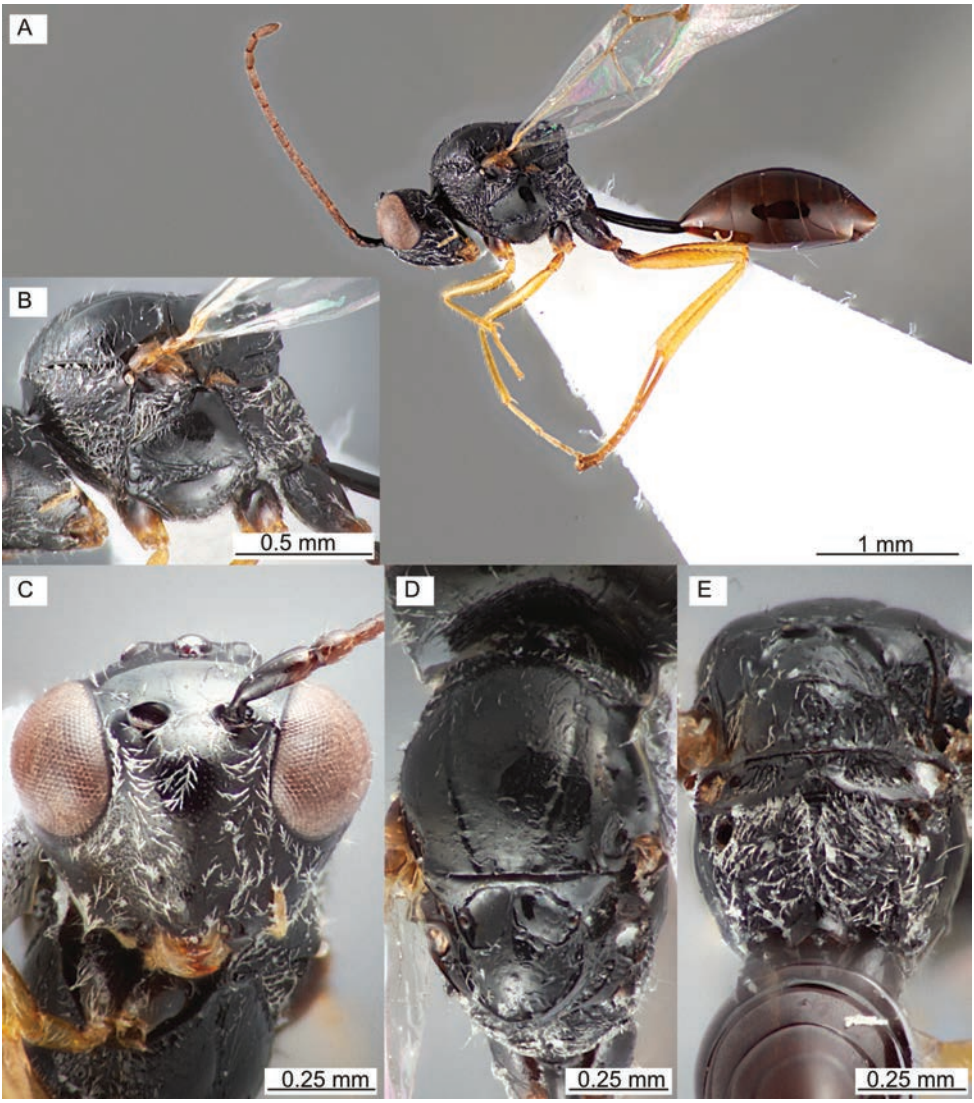

Figure 15. *Anacharis petiolata*, female (ZFMK-TIS-2629285) **A** habitus **B** mesosoma lateral **C** face **D** mesosoma dorsal **E** mesosoma posterior view.

2030 m a.s.l.; 6 Aug. 2014; BC-ZSM-HYM-24066-H09 (ZSM). • 1 ♀, 1 ♂; Bavaria, Garmisch-Partenkirchen, Zugspitze, mountain; 47.4062°N, 11.0095°E; ca 1970 m a.s.l.; 20 Jun.-5 Jul. 2018; Doczkal, D., Voith, J. leg.; Malaise trap; female - ZFMK-TIS-2637891; male - ZFMK-TIS-2637890. • 2 ♀♀, 1 ♂; Bavaria, Garmisch-Partenkirchen, Zugspitze, mountain; 47.4068°N, 11.008°E; ca 2010 m a.s.l.; 20 Jun.-5 Jul. 2018; Doczkal, D., Voith, J. leg.; Malaise trap; females - ZFMK-TIS-2628236, ZFMK-TIS-2629285; male - ZFMK-TIS-2628237. • 1 ♀; same collection data as for preceding; 2–13 Aug. 2018; ZFMK-TIS-2637893.

Greenland • 1 ♀, 2 ♂♂; SouthWest Greenland, Evighedsfjord, Kangiussaq; 65.8667°N, -52.2°E; ca 30 m a.s.l.; 19 Jul.-20 july 2003; Kissavik Exp., ZMUC leg.; female - zmuc00023359 (ZMUC); males - zmuc00023357 (ZMUC), zmuc00023358 (ZMUC).

Material without DNA barcode. Germany • 1 ♂; Bavaria, Garmisch-Partenkirchen, Zugspitze, mountain; 47.4053°N, 11.0091°E; ca 1980 m a.s.l.; 18 Jul.-2 Aug. 2018; Dieter Doczkal | Johannes Voith leg.; Malaise trap; ZFMK-HYM-00039678. • 4 ♀♀; Bavaria, Garmisch-Partenkirchen, Zugspitze, mountain; 47.4062°N, 11.0095°E; ca 1970 m a.s.l.; 20 Jun.-5 Jul. 2018; Dieter Doczkal | Johannes Voith leg.; Malaise trap; ZFMK-HYM-00039679, ZFMK-HYM-00039680, ZFMK-HYM-00039681, ZFMK-HYM-00039682. • 1 ♂; same collection data as for preceding 5–18 Jul. 2018; ZFMK-TIS-2642567. • 2 ♀♀; same collection data as for preceding 18 Jul.-2 Aug. 2018; ZFMK-TIS-2642535, ZFMK-TIS-2642547. • 1 ♂; Bavaria, Garmisch-Partenkirchen, Zugspitze, mountain; 47.4068°N, 11.008°E; ca 2010 m a.s.l.; 5–18 Jul. 2018; Dieter Doczkal | Johannes Voith leg.; Malaise trap; ZFMK-TIS-2642544. • 2 ♂♂; Bavaria, Garmisch-Partenkirchen, Zugspitze, Platt, mountain; 47.4053°N, 11.0091°E; ca 1980 m a.s.l.; 5–18 Jul. 2018; Dieter Doczkal | Johannes Voith leg.; Malaise trap; ZFMK-TIS-2640706, ZFMK-TIS-2640707. • 1 ♂; same collection data as for preceding 18 Jul.-2 Aug. 2018; ZFMK-HYM-00039678.

Greenland • 1 ♀; Narssarssuaq; 61.1°N, -45.25°E; ca 0 m a.s.l.; 5 Jul. 1983; Peter Nielsen leg.; NHMD918327 (ZMUC). • 2 ♂♂; same collection data as for preceding 1 Aug. 1983; NHMD918299 (ZMUC), NHMD918313 (ZMUC). • 1 ♀; same collection data as for preceding 13 Aug. 1983; NHMD918341 (ZMUC). • 1 ♀3 ♂♂; SouthWest Greenland, Evighedsfjord, Kangiussaq; 65.8667°N, -52.2°E; ca 30 m a.s.l.; 19–20 Jul. 2003; Kissavik Exp., ZMUC leg.; female - zmuc00023359 (ZMUC); males - NHMD918215 (ZMUC), zmuc00023357 (ZMUC), zmuc00023358 (ZMUC). • 1 ♂; same collection data as for preceding 24–25 Jul. 2003; NHMD918229 (ZMUC). • 1 ♀; SouthWest Greenland, Itivleq, eastern end; 66.55°N, -52.4333°E; ca 0 m a.s.l.; 22–23 Jul. 2003; Kissavik Exp., ZMUC leg.; NHMD918285 (ZMUC). • 1 ♀; SouthWest Greenland, Kangerdluarssuk east; 66.9833°N, -53.2°E; ca 20 m a.s.l.; 24–25 Jul. 2003; Kissavik Exp., ZMUC leg.; NHMD918271 (ZMUC). • 1 ♀, 1 ♂; West Greenland, Qarássap munatâ; 70.75°N, -53.62°E; ca 710 m a.s.l.; 18–19 Jul. 1969; Jens Böcher leg.; female - NHMD918243 (ZMUC); male - NHMD918257 (ZMUC).

Switzerland • 1 ♀; Neuchâtel, Auvernier; 16 Aug. 1956; Jacques de Beaumont leg.; specimen at MHNG. • 2 ♂♂; same collection data as for preceding 26 Aug. 1956; specimens at MHNG. • 1 ♂; Vaud, Ferreyres; 22 Aug. 1952; Jacques de Beaumont

Figure 16. Lectotype of *A. typica* (**A-C**) and holotype of *A. gracilipes* (**D, E**) **A** labels, frontal **B** lectotype ventral **C** lectotype dorsal **D** holotype dorsal **E** holotype labels frontal, above and the back, below.

leg.; specimen at MHNG. • 1 ♂; Vaud, La Sauge; 10 Aug. 1959; Jacques de Beaumont leg.; specimen at MHNG. • 2 ♂♂; same collection data as for preceding 29 Aug. 1956; specimens at MHNG. • 1 ♀; Vaud, Lioson Sep. 1956; Jacques de Beaumont leg.; specimen at MHNG. • 1 ♀; Vaud, Marchairuz; 21 Jul. 1960; Jacques de Beaumont leg.; specimen at MHNG. • 1 ♀; Vaud, Sta Catharina; 17 Sep. 1955; Jacques de Beaumont leg.; specimen at MHNG.

Biology. Summer species, flying from July to September, peak in July. Seems confined to alpine, arctic or boreal habitats.

Distribution. Finland (locus typicus of *A. petiolata*: Lapland, Muonio, likely on Finnish side of Muonio River, see remarks), Germany (Alps), Greenland, Romania (locus typicus of *A. gracilipes*: Rarău massif (Eastern Romanian Carpathians) at "1,950 m" altitude according to Ionescu (1969) [highest peak according to Wikipedia is at 1651 m]), Switzerland.

DNA barcode matches with publicly available sequences from Canada (e.g. ABINP3207-21) and Norway (e.g. GWNWG2160-14).

In Central Europe restricted to elevations above 1900 m a.s.l. but occurring at lower altitudes in arctic and subarctic, boreal landscapes.

Remarks. *A. petiolata* (Zetterstedt, 1838, often erroneously cited as Zetterstedt, 1840) was synonymised with *A. euchariodes* by Fergusson (1986) and was erroneously listed as synonym of *A. immunis* in Mata-Casanova et al. (2018). The type locality of *A. petiolata* is Muonio, Lapland (in the description: "Pinetis Lapponiae ad Muonioniska" (Zetterstedt 1838)). Muonio is a municipality in present-day Finland (belonging to Russia at the time of Zetterstedt's visit), where Zetterstedt visited local entomologist Kolström during his 1821 Lapland journey. The Muoniojoki river, which flows indirectly downstream into the Torne river, marks the border between Finland and Sweden near the municipality of Muonio and it is unclear whether Zetterstedt crossed it to collect insects from both sides of the river, though he mentions how scary it is to cross the river, making it unlikely that he frequently did so (Zetterstedt 1822). In conclusion, whether the lectotype was collected in modern day Finland or Sweden is probably impossible to tell and the question itself of minor significance.

There are no descriptive labels on the lectotype. Fergusson (1986) stated that the lectotype was held at NHRS, but it is actually deposited at the MZLU. The sex of the lectotype is difficult to discern, due to the missing antennae and only images available to us. We consider it a male, as the original label shows, though that is in contrast to what Fergusson (1986) wrote. Apparently, the specimen was already in a poor condition when Fergusson studied it and he could not reliably identify the sex either.

On the primary type of *A. gracilipes*: Mata-Casanova et al. (2018) cites a lectotype of *A. gracilipes* as primary type. However, Ionescu specifically mentions a holotype in his publication, though without giving unambiguous details about the actual specimen (Ionescu 1969). The ICZN states in 73.1.2., that "If the taxon was established before 2000 evidence derived from outside the work itself may be taken into account [Art. 72.4.1.1] to help identify the specimen." The loaned specimen from MGAB with the Museum ID "GAL 340/9" bears the word "holotip" on its label, along with informa-

tion on locality and time that match the description of the type series. The specimen thereby constitutes the holotype.

The holotype was kept in a vial with ethanol, already damaged, lacking head and wings, legs incomplete. We mounted the specimen on a white pointed card with Shellac Gel glue on the right side of its mesosoma after asking permission from MGAB. All coxae are present, fore trochanters and femora present, trochanter and femora of right hind leg mounted separately along with a tibia. The specimen was about 2.8 mm in body length (measurements on holotype combined with proportions from photograph in Ionescu, 1969) and that falls into the average body size of most *Anacharis* species.

A. petiolata is morphologically very similar to *A. typica*. The morphological differences are rather subtle differences in colouration and morphological diagnoses for both species are rather weak. Still, we differentiate between the two species based on the distinct difference in CO1 barcode sequences as well as a difference in habitat type/distribution. All known specimens of *A. petiolata* were collected in alpine or boreal environments, specimens of *A. typica* were collected in temperate environments below 700 meters above sea level.

***Anacharis typica* Walker, 1835, stat. rev.**

Figs 2D, 3D, 17A–E

Anacharis typicus Walker, 1835:520 - lectotype (NHMUK) ♀, photographs examined (Fig. 16A–C).

Diagnosis (n = 10). Belongs to the *euchariodes species group*. Medium sized species (2.9–3.5, mean 3.2 mm, similar to *A. euchariodes*, *A. martinae* and *A. petiolata*). Differing from *A. euchariodes* and *A. martinae* by having a centrally smooth mesoscutellum (Fig. 17D, E, centrally carinate in *A. euchariodes* and *A. martinae*) and a smooth lateromedial area of the pronotum (Fig. 17B, rugose to obliquely carinate in *A. euchariodes* and *A. martinae*). Differs from *A. petiolata* mainly by having the hind coxa often distinctly bicoloured, with noticable paling apically (Fig. 17A, hind coxa less distinctly bicoloured, though weak paling is notable apically in *A. petiolata*). The hind trochanter in *A. typica* has a similar pattern of paling as hind coxa or is as pale as in hind femur (hind trochanter similarly dark as the hind coxa in *A. petiolata*). Additional to morphological differences, *A. typica* is exclusively collected in temperate environments below 700 meters above sea level (whilst *A. petiolata* is collected from boreal environments above 1,000 meters above sea level).

CO1 barcode. n=10. Maximum intraspecific distance: 0.5%. Minimum distance to closest species (*A. euchariodes*): 5.7%. CO1 barcode consensus sequence:

AATTTTATACTTTATTTTAGGAATTTGATCAGGAATAATAGGATCAAGATTAAGAATAATTATTCGAATAGAATTAGGGACCCCCTCTCAATTAATTATAAATGATCAAATTTATAACTCAATTGTAACTGCTCATGCATTTATTATAATTTTCTTTATAGTCATACCTATTATAGTAGGAGGATTCGGAAATTATTTAGTGCCTTTAATATTAATCTCTCCTGATATAGCTTTCC-

CCCGATTAAATAATTTAAGATTTTGATTTTTAATCCCCTCTTTATTTT-
TAATAACAATTAATTTATTTATTGACCAAGGAGCAGGAACAGGGTGAACT-
GTATACCCCCCATTATCATCACTCACAGGTCATCCATCTATATCGGTA-
GATTTAGTTATTTATTCATTACATTTAAGTGGAATTTCCTCAATTCTTG-
GTTCTATTAATTTTATTGTAACCATTTTAAATATACGAATAACTGTTA-
TATCTATAGACAAAATTTCATTATTTATTTGATCTATTTTTTTTAACTA-
CAATTTTATTATTATTATCTTTACCAGTACTAGCAGGAGGTTTAACTAT-
ATTACTATTTGATCGAAATTTAAATACATCTTTTTTTTGACCCTACAGGAG-
GAGGGGATCCAATCCTTTATCAACACTTATTT

Type material.

Lectotype of *Anacharis typicus* Walker, 1835

81 61 [on backside of mounting board]

2.

Type

In Coll under typical

B.M.1981 . Under typica

LECTOTYPE

LECTOTYPE Anacharis typica Walker det. N.D.M.Fergusson, 1981

B.M. TYPE HYM 7. 163

[QR code] NHMUK 012858913

[for images, see Fig. 16A–C and https://data.nhm.ac.uk/dataset/56e711e6-c847-4f99-915a-6894bb5c5dea/resource/05ff2255-c38a-40c9-b657-4ccb55ab2feb/record/10470199]

Other material examined. DNA barcode vouchers. Austria • 1 ♂; Styria, NP Gesäuse, Gsengquelle; 47.5683°N, 14.5902°E; ca 680 m a.s.l.; 2 Sep. 2015; Haseke leg.; ZFMK-TIS-2640691.

Belgium • 1 ♀; West Flanders, Beernem, Centrum; 51.1259°N, 3.3202°E; ca 10 m a.s.l.; 8 May 2022; De Ketelaere, Augustijn leg.; hand picked; ZFMK-TIS-2640858. • 1 ♀; West Flanders, Beernem, Gevaerts; 51.1411°N, 3.3215°E; ca 10 m a.s.l.; 24 Apr. 2022; De Ketelaere, Augustijn leg.; hand picked; ZFMK-TIS-2640857.

Germany • 1 ♀; Hesse, Waldeck-Frankenberg, National park Kellerwald-Edersee, Maierwiesen; 51.1555°N, 9.0015°E; ca 370 m a.s.l.; 22 Jun.-8 Jul. 2021; GBOL III leg.; Malaise trap (Krefeld version); ZFMK-TIS-2640806. • 3 ♂♂; Hesse, Waldeck-Frankenberg, NP Kellerwald-Edersee, „Banfe-Haus“; 51.167°N, 8.9749°E; ca 270 m a.s.l.; 7–21 Jul. 2022; GBOL III leg.; Malaise trap; ZFMK-TIS-2640757, ZFMK-TIS-2640758, ZFMK-TIS-2640760. • 1 ♀; Mecklenburg-Vorpommern, Vorpommern-Rügen, Großer Vilm, Biosphärenreservat; 54.325°N, 13.539°E; ca 30 m a.s.l.; 24 May-3 Jun. 2016; Rulik, Björn et al. leg.; Malaise trap; ZFMK-TIS-2629503. • 1 ♀; North Rhine-Westphalia, Rhein-Sieg-Kreis, Schladern near Windeck, Sieg river, right river bank; 50.8°N, 7.585°E; ca 130 m a.s.l.; 4–11 Jul. 2017; ZFMK et al. leg.; Malaise trap; ZFMK-TIS-2629276.

Lithuania • 1 ♀; Silute distr., Sysa, Sysa, control plot; 55.3127°N, 21.4049°E; ca 0 m a.s.l.; 14–25 Jun. 2020; Petrasiunas, Andrius leg.; Malaise trap; ZFMK-TIS-2637717.

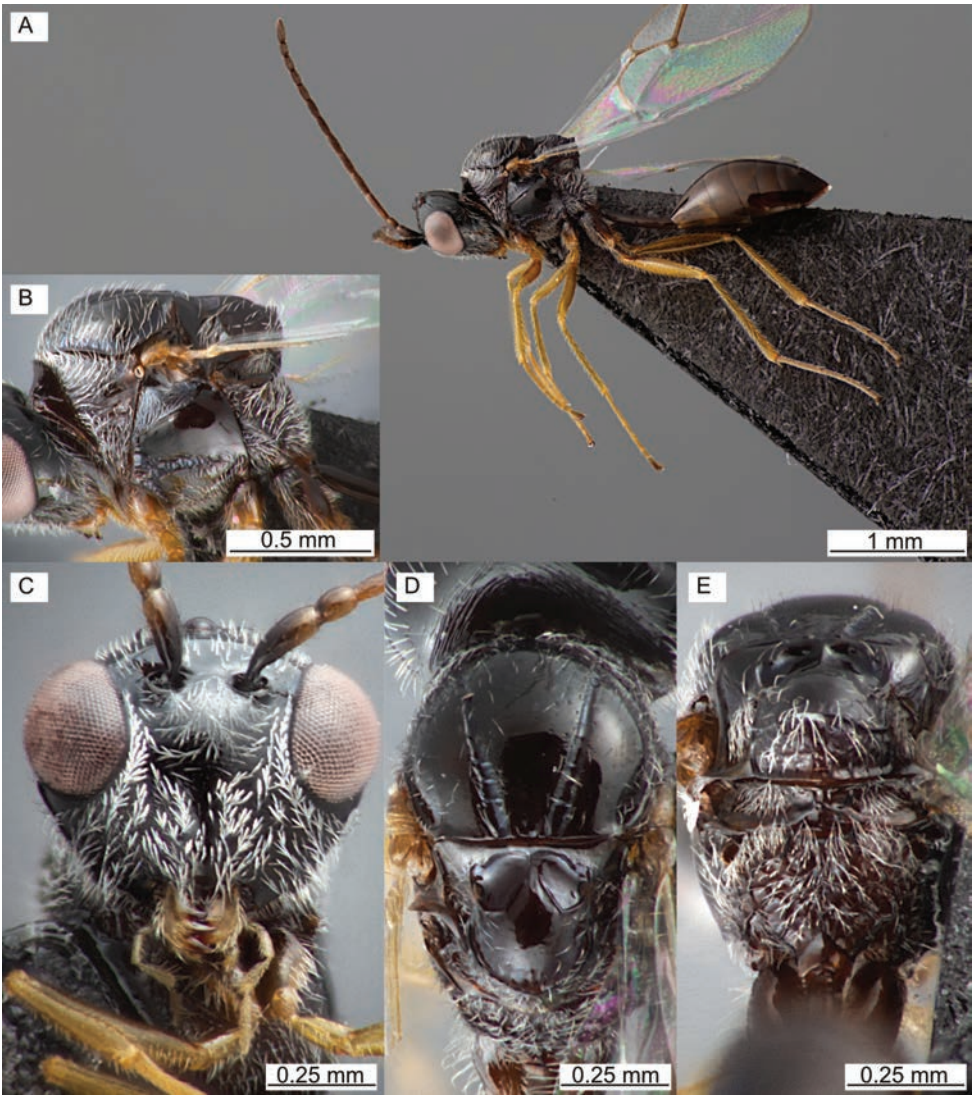

Figure 17. *Anacharis typica*, female (ZFMK-TIS-2640806) **A** habitus **B** mesosoma lateral **C** face **D** mesosoma dorsal **E** mesosoma posterior view.

Material without DNA barcode. Belgium • 2 ♂♂; Walloon Brabant, Ottignies; 9–16 Jul. 1983; Paul Dessart leg.; Malaise trap; JV_Prel_0074 (RBINS), JV_Prel_0045 (RBINS). • 2 ♂♂; same collection data as for preceding 28 May-4 Jun. 1983; JV_Prel_0075 (RBINS), JV_Prel_0076 (RBINS). • 1 ♂; West Flanders, Harelbeke, Gavers, Wetland with pools; 50.8379°N, 3.3215°E; ca 10 m a.s.l.; 11 Jun. 2022; Bart Lemey leg.; hand caught; JV_Prel_0052 (RBINS).

Germany • 1 ♂; Hesse, Werra-Meißner-Kreis, Großalmerode, Private garden, Siedlerweg, semi-abandoned garden with wet spot, ivy hedge and salix; 51.2591°N, 9.7871°E; ca 380 m a.s.l.; 12–20 Jul. 2022; Jonathan Vogel leg.; Malaise trap; ZFMK-

TIS-2640704. • 1 ♂; North Rhine-Westphalia, Rhein-Sieg-Kreis, Schladern near Windeck, Sieg river, right river bank; 50.8°N, 7.585°E; ca 130 m a.s.l.; 18–25 Jul. 2017; ZFMK et al. leg.; Malaise trap; ZFMK-HYM-00039677. • 2 ♂♂; same collection data as for preceding 1–8 Aug. 2017; ZFMK-HYM-00039674, ZFMK-HYM-00039675.

Italy • 1 ♂; Val d'Aoste, Boertolaz, (Villeneuve); ca 800 m a.s.l.; 15 Sep. 1978; L. Martile leg.; Malaise trap; NHRS-HEVA 000023180 (NHRS).

Sweden • 1 ♂; Gotland, Eksta sn, Stora Karlsö, calcarous low herb pasture; 57.2873°N, 17.9775°E; ca 40 m a.s.l.; 26–29 Aug. 2014; Hymenoptera Inventory 2014 leg.; Malaise trap; MT Loc#2; NHRS-HEVA 000023181 (NHRS). • 1 ♂; Gotska sandön, Kapellängen; 7 Jul. 1964; Bror Hanson leg.; NHRS-HEVA 000023182 (NHRS). • 1 ♂; Öland, Glömminge, Gillsättra; 4 Aug. 2004; Mattias Forshage leg.; specimen in coll MF. • 1 ♀; Öland, Kastlösa; 26 Jun. 1962; Karl-Johan Hedqvist leg.; NHRS-HEVA 000023198 (NHRS). • 1 ♂; Öland, Kastlösa; 28 Jun. 1962; Tor-Erik Leiler leg.; NHRS-HEVA 000023197 (NHRS). • 2 ♂♂; Scania, Kristianstads kommun, Trunelän, Degeberga, Grazed meadow at alder stand along stream; 55.7746°N, 14.2156°E; ca 80 m a.s.l.; 1–13 Aug. 2019; Swedish Insect Inventory Programme (SIIP), Station Linné leg.; Malaise trap; NHRS-HEVA 000023184 (NHRS), NHRS-HEVA 000023185 (NHRS). • 1 ♂; Scania, Lomma; 10 Jul. 1963; Hans von Rosen leg.; NHRS-HEVA 000023188 (NHRS). • 1 ♂; same collection data as for preceding 13 Aug. 1963; NHRS-HEVA 000023189 (NHRS). • 2 ♀♀; same collection data as for preceding 14 Aug. 1963; NHRS-HEVA 000023186 (NHRS), NHRS-HEVA 000023187 (NHRS). • 1 ♂; Scania, Saxtorp; 5 Jun. 1961; Karl-Johan Hedqvist leg.; NHRS-HEVA 000023183 (NHRS). • 1 ♂; Scania, Stenshuvuds NP, lush mixed oak forest; 55.6603°N, 14.2755°E; ca 30 m a.s.l.; 22 Sep.-1 Nov. 2004; Swedish Malaise Trap Project (Swedish Museum of Natural History) leg.; Malaise trap; NHRS-HEVA 000023190 (NHRS). • 1 ♀, 1 ♂; Småland; [18xx]; Carl Henning Boheman leg.; female - NHRS-HEVA 000023191 (NHRS); male - NHRS-HEVA 000023192 (NHRS). • 1 ♂; Södermanland, Tockenön Jul. 1950; Anton Jansson leg.; NHRS-HEVA 000023193 (NHRS). • 1 ♂; Uppland, Vallentuna; 7 Jun. 1959; Karl-Johan Hedqvist leg.; NHRS-HEVA 000023195 (NHRS). • 1 ♀; same collection data as for preceding 15 Sep. 1962; NHRS-HEVA 000023194 (NHRS). • 1 ♂; Västmanland, Köping; 18 May 1975; Walter Siering leg.; NHRS-HEVA 000023196 (NHRS).

Switzerland • 1 ♀; Grisons, Pontresina; unknown leg.; specimen at NMBE.

Biology. Summer species, flying mainly from April to September, peak in July. No clear preferences in terms of habitat.

Distribution. Austria, Belgium, Germany, Italy, Lithuania, Sweden, Switzerland, United Kingdom (locus typicus of *A. typica*: southern England, near London or Isle of Wight).

Found in elevations up to 400 m a.s.l., rarely up to 800 m a.s.l.

Remarks. The specimen labelled as lectotype is clearly a female, not a male as stated by Fergusson (1986). Despite this incongruence we acknowledge the specimen labelled as lectotype by Fergusson as such.

The lectotype is glued to its ventral side on cardboard, face down, wings also glued to the board. It is overall intact, though the 13th antennal segment is either broken in half and the fragment is lost, or the segment is malformed. The tarsomeres of the right

fore leg are missing from second tarsomere onwards. Both wings and legs obscure the lateral mesosoma on both sides.

With 2.6 mm body length, the lectotype is a comparably small specimen of this species (average body length 3.2 mm). Additionally, the lectotype is unusual by its overall reddish colouration, which may have been caused by ageing. Otherwise, it is morphologically well-fitting with the specimens we examined.

For a comparison of the similar *A. typica* and *A. petiolata*, see the remarks section of *A. petiolata*.

One specimen from Belgium (JV_Prel_0076) was similarly coloured as the Bavarian specimens (BC-ZSM-HYM-27596-F10 & BC-ZSM-HYM-27596-F09, see variation section in description of *A. martinae*) of *A. martinae*, having the head distinctly darker than the otherwise pale body.

In the distribution section we only list those records that we can verify by having seen actual specimens. Additional distribution records can be inferred from sequences from BOLD, if they match with our species cluster of *A. typica*. They were obtained from specimens originating from Canada (e.g. SMTPI9646-14). The identities of these sequences as *A. typica* need to be confirmed by examination of the physical specimens before reliably citing *A. typica* for Canada.

Key to the Northwestern European species of *Anacharis* (females and males)

The characters used in this key are, in part, based on the comparison of a small number of specimens (most notably *A. minima*, *A. petiolata* and *A. typica*). Note especially our concern that the colouration of specimens may be sensitive to the method of killing and the state of the specimen's preservation. Due to the high degree of inter- and intraspecific variability, we stress that the most reliable way to identify the species of *Anacharis* is via comparison of DNA barcode data.

1 Occiput smooth (Fig. 18A); notauli weak, fading in anterior region, inside not carinate (Fig. 11D); placodeal sensilla in females starting at fourth flagellomere; inner side of hind coxa with equally distributed pubescence on entire length; petiole relatively short (Fig. 11A) (*immunis* species group) **2**

– Occiput with at least some noticeable transversal striolation to striation laterally to medially (Fig. 18B); notauli usually strong, not fading in anterior region and often inside carinate (Fig. 10D); placodeal sensillae in females starting at first flagellomere; inner side of the hind coxa with no continuous pubescence along its entire length; petiole relatively long (Fig. 10A) (*euchari-oides* species group) **4**

2 Dorsal surface of mesoscutellum largely smooth and even, especially centrally (Fig. 11D). Fore and mid coxa often noticeably darker than rest of legs and generally appearing darker (difficult to see in old/paled specimens, Fig. 11A) ..... ***A. immunis* Walker, 1835**

– Dorsal surface of mesoscutellum with an uneven to reticulate-foveate sculpture centrally (Fig. 9D). Fore and mid coxa usually as pale as rest of legs and

generally appearing paler (difficult to see in old/paled specimens, Fig. 9A). **3**

3 Dorsal and posterior surface of mesoscutellum heavily foveate, usually with small foveae that continue on posterior surface of mesoscutellum (Fig. 4E in Mata-Casanova et al. 2018). Circumscutellar carina not distinctly flanged upwards, apically not appearing like a tooth in lateral view (Fig. 4E in Mata-Casanova et al. 2018). Mesopleural sculpture rugose, diffusing the mesopleural line dorsally in its anterior half. Strong wrinkles on mesoscutum, especially in anteromedian area, making the anteroadmedian signa distinct (Fig. 4D in Mata-Casanova et al. 2018) ..... ***A. norvegica*** **Mata-Casanova & Pujade-Villar, 2018**

– Dorsal surface of mesoscutellum reticulate-foveate (Fig. 9D), never with small foveae that continue on the posterior surface of mesoscutellum. Circumscutellar carina usually distinctly flanged upwards, apically appearing like a tooth in lateral view (Fig. 9B). Mesopleural sculpture smooth to rugose, not diffusing the mesopleural line in most of its anterior half (Fig. 9B). Less to no wrinkles on mesoscutum and thereby less distinct anteroadmedian signa (Fig. 9D)..... ***A. ensifer*** **Walker, 1835, stat. rev.**

4 Dorsal surface of mesoscutellum centrally with sculpture (Fig. 10D). Lateromedial area of pronotum variable (Fig. 12B). Nuchal collar variable **5**

– Dorsal surface of mesoscutellum largely smooth and even (Fig. 17D). Lateromedial area of pronotum smooth (Fig. 14B). Nuchal collar dorsally broadly projecting into a point (Fig. 6D–F) **7**

5 Dorsal surface of mesoscutellum with well-defined reticulate carinae in the anterior half between the mesoscutellar foveae, in other areas largely smooth or variable (Fig. 13D); large species, 3.5 mm or larger ..... ***A. maxima*** **Vogel, Forshage & Peters, sp. nov.**

– Sculpture of mesoscutellum different; medium sized species, 2.6–3.4 mm body size **6**

6 Lateromedial area of pronotum smooth to rugose (Fig. 10B); mesoscutum centrally more sparsely pubescent than in other areas of the mesoscutum; space between toruli often without striolation; mesoscutellar sculpture usually with median carina centrally interrupted, lateral carinae dissolved into general reticulation (Fig. 10D); nuchal collar usually broadly forming a dorsal tooth (Fig. 6D–F); metasoma usually black..... ***A. eucharioides*** **Dalman, 1818**

– Lateromedial area of pronotum sculptured with parallel longitudinal carinae like ventrally (Fig. 12B); mesoscutum more evenly pubescent; space between toruli often with transversal striolation; mesoscutellar sculpture often with median carina reaching posterior margin and two lateral carinae or low crests that delineate a longitudinal median field (Fig. 12D); nuchal collar usually forming a narrow dorsal tooth (Fig. 6C); metasoma brown to dark-brown ... ***A. martinae*** **Vogel, Forshage & Peters, sp. nov.**

7 Small sized species, around 2.4 mm body size; carination of notauli absent; with narrow coriaceous texture of the malar space that extends only around the dorsal corner of the mandibular base (Fig. 19A); mesopleural line usually reaching posteroventral hypocoxal furrow (Fig. 14B). Rare species..... .....***A. minima*** **Vogel, Forshage & Peters, sp. nov.**

– Medium sized species, around 3 mm body size; carination of notauli variable; band of coriaceous texture of malar space extending along entire length of mandibular base (Fig. 19B); mesopleural line usually not reaching posteroventral hypocoxal furrow (Fig. 15B).....**8**

8 Collected in boreal environments or above 1,000 meters above sea level; hind coxa less distinctly bicoloured, though weak paling is notable apically, hind trochanter usually as dark as hind coxa (Fig. 15A)..... .....***A. petiolata*** **Zetterstedt, 1838, stat. rev.**

– Collected in nemoral environments, below 700 meters above sea level; hind coxa often distinctly bicoloured, with noticable paling apically, hind trochanter in has a similar pattern of paling as hind coxa or is as pale as in hind femur (Fig. 17A).....***A. typica*** **Walker, 1835, stat. rev.**

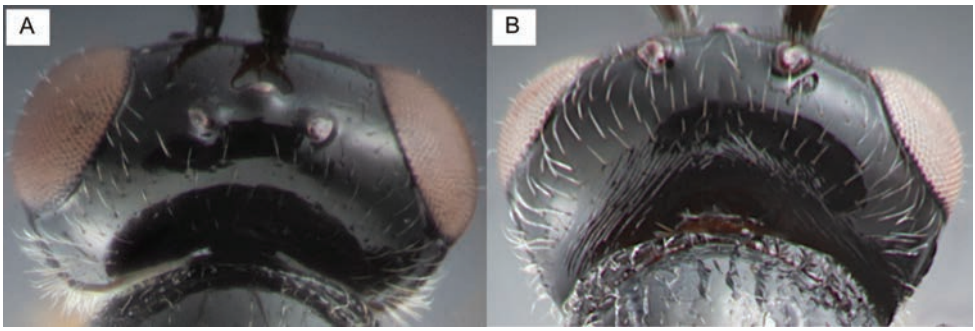

Figure 18. (postero-)dorsal view of the head **A** occiput smooth (*A. immunis*, ♀, ZFMK-TIS-2640709) **B** occiput striate (*A. martinae* sp.nov., holotype (ZFMK-TIS-2640787), ♀).

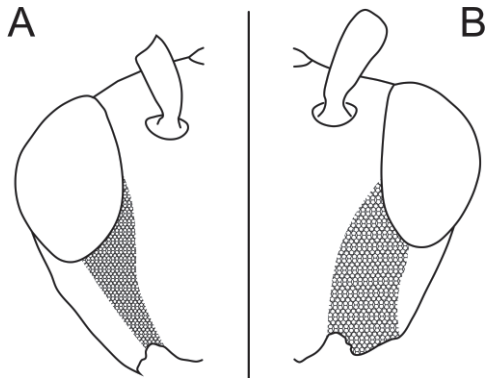

Figure 19. Frontal view of head, showing the extent of the coriaceous texture of the malar area in **A** *A. minima* sp.nov. **B** *A. maxima* sp.nov.

Discussion

By integrating analyses of CO1 barcode data, morphological examination, multivariate morphometrics, WIPs and male genitalia dissections, we were able to detect and delimit nine species of *Anacharis* in Northwestern Europe, belonging to two species groups. The presence of more than two species is in line with the findings of Mata-Casanova et al. (2018) and in contrast to the broad species circumscriptions for *A. eucharioides* and *A. immunis* of Fergusson (1986).

Delimiting species based on morphology proved comparatively difficult due to overall similarity of the species, and strong intraspecific variation. We acknowledge that previous studies which did not include analyses of molecular sequence data, and thereby not having a chance of being informed by a reverse taxonomy approach, were not able to fully delimit the Northwestern European species. Specifically, we found the following previously used characters to vary considerably intraspecifically: The setosity of the eyes, the parascutal sulcus, the depth and carination of the notauli, the mesoscutellar sculpture, the propodeal sculpture, and the petiole length:hind coxa length ratio. We briefly discuss the states of each of these characters as well as their diagnostic value.

Regarding the setosity of the eyes, all species treated in Mata-Casanova et al. (2018) were described as having glabrous eyes. In contrast to that, we found all species to have setose eyes, the setae being either merely stubs, or considerably long (e.g. Fig. 4E, F). It is likely that they fall off during preservation and preparation or are overlooked. Especially with a light background, they are very difficult to see.

Regarding the parascutal sulcus, it was used in couplet three of the key, in the (re-) descriptions of the species, but not in the diagnoses in Mata-Casanova et al. (2018). We found it varying in both presence and extent in all of the species within the *eucharioides* species group (except *A. minima* where n=1). It is sometimes clearly present, with anterior transversal carination, and sometimes it lacks this carination and varies in extent, either reaching the notauli or only being impressed in the posterior half. We did not observe a clear allometric effect. As a result, we conclude that this character is not suitable as a diagnostic character.

The notauli can be shallow and weak with no carination inside, as well as distinct and deep, with strong carination in the same species. The expression of the notauli may serve to exemplarily describe intraspecific variability of characters that we observed in *Anacharis*: Most specimens share what can be called a "typical pattern" but others contribute to the strong variation, either being more or less pronounced in the expression of the character. This makes it seemingly easy when studying a limited number of specimens but adds to an increasingly blurry piucture when studying a large number of specimens before being finally able to correctly evaluate and describe a character. Again, note that this would have been tremendously difficult if not impossible without the reciprocal information from analyses of sequence data.

Regarding the mesoscutellar sculpture – on both dorsal and posterior face – we see a pattern similar to what we described above for the notauli. However, when generally smooth and even (as in *A. typica*, *A. petiolata*, *A. immunis* and *A. minima*) or when

distinctly carinate (as in *A. ensifer*, *A. eucharioides*, *A. martinae*, *A. maxima* and *A. norvegica*), mesoscutellar sculpture can be of diagnostic value.

The propodeal sculpture is intraspecifically variable, especially in the median part of the propodeum. From our examination, it cannot be used diagnostically between species.

Especially if qualitative characters are difficult to find, multivariate morphometric analyses can be executed. Our results, however, show that – generally – morphometric characters in *Anacharis* are of very limited use (Figs 7, 8). Exceptions are the differentiation between species groups and the partial or full delimitation of *A. martinae* (Fig. 8B) and *A. maxima* (Fig. 8C) which showcase the power of multivariate statistics in delimiting taxonomically challenging species.

The analyses of molecular sequence data, implementing more than one automated species delimitation method as should be common practice (Meier et al. 2022), gave results widely congruent between methods and also congruent with morphological examinations, including morphometric analyses. When using only DNA barcode data, interspecific haplotype-sharing goes undetected. Accordingly, taxonomic acts should be taken integrating various traits into forming species hypotheses. Ideally, mitochondrial DNA barcode sequence data will be complemented by nuclear markers (e.g. Dietz et al. 2022), especially if diagnoses are weak or results from DNA barcodes and morphology are incongruent.

In addition to molecular sequence data, morphology and morphometrics, we further explored the use of WIPs in the alpha taxonomy of Figitidae. We found it to be useful for species group diagnostics and potentially also for separating species, as shown for the newly described species *A. martinae* and *A. maxima*. With an optimised protocol, the WIPs on areas like the radial and median areas of fore and hind wing could potentially emerge better and be further evaluated for their use in species delimitation. However, to do that reliably, larger series of better-quality images are required for each species. Once established, ideally on species level, WIPs might also be used for automated species recognition. This has great potential, especially when applying a trained AI to recognise the species (Cannet et al. 2022, 2023; Jin et al. 2023).

From our first steps in evaluating male genitalia for their specific diagnostic power in Figitidae, we report some interspecific differences, most notably between the *eucharioides* and *immunis* species groups. On the species level, we could find differences in male genitalia morphology in the cases of *A. eucharioides* and *A. maxima* only. The differences are however subtle and nowhere close to the diversity of male genitalia morphology of the Ceraphronoidea (Salden & Peters, 2023). Like in other groups of microhymenoptera, the dissection of the male genitalia is difficult and yet we would argue that consulting male genitalia generally is a strategy worth investigating in parasitoid wasp taxonomy when there is a shortage of diagnostic characters.

Hemerobiiform Neuroptera are comparably poor in natural enemies (Aspöck et al. 1980). Several taxa which are parasitoids of defensible hosts share similar adaptations, which are often striking in these neuropteran parasitoids, including a short compact mesosoma, a strongly petiolate metasoma and comparably long and slender legs. This facilitates quick movements in general and specifically those associated with "quick-strike" oviposition maintaining a distance to the host to avoid being injured by

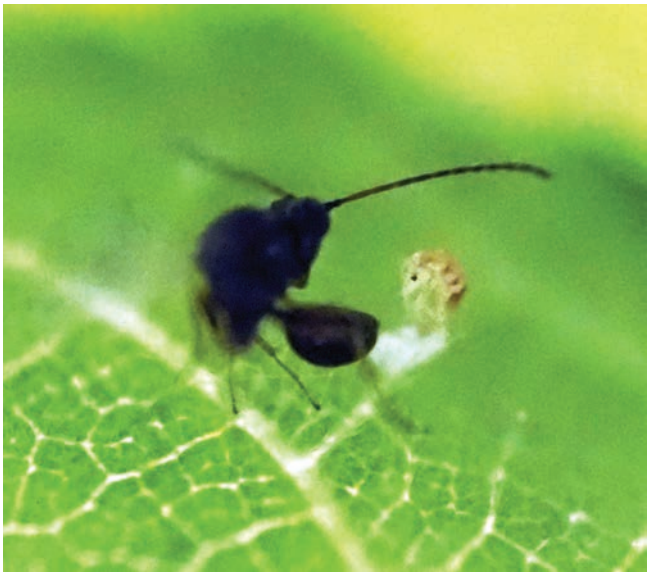

Figure 20. *Anacharis* sp. in action. A female *Anacharis* sp. attacking a hemerobiid early instar larva by bending its metasoma through the legs in the style of aphidiine braconids (photo by Kim Neubauer).

it (Buffington et al. 2007). Among these taxa are the A-wasps (Heloridae, larval-cocoon parasitoids of Chrysopidae), braconids in the genus *Chrysopophthorus* (adult parasitoids of Chrysopidae), Brachycyrtinae (Ichneumonidae, (pre-)pupal parasitoids of Chrysopidae) and the Anacharitinae. The Anacharitinae are the only group within the Cynipoidea that show these adaptations and are the only ones which are associated with obviously defensible hosts. Field observations in the US (Arizona) on *Anacharis* specimens of unknown species show a characteristic positioning of the metasoma for oviposition that resembles that of aphidiine braconids (aphid parasitoids). The metasoma is bent downwards through the prancing legs, pointing forward in the direction of the host (Fig. 20). In this instance, the wasp was striking about five times over the course of one full minute, taking less than three seconds per strike (Kim Neubauer, pers. comm.).

Among the Anacharitinae in Northwestern Europe, *Anacharis* is the most commonly occurring genus. Yet, the taxonomic turmoil (Fergusson 1986; Mata-Casanova et al. 2018 and this study) has blurred the knowledge about life history of each species significantly, i.e. it is impossible to assign the few existing host records beyond species group level. As parasitoids of brown lacewing larvae, they play an arguably important role as natural regulators of these common aphidivorous insects that are also of economic importance (Stelzl and Devetak 1999). In order to understand the trophic interactions of aphids, their predators and parasitoids, knowledge about host-parasitoid relationships is fundamental, which in turn requires taxonomically stable taxa and unambiguously vouchered host records.

The DNA barcode dataset we provide is currently the most comprehensive dataset of *Anacharis* sequences worldwide and enabled us to connect European barcode data

of *A. eucharioides*, *A. petiolata* and *A. typica* with that of Nearctic (mainly Canadian) records that are publicly available on BOLD. As the available data grows, along with continued revisionary work, the barcode datasets will become increasingly useful to accelerate the accumulation of life history and distribution knowledge about the species treated herein as well as of currently unknown species in Europe and worldwide.

Acknowledgements

The Federal Ministry of Education and Research of Germany (Bundesministerium für Bildung und Forschung, BMBF) is funding the project "GBOL III: Dark Taxa" as Research for Sustainable Development (Forschung für Nachhaltige Entwicklung, FONA; www.fona.de) under the funding reference 16LI1901A.

We sincerely appreciate the invaluable input from the reviews of Louis Nastasi and Simon van Noort that led to the final version of this manuscript.

We want to express our gratitude to Ximo Mengual, Tobias Salden and Santiago Jaume Schinkel for practical advice regarding the preparation of the male genitalia. Ximo Mengual proved most helpful for introducing and troubleshooting the camera setup. Juliane Vehof gave a comprehensive introduction into and was available for constant troubleshooting with the Zeiss imaging setup.

For the procession of the data into the GBOL and BOLD databases, we are indebted to the GBOL core team at the ZFMK and want to specifically thank Jana Thormann.

We thank the administrative body and the research department of the Kellerwald Edersee National Park, in particular Carsten Morkel, for allowing the sampling with ten Malaise traps over a long period that yielded many interesting specimens.

We are grateful for the provision of samples by Andrius Petrašiūnas for the Lithuanian samples, Fons Verheyde, Augustijn de Ketelaere and Wouter Dekoninck for the Belgian and Dutch samples and Alf Tore Mjös for the Norwegian samples. We thank the staff of the Swedish Malaise Trap Project, Martti Koponen in Otava, Thorkhild Munk in Aarhus (+), and curators of several Swiss museums (Giulio Cuccodoro at MHNG, Anne Freitag at MZL, Hannes Baur at NMBE), who had all provided samples in other connections years ago which turned out useful here. For the kind loan of barcode voucher specimens, we want to thank Lars Vilhemsen (ZMUC) & Stefan Schmidt (ZSM). In short, we want to thank all the collectors and curators, specifically mentioned or not, that made the study of the material possible.

We want to thank Alexandra Popa (MGAB) for the gratuitous loan of the holotype and a paratype of *A. gracilipes* and the permission to mount the specimens, Joseph Monks (NHMUK) for organising images of the Walker type specimens, the team at the CNC, especially Andrew Bennett and Amber Bass, for making the type images of *A. fergussoni* accessible, the team of the entomology section at the MZLU, especially Rune Bygebjerg and Christoffer Fägerström for the images of the MZLU type material and Stefan Schmidt, Olga Schmidt and Jeremy Hübner (ZSM) for making the Hartig types accessible.

We want to express our thanks for the support by Hege Vårdal (NHRS) for her help at several different stages of the manuscript's development, including the utterly kind hospitability during JV's visits to Stockholm.

We are grateful to Göran Nordlander and Matt Buffington for the continuous and exciting discussions about Cynipoid taxonomy and more.

We thank Santiago Jaume Schinkel and Fons Verheyde for testing the key and their precious comments that lead to its much-improved state.

For sharing her observations and images with us and allowing us to further share one of her images within this manuscript, we want to sincerely thank Kim Neubauer.

We are grateful to the International Society of Hymenopterists for their support.

References

van Achterberg C, Shaw MR (2016) Revision of the Western Palaearctic species of *Aleiodes* Wesmael (Hymenoptera, Braconidae, Rogadinae). Part 1: Introduction, key to species groups, outlying distinctive species, and revisionary notes on some further species. ZooKeys 639: 1–164. https://doi.org/10.3897/zookeys.639.10893

Aspöck H, Aspöck U, Hölzel H (1980) 1 Die Neuropteren Europas: Eine zusammenfassende Darstellung der Systematik, Ökologie und Chorologie der Neuropteroidea (Megaloptera, Raphidioptera, Planipennia) Europas. Goecke & Evers, Krefeld, 495 pp.

Astrin JJ, Stüben PE (2008) Phylogeny in cryptic weevils: molecules, morphology and new genera of Western Palaearctic Cryptorhynchinae (Coleoptera: Curculionidae). Invertebrate Systematics 22(5): 503–522. https://doi.org/10.1071/IS07057

Awad J, Höcherl A, Hübner J, Jafari S, Moser M, Parsa M, Vogel J, Schmidt S, Krogmann L, Peters RS (2020) Just launched! GBOL III: Dark Taxa, a large research initiative focusing on German and Central European parasitoid wasps (and lower Diptera). Hamuli 11(2): 5–8.

Baur H (2015) Pushing the limits – two new species of *Pteromalus* (Hymenoptera, Chalcidoidea, Pteromalidae) from Central Europe with remarkable morphology. ZooKeys 514: 43–72. https://doi.org/10.3897/zookeys.514.9910

Baur H, Leuenberger C (2011) Analysis of ratios in multivariate morphometry. Systematic Biology 60(6): 813–825. https://doi.org/10.1093/sysbio/syr061

Baur H, Leuenberger C (2020) Multivariate Ratio Analysis (MRA): R-scripts and tutorials for calculating Shape PCA, Ratio Spectra and LDA Ratio Extractor. https://doi.org/10.5281/ZENODO.4250142

Buffington ML, Nylander JAA, Heraty JM (2007) The phylogeny and evolution of Figitidae (Hymenoptera: Cynipoidea). Cladistics 23 (5): 403–431. https://doi.org/10.1111/j.1096-0031.2007.00153.x

Buffington ML, Sandler RJ (2011) The Occurrence and Phylogenetic Implications of Wing Interference Patterns in Cynipoidea (Insecta: Hymenoptera). Invertebrate Systematics 25(6): 586. https://doi.org/10.1071/IS11038

Buffington ML, Condon M (2013) The description and bionomics of *Tropideucoila blepharoneurae* Buffington and Condon, new species (Hymenoptera: Figitidae: Zaeucoilini), para-

sitoid of *Blepharoneura* Loew Fruit Flies (Tephritidae). Proceedings of the Entomological Society of Washington 115(4): 349–357. https://doi.org/10.4289/0013-8797.115.4.349

Buffington ML, Forshage M (2014) The description of *Garudella* Buffington and Forshage, new genus (Hymenoptera: Figitidae: Eucoilinae). Proceedings of the Entomological Society of Washington 116(3): 225–242. https://doi.org/10.4289/0013-8797.116.3.225

Buuren SV, Groothuis-Oudshoorn K (2011) mice: Multivariate Imputation by Chained Equations in R. Journal of Statistical Software 45(3): 1–67. https://doi.org/10.18637/jss.v045.i03

Cameron P (1890) A monograph of the British phytophagous Hymenoptera (*Tenthredo*, *Sirex* and *Cynips*, Linné.) Vol. III. Ray Society, London, 341 pp.

Cannet A, Simon-Chane C, Akhoundi M, Histace A, Romain O, Souchaud M, Jacob P, Delaunay P, Sereno D, Bousses P, Grebaut P, Geiger A, De Beer C, Kaba D, Sereno D (2022) Wing Interferential Patterns (WIPs) and machine learning, a step toward automatized tsetse (*Glossina* spp.) identification. Scientific Reports 12(1): 20086. https://doi.org/10.1038/s41598-022-24522-w

Cannet A, Simon-Chane C, Akhoundi M, Histace A, Romain O, Souchaud M, Jacob P, Sereno D, Mouline K, Barnabe C, Lardeux F, Boussès P, Sereno D (2023) Deep learning and wing interferential patterns identify *Anopheles* species and discriminate amongst Gambiae complex species. Scientific Reports 13(1): 13895. https://doi.org/10.1038/s41598-023-41114-4

Cave RD, Miller GL (1987) Notes on *Anacharis melanoneura* (Hymenoptera: Figitidae) and *Charitopes mellicornis* (Hymenoptera: Ichneumonidae) Parasitizing *Micromus posticus* (Neuroptera: Hemerobiidae). Entomological News 98(5): 211–216.

Dalman JW (1823) Analecta entomologica. Typis Lindhianis, Holmiae, 104 pp. https://doi.org/10.5962/bhl.title.66069

Dal Pos D, Mikó I, Talamas EJ, Vilhelmsen L, Sharanowski BJ (2023) A revised terminology for male genitalia in Hymenoptera (Insecta), with a special emphasis on Ichneumonoidea. PeerJ 11: e15874. https://doi.org/10.7717/peerj.15874

von Dalla-Torre KW, Kieffer J-J (1910) Das Tierreich: Cynipidae. R. Friedländer und Sohn, Berlin. https://doi.org/10.5962/bhl.title.1077

De Queiroz K (2007) Species concepts and species delimitation. Systematic Biology 56(6): 879–886. https://doi.org/10.1080/10635150701701083

Dietz L, Eberle J, Mayer C, Kukowka S, Bohacz C, Baur H, Espeland M, Huber BA, Hutter C, Mengual X, Peters RS, Vences M, Wesener T, Willmott K, Misof B, Niehuis O, Ahrens D (2022) Standardized nuclear markers improve and homogenize species delimitation in Metazoa. Methods in Ecology and Evolution 14(2): 543–555. https://doi.org/10.1111/2041-210X.14041

Edgar RC (2004) MUSCLE: A multiple sequence alignment method with reduced time and space complexity. BMC Bioinformatics 5(1): 113. https://doi.org/10.1186/1471-2105-5-113

Fergusson NDM (1986) Handbook for the Identification of British Insects: Charipidae, Ibaliidae & Figitidae. Royal Entomological Society of London, London, 55 pp.

Fontal-Cazalla FM, Buffington ML, Nordlander G, Liljeblad J, Ros-Farre P, Nieves-Aldrey JL, Pujade-Villar J, Ronquist F (2002) Phylogeny of the Eucoilinae (Hymenoptera: Cynipoidea: Figitidae). Cladistics 18(2): 154–199. https://doi.org/10.1111/j.1096-0031.2002.tb00147.x

German Barcode of Life Consortium [Wägele W, Haszprunar G, Eder J, Xylander W, Borsch T, Quandt D, Grobe P, Pietsch S, Geiger M, Astrin J, Rulik B, Hausmann A, Moriniere J, Holstein J, Krogmann L, Monje C, Traunspurger W, Hohberg K, Lehmitz R, Müller K, Nebel M, Hand R] (2011) GBOL. https://www.bolgermany.de

Handlirsch A (1886) Die Metamorphose zweier Arten der Gattung *Anacharis* Dalm.

Harris RA (1979) A glossary of surface sculpturing. Occasional Papers in Entomology 28: 1–31.

Hausmann A, Krogmann L, Peters RS, Rduch V, Schmidt S (2020) GBOL III: DARK TAXA. iBOL Barcode Bulletin 10(1): 1–4. https://doi.org/10.21083/ibol.v10i1.6242

Hawkes MF, Duffy E, Joag R, Skeats A, Radwan J, Wedell N, Sharma MD, Hosken DJ, Troscianko J (2019) Sexual selection drives the evolution of male wing interference patterns. Proceedings of the Royal Society B: Biological Sciences 286(1903): 20182850. https://doi.org/10.1098/rspb.2018.2850

Hayat M (2009) Records and descriptions of Trichogrammatidae from India (Hymenoptera: Chalcidoidea). Oriental Insects 43 (1): 201–227. https://doi.org/10.1080/00305316.2009.10417583

Hoang DT, Chernomor O, Von Haeseler A, Minh BQ, Vinh LS (2018) UFBoot2: Improving the Ultrafast Bootstrap Approximation. Molecular Biology and Evolution 35 (2): 518–522. https://doi.org/10.1093/molbev/msx281

Hosseini F, Lotfalizadeh H, Norouzi M, Dadpour M (2019) Wing interference colours in *Eurytoma* (Hymenoptera: Eurytomidae): Variation in patterns among populations and sexes of five species. Systematics and Biodiversity 17(7): 679–689. https://doi.org/10.1080/14772000.2019.1687603

ICZN [International Commission on Zoological Nomenclature] (1999) International Code of Zoological Nomenclature. 4th edn. The International Trust for Zoological Nomenclature, London.

Ionescu MA (1969) Hymenoptera Cynipoidea. Fauna Republicii Socialiste Romania Vol. 9 Fasc. 6: 290 pp.

Janšta P, Delvare G, Baur H, Wipfler B, Peters RS (2020) Data–rich description of a new genus of praying mantid egg parasitoids, *Lasallegrion* gen. n. (Hymenoptera: Torymidae: Podagrionini), with a re-examination of *Podagrion* species of Australia and New Caledonia. Journal of Natural History 54(9–12): 755–790. https://doi.org/10.1080/00222933.2020.1778112

Jafari S, Müller B, Rulik B, Rduch V, Peters RS (2023) Another crack in the Dark Taxa wall: a custom DNA barcoding protocol for the species-rich and common Eurytomidae (Hymenoptera, Chalcidoidea). Biodiversity Data Journal 11: e101998: 1–13. https://doi.org/10.3897/BDJ.11.e101998

Jin S, Parks KS, Janzen DH, Hallwachs W, Dyer LA, Whitfield JB (2023) The wing interference patterns (WIPs) of *Parapanteles* (Braconidae, Microgastrinae): demonstrating a powerful and accessible tool for species-level identification of small and clear winged insects. Journal of Hymenoptera Research 96: 967–982. https://doi.org/10.3897/jhr.96.111382

Kapli P, Lutteropp S, Zhang J, Kobert K, Pavlidis P, Stamatakis A, Flouri T (2017) Multirate Poisson tree processes for single-locus species delimitation under maximum likelihood and Markov chain Monte Carlo. [Valencia A (Ed.)] Bioinformatics 33(11): 1630–1638. https://doi.org/10.1093/bioinformatics/btx025

Katayama N, Abbott JK, Kjærandsen J, Takahashi Y, Svensson EI (2014) Sexual Selection on Wing Interference Patterns in *Drosophila melanogaster*. Proceedings of the National Academy of Sciences 111(42): 15144–15148. https://doi.org/10.1073/pnas.1407595111

Kierych E (1984) Notes on the Genus *Prosynapsis* D.T. et Kieff. (*Synapsis* Forst.), with a List of *Anacharis* Dalm. Species Occurring in Poland (Hymenoptera, Cynipoidea, Anacharitidae). Annales Zoologici 37 (11): 335–340.

Markmann M, Tautz D (2005) Reverse taxonomy: an approach towards determining the diversity of meiobenthic organisms based on ribosomal RNA signature sequences. Philosophical Transactions of the Royal Society B: Biological Sciences 360(1462): 1917–1924. https://doi.org/10.1098/rstb.2005.1723

Mata-Casanova N, Selfa J, Pujade-Villar J (2018) Three new species of *Anacharis* Dalman, 1823 (Hymenoptera: Figitidae), with revised taxonomy and distribution records of palaearctic and indomalayan species. European Journal of Taxonomy 414: 1–25. https://doi.org/10.5852/ejt.2018.414

Mata-Casanova N, Selfa J, Wang Y, Chen X-X, Pujade-Villar J (2016) Diversity of subfamily Anacharitinae (Hymenoptera: Cynipoidea: Figitidae) in China with description of a new species of *Xyalaspis* Hartig, 1843. Journal of Asia-Pacific Entomology 19(1): 9–14. https://doi.org/10.1016/j.aspen.2015.11.007

Meier R, Shiyang K, Vaidya G, Ng PKL (2006) DNA barcoding and taxonomy in diptera: A tale of high intraspecific variability and low identification success. [Hedin M (Ed.)] Systematic Biology 55(5): 715–728. https://doi.org/10.1080/10635150600969864

Meier R, Blaimer BB, Buenaventura E, Hartop E, vonRintelen T, Srivathsan A, Yeo D (2022) A re-analysis of the data in Sharkey et al.'s (2021) minimalist revision reveals that BINs do not deserve names, but BOLD Systems needs a stronger commitment to open science. Cladistics 38: 264–275. https://doi.org/10.1111/cla.12489

Mikó I, Masner L, Johannes E, Yoder MJ, Deans AR (2013) Male terminalia of Ceraphronoidea: morphological diversity in an otherwise monotonous taxon. Insect Systematics & Evolution 44(3–4): 261–347. https://doi.org/10.1163/1876312X-04402002

Miller GL, Lambdin PL (1985) Observations on *Anacharis melanoneura* (Hymenoptera: Figitidae), a Parasite of *Hemerobius stigma* (Neuroptera: Hemerobiidae). Entomological News 96(3): 93–97.

Minh BQ, Schmidt HA, Chernomor O, Schrempf D, Woodhams MD, Von Haeseler A, Lanfear R (2020) IQ-TREE 2: New Models and Efficient Methods for Phylogenetic Inference in the Genomic Era. Molecular Biology and Evolution 37(5): 1530–1534. https://doi.org/10.1093/molbev/msaa015

Moser M, Ulmer JM, Van De Kamp T, Vasiliţa C, Renninger M, Mikó I, Krogmann L (2023) Surprising morphological diversity in ceraphronid wasps revealed by a distinctive new species of *Aphanogmus* (Hymenoptera: Ceraphronoidea). European Journal of Taxonomy 864: 146–166. https://doi.org/10.5852/ejt.2023.864.2095

van Noort S, Buffington ML, Forshage M (2015) Afrotropical Cynipoidea (Hymenoptera). ZooKeys 494: 1–176. https://doi.org/10.3897/zookeys.493.6353

Polaszek A, Fusu L, Viggiani G, Hall A, Hanson P, Polilov AA (2022) Revision of the World Species of *Megaphragma* Timberlake (Hymenoptera: Trichogrammatidae). Insects 13(6): 561. https://doi.org/10.3390/insects13060561

Puillandre N, Brouillet S, Achaz G (2021) ASAP: assemble species by automatic partitioning. Molecular Ecology Resources 21(2): 609–620. https://doi.org/10.1111/1755-0998.13281

Ratnasingham S, Hebert PDN (2007) Barcoding BOLD: The Barcode of Life Data System (www.barcodinglife.org). Molecular Ecology Notes 7(3): 355–364. https://doi.org/10.1111/j.1471-8286.2007.01678.x

Ratnasingham S, Hebert PDN (2013) A DNA-Based Registry for All Animal Species: The Barcode Index Number (BIN) System. [Fontaneto D (Ed.)] PLoS ONE 8(7): e66213. https://doi.org/10.1371/journal.pone.0066213

Reinhard H (1860) Die Figitiden des mittlern Europa. Berliner Entomologische Zeitschrift 4: 204–245.

Ronquist F, Nordlander G (1989) Skeletal morphology of an archaic cynipoid, *Ibalia rufipes* (Hymenoptera: Ibaliidae). Entomologica Scandinavica Supplement No. 33: 1–62.

Salden T, Peters RS (2023) Afrotropical Ceraphronoidea (Insecta: Hymenoptera) put back on the map with the description of 88 new species. European Journal of Taxonomy 884: 1–386. https://doi.org/10.5852/ejt.2023.884.2181

Schulmeister S, Wheeler WC, Carpenter JM (2002) Simultaneous analysis of the basal lineages of Hymenoptera (Insecta) using sensitivity analysis. Cladistics 18 (5): 455–484. https://doi.org/10.1111/j.1096-0031.2002.tb00287.x

Shevtsova E, Hansson C (2011) Species recognition through wing interference patterns (WIPs) in *Achrysocharoides* Girault (Hymenoptera, Eulophidae) including two new species. ZooKeys 154: 9–30. https://doi.org/10.3897/zookeys.154.2158

Shevtsova E, Hansson C, Janzen DH, Kjærandsen J (2011) Stable structural color patterns displayed on transparent insect wings. Proceedings of the National Academy of Sciences 108(2): 668–673. https://doi.org/10.1073/pnas.1017393108

Stelzl M, Devetak D (1999) Neuroptera in agricultural ecosystems. Agriculture, Ecosystems and Environment 74(1–3): 305–321. https://doi.org/10.1016/S0167-8809(99)00040-7

Thomson CG (1862) Försök Till Uppställning och Beskrifning af Sveriges Figiter. Öfversigt af Kongl. Vetenskaps-akademiens förhandlingar 18: 395–420.

Trietsch C, Mikó I, Notton D, Deans A (2018) Unique extrication structure in a new megaspilid, *Dendrocerus scutellaris* Trietsch & Mikó (Hymenoptera: Megaspilidae). Biodiversity Data Journal 6: e22676. https://doi.org/10.3897/BDJ.6.e22676

Verhandlungen Der Kaiserlich-Königlichen Zoologisch-Botanischen Gesellschaft in Wien 36: 235–238.

Walker F (1835) Description of Some British Species of *Anacharis*. Entomological Magazine 2: 518–522.

Weld LH (1952) Cynipoidea (Hym.) 1905–1950 Being a Supplement to the Dalla-Torre and Kieffer Monograph - the Cynipidae in Das Tierreich, Lieferung 24, 1910 and Bringing the Systematic Literature of the World up to Date, Including Keys to Families and Subfamilies and Lists of New Generic, Specific and Variety Names. Privately printed, Ann Arbor, Michigan, 351 pp.

Westwood JO (1833) Notice of the habits of a cynipideous insect, parasitic upon the rose louse (*Aphis rosae*); with descriptions of several other parasitic hymenoptera. Magazine of Natural History 6: 491–497.

Zetterstedt JW (1822) Resa genom Sweriges och Norriges lappmarker, förrättad år 1821. Berling, Lund, 1–2[: 266 + 232 pp].

Zetterstedt JW (1838) pt. 2. In: Insecta Lapponica. Lipsiae [Leipzig], 220 pp.

Žikić V, Van Achterberg C, Stanković SS, Ilić M (2011) The male genitalia in the subfamily Agathidinae (Hymenoptera: Braconidae): Morphological information of species on generic level. Zoologischer Anzeiger - A Journal of Comparative Zoology 250(3): 246–257. https://doi.org/10.1016/j.jcz.2011.04.006

Supplementary material 1

Material examined

Authors: Jonathan Vogel, Mattias Forshage

Data type: xlsx

Explanation note: Listing all material examined, including BOLD IDs if available. Was used as a basis for the material examined sections of each respective species. Contains all nine species.

Link: https://doi.org/10.3897/jhr.97.131350.suppl1

Supplementary material 2

Foreign BOLD IDs

Author: Jonathan Vogel

Data type: xlsx

Explanation note: BOLD IDs of the sequences accessed via BOLD that were neither examined morphologically, nor produced herein.

Link: https://doi.org/10.3897/jhr.97.131350.suppl2

Supplementary material 3

Morphometry analysis: Raw data
Authors: Jonathan Vogel, Christoph Braun
Data type: xlsx
Explanation note: The raw data that was used to run the morphometric analyses, prior to the imputation script.

Link: https://doi.org/10.3897/jhr.97.131350.suppl3

Supplementary material 4

Imputed morphometric data
Author: Christoph Braun
Data type: xlsx
Explanation note: The imputed morphometric data that was used for the morphometric analyses.

Link: https://doi.org/10.3897/jhr.97.131350.suppl4

Supplementary material 5

Additional results from morphometry
Author: Christoph Braun
Data type: pdf
Explanation note: Documentation of additional results from morphometry: PCA and ratio extractor results of the species-level analyses not shown in the manuscript as well as the results of the allometry tests of all sspecies group- and species-level comparisons.

Link: https://doi.org/10.3897/jhr.97.131350.suppl5

JHR 97: 699–720 (2024)
doi: 10.3897/jhr.97.128234
https://jhr.pensoft.net

RESEARCH ARTICLE

JOURNAL OF Hymenoptera RESEARCH
A peer-reviewed open-access journal
The International Society of Hymenopterists

Phenology of microhymenoptera and their potential threat by insect decline

Maura Haas-Renninger[1,2,3], Sonia Bigalk[1], Tobias Frenzel[1], Raffaele Gamba[1], Sebastian Görn[1], Michael Haas[1], Andreas Haselböck[4], Thomas Hörren[5], Martin Sorg[5], Ingo Wendt[1], Petr Jansta[6], Olaf Zimmermann[7], Johannes L. M. Steidle[2,3], Lars Krogmann[1,2,3]

1 *State Museum of Natural History Stuttgart, Department of Entomology, Rosenstein 1, 70191 Stuttgart, Germany* **2** *University of Hohenheim, Institute of Biology, Biological Systematics (190w), Garbenstraße 30, 70599 Stuttgart, Germany* **3** *Center of Excellence for Biodiversity and integrative Taxonomy (KomBioTa), Wollgrasweg 23, 70599 Stuttgart, Germany* **4** *Entomological Society Stuttgart e.V., Wild Bee Cadastre, Rosenstein 1, D-70191 Stuttgart, Germany* **5** *Entomological Society Krefeld, Magdeburger Straße 30-40, 47800 Krefeld, Germany* **6** *Faculty of Science, Charles University, Prague, Czech Republic* **7** *Agricultural Research Centre Augustenberg (LTZ), Nesslerstraße 25, 76227 Karlsruhe, Germany*

Corresponding author: Maura Haas-Renninger (maura.haas-renninger@smns-bw.de)

Academic editor: Miles Zhang | Received 24 May 2024 | Accepted 30 July 2024 | Published 30 August 2024

https://zoobank.org/4AB1A598-7346-459F-B9C5-793EA8495B19

Citation: Haas-Renninger M, Bigalk S, Frenzel T, Gamba R, Görn S, Haas M, Haselböck A, Hörren T, Sorg M, Wendt I, Janšta P, Zimmermann O, Steidle JLM, Krogmann L (2024) Phenology of microhymenoptera and their potential threat by insect decline. Journal of Hymenoptera Research 97: 699–720. https://doi.org/10.3897/jhr.97.128234

Abstract

Although microhymenoptera are highly abundant in all terrestrial ecosystems, they are overlooked in most of insect monitoring studies due to their small-size and demanding identification linked with lack of taxonomic experts. Until now, it is unclear to what extent microhymenoptera are affected by insect decline, as there is a huge knowledge gap on their abundance. To fill this knowledge gap, we used Malaise trap samples from three study sites of a complete vegetation period (March to November) of an ongoing insect monitoring study in south-western Germany (i) to study the relationship of insect total biomass, and abundance and diversity of microhymenoptera, and (ii) to assess the phenology of microhymenoptera families. Our results show that microhymenoptera abundance and diversity are positively correlated with total insect biomass, indicating that insect biomass is a valuable proxy for insect abundancy trends even for small-sized insects. In total, we counted 90,452 specimens from 26 families belonging to 10 superfamilies of Hymenoptera. Microhymenoptera numbers peaked twice during the year, first between June and July and second between July and August. Interestingly, egg-parasitoids, such as Scelionidae, Mymaridae and

Trichogrammatidae had a slightly shifted second activity period in August and September. Our data provides a baseline for the occurrence of microhymenoptera in meadow ecosystems in south-western Germany and underlines the potential of mass samples to study microhymenoptera in the context of insect decline.

Keywords
Activity pattern, biodiversity, biomass, fractionator, insect decline, malaise trap, seasonality

Introduction

The global decline of insects (Hallmann et al. 2017; Sánchez-Bayo and Wyckhuys 2019; Seibold et al. 2019; Wagner et al. 2021) poses a major threat to humankind, as insects play an essential role for our ecosystems through providing functions such as pollination (Klein et al. 2007), natural balance of populations (DeBach and Rosen 1991), and nutrient cycling (Yang and Gratton 2014). Therefore, long-term assessments of insect population trends are necessary to implement and adapt conservation measures to preserve insects in the future. In recent years, several insect monitoring studies were conducted (e.g. Seibold et al. 2019; Karlsson et al. 2020; Lehmann et al. 2021; Staab et al. 2023), which are all facing various constraints. First, they are limited through funding sources (often granted only for a few years) and trained personnel for insect identification. Second, many long-term studies focus only on specific target groups, such as butterflies (Thomas 2005), wild bees (Turley et al. 2022), beetles, true bugs, grasshoppers and spiders (Seibold et al. 2019). Such groups are relatively well studied, easy to identify and historically used as indicators for diversity and landscape changes. In addition, calibrating estimates of abundance for long term studies can be difficult even for target groups as it highly depends on the trapping type used for the assessment (Battles et al. 2024).

An alternative to focusing on specific insect taxa is to use biomass as a proxy for abundance of insects. This has been done in the landmark study by Hallmann et al. (2017), in which biomass of flying insects was used to monitor insect population trends, showing a decline of 76% in insect biomass over 27 years on the study sites, but also in several other studies (Lister and Garcia 2018; Uhler et al. 2021; Welti et al. 2021; Müller et al. 2023). The benefits of using biomass is that the weighing setup is cheap, it can be done in a standardized way, and there is no need for time-consuming counting of specimens or taxonomic identification. However, the use of biomass as a proxy for diversity is also highly controversial (Hallmann et al. 2021b; Redlich et al. 2021). Intensive land use can lead to the mass occurrence of few insect species, compromising the relationship between biomass and diversity. In addition, the assessment of insect diversity using metabarcoding results still has methodological weaknesses that lead to bias in the data patterns (Zizka et al. 2022). Consequently, it depends on many factors to derive statements on species diversity from biomass information.

Malaise traps are used widely to assess biomass of flying insects in a standardized way. The two insect orders that are most abundant in such Malaise trap samples are Diptera and Hymenoptera (Geiger et al. 2016; Srivathsan et al. 2023). Although

numerous, especially small-sized parasitoid Hymenoptera (microhymenoptera) represent only a small fraction of the total biomass, where they are mostly considered 'by-catch' and remain unprocessed. This is problematic, because Hymenoptera are assumed to be the most diverse animal order in the world (Forbes et al. 2018), and play an important role in many terrestrial ecosystems. Ecologically, parasitoid Hymenoptera are important as top-down regulators of their specific hosts, often herbivorous insects (LaSalle 1993; Heraty 2017) and are essential for the resilience of ecosystems (LaSalle and Gauld 1991; Grissell 1999). In ecological studies, they can serve as indicators for the presence of their hosts (Anderson et al. 2011). Due to their high position in the food web, parasitoids are also particularly prone to extinction (Hassell 2000; Wagner et al. 2021; Klaus et al. 2023), although only few studies focused on their potential decline (but see Gatter et al. 2020; Janzen and Hallwachs 2021).

One reason for the neglect of parasitoid Hymenoptera in biodiversity studies is that they harbour many so-called 'dark taxa', which are extremely species-rich groups of small-sized insects that are hard to identify and that harbour mostly undescribed taxa (Shaw and Hochberg 2001; Hausmann et al. 2020a; Hartop et al. 2022). The taxonomic work that would be necessary to describe and identify dark taxa often lacks funding sources as taxonomy is poorly recognized in science and the public (but see Behm 2018). As a consequence, the scarcity of experts contributes to the taxonomic impediment (Engel et al. 2021). Altogether, this leads to a huge knowledge gap not only on the diversity of parasitoid Hymenoptera in terrestrial ecosystems, but also on their potential threat through agricultural activities (Sánchez-Bayo and Wyckhuys 2019), like mowing or pesticide application (Brühl et al. 2021; Schöfer et al. 2023).

To fill this gap, we studied microhymenoptera in Malaise trap samples of an ongoing insect monitoring program in south-western Germany. As Hallmann et al. (2017) highlighted the relevance of insect biomass for monitoring insect abundance trends, we studied the relationship of insect total biomass, and abundance and diversity of microhymenoptera to see, if a decrease in insect total biomass of Malaise trap samples, can be also indicatory of a decrease of microhymenoptera. Moreover, we provide a phenology for different families of microhymenoptera of semi-arid grassland of south-western Germany. These data can be used for the timing of potentially harmful agricultural activities, e.g. mowing (Haas-Renninger et al. 2023b) or pesticide application, to avoid high activity periods of microhymenoptera.

Methods

Site selection and environmental data

To obtain data on microhymenoptera families from sites that have a comparably high potential to harbour intact insect communities including rare or endangered species, three sites with high conservation values (CV) were selected out of twelve study sites sampled in 2019 within the project "Aerial Biomass" of the insect monitoring program

(see Sampling and specimen handling). We used the CV according to Görn and Fischer (2011), calculated from the number and threat level of wild bees as indicator species. Wild bees are considered useful indicators on the landscape level, as they are dependent on specific habitat requirements for reproduction and nesting (Schindler et al. 2013; Twerd et al. 2021). The data were obtained from the project "Aerial Biomass" (LUBW, unpublished). Threat levels are based on the German Red List (Westrich et al. 2011) and the Red List for bees in Baden-Wuerttemberg (Westrich et al. 2000). We use the term "trap location" for the exact location of the Malaise trap and the term "study site" for the trap location including a 500 m radius around the trap.

Statistical analyses were performed using the software 'R', version 4.0.4 (R Core Team 2021). To select three similar study sites from the twelve study sites that were sampled in 2019, we used available data on wild bee abundance. We calculated a hierarchical cluster analysis, method 'binary' data with complete linkage, to identify those study sites that cluster together. For climate data, we used daily station observations of mean temperature at 2 m above ground in °C and precipitation height in mm from the Climate Data Centre (DWD 2023; see above) from weather stations close to the study sites (< 17 km). We calculated the means over our two-week collecting periods. The proportion of land use around the trap location was calculated in QGIS (ver. 3.32.3-Lima, http://www.qgis.org). Therefore, different land uses were identified and mapped through georeferenced, digital orthophotos (resolution of 20 cm per pixel, imaged in 2018 by the Landesamt für Geoinformation und Landentwicklung Baden-Wuerttemberg) in a radius of 500 m around the trap location. The area for each land use type was then calculated within QGIS and converted in percentages.

Sampling and specimen handling

We used Malaise trap samples from the project "Aerial Biomass" of the insect monitoring program in south-western Germany at the Stuttgart State Museum of Natural History (SMNS), which was launched in 2018 by the State Institute for Environment Baden-Wuerttemberg (LUBW, https://www.lubw.baden-wuerttemberg.de/natur-und-landschaft/insektenmonitoring). The aim of this program is to monitor long-term insect population trends using total insect biomass, and abundance and species richness of wild bees in protected and non-protected sites. The traps and methods are standardized and based on the recommendations by the Entomological Society Krefeld (Ssymank et al. 2018). The Malaise traps were set up in 2019 from the end of March until the beginning of November and emptied every two weeks, resulting in 16 samples per study site. Malaise traps according to the model by Henry Townes (Townes 1972) adapted after Schwan et al. (1993) were placed in the sites by members of the Entomological Society of Krefeld.

We used the samples from the three sites from the whole collecting period in 2019, resulting in 48 samples. We used the fractionator method based on Buffington and Gates (2008) with an adapted protocol (Haas-Renninger et al. 2023a) to more easily obtain our target taxa of microhymenoptera. This method is based on a sieve (2 mm mesh size) in a plastic tub into which a full fluid-conserved insect sample can be

poured in and carefully size fractioned on an orbital shaker. Both size fractions (macro and micro) were stored in a freezer at -20 °C at Stuttgart State Museum of Natural History (SMNS) until further processing. Only the micro fraction was used for further analyses. Therefore, larger-sized species of certain families remained in the macro fraction and thus might not be covered in the phenology of the Hymenoptera families.

Hymenoptera specimens from all micro fractions were sorted out, counted and identified at least to family level using Goulet and Huber (1993). Formicidae were not investigated. Wild bees had been sorted out before the fractioning process. The microhymenoptera were stored in 99.6% pure ethanol and remained in the freezer until further processing. As not all families that we obtained have a parasitoid lifestyle, we use the term 'microhymenoptera' instead of 'parasitoid Hymenoptera' for our data. We use the term 'abundance' for the total number of counted specimens of a specific taxon.

Insect biomass, microhymenoptera abundance and diversity

Insect biomass data are unpublished and were obtained from the project "Aerial Biomass". To test how total microhymenoptera abundance and diversity relate to insect biomass, we used statistical models. As our data were count data, we calculated a general linear model (family 'poisson') with total abundance of microhymenoptera as dependent variable, total insect biomass (in grams per sample) as explanatory variable, Julian Day number (JDN, end date of each two-week collecting interval), mean temperature and precipitation as covariates, and study site (n = 3) as factor. To study the relationship of microhymenoptera diversity and insect biomass, we calculated a linear model. We used the R package 'vegan' version 2.6-4 (Oksanen et al. 2022) to calculate the Shannon diversity index (H') of every sample using microhymenoptera abundance on family level. Data were checked for normal distribution using Shapiro–Wilk normality test. Residual plots were optically checked for homogeneity of variances. We used family diversity as dependent variable, total insect biomass as explanatory variable, Julian Day number (JDN, end date of two week collecting interval), mean temperature and precipitation as covariates, and study site (n = 3) as factor. For fitting the model, we used ANOVA to gradually subtract explanatory variables that had no significant effect. In addition, we created a model selection table based on small sample corrected AICc (package 'AICcmodavg', Suppl. material 1: table S3). Our final model included total insect biomass as explanatory variable and study site as factor.

Results

Site selection

From all twelve study sites from 2019, conservation values were highest for study site Apfelberg (CV = 237.5), Steiner Mittelberg (CV = 157.5), Weissach (CV = 132.5) and Köllbachtal (CV = 200) (Suppl. material 1: fig. S1). In a hierarchical cluster analysis

based on conservation values sites Apfelberg and Steiner Mittelberg clustered together and were closer to Weissach than to Köllbachtal (Suppl. material 1: fig. S2). Probably, this is because study site Köllbachtal differs markedly from the other three sites in terms of habitat characteristics (e.g., high moisture). Therefore, study sites Apfelberg, Steiner Mittelberg, and Weissach were chosen for our analysis. These sites are characterized by dry, low-intensity managed meadows and were mown or grazed only twice a year.

A) Apfelberg

The study site on the nature conservation area "Apfelberg" Schutzgebiets-Nr. 2.217 near Karlsruhe, Baden-Wuerttemberg (Table 1) is characterized by an extensively managed meadow with southern exposure (Fig. 1A). The study site was mown once between mid-July and end of July without removal of cut grass. Between end of September and beginning of October, sheep were grazing on the site. The trap location is surrounded by densely growing woody plants towards the north and west, including fruit trees and bushes (Fig. 2A). The study site is surrounded by vineyards and agricultural fields and towards the east, it is richly structured with woodlands and small patches of grassland. The site slopes southwards, where it is dominated by meadows and agricultural sites. Within a radius of 50 m surrounding the trap, the plant community is characterized by an oat grass meadow with elements of a semi-arid grassland.

B) Steiner Mittelberg

The study site on the nature conservation area "Beim Steiner Mittelberg" Schutzgebiets-Nr. 2.119, thereafter referred to as "Steiner Mittelberg" near Karlsruhe, Baden-Wuerttemberg (Table 1), is an extensively managed meadow. It is located in a dry valley surrounded by agricultural sites, that are managed organically (Fig. 1B). The site was mown between end of May and beginning of June and between mid- and end of August with the cut grass having been partly removed. Northwards, there are meadow orchards and gardens located close to a small forest (Fig. 2B). Westwards, there are managed meadows and an extensive forest. The site slopes towards the south, bordering on agricultural sites with wheat fields and smaller forest patches. The plant community is not fully developed and shows an interrupted stock of semi-arid grassland and oat grass meadow elements.

C) Weissach

This study site is on a grassland area near Weissach, ÖFS 124 (Fig. 1C) located between Stuttgart and Karlsruhe, Baden-Wuerttemberg (Table 1). In contrast to the others, it does not belong to a nature conservation area and is a low-intensity managed meadow, near a test track for cars (Fig. 2C). This might influence the comparability with the other sites (Hausmann et al. 2020b). The site was mown between end of May and beginning of June, with removal of cut grass, and a second time in June, with the cut grass

removed around two weeks later. North of the site, there is a small wood patch, which is surrounded by intensively managed agricultural areas (Fig. 2C). Towards the East, a heap of stones separates the site from a small wood patch, which is surrounded by further agricultural sites and woodland. The area slopes towards southeast, where there is a row of fruit trees alongside the meadow, followed by small wood patches and meadow areas. Westwards, the meadow is bordered by the test track. The plant community can be described as an *Onobrychido-Brometum erecti*, a sainfoin-brome grass semi-arid grassland, which is strongly impoverished, and that develops into ruderal vegetation.

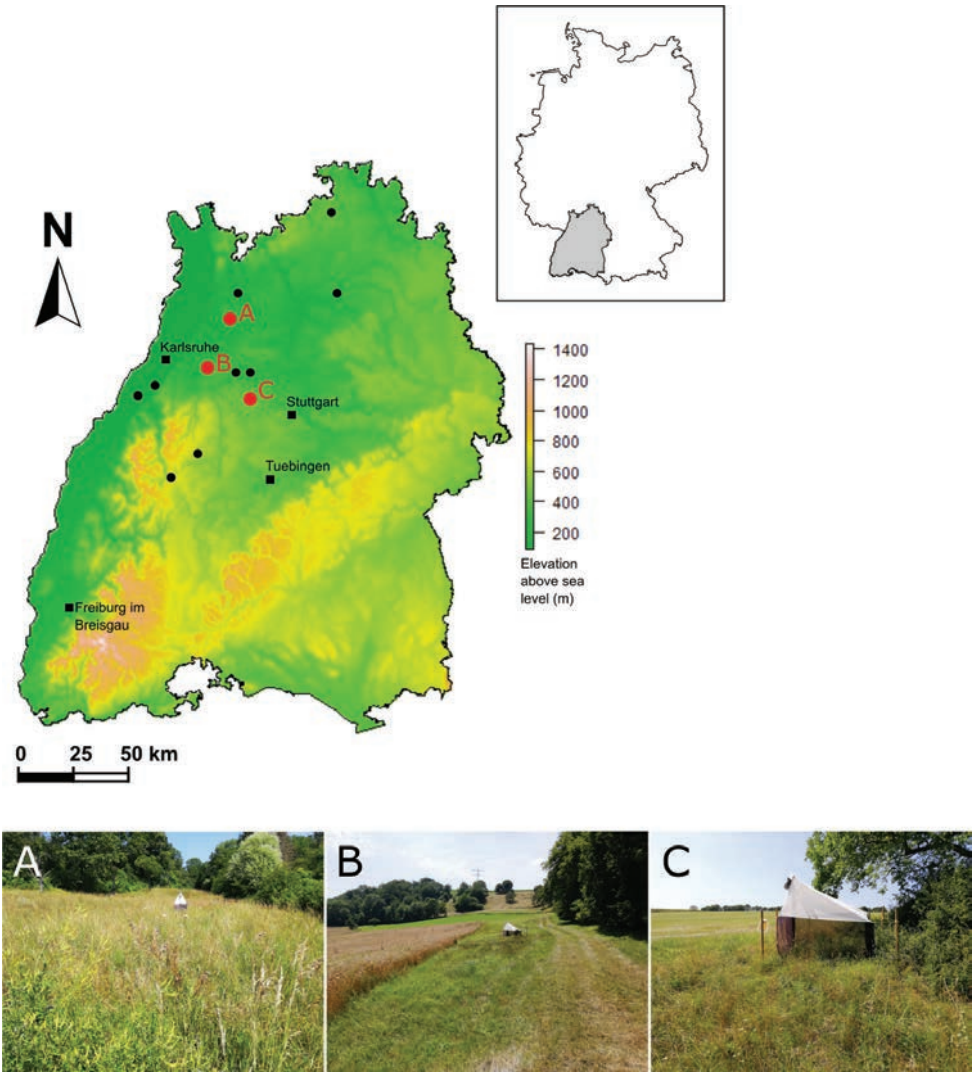

Figure 1. Malaise traps on semi-arid meadows in Baden-Wuerttemberg, south-western Germany, with two protected areas (**A** Apfelberg **B** Steiner Mittelberg) and one non-protected area (**C** Weissach). Black dots symbolize other study sites that were not further analysed in this study (for details, see Suppl. material 1: table S1).

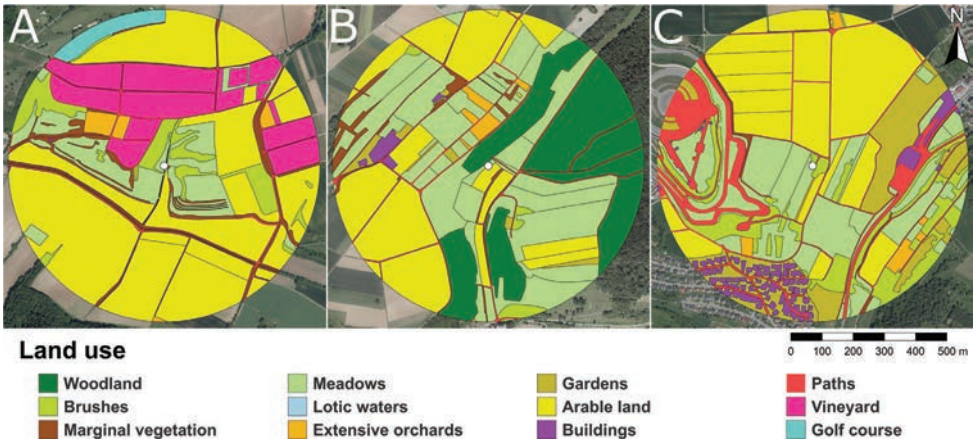

Figure 2. Land use types in a radius of 500 m around the Malaise trap of the three study sites **A** Apfelberg **B** Steiner Mittelberg and **C** Weissach in Baden-Wuerttemberg, south-western Germany. The white dots in the centre of each circle symbolize the Malaise trap location. For land use proportions per study site in percent, see Suppl. material 1: table S2. Geobasisdaten © LGL, www.lgl-bw.de; RIPS, LUBW.

Table 1. Details on selected study sites. Start date: set up of Malaise trap; End date: dismantling of Malaise trap; DWD weather station: accessed using the Climate Data Centre (DWD 2023, https://www.dwd.de/DE/Home/home_node.html).

Study site		A) Apfelberg	B) Steiner Mittelberg	C) Weissach
Trap location		49.16754°N, 8.7903°E; 178 m AMSL	48.97039°N, 8.65899°E; 240 m AMSL	48.84296°N, 8.91448°E; 438 m AMSL
Start date		23.03.2019	23.03.2019	23.03.2019
End date		05.11.2019	06.11.2019	05.11.2019
DWD weather station	Temperature data	"Waibstadt"; Germany, 49.2943°N, 8.9053°E; 237 AMSL; linear distance to trap: 16.38 km	"Pforzheim-Ispringen"; Germany, 48.9329°N, 8.6973°E; 332 m AMSL; linear distance to trap: 5.02 km	"Renningen-Ihinger Hof"; Germany, 48.7425°N, 8.9240°E; 478 m AMSL; linear distance to trap: 11.19 km
	Precipitation data	See Temperature data	See Temperature data	"Weissach"; Germany, 48.8457°N, 8.9073°E; 455 m AMSL; linear distance to trap: 0.61 km

Insect biomass, microhymenoptera abundance and diversity

In total, we counted 90,452 microhymenoptera specimens that we could assign to 26 families in 10 superfamilies. We found a significant relationship between insect biomass, study site, JDN, temperature, precipitation, and microhymenoptera abundance (Table 2). The linear model to study the relationship of insect biomass and diversity was also significant (Table 2). There was a significant relationship between diversity of microhymenoptera families, total insect biomass and study site (Table 2), while JDN and temperature were not significant.

Table 2. The results of linear models for abundance of microhymenoptera and diversity of microhymenoptera families.

Abundance	Estimate	Std. Error	z value	*p*
(Intercept)	-4414.00	205.70	-21.46	
Insect total biomass	0.00	0.00	-6.00	**<0.001*****
Study site	0.93	0.01	92.22	**<0.001*****
JDN	0.42	0.01	43.15	**<0.001*****
Temperature	0.00	0.00	21.48	**<0.001*****
Precipitation	0.18	0.00	100.00	
Null deviance: 61345.1 on 47 degrees of freedom				
Residual deviance: 4668.6 on 41 degrees of freedom				
Diversity	**Df**	**Sum Sq**	**Mean Sq**	**F value**	***p***
Insect total biomass	1	0.16	0.16	8.85	**0.005****
Study site	2	0.16	0.08	4.48	**0.017***
Residuals	44	0.77	0.02	-	-
Observations	48				
Multiple R^2	0.29				
Adjusted R^2	0.24				
p	**0.002**				

Seasonal changes in microhymenoptera

The study site Steiner Mittelberg had the highest abundance with 45,678 specimens, followed by Weissach with 24,037 specimens and Apfelberg with 20,737 specimens. The microhymenoptera family with the highest abundance was the family Mymaridae. It dominated throughout the year at Steiner Mittelberg and was outnumbered at Apfelberg only from April to June by Platygastridae, in July to August by Scelionidae and in September by Trichogrammatidae. At Weissach, Mymaridae was only outnumbered from July to August by Scelionidae and in September by Trichogrammatidae (Suppl. material 1: fig. S3).

The lowest abundance of microhymenoptera were observed at all three study sites between March and April in spring, and between Mid-September and October in autumn. The abundance reached a first peak between June and July, a second peak between July and August and a final small peak in October (Fig. 3). At Steiner Mittelberg, there was an additional forth peak mid-August (Fig. 3b). Some families peaked early in the season (e.g. Platygastridae) and some showed high activity also in the late season (e.g. Figitidae, Trichogrammatidae). Some families had only one activity peak (e.g. Scelionidae, Mymaridae), whereas others had two (e.g. Figitidae, Eulophidae), or three (e.g. Trichogrammatidae). Also, timing and number of peaks of the families differed between the three sites. Families that were rarely found in the micro fractions, such as Proctotrupidae, Cynipidae, Ormyridae, Signiphoridae, Tetracampidae, Torymidae, Mymarommatidae and Crabronidae are shown in Suppl. material 1: fig. S4.

Interestingly, there was no consistent decline in microhymenoptera after mowing neither for total abundance (Fig. 3), nor for abundance of the different families (Figs 4, 5). For the total number of specimens, mowing was followed by a sharp de-

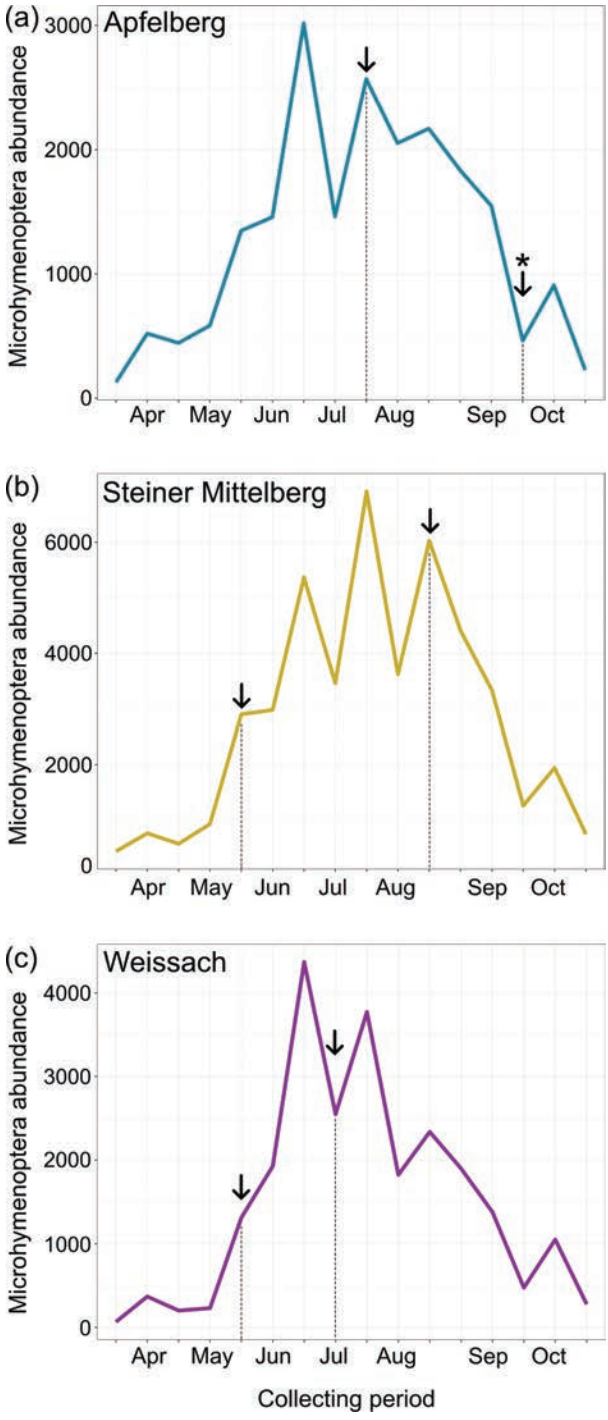

Figure 3. Seasonal abundance of microhymenoptera from Malaise traps at three study sites **a** Apfelberg **b** Steiner Mittelberg and **c** Weissach in Baden-Wuerttemberg, south-western Germany. The arrows mark mowing events and the asterisk marks grazing activities.

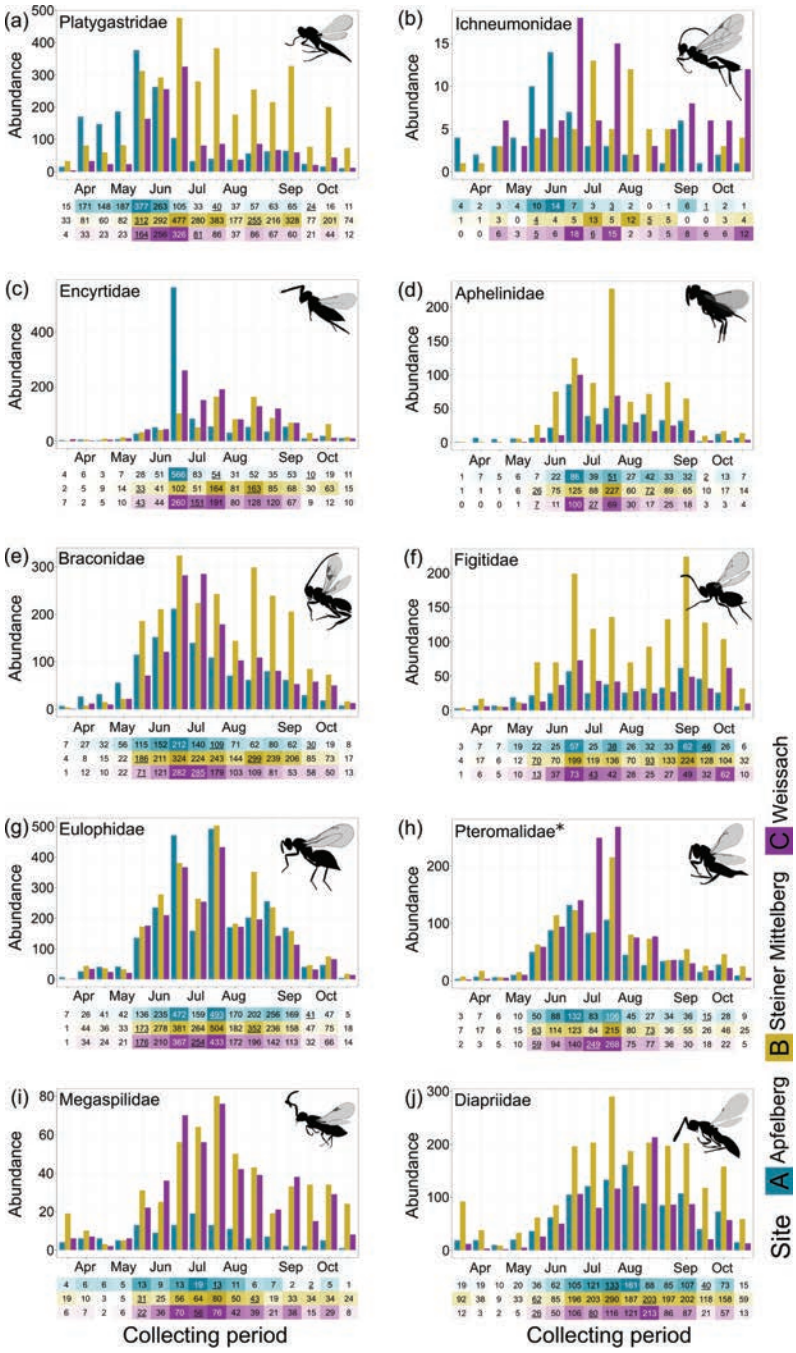

Figure 4. Seasonal abundance patterns of different microhymenoptera families from Malaise traps at three study sites in Baden-Wuerttemberg, south-western Germany. Families are sorted by the time of the first activity peak. Only families with n > 20 during their activity peak are shown. Underlined values indicate mowing activity, except for one sheep grazing event at Apfelberg in September/October. *: Family definition of 'Pteromalidae' is based on Goulet and Huber (1993) as specimen identification was done before Burks et al. (2022).

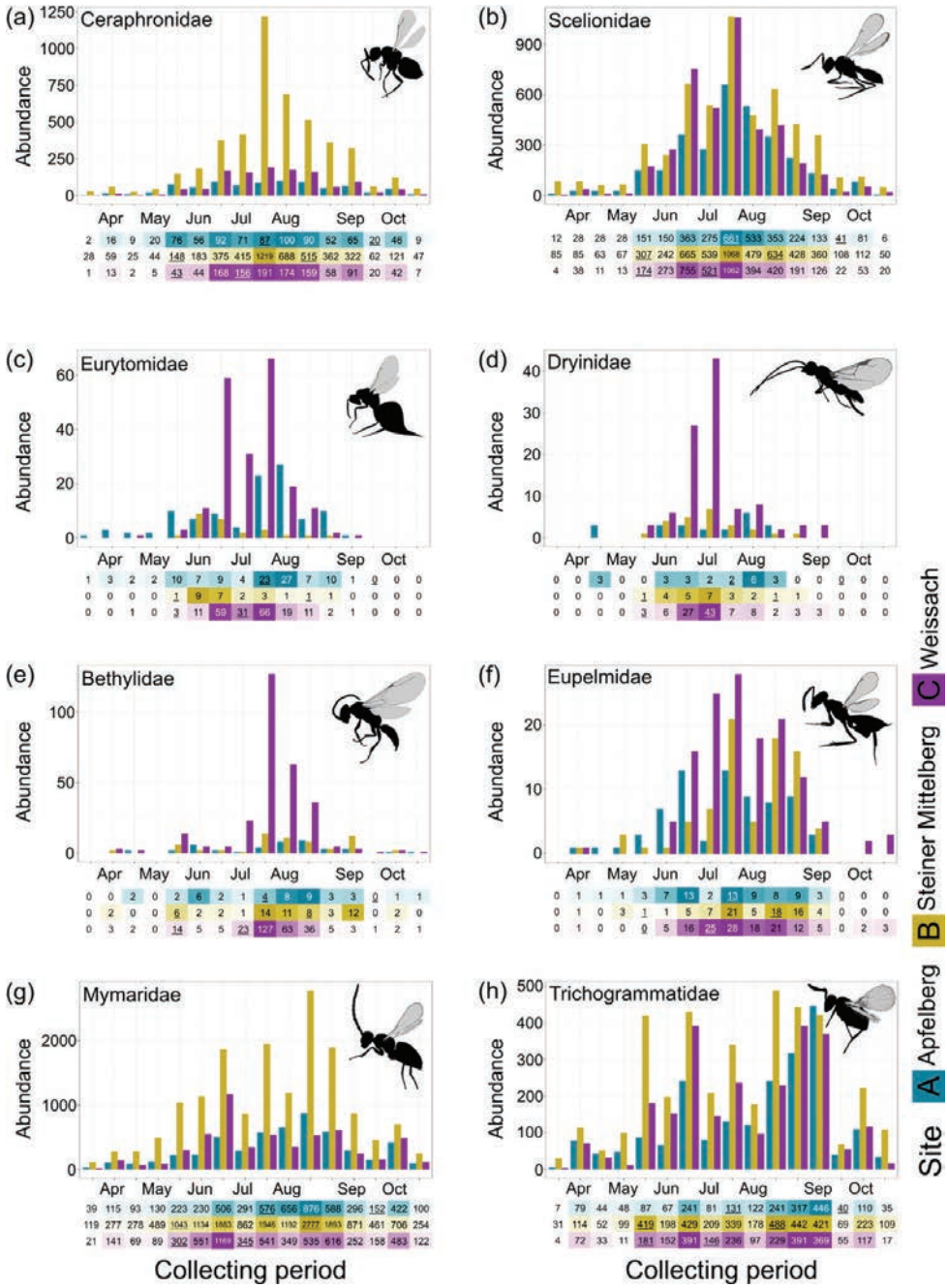

Figure 5. Seasonal abundance patterns of different microhymenoptera families from Malaise traps at three study sites in Baden-Wuerttemberg, south-western Germany. Families are sorted by the time of the first activity peak. Only families with n > 20 during their activity peak are shown. Underlined values indicate mowing activity, except for one sheep grazing event at Apfelberg in September/October.

crease at Apfelberg in July and in Steiner Mittelberg in August, but an increase after grazing in Apfelberg in September, and after mowing in May in Steiner Mittelberg, and in Weissach in May and July.

Discussion

To the very best of our knowledge, this is the first study on the diversity and the phenology of different families of microhymenoptera in meadow ecosystems using Malaise traps. Because it is currently not possible to study the abundance and the diversity of taxonomic groups in parallel at the same time using molecular methods, several thousands of microhymenoptera had to be sorted manually on family level, which took 18 person-months in the present study. Therefore, we restricted our analysis to data from one year and three sites. However, because all three sites are very similar, we consider it likely that these data are representative for insect communities in semi-arid grasslands of south-western Germany.

A current discussion revolves around the relationship between biomass of insects and biodiversity, and the potential of certain taxa to serve as indicators for biomass or species richness (Redlich et al. 2021; Uhler et al. 2021). This is important for the interpretation of recent data on insect decline and its ecological consequences, based on biomass data from malaise trap catches (Hallmann et al. 2017; Uhler et al. 2021). Recently, Hallmann et al. (2021a) found a significant relationship between hoverfly abundance and species richness with the total biomass of insects in malaise trap catches from six locations in North Rhine-Westphalia, Germany. These locations were also studied in the Krefeld study (Hallmann et al. 2017), at two time points, 1989 and 2014. From this, Hallmann et al. (2021a) concluded that the biomass decline reported by Hallmann et al. (2017) is in fact associated with a decline in abundance and diversity of hoverflies, and possibly other taxa as well. A positive correlation with hoverflies was confirmed by Redlich et al. (2021), and Uhler et al. (2021), using insect biomass data from malaise traps at 179 locations in South Germany from different habitats. Interestingly, the correlation of total insect biomass with species richness differed depending on temperature and habitat but was significantly positive in all habitats for Diptera, Lepidoptera and Orthoptera, but not for other groups on all studied habitats. From this, it was concluded that hoverflies might be indicators for large-bodied insect taxa such as Orthoptera and Lepidoptera, while taxa with small body size, but high diversity have less impact on biomass (Redlich et al. 2021). In contrast to this idea, our data on microhymenoptera from low-intensity managed meadows revealed not only a significant correlation between total insect biomass and diversity, but also with abundance. We assume that this is caused by the dependence of microhymenoptera on the abundance of their hosts, which at least partially belong to the Lepidoptera and Diptera. This finding indicates that the decline of insect biomass reported by Hallman et al. (2017) may also affect microhymenoptera.

There was a positive correlation between temperature, precipitation and abundance of microhymenoptera, which has been observed also in previous studies for insects (Pilotto et al. 2020; Uhler et al. 2021; Welti et al. 2021; Müller et al. 2023). This finding is reasonable considering the fact that insects are ectothermic organisms, which means that with increasing temperature, their metabolism increases, which can lead to higher flight activity (Klowden 2013). In his study on the influence of different climatic factors on parasitoid Hymenoptera, Ulrich (2000) identified precipitation as the most important climatic factor. In contrast, Juillet (1964) concluded that temperature and wind velocity are the main indicators of activity of Ichneumonoidea, and that precipitation is not an informative indicator, because of its occasional occurrence. Still, it remains unclear if microhymenoptera abundance and activity are affected by the weather directly or via their host densities.

At all sites, wasps were collected in larger numbers only after end of May in spring, and after September in autumn and had between one and four peaks in activity over the year, mostly between June and July, in July, and between July and August. It is unclear, if these peaks represent several generations of wasps throughout the year or are caused by different species within each family with non-matching peaks. As mowing showed to be harmful for microhymenoptera (Haas-Renninger et al. 2023b), our phenology data indicates two periods in the year which might be suitable for activities such as mowing, up to end of May in spring, and after September in autumn. However, our data do not provide evidence for a decline of microhymenoptera due to mowing. In fact, from the five mowing events and one grazing event observed during our study, only two were associated with a subsequent decline in abundance, while an increase was observed in four cases (Fig. 3). The large losses of up to 64% in individuals caused by mowing (Haas-Renninger et al. 2023b) may not affect the population sizes in the field. It can be suggested that mowing had no impact because microhymenoptera have a short lifespan and their population sizes strongly depend on newly emerged specimens. It might be possible that our study sites were quickly re-populated after mowing by wasps, which emerged from unmown habitats from surrounding areas (Fig. 2).

In our study, the most abundant microhymenopteran families were egg parasitoids of the families Mymaridae, Scelionidae and Trichogrammatidae, and Platygastridae. Boness (1953), who used sweep netting, ground eclectors and vegetation beating found that Chalcidoidea, the superfamily of Mymaridae and Trichogrammatidae, are the most abundant parasitoid wasps in meadows. This is consistent with Haas-Renninger et al. (2023b), which found that Chalcidoidea in general and especially Mymaridae dominated. However, Haas-Renninger et al. (2023b) found Ceraphronidae to be the family with the second largest abundance, which were found in much lower number in this study. This might be due to the different trapping methods, as Haas-Renninger et al. (2023b) used insect suction samplers. The egg-parasitoids in the families Scelionidae, Mymaridae and Trichogrammatidae show two main activities, the first between June and July and the second between August and September. This pattern was also observed by Ulrich (2005) for egg-parasitoid using emergence traps. Other endoparasitoids, such as some Braconidae, Encyrtidae and Ceraphronidae, that use various hosts,

show a high activity already in mid-May, and in the case of Platygastridae even earlier in April. In the case of Braconidae, of which around one quarter of specimens are expected in the micro fraction (Haas-Renninger et al. 2023a), the observed phenology might be due to the activity of small-sized Aphidiinae, that are parasitoids of aphids. The high abundance of Encyrtidae between June and July at Apfelberg might be due to the mass-emergence of a few species. This is for example known from the genus *Copidosoma*, which are polyembryonic parasitoids of Lepidoptera and produce a high number of offspring (Smith et al. 2017). For the families that we found in the samples but did not discuss here, their biology comprises too many different host orders or life stages of hosts (Figitidae, Aphelinidae, Eulophidae, Eupelmidae, Eurytomidae, Pteromalidae), or they occurred in numbers that were too low to see a clear phenology (Cynipidae, Ormyridae, Signiphoridae, Tetracampidae, Mymarommatidae), partly due to the fractioning process (Ichneumonidae, Torymidae, Proctotrupidae, Aculeata) (Haas-Renninger et al. 2023a).

In our study, we used size-fractioned samples to separate small-sized specimens from larger ones and focused solely on the micro fraction, as we were interested in microhymenoptera. The efficiency of the fractionator to separate Hymenoptera families has already been tested (Haas-Renninger et al. 2023a) and has shown to be very useful in terms of specimen handling and expenditure of time considering the high number of sorted Malaise trap samples in this study. Our focus on the micro fraction explains the low numbers of Ichneumonoidea and Aculeata, which are generally very numerous in whole Malaise trap samples (Srivathsan et al. 2023). Another constraint of our study is the focus on the family level. Different genera and species within a family can have different phenologies depending on the host stages they are associated with (Gaasch et al. 1998). Nevertheless, we are confident that our results can show general activity patterns of microhymenopteran families, which might be interesting not only for hymenopterists focusing on a specific family, but also for conservation management. Therefore, this might be the first step towards assessing parasitoid Hymenoptera in a long-term monitoring approach and to consider them as useful indicators for biodiversity (LaSalle and Gauld 1993; Fraser et al. 2008; Anderson et al. 2011; Stevens et al. 2013). Species of higher trophic levels such as parasitoids are at particularly high risk of extinction due to habitat loss and landscape homogenisation (Hassell 2000; Wagner et al. 2021; Klaus et al. 2023). Another critical factor is climate change which was suggested by Janzen and Hallwachs (2021) as the main driver for a decline of parasitoid Hymenoptera species richness in a protected rain forest over 34 years.

We selected our study sites dependent on the conservation value which is based on the number and conservation status of indicator species, in our case wild bees, in a specific habitat (Görn and Fischer 2011). The microhymenoptera abundance at the protected area Apfelberg showed more similar patterns to the non-protected area Weissach than to the protected area Steiner Mittelberg, where abundance was nearly twice as high. This might be due to the location of the Malaise trap at Steiner Mittelberg, where the trap was placed in a low-intensity managed meadow, between an organically cultivated field and a forest edge (Fig. 1B). Therefore, many specimens might have

been trapped while migrating from meadow to forest and vice versa, or while migrating through the corridor between field and forest, especially as the Malaise trap was oriented orthogonally to this corridor. Edges of forests are known as insect flyways (Townes 1972) and trap locations directly at such border lines can massively influence the trap result (Hausmann et al. 2020b), which is especially the case for Weissach (Fig. 1C). By contrast, the Malaise traps at Apfelberg (Fig. 1A) was placed more centrally in the meadow. As we could not see strong differences in the phenology of the different microhymenoptera families as well as the family composition between the sites, we believe that our site selection based on conservation values of wild bees together with the hierarchical cluster analysis was reasonable for the purpose of our study.

Our data set forms the baseline for microhymenoptera occurrence in low-intensity managed meadows in south-western Germany. Our pre-sorted microhymenoptera specimens are a valuable resource for taxonomical approaches, such as Large-Scale Integrative Taxonomy (LIT) (Hartop et al. 2022), which aims to enable fast and reliable species delimitation based on preliminary species hypotheses acquired through inexpensive data, such as pictures and barcodes. Parts of the microhymenoptera specimens sampled in our study have already been taxonomically treated in the project GBOL III: Dark Taxa (https://gbol.bolgermany.de/gbol3/de/gbol-dark-taxa/) resulting in new microhymenopteran species descriptions (Moser et al. 2023). With our study, we want to raise awareness for the importance of standardized long-term monitoring projects to observe population trends of insects. Our study also highlights the value of the 'black gold' of mass samples, containing an unknown diversity of microhymenoptera waiting to be discovered.

Acknowledgments

We want to thank Florian Theves for helpful comments on the first draft of this paper. We also thank the regional administrative authorities of Karlsruhe for granting sampling permissions. Funding for Maura Haas-Renninger was provided by the Ministry of Science and Art of Baden-Wuerttemberg through a graduate scholarship from the State Graduate Sponsorship Program. The Malaise trap samples were obtained from an ongoing biodiversity monitoring initiative coordinated by the LUBW (Landesanstalt für Umwelt Baden-Wuerttemberg) and funded by the state government of Baden-Wuerttemberg within the "Sonderprogramm zur Stärkung der biologischen Vielfalt". We also thank three unknown reviewers for their helpful comments.

References

Anderson A, McCormack S, Helden A, Sheridan H, Kinsella A, Purvis G (2011) The potential of parasitoid Hymenoptera as bioindicators of arthropod diversity in agricultural grasslands. Journal of Applied Ecology 48: 382–390. https://doi.org/10.1111/j.1365-2664.2010.01937.x

Battles I, Burkness E, Crossley MS, Edwards CB, Holmstrom K, Hutchison W, Ingerson-Mahar J, Owens D, Owens AC (2024) Moths are less attracted to light traps than they used to be. Journal of Insect Conservation, 12 pp. https://doi.org/10.1007/s10841-024-00588-x

Behm J (2018) Das Sonderprogramm zur Stärkung der biologischen Vielfalt. Landesanstalt für Umwelt Baden-Württemberg 2.

Boness M (1953) Die Fauna der Wiesen unter besonderer Berücksichtigung der Mahd. Ein Beitrag zur Agrarökologie. Zeitschrift für Morphologie und Ökologie der Tiere 42: 225–277. https://doi.org/10.1007/BF00412995

Brühl CA, Bakanov N, Köthe S, Eichler L, Sorg M, Hörren T, Mühlethaler R, Meinel G, Lehmann GU (2021) Direct pesticide exposure of insects in nature conservation areas in Germany. Scientific reports 11: 24144. https://doi.org/10.1038/s41598-021-03366-w

Buffington M, Gates M (2008) The Fractionator: a simple tool for mining 'Black Gold'. Skaphion 2: 1–4.

Burks R, Mitroiu M-D, Fusu L, Heraty JM, Janšta P, Heydon S, Papilloud ND-S, Peters RS, Tselikh EV, Woolley JB, van Noort S, Baur H, Cruaud A, Darling C, Haas M, Hanson P, Krogmann L, Rasplus J-Y (2022) From hell's heart I stab at thee! A determined approach towards a monophyletic Pteromalidae and reclassification of Chalcidoidea (Hymenoptera). Journal of Hymenoptera Research 94: 13–88. https://doi.org/10.3897/jhr.94.94263

DeBach P, Rosen D (1991) Biological control by natural enemies, 2nd edn. Cambridge University Press, Cambridge England, New York.

Engel MS, Ceríaco LM, Daniel GM, Dellapé PM, Löbl I, Marinov M, Reis RE, Young MT, Dubois A, Agarwal I, Lehmann A. P, Alvarado M, Alvarez N, Andreone F, Araujo-Vieira K, Ascher JS, Baêta D, Baldo D, Bandeira SA, Barden P, Barrasso DA, Bendifallah L, Bockmann FA, Böhme W, Borkent A, Brandão CR, Busack SD, Bybee SM, Channing A, Chatzimanolis S, Christenhusz MJ, Crisci JV, D'elía G, Da Costa LM, Davis SR, Lucena CA de, Deuve T, Fernandes Elizalde S, Faivovich J, Farooq H, Ferguson AW, Gippoliti S, Gonçalves FM, Gonzalez VH, Greenbaum E, Hinojosa-Díaz IA, Ineich I, Jiang J, Kahono S, Kury AB, Lucinda PH, Lynch JD, Malécot V, Marques MP, Marris JW, Mckellar RC, Mendes LF, Nihei SS, Nishikawa K, Ohler A, Orrico VG, Ota H, Paiva J, Parrinha D, Pauwels OS, Pereyra MO, Pestana LB, Pinheiro PD, Prendini L, Prokop J, Rasmussen C, Rödel M-O, Rodrigues MT, Rodríguez SM, Salatnaya H, Sampaio Í, Sánchez-García A, Shebl MA, Santos BS, Solórzano-Kraemer MM, Sousa AC, Stoev P, Teta P, Trape J-F, Dos Santos CV-D, Vasudevan K, Vink CJ, Vogel G, Wagner P, Wappler T, Ware JL, Wedmann S, Zacharie CK (2021) The taxonomic impediment: a shortage of taxonomists, not the lack of technical approaches. Zoological Journal of the Linnean Society 193: 381–387. https://doi.org/10.1093/zoolinnean/zlab072

Forbes AA, Bagley RK, Beer MA, Hippee AC, Widmayer HA (2018) Quantifying the unquantifiable: why Hymenoptera, not Coleoptera, is the most speciose animal order. BMC ecology 18: 21. https://doi.org/10.1186/s12898-018-0176-x

Fraser SE, Dytham C, Mayhew PJ (2008) The effectiveness and optimal use of Malaise traps for monitoring parasitoid wasps. Insect Conservation and Diversity 1: 22–31. https://doi.org/10.1111/j.1752-4598.2007.00003.x

Gaasch CM, Pickering J, Moore CT (1998) Flight Phenology of Parasitic Wasps (Hymenoptera: Ichneumonidae) in Georgia's Piedmont. Environmental Entomology 27: 606–614. https://doi.org/10.1093/ee/27.3.606

Gatter W, Ebenhöh H, Kima R, Gatter W, Scherer F (2020) 50-jährige Untersuchungen an migrierenden Schwebfliegen, Waffenfliegen und Schlupfwespen belegen extreme Rückgänge (Diptera: Syrphidae, Stratiomyidae; Hymenoptera: Ichneumonidae). Entomologische Zeitschrift 130: 131–142.

Geiger MF, Moriniere J, Hausmann A, Haszprunar G, Wägele W, Hebert PD, Rulik B (2016) Testing the Global Malaise Trap Program - How well does the current barcode reference library identify flying insects in Germany? Biodiversity data journal 4: e10671. https://doi.org/10.3897/BDJ.4.e10671

Görn S, Fischer K (2011) Niedermoore Nordostdeutschlands bewerten. Vorschlag für ein faunistisches Bewertungsverfahren. Naturschutz und Landschaftsplanung 43: 211–217.

Goulet H, Huber JT (1993) Hymenoptera of the world: an identification guide to families. Agriculture Canada.

Grissell EE (1999) Hymenopteran Biodiversity: Some Alien Notions. American Entomologist 45: 235–244.

Haas-Renninger M, Schwabe N, Moser M, Krogmann L (2023a) Black gold rush - Evaluating the efficiency of the Fractionator in separating Hymenoptera families in a meadow ecosystem over a two week period. Biodiversity data journal 11: e107051. https://doi.org/10.3897/BDJ.11.e107051

Haas-Renninger M, Weber J, Felske I, Kimmich T, Csader M, Betz O, Krogmann L, Steidle JL (2023b) Microhymenoptera in roadside verges and the potential of arthropod-friendly mowing for their preservation. Journal of Applied Entomology 147(10): 1035–1044. https://doi.org/10.1111/jen.13199

Hallmann CA, Sorg M, Jongejans E, Siepel H, Hofland N, Schwan H, Stenmans W, Müller A, Sumser H, Hörren T, Goulson D, Kroon H de (2017) More than 75 percent decline over 27 years in total flying insect biomass in protected areas. PLoS ONE 12(10): e0185809. https://doi.org/10.1371/journal.pone.0185809

Hallmann CA, Ssymank A, Sorg M, Kroon H de, Jongejans E (2021a) Insect biomass decline scaled to species diversity: General patterns derived from a hoverfly community. Proceedings of the National Academy of Sciences of the United States of America 118(2): e2002554117. https://doi.org/10.1073/pnas.2002554117

Hallmann CA, Ssymank A, Sorg M, Kroon H de, Jongejans E (2021b) Reply to Redlich et al.: Insect biomass and diversity do correlate, over time. Proceedings of the National Academy of Sciences of the United States of America 118(49): e2114567118. https://doi.org/10.1073/pnas.2114567118

Hartop E, Srivathsan A, Ronquist F, Meier R (2022) Towards Large-scale Integrative Taxonomy (LIT): resolving the data conundrum for dark taxa. Systematic biology 71: 1404–1422. https://doi.org/10.1093/sysbio/syac033

Hassell MP (2000) Host–parasitoid population dynamics. Journal of Animal Ecology 69: 543–566. https://doi.org/10.1046/j.1365-2656.2000.00445.x

Hausmann A, Krogmann L, Peters R, Rduch V, Schmidt S (2020a) GBOL III: Dark Taxa - iBOL Barcode Bulletin. 2020. GBOL III: dark taxa. https://doi.org/10.21083/ibol.v10i1.6242

Hausmann A, Segerer AH, Greifenstein T, Knubben J, Morinière J, Bozicevic V, Doczkal D, Günter A, Ulrich W, Habel JC (2020b) Toward a standardized quantitative and quali-

tative insect monitoring scheme. Ecology and Evolution 10: 4009–4020. https://doi.org/10.1002/ece3.6166

Heraty J (2017) Parasitoid Biodiversity and Insect Pest Management. In: Foottit RG (Ed.) Insect Biodiversity. Wiley, 603–625. https://doi.org/10.1002/9781118945568.ch19

Janzen DH, Hallwachs W (2021) To us insectometers, it is clear that insect decline in our Costa Rican tropics is real, so let's be kind to the survivors. Proceedings of the National Academy of Sciences of the United States of America 118(2) e2002546117. https://doi.org/10.1073/pnas.2002546117

Juillet JA (1964) Influence of weather on flight activity of parasitic Hymenoptera. Canadian Journal of Zoology 42: 1133–1141. https://doi.org/10.1139/z64-110

Karlsson D, Hartop E, Forshage M, Jaschhof M, Ronquist F (2020) The Swedish Malaise trap project: a 15 year retrospective on a countrywide insect inventory. Biodiversity data journal 8: e47255. https://doi.org/10.3897/BDJ.8.e47255

Klaus F, Tscharntke T, Grass I (2023) Trophic level and specialization moderate effects of habitat loss and landscape diversity on cavity-nesting bees, wasps and their parasitoids. Insect Conservation and Diversity 17(1): 65–76. https://doi.org/10.1111/icad.12688

Klein A-M, Vaissière BE, Cane JH, Steffan-Dewenter I, Cunningham SA, Kremen C, Tscharntke T (2007) Importance of pollinators in changing landscapes for world crops. Proceedings of the Royal Society B: Biological Sciences 274: 303–313. https://doi.org/10.1098/rspb.2006.3721

Klowden MJ (2013) Physiological systems in insects. Academic press. https://doi.org/10.1016/C2011-0-04120-0

LaSalle J (1993) Parasitic Hymenoptera, biological control and biodiversity. In: LaSalle J, Gauld ID (Eds) Hymenoptera and biodiversity. C.A.B. International, Wallingford, Oxon, 197–215.

LaSalle J, Gauld ID [Eds] (1993) Hymenoptera and biodiversity. C.A.B. International, Wallingford, Oxon.

LaSalle J, Gauld ID (1991) Parasitic Hymenoptera and the biodiversity crisis. Redia 74: 315–334.

Lehmann GU, Bakanov N, Behnisch M, Bourlat SJ, Brühl CA, Eichler L, Fickel T, Geiger MF, Gemeinholzer B, Hörren T, Köthe S, Lux A, Meinel G, Mühlethaler R, Poglitsch H, Schäffler L, Schlechtriemen U, Schneider FD, Schulte R, Sorg M, Sprenger M, Swenson SJ, Terlau W, Turck A, Zizka VM (2021) Diversity of Insects in Nature protected Areas (DINA): an interdisciplinary German research project. Biodiversity and Conservation 30: 2605–2614. https://doi.org/10.1007/s10531-021-02209-4

Lister BC, Garcia A (2018) Climate-driven declines in arthropod abundance restructure a rainforest food web. Proceedings of the National Academy of Sciences of the United States of America 115: E10397-E10406. https://doi.org/10.1073/pnas.1722477115

Moser M, Ulmer JM, van de Kamp T, Vasiliţa C, Renninger M, Mikó I, Krogmann L (2023) Surprising morphological diversity in ceraphronid wasps revealed by a distinctive new species of *Aphanogmus* (Hymenoptera: Ceraphronoidea). European Journal of Taxonomy 864: 146–166. https://doi.org/10.5852/ejt.2023.864.2095

Müller J, Hothorn T, Yuan Y, Seibold S, Mitesser O, Rothacher J, Freund J, Wild C, Wolz M, Menzel A (2023) Weather explains the decline and rise of insect biomass over 34 years. Nature. https://doi.org/10.1038/s41586-023-06402-z

Oksanen J, Simpson GL, Blanchet FG, Kindt R, Legendre P, Minchin PR, O'Hara RB, Solymos P, Stevens MH, Szoecs E, Wagner H, Barbour M, Bolker M, Bolker B, Borcard D, Carvalho G, Chirico M, Caceres M de, Durand S, Evangelista HB, FitzJohn R, Friendly M, Furneaux B, Hannigan G, Hill MO, Lahti L, McGlinn D, Ouellette M-H, Cunha ER, Smith T, Stier A, Braak JC ter, Weedon J (2022) vegan: Community Ecology Package. R package version 2.6-4. https://CRAN.R-project.org/package=vegan

Pilotto F, Kühn I, Adrian R, Alber R, Alignier A, Andrews C, Bäck J, Barbaro L, Beaumont D, Beenaerts N, Benham S, Boukal DS, Bretagnolle V, Camatti E, Canullo R, Cardoso PG, Ens BJ, Everaert G, Evtimova V, Feuchtmayr H, García-González R, Gómez García D, Grandin U, Gutowski JM, Hadar L, Halada L, Halassy M, Hummel H, Huttunen K-L, Jaroszewicz B, Jensen TC, Kalivoda H, Schmidt IK, Kröncke I, Leinonen R, Martinho F, Meesenburg H, Meyer J, Minerbi S, Monteith D, Nikolov BP, Oro D, Ozoliņš D, Padedda BM, Pallett D, Pansera M, Pardal MÂ, Petriccione B, Pipan T, Pöyry J, Schäfer SM, Schaub M, Schneider SC, Skuja A, Soetaert K, Spriņģe G, Stanchev R, Stockan JA, Stoll S, Sundqvist L, Thimonier A, van Hoey G, van Ryckegem G, Visser ME, Vorhauser S, Haase P (2020) Meta-analysis of multidecadal biodiversity trends in Europe. Nature communications 11: 3486. https://doi.org/10.1038/s41467-020-17171-y

R Core Team (2021) R: A language and environment for statistical computing. https://www.R-project.org/

Redlich S, Steffan-Dewenter I, Uhler J, Müller J (2021) Hover flies: An incomplete indicator of biodiversity. Proceedings of the National Academy of Sciences of the United States of America 118(49): e2112619118. https://doi.org/10.1073/pnas.2112619118

Sánchez-Bayo F, Wyckhuys KA (2019) Worldwide decline of the entomofauna: A review of its drivers. Biological Conservation 232: 8–27. https://doi.org/10.1016/j.biocon.2019.01.020

Schindler M, Diestelhorst O, Haertel S, Saure C, Scharnowski A, Schwenninger HR (2013) Monitoring agricultural ecosystems by using wild bees as environmental indicators. BioRisk 8: 53–71. https://doi.org/10.3897/biorisk.8.3600

Schöfer N, Ackermann J, Hoheneder J, Hofferberth J, Ruther J (2023) Sublethal Effects of Four Insecticides Targeting Cholinergic Neurons on Partner and Host Finding in the Parasitic Wasp *Nasonia vitripennis*. Environmental toxicology and chemistry 42: 2400–2411. https://doi.org/10.1002/etc.5721

Schwan H, Sorg M, Stenmans W (1993) Naturkundliche Untersuchungen zum Naturschutzgebiet Die Spey (Stadt Krefeld, Kreis Neuss). I. Untersuchungsstandorte und Methoden. Natur am Niederrhein (NF) 8: 1–13.

Seibold S, Gossner MM, Simons NK, Blüthgen N, Müller J, Ambarlı D, Ammer C, Bauhus J, Fischer M, Habel JC, Linsenmair KE, Nauss T, Penone C, Prati D, Schall P, Schulze E-D, Vogt J, Wöllauer S, Weisser WW (2019) Arthropod decline in grasslands and forests is associated with landscape-level drivers. Nature 574: 671–674. https://doi.org/10.1038/s41586-019-1684-3

Shaw MR, Hochberg ME (2001) The Neglect of Parasitic Hymenoptera in Insect Conservation Strategies: The British Fauna as a Prime Example. Journal of Insect Conservation 5: 253–263. https://doi.org/10.1023/A:1013393229923

Smith MS, Shirley A, Strand MR (2017) *Copidosoma floridanum* (Hymenoptera: Encyrtidae) Rapidly Alters Production of Soldier Embryos in Response to Competition. Annals of the Entomological Society of America 110: 501–505. https://doi.org/10.1093/aesa/sax056

Srivathsan A, Ang Y, Heraty JM, Hwang WS, Jusoh WF, Kutty SN, Puniamoorthy J, Yeo D, Roslin T, Meier R (2023) Convergence of dominance and neglect in flying insect diversity. Nature Ecology & Evolution 7: 1012–1021. https://doi.org/10.1038/s41559-023-02066-0

Ssymank A, Sorg M, Doczkal D, Rulik B, Merkel-Wallner G, Vischer-Leopold M (2018) Praktische Hinweise und Empfehlungen zur Anwendung von Malaisefallen für Insekten in der Biodiversitätserfassung und im Monitoring. Series Naturalis 1. http://www.entomologica.org/sn/naturalis2018_1.pdf

Staab M, Gossner MM, Simons NK, Achury R, Ambarlı D, Bae S, Schall P, Weisser WW, Blüthgen N (2023) Insect decline in forests depends on species' traits and may be mitigated by management. Communications biology 6: 338. https://doi.org/10.1038/s42003-023-04690-9

Stevens NB, Rodman SM, O'Keeffe TC, Jasper DA (2013) The use of the biodiverse parasitoid Hymenoptera (Insecta) to assess arthropod diversity associated with topsoil stockpiled for future rehabilitation purposes on Barrow Island, Western Australia. Records of the Western Australian Museum, Supplement 83: 355. https://doi.org/10.18195/issn.0313-122x.83.2013.355-374

Thomas JA (2005) Monitoring change in the abundance and distribution of insects using butterflies and other indicator groups. Philosophical Transactions of the Royal Society B: Biological Sciences 360: 339–357. https://doi.org/10.1098/rstb.2004.1585

Townes H (1972) A light-weight Malaise trap. Entomological news 83: 239–247.

Turley NE, Biddinger DJ, Joshi NK, López-Uribe MM (2022) Six years of wild bee monitoring shows changes in biodiversity within and across years and declines in abundance. Ecology and Evolution 12:e9190. https://doi.org/10.1002/ece3.9190

Twerd L, Banaszak-Cibicka W, Sobieraj-Betlińska A, Waldon-Rudzionek B, Hoffmann R (2021) Contributions of phenological groups of wild bees as an indicator of food availability in urban wastelands. Ecological Indicators 126: 107616. https://doi.org/10.1016/j.ecolind.2021.107616

Uhler J, Redlich S, Zhang J, Hothorn T, Tobisch C, Ewald J, Thorn S, Seibold S, Mitesser O, Morinière J, Bozicevic V, Benjamin CS, Englmeier J, Fricke U, Ganuza C, Haensel M, Riebl R, Rojas-Botero S, Rummler T, Uphus L, Schmidt S, Steffan-Dewenter I, Müller J (2021) Relationship of insect biomass and richness with land use along a climate gradient. Nature communications 12: 5946. https://doi.org/10.1038/s41467-021-26181-3

Ulrich W (2000) Influence of weather conditions on populations of parasitic Hymenoptera in a beech forest on limestone. Polish Journal of Entomology 69: 47–64.

Ulrich W (2005) Die Hymenopteren einer Wiese auf Kalkgestein: Ökologische Muster einer lokalen Tiergemeinschaft. Schriftenreihe Forschungszentrum Waldökosysteme A 195, Göttingen.

Wagner DL, Grames EM, Forister ML, Berenbaum MR, Stopak D (2021) Insect decline in the Anthropocene: Death by a thousand cuts. Proceedings of the National Academy of Sciences of the United States of America 118(2): e2023989118. https://doi.org/10.1073/pnas.2023989118

Welti EA, Zajicek P, Frenzel M, Ayasse M, Bornholdt T, Buse J, Classen A, Dziock F, Engelmann RA, Englmeier J, Fellendorf M, Förschler MI, Fricke U, Ganuza C, Hippke M, Hoenselaar G, Kaus-Thiel A, Kerner J, Kilian D, Mandery K, Marten A, Monaghan MT, Morkel C, Müller J, Puffpaff S, Redlich S, Richter R, Rojas-Botero S, Scharnweber T, Scheiffarth G, Yáñez PS, Schumann R, Seibold S, Steffan-Dewenter I, Stoll S, Tobisch C,

Twietmeyer S, Uhler J, Vogt J, Weis D, Weisser WW, Wilmking M, Haase P (2021) Temperature drives variation in flying insect biomass across a German malaise trap network. Insect Conservation and Diversity 15(2): 168–180. https://doi.org/10.1111/icad.12555

Westrich P, Schwenninger HR, Herrmann M, Klatt M, Klemm M, Prosi R, Schanowski A (2000) Rote Liste der Bienen Baden-Württembergs. Naturschutz-Praxis, Artenschutz 4.

Westrich P, Frommer U, Mandery K, Riemann H, Ruhnke H, Saure C, Voith J (2011) Rote Liste und Gesamtartenliste der Bienen (Hymenoptera, Apidae) Deutschlands. 5. Fassung. Naturschutz und Biologische Vielfalt 70(3): 373–416.

Yang LH, Gratton C (2014) Insects as drivers of ecosystem processes. Current Opinion in Insect Science 2: 26–32. https://doi.org/10.1016/j.cois.2014.06.004

Zizka VM, Geiger MF, Hörren T, Kirse A, Noll NW, Schäffler L, Scherges AM, Sorg M (2022) Repeated subsamples during DNA extraction reveal increased diversity estimates in DNA metabarcoding of Malaise traps. Ecology and Evolution 12: e9502. https://doi.org/10.1002/ece3.9502

Supplementary material 1

Supplementary information

Authors: Maura Haas-Renninger, Sonia Bigalk, Tobias Frenzel, Raffaele Gamba, Sebastian Görn, Michael Haas, Andreas Haselböck, Thomas Hörren, Martin Sorg, Ingo Wendt, Petr Janšta, Olaf Zimmermann, Johannes L. M. Steidle, Lars Krogmann

Data type: docx

Explanation note: **figure S1.** Conservation value for study sites based on wild bee species occurrence. **figure S2.** Cluster dendrogram for wild bee species presence at twelve different study sites. **figure S3.** Composition of microhymenoptera families in the micro fractions of Malaise trap samples from three study sites in Baden-Wuerttemberg, south-western Germany. **figure S4.** Seasonal abundance of different microhymenoptera families from Malaise traps at three study sites in Baden-Wuerttemberg, south-western Germany. **table S1.** Study sites in Baden-Wuerttemberg, Germany, that were sampled in 2019 within the insect monitoring project "Aerial Biomass". **table S2.** Area proportions of land use of the three study sites in a 500 m radius around the Malaise trap. **table S3.** Model selection table of linear models for diversity of microhymenoptera families.

Link: https://doi.org/10.3897/jhr.97.128234.suppl1

JHR 97: 721–739 (2024)
doi: 10.3897/jhr.97.127500
https://jhr.pensoft.net

RESEARCH ARTICLE

JOURNAL OF Hymenoptera RESEARCH
A peer-reviewed open-access journal
The International Society of Hymenopterists

Solitary folded-winged wasps of the genus *Zethus* Fabricius (Vespidae, Zethinae) parasitised by two new species of Strepsiptera on different continents

Daniel Benda[1,2], Hans Pohl[3], Rolf Beutel[3], Jakub Straka[2]

1 *Department of Entomology, National Museum of the Czech Republic, Prague, Czech Republic* **2** *Department of Zoology, Faculty of Science, Charles University, Prague, Czech Republic* **3** *Institut für Zoologie und Evolutionsforschung, Friedrich-Schiller-Universität, Jena, Germany*

Corresponding author: Daniel Benda (benda.daniel@email.cz)

Academic editor: Michael Ohl | Received 14 May 2024 | Accepted 11 August 2024 | Published 9 September 2024

https://zoobank.org/F340D011-940A-47BB-9A5B-78D9B3DE1833

Citation: Benda D, Pohl H, Beutel R, Straka J (2024) Solitary folded-winged wasps of the genus *Zethus* Fabricius (Vespidae, Zethinae) parasitised by two new species of Strepsiptera on different continents. Journal of Hymenoptera Research 97: 721–739. https://doi.org/10.3897/jhr.97.127500

Abstract

Two new species of Strepsiptera from the genus *Zethus* Fabricius, 1804 (Hymenoptera: Vespidae) are described. Although the stylopisation of the genus *Zethus* has been known for almost a century, we provide the first description of its strepsipteran parasites. *Zethus brasiliensis fuscatus* R. Bohart & Stange, 1965 is parasitised by *Eupathocera zethi* **sp. nov.** in the Neotropical Region (French Guiana) and *Zethus favillaceus* Walker, 1871 by *Deltoxenos impressus* **sp. nov.** in the Afrotropical Region (Kenya). An independent switch to the same host genus is supported by molecular and morphological data. Diagnoses and detailed descriptions of the species are provided based on characters of the female cephalothorax and male cephalotheca. Diagnostic characters are discussed.

Keywords

Cephalothorax, morphology, parasite association, Strepsiptera, taxonomy, wasp parasites, *Zethus*

Introduction

Zethus Fabricius, 1804 is the most species-rich genus in Vespidae and comprises 279 out of the 363 species of Zethini (Lopes et al. 2021). Although a recent phylogenomic study supported the subfamily status of Zethinae as sister to Polistinae + Vespinae

(Piekarski et al. 2018), the original "Zethini" were revealed as a paraphyletic grouping with two major clades Raphiglossinae and Zethinae (Bank et al. 2017). The close phylogenetic relationship between Zethinae and Polistinae + Vespinae also has implications for the interpretation of the evolution of traits such as nest-building (Bank et al. 2017). Polistinae and Vespinae are well known for building nests from paper-like material (Evans and West-Eberhard 1970). Intriguingly, some members of Zethinae use old insect burrows in twigs, branches or in the ground, which is possibly an ancestral behaviour. However, other species in the subfamily construct new nests from masticated and salivated plant material (usually leaves) pasted together with a resinous substance (Bohart and Stange 1965). Advanced nesting behaviour has arguably contributed to the evolutionary success of Polistinae and Vespinae after their solitary ancestors evolved the ability to exploit masticated and salivated plant material for constructing nests (Bank et al. 2017). Some species of Zethinae even have preserved a plesiomorphic form of social behaviour, with several females sharing a nest but each one tending their own brood, but with complex interactions such as nest usurpation, nest defence, or adoption of orphaned nests (Lopes and Noll 2014; Kelstrup et al. 2023).

The genus *Zethus* is widespread throughout the New World and the Ethiopian and Oriental Regions (Nguyen and Carpenter 2017). It reaches its greatest diversity in the Neotropics, where over 230 species are known (Tan et al. 2018). The genus is characterised by the following features: propodeum with elongate orifice and acutely pointed dorsally, propodeal valvula elongate and quadrate, separate from propodeal lamella; labial palp four-segmented; mid-tibia usually with two spurs (Bohart and Stange 1965; Nguyen and Carpenter 2017; Tan et al. 2018). A recent cladistic analysis based on morphological characters supported 9 subgenera within the genus *Zethus* (Lopes et al. 2021).

Regarding interactions with other organisms, only fragmentary information is available on parasites of *Zethus* species. Pereira et al. (2018) reported 8 genera of phoretic and parasitic mites (Acari) found on *Zethus*. Salt (1927) and Salt and Bequaert (1929) recorded *Zethus pubescens* Smith, 1857, *Z. spinipes variegatus* Saussure, 1852, and *Z. romandinus* Saussure, 1852) as hosts of Strepsiptera. Almost a century later Benda et al. (2019) recorded stylopised *Zethus* sp. from French Guiana. The undescribed strepsipteran species was assigned to *Pseudoxenos* Saunders, 1872 (Xenidae), following the traditional taxonomy of Strepsiptera with species parasitising solitary wasps included in this genus. Benda et al. (2021) published a molecular phylogeny of Xenidae based on an extended dataset with a focus on species diversity. They recorded *Zethus brasiliensis fuscatus* R. Bohart & Stange, 1965 as a host for an undescribed putative species of *Pseudoxenos*. Benda et al. (2022b) published a new generic classification of Xenidae and included the undescribed species from *Z. brasiliensis fuscatus* in the genus *Eupathocera* Pierce, 1908 which was restituted from synonymy.

In the present study we describe two new species of Strepsiptera from two host species from two continents, *Z. brasiliensis fuscatus* and *Z. favillaceus* Walker, 1871. We provide diagnoses and descriptions of the species in accordance with a previous phylogenetic study (Benda et al. 2021) and an updated generic classification based on characters of the female cephalothorax and male cephalotheca Benda et al. (2022b).

Materials and methods

Taxon sampling

The material of Strepsiptera from *Zethus brasiliensis fuscatus* and *Z. favillaceus* comprised a total of 11 females, 3 empty male puparia and 1 occupied male puparium. Material from the following public and private collections was examined:

NMPC National Museum of the Czech Republic, Prague, Czech Republic;
OLML Oberösterreichisches Landesmuseum, Linz, Austria;
YNPC Yuta Nakase personal collection, Matsumoto, Japan.

Fixation and preparation

The host individuals were relaxed in water vapour and then immediately dissected. The dissected endoparasitic female and male puparium were removed from the host body and cleared using a mixture of lysis buffer ATL and proteinase K (Qiagen) at 56 °C for several hours. The cleared specimen was cleaned in distilled water several times and then stored in a vial with 96% ethanol. The female cephalothorax was air-dried or dried by using absolute ethanol and hexamethyldisilazane (HMDS method) (Heraty 1998) to prevent the cuticle from collapsing during the drying process. The female body was extracted from the cephalothorax before drying. After this step, the dried specimens were glued onto card mounting points, which were pinned afterwards.

Measurements

The width and length of the female cephalothorax, the female head capsule and the male cephalotheca were measured using a Leica S9D Stereomicroscope with a calibrated ocular micrometer. The cephalothorax length was measured from the apex of the clypeal lobe to the constriction of abdominal segment I; the cephalothorax width is the maximum distance between its lateral margins.

Photomicrography

The general habitus of stylopised host specimens and the host abdomen with protruding strepsipterans were documented with multifocus images, taken with Canon EOS 550D or 70D cameras equipped with EF 50 mm and MP-E 65 mm macro lenses. Lateral lights and a diffuser were used.

For the documentation of the original colouration of the female larval cephalothorax and the male cephalotheca, specimens glued to card mounting points were used. They were photographed with a Canon EOS 7D digital SLR equipped with a Canon MP-E 65 mm macro lens (Canon, Krefeld, Germany) fitted with a StackShot macro rail (Cognisys, Traverse City, MI, USA). Each specimen was illuminated with two

flashlights (Yongnuo Photographic Equipment, Shenzhen, China) fitted to a transparent cylinder for even and soft light. For the documentation of tiny structures on the head capsule, we used a Canon EOS 70D camera attached to an Olympus BX40 microscope. The microscope was equipped with lateral lights and a diffuser. Zerene Stacker (Zerene Systems LLC, Richland, USA) was used to process stacks of images with different focus.

Scanning electron microscopy (SEM)

Dried female cephalothoraces glued to card points were mounted on a rotatable specimen holder (Pohl 2010). Each specimen was sputter coated with gold with an Emitech K 500 (Sample preparation division, Quorum Technologies Ltd., Ashford, England). The SEM micrographs were taken with an ESEM XL30 (Philips, Amsterdam, Netherlands) equipped with Scandium FIVE (Olympus, Münster, Germany).

Image processing

All images were processed and arranged into plates with Adobe Photoshop® CS5 (Adobe System Incorporated, San Jose, USA) software. CorelDraw® X8 (CorelDraw Corporation, Ottawa, ON, Canada) was used for the lettering of the plates.

Terminology and description style

The terminology used for the female cephalothorax was adopted from Benda et al. (2022), Richter et al. (2017), Löwe et al. (2016), and Kinzelbach (1971a). The cephalothorax is described in morphological orientation in figures, although its functional orientation in the host's body is inverted.

Results

***Eupathocera zethi* Benda & Straka, sp. nov.**
https://zoobank.org/8AD765DD-069C-44E2-BAAA-46020E29AC56

Type material. ***Holotype*** • French Guiana: 1♀; Cayenne, Roura env., 18 Oct. 2015; Naoki Ogawa leg.; NMPC; host: *Zethus brasiliensis fuscatus* R. Bohart & Stange, 1965.

Paratypes • French Guiana: 1♀; same host specimen (collection data) as for holotype, 18 Oct. 2015; Naoki Ogawa leg.; YNPC; 1♀ + 1 empty male puparium (EMP), 2♀; 35 km S of Roura, Relais de Patawa, 16 July 2000; Ji. Kadlec leg.; OLML; same host species as holotype; 1♀; NE Mount de Kaw Fourgassie, 5. Aug. 2006; M. Snížek; OLML; same host species as holotype.

Diagnosis of female cephalothorax. This species is diagnosed by a combination of characters. It differs from all remaining species of *Eupathocera* by the presence of very

conspicuously imprinted mesal furrows indicating the pro-mesothoracic and meso-metathoracic borders on the ventral side (sbpm, sbmm; Figs 1C, 2A), and inconspicuous mandibles fused with the labial area and bearing a rounded (not distinctly raised) mandibular bulge (mdb; Fig. 3E). The clypeal surface is completely smooth with distinctly exposed sensilla, in contrast to *Eupathocera luctuosae* Pierce, 1911 and *E. insularis* (Kifune, 1983), which display a wrinkled, lamellar clypeal area, with scarcely visible sensilla. The number of clypeal sensilla is very high in the new species, more than 60. A larger number occurs only in species utilising *Sphex* L., 1758 – *Eupathocera fuliginosi* (Brethes, 1923) (more than 60) and *E. westwoodi* (Templeton, 1841) (more than 80). The border between the clypeal area and frontal region is indistinct in comparison to *Eupathocera luctuosae* Pierce, 1911 and *E. insularis* (Kifune, 1983) where it is clearly recognisable.

Description of female cephalothorax. ***Shape and colouration.*** Size of holotype cephalothorax: length 1.8 mm, width 1.74 mm; slightly variable, as long as wide or slightly wider than long, length 1.78–2.03 mm, width 1.74–1.83 mm. Abdominal segment I not protruding laterally, corner below spiracles rounded. Anterior head margin rounded, not protruding from head capsule. Thorax slightly widening posteriorly. Colouration of cephalothorax mostly dark with light brown pattern on ventral side, but mostly light brown dorsomedially with specific contrast pattern.

Head capsule. Approximately ⅓ as long as entire cephalothorax including lateral extensions. Colouration mostly dark with specific pattern with paler lateral extensions, mandibular bases and ventral labral field. Clypeal area distinctly delimited from labral area. Clypeal lobe rather indistinct but visible. Clypeal surface completely smooth with distinctly exposed sensilla. Number of clypeal sensilla slightly over 60. Border between clypeal and frontal region indistinct but still present. Frontal region smooth or very slightly wrinkled (fr, Fig. 2F). Segmental border between head and prothorax indicated by dark transverse stripe on dorsal side (sbhp, Fig. 1D), in SEM pictures visible by change in cuticular sculpture (sbhp, Fig. 3B). Head and prothorax distinctly separated by birth opening ventromedially (bo, Fig. 3A) and laterally by suture (sbhp, Fig. 3A).

Supra-antennal sensillary field. Smooth or very slightly wrinkled, with dispersed sensilla (Fig. 2C, D). Not distinctly delimited by furrow medially, but border marked by different surface structure of supra-antennal sensillary field and smooth frontal region (Fig. 3B).

Antenna. Vestigial antenna bulging, preserved as more or less clearly defined area, with distinct plates (pra, Fig. 2C, D). Antennal torulus reduced (Fig. 2C, D). Periantennal area expanded, smooth (paa, Fig. 2C, D). Distance between antennal area and supra-antennal sensillary field relatively large.

Labrum. Ventral field wider than long, elliptic, completely smooth, shiny, and pale, contrasting with dark dorsal labral field and labium. Dorsal labral field slightly arcuate, 5× wider than long in midline. Setae on dorsal field blunt, sensilla-like, spines lacking.

Mandible. Anteromedially directed at an angle of 30°, enclosed in mandibular capsule. Mandibular bulge not distinctly raised, rounded, with several inconspicuous sensilla. Cuticle of mandible smooth posteriorly, with longitudinal grooves dorsolaterally (md; Fig. 3E, F). Mandibular tooth narrow, anteriorly oriented, with or without spines (mdt; Fig. 3E, F).

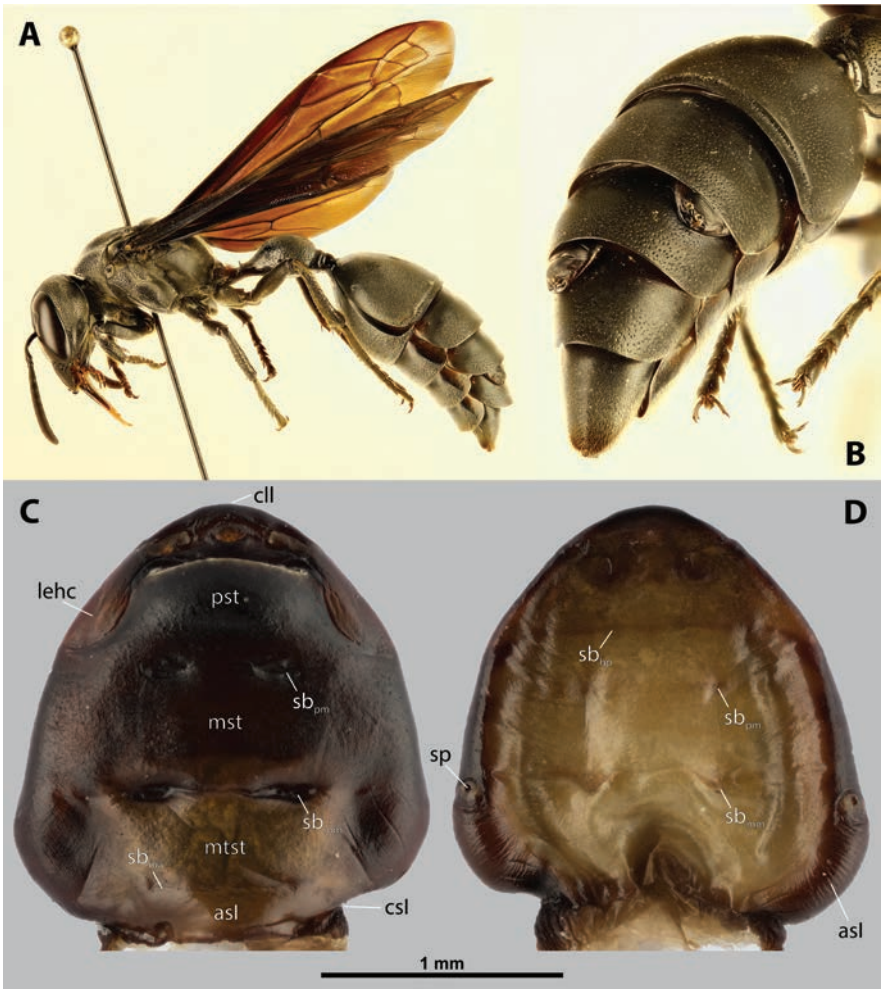

Figure 1. *Eupathocera zethi* Benda & Straka, sp. nov., host, female cephalothorax **A** *Zethus brasiliensis fuscatus* R. Bohart & Stange, 1965 stylopised by *E. zethi* sp. nov., lateral view **B** detail of host abdomen of *Z. brasiliensis fuscatus*, with two female cephalothoraces **C–D** holotype of *E. zethi* sp. nov., ♀ (NMPC) from *Z. brasiliensis fuscatus* **C** ventral side of cephalothorax **D** dorsal side of cephalothorax. Abbreviations: asI – abdominal segment I, cll – clypeal lobe, csI – constriction of abdominal segment I, lehc – lateral extension of head capsule, mst – mesosternum, mtst – metasternum, pst – prosternum (prosternal extension), sbhp – segmental border between head and prothorax, sbma – segmental border between metathorax and abdomen, sbmm – segmental border between mesothorax and metathorax, sbpm – segmental border between prothorax and mesothorax, sp – spiracle.

Maxilla. Distinctly reduced and only very slightly protruding, not projecting beyond mandible anteriorly. Partially fused to labial area, both regions not clearly separated. Cuticle reticulated, with smooth areas, not distinctly wrinkled (mx; Fig. 3E, F). Vestige of palp inconspicuous, forming small bulge with impression, located medially on ventral side of maxilla. Submaxillary groove indistinctly produced posterolaterally towards maxillary base.

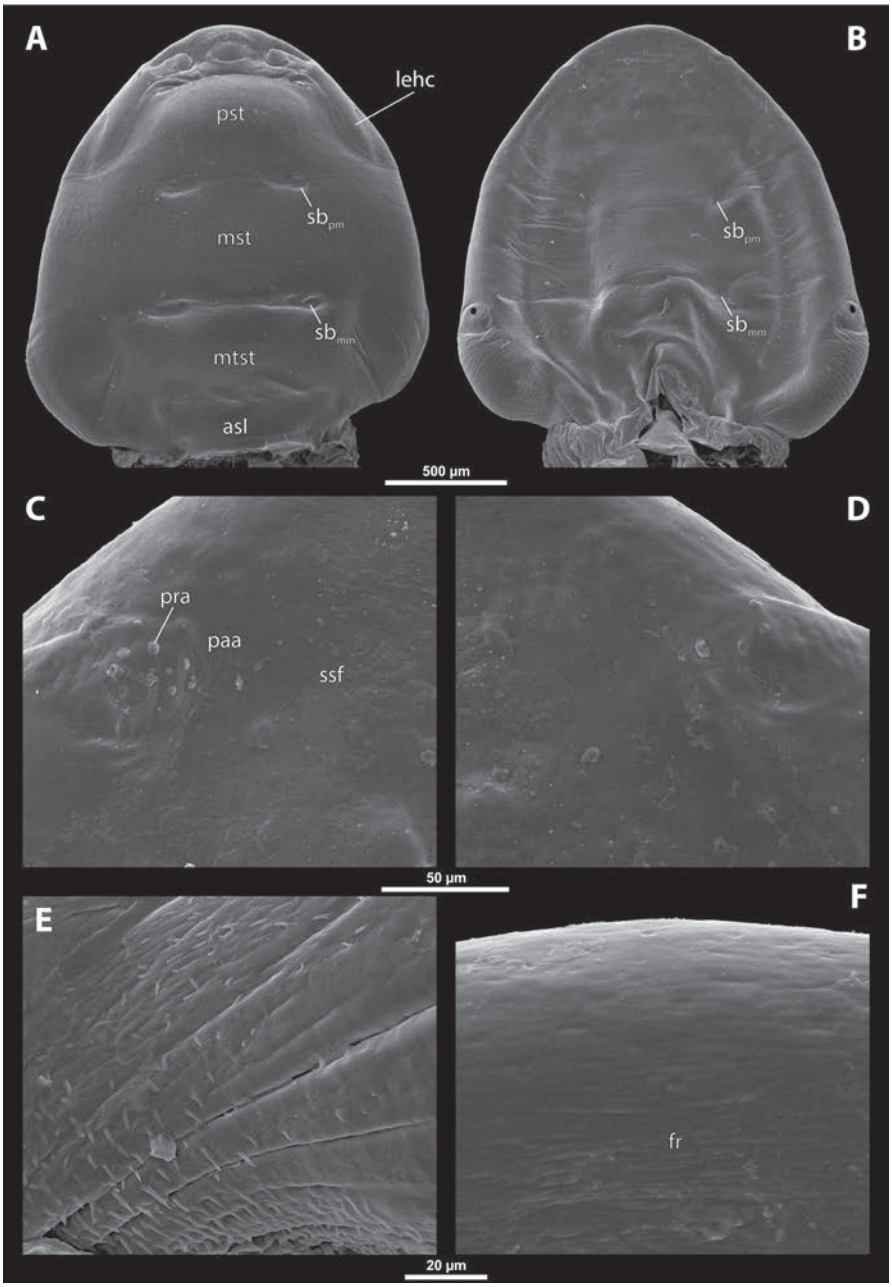

Figure 2. Holotype of *Eupathocera zethi* Benda & Straka, sp. nov., ♀ (NMPC), SEM micrographs of cephalothorax **A** ventral side **B** dorsal side **C** right vestigial antenna, dorsal side **D** left vestigial antenna, dorsal side **E** left lateral border of abdominal segment I below spiracle, dorsal side **F** detail of anterior border of cephalothorax, dorsal side. Abbreviations: asI – abdominal segment I, fr – frontal region, lehc – lateral extension of head capsule, mst – mesosternum, mtst – metasternum, paa – periantennal area, pra – plate of vestigial antenna, pst – prosternum (prosternal extension), sbmm – segmental border between mesothorax and metathorax, sbpm – segmental border between prothorax and mesothorax, ssf – supra-antennal sensillary field.

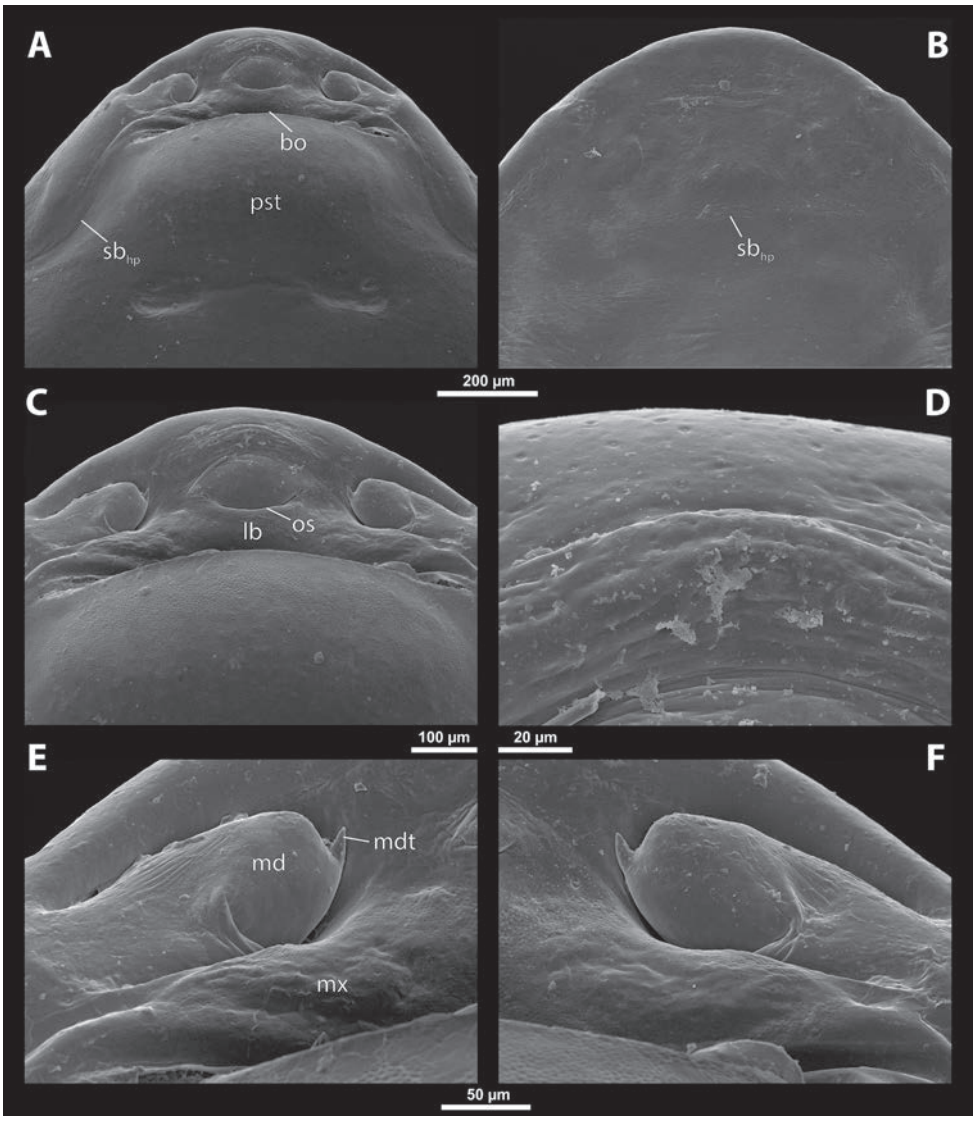

Figure 3. Holotype of *Eupathocera zethi* Benda & Straka, sp. nov., ♀ (NMPC), SEM micrographs of cephalothorax **A** anterior part of cephalothorax, ventral side **B** anterior part of cephalothorax, dorsal side **C** mouthparts, ventral side **D** detail of anterior border of cephalothorax, ventral side **E** right mandible and maxilla, ventral side **F** left mandible and maxilla, ventral side. Abbreviations: bo – birth opening, lb – labial area, md – mandible, mdt – mandibular tooth, mx – vestige of maxilla (maxilla), pst – prosternum (prosternal extension), os – mouth opening, sbhp – segmental border between head and prothorax.

Labium. Labial area not distinctly recognisable between maxillae, flat, slightly longer than wide in midline (lb; Fig. 3C). Anteriorly delimited by mouth opening, posteriorly by birth opening. Cuticular surface very slightly reticulated.

Mouth opening. Slightly arcuate, sclerotised along margin (os; Fig. 3C).

***Thorax*.** Pro-mesothoracic and meso-metathoracic borders distinct on ventral side, separated by mesal furrows (sbpm, sbmm; Figs 1C, 2A). On dorsal side separated by less conspicuous dark mesal furrows (sbpm, sbmm; Figs 1D, 2B). Border between metathorax and abdomen marked by change in cuticular surface structure or pigmentation. Cuticle of thoracic segments reticulate on ventral side, often with scattered small papillae. Dorsal side of thorax predominantly smooth, only slightly wrinkled. Prosternal extension undifferentiated. Prosternum bulging, distinctly elevated above head medially and laterally (pst; Fig. 3A). Shape of meso- and metathorax unmodified, transverse. Prosternum and mesosternum on ventral side with dark colouration, but metasternum medially pale. All thoracic segments pale on dorsal side, but dark laterally.

***Abdominal segment I and spiracles*.** Setae and cuticular spines present on lateral region of abdominal segment I (Fig. 2E). Spiracles on posterior ~ ⅓ of cephalothorax slightly elevated, with anterolateral or anterodorsal orientation. Cephalothoracic part of abdominal segment I below spiracles dark on dorsal side, medially paler on ventral side (asI; Figs 1C, 2A).

Etymology. The name refers to the host genus *Zethus*. From Greek *Zethus* – the son of Zeus in ancient Greek mythology. Adjective.

***Deltoxenos impressus* Benda & Straka, sp. nov.**
https://zoobank.org/9FE257A5-8010-4607-9285-7364594430E2

Type material. *Holotype*. Kenya • 1♀; Mwingi, Kangonde vadi, 18 Apr. 2007; M. Halada leg.; OLML; host: *Zethus favillaceus* Walker, 1871.

***Paratypes*.** Kenya • 2♀; 1♀ + 2 empty male puparia; 1♀ + 1 male puparium; 1♀ + 1 male puparium + 2 empty male puparia; same locality and host as for holotype, 18 Apr. 2007; M. Halada leg.; OLML.

Diagnosis of female cephalothorax. This species is easily distinguished from other representatives of the genus *Deltoxenos* by mandibles distinctly anteromedially directed (angle of 65°) and by conspicuous impressions on the surface of the lateral extensions at the site of the reduced compound eyes. These impressions are best visible on SEM images (im; Fig. 6A) but also recognizable with a light microscope. The surface of the lateral extensions is slightly wrinkled or smooth in other species of *Deltoxenos*. The anterior head margin is rounded, and the clypeal lobe is merged with the head capsule, in contrast to *Deltoxenos rueppelli* (Kinzelbach, 1971), where the clypeal lobe protrudes distinctly from the head capsule but is blunted on top. On the ventral side the clypeal area is very smooth and lacks sensilla (cl; Fig. 6D), whereas sensilla are present ventrally in *Deltoxenos bidentatus* (Pasteels, 1950) and *D. rueppelli*. In contrast to *Deltoxenos bequaerti* (Luna de Carvalho, 1956), the cuticle of the thoracic segments on the ventral side is reticulate, with scattered inconspicuous or more distinct and pigmented papillae, mainly visible on the metasternum. In contrast, the thoracic segments on the ventral side are evenly scattered with conspicuous papillae in *D. bequaerti*.

Other characters that distinguish *D. impressus* sp. nov. from *D. bidentatus* and *D. rueppelli*: ventral field wider than long, elliptic, nearly circular versus more flattened and not nearly circular; dorsal field arcuate, slightly raised versus dorsal field distinctly arcuate and distinctly raised; mandible anteromedially directed at angle of 65° versus a maximum of 45° in *D. rueppelli*; mandibular bulge distinctly raised, elongated, slightly curved laterally versus mandibular bulge slightly raised and anteriorly directed; cuticle of mandible completely smooth versus almost completely wrinkled.

Description of female cephalothorax. ***Shape and colouration.*** Size of holotype cephalothorax: length 1.06 mm, width 0.9 mm. Cephalothorax variable in size but always distinctly longer than wide, length 0.9–1.06 mm, width 0.74–0.9 mm. Promesothoracic and meso-metathoracic segmental border only slightly constricted laterally (Fig. 4C, D). Abdominal segment I not protruding laterally, corner below spiracles rounded. Anterior head margin rounded, not distinctly protruding from remaining head capsule. Thorax elongated, very slightly widening posteriorly. Cephalothorax with conspicuously contrasting light and dark colour pattern.

Head capsule. Ca ⅔ as long as entire cephalothorax including lateral cephalic extension. Colouration forming specific pattern with dark brown anterior part and pale lateral extensions. Surface of lateral extensions at site of reduced compound eyes smooth, with conspicuous impressions visible on SEM images (im; Fig. 6A). Clypeal area well delimited from labral area, arcuate, clypeal lobe merged with head capsule. Surface completely smooth with slightly more than 40 distinctly exposed sensilla on dorsal side (cls; Fig. 5F). Ventral side of clypeal area smooth and lacking sensilla (cl; Fig. 6D). Border between clypeal and frontal region indistinct but still present. Frontal region smooth (fr; Fig. 6B). Segmental border between head and prothorax indicated by distinct mesal furrow on dorsal side (sbhp; Fig. 6B) and by dorsal transverse stripe of frontal and occipital papillae (p; Fig. 6B). Head and prothorax distinctly separated by birth opening ventromedially (bo; Fig. 6A) and laterally by suture (sbhp; Fig. 6A).

Supra-antennal sensillary field. Completely smooth, with dispersed sensilla (Fig. 2C, D). Distinctly delimited by furrow on medial side (fssf; Fig. 6B), surface of supra-antennal sensillary field and frontal region with same sculpture.

Antenna. Preserved as poorly defined area, with several distinct rounded plates and an inconspicuous cavity (Fig. 5C, D). Antennal torulus reduced. Periantennal area expanded, smooth (paa; Fig. 5C, D). Border between antennal area and supra-antennal sensillary field indistinct.

Labrum. Ventral field wider than long, elliptic, nearly circular. Dorsal field arcuate, slightly raised, laterally narrower than medially, 6× wider than long in midline (vlf, dlf; Fig. 6C, D). Dorsal field with 16 sensilla inserted in cavities.

Mandible. Mandibles anteromedially directed at angle of 65°, enclosed in mandibular capsule. Mandibular bulge distinctly raised, elongated, slightly curved laterally, with several sensilla (mdb; Fig. 6E, F). Cuticle of mandible completely smooth. Mandibular tooth slightly curved, pointed apically, almost completely lacking spines (mdt; Fig. 6E, F).

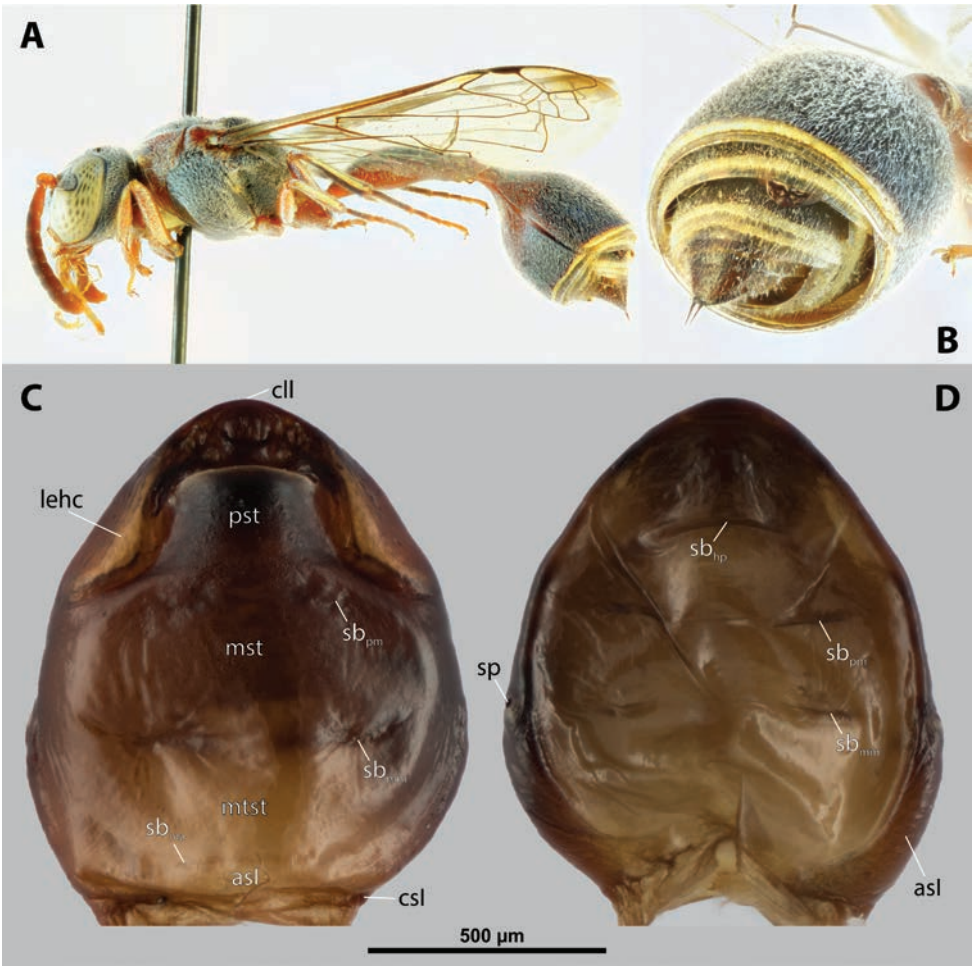

Figure 4. *Deltoxenos impressus* Benda & Straka, sp. nov., host, female cephalothorax **A** *Zethus favillaceus* Walker, 1871 stylopised by *D. impressus* sp. nov., lateral view **B** detail of host abdomen of *Z. favillaceus*, with female cephalothorax **C–D** holotype of *D. impressus* sp. nov., ♀ (OLML) from *Z. favillaceus* **C** ventral side of cephalothorax **D** dorsal side of cephalothorax. Abbreviations: asI – abdominal segment I, cll – clypeal lobe, csI – constriction of abdominal segment I, lehc – lateral extension of head capsule, mst – mesosternum, mtst – metasternum, pst – prosternum (prosternal extension), sbhp – segmental border between head and prothorax, sbma – segmental border between metathorax and abdomen, sbmm – segmental border between mesothorax and metathorax, sbpm – segmental border between prothorax and mesothorax, sp – spiracle.

Maxilla. Only slightly raised, almost fused with labial area (mx; Fig. 6C). Cuticle smooth, with longitudinal furrow. Apical maxillary region not projecting beyond mandibular apex. Basal part firmly connected with labium and not overlapping with mandible (mxb; Fig. 6C). Vestige of palp indistinct. Maxillary base distinctly produced anterolaterally as submaxillary groove. Space between prothoracic extension and head extended (sbhp, mxb; Fig. 6A).

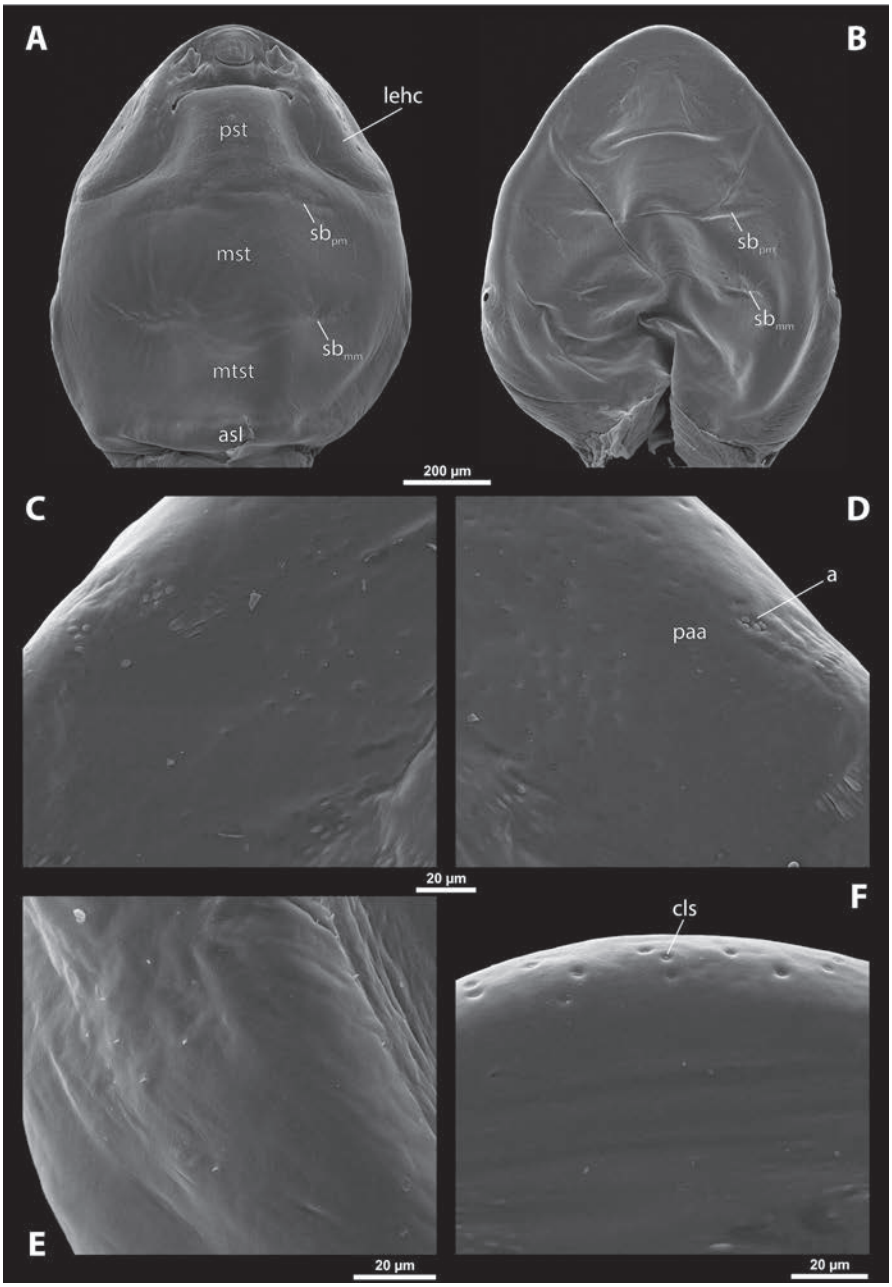

Figure 5. Holotype of *Deltoxenos impressus* Benda & Straka, sp. nov., ♀ (OLML), SEM micrographs of cephalothorax **A** ventral side **B** dorsal side **C** right vestigial antenna, dorsal side **D** left vestigial antenna, dorsal side **E** left lateral border of abdominal segment I below spiracle, dorsal side **F** detail of anterior border of cephalothorax, dorsal side. Abbreviations: a – vestigial antenna, asI – abdominal segment I, cls – clypeal sensillum, lehc – lateral extension of head capsule, mst – mesosternum, mtst – metasternum, paa – periantennal area, pst – prosternum (prosternal extension), sbmm – segmental border between mesothorax and metathorax, sbpm –segmental border between prothorax and mesothorax.

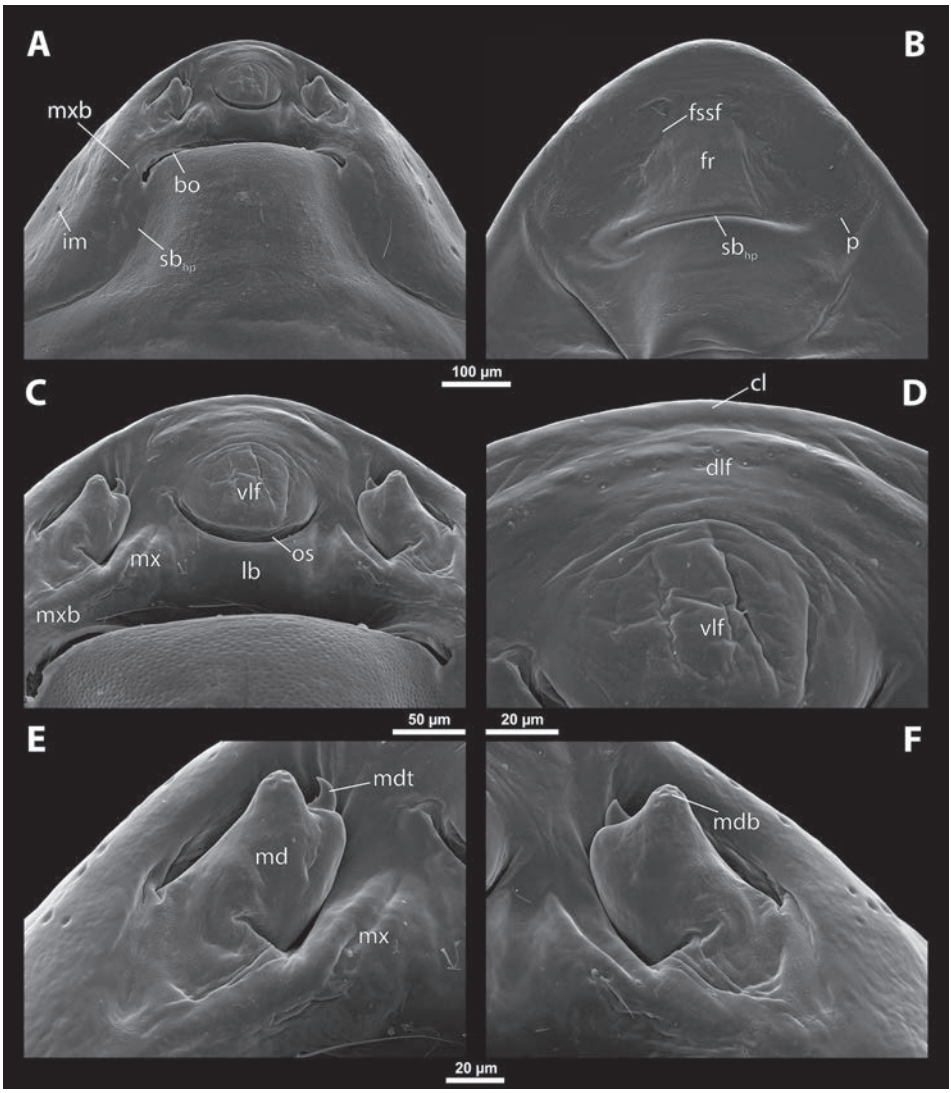

Figure 6. Holotype of *Deltoxenos impressus* Benda & Straka, sp. nov., ♀ (OLML), SEM micrographs of cephalothorax **A** anterior part of cephalothorax, ventral side **B** anterior part of cephalothorax, dorsal side **C** mouthparts, ventral side **D** detail of anterior border of cephalothorax, ventral side **E** right mandible and maxilla, ventral side **F** left mandible and maxilla, ventral side. Abbreviations: bo – birth opening, cl – clypeal area, dlf – dorsal labral field of labral area, im – impression, lb – labial area, md – mandible, mdb – mandibular bulge, mdt – mandibular tooth, mx – vestige of maxilla (maxilla), mxb – maxillary base (at mandible base), os – mouth opening, p – papilla, sbhp – segmental border between head and prothorax, vlf – ventral labral field of labral area.

Labium. Labial area quite indistinct between maxillae, delimited anteriorly by mouth opening and posteriorly by birth opening (lb; Fig. 6C). Flat, approximately as long as wide. Cuticular surface smooth.

Mouth opening. Widely arcuate, almost semicircular, sclerotised along margin (os; Fig. 6C).

Thorax. Pro-mesothoracic and meso-metathoracic borders visible ventrally as slightly imprinted mesal furrows (sbpm, sbmm; Figs 4C, 5A). On dorsal side separated by conspicuous dark mesal furrows, distinctly contrasted with pale thoracic segments (sbpm, sbmm; Figs 4D, 5B). Border between metathorax and abdomen indicated by ventral ridge on ventral side or indicated by change in colour and cuticular sculpture. Cuticle of thoracic segments on ventral side reticulate with scattered inconspicuous or more distinct pigmented papillae, mainly visible on metasternum. Prosternum conspicuously dark, mesosternum brown, and metasternum light brown. Prosternal extension undifferentiated. Dorsal side of thorax usually completely smooth, rarely with papillae on prothorax. All thoracic segments dorsally pale, but dark laterally. Meso- and metathorax transverse, rarely slightly elongated.

Abdominal segment I and spiracles. Setae and cuticular spines present on lateral region of abdominal segment I posterior to spiracle (Fig. 5E). Spiracles on posterior ~ ⅔ of cephalothorax slightly elevated, with anterolateral orientation. Cephalothoracic part of abdominal segment I below spiracles dark brown and medially light brown on both sides (asI, Fig. 4C).

Diagnosis of male cephalotheca. This species is distinguished from other representatives of the genus *Deltoxenos* by a combination of the following characters: clypeal lobe distinctly arcuate in frontal view versus conspicuously bulging as in *D. rueppelli*; shape of cephalotheca rounded in frontal view, very slightly flattened (Fig. 7C) versus more flattened in *D. rueppelli*; frontal region with distinct impression versus impression not visible in *D. rueppelli* and *D. bequaerti*; occipital bulge not protruding from elliptic shape of cephalotheca versus occipital bulge protruding in *D. rueppelli* and *D. bequaerti*.

Other characters that distinguish *D. impressus* sp. nov. from *D. rueppelli*: clypeal lobe as wide as mandible versus clypeal lobe distinctly wider than mandible; gena completely dark (gn; Fig. 7C) versus light brown.

Description of male cephalotheca. ***Shape and colouration.*** In frontal view rounded, very slightly flattened, elliptic, length 0.6 mm, width 0.86 mm, in lateral view protruding anteriorly, pointed apically (Fig. 7C, D). Colouration predominantly dark with paler areas.

Cephalothecal capsule. Compound eyes visible, pale to dark, with dark individual cornea lenses. Clypeal lobe distinctly arcuate in frontal view, prominent in lateral view (cl; Fig. 7C, D). Clypeal area completely dark, clypeal sensilla indistinct. Clypeal lobe as wide as mandible.

Frontal region with paired furrow of supra-antennal sensillary field, distinct impression and slightly raised occipital bulge (ssf, fi, ob; Fig. 7C). Occipital bulge not protruding from elliptic outline of cephalotheca. Gena completely dark (gn; Fig. 7C). Diameter of genae between maxillary base and compound eye approximately 3× larger than diameter of vestigial antenna.

Supra-antennal sensillary field. Dark, kidney-shaped and bulging, not delimited medially by distinct furrow (ssf; Fig. 7). Dark sensilla well visible.

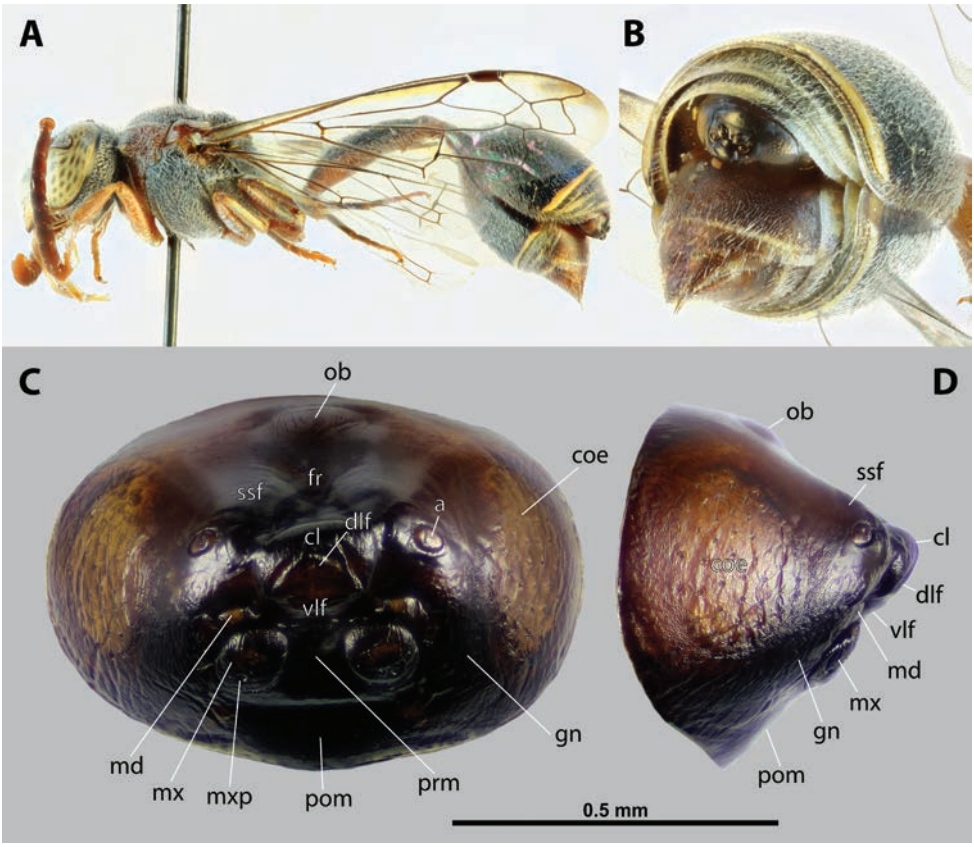

Figure 7. *Deltoxenos impressus* Benda & Straka, sp. nov., host, male cephalotheca **A** *Zethus favillaceus* Walker, 1871 stylopised by *D. impressus* sp. nov., lateral view **B** detail of host abdomen of *Z. favillaceus*, with male cephalotheca **C–D** paratype of *D. impressus* sp. nov., ♀ (OLML) from *Z. favillaceus* **C** ventral side of cephalothorax **D** dorsal side of cephalothorax. Abbreviations: a – vestigial antenna, cl – clypeal area, coe – compound eye, dlf – dorsal labral field of labral area, fr – frontal region, gn – gena, md – mandible, mx – vestige of maxilla, mxp – vestige of maxillary palp, ob – occipital bulge, pom – postmentum, prm – praementum, ssf – supra-antennal sensillary field, vlf – ventral labral field of labral area.

Antenna. Of standard shape, dark, small, with small plates or sensilla and complete torulus (a; Fig. 7C). Periantennal area not clearly delimited from supra-antennal sensillary field. Small plates and sensilla present.

Labrum. Labral area distinct, slightly less dark medially. Dorsal field arcuate, with dispersed setae visible (dlf; Fig. 7C). Ventral field elliptic.

Mandible. Nearly medially directed (md; Fig. 4E). Colouration predominantly dark but slightly lighter medially. Distance between mandibles very distinctly exceeding mandibular length. ***Maxilla.*** Distinct, prominent, completely dark with inconspicuous paler spot anteriorly. Wide at base, approximately 2× as wide as mandible (mx; Fig. 7C). Vestige of palp present, conspicuous (mxp; Fig. 7C).

Labium and hypopharynx. Labium distinct between and below maxillae, completely dark. Praementum and postmentum separated by furrow. Hypopharyngeal protuberance present but very indistinct (hyp; Fig. 7C). Mouth opening well visible, not covered by ventral labral field, distinctly arcuate.

Etymology. From the Latin substantive *impressio*, meaning an impression or hole. The specific epithet refers to conspicuous impressions on the lateral extensions of the female cephalothorax. Adjective.

Discussion

Although *Zethus* belongs to the most diverse and widespread genera of the family Vespidae (with 279 described species), very little is known about the spectrum of its parasites. The evolution of the highly diverse genus is also insufficiently known, even though an extensive phylogeny at the subgeneric level was presented recently (Lopes et al. 2021). From all established nine subgenera of *Zethus*, three are known to be parasitised by Strepsiptera (*Madecazethus*, *Zethus*, *Zethusculus*) (Table 1). Not surprisingly, both xenid species described in this work from different continents parasitise species of phylogenetically very distinctly separated *Zethus* subgenera. The host of *Deltoxenos impressus* sp. nov. belongs to the most ancestral subgenus *Madecazethus*, which is distributed in the Afrotropical realm and part of the Palearctic region. In clear contrast, *Eupathocera zethi* sp. nov. parasitises species of the subgenus *Zethusculus*, which is deeply nested within *Zethus* and is distributed in the New World.

Although parasites can be good models to track the biogeography of their hosts on the species and population level on a small geographical scale (Štefka et al. 2011), the situation is more complicated on higher taxonomic levels. In the case of the evolution of Xenidae, switches to a new host lineage, often connected with long-distance dispersal, play a prominent role (Benda et al. 2022b). Many xenid subgroups are rather opportunistic with some level of host group conservatism rather than host-parasite coevolution. Previously, we indicated many other parallel switches to the same group of Hymenoptera (e.g. Ammophilini, Sphecini, *Ancistrocerus* Wesmael, 1836) (Benda et al. 2021).

Table 1. Overview of *Zethus* species stylopised by Xenidae with general information about distribution, parasitic species, and original study.

Species	Subgenus	Distribution	Strepsiptera species	Publication
Zethus brasiliensis fuscatus R. Bohart & Stange, 1965	*Zethusculus*	French Guiana	*Eupathocera zethi* sp. nov.	Benda et al. (2021), this study
Zethus favillaceus Walker, 1871	*Madecazethus*	Kenya	*Deltoxenos impressus* sp. nov.	this study
Zethus pubescens Smith, 1857	*Madecazethus*	Republic of South Africa	Unknown	Salt and Bequaert (1929)
Zethus spinipes variegatus Saussure, 1852	*Zethus*	Texas, Florida (USA)	Unknown	Salt and Bequaert (1929)
Zethus romandinus Saussure, 1852	*Zethusculus*	Peru	Unknown	Salt and Bequaert (1929)

Within Vespidae, *Polistes* Latreille, 1802 − a widely distributed and large genus of social wasps, with 237 described species (Silveira et al. 2021) − is parasitised by the maximum number of species of Strepsiptera. The genus typically associated with it, *Xenos* Rossi, 1793, presently comprises 33 described species of the Old and New World (Benda et al. 2022b). In contrast, other very diverse vespid genera such as *Mischocyttarus* Saussure, 1853 or *Zethus* have a scarce record of being parasitised by strepsipterans. *Mischocyttarus* is a large genus of the New World that comprises approximately 250 described species (Silveira 2008), but only three strepsipteran parasites are described (Benda et al. 2022a). Like in the case of *Zethus*, there are probably many more undescribed species of Strepsiptera that have escaped notice due to their inconspicuousness or rarity.

The xenid genus *Eupathocera* has a very wide range of hosts. It parasitises wasps from three families: Sphecinae, Ammophilinae (Sphecidae); *Tachytes* (Crabronidae: Crabroninae); *Zethus* (Vespidae: Zethinae); and *Pachodynerus* (Vespidae: Eumeninae) (Benda et al. 2022b). According to the phylogeny of Benda et al. (2021), *Eupathocera* from *Zethus* is the sister lineage of the monophyletic group parasitising digger wasps with a divergence of about 20 million years ago. Folded-winged wasps of the genus *Zethus* could have played a key role in the evolution of Xenidae during the switch from solitary wasps (Eumeninae) to sphecid wasps (Sphecidae) that occurred in parallel in the New and Old World (Benda et al. 2019). Due to a wide host range connected with morphological variability within the genus, the diagnosis of *Eupathocera zethi* sp. nov. is complicated and a combination of characters is required. In contrast, *Deltoxenos impressus* sp. nov. can be very easily distinguished from other *Deltoxenos* species by the orientation of the mandibles and lacking impressions at the site of the compound eyes. Although we were not able to obtain DNA sequences due to the age of the material, the species can be easily assigned to a genus using a key to the genera of Xenidae (Benda et al. 2022b).

Our work and data in the literature (Salt and Bequaert 1929) suggest that the genus *Zethus* is more frequently parasitised than expected and more vigilance is needed when handling material of its species. It is also very likely that both described species have a distinctly larger distribution than we recorded in this work, which is tentatively suggested by the distribution area of *Zethus favillaceus* that ranges from South Africa to Saudi Arabia (Tan et al. 2018).

Acknowledgements

We are very grateful to Yuta Nakase for providing a part of the material. We are also deeply indebted to Esther Ockermüller and Martin Schwarz for access to the Hymenoptera Collection and hospitality in Linz, and Josef Gusenleitner for the identification of wasp species. Daniel Tröger and one anonymous carefully reviewed the manuscript and made very helpful suggestions. This is greatly appreciated. We also cordially thank Kateřina Bezányiová for language proofreading. This project was supported by the Ministry of Culture of the Czech Republic (DKRVO 2024-2028/5.I.a, National Museum, 00023272). The authors declare no conflict of interest.

References

Bank S, Sann M, Mayer C, Meusemann K, Donath A, Podsiadlowski L, Kozlov A, Petersen M, Krogmann L, Meier R, Rosa P, Schmitt T, Wurdack M, Liu S, Zhou X, Misof B, Peters RS, Niehuis O (2017) Transcriptome and target DNA enrichment sequence data provide new insights into the phylogeny of vespid wasps (Hymenoptera: Aculeata: Vespidae). Molecular Phylogenetics and Evolution 116: 213–226. https://doi.org/10.1016/j.ympev.2017.08.020

Benda D, Nakase Y, Straka J (2019) Frozen Antarctic path for dispersal initiated parallel host-parasite evolution on different continents. Molecular Phylogenetics and Evolution 135: 67–77. https://doi.org/10.1016/j.ympev.2019.02.023

Benda D, Votýpková K, Nakase Y, Straka J (2021) Unexpected cryptic species diversity of parasites of the family Xenidae (Strepsiptera) with a constant diversification rate over time. Systematic Entomology 46: 252–265. https://doi.org/10.1111/syen.12460

Benda D, Pohl H, Beutel R, Straka J (2022a) Two new species of *Xenos* (Strepsiptera: Xenidae), parasites of social wasps of the genus *Mischocyttarus* (Hymenoptera: Vespidae) in the New World. Acta Entomologica Musei Nationalis Pragae 62: 1–11. https://doi.org/10.37520/aemnp.2022.014

Benda D, Pohl H, Nakase Y, Beutel R, Straka J (2022b) A generic classification of Xenidae (Strepsiptera) based on the morphology of the female cephalothorax and male cephalotheca with a preliminary checklist of species. ZooKeys 1093: 1–134. https://doi.org/10.3897/zookeys.1093.72339

Bohart R, Stange L (1965) A Revision of the Genus Zethus Fabricius in the Western Hemisphere (Hymenoptera: Eumenidae). University of California Publications in Entomology 40: 1–216.

Evans HE, West-Eberhard MJ (1970) The wasps. University of Michigan. Ann Arbor: 1–265.

Heraty JM (1998) Hexamethyldisilazane: A chemical alternative for drying insects. Entomological news 109: 369–374.

Kelstrup H, West-Eberhard M, Nascimento F, Riddiford L, Hartfelder K (2023) Behavior, ovarian status, and juvenile hormone titer in the emblematic social wasp *Zethus miniatus* (Vespidae, Eumeninae). Behavioral Ecology and Sociobiology 77: 58. https://doi.org/10.1007/s00265-023-03334-6

Lopes RB, Noll FB (2014) Notes on the Neotropical *Zethus* Fabricius, 1804 (Hymenoptera, Vespidae, Eumeninae) with the description of two new species from Brazil. Zootaxa 3784: 179–186. https://doi.org/10.11646/zootaxa.3784.2.7

Lopes RB, Carpenter JM, Noll FB (2021) Cladistic analysis of *Zethus* Fabricius, 1804 (Hymenoptera, Vespidae): a new subgeneric classification. Journal of Hymenoptera Research 82: 253–283. https://doi.org/10.3897/jhr.82.65760

Nguyen LTP, Carpenter JM (2017) Taxonomic review of the genus *Zethus* Fabricius (Hymenoptera: Vespidae: Eumeninae) from Vietnam with descriptions of four new species. Entomological Science 20: 24–32. https://doi.org/10.1111/ens.12218

Pereira MCSA, Hermes MG, Bernardi LFO (2018) An overview of the mite fauna (Acari) associated with eumenine wasps (Hymenoptera: Vespidae) found in Brazilian collections. Journal of Natural History 52: 3017–3038. https://doi.org/10.1080/00222933.2019.1568602

Piekarski PK, Carpenter JM, Lemmon AR, Moriarty Lemmon E, Sharanowski BJ (2018) Phylogenomic Evidence Overturns Current Conceptions of Social Evolution in Wasps (Vespidae). Molecular Biology and Evolution 35: 2097–2109. https://doi.org/10.1093/molbev/msy124

Salt G (1927) Notes on the Strepsiptera and their hymenopterous hosts. Psyche: A Journal of Entomology 34: 182–192. https://doi.org/10.1155/1927/25470

Salt G, Bequaert J (1929) Stylopized Vespidæ. Psyche: A Journal of Entomology 36: 249–282. https://doi.org/10.1155/1929/78563

Silveira OT (2008) Phylogeny of wasps of the genus *Mischocyttarus* de Saussure (Hymenoptera, Vespidae, Polistinae). Revista Brasileira de Entomologia 52: 510–549. https://doi.org/10.1590/S0085-56262008000400004

Silveira OT, Andena SR, Somavilla A, Carpenter JM (2021) Phylogeny and classification of the Neotropical social wasps. In: Prezoto F, Nascimento FS, Barbosa BC, Somavilla A (Eds) Neotropical Social Wasps: Basic and applied aspects. Springer International Publishing, Cham, 267–291. https://doi.org/10.1007/978-3-030-53510-0_15

Štefka J, Hoeck PE, Keller LF, Smith VS (2011) A hitchhikers guide to the Galápagos: co-phylogeography of Galápagos mockingbirds and their parasites. BMC Evolutionary Biology 11: 284. https://doi.org/10.1186/1471-2148-11-284

Tan J-L, Carpenter JM, van Achterberg C (2018) Most northern Oriental distribution of *Zethus* Fabricius (Hymenoptera, Vespidae, Eumeninae), with a new species from China. Journal of Hymenoptera Research 62: 1–13. https://doi.org/10.3897/jhr.62.23196

JHR 97: 741–754 (2024)
doi: 10.3897/jhr.97.127622
https://jhr.pensoft.net

RESEARCH ARTICLE

JOURNAL OF Hymenoptera RESEARCH
A peer-reviewed open-access journal
The International Society of Hymenopterists

Parasitoid wasps associated with *Antigastra catalaunalis* (Lepidoptera, Crambidae) in Northern Sinaloa, Mexico

Ramón A. Sarazú-Pillado[1], Héctor González-Hernández[1], J. Refugio Lomeli-Flores[1], Jorge M. Valdez-Carrasco[1], Edgardo Cortez-Mondaca[2], Ariel Guzmán-Franco[1]

1 *Colegio de Postgraduados, Posgrado en Fitosanidad, Programa de Entomología y Acarología, Montecillo, CP 56230, Texcoco, Estado de México, Mexico* **2** *INIFAP-Campo Experimental Valle del Fuerte, Km 1609 carretera Internacional México-Nogales, Juan José Ríos, Sinaloa, 81110, Mexico*

Corresponding author: J. Refugio Lomeli-Flores (jrlomelif@hotmail.com)

Academic editor: Miles Zhang | Received 16 May 2024 | Accepted 23 July 2024 | Published 16 September 2024

https://zoobank.org/24F320B5-65F4-4952-AC18-8E0AD8A2CD82

Citation: Sarazú-Pillado RA, González-Hernández H, Lomeli-Flores JR, Valdez-Carrasco JM, Cortez-Mondaca E, Guzmán-Franco A (2024) Parasitoid wasps associated with *Antigastra catalaunalis* (Lepidoptera, Crambidae) in Northern Sinaloa, Mexico. Journal of Hymenoptera Research 97: 741–754. https://doi.org/10.3897/jhr.97.127622

Abstract

New records of Hymenoptera parasitoids of the sesame webworm, *Antigastra catalaunalis* Duponchel (Lepidoptera: Crambidae), are presented for Northwest Mexico. Taxonomic assignation was based on morphological features. Partial sequences of the COI region from the most common parasitoids were deposited in GenBank. Six species of wasps were obtained: *Bracon* (*Habrobracon*) *platynotae* Cushman (Braconidae), *Eiphosoma dentator* Fabricius (Ichneumonidae), *Perilampus platigaster* species group (Perilampidae), *Brachymeria annulata* Walker, *Conura side* Walker, *Conura maculata* Fabricius (Chalcididae) and *Goniozus punctaticeps* Kieffer (Bethylidae). Partial sequences of the COI region obtained from the most common parasitoids helped to confirm at genus level but not species. This is the first record of the association of all these parasitoid species with *A. catalaunalis*.

Keywords

Braconidae, Chalcididae, molecular biology, Sesame webworm

Introduction

The sesame webworm, *Antigastra catalaunalis* Duponchel (Lepidoptera: Crambidae), is native in the tropical and subtropical areas of Africa, although it was first reported in South America on sesame crops (Hallman and Sanchez 1982), and it has recently

established in North America (Sarazú-Pillado et al. 2020). The second instar larva produces silk with which it binds leaves, branches, and flowers to form a shelter to protect itself from adverse abiotic conditions such as temperature and natural enemies, including parasitoids and predators (Simoglou et al. 2017). It is considered as a pest as it feeds on most parts of the plant except the root, and generally, it attacks the crop since the seedling stage (Gebregergis et al. 2016; Sarazú-Pillado et al. 2020).

Antigastra catalaunalis is a significant pest of sesame in the main producing countries in Asia and Africa. Gupta et al. (2002), reported losses from 6.2 to 43.1% in Madhya Pradesh, India; while Simoglou et al. (2017), in Drama, Northern Greece, reported losses exceeding 50% of production, with 80% of plants infested and 50% of capsules damaged. In South America, this pest was first detected in Colombia in 1971 (Hallman and Sanchez 1982). Recently, according to Sarazú-Pillado et al. (2020), it was found in Sinaloa, the main sesame-producing state in Mexico.

Currently, chemical control is the most widely used tactic against *A. catalaunalis*. However, its use also results in an imbalance in agroecosystems, environmental contamination, and a negative impact on beneficial fauna. There are 39 species of parasitoids associated with *A. catalaunalis* (Table 1), some of them are present in India (Jakhmola 1983; Naveen et al. 2019), Tanzania (Robertson 1973), Nigeria (Chadha 1974), and Colombia (Hallman and Sanchez 1982). Although, few of these parasitoids have been proposed for augmentative biological control programs, a strategy that may imply laboratory rearing and periodic mass release of the parasitoid species; for example, *Elasmus* sp. (Eulophidae) in Vietnam (Tung et al. 2011); *Trathala flavoorbitalis* Cameron (Ichneumonidae) in India (Baskaran and Thangavelu 1990); and *Bracon* (*Habrobracon*) *hebetor* Say (Braconidae) in Egypt (El-Basha 2015). However, it is necessary to identify, by morphological and molecular taxonomy, parasitoid that could be associated to *A. catalaunalis* in sesame field in northern Sinaloa, Mexico.

Materials and methods

Field collections

The collections were carried out from August to October 2020, in commercial sesame fields in the municipalities of El Fuerte (26°16'20"N, 108°54'49"W), Sinaloa (25°44'9"N, 108°15'30"W), and Mocorito (25°29'50"N, 107°53'42"W), where the highest sesame production in the state of Sinaloa is concentrated. Through the experiments these fields were under agronomic management by the producer. In El Fuerte, the Pata de Gallo variety was used, which was planted on residual moisture on July 21, 2020, with a row spacing of 80 cm and 17 plants per linear meter. A tractor was used for soil cultivation 33 days after planting for soil movement and weed elimination. An aerial application of insecticide against the sesame webworm was applied 45 days after planting, at a rate of 500 ml of Chlorpyrifos + 300 ml of Lambda Cyhalothrin/ha.

Table 1. Records of parasitoids associated with *Antigastra catalaunalis* around the world.

Order: Family Species	Distribution	References
Hymenoptera: Ichneumonidae		
Charops sp.	Tanzania	(Robertson 1973).
Diadegma sp.	India	(Jakhmola 1983; Nair 1986; Patel and Bhalani 1989).
Doliphocerus gricilis Hayat	India	(Din-Gurs and Husain 1997).
Eriborus sp.		(Ramakrishna 1927; Jakhmola 1983; Naveen et al. 2019).
Eriborus trochanteratus (Morley)	India	(Din-Gurs and Husain 1997; Kapadia 1997).
Pristomerus sp.	Nigeria and Tanzania	(Robertson 1973; Chadha 1974).
Temelucha biguttula (Matsumura)	Bangladesh	(Biswas et al. 2001).
Trathala flavoorbitalis (Cameron)	Asia, from India to Japan, Australia and Hawaii	(Ramdas-Menon et al. 1960; Jakhmola 1983; Choudhary et al. 1986; Kalra 1989; Baskaran and Thangavelu 1990; Kumar and Goel 1994; Behera 2011; Naveen et al. 2019).
Hymenoptera: Braconidae		
Agathidinae undetermined	India	(Naveen et al. 2019).
Agathis sp.	India	(Jakhmola 1983).
Apanteles sp.	India, Tanzania, and Nigeria	(Robertson 1973; Chadha 1974; Choudhary et al. 1986; Kalra 1989; Kumar and Goel 1994).
Apanteles aethiopicus Wilkinson	West Africa, Cameroon, and Somalia	(Wilkinson 1931, 1932; Walker 1994).
Bassus sp.	India	(Naveen et al. 2019).
Bassus antigastrae Wilkinson	Sudan	(Wilkinson 1931).
Bracon sp.	Colombia	(Hallman and Sanchez 1982).
Bracon (*Habrobracon*) *brevicornis* Wesmael	West and South Africa, the Middle East, India, and Europe	(Shenefelt 1978).
Bracon (*Habrobracon*) *gelechiae* Ashmead	India	(Jakhmola 1983).
Bracon (*Habrobracon*) *hebetor* Say	Egypt, India, Cosmopolitan	(Negi et al. 1944; Jakhmola 1983; Nair 1986; Patel and Bhalani 1989; El-Basha 2015; Naveen et al. 2019).
Camptothlipsis luteostigmalis van Achterberg	United Arab Emirates	(van Achterberg 2011).
Chelonus curvimaculatus Cameron	India, Sudan, West and Southern Africa	(Risbec 1950).
Hormius sp.	Senegal	(Risbec 1960).
Phanerotoma sp.	India	(Kumar and Goel 1994; Naveen et al. 2019).
Phanerotoma hendecasisella Cameron	India, Egypt, Australia, Sri Lanka, Java and Myanmar	(Bhatnagar and Davies 1979; Nair 1986; Patel and Bhalani 1989).
Hymenoptera: Chalcididae		
Brachymeria sp.		
Conura sp. (Spilochalcis)	Colombia	(Hallman and Sanchez 1982).
B. nigricorporis Husain & Agarwal	India	(Din-Gurs and Husain 1997).
Hymenoptera: Eulophidae		
Elasmus sp.	Vietnam	(Tung et al. 2011).
Elasmus brevicornis Gahan	India	(Nair 1986; Kalra 1989; Patel and Bhalani1989; Kumar and Goel 1994).
Euplectrus sp.	Colombia	(Hallman and Sanchez 1982).
Tetrastichus sp.	India	(Din-Gurs and Husain 1997).
Hymenoptera: Trichogrammatidae		
Trichogramma chilonis Ishii	India	(Choudhary et al. 2017).
Trichogramma sp.	India	(Choudhary et al. 1986).
Hymenoptera: Scelionidae		
Telenomus thestor Nixon	Uganda	(Risbec 1960).
Diptera: Tachinidae		
Cadurcia lucens Villeneuve	Nigeria	(Chadha 1974).
Exorista ebneri Villeneuve	Egypt, Sudan y Tunisia	(Risbec 1950).
Pseudoperichaeta laevis Villeneuve	Tanzania	(Robertson 1973).
Tachina sp.	Somalia	(Risbec 1960).
Zygobothria sp.	India	(Choudhary et al. 1986).

In the Sinaloa field, the Breve Doble variety was used, which was planted using residual moisture on July 19, 2020, with a row spacing of 75 cm and 17 plants per linear meter. Soil cultivation was carried out 23 days after planting for soil movement and weed elimination. No insecticide applications were made in this field.

In Mocorito, the Breve Doble variety was planted under residual moisture on July 21, 2020, with a row spacing of 75 cm and an average of 18 plants per linear meter. Soil cultivation was carried out 25 days after planting for soil movement and weed elimination. Additionally, two applications of insecticide against *A. catalaunalis* were made using a tractor. The first application was made 22 days after planting at a rate of 500 ml/ha of Emamectin Benzoate, and the second application was made 37 days after planting, using the same product and dose.

Seven samplings were made on each commercial sesame field. On each experimental field, five points were selected, one on each corner and one in the center of the field, and from each point, 35 plants were randomly selected for examination. Larvae and pupae of *A. catalaunalis* were collected from each plant. The larvae were placed in a plastic container (30 cm × 30 cm × 20 cm) covered with organza fabric with sesame leaves as food. The pupae were collected with plant tissue attached to avoid damage. Once in the laboratory, the larvae were individually placed in Petri dishes (15 cm × 2 cm) with sesame leaves as food, the pupae were separated from the plant tissue and individually placed in Petri dishes. All Petri dishes were kept at room temperature of 29 ± 4 °C, 76 ± 23% relative humidity, and a 12:12 h (light-dark) photoperiod. The material was checked daily for evidence of parasitism. The emerging parasitoids were preserved with 70% ethanol in 1.5 ml Eppendorf tubes and transferred to the Biological Control Laboratory at the Colegio de Postgraduados, Montecillo Campus, for identification.

Identification of parasitoids

The parasitoids were dehydrated in graded alcohols (80, 90, and 96%) and then placed in amyl acetate for 24 hours before being dry mounted. Photographs of the diagnostic structures (head, antennae, wings, thorax, and abdomen) and the general appearance of the adults were taken using a Carl Zeiss Discovery V20 stereoscopic microscope (White Plains, NY, USA) equipped with a Canon EOS 5D Mark II camera (Ōta, Tokyo, Japan). The images were edited using GLIMP software (version 2.10.24, free software) and stacked using ZERENE STACKER software (version T2021, Zerene Systems LLC). Morphological identification of the adults was carried out using the follow identification keys: for Braconidae Cushman (1914) and Goulet and Huber (1993); for Bethylidae Evans (1979); for Ichneumonidae Dasch (1979) and Gauld (2000); for Perilampidae Darling (1997); and for Chalcididae Boucek and Halstead (1997). Experts in each taxonomic group confirmed species identifications. Taxa names of Ichneumonoidea are according to Yu et al. (2016). Reference specimens of the parasitoids and adults of *A. catalaunalis* were deposited in the entomological collections of the Colegio de Postgraduados (CEAM) and the MIFA, Faculty of Engineering and Sciences, Universidad Autónoma de Tamaulipas, Cd. Victoria, Tamaulipas, Mexico (MIFA-UAT).

DNA extraction and COI amplification

DNA extractions from the parasitoids were performed using the Quick-DNA Tissue/Insect Miniprep Kit (Zymo Research), following the manufacturer's instructions. Quality and quantity of the extracted DNA were determined by visualization on agarose gels and using the NanoDrop, respectively.

PCR reactions to amplify a 650–700 bp region of the cytochrome oxidase subunit I (COI) gene were performed using the HCO-2198 primers (TAA ACT TCA GGG TGA CCA AAA AAT CA) and LCO-1490 (GGT CAA CAA ATC ATA AAG ATA TTG G) (Hebert et al. 2003). For a final reaction volume of 30 µL, 3 µL of buffer (10X), 1.2 µL of $MgCl_2$ (25 mM), 0.6 µL of dNTPs (10 mM), 0.9 µL of each primer (10 µM), 0.1 µL of Taq polymerase (5 U µL-1), 5 µL of DNA (10–20 ng µL-1), and 18.3 µL of 6% trehalose were used. The thermal conditions for amplification were as follows: an initial denaturation step of 60 sec at 94 °C; followed by five cycles of 60 sec at 94 °C, 90 sec at 45 °C, and 90 sec at 72 °C, then 35 cycles of 60 sec at 94 °C, 90 sec at 60 °C, and 60 sec at 72 °C, ending with a final extension of 5 min at 72 °C. The PCR products were visualized on an agarose gel and photographed using the Infinity VX2 System device (Vilber Lourmat, France). The PCR products were sent to the Company Macrogen (Seoul, Korea) for sequencing. The resulting sequences were edited using BioEdit v. 7.1.9. The sequences were compared against the GenBank database using the BLAST search engine. From the BLAST results list, the species with the highest score, 98–100%, was used to assign species, or 93–98% to assign the higher taxon group (Hebert et al. 2003). COI sequences obtained were deposited in GenBank, and the accession numbers are indicated in Table 2.

Table 2. Relationship of parasitoids of *Antigastra catalaunalis* collected in three municipalities of Northern Sinaloa, Mexico.

	Localities							Total specimen	Total Localities
	Mocorito		El Fuerte		Sinaloa				
Collection date	**1**	**4**	**2**	**6**	**3**	**5**	**7**		
Parasitoid species (PS)									
*Brachymeria annulata**	-	2	-	1	1	-	2	6	4
Bracon (*Habrobracon*) *platynotae**	-	8 (2)	10 (3)	7 (2)	4 (1)	3 (2)	7 (2)/ MZ196440 MZ196441 MZ196442 MZ196443	39(12)	6
*Conura maculata**	-	-	2	2	-	1	3	8	4
*Conura side**	-	-	1	-	1	-	1	3	3
*Eiphosoma dentator**	-	2/MZ196444	1	-	1/MZ196445	1	-	5	4
*Goniozus punctaticeps**	-	-	4 (1)	3 (1)	-	4 (1)	4 (1)	15 (04)	4
Perilampus platigaster species group*	-	1	-	-	-	-	-	1	1
Total specimens	0	13 (2)	18 (4)	13 (3)	7 (1)	9 (3)	17 (3)		
		13 (2)	31 (7)			33 (7)		77 (16)	

*New record association host-parasitoid; Collection date (2020): 1) 13/VIII, 2) 19/VIII, 3) 21/VIII, 4) 22/VIII, 5) 12/IX, 6) 26/IX, 7) 27/IX; Number of specimens: The number of parasitized *A. catalaunalis* immature stage is noted in parentheses; GenBank access number: MZ196440 to MZ196445.

Results

In the present study a total of 77 parasitoid specimens from seven species were obtained associated to *A. catalaunalis* in commercial sesame fields of Sinaloa. Among these, three species emerged from larvae and four from pupae. The highest number and diversity of parasitoids were found in the municipalities of Sinaloa and El Fuerte, with six species each, while four species were collected in Mocorito. *Bracon* (*Habrobracon*) *platynotae* Cushman (Braconidae) was the most abundant species (39 specimens), followed by *Goniozus punctaticeps* (Bethylidae) (15 specimens), *Conura maculata* (Chalcididae) (8 specimens), *Brachymeria annulata* (Chalcididae) (6 specimens), *Eiphosoma dentator* (Ichneumonidae) (5 specimens), *Conura side* (Chalcididae) (3 specimens), and *Perilampus platigaster* species group (Perilampidae) (one specimen).

When the obtained sequences were compared to the GenBank database, no similarity above 98% was obtained, which could have helped to confirm species. However, for the sequences of *E. dentator*, the closest match was with a sequence of *E. tantalium* (JF793018.1) with a 91.32% identity, an E-value of 0.0 and 95% query cover, which confirmed the correct genus identification. For the sequences of *B. platynotae*, the closest match obtained was 92.24% similarity with a sequence of *Habrobracon* sp. (MG439564.1), an E-value of 0.0 and 95% query cover, confirming the correct genus identification.

Discussion

The species complex of parasitoids associated with *A. catalaunalis* in northern Sinaloa (Fig. 1) could be an important component for the integrated management of this pest in sesame. Below are some details of the collected species.

Bracon (*Habrobracon*) *platynotae* Cushman (Braconidae) (Fig. 1C, D) was the most abundant parasitoid species from the three municipalities, except for one collection date in Mocorito, where the parasitoid was absent, possibly due to insecticide application before collection. Up to four parasitoid adults were obtained from a single *A. catalaunalis* larva, indicating it is a gregarious ectoparasitoid (Table 2). Although it only parasitizes large larvae of the 4th and 5th instars, it was observed to cause permanent paralysis and death of small larvae, possibly for feeding, like what was observed with *B. hebetor* on *A. catalaunalis* larvae, in Egypt (El-Basha 2015). This species has only been reported in Mexico on *Pectinophora gossypiella* Saunders (Gelechiidae), under the synonym *Microbracon platynotae* Cushman, in Durango (Muesebeck 1925). This study reports for the first time *B. platynotae* as a parasitoid of *A. catalaunalis* in Sinaloa, Mexico. Given that several species of the subgenus *Habrobracon* have shown success in biological control programs, *B. platynotae* would be a viable option for laboratory and field evaluation studies; considering that it also has *P. gossypiella* as host (Muesebeck 1925).

Goniozus punctaticeps Kieffer (Bethylidae) (Fig. 1E, F) is a gregarious ectoparasitoid of lepidopteran larvae (Evans 1979). It was found in the municipalities of El Fuerte and Sinaloa, with up to four adults obtained from one *A. catalaunalis* larva (Table 2). The parasitized larvae exhibited permanent paralysis. This parasitoid has been reared

in Texas, USA on *Acrobasis nuxvorella* Neunzig (Pyralidae) and *Cidia caryana* Fitch (Tortricidae) on pecan (Nickels et al. 1950), also in *Coleotechnites* (=*Evagora*) *milleri* Busck (Gelechiidae), *C.* (=*Lespeyresia*) *caryana*, *A. nuxvorella* and *Etiella zinckenella* Treitschke (Pyralidae) also in the USA (Evans 1979). In Mexico, *G. punctaticeps* (cited as *P. cellularis*) has only been reported on *A. nuxvorella* and *C. caryana* in walnut trees

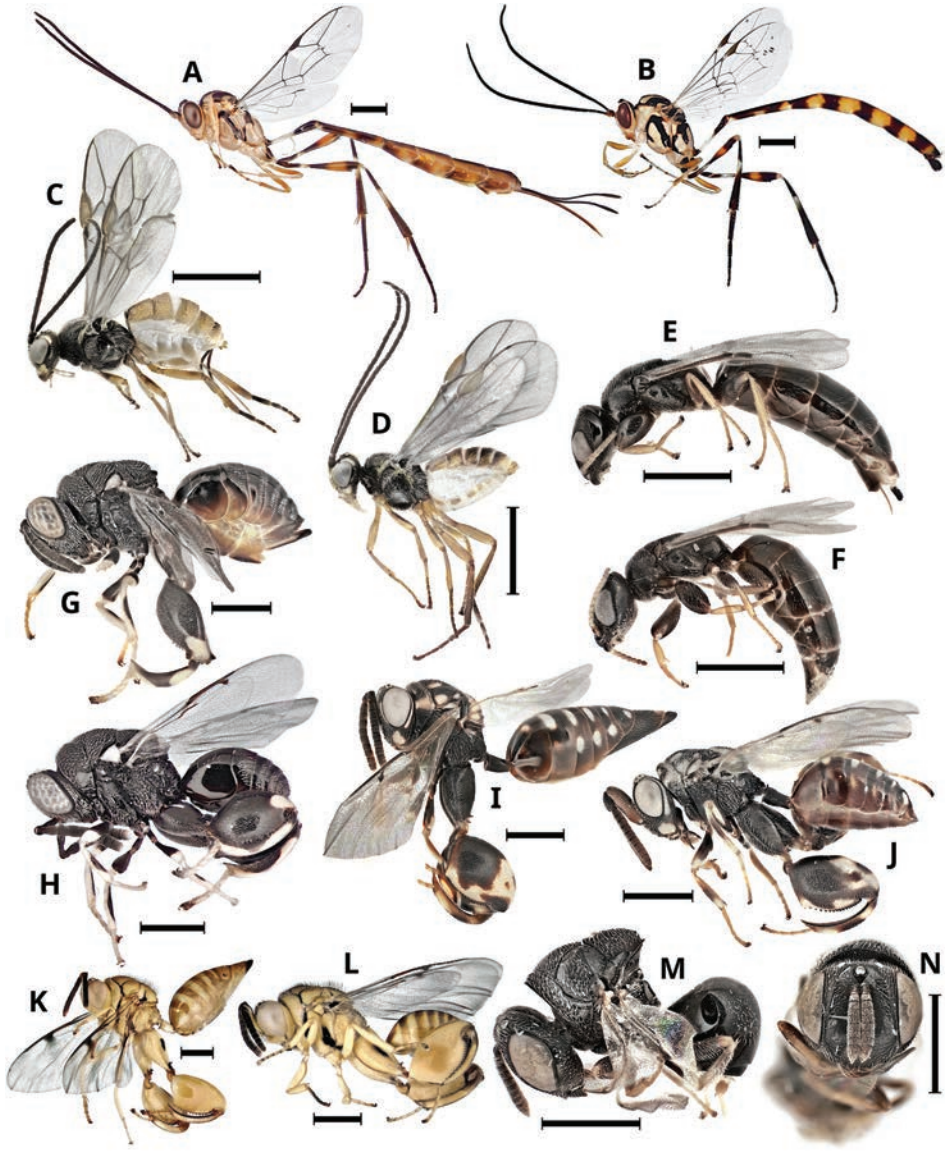

Figure 1. *Eiphosoma dentator* **A** female lateral view **B** male lateral view; *Bracon* (*Habrobacon*) *platynotae* **C** female lateral view **D** male lateral view; *Goniozus punctaticeps* **E** female lateral view **F** male lateral view; *Brachymeria annulata* **G** female lateral view **H** male lateral view; *Conura side* **I** female lateral view **J** male lateral view; *Conura maculata* **K** female lateral view **L** male lateral view; *Perilampus platigaster* species group **M** male lateral view **N** male Front view. Scale bars: 1 millimeter.

in Nuevo León (Reyes-Villanueva 1987). There are no previous records of Bethylidae species associated with *A. catalaunalis*, so *G. punctaticeps* is reported for the first time as a parasitoid on this host in northern Sinaloa, Mexico.

Eiphosoma dentator Fabricius (Ichneumonidae) (Fig. 1A, B) is a solitary ectoparasitoid of lepidopteran larvae (Dasch 1979). It was reared in all three municipalities, but in low numbers (Table 2). *A. catalaunalis* larvae parasitized by *E. dentator* exhibited permanent paralysis. It was first reported in Texas, USA, by Mann (1969), parasitizing *Loxomorpha flavidissimalis* Grote (Crambidae), a potential pest in prickly pear crops. In South Florida, USA, it was found parasitizing *Lineodes interga* Zeller (Crambidae), a pest of eggplant (Dasch 1979). In Barbados, it is also associated with a pest of the family Crambidae, such as *Diaphania hyalinata* L. (Alam 1989). Recently, it was also reported in Tamaulipas, Mexico, on *L. flavidissimalis* (Gaona-García et al. 2020). In this study, *E. dentator* is reported for the first time as a parasitoid of *A. catalaunalis* in Sinaloa, Northwest Mexico. In some studies, it is reported without major impact on pest lepidopteran populations (Mann 1969; Dasch 1979; Alam 1989; Gaona-García et al. 2020). However, based on observations in this study, this parasitoid is considered an additional regulatory factor for *A. catalaunalis* populations in sesame, which could be exploited in conservation biological control programs.

Brachymeria annulata Walker (Chalcididae) (Fig. 1G, H), adults were collected individually from *A. catalaunalis* pupae, one specimen in El Fuerte, two specimens in Mocorito and three specimens in Sinaloa municipality (Table 2). There exist records of *B. annulata* parasitizing *Talides hispa* Evans (Hesperiidae) in Panama (Santos-Murgas et al. 2021); *Erinnys ello* L. (Sphingidae) in Acre, Brazil, *Alabama argillacea* Hubner (Noctuidae) in Paraguay (Silvie et al. 2007), and as a hyperparasitoid associated with *Diadegma leontiniae* Brèthes (Ichneumonidae) in the Brasilia region, Brazil (Guilloux et al. 2002), parasitoid released in cruciferous crops. *Brachymeria* sp. (Hallman and Sanchez 1982) and *Brachymeria nigricorporis* (Din-Gurs and Husain 1997) (Table 1) are the only previous records of association between wasps of the genus *Brachymeria* as parasitoids of *A. catalaunalis*. In this study, *B. annulata* is reported for the first time as a parasitoid of *A. catalaunalis* pupae in Sinaloa, Northwest Mexico.

Three specimens of *Conura side* Walker (Chalcididae) (Fig. 1I, J) were obtained from *A. catalaunalis* pupae (Fig. 2I, H), one from El Fuerte and two from Sinaloa. As a primary parasitoid, it has been associated with some species of Chrysomelidae (Coleoptera), such as *Gratiana boliviana* Spaeth, a beetle released in Florida and other parts of the USA as a biological control agent against *Solanum viarum* Dunal (Solanaceae) (Diaz et al. 2012). It was also released in Maryland, USA, for biological control of *Cassida rubiginosa* Muller, a chrysomelid considered an invasive pest and defoliator of some *Carduus* species (Tipping 1993). As primary parasitoid it was reared from pupae of *Anagasta kuhniella* Zeller and *Galleria mellonella* L. (Pyralidae) in Belleville, Canada (Arthur 1958). As a hyperparasitoid it was collected on *Campoletis sonorensis* Cameron, parasitoid of important pests of maize (Vinson and Iwantsch 1980); also, on *Diadegma insulare* Cresson on cruciferous pests (Lee and Heimpel 2005).

Conura maculata Fabricius (Chalcididae) (Fig. 1K, L) was collected as a solitary parasitoid in *A. catalaunalis* pupae, with four specimens in El Fuerte and Sinaloa, respectively (Table 2). As a primary parasitoid, it has been reported on chrysalids of *Opsiphanes invirae*

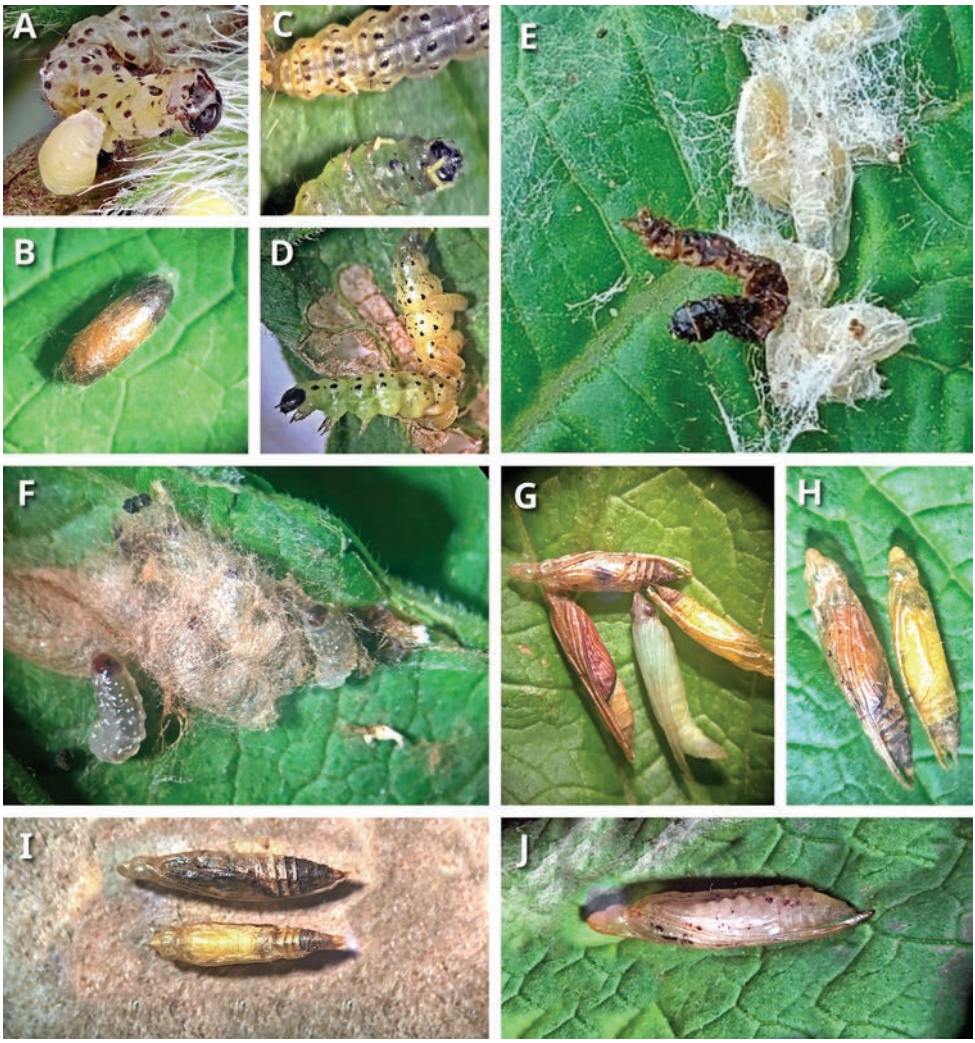

Figure 2. *Eiphosoma dentator* **A** larva feeding on an *Antigastra catalaunalis* larvae **B** cocoon; *Bracon* (*Habrobracon*) *platynotae* **C** eggs **D** larvae on *A. catalaunalis* larva; **E** cocoon **F** *Goniozus punctaticeps* larvae and cocoon on *A. catalaunalis* larvae; *C. maculata* **G** healthy pupae of *A. catalaunalis* (below) and pupae parasitized **H** parasitized pupae; *Conura* spp. **I** pupae parasitized by *C. side* (above) *C. maculata* (below); *C. side* **J** pupae of *A. catalaunalis* parasitized.

amplificatus Stichel, a pest of palm oil in Argentina (Gervazoni and Arbino 2018), and Rio Grande do Sul, Brazil (Salgado-Neto and Lopes-Da-Silva 2011). *Conura maculata* has been recorded as a hyperparasitoid on *Cotesia rubecula* Marshall and *C. glomerata* L. (McDonald and Kok 1991). This parasitoid species is widely recorded in America, mostly from tropical areas (Delvare 1992). Özdikmen (2011), noted that *C. maculata* is distributed from Mexico to Paraguay. Recently, Huber et al. (2021), reported the presence of *C. maculata* in Canada and the USA. *Conura* (=*Spilochalcis*) sp. (Hallman and Sanchez 1982) was the only record of association between this genus of parasitoid wasp on *A. catalaunalis* in

Colombia (Table 1). Thus, in the present study, the association of *C. side* and *C. maculata* with *A. catalaunalis* in sesame in Sinaloa, Northwest Mexico, is reported for the first time.

Only one specimen of *Perilampus platigaster* species group (Smulyan 1936), (Perilampidae) (Fig. 1M, N), was obtained in Mocorito (Table 2). Members of this genus are known to be hyperparasitoids, mainly of Tachinidae (Diptera) and Ichneumonoidea (Hymenoptera) (Darling 1997). This is the first report of *Perilampus platigaster* species group associated with *A. catalaunalis* pupae.

The lack of sequences of *E. dentator* and *H. platynotae* in the GenBank database, did not allow a molecular confirmation at the species level; however, it helped to confirm the genus, and because these sequences were deposited in this database, they can be used as references in future research on this species.

Conclusions

Among the three species of *A. catalaunalis* larval parasitoids, only *Bracon* (*Habrobracon*) *platynotae* was more abundant in all three collection sites and throughout the crop cycle (Table 2), with a higher presence in August, consistent with the population peaks of *A. catalaunalis*. This parasitoid has attributes that could position it as a candidate for mass-rearing studies and for use as a biological control agent. In this study, no apparent hyperparasitism was found on its larvae, nor on the larvae of the other larval parasitoids such as *Goniozus punctaticeps* and *Eiphosoma dentator*. The most abundant pupal parasitoids were *Conura maculata* and *Brachymeria annulata*. The four wasps reared from pupae also can act as hyperparasitoids of Ichneumonoidea (Hymenoptera) and Tachinidae (Diptera). In this study, all specimens of the families Chalcididae were obtained from *A. catalaunalis* pupae, and it is very likely that *Perilampus platigaster* species group is a hyperparasitoid of the collected Ichneumons, due to the background we have on this species group.

The obtained results offer alternatives for using several parasitoid species in an integrated management program for sesame cultivation in Sinaloa, Mexico. This includes the proposal of using *B. platynotae* as a biological control agent through augmentation, or the use of the parasitoid complex in conservation strategies for beneficial parasitoid and predator fauna.

References

Alam MM (1989) Vegetable pests and their natural enemies in Barbados. Proc. 22nd CFCS annual meeting in St. Lucia, 1986 Vol. XXII, 295–302.

Arthur AP (1958) Development, behaviour, and descriptions of immature stages of *Spilochalcis side* (Walk.) (Hymenoptera: Chalcididae). Canadian Entomologist 90: 590–595. https://doi.org/10.4039/Ent90590-10

Baskaran RKM, Thangavelu S (1990) Studies on the incidence of sesame shoot webber, *Antigastra catalaunalis* Duponchel and its parasitoid *Trathala flavo-orbitalis* Cameron. Sesame and Safflower Newsletter 5: 29–32. https://doi.org/10.9734/JAERI/2016/28483

Behera PK (2011) *Trathala flavo-orbitalis*, natural enemy of sesame shoot webber and capsule borer in Coastal Odisha. Insect Environment 17: 133–134. https://www.cabidigitallibrary.org/doi/pdf/10.5555/20123330846

Bhatnagar VS, Davies JC (1979) Arthropod endoparasites of insect pests (excluding *Heliothis* spp.) recorded at ICRISAT Center Andhra Pradesh, India, 1974–1979. Progress Report 3, 17 pp.

Biswas GC, Kabir SMH, Das GP (2001) Insect pests of sesame, *Sesamum indicum* Linn. in Bangladesh, their succession and natural enemies. Indian Journal of Entomology 63(2): 117–124.

Boucek Z, Halstead JA (1997) Chalcididae. In: Gibson GPA, Huber JT, Woolley JB (Eds) Annotated keys to the genera of Nearctic Chalcidoidea (Hymenoptera). NRC Research Press, Ottawa, Ontario, 151–164.

Chadha SS (1974) Effect of some climatic factors on the fluctuation of populations of *Antigastra catalaunalis* Duponchel [Lepidoptera: Pyralidae] a pest of *Sesamum indicum* L. Samaru Misc. 48, 23 pp.

Choudhary MD, Kumawat KC, Samota RG, Bajaya T (2017) Evaluation of sequences of integrated pest management practices against sesame Leaf and Capsule Borer, *Antigastra catalaunalis*. Journal of Pharmacognosy and Phytochemistry 6: 1440–1444.

Choudhary R, Singh KM, Singh RN (1986) Pest complex and succession of insect pests in *Sesamum indicum* (Linn). Indian Journal of Entomologist 48: 428–434.

Cushman RA (1914) A revision of the North American species of the Braconid genus *Habrobracon* Johnson (Ashmead). Proceedings of the Entomological Society of Washington 16: 99–108. https://www.biodiversitylibrary.org/partpdf/7071

Darling DC (1997) Perilampidae. In: Gibson GPA, Huber JT, Woolley JB (Eds) Annotated keys to the genera of Nearctic Chalcidoidea (Hymenoptera). NRC Research Press, Ottawa, Ont., 534–540.

Dasch CE (1979) Ichneumon-flies of America North of Mexico: 8. Subfamily Cremastinae. Memoirs of the American Entomological Institute 29: 1–702.

Delvare G (1992) Les Chalcididae (Hymenoptera) d'importance économique dans les palmeraies d'Amérique tropicale. Bulletin de la Société entomologique de France 97: 349–372. https://doi.org/10.3406/bsef.1992.17828

Diaz R, Hibbard K, Samayoa A, Overholt WA (2012) The arthropod community associated with tropical soda apple and natural enemies of *Gratiana boliviana* (Coleoptera: Chrysomelidae) in Florida. Florida Entomologist 95: 228–232. https://doi.org/10.1653/024.095.0141

Din-Gurs S, Husain T (1997) A note on natural enemies of *Antigastra* catalaunalis a major pest of sesamum. Shashpa. 4: 167–168.

El-Basha NA (2015) Developmental and reproductive biology of the ecto-larval parasitoid *Bracon hebetor* Say (Hymenoptera: Braconidae) on sesame capsule borer, *Antigastra catalaunalis* (Duponchel) (Lepidoptera: Pyralidae). Egyptian Academic Journal of Biological Sciences 8: 69–78. https://doi.org/10.21608/eajbsa.2015.12870

Evans HE (1979) The Bethylidae of America North of Mexico. Memoirs of the American Entomological Institute 27: 1–332.

Gaona-García G, Vanoye-Eligio V, Lara-Villalón M, Ruíz-Cancino E, Sánchez-Ramos G, Alma SM (2020) First report in Mexico of *Eiphosoma dentator* (Fabricius) (Hymenoptera: Ichneumonidae) as a parasitoid of the cactus-feeding *Loxomorpha flavidissimalis* (Grote)

(Lepidoptera: Crambidae). Proceedings of the Entomological Society of Washington 122: 515–518. https://doi.org/10.4289/0013-8797.122.2.515

Gauld ID (2000) The Ichneumonidae of Costa Rica, 3. Introduction and keys to species of the subfamilies Brachycyrtinae, Cremastinae, Labeninae and Oxytorinae, with an appendix on the Anomaloninae. Memoirs of the American Entomological Institute 63: 1–453.

Gebregergis Z, Dereje A, Fitwy I (2016) Assessment of Incidence of Sesame Webworm *Antigastra catalaunalis* (Duponchel) in Western Tigray, North Ethiopia. Journal of Agriculture and Ecology Research International 9(4): 1–9. https://doi.org/10.9734/JAERI/2016/28483

Gervazoni PB, Arbino MO (2018) First record of *Conura* (*Conura*) *maculata* (Fabricius, 1787) (Hymenoptera: Chalcididae) parasitizing *Opsiphanes invirae amplificatus* (Stichel, 1904) (Lepidoptera: Nymphalidae) in the province of Corrientes, Argentina. Check List 14: 1155–1159. https://doi.org/10.15560/14.6.1155

Goulet H, Huber JT (1993) Hymenoptera of the world: an identification guide to families. Agriculture of Canada, Publ. 1894, 668 pp.

Guilloux T, Monnerat R, Castelo-Branco M, Kirk A, Bordat D (2002) Population dynamics of *P. xylostella* (Lepidoptera: Yponomeutidae) and its parasitoids in the region of Brasilia. In improving biocontrol of *Plutella xylostella*. Proceedings of the International Symposium, 21–24 October, 184 pp. https://doi.org/10.1046/j.1439-0418.2003.00746.x

Gupta MP, Rai HS, Chaurasia SK (2002) Incidence and Avoidable Loss due to Leaf Roller/ Capsule Borer, *Antigastra catalaunalis* Dup. in Sesame. Annals of Plant Protection Sciences 10: 202–206.

Hallman GJ, Sanchez GG (1982) Possibilities for biological control of *Antigastra catalaunalis* (Lepidoptera: Pyralidae), a new pest of sesame in the western hemisphere. Entomophaga 27: 425–429. https://doi.org/10.1007/BF02372065

Hebert PDN, Cywinska A, Ball SL, de Waard JR (2003) Biological identifications through DNA barcodes. Proceedings of the Royal Society, Biological Sciences 270: 313–322. https://doi.org/10.1098/rspb.2002.2218

Huber JT, Bennett AMR, Gibson GAP, Zhang YM, Darling DC (2021) Checklist of Chalcidoidea and Mymarommatoidea (Hymenoptera) of Canada, Alaska and Greenland. Journal of Hymenoptera Research 82: 69–138. https://doi.org/10.3897/jhr.82.60058

Jakhmola SS (1983) Natural enemies of til leafroller and capsule borer, *Antigastra catalaunalis* Dup. Journal Bulletin of Entomology 24: 147–148.

Kalra VK (1989) Natural parasitism of sesame leaf webber and pod borer, *Antigastra catalaunalis* Duponchel. Indian Journal of Plant Protection 17: 9–11. https://www.phytojournal.com/archives/2019/vol8issue2S/PartG/Sp-8-2-101-178.pdf

Kapadia MN (1997) Biology of sesamum leaf roller and capsule borer *Antigastra catalaunalis* (Duponchel) in Gujarat. Gujarat Agricultural University Research Journal 22(2): 144–146.

Kumar S, Goel SC (1994) Record of a new larval parasitoid associated with *Antigastra catalaunalis* (Dup.) (Lepidoptera: Pyralidae). Journal of the Bombay Natural History Society 91: 331.

Lee JC, Heimpel GE (2005) Impact of flowering buckwheat on Lepidopteran cabbage pests and their parasitoids at two spatial scales. Biological Control 34: 290–301. https://doi.org/10.1016/j.biocontrol.2005.06.002

Mann J (1969) Cactus-feeding insects and mites. United States National Museum Bulletin 256: 1–158. https://doi.org/10.5479/si.03629236.256.1

McDonald RC, Kok LT (1991) Hyperparasites attacking *Cotesia glomerata* (L) and *Cotesia rubecula* (Marshall) (Hymenoptera: Braconidae) in Southwestern Virginia. Biological Control 1: 170–175. https://doi.org/10.1016/1049-9644(91)90116-H

Muesebeck CFW (1925) A revision of the parasitic wasps of the genus *Microbracon* occurring in America North of Mexico. No. 2580- Proceedings of the United States National Museum 67: 1–85. https://doi.org/10.5479/si.00963801.67-2580.1

Nair MRGK (1986) Insect and mite pests of crops in India. Indian Council of Agricultural Research, New Delhi, India, 99–102.

Naveen B, Nadagouda S, Ashoka J, Kariyanna B (2019) Natural enemies for sesame leaf webber *Antigastra catalaunalis* (Duponchel) (Lepidoptera: Pyralidae) on sesame. Journal of Pharmacognosy and Phytochemistry SP2: 257–259. https://www.phytojournal.com/archives/2019/vol8issue2S/PartG/Sp-8-2-101-178.pdf

Negi PS, Venkatraman TV, Chatterjee KC (1944) The mass breeding of the braconid *Microbracon hebetor* Say in India. Current Science 13: 136–136. https://www.jstor.org/stable/24209399

Nickels CB, Pierce WC, Pinkney CC (1950) Parasites of the pecan nut casebearer in Texas. Technical Bulletin of the Texas Department of Agriculture No. 1011, 21 pp.

Özdikmen H (2011) New names for some preoccupied specific epithets in Chalcidoidea I: families Agaonidae, Aphelinidae, Chalcididae, Encyrtidae, Eulophidae (Hymenoptera: Parasitica). Munis Entomology & Zoology 6: 796–814.

Patel AA, Bhalani PA (1989) A new record of *Diadegma* sp. as larval parasites of sesamum leaf roller in Gujarat. Indian Journal of Entomologist 51: 474.

Ramakrishna ATV (1927) The parasitic Hymenoptera of economic importance noted from south India. Bulletin of Entomological Research 18: 73–78. https://doi.org/10.1017/S0007485300019714

Ramdas-Menon MG, Rattan L, Bhatacherjee NS (1960) Studies on *Antigastra catalaunalis* (Dduponchel), the til leaf-roller. II Bionomics and biology. Indian Journal of Entomologist 22: 1–6.

Reyes-Villanueva F (1987) Insectos parásitos de los lepidópteros plaga del nogal en Nuevo León, análisis de su potencial como agentes de control biológico. Folia Entomológica Mexicana 72: 111–120.

Risbec J (1950) Etat actuel des recherches entomologiques agricoles dans la region correspondant au secteur soudanais de recherches agronomiques. In C r. 1er Conf. int. Af rie. Ouest 1: 317–375.

Risbec J (1960) Les parasites des insectes d'importance economique en Afrique tropicale et a Madagascar. Agronomie Tropicale 15: 624–655. https://agritrop.cirad.fr/375765/1/ID375765.pdf

Robertson IAD (1973) Notes on the insect parasites of some lepidopteran pests in Tanzania. East African Agricultural and Forestry Journal 39: 82–93. https://doi.org/10.1080/00128325.1973.11662621

Salgado-Neto G, Lopes-da-Silva M (2011) First report of parasitism on pupae of *Opsiphanes invirae amplificatus* Stichel (Lepidoptera, Nymphalidae) by *Conura* (*Conura*) *maculata* (Fabricius)(Hymenoptera, Chalcididae) in Rio Grande do Sul, Brazil. Revista Brasileira de Entomologia, 55: 285–286. https://doi.org/10.1590/S0085-56262011005000016

Santos-Murgas A, Gutiérrez-Lanzas JJ, Lanuza-Garay A (2021) Registro de parasitismo de *Brachymeria annulata* (Hymenoptera: Chalcididae) en pupas de *Talides hispa* Evans, 1955 (Lepidoptera: Hesperiidae) en Panamá. Poeyana (512). [Recuperado a partir de] http://revistasgeotech.com/index.php/poey/article/view/343

Sarazú-Pillado RA, González-Hernández H, Cortez-Mondaca E, Valdez-Carrazco J, Almela JB, Lomeli-Flores R (2020) First Report of Sesame Leaf Webber in Sesame in Northern Sinaloa, Mexico. Southwestern Entomologist 45: 575–578. https://doi.org/10.3958/059.045.0228

Shenefelt RD (1978) Braconidae, 10. In: Van Achtenbeerg C, Shenefelt RD (Eds) Hymenopterorum Catalogus. Dr. W Junk BV, The Hague, 1425–1872.

Silvie PJ, Delvare G, Aberlenc HP, Cardozo R, Gomez V (2007) Novos parasitóides das pragas do algodoeiro recem identificados no Paraguai. In: X Simpósio de Controle Biológico, Brasília – DF. ID – 024.

Simoglou KB, Anastasiades AI, Baixeras J, Roditakis E (2017) First report of *Antigastra catalaunalis* on sesame in Greece. Entomologia Hellenica 26: 6–12. https://doi.org/10.12681/eh.14824

Smulyan MT (1936) A revision of the chalcid flies of the genus *Perilampus* Latreille occurring in America north of Mexico. Proceedings of the United States National Museum 83: 369–412. https://doi.org/10.5479/si.00963801.2990.369

Tipping PW (1993) Field studies with *Cassida rubiginosa* (Coleoptera: Chrysomelidae) in Canada thistle. Environmental Entomology 22: 1402–1407. https://doi.org/10.1093/ee/22.6.1402

Tung PT, Dung DT, Long KD (2011) Some bio-ecological characteristics of larval ectoparasitoid *Elasmus* sp. (Hymenoptera: Eulophidae) on sesami leaffolder *Antigastra catalaunalis* (Dup.) (Lepidoptera: Pyralidae) In Nghi Loc, Vietnam. J. Sci. Dev. 9: 129–138.

van Achterberg C (2011) Order Hymenoptera, family Braconidae. The subfamily Agathidinae from the United Arab Emirates, with a review of the fauna of the Arabian Peninsula. Arthropod fauna of the United Arab Emirates 4: 286–352.

Vinson SB, Iwantsch GF (1980) Host suitability for insect parasitoids. Annual Review of Entomology 25: 397–419. https://doi.org/10.1146/annurev.en.25.010180.002145

Walker AK (1994) Species of Microgastrinae (Hymenoptera: Braconidae) parasitizing lepidopterous cereal stem borers in Africa. Bulletin of Entomological Research 84: 421–434. https://doi.org/10.1017/S0007485300032557

Wilkinson DS (1931) Braconidae: Notes and new species. Bulletin of Entomological Research 22: 75–82. https://doi.org/10.1017/S000748530002976X

Wilkinson DS (1932) A revision of the Ethiopian species of the genus *Apanteles* (Hymenoptera: Braconidae). Transactions of The Royal Entomological Society of London 80: 301–344. https://doi.org/10.1111/j.1365-2311.1932.tb03312.x

Yu DS, van Achterberg C, Horstmann K (2016) Taxapad 2016. Ichneumonoidea 2015 (Biological and taxonomical information), Taxapad Interactive Catalogue Database on flash-drive. Nepean, Ottawa.

JHR 97: 755–780 (2024)
doi: 10.3897/jhr.97.129470
https://jhr.pensoft.net

RESEARCH ARTICLE

JOURNAL OF Hymenoptera RESEARCH
A peer-reviewed open-access journal
The International Society of Hymenopterists

Integrative taxonomy of a new species of a bumble bee-mimicking brood parasitic bee, *Tetralonioidella mimetica* (Hymenoptera, Apoidea, Apidae), investigated through phylogenomics

Michael C. Orr[1,2], Douglas Chesters[1], Paul H. Williams[3], Thomas J. Wood[4,5], Qingsong Zhou[1], Silas Bossert[6], Trevor Sless[7], Natapot Warrit[8], Pierre Rasmont[5], Guillaume Ghisbain[5], Mira Boustani[5], A'rong Luo[1], Yuan Feng[1], Ze-Qing Niu[1], Chao-Dong Zhu[1,9,10]

1 *Key Laboratory of Zoological Systematics and Evolution, Institute of Zoology, Chinese Academy of Sciences, Beijing, China* **2** *Entomologie, Staatliches Museum für Naturkunde Stuttgart, Stuttgart, Germany* **3** *Department of Life Sciences, Natural History Museum, London, UK* **4** *Naturalis Biodiversity Center, Darwinweg, Leiden, Netherlands* **5** *Laboratory of Zoology, Research Institute of Biosciences, University of Mons, Mons, Belgium* **6** *Department of Entomology, Washington State University, Pullman, USA* **7** *Department of Biology, York University, Toronto, Canada* **8** *Center of Excellence in Entomology, Department of Biology, Faculty of Science, Chulalongkorn University, Bangkok, Thailand* **9** *College of Life Sciences/International College, University of Chinese Academy of Sciences, Beijing, China* **10** *Key Laboratory of Animal Biodiversity Conservation and Integrated Pest Management, Institute of Zoology, Chinese Academy of Sciences, Beijing, China*

Corresponding authors: Chao-Dong Zhu (zhucd@ioz.ac.cn); Michael C. Orr (michael.christopher.orr@gmail.com)

Academic editor: Jack Neff | Received 15 June 2024 | Accepted 6 August 2024 | Published 24 September 2024

https://zoobank.org/9923889C-6C6C-42F6-8A08-DB42C200D7CC

Citation: Orr MC, Chesters D, Williams PH, Wood TJ, Zhou Q, Bossert S, Sless T, Warrit N, Rasmont P, Ghisbain G, Boustani M, Luo A'rong, Feng Y, Niu Z-Q, Zhu C-D (2024) Integrative taxonomy of a new species of a bumble bee-mimicking brood parasitic bee, *Tetralonioidella mimetica* (Hymenoptera, Apoidea, Apidae), investigated through phylogenomics. Journal of Hymenoptera Research 97: 755–780. https://doi.org/10.3897/jhr.97.129470

Abstract

A new species of bumble bee-mimicking brood parasitic bee, *Tetralonioidella mimetica* Orr & Zhu, **sp. nov.**, is described from China. The systematic placement of this species was initially challenging but was resolved using a combination of phylogenomic and COI barcode analyses, which strongly support the new species as a member of the genus *Tetralonioidella* Strand. Interestingly, the new species mimics the color pattern of both a bumble bee (*Bombus* Latreille), and its host *Habropoda* Smith species, a mimicry format previously unknown for bees. A review of the other *Tetralonioidella* species revealed three additional bee mimics, including two further likely model-host-brood parasite mimicry complexes. To

our knowledge, these represent the first documented three-tiered mimetic systems in bees. Several additional taxonomic actions recently became necessary in these and related taxa: *Tetralonioidella meghalayensis* Dohling & Dey, 2024 is synonymized **syn. nov.** with *Habropoda radoszkowskii* (Dalla Torre, 1896) and *Varthemapistra* Engel, **stat. rev.** is again synonymized with *Habrophorula* Lieftinck. Our results also highlight issues with the generic classification of the tribe Melectini as currently used, as *Melecta* Latreille was found paraphyletic in relation to the remaining melectine genera. As a first step toward resolving this issue, we return the *Melecta* subgenus *Eupavlovskia* Popov, **stat. rev.** to genus level and discuss the ongoing systematic uncertainties regarding melectine taxonomy.

Keywords
Anthophila, brood parasite, Melectini, mimicry, Nomadinae, taxonomy

Introduction

The inner workings of mimicry have long fascinated scientists, but relatively few systems have been studied in detail in insects. Special focus has targeted Lepidoptera such as the genus *Heliconius* Kluk, 1780 and its relatives (Dasmahapatra et al. 2012; Kronforst and Papa 2015). Similarly in bees, work has predominantly focused on the bumble bees (*Bombus* Latreille, 1802) (Williams 2007; Ezray et al. 2019; Chatelain et al. 2023). However, much remains unstudied even in those better-known systems, and the genomic underpinnings of the complex color polymorphisms of this group are only now beginning to be understood (Owen and Plowright 1980; Williams 2007, 2008; Pimsler et al. 2017; Tian et al. 2019). Solitary bees are understudied in comparison, typically with mimetic relationships merely suggested but not definitively demonstrated (Blaimer et al. 2018; Bossert et al. 2020), such that many additional examples are expected across the bee tree of life (Chatelain et al. 2023).

The tribe Melectini contains >200 species of obligately brood parasitic bees worldwide, with especially high species and generic diversity in Asia (Ascher and Pickering 2023) where bumble bees also attain their peak richness (Williams 1998). There has been relatively little recent taxonomic research focused on this group compared to the second half of the 20th century (e.g., the works of Lieftinck), although Griswold and Parker (1999) and Onuferko et al. (2021) both provided valuable insights into their systematics. This group is dominated by the large genera *Thyreus* Panzer, 1806 (around 112 valid species) and *Melecta* Latreille, 1802 (around 55 valid species). The third largest genus, *Tetralonioidella* Strand, 1914, currently includes 19 species and has been repeatedly suggested to be the sister group to the remaining Melectini (Dubitzky 2007; Michener 2007; Niu et al. 2017; Sless et al. 2022). Far more restricted in its distribution than the near-Holarctic *Melecta* and the Eastern Hemisphere *Thyreus*, *Tetralonioidella* is known primarily from Eastern Asia, ranging from north China southward to Indonesia and from India into easternmost China.

Interestingly, the distribution of *Tetralonioidella* is concordant with the Asian-Oceanic hotspot of *Habropoda* Smith, 1854 species richness, and also corresponds closely to the range of *Elaphropoda* Lieftinck, 1966, which together encompass the known hosts of these brood parasites (Lieftinck 1972; Wu 2000; Michener 2007). Based pri-

Table 1. Suggested host associations of *Tetralonioidella* (=*T.*). *Elaphropoda* = *E.*, *Habropoda* = *H.* Note that one species may use multiple hosts as seen in other Melectini (Lieftinck 1972).

Host	Host author	Parasite	Parasite author	Evidence	Source
H. sutepensis	(Cockerell, 1929)	*T. habropodae*	(Cockerell, 1929)	Co-flight	Cockerell 1929
H. christineae	Dubitzky, 2007	*T. heinzi*	Dubitzky, 2007	Elev., phenology, dist.	Dubitzky 2007
H. bucconis	(Friese, 1911)	*T. himalayana*	(Bingham, 1897)	Distribution	Dubitzky 2007
E. erratica	(Lieftinck, 1944)	*T. insidiosa*	(Lieftinck, 1944)	Co-flight	Lieftinck 1944
E. impatiens	(Lieftinck, 1944)	*T. vulpecula*	(Lieftinck, 1944)	Co-flight	Lieftinck 1944
H. xizangensis	Wu, 1979	*T. himalayana*	(Bingham, 1897)	Co-flight, abund., dist.	This study
H. mimetica	Cockerell, 1929	*T. mimetica*	Orr & Zhu, sp. nov.	Co-flight, abund., dist.	This study

marily on range overlap and concurrent collections, a total of five specific host-parasite associations have been suggested for *Tetralonioidella* (Table 1). Unfortunately, direct evidence of host associations remains elusive for this group due to their rarity.

Although *Tetralonioidella* was originally described as a genus over a century ago (Strand 1914), it was not until Lieftinck (1983) rediscovered the name and moved ten species into this taxon that it was widely used. More recently, Dubitzky (2007) and Niu et al. (2017) treated the species of Taiwan and mainland China, respectively. Unfortunately, despite recent efforts, the taxonomy of this rare genus remains problematic, as is exemplified by the fact that 9/19 species of *Tetralonioidella* lack female descriptions while another 2/19 lack descriptions for males in recent work (Niu et al. 2017; note there are 20 total with this paper). These various issues are further compounded by the large number of additional species expected to be recorded in China (Orr et al. 2022). For difficult groups such as these, integrative taxonomic methods incorporating multiple lines of evidence such as morphological and molecular data becomes especially valuable (Orr et al. 2020).

As part of an initial, systematic treatment of the group we here describe a new mimetic species, *Tetralonioidella mimetica* Orr & Zhu, sp. nov., and confirm its generic placement based on morphological and molecular analyses, the latter of which is also used to preliminarily investigate the relationships of the genera within Melectini. The remaining *Tetralonioidella* are then reviewed for additional mimics and potential hosts and mimicry models are discussed for these species. Where relevant, these are assigned to bumble bee color patterns to enable comparison with their geographic ranges. Finally, we briefly consider the phenomenon of mimicry among other Asian bees, with special focus on the Chinese fauna.

Materials and methods

Systematics

A total of seven specimens (three females, four males) of the new species were examined. All specimens directly examined are deposited in the Institute of Zoology, Chinese Academy of Sciences, Beijing (IZCAS), including the holotype and paratype of the new species. Where possible, type specimens were directly examined for other

species (9/19 species, the Chinese species), and otherwise reference was made to imaged type specimens (2/19: *Tetralonoidella habropodae* (Cockerell, 1929) and *Tetralonioidella pendleburyi* (Cockerell, 1926)), specimens (2/19), other images (4/19), and original descriptions (2/19) to ensure that the species focused on here is new and to discern whether other species represent mimics.

The terminology used largely follows that of Michener (2007) and Niu et al. (2017). Abbreviations used include: F = flagellomere, T = tergum, S = sternum. Images were taken using various equipment as follows: description and general morphological characters of the new species with an Olympus OMD EM1 firmware 4.4 using an Olympus Zuiko 60mm f:2.8 macro, other images including genitalia with a Canon EOS80D. Some images were brightened in post-processing to better approximate real-life color depth.

Sampling of sequence data

We constructed a backbone phylogenetic hypothesis using character-rich Ultra-Conserved Element (UCE) data, which was subsequently expanded with placement of additional species represented by COI barcodes only. For UCEs, nine species of Melectini were acquired from Sless et al. (2022) and re-analyzed with *Tetralonioidella* as the sister-group of the remaining melictine taxa, given its accepted phylogenetic placement (Sless et al. 2022). For COI, a total of 12 sequences representing minimally 10 species across five genera was taken from GenBank (NCBI) and the Barcode of Life Database (BOLD), including an outgroup from Anthophorinae (Table 2). Eight additional COI sequences were taken from a recent UCE study on the apid subfamily Nomadinae (Sless et al. 2022). An additional four new COI sequences of rare species were generated for this study using standard barcoding approaches (as in Orr et al. 2018). Accession numbers for all sequences are given in Table 2.

Phylogenetic analyses

We used the aligned UCE matrix of Sless et al. (2022) and parameters are given therein. Maximum likelihood reconstructions of the UCE data were performed using IQ-TREE v1.6.12 (Nguyen et al. 2015) with 1,000 ultrafast bootstraps (UFBoot, Hoang et al. 2018), 1,000 SH-aLRT replicates (Guindon et al. 2010), and best substitution model "GTR+F+R2" within IQ-TREE. A secondary phylogenetic analysis was conducted with the COI data, using the UCE result as a backbone. Effectively, the UCE data were used to constrain the relationships recoverable in a barcode tree, with special focus on older nodes where barcode data generally provide unreliable results. Nine species were represented in both the barcode and UCE data. Barcodes were aligned using Clustal Omega version 1.2.4 (Madeira et al. 2022), with the alignment of 26 sequences totaling 737 columns (365 distinct patterns, 290 parsimony-informative, 60 singleton sites, and 387 invariant sites). These were constrained in the COI inference (Zhou et al. 2016) by inputting the Newick format result of the UCE analysis as a partial constraint tree with the –g switch of IQ-TREE.

Table 2. Specimens sequenced. Columns given include published ID number, tribe, genus, species, and the source via which it can be queried. In the source, "here" refers to this paper and in such cases provides the pre-upload voucher code of the sample. GB refers to uploads on GenBank, and BOLD refers to uploads on the Barcode of Life Database.

ID	Tribe	Species	Source
CCDB-15281	Anthophorini	*Pachymelus peringueyi*	BOLD
BEECC863-09	Melectini	*Melecta alexanderi*	BOLD
BBHYG927-10	Melectini	*Melecta pacifica*	BOLD
BEECC859-09	Melectini	*Melecta separata*	BOLD
BEECC754-09	Melectini	*Melecta thoracica*	BOLD
BEECB476-07	Melectini	*Brachymelecta californica*	BOLD
BEECC854-09	Melectini	*Zacosmia maculata*	BOLD
KJ839671	Melectini	*Melecta albifrons*	NCBI
KJ839507	Melectini	*Melecta luctuosa*	NCBI
HM401245	Melectini	*Thyreus orbatus*	NCBI
EX037	Melectini	*Melecta albifrons*	Sless et al. 2022
EX036	Melectini	*Melecta italica* cf.	Sless et al. 2022
BLX881	Melectini	*Melecta thoracica*	Sless et al. 2022
EX042	Melectini	*Tetralonioidella pendleburyi*	Sless et al. 2022
EX044	Melectini	*Thyreomelecta sibirica*	Sless et al. 2022
EX088	Melectini	*Thyreus delumbatus*	Sless et al. 2022
EX090	Melectini	*Thyreus quinquefasciatus*	Sless et al. 2022
EX029	Melectini	*Brachymelecta californica*	Sless et al. 2022
D0863	Melectini	*Eupavlovskia obscura*	Here: MGPCC007-21 (BOLD)
D08632	Melectini	*Eupavlovskia obscura*	Here: MGPCC008-21 (BOLD)
IOZ(E)2148081	Melectini	*Tetralonioidella mimetica*	Here: MGPCC191-24 (BOLD)
IOZ(E)2148051	Melectini	*Tetralonioidella wuae*	Here: MGPCC192-24 (BOLD)
BSRUAA6806	Melectini	*Thyreus callurus*	Here: PQ074116 (GB)
BSRUAA6807	Melectini	*Thyreus centrimaculata*	Here: PQ074117 (GB)
BSRUAA6787	Melectini	*Thyreus ceylonicus*	Here: PQ074119 (GB)
BSRUAA6780	Melectini	*Thyreus himalayensis*	Here: PQ074118 (GB)
BSRUAA6801	Melectini	*Thyreus cyathiger* cf.	Here: PQ074120 (GB)

We compared the likelihood of this result with other hypotheses to evaluate the generic associations and validity of the taxa included here (with our tree considered ***hypothesis 1***, to see whether alternative scenarios were significantly better supported than our reconstruction when they were imposed via constraints). First, we tested whether *Melecta* was monophyletic without the tentative subgenus *Melecta* (*Eupavlovskia*) Popov, 1955 (***hypothesis 2:*** *Melecta* monophyletic). We then tested whether (*Eupavlovskia*) also belonged within the genus *Melecta* as considered by Michener (2000, 2007) (***hypothesis 3:*** *Melecta* monophyletic, with (*Eupavloskia*) as a subgenus). The latter two hypothesis scenarios were implemented with manually defined constraint files input to IQ-TREE as previous. Each of the three inferences incorporated model testing (Kalyaanamoorthy et al. 2017), with model TIM+F+I+G4 selected based on both the Akaike Information Criterion and Bayesian Information Criterion. The likelihood of the three hypotheses was compared with the approximately unbiased (AU) test, with 10,000 multiscale bootstrap replicates (Shimodaira 2002).

Results

Phylogeny

The backbone phylogeny provided generally reliable results for the groups of interest in Melectini (Fig. 1). As according to Sless et al. (2022), the genus *Tetralonioidella* was sister to the genus *Eupavlovskia* and both lineages together form the sister group to the remaining Melectini. The small genus *Zacosmia* Ashmead, 1898 was then sister to a well-supported group with the remaining melectine genera, where *Thyreomelecta* Rightmyer & Engel, 2003 was sister to *Thyreus*, with those two genera sister to *Melecta* + *Brachymelecta* Linsley, 1939. This latter group appears problematic, with a poorly supported grouping of several Eastern and Western Hemisphere species of *Melecta* recovered as sister to a clade comprising *Brachymelecta* and another clade of *Melecta* from both the Eastern and Western hemispheres. These results were generally consistent with Sless et al. (2022), save for the issues in *Melecta*, which is expected given that a subset of those data was used for the backbone.

Topological tests provided definitive insight into the placement of *Eupavlovskia*, strongly supporting it as separate from *Melecta* (Suppl. material 1: table S1, note S1), where it had previously been considered as only a subgenus by Michener (2000; 2007). However, as well as being originally described as a distinct genus, *Eupavlovskia* was also considered to be a valid genus by Lieftinck (1969; 1972; 1983), the last major reviser of Old World Melectini. Consequently, we return to the position of Lieftinck and restore *Eupavlovskia* to the generic level now with a phylogenetic justification, providing an account below in the Systematics subsection. Contrastingly, the results for whether or not *Melecta* was paraphyletic in relation to *Brachymelecta* were inconclusive (Suppl. material 1: table S1, note S1). As such, we choose not to take formal action on the status of *Melecta*; instead, we prefer to improve taxon sampling in future efforts to address the lingering possibility of *Melecta* not representing a monophyletic group.

Generic placement of the new species

The placement of the new species was initially difficult because it exhibited characteristics of both *Tetralonioidella* and *Eupavlovskia*. The exceptionally long forewing marginal cell supports the placement of this species in *Tetralonioidella*, following Michener's (2007) interpretation. However, a specimen of this species collected in 1993 from the IZCAS collection was labeled as "*Eupavlovskia* sp.". Both sexes were present, and this error was likely based on the distally enlarged and flattened hind basitarsus of the male (Fig. 2). As this character can also be found in *Melecta* (*Melecta*) and *Melecta* (*Paracrocisa*) Alfken, 1937, it does not appear to be uncommon or phylogenetically conserved in Melectini. Further, this species clearly agrees with the generic diagnoses of *Tetralonioidella* in Dubitzky (2007), Michener (2007), and Niu et al. (2017). Finally, the phylogenetic evidence presented herein clearly places the new species within *Tetralonioidella* with strong support, as detailed above, giving us confidence in this placement and highlights the need to better delineate *Eupavlovskia*.

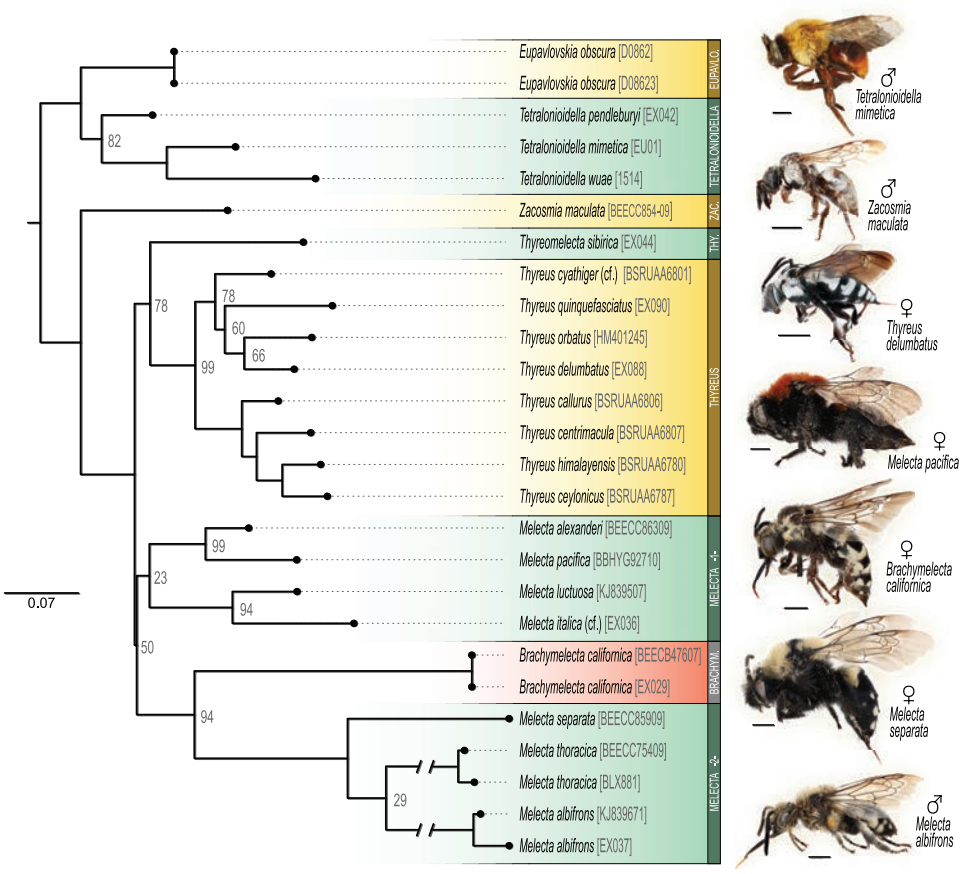

Figure 1. Phylogeny of Melectini. The tree was inferred using UCE and COI sequence data. Values at nodes are bootstrap support values and left scale bar refers to substitutions per site. Scale bars next to specimens indicate 2 mm length. Sequence identifiers are giving following species names.

Systematics

Superfamily Apoidea
Family Apidae
Subfamily Nomadinae
Tribe Melectini

Eupavlovskia Popov, 1955, stat. rev.

Melecta, sensu Michener 2000, 2007 (former subgenus).

Diagnosis. Diagnosis is best made in the male sex, as there are no known characters present in the female sex which allow unambiguous separation from all other melectine genera. Generally robust, moderately large bees, 12.5–16 mm in length. Mesosoma

covered with long and dense pubescence, this particularly evident on the dorsal surface where it covers and obscures the pronotal tubercules, scutum, scutellum, and scutellar spines. Marginal cell of forewing short, three times as long as broad, only slightly exceeding the third submarginal cell. Labrum almost square, widest basally, surface slightly concave, anterior border entire, little upturned, with rounded side edges, basal tubercles only weakly projecting but generally large. Hind tibia of the male strongly broadened and expanded at its apex, with strong ventroapical process extending laterally beyond the base of the tibial spurs. Inner hind tibial spur noticeably longer than the outer, gently and variably curved in different directions, appearing weakly undulate. Hind basitarsis of the male strongly to moderately broadened in its apical half to two-thirds. Male antennae without rhinarial pits on their posterior faces (sensu Lieftinck). T7 of male subtruncate, apex clothed with appressed tomentum. S7 very slender, with narrow, widely divergent arms and bilobed apex, the lobes fringed with strong bristles; S8 with well-developed ridges in apical half, apex itself with tufts of long feathery hairs.

Due to the thickly hairy mesosoma, *Eupavlovskia* can appear superficially quite similar to *Tetralonioidella*, but they may be separated by a short marginal cell (the most common character state for melectine bees) that only extends slightly beyond the apex of the third submarginal cell, the marginal cell itself being clearly shorter in maximum length than the length of the three submarginal cells combined; it is also shorter than the distance between its apex and the apex of the forewing. In *Tetralonioidella* the marginal cell is much longer, exceeding the third marginal cell and only slightly shorter than the length of the three submarginal cells combined; it is longer than the distance between its apex and the apex of the forewing. From other Eastern Hemisphere melectine bees, *Eupavlovskia* is separated by the scutellum, which is not flattened into a plate that overhangs the declivity of the propodeum and by the presence of arolia (with a plate-like scutellum and without arolia in *Thyreus*), by the three submarginal cells (two submarginal cells in *Sinomelecta* Baker, 1997), by the length of T1, which is dorsally shorter than T2 and the presence of arolia (T1 longer than to scarcely shorter than T2 dorsally and with arolia absent or nearly so in *Afromelecta* Lieftinck, 1972 and *Thyreomelecta*), from all *Melecta* or currently recognized *Melecta* subgenera by the combination of the long and dense mesosomal pilosity, the shape of the male legs, the absence of rhinaria on the antennal segments, and the structure of the male S7–8.

Distribution. From Spain in the west across the Western Palearctic to Central Asia (Uzbekistan, Bukhara; Lieftinck 1969). Not present in Africa or the Levant. Composed of two species, *Eupavlovskia funeraria* (Smith, 1854) from Spain to the Caucasus and *Eupalvovskia obscura* (Friese, 1895) from Italy to Uzbekistan.

Comments. *Eupavlovskia*, *Paracrocisa* and *Pseudomelecta* Radoszkowski, 1865 were separated from *Melecta* at the generic level by Lieftinck (1969; 1972; 1983), but Michener (2007) considered the given characters insufficiently distinctive and instead considered them as subgenera. We show here that *Eupavlovskia* is valid and separate from *Melecta* and its other groups (via molecular work here and prior morphological accounts), and formally return it to the generic level once more; further work is necessary on the rare groups *Melecta* (*Paracrocisa*) and *Melecta* (*Pseudomelecta*) to ascertain whether they also warrant generic-level treatment.

***Tetralonioidella mimetica* M. C. Orr & C. D. Zhu, sp. nov.**
https://zoobank.org/DE741BE9-30F8-4C28-A16C-CB22D673E2F3

Tetralonioidella mimetica Orr & Zhu, 2023: holotype (IOZ(E)2148141): male: male, holotype: China, Sichuan Province, Wenchuan City, Yingxiu County, 900 m, 1983.8.3, coll. Zhang Huaicheng. Verbatim: 四川汶川映秀 900m // 1983, 8.3张怀成 // IOZ(E)2148141. Translation: Sichuan Province, Wenchuan City, Yingxiu, 900m // 1983.8.3 Zhang Huaicheng // IOZ(E)2148141. Coordinates from Google Earth retroactive georeferencing: 31.05, 103.49.

Diagnosis. The forewing marginal cell is clearly longer than the distance from its apex to the apex of the forewing, and this character separates it from other melectine genera. Additionally, both sexes are immediately recognizable from nearly all other Melectini by color, specifically the yellow scutellar hair followed by a largely black metasoma tipped with reddened terga and hairs. Among melectines, it may still be confused with *Tetralonioidella tricolor*, from which both sexes can be distinguished by a transverse black stripe of hair on the scutum, and in males additionally by the unmodified hindleg of *T. tricolor* compared to the enlarged, flattened hindbasitarsus of the new species.

In the key of Niu et al. (2017), females run to couplet 7 but clearly do not fit the color patterns described. Males key to couplet 19 and their S8 more closely resembles that of *T. tianmuensis*, though with a much stronger medial point. Some males with brighter scutal setae color may key instead to *Tetralonioidella fukienensis* Lieftinck, 1983. In both cases, pubescence color of *T. mimetica* clearly distinguishes it from the alternatives.

Description. Male: pubescence and integumental color: See Figs 2, 3. Closely resembling bumble bee coloration, specifically group 134 of Williams (2007). Head black, integument of galea medium brown, mandibles dark brown, labrum medium brown-reddish, and sometimes clypeal edges dark brown. Mesosoma yellow over largely black integument. Legs brown to light brown, slightly lighter than primarily dark brown integument. Metasomal T1-2 black, sometimes reddened slightly on edge of T2. T3 onward increasingly reddish-orange in integument and pubescence, wholly so typically by T4. Metasomal sterna following terga, though starting at dark brown.

Males smaller, body size 12–13mm.

***Head*:** Galea only slightly longer than height of eye, shiny throughout, with minute single-sized punctures, tip angularly pointed but sides rounded to tip. Mandible unmodified, with weak but distinct inferior blade running parallel to main blade. Labrum shiny but somewhat craggy, large punctures indistinct from various angles, rim shallowly but obviously, roundly indented medially, with distinct row of hairs along rim though not forming dense brush. Lacking facial maculations. Clypeus strongly protuberant, by about half max eye width. Clypeus shiny medially near rim, tessellate elsewhere, with distinct rounding outward above shiny rim, with irregular but dense pitting throughout. Cheek immediately slanted inward from rear of compound eye. Antennal F1-2 roughly equal length, slightly longer than subsequent flagellomeres. Ocelli nearly linear, medial ocellus only slightly lower than lateral ocelli. Integumental

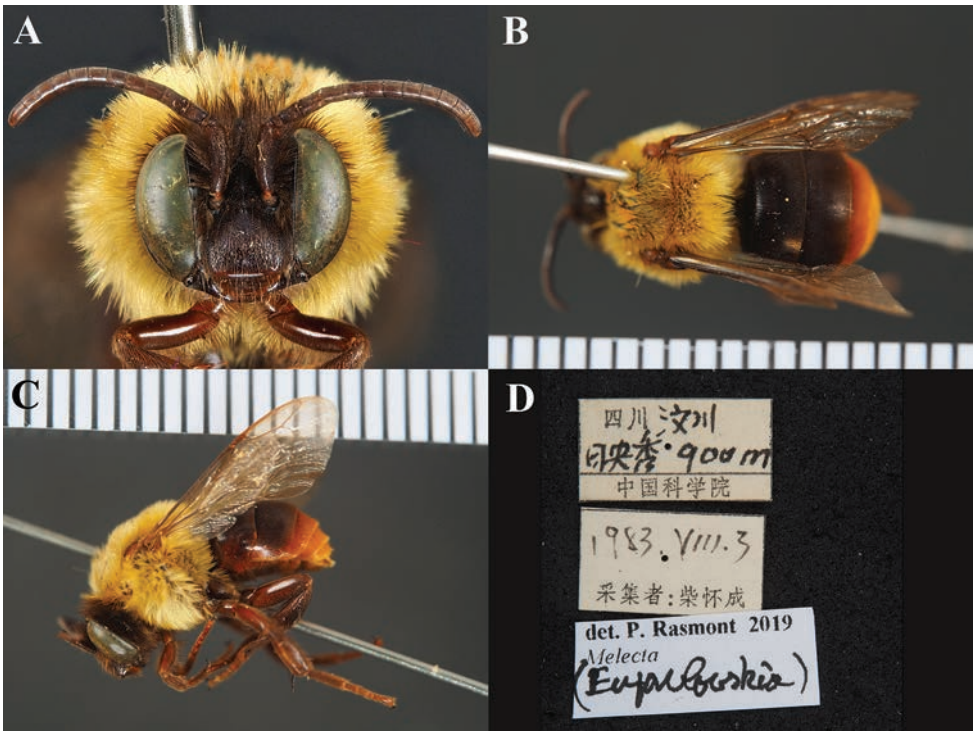

Figure 2. Male external morphology of *Tetralonioidella mimetica* sp. nov. Imaged from the holotype (IOZ(E)2148141) **A** face **B** dorsal **C** habitus **D** labels excluding identification label. Lines represent mm. Images by PR.

surface near ocelli shiny, strongly pitted below, slightly tessellate and sparsely, minutely pitted between lateral ocelli and compound eye.

***Mesosoma*:** Intertegular distance (at rear) averaging 3.58 mm based on four specimens (3.5, 3.6, 3.5, 3.7). Wings only very slightly darkened, hairy within cells along fore edge and decreasingly so posteriorly, apical papillae strongly apparent. Scutum, scutellum, metanotum typically obscured by dense, plumose hair. Below, integument densely punctured, interspaces weakly tessellate. Tegula translucent, medium brown, somewhat orange. Scutellar spines large, strongly pointed and directed posteriorly and slightly laterally, still obvious through dense hairs although eclipsed by them. Legs largely unmodified, save for hindleg: tibia in profile increasing in width from unmodified base to tip that is over twice its initial width, vaguely triangular overall, not flattened, broadest apically. Hindbasitarsus similarly narrow proximally, though flattened and broadened to tip like a paddle. Basitibial plate absent.

***Metasoma*:** T1-2 longer from above, about equal, with T3 at most roughly 2/3 of either. Terga covered in small hairs, largely simple medially but increasingly plumose laterally and apically, largely plumose by T4. Terga weakly tessellate between punctures, with weak reflections; usually apparent through appressed setae for T1-2 and often T3. Tergal rims unmodified, of similar opacity, color to rest. Male T6 unmodified.

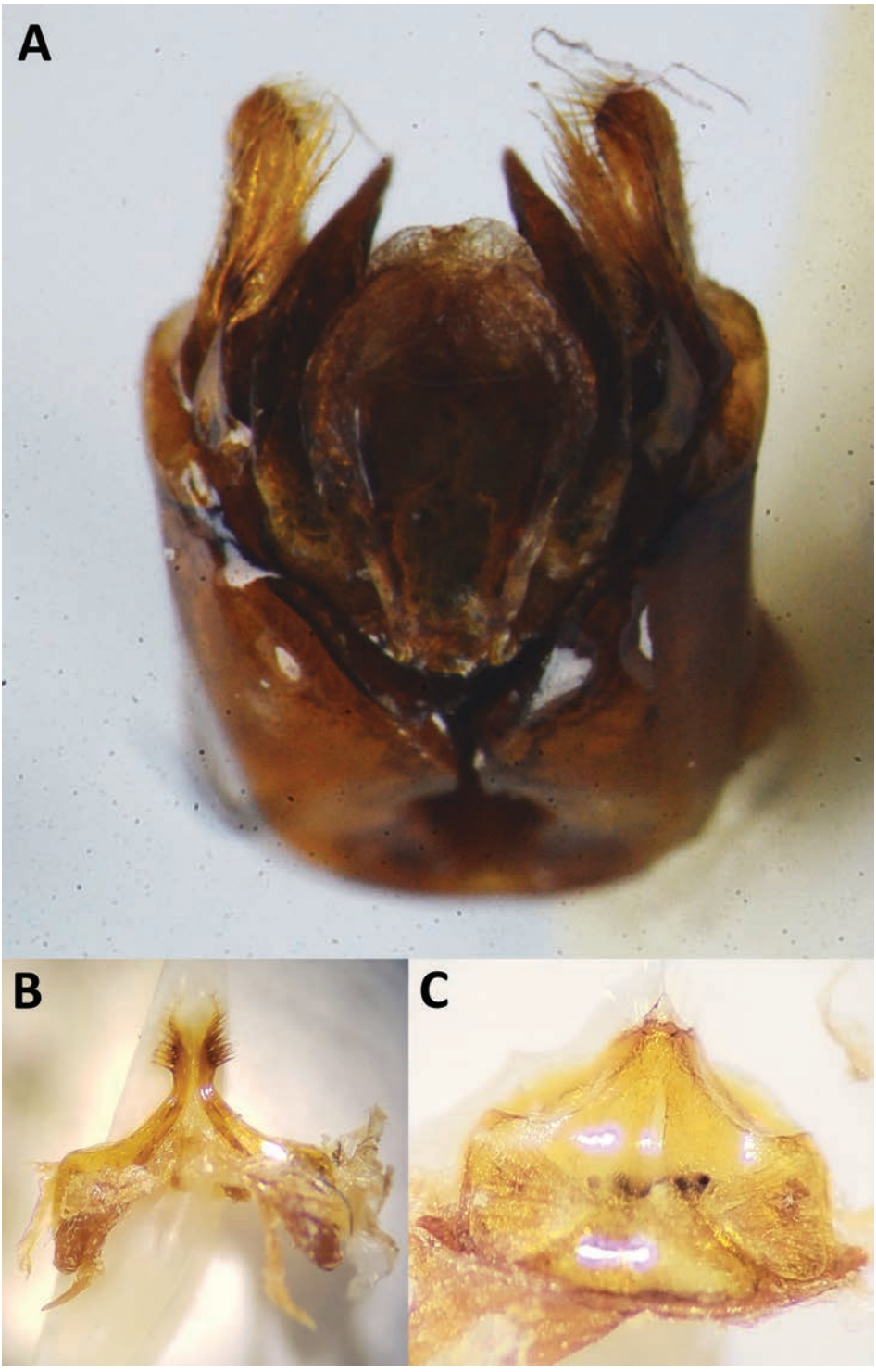

Figure 3. Male genitalia of *Tetralonioidella mimetica* sp. nov. Imaged from IOZ(E)2148161 **A** genital capsule (brightened, ~80×) **B** S7 (50×) **C** S8 (50×).

Male T7 in profile gradually thinning to tip with slight abrupt dip medially; without medial longitudinal carina, but covered in dense hairs beyond base; lacking lateral projections or flanges; tip from above bilobed with medial indentation similar in size to each of the lobes, with rounded tip. Male S6 unmodified and lacking distinctive hair patches, very slightly and gradually shallowed medially along rim. Male S7 overall initially appearing disconnected medially given weak medial scleritization contrasting with stronger tan integumental color laterally; with distinct lateral corners nearing 90°, but rounded; with strong subapical hair tufts directed laterally; tip broadly bifid with wide pointed tips, lateral to broad apical, V-shaped emargination. Male S8 shield-like, laterally gradually declivous in latter half though maintaining overall rounded outline until near tip, there projected forward and narrowing to tip, sharply pointed medially with long hairs arising from below. Male genital capsule with outer corners, where gonocoxite tips curve inward to gonostylus, lacking any flange, instead marked by narrowing toward tip, though again slightly expanded terminally, largely without hairs. Interior projection between gonostylus and penis valves also narrowed to tip, but entirely covered in long, plumose hairs largely obscuring form.

Female: highly similar to males overall, differing as given: Pubescence and integumental color: See Fig. 4. Head generally slightly darker through, save glossa and labrum. Leg hairs darker, more often black or dark brown, integument similar.

Females slightly larger, in part due to more tapering, elongate metasoma, body size 13–14mm, largest nearing 16mm.

***Head*:** labrum more narrowly and abruptly indented medially, forming clearer corners.

***Mesosoma*:** Intertegular distance (at rear) similar, averaging 3.63mm based on three specimens (3.8, 3.5, 3.6). Legs unmodified, hind tibia only slightly expanded apically, with widest point clearly before tip.

***Metasoma*:** Overall shape roughly similar but tapering to more distinct point terminally. T1-5 visible from above, T6 typically only visible for pygidial plate, itself triangular near base, coming to narrow tip with near-parallel sides. Sterna largely unmodified, last visible sterna narrowed and curled upward, elongate, forming support for very long sting.

Distribution. This species is recorded from Sichuan (four sites), Guangzhou (one site), and Hunan (one site) at elevations of 700 m, 700–900 m, 900 m, 1150–1200 m, 1270 m, and 1300 m (relatively low for Sichuan bumble bees, Williams et al. 2009). Notably, this species has not been found on the Qinghai-Tibetan Plateau or the lower elevations of the Sichuan depression (the latter absence could in part be due to local landscape alteration). This bee might be restricted to mid-elevations as such, below the edge of the nearby Qinghai-Tibetan Plateau, although we cannot yet determine any type of habitat specificity with the little data available.

Phenology. This bee has been collected from July 24 through August 18.

Bee hosts. *Habropoda mimetica* Cockerell, 1927 is the most likely host, based on similarities in known distribution (mid-elevation ringing Sichuan depression and adjacent similar habitat), phenological matching, and elevational similarity. This association was especially evident at the Baishuihe National Nature Reserve in Sichuan, where

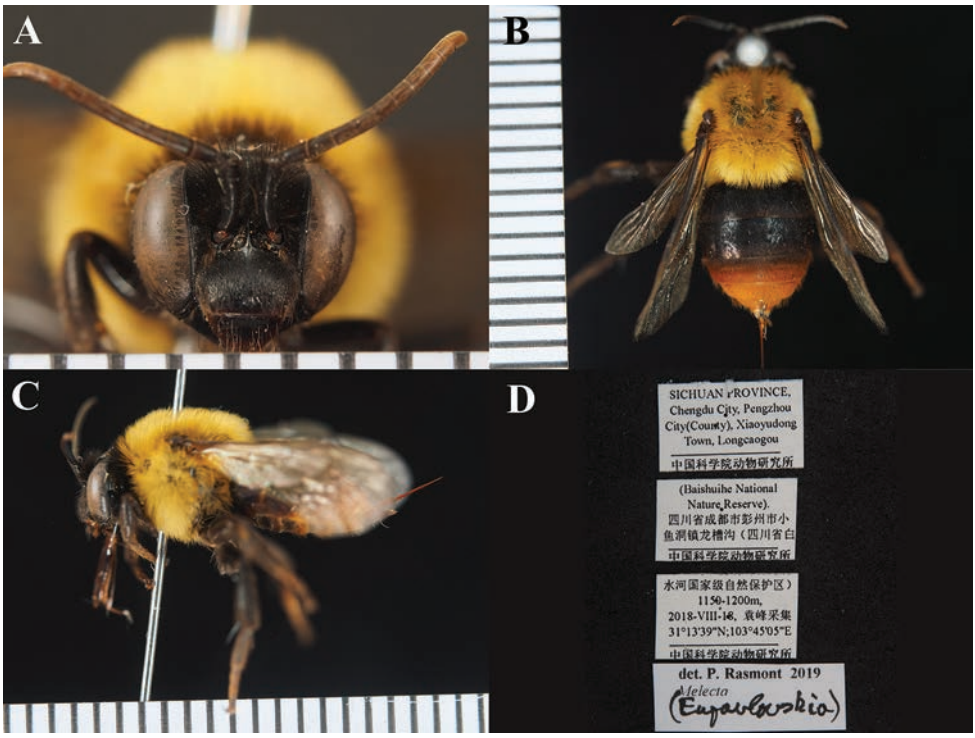

Figure 4. Female external morphology of *Tetralonioidella mimetica* sp. nov. Imaged from IOZ(E)2148071 **A** face **B** dorsal **C** habitus **D** labels excluding ID label. Lines represent mm. Images by PR.

H. mimetica was exceedingly common, while other species of *Habropoda* were rarer (*Habropoda omeiensis* Wu, 1979, *Habropoda sinensis* Alfken, 1937). It may be that this species targets multiple hosts, but among these *H. mimetica* is almost certainly utilized.

Floral visitation. No floral data are available for this species. Brood parasites are generally considered relatively generalist, given that they need not collect pollen for their offspring, but tracking specific resources may benefit a brood parasite in finding specialized hosts.

Etymology. The name "*mimetica*" is given to reference its mimicry and also its likely host, *Habropoda mimetica*. This name derives from the Ancient Greek adjective *mimetikos* (that which imitates), and is in the feminine singular nominative form.

Material examined. All are paratypes except for the holotype: IOZ(E)2148141: male, holotype: China, Sichuan Province, Wenchuan City, Yingxiu City, 900 m, 1983.8.3, coll. Zhang Huaicheng; IOZ(E)2142171: male: China, Chongqing City, Wanzhou District, Wangerbao National Nature Reserve, 1300 m, 1993.8.15, Song Shimei; IOZ(E)2148161: male, genitalia pulled: China, Guizhou Province, Tongren City, Shiqian County, Jinxing village, 700 m, 1988.7.24, coll. Yang Longlong; IOZ(E)2148151: male: China, Hunan Province, Xiangxi Tujia and Miao Autonomous Prefecture, Yongshun County, Muhe Forest farm, 700–900 m, 1988.8.8, coll.

Yang Longlong; IOZ(E)2148081: female, EU1 COI voucher: China, Sichuan Province, Baishuihe National Nature Reserve, 31°15'56"N, 103°50'02"E. 2018.8.17, coll. Feng Yuan; IOZ(E)2148071: female: Sichuan province, Chengdu City, Pengzhou City, Xiaoyudong Town, Longcaogou (Baishuihe National Nature Reserve), 31°13'39"N, 103°45'05"E, 1150–1200 m, 2018-VIII-18; IOZ(E)2148061: female: Sichuan Province, Wenchuan City, Yingxiu County, 900 m,1983.8.3, coll. Zhang Huaicheng.

Comments. The new species was originally set aside by Yan-Ru Wu as a member of *Eupavlovskia*, later identified as a possible *Tetralonioidella* by MCO and ZN and then hypothesized to be *Eupavlovskia* again by PR.

Review of mimicry patterns of species of *Tetralonioidella*

Bumble bees seem the most likely model in this system. Given the complexity of the color patterns detailed herein, it seems unlikely that they have arisen and been maintained by chance, or by aposematism as might be the case for some all-black, red-tailed species (Williams 2007). Bumble bees are commonly mimetic models for a wide range of taxa (Willadsen 2022; Chatelain et al. 2023), including for each other (Williams 2007; Williams 2008). This is likely a consequence of their sociality and defensiveness at nests, their generally high willingness to sting compared to solitary bees, the distinctiveness of their often-vibrant color patterns, and their high abundance in some environments. As another social and abundant group of bees, honey bees are similarly mimicked by a wide variety of taxa (Rettenmeyer 1970; Chatelain et al. 2023), and the same happens with various social wasps (Chatelain et al. 2023). From these facts, when mimetic systems exist incorporating bumble bee color patterns, it seems reasonable to assume that bumble bees serve as models (so long as other aggressive, social, abundant species are not involved).

If we accept that *H. mimetica* is the host or one of the hosts of *T. mimetica*, and that *Bombus* are the likely models in this system, then this species represents a three-tiered mimicry complex, comprised of the model bumble bee(s), the host *H. mimetica*, and the brood parasite *T. mimetica*. In this case, there are many potential bumble bee models, but the most likely models are species including *Bombus breviceps* Smith, 1852 and *Bombus trifasciatus* Smith, 1852, based on coloration, distribution, and commonness (Williams et al. 2009). To our knowledge, this is the first documented case of three-tiered mimicry in bees, comprised of model host-brood parasite. An additional potential member of this mimicry ring at the brood parasite level is the species *Tetralonioidella tricolor* (Lieftinck, 1972), which may be separated from *T. mimetica* by the transverse black hair band across the scutum and the unmodified male hind leg, but the host of that species remains unknown although both *Tetralonioidella* species are found in the same general region.

Further investigation of other *Tetralonioidella* species revealed two additional potential examples of three-tiered mimicry (Fig. 5). The first of these is detailed by Cockerell (1929), where he documented *Tetralonioidella habropodae* flying with *Habropoda sutepensis* Cockerell, 1929 at Doi Sutep mountain in Thailand, from which he infers not only resemblance but also a host association between the two. Although he does not note it, these two species also strongly resemble lighter individuals of *Apis cerana* Fabricius, 1793 which is found in

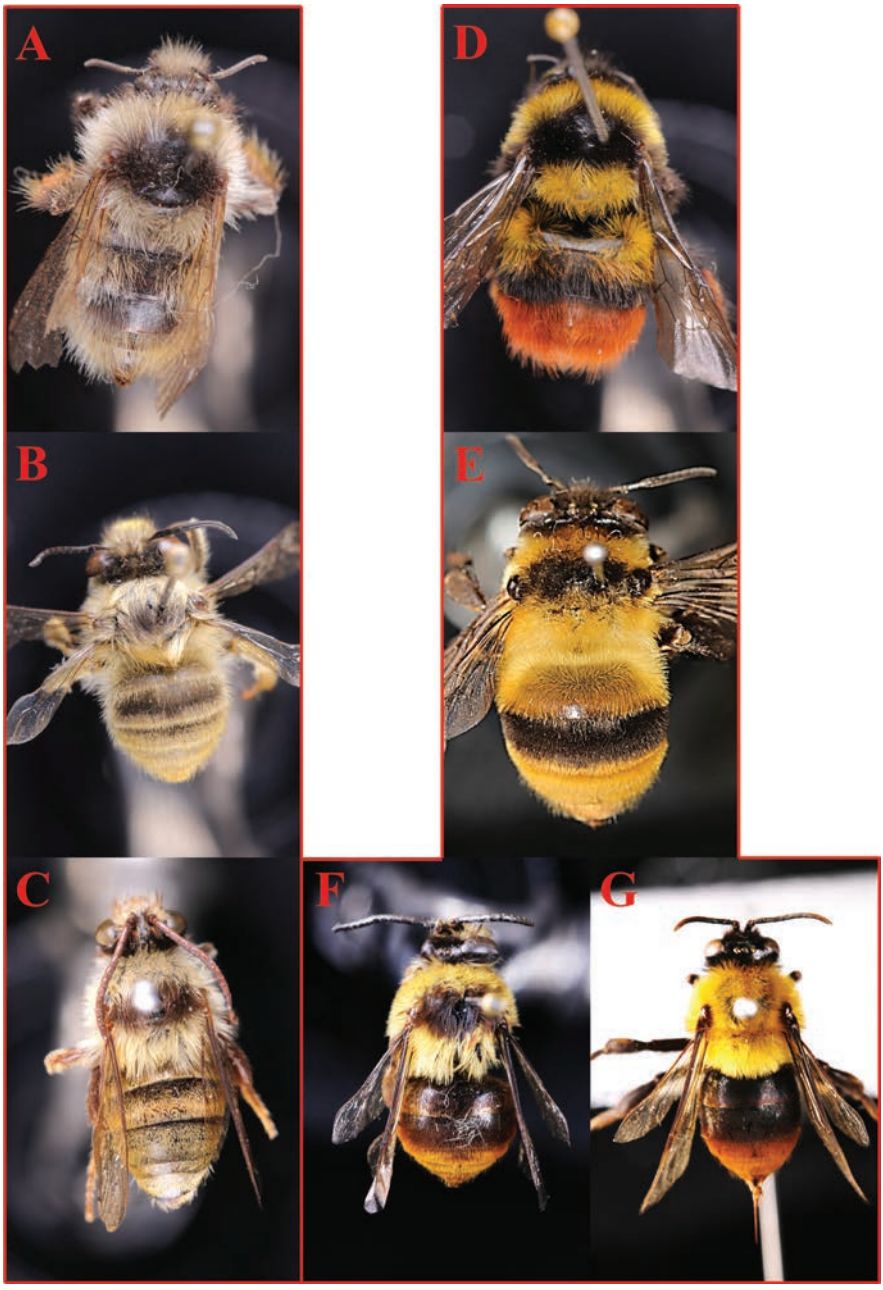

Figure 5. Hypothesized examples of three-tiered mimicry systems in bees. Given are the model (top), likely host (middle), and brood parasite (bottom). System 1: likely model **A** *Bombus lepidus* worker (IOZ(E)1429818); likely host **B** *Habropoda xizangensis* male (IOZ(E)2051720); and brood parasite **C** *Tetralonioidella himalayana* male (IOZ(E)2148111). System 2: likely model **D** *Bombus friseanus* worker (IOZ(E)1429817); likely host **E** *Habropoda mimetica* female (IOZ(E)2148091); and brood parasites **F** *Tetralonioidella tricolor* male (IOZ(E)2148051) **G** *Tetralonioidella mimetica* female (IOZ(E)2148071). Note that multiple species may act as models or hosts.

the region, making this a potential three-tiered mimicry system. The third example is newly proposed here and more tenuous, focused on the unusually widespread *Tetralonioidella himalayana* (Bingham, 1897) (found in the Himalaya, and inexplicably also Taiwan, with few records in-between). Because of its large range, this parasite must be attacking multiple *Habropoda* species. Among these, the Himalayan *Habropoda xizangensis* Wu, 1979 presents one of few host options covering the western range of *T. himalayana*, and notably that species exhibits an unusual olive-colored hair patterning similar both to and bumble bees of the *Bombus lepidus* Skorikov, 1912 group.

The species of *Tetralonioidella* with yellow scutal hair and largely black metasomas (e.g., *T. pendleburyi*, etc.) may also represent mimics of other bees such as *Xylocopa appendiculata* Smith, 1852, which can be quite common (although more so in or near human habitats). However, this will require further study, as it is an exceedingly common color pattern across various groups of bees, and it is unclear whether this is a result of mimicry (although suggested as such in Wilson et al. 2022).

Discussion

Systematics

The present study highlights the need to solidify and expand our understanding of melectine systematics and taxonomy. As an important first step, we provide a framework and method for integrating data types, which, going forward, will enable quicker and more efficient phylogenomic works on this and other understudied groups for which phylogenomic data are lacking but where many barcodes are available. This is especially important in developing countries where many new species are expected to be present, but where the capacity for phylogenomic sequencing and analysis remains limited (Orr et al. 2020). The biggest remaining challenge is to understand the true limits of the genus *Melecta*, as the name is ascribed to the genus type-species *Melecta albifrons* (Forster, 1771) (West Palearctic), which we found to group most closely related to several Western Hemisphere species (Fig. 1, *Melecta* clade '1'). This clade forms the sister group to the Western Hemisphere genus *Brachymelecta*, which renders *Melecta* paraphyletic: an additional clade of primarily Eastern Hemisphere species (Fig. 1, *Melecta* clade '2') form the sister group to *Melecta* clade 1 + *Brachymelecta*. Given the comparatively low supports in this region of the tree, however, we must sample additional taxa and ideally generate more UCEs or low-coverage genome data to better solidify these relationships and understand what other names, if in fact necessary, must be raised to the generic level. *Thyreus* should also be further investigated, as there are many species (>200), and it remains uncertain if the much smaller genus *Thyreomelecta* is valid and distinct.

There are some additional, more recent taxonomic actions which also require further treatment. This year, Dohling and Day (2024) described *Tetralonioidella meghalayensis* Dohling & Day, 2024 from four female specimens from north-eastern India (Meghalaya state), but the holotype specimen that they imaged is a pollen-collecting bee

based upon its visible scopa on the hind legs (see their figs 1, 3). It cannot be *Tetralonioidella*, as all these brood parasitic species lack scopae. From the character examination (including wing venation, with the 1st and 2nd recurrent veins meeting the 2nd and 3rd submarginal cross veins, respectively) and myriad other features, it clearly belongs to the anthophorine genus *Habropoda*. Further comparison with Lieftinck (1974) and pinned reference material at Naturalis by TJW confirms that not only is it *Habropoda*, but that it fits clearly within the distribution of, and morphological variation seen in *Habropoda radoszkowskii* (Dalla Torre, 1896) (clypeus medioapically with a small but distinct and narrowly triangular yellow mark (not transverse), face with dense adpressed to erect whitish hairs on paraocular areas and frons, terga without clearly defined pale apical hairbands, body pubescence reddish, without broad unicolorous patches of black or yellow hairs, eyes non-globular, tergal margins slightly lightened hyaline, hind basitarsis with mixture of black hairs), a species known from the Eastern Himalayas including the neighboring Indian state of Assam (Lieftinck 1974). Consequently, we synonymize *Tetralonioidella meghalayensis* with *Habropoda radoszkowskii* syn. nov. Hopefully, further efforts at imaging type specimens held outside of their home countries by various institutions will help avoid similar issues in the future (Orr et al. 2020, Warrit et al. 2023).

Additionally, the taxonomy of the relatively closely related subfamily Anthophorinae is also in need of clarification. Per Orr et al. (2022), the genus *Varthemapistra* Engel, 2018 was synonymized with *Habrophorula* based on several lines of evidence. Tran et al. (2024) later reversed this decision based on no additional data and the incorrect assertion that the "simple mandible" of the single described female representing *Varthemapistra* is unique (autapomorphic) among anthophorines, despite the fact that the genus is only documented from one sex and that females of *Anthophora peritomae* Cockerell, 1905 also have simple mandibles (noted in Orr et al. 2022, but not mentioned by Tran et al. 2024). To avoid moving *A. peritomae* to a monotypic genus on the other side of the world based on a single character (as the other defining characters of *Varthemapistra* are neither unique nor compelling, including even the color of the metatibial pubescence), and to avoid overcomplicating the taxonomy of a region most needing of taxonomic stability (Warrit et al. 2023), we continue to follow the conclusions of Orr et al. (2022), treating *Varthemapistra* as a junior synonym of *Habrophorula*. We further hope that taxonomists working in these and other groups can, going forward, focus on stability and make only necessary change rather than promulgating unnecessary new higher-level names for single species.

Mimicry

The three-tiered mimicry systems described here raise several interesting new questions that require further investigation. First and foremost, are the selective pressures that resulted in brood parasitic mimics being exerted by predators, or by the hosts themselves? The case for predation driving mimicry has long been established, but it may be initially unclear how hosts could also select for color patterns. In the case of Anthophorinae, they are highly visual bees known to actively come and visually inspect people in the field (Thorp 1969). When encountering brood parasites and other nest invaders, violent

reactions have been documented in multiple instances for numerous species, including actively chasing various flies and brood parasitic bees away from nest sites (Thorp 1969; Batra 1978; Orr et al. 2016). By appearing similar to their hosts, brood parasites might be able to avoid these defensive behaviors when attempting to invade the nests of *Anthophora* and relatives; this would be especially useful at large aggregations, where numerous active females could inadvertently protect other nests by chasing brood parasites away from their own. Another potential example of at least host and brood parasite mimicking each other includes some South American brood parasites of *Epiclopus* Spinola, 1851 (Vivallo 2014) and their potential host *Centris cineraria* Smith, 1854, which also belongs to a group with high visual acuity (notably, the color pattern is also exhibited by some nearby members of *Alloscirtetica* Holmberg, 1903, *Megachile saulcyi* Guérin-Méneville, 1845, and *Svastrides* Michener, LaBerge, & Moure, 1955; it is also a rather simpler color form that might arise more easily by chance). The model in this example remains unclear, however, as suitable *Bombus* color patterns do not overlap, at least not with the range of *Epiclopus*. In contrast, the solitary bees *Andrena* (Andrenidae) are generally considered to rely less on vision when foraging, likely requiring less intense visual capability compared to fast-flying species. Their principal brood parasites in the genus *Nomada* (Apidae: Nomadinae) show no form of color similarity to them, and indeed *Nomada* may be under selective pressure to chemically mimic *Andrena* species instead (Tengö and Bergstrom 1977), or there may be less pressure since many *Andrena* do not or weakly sting, though evidence for this conjecture overall is extremely limited. Experimental manipulations including color alteration of brood parasitic bees could prove useful for testing whether hosts in these systems might be exerting selective pressures leading to mimicry as a means to escape them (although some interactions are limited to the confines of dark nests where visual features would be less useful).

Of interest is also that all confirmed melectine mimics fall within *Tetralonioidella*. Though almost all melectine bees are associated strictly with Anthophorinae, and therefore, they might benefit from resembling their often violent hosts as described above, no other melectine species conclusively exhibit such coloration. However, Lieftinck (1972: 301) mentions remarks by Popov (1955), who associated *M.* (*Paracrocisa*) *kuschakewiczi* (Radoszkowski, 1890) with "*Anthophora semperi* Morawitz" the latter being a large, black bee with white spots on the metasoma. However, *A. semperi* Morawitz does not exist, and should rightfully be *A. semperi* Fedtschenko, 1875 which may be a junior synonym of *A. dubia* Eversmann, 1852 depending on the identity of the type material of *A. dubia*, which is currently unavailable for study. In any case, given the abundance of black and white color patterns in melectines, it remains unclear whether any association is biologically meaningful; there are no black and white-spotted anthophorine hosts in most of the Old-World Mediterranean basin, where black-and-white melectines are diversified. It is, therefore, possible that some other melectine genera mimic their anthophorine hosts, but this should be conclusively established with new studies. Notably, *Melecta* and other melectine genera in Asia can be found in proximity with many bumble bee species but do not mimic them, so we would suggest that proximity alone does not make mimicry inevitable. It may simply be that the unusual hairiness of many of the *Tetraloni-*

oidella, in comparison to nearly all other Melectini, made them pre-adapted to the use of color for mimicry of bumble bees, as most bumble bees also have at least medium-length hairs. *Eupavlovskia* is an exception, also with much longer and denser hair on the mesoscutum, but predation pressures may simply vary by region, their genomic architecture may not include the type of variation necessary, and it has not mutated sufficiently, or the evolutionary chance of engaging in mimicry has simply not occurred.

The habitats of the brood parasites, their hosts, and likely *Bombus* models generally seem to align, especially given that most have been collected together, but this may be due to limited distributional records and collecting effort. The distribution of *Tetralonioidella mimetica*, its likely host, and potential *Bombus* models are interesting from the perspective of color pattern matching. The new species *T. mimetica* differs slightly from its likely host (*H. mimetica*) in that the former does not have the transverse black scutum hair stripe of the latter, nor does it have yellow hair on any of the first several terga (Fig. 5). Conversely, *H. mimetica* and *T. tricolor* more closely align with group 133 (Williams 2007), which are more common and species-rich in the region and overall compared to other groups (Williams et al. 2009). Instead, the best match for *T. mimetica* is group 134 of Williams (2007), which is unexpectedly most species-rich and abundant in the Transhimalaya of Ladakh and Zanskar and adjacent westward areas, from which *T. mimetica* is currently not known. In Sichuan, where *T. mimetica* appears most common, *Bombus* with similar color patterns are still found, but they are rare and generally at higher elevations (Williams et al. 2009). One possible explanation is that *T. mimetica* is present in the western Himalaya but has yet to be documented there, which seems feasible considering the rarity of the species and the considerable distribution of the related *T. himalayana* (from the eastern Himalayan to Taiwan, although it appears disjunct). It is also possible that they co-occurred in the past, as distributions are likely to have changed with climatic shifts. In the absence of this potential larger distribution, it is not immediately clear why it does not more closely match local model species (or its host). It may simply be that this is a case of imperfect mimicry, such that benefits are had without too closely matching a given model (Kikuchi and Pfennig 2013).

The interplay of various factors on the quality of mimicry is also a topic worthy of further consideration, as it could help to explain distributional mismatches or some cases of imperfect mimicry. *Tetralonioidella* are generally medium-sized bees, so under the theory that larger prey animals must better resemble the protected species they imitate (Penney et al. 2012), we would expect them to show close matching to their models. The black line of hairs on the scutum seen in *T. tricolor* but not in *T. mimetica*, which is also seen or not in some bumble bees, may also have physiological effects of helping to dissipate heat (Williams 1991; Williams 2007). These types of systems, especially bumble bees with their high intraspecific variation, offer an interesting natural lab for testing the various potential trade-offs involved in mimicry, and could prove increasingly useful to study as ongoing climatic changes might amplify the influence of physiological considerations in such systems.

The bees of Asia present a unique and interesting opportunity for the further exploration of mimicry in bees. For example, the carpenter bees of the subgenus *Bombioxylocopa*

Maa, 1939 all appear to be mimics, and numerous other species have epithets referring to their color patterns resembling bumble bees, such as *Amegilla bombiomorpha* Wu, 1983 (similar to *T. tricolor*). However, questions remain as to whether some color forms indicate mimicry or simple aposematism. For instance, there are many Hymenoptera and other insects (potential mimics) that exhibit an all-black form with a red tail, which for aculeate Hymenoptera would clearly indicate the location of the sting. Simple color forms such as this are considerably more difficult to link to mimicry than are the more complex types exhibited by bees such as *T. mimetica*, given the number of coordinated changes necessary for the latter to evolve, and more work is clearly necessary to further explore these phenomena.

Funding statement

MCO was supported by the National Science Foundation of China's International Young Scholars Program (31850410464) and The National Science Fund for Distinguished Young Scholars (No. 31625024), and partially by the Chinese Academy of Sciences President's International Fellowship Initiative (PIFI) (2018PB0003, 2020PB0142, 2024PVC0046). CDZ's lab is supported by grants from the Key Laboratory of the Zoological Systematics and Evolution of the Chinese Academy of Sciences (grant number 2008DP173354) and the Key Program of the National Natural Science Foundation of China (Grant No. 32330013).

Acknowledgements

Laurence Packer and Petr Bogusch are thanked for their input on the paper, including photographs from the latter of several species, especially *Tetralonioidella tricolor*. Yiwei Lu and Mwinzi Duncan Kioko are thanked for logistics support. Author contributions: MCO, PHW, TJW, & CDZ conceived the study; MCO, TJW, SB, TS, NW, PR, GG, MB, AL, FY, & ZN provided specimens and/or data; MCO, PR, AL, & CDZ secured funding; MCO, DC, QZ, & SB conducted analyses; MCO, DC, & SB visualized results; MCO, DC, PHW, & TJW wrote the initial draft; all authors discussed or directly commented on drafts; all authors read and approved the paper.

References

Alfken JD (1937) Zur Unterscheidung der Bienengattungen *Crocisa* Jur. und *Melecta* Latr. Konowia 16: 172–175.

Ascher JS, Pickering J (2023) Discover Life bee species guide and world checklist (Hymenoptera: Apoidea: Anthophila). http://www.discoverlife.org/mp/20q?guide=Apoidea_species [accessed 23 February 2023]

Ashmead WH (1898) Some new genera of bees. Psyche 8: 282–285. https://doi.org/10.1155/1898/70320

Batra SW (1978) Aggression, territoriality, mating and nest aggregation of some solitary bees (Hymenoptera: Halictidae, Megachilidae, Colletidae, Anthophoridae). Journal of the Kansas Entomological Society, 547–559.

Bingham CT (1897) The Fauna of British India Including Ceylon and Burma, Hymenoptera. Vol. I. Wasps and Bees. Taylor and Francis, London. xxix + 577 pp. [4 pls] https://doi.org/10.5962/bhl.title.100738

Bossert S, Copeland RS, Sless TJL, Branstetter MG, Gillung JP, Brady SG, Danforth BN, Policarová J, Straka J (2020) Phylogenomic and morphological reevaluation of the bee tribes Biastini, Neolarrini, and Townsendiellini (Hymenoptera: Apidae) with description of three new species of Schwarzia. Insect Systematics and Diversity 4: 1–29. https://doi.org/10.1093/isd/ixaa013

Chatelain P, Elias M, Fontaine C, Villemant C, Dajoz I, Perrard A (2023) Müllerian mimicry among bees and wasps: a review of current knowledge and future avenues of research. Biological Reviews 98(4): 1310–1328. https://doi.org/10.1111/brv.12955

Cockerell TDA (1911) Descriptions and records of bees – XXXIV. Annals and Magazine of Natural History (8)7: 225–237. https://doi.org/10.1080/00222931108692933

Cockerell TDA (1926) XXX. – Descriptions and records of bees. – CXII. Journal of Natural History 18(104): 216–227. https://doi.org/10.1080/00222932608633504

Cockerell TDA (1927) Some bees, principally from Formosa and China. American Museum Novitates 274: 1–16.

Cockerell TDA (1929) Descriptions and records of bees – CXVII. Annals and Magazine of Natural History (10)4: 132–141. https://doi.org/10.1080/00222932908673035

Dalla Torre KW (1896) Catalogus hymenopterorum hucusque descriptorum systematicus et synonymicus: Apidae (Anthophila) (Vol. 10). G. Engelmann.

Dasmahapatra KK, Walters JR, Briscoe AD, Davey JW, Whibley A, Nadeau NJ, et al. (2012) Butterfly genome reveals promiscuous exchange of mimicry adaptations among species. Nature 487(7405): 94. https://doi.org/10.1038/nature11041

Dohling PNK, Dey D (2024) Description of a new species of the cleptoparasitic bee genus *Tetralonioidella* Strand, 1914 (Hymenoptera: Apidae: Melectini) from India. Animal Taxonomy and Ecology. https://doi.org/10.1556/1777.2024.12683

Dubitzky A (2007) Revision of the *Habropoda* and *Tetralonioidella* species of Taiwan with comments on their host-parasitoid relationships (Hymenoptera: Apoidea: Apidae). Zootaxa 1483: 41–68. https://doi.org/10.11646/zootaxa.1483.1.3

Engel MS (2018) A new genus of anthophorine bees from Brunei (Hymenoptera: Apidae). Journal of Melittology 78: 1–13. https://doi.org/10.17161/jom.v0i78.7488

Fabricius JC (1793) Entomologia Systematica Emendata et Aucta. . . ., Vol. 2, viii 519 pp. Hafniae: Proft.

Forster JR (1771) A catalogue of the animals of North America. To which are added short directions for collecting, preserving and transporting all kinds of natural history curiosities. B. White. Friese, H. 1911. Neue Bienenarten von Formosa und aus China (Kanton). Verhandlungen der Zoologisch-Botanischen Gesellschaft in Wien 61: 123–128.

Griswold T, Parker FD (1999) *Odyneropsis*, a genus new to the United States, with descriptions of other new cleptoparasitic Apidae (Hymenoptera: Apoidea). Entomological contributions in memory of Byron A. Alexander., 217–219.

Guindon S, Dufayard JF, Lefort V, Anisimova M, Hordijk W, Gascuel O (2010) New algorithms and methods to estimate maximum-likelihood phylogenies: assessing the performance of PhyML 3.0. Systematic biology 59(3): 307–321. https://doi.org/10.1093/sysbio/syq010

Guérin-Méneville F E (1845) Description de quelques-uns des Insectes les plus remarquable découverts par MA Delegorgue dans les pays des Boschimans, des Ama Zoulous, des Massilicatzi et au Port Natal, pendant les années 1838, 39, 40, 41, 42, 43 et 44. Revue Zoologique, par la Société Cuvierienne 18: 283–286.

Hoang DT, Chernomor O, Von Haeseler A, Minh BQ, Vinh LS (2018) UFBoot2: improving the ultrafast bootstrap approximation. Molecular biology and evolution 35(2): 518–522. https://doi.org/10.1093/molbev/msx281

Holmberg EI (1903) Delectus Hymenopterologicus Argentinus. Anales del Museo Nacional de Buenos Aires (3)2: 377–512.

Kalyaanamoorthy S, Minh BQ, Wong TK, Von Haeseler A, Jermiin LS (2017) ModelFinder: fast model selection for accurate phylogenetic estimates. Nature methods 14(6): 587–589. https://doi.org/10.1038/nmeth.4285

Kikuchi DW, Pfennig DW (2013) Imperfect mimicry and the limits of natural selection. The Quarterly review of biology 88(4): 297–315. https://doi.org/10.1086/673758

Kluk K (1780) Zwierzat histotyi naturalney Poczatki i gospodarstwo. Vol. 4. – Warsaw, Xiçzy Piiarów, [10] + 502 pp. [+ 4 double plates]

Kronforst MR, Papa R (2015) The functional basis of wing patterning in *Heliconius* butterflies: the molecules behind mimicry. Genetics 200(1): 1–19. https://doi.org/10.1534/genetics.114.172387

Latreille PA (1802) Histoire Naturelle des Fourmis, et Recueil de Mèmoire er d'Observations sur les Abeille, les Araignèes, les Faucheurs, et Autres Insectes, xvi. 445 pp. [12 pls] https://doi.org/10.5962/bhl.title.65810

Lieftinck MA (1944) Some Malaysian bees of the family Anthophoridae. Treubia (Dobutu-Gaku-Iho), hors serie: 57–138. [pl. 42]

Lieftinck MA (1966) Notes on some anthophorine bees, mainly from the Old World. Tijdschrift voor Entomologie 109: 125–161.

Lieftinck MA (1969) The melectine genus *Eupavlovskia* Popov, 1955, with notes on its distribution and host relations (Hymenoptera, Apoidea, Anthophoridae). Tijdschrift voor Entomologie 112(4): 101–122.

Lieftinck MA (1972) Further studies on Old World melectine bees, with stray notes on their distribution and host relationships (Hymenoptera, Anthophoridae). Tijdschrift voor Entomologie 115: 1–55.

Lieftinck MA (1974) Review of Central and East Asiatic *Habropoda* F. Smith, with *Habrophorula*, a new genus from China (Hymenoptera, Anthophoridae). Tijdschrift voor Entomologie 117(5): 157–224.

Lieftinck MA (1983) Notes on the nomenclature and synonymy of Old World Melectine and anthophorine bees (Hymenoptera, Anthophoridae). Tijdschrift voor Entomologie 126: 269–284.

Linsley EG (1939) A revision of the nearctic Melectinae. Annals of the Entomological Society of America 32: 429–468. https://doi.org/10.1093/aesa/32.2.429

Maa T-C (1939) *Xylocopa orientalia critica* (Hymen.), I. Subgenus *Bomboixylocopa* novum. Lingnan Science Journal 18: 155–160.

Madeira F, Pearce M, Tivey AR, Basutkar P, Lee J, Edbali O, et al. (2022) Search and sequence analysis tools services from EMBL-EBI in 2022. Nucleic acids research, 50(W1), W276–W279. https://doi.org/10.1093/nar/gkac240

Michener CD, LaBerge WE, Moure JS (1955) Some American Eucerini bees. Dusenia 6(6): 213.

Michener CD (2000) The Bees of the World (1st edition). The Johns Hopkins University Press, Baltimore and London.

Michener CD (2007) The Bees of the World (2nd edition). The Johns Hopkins University Press, Baltimore and London, xvi+953 pp.

Nguyen LT, Schmidt HA, Von Haeseler A, Minh BQ (2015) IQ-TREE: a fast and effective stochastic algorithm for estimating maximum-likelihood phylogenies. Molecular biology and evolution 32(1): 268–274. https://doi.org/10.1093/molbev/msu300

Niu Z, Feng Y, Zhu C (2017) Taxonomic study of the genus *Tetralonioidella* Strand from China (Hymenoptera: Apidae: Melectini). Zoological Systematics 42(4): 418–445.

Onuferko TM, Packer L, Genaro JA (2021) *Brachymelecta* Linsley, 1939, previously the rarest North American bee genus, was described from an aberrant specimen and is the senior synonym for *Xeromelecta* Linsley, 1939. European Journal of Taxonomy 754: 1–51. https://doi.org/10.5852/ejt.2021.754.1393

Orr MC, Griswold T, Pitts JP, Parker FD (2016) A new bee species that excavates sandstone nests. Current Biology 26(17): R792–R793. https://doi.org/10.1016/j.cub.2016.08.001

Orr MC, Pitts JP, Griswold T (2018) Revision of the bee group *Anthophora* (*Micranthophora*) (Hymenoptera: Apidae), with notes on potential conservation concerns and a molecular phylogeny of the genus. Zootaxa 4511(1): 1–193. https://doi.org/10.11646/zootaxa.4511.1.1

Orr MC, Ascher JS, Bai M, Chesters D, Zhu CD (2020) Three questions: How can taxonomists survive and thrive worldwide? Megataxa 1(1): 19–27. https://doi.org/10.11646/megataxa.1.1.4

Orr MC, Hughes AC, Chesters D, Pickering J, Zhu CD, Ascher JS (2021) Global patterns and drivers of bee distribution. Current Biology 31(3): 451–458. https://doi.org/10.1016/j.cub.2020.10.053

Orr MC, Branstetter MG, Straka J, Yuan F, Leijs R, Zhang D, et al. (2022) Phylogenomic interrogation revives an overlooked hypothesis for the early evolution of the bee family Apidae (Hymenoptera: Apoidea), with a focus on the subfamily Anthophorinae. Insect Systematics and Diversity 6(4): 7. https://doi.org/10.1093/isd/ixac022

Owen RE, Plowright RC ((1980) Abdominal pile color dimorphism in the bumble bee, *Bombus melanopygus*. Journal of Heredity 71(4): 241–247. https://doi.org/10.1093/oxfordjournals.jhered.a109357

Panzer GWF (1806) Kritische Revision der Insektenfauna Deutschlands, Vol. 2. [14] + 271 pp. [2 pls. Nürnberg: Felssecker.]

Penney HD, Hassall C, Skevington JH, Abbott KR, Sherratt TN (2012) A comparative analysis of the evolution of imperfect mimicry. Nature 483(7390): 461–464. https://doi.org/10.1038/nature10961

Pimsler ML, Jackson JM, Lozier JD (2017) Population genomics reveals a candidate gene involved in bumble bee pigmentation. Ecology and evolution 7(10): 3406–3413. https://doi.org/10.1002/ece3.2935

Popov VB (1955) Generic groupings of the palearctic Melectinae. Trudy Zoologicheskova Instituta, Akademii Nauk SSSR 21: 321–334. [In Russian]

Radoszkowski O (1865) [Tribu des Mélectides.] Horae Societatis Entomologicae Rossicae 3: 53–60.

Rettenmeyer CW (1970) Insect mimicry. Annual review of entomology 15(1): 43–74. https://doi.org/10.1146/annurev.en.15.010170.000355

Rightmyer MG, Engel MS (2003) A new Palearctic genus of melectine bees (Hymenoptera: Apidae). American Museum Novitates 2003(3392): 1–22. https://doi.org/10.1206/0003-0082(2003)392<0001:ANPGOM>2.0.CO;2

Shimodaira H (2002) An approximately unbiased test of phylogenetic tree selection. Systematic Biology 51(3): 492–508. https://doi.org/10.1080/10635150290069913

Skorikov AS (1912) Neue Hummelformen (Hymenoptera, Bombidae). IV. Russkoe Entomologicheskoe Obozrenie 12: 606–610.

Sless TJ, Branstetter MG, Gillung JP, Krichilsky EA, Tobin KB, Straka J, et al. (2022) Phylogenetic relationships and the evolution of host preferences in the largest clade of brood parasitic bees (Apidae: Nomadinae). Molecular Phylogenetics and Evolution 166: 107326. https://doi.org/10.1016/j.ympev.2021.107326

Smith F (1852) IX. Descriptions of some Hymenopterous Insects from Northern India. Transactions of The Royal Entomological Society of London 7(2): 45–48. https://doi.org/10.1111/j.1365-2311.1852.tb02209.x

Smith F (1854) Catalogue of Hymenopterous Insects in the Collection of the British Museum, Part 2, London, 199–465. [pls. vii–xii]

Spinola M (1851) Hymenópteros In: Gay C (Ed.) Historia Fisica y Politica de Chile . . . , Zoologia, Vol. 6. Paris: Casa del autor, 153–569.

Strand E (1914) H. Sauter's Formosa-Ausbeute, Apidae III. Archiv für Naturgeschichte, Abt. A 80(1): 136–144. https://doi.org/10.5962/bhl.part.26478

Tengö J, Bergström G (1977) Cleptoparasitism and odor mimetism in bees: do *Nomada* males imitate the odor of *Andrena* females? Science 196(4294): 1117–1119. https://doi.org/10.1126/science.196.4294.1117

Thorp RW (1969) Ecology and behavior of *Anthophora edwardsii* (Hymenoptera: Anthophoridae). American Midland Naturalist, 321–337. https://doi.org/10.2307/2423781

Tian L, Rahman SR, Ezray BD, Franzini L, Strange JP, Lhomme P, Hines HM (2019) A homeotic shift late in development drives mimetic color variation in a bumble bee. Proceedings of the National Academy of Sciences 116(24): 11857–11865. https://doi.org/10.1073/pnas.1900365116

Tran NT, Engel MS, Nguyen LTP (2024) A new species of *Habrophorula* from Vietnam and an updated key to species of the genus (Hymenoptera, Apidae). ZooKeys 1197: 261. https://doi.org/10.3897/zookeys.1197.118126

Vivallo F (2014) Taxonomic revision of the cleptoparasitic bee genus *Epiclopus* Spinola, 1851 (Hymenoptera: Apidae: Ericrocidini). Zootaxa 3857(1): 041–070. https://doi.org/10.11646/zootaxa.3857.1.2

Warrit N, Ascher J, Basu P, Belavadi V, Brockmann A, Buchori D, et al. (2023) Opportunities and challenges in Asian bee research and conservation. Biological Conservation 110173. https://doi.org/10.1016/j.biocon.2023.110173

Willadsen PC (2022) Aculeate hymenopterans as aposematic and mimetic models. Frontiers in Ecology and Evolution 10: 827319. https://doi.org/10.3389/fevo.2022.827319

Williams PH (1991) The bumble bees of the Kashmir Himalaya (Hymenoptera: Apidae, Bombini). Bulletin of British Museum 60(1): 1–204.

Williams PH (1998) An annotated checklist of bumble bees with an analysis of patterns of description (Hymenoptera: Apidae, Bombini). Bulletin of The Natural History Museum (Entomology) 67: 79–152. www.nhm.ac.uk/bombus/ [accessed 2023]

Williams P (2007) The distribution of bumblebee colour patterns worldwide: possible significance for thermoregulation, crypsis, and warning mimicry. Biological Journal of the Linnean Society 92(1): 97–118. https://doi.org/10.1111/j.1095-8312.2007.00878.x

Williams PH (2008) Do the parasitic *Psithyrus* resemble their host bumblebees in colour pattern? Apidologie 39: 637–649. https://doi.org/10.1051/apido:2008048

Williams P, Tang Y, Yao J, Cameron S (2009) The bumblebees of Sichuan (Hymenoptera: Apidae, Bombini). Systematics and Biodiversity 7(2): 101–189. https://doi.org/10.1017/S1477200008002843

Wilson JS, Pan AD, Alvarez SI, Carril OM (2022) Assessing Müllerian mimicry in North American bumble bees using human perception. Scientific Reports 12(1): 17604. https://doi.org/10.1038/s41598-022-22402-x

Wu Y-R (1979) A study on the Chinese *Habropoda* and *Elaphropoda* with descriptions of new species. Acta Entomologica Sinica 22: 343–348.

Wu YR (1983) Two new species of *Amegilla* from China (Apoidea: Anthophoridae)[*Amegilla bombiomorpha*, *Amegilla yunnanensis*]. Acta entomologica Sinica.

Wu YR (2000) Fauna Sinica Insecta Vol. 20. Hymenoptera. Melittidae, Apidae [in Chinese]. Science Press, Beijing. 442 pp. [9 plts]

Zhou X, Frandsen PB, Holzenthal RW, Beet CR, Bennett KR, Blahnik RJ, Bonada N, Cartwright D, Chuluunbat S, Cocks GV, Collins GE, deWaard J, Dean J, Flint OS, Hausmann A, Hendrich L, Hess M, Hogg ID, Kondratieff BC, Malicky H, Milton MA, Morinière J, Morse JC, Mwangi FN, Pauls SU, Gonzalez MR, Rinne A, Robinson JL, Salokannel J, Shackleton M, Smith B, Stamatakis A, StClair R, Thomas JA, Zamora-Muñoz C, Ziesmann T, Kjer KM (2016) The Trichoptera barcode initiative: a strategy for generating a species-level Tree of Life. Philosophical Transactions of the Royal Society B 371: 20160025. https://doi.org/10.1098/rstb.2016.0025

Supplementary material 1

Supplemental text and details

Authors: Michael C. Orr, Douglas Chesters, Paul H. Williams, Thomas J. Wood, Qingsong Zhou, Silas Bossert, Trevor Sless, Natapot Warrit, Pierre Rasmont, Guillaume Ghisbain, Mira Boustani, A'rong Luo, Yuan Feng, Ze-Qing Niu, Chao-Dong Zhu

Data type: docx

Link: https://doi.org/10.3897/jhr.97.129470.suppl1

Supplementary material 2

RaxML tree file

Authors: Michael C. Orr, Douglas Chesters, Paul H. Williams, Thomas J. Wood, Qingsong Zhou, Silas Bossert, Trevor Sless, Natapot Warrit, Pierre Rasmont, Guillaume Ghisbain, Mira Boustani, A'rong Luo, Yuan Feng, Ze-Qing Niu, Chao-Dong Zhu

Data type: barcodes_constrained

Link: https://doi.org/10.3897/jhr.97.129470.suppl2

JHR 97: 781–805 (2024)
doi: 10.3897/jhr.97.115489
https://jhr.pensoft.net

RESEARCH ARTICLE

JOURNAL OF Hymenoptera RESEARCH
A peer-reviewed open-access journal
The International Society of Hymenopterists

Five new species of *Metapolybia* Ducke, 1905, with the description of the male genitalia of seven species of the genus (Hymenoptera, Vespidae, Polistinae)

Gustavo B. Cortes[1], Fernando B. Noll[1], James M. Carpenter[2], Sergio R. Andena[3]

1 *Departamento de Ciências Biológicas, Instituto de Biociências, Letras e Ciências Exatas (IBILCE), Universidade Estadual Paulista (UNESP), São José do Rio Preto, SP, Brazil* **2** *Division of Invertebrate Zoology, American Museum of Natural, New York, NY, USA* **3** *Universidade Estadual de Feira de Santana, Departamento Ciências Biológicas, Museu de Zoologia, Feira de Santana, BA, Brazil*

Corresponding author: James M. Carpenter (carpente@amnh.org)

Academic editor: Michael Ohl | Received 8 November 2023 | Accepted 29 January 2024 | Published 26 September 2024

https://zoobank.org/32C3301F-70AF-4241-8B12-B4555F0AFA2B

Citation: Cortes GB, Noll FB, Carpenter JM, Andena SR (2024) Five new species of *Metapolybia* Ducke, 1905, with the description of the male genitalia of seven species of the genus (Hymenoptera, Vespidae, Polistinae). Journal of Hymenoptera Research 97: 781–805. https://doi.org/10.3897/jhr.97.115489

Abstract

Five new species of *Metapolybia* are described, *Metapolybia carpenteriana*, Andena & Noll, **sp. nov.** (Ecuador, Peru), *Metapolybia pseudodocilis* Cortes, **sp. nov.** (Bolivia), *Metapolybia richardsi* Andena, **sp. nov.** (Ecuador), *Metapolybia sulamerica* Carpenter, **sp. nov.** (Colombia), *Metapolybia zucchiana* Andena & Carpenter, **sp. nov.** (Panama), in addition to the hitherto unknown males of *M. bromelicola*, *M. encantata*, *M. mesoamerica*, *M. servilis* and *M. rufata* plus two new species. Comparative remarks for the species are given.

Keywords

Epiponini, Paper wasps, Social wasps

Introduction

Metapolybia Ducke is an epiponine genus with eighteen species described, strictly neotropical, extending from Mexico to the middle-southern part of Brazil and Paraguay, with most species found in the Amazon (Richards 1978; Cooper 1999; Andena and Carpenter 2011; Somavilla and Andena 2018; Andena et al. 2019).

Some species of *Metapolybia* have been studied in detail concerning behavior (West-Eberhard 1978; Karsai and Wenzel 2000; Baio et al. 2003; Chavarría and Noll 2013). The castes are hardly detectable by external morphology (Richards 1978; Carpenter and Ross 1984). Baio et al. (2003), studying *M. docilis*, found slight differentiation between queens and workers, at least in the early stages of nest development. In *M. aztecoides* it was found that castes are apparently determined by disputes among adults rather than by larval manipulation (West-Eberhard 1978, 2000). This process was later confirmed not only for the genus, but for the whole tribe (Chavarría-Pizzaro et al. 2023).

Richards (1978) considered the nest of *Metapolybia* as astelocyttarus, usually on a tree-trunk where the flat envelope is made of local material, often highly cryptic, but also on buildings where they may be relatively conspicuous. The nest is characterized by a single comb expanded suddenly in blocks, with new cells built on the substrate adjacent to earlier ones and on any side of them when the nest is on a horizontal surface, growing upwards on vertical surfaces and around curved surfaces (Wenzel 1998). The envelope is built up from the substrate or from fully elongated cell walls (*M. docilis*), with a single sheet and secretion forming clear windows; the entrance is peripheral and curved upward (Richards 1978; Wenzel 1998); however, two species lack an envelope (*M. bromelicola* and *M. encantata*).

According to Richards (1978) the genus is characterized by the absence of a pronotal keel or fovea; the entrance to the spiracular chamber high and very narrow; the occiput somewhat emarginate with the head produced behind the eyes; the gena not margined; the metasomal petiole long and narrow, being widened and convex at its posterior end. The species "*Metapolybia alfkenii*" once cited in a list of species recorded to Brazil (Barbosa et al. 2016), is, in fact, an erroneous contraction of *Mischocyttarus alfkenii* (Ducke 1904). Since the last revision (Richards 1978), seven species were described: *Metapolybia mesoamerica* Smethurst & Carpenter, 1998, *M. encantata* Cooper, 1999, *M. silvicola* Cooper, 1999, *M. servilis* Cooper 1999, *M. miltoni* Andena & Carpenter, 2011, *M. araujoi* Somavilla & Andena, 2018 and, *M. fraudator* Carpenter & Andena, 2019.

Here, we describe five new species of *Metapolybia*. Also, the male genitalia of seven species are depicted and re/described.

Methods

The specimens analyzed were borrowed from the following institutions: **AMNH**—Americam Museum of Natural History, New York, USA; **MPEG**—Museu Paraense Emílio Goeldi, Belém, Brazil; and **NHM**—Natural History Museum, London, UK.

The external morphology of dry pinned adult specimens was observed under the stereo microscope Leica MZ75. Photographs were taken using the stereo microscope Leica M205 C with attached Flexacam C1 camera and LASx software. Male genitalia were extracted, treated in a 10% KOH solution and observed under stereo microscope. Illustrations were produced for each specimen employing the Inkscape v. 1.3 software.

The terminology and standardization follow Richards (1978), Andena and Carpenter (2011), and Somavilla et al. (2018).

Results

***Metapolybia carpenteriana* Andena & Noll, sp. nov.**
https://zoobank.org/4ABBB23F-BEE8-4133-A843-2D29A13A5A5A
Figs 1–5

Diagnosis. Very like *M. suffusa* in color and general aspects, but with yellow markings more isolated with only the metasoma being more extensively reddish resembling the *M. suffusa* pattern, the head is more distinctly excavated and emarginated behind, lateral pronotal carina more raised and somewhat sharp, propodeum with fewer and shorter bristles and most of them concentrated on the posterior region, and tergum I more produced after spiracles.

Description. Female. ***Size*****:** 5.5 mm. Length of fore wing 5.5 mm.

Color**:** Blackish species with yellow markings as follows: spot in U-shape on clypeus, inner orbits, and bottom of gena; mandibles with a yellow band extending longitudinally; broad band on anterior margin of pronotum, covering the lateral pronotal carina, interrupted medially and posterior margin of pronotum, fading to sides, both connected dorsally forming an X shape; two lateral spots on scutellum, metanotum and bottom of propodeum; axilla yellow; Antennal articles blackish, last three antennomeres brownish/reddish beneath, scape brownish above and yellowish beneath; Fore legs blackish, coxae with yellow spots, tibia and tarsus orange, mid and hind legs blackish, coxae sometimes with yellow spots. Metasoma orange/reddish, yellow bands on tergum and sternum I to V. Body surface covered with yellowish tomentum. Wings hyaline, venation brown.

Head**:** (1) clypeus 1.8 times wider than longer with punctures shallow, scattered, separated by more than 2.0 diameters; (2) inter-antennal prominence moderately raised, subacute with weak medial furrow; (3) frons and vertex with punctures denser than clypeus, shallow separated by about 1.0–2.0 diameters; (4) gena 0.75–0.8 wider than width of the eyes, slightly narrowing to mandibular condyle, punctures very shallow and scattered; (5) tempora narrowing to vertex; (6) posterior region of the head excavated, moderately emarginated.

Mesosoma**:** (1) pronotum with very shallow and scattered punctures, lateral pronotal carina raised, subacute to acute; (2) humeri do not at all projected in front of tegula, rounded; (3) pretegular carina acute on upper region, curved, not interrupted; (4) scutum 1.1 times wider than longer with very small and scattered punctures; (5) mesopleura with shallow punctures separated by more than 2.0 diameters, like those on frons and vertex; (6) scutellum very slightly concave, almost flat, with shallow punctures or absent, indistinct, medial line raised anteriorly, weakly marked posteriorly; (7) metanotum slightly concave, slightly pointed posteriorly; (8) metapleuron with scattered punctures, upper plate 1.5 times longer than wide; (9) propodeum, with moderately long and sparse outstanding hairs, predominantly on posterior region; (10) propodeal concavity narrow and moderately deep, developed anteriorly, weakly striate, not extending laterally, scattered punctuation; (11) prestigma as long as wide, tip rounded-truncate.

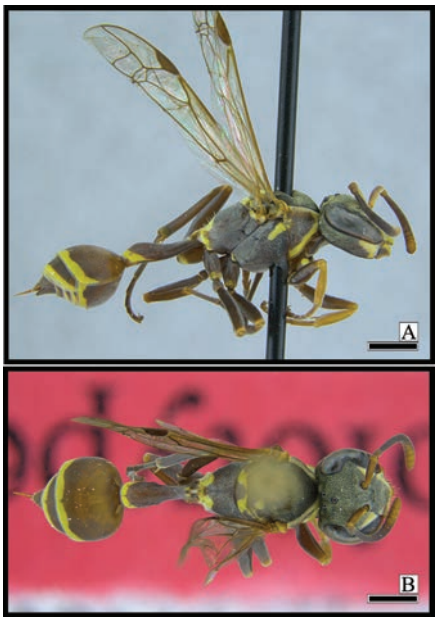

Figure 1. *Metapolybia carpenteriana* **A** lateral view **B** dorsal view. Scale bars: 1.0 mm.

Figure 2. *Metapolybia carpenteriana* **A** head, frontal view **B** pronotum, lateral view. Scale bars: 0.5 mm.

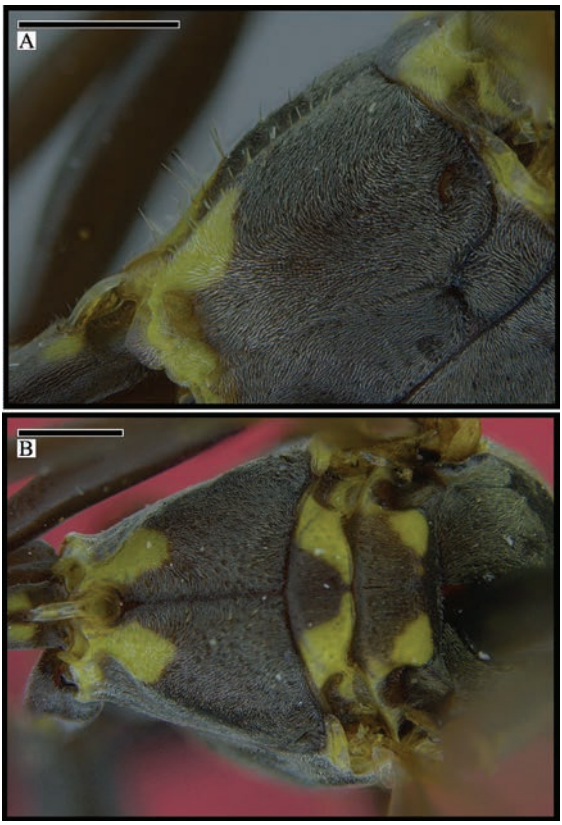

Figure 3. *Metapolybia carpenteriana* **A** propodeum, lateral view **B** propodeum, dorsal view. Scale bars: 0.5 mm.

***Metasoma*:** (1) first metasomal tergum filiform, widening little after the prominent spiracles, slightly convex in lateral view, moderately prominent after spiracles; (2) second metasomal tergum 1.5 times wider than long, coriaceous (3) tergum three to six moderately to densely punctured.

Male. Like female except for the more extensive yellow spots; mandibles entirely yellow; clypeus yellow with a very small brown spot dorsally; tip of clypeus rounded–truncate, compressed, narrower with silvery pubescence, and fewer and shorter bristles; fore coxae almost entirely yellow; dorsal region of mid and hind coxae also yellow; gena narrower; excavation on posterior region of head less distinct, more rounded.

***Male genitalia*:** see male genitalia description section below.

Nest. Unknown.

Distribution. Ecuador: Napo; Peru: Loreto.

Type material. *Holotype*. Ecuador • 1 female; Prov. Napo, 10 km W Misahualli; 16 Dec. 1990; Carpenter & Wenzel; Nest 901216-4; **AMNH**.

***Paratype*.** Ecuador • 19 females, 2 males; same data as for holotype; one male with extracted genitalia pinned together; **AMNH**.

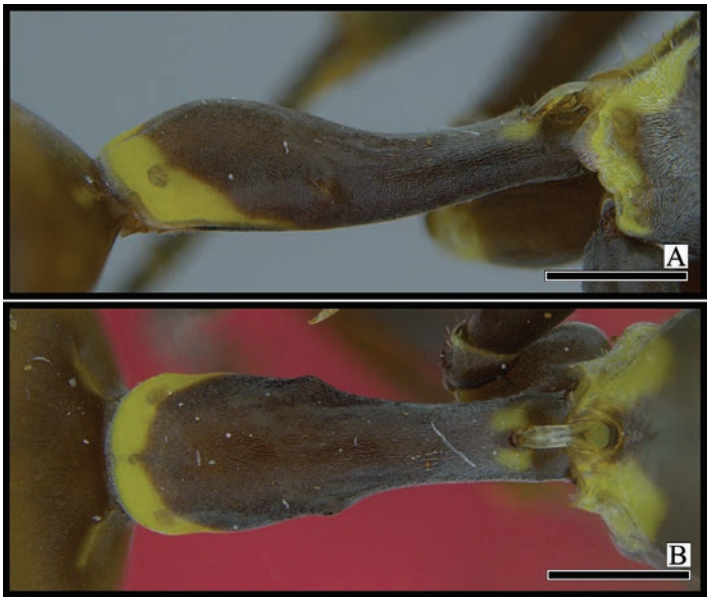

Figure 4. *Metapolybia carpenteriana* **A** tergum I, lateral view **B** tergum I, dorsal view. Scale bars: 0.5 mm.

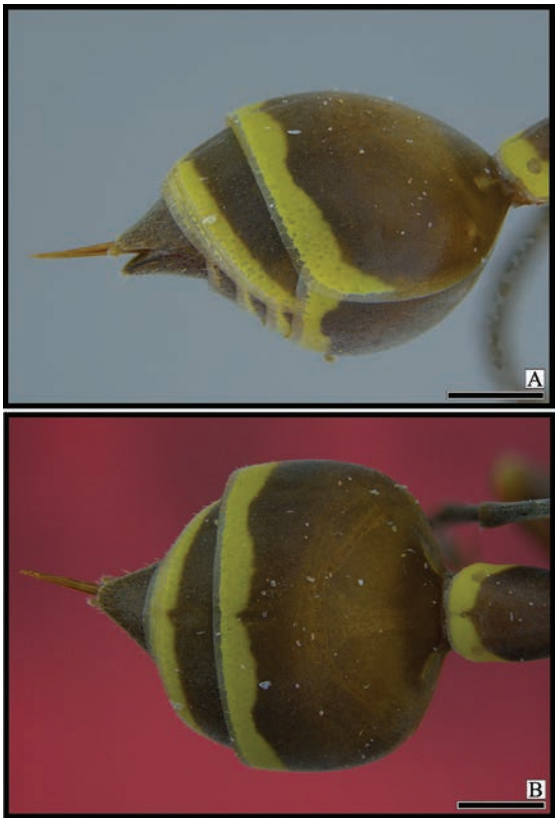

Figure 5. *Metapolybia carpenteriana* **A** metasoma, lateral view **B** metasoma, dorsal view. Scale bars: 0.5 mm.

Other material. Ecuador • 51 females, 4 males; same data as for holotype. Peru • 15 females; Loreto, Iquitos, Rio Nanay; 2 Jan. 1991; Carpenter & Wenzel; Nest 910102-3; **AMNH**.

Etymology. The specific name honors Dr. James M. Carpenter, who recognized all these new species described in this work and asked us to describe them, and also for his contribution to the knowledge on the systematics of Vespidae around the world.

***Metapolybia pseudodocilis* Cortes, sp. nov.**

https://zoobank.org/47ADD83B-B7A3-442B-9F00-6B2D6A52A5A0

Figs 6–9

Diagnosis. Brownish species, head blackish. Very similar to the reddish form of *M. docilis* which can be separated by its broader and more strongly striated propodeal concavity and the lateral pronotal carina more raised and acute. Also, this species is similar in color to *M. rufata*, *M. encantata*, *M. suffusa* and *M. carpenteriana* but with a strong sculpture overall, especially on mesosoma and propodeum, and the yellow markings reduced compared to the latter two.

Description. Female. ***Size*:** 6.6 mm. Length of fore wing 4.5 mm.

***Color*:** Brownish species, head blackish with yellow markings as follows: spot on dorsal margin of mandibles, near base; band on apical margin of clypeus, almost reaching the yellow lateral lobes; spots on inner orbits; antennae reddish brown dorsally

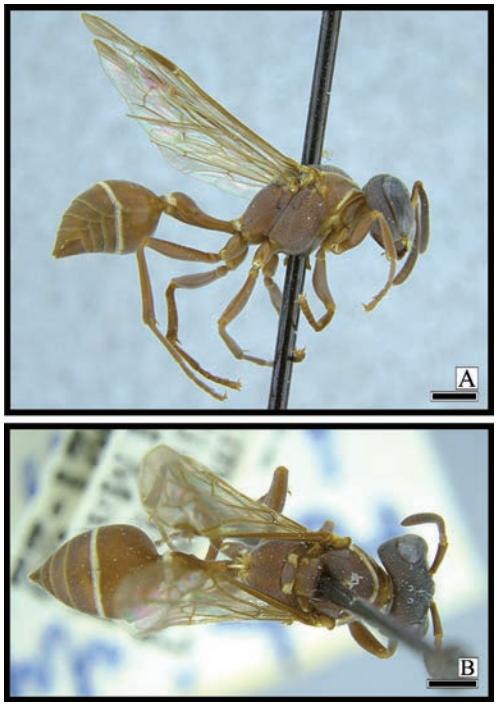

Figure 6. *Metapolybia pseudodocilis* **A** lateral View **B** dorsal view. Scale bars: 1.0 mm.

Figure 7. *Metapolybia pseudodocilis* **A** head, frontal view **B** pronotum, lateral view, Scale bars: 1.0 mm (**A**); 0.5 mm (**B**).

Figure 8. *Metapolybia pseudodocilis.* Propodeum, dorsal view. Scale bar: 0.5 mm.

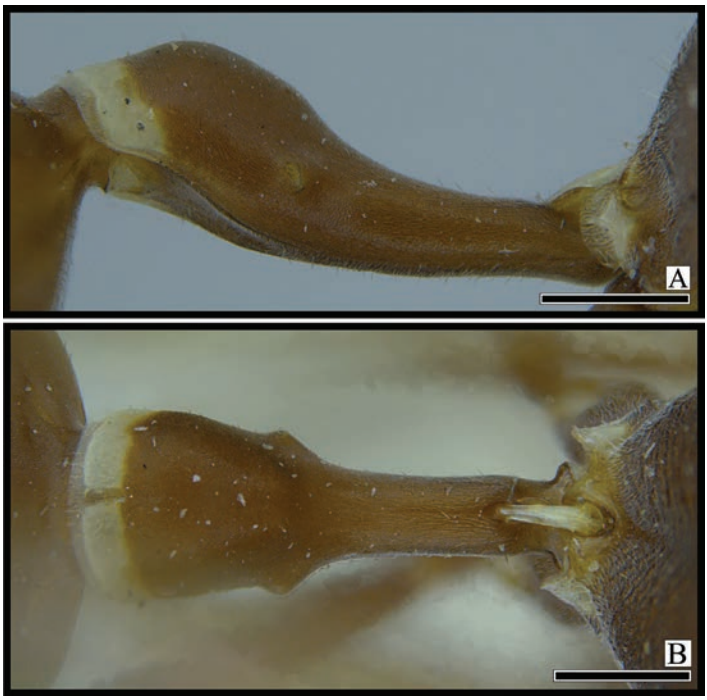

Figure 9. *Metapolybia pseudodocilis* **A** tergum I, lateral view **B** tergum I, dorsal view. Scale bars: 0.5 mm.

and yellowish beneath; small spot on inferior end of anterior margin of pronotum; lateral pronotal carina entirely yellow; band on posterior dorsal margin of pronotum, reaching both tegulae; lamellae behind pretegular carina yellow; sometimes small spot on metapleura by the dorsal end of scrobal furrow; two lateral, sometimes evanescent, yellow spots on scutellum and metanotum; propodeum with two spots on posterior margin near the yellow propodeal valves; legs reddish; wings hyaline, venation white brown; metasoma with yellow bands on tergum I–II and sternum I–II, and evanescent bands on tergum III and sternum III. Body covered with a whitish tomentum. Wings hyaline, venation brown.

***Head*:** (1) clypeus 1.5 times wider than longer, punctures dense, separated by 1.0 diameter or less; (2) inter-antennal prominence raised and acute, with a marked medial furrow; (3) frons and vertex with dense punctures, separated by less than 1.0 diameter (4) gena 0.90–0.95 wider than width of eyes, strongly narrowing to mandibular condyle; punctures dense and coarse; (5) tempora slightly narrowing to vertex; (6) posterior region of head rounded, moderately emarginated.

***Mesosoma*:** (1) lateral pronotal carina raised, subacute; (2) humeri not produced at all in front of tegula; (3) pretegular carina rounded on upper region, curved, not interrupted; (4) scutum 1.3 times wider than longer with punctures small, moderately deep, separated by about 1–2 diameters; (5) mesopleuron with dense and coarse punctures, separated by 1.0 diameter or less; (6) scutellum with deep punctures, spaced,

moderately concave posteriorly, medial line raised anteriorly, vanishing posteriorly; (7) metanotum strongly concave; (8) metapleuron with scattered and shallow punctures, upper plate rugose, 1.5 times longer than wide; (9) propodeum strongly punctured with short and scattered hairs; (10) propodeal concavity broad and deep, weakly developed anteriorly, striation very strong, extending laterally; (11) prestigma as long as wide, tip rounded.

***Metasoma*:** (1) first metasomal tergum filiform, widening little after the prominent spiracles; posteriorly convex in lateral view, strongly prominent; (2) second metasomal tergum 1.8 times wider than longer, coriaceous, finely punctured on posterior fifth; (3) terga three to six brownish, densely punctured.

***Variation*:** One paratype with more extensive yellow markings. Lateral spots on scutellum and metanotum are brighter and bigger, scutellum with an additional small spot on the center. Spots on propodeum are larger, reaching half of posterior face length.

Male. Unknown.

Nest. Unknown.

Distribution. Bolivia: La Paz.

Type material. *Holotype*: Bolivia • female; La Paz, Tumupasa; Dec.; W. M. Mann; Mulford Biol. Expl. 1921-22 (**AMNH**).

***Paratype*:** Bolivia • 3 females; same locality as holotype.

Etymology. Due to the similarities of this species with *M. docilis*, the prefix *pseudo* means 'false' *docilis*.

***Metapolybia richardsi* Andena, sp. nov.**

https://zoobank.org/85763BAD-1611-4601-B4B7-EAE4C39562C4

Figs 10–12

Diagnosis. Very similar to *M. fraudator*, except its scutum narrower, the lateral pronotal carina not effaced on ventral corner, metapleural-propodeal furrow vanishing and the evanescent weak yellow markings overall; pretegular carina like in *M. fraudator.*

Description. Female. *Size*: 8.3 mm. Length of fore wing: 5.0 mm

***Color*:** Black species with yellow markings as follows: spots on inner orbits and tip of clypeus; Tergum I with weak yellow band; Sternites II–III with weak yellow bands; terga III–VI, without yellow bands. Mandibles, antennal articles and scape blackish/brownish. Wings hyaline, venation brown.

***Head*:** (1) clypeus 1.3 times wider than longer, punctures shallow, scattered, separated by more than 2.0 diameters; bristles extending all the way down, not forming a polished rim; (2) internantennal prominence raised, subacute, with a marked medial furrow; (3) frons and vertex covered with yellowish pubescence; punctures small, distinct, separated by 1–1.5 diameters, becoming sparser on vertex; (4) gena 0.7 wider than width of the eyes, strongly narrowing to mandibular condyle; punctures very small, scattered, pubescence very reduced; (5) tempora narrowing to vertex; (6) posterior region of the head excavated, strongly emarginated behind.

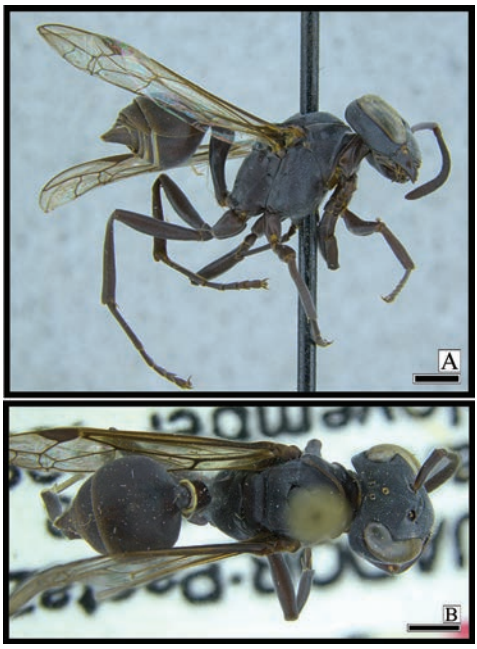

Figure 10. *Metapolybia richardsi* **A** lateral view **B** dorsal view. Scale bars: 1.0 mm.

Figures 11. *Metapolybia richardsi* **A** scutum, dorsal view **B** pronotum, lateral view. Scale bars: 0.5 mm.

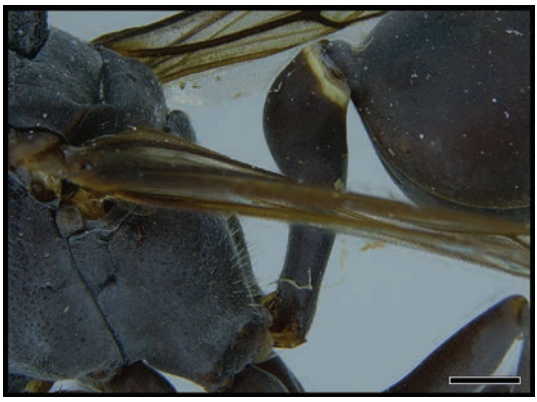

Figure 12. *Metapolybia richardsi.* Propodeum and tergum I, lateral view. Scale bar: 0.5 mm.

***Mesosoma*:** (1) lateral pronotal carina raised, acute; pronotum with shallow and scattered punctures; (2) humeri produced in front of tegula, subacute; (3) pretegular carina acute on upper region, curved, not interrupted, not prominent; (4) scutum as long as wide, punctures small, shallow, scattered; (5) mesopleuron with shallow punctures separated by more than 2.0 diameters; (6) scutellum with small, though distinct punctures, separated by 1.0 diameter, slightly concave posteriorly, medial line raised anteriorly, vanishing posteriorly; (7) metanotum strongly concave with scattered punctures; (8) metapleuron with few scattered punctures, upper plated 1.3 times longer than wide; (9) propodeum with shallow scattered punctures with moderate long and sparse hairs on posterior region; (10) propodeal concavity broad, moderately deep, weakly developed anteriorly, striation distinct, extending laterally; (11) prestigma as long as wide, tip truncate.

***Metasoma*:** (1) first metasomal tergum filiform, widening little after the prominent spiracles; prominent (2) tergum II 1.2 times wider than longer, coriaceous, punctures distinct on posterior fifth; (3) terga III–VI densely punctured.

Male. Unknown.

Nest. Unknown.

Distribution. Ecuador: Pastaza.

Holotype. Ecuador • 1 female; Pastaza, Jibaria, Shurupe; 7 Nov. 1987; Mike Huybensz; **AMNH**.

Etymology. The specific name honors O.W. Richards for his contribution of the knowledge of the social wasps.

Metapolybia sulamerica Carpenter, sp. nov.

https://zoobank.org/F3A53BE5-1A87-4ACD-8071-951B80FD9F01
Figs 13–16

Diagnosis. This species is like *M. servilis*, however the lateral pronotal carina its less raised and somewhat sharp; propodeal concavity broader and deeper; clypeus wider.

Plus, *M. sulamerica* has the integument of the mesosoma and metasoma brownish with yellow markings reduced and less distinct than the blackish *M. servilis.*

Description. Female. ***Size*****:** 5.5 mm. Length of fore wing 5.0 mm

Color**:** Brownish species, head blackish with yellow markings as follows: spots on mandibles near condyle andventral margin of clypeus; weak spots on inner orbits, anterior region of pronotal carina, axilae, metanotum.; bands on posterior region of tergum I–II and sternum I; weak bands on tergum III–IV. Tegula yellowish with brown spots. Antennal articles brownish, scape yellowish beneath. Legs brown. Wings hyaline, venation brown.

Head**:** (1) clypeus 1.2 times wider than longer; ventral margin with a reduced yellow band; punctures very shallow, scattered, separated by more than 2.0 diameters; erect hairs on first 2/3; (2) inter-antennal prominence little raised, truncate to subacute, with a weak medial furrow; (3) frons and vertex covered with a yellowish pubescence, punctures shallow, dense, separated by about 1 diameter, becoming sparser on vertex; (4) gena 0.85–0.90 wider than width of the eyes, strongly narrowing to mandibular condyle, punctures weak, scattered, pubescence yellowish; (5) tempora narrowing to vertex; (6) posterior region of the head rounded, moderately emarginated.

Mesosoma**:** (1) lateral pronotal carina little raised, subacute,; punctures shallow, small, though distinct, separated by more than 2.0 diameters; (2) humeri scarcely

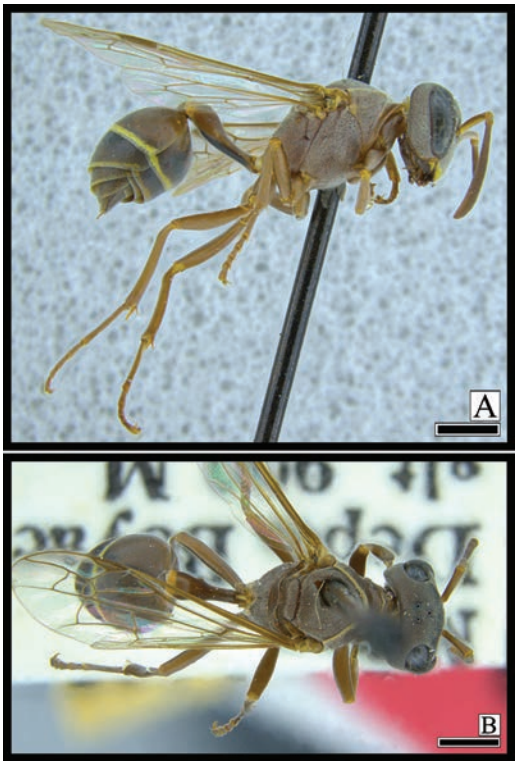

Figure 13. *Metapolybia sulamerica* **A** lateral view **B** dorsal view. Scale bars: 1.0 mm.

produced in front of tegula, gently rounded; (3) pretegular carina rounded, not acute, not interrupted; (4) scutum 1.2 times wider than long with scattered punctures; (5) mesopleura with punctures separated by about 1.0–1.4 diameters mostly concentrated on posterior region; (6) scutellum with distinct punctures, slightly concave posteriorly; medial line raised anteriorly, complete posteriorly; (7) metanotum strongly concave, punctures sparse; (8) metapleuron with scattered punctures, upper plate as long as wide or 1.3 times longer than wide, punctures denser than lower plate; (9) propodeum with scattered short hairs, propodeal concavity shallow, almost flat, weakly striate, not extending laterally; (10) prestigma as long as wide, tip truncate.

***Metasoma*:** (1) First metasomal tergum filiform, widening little after strong spiracles, strongly convex posteriorly in lateral view, prominent; (2) second metasomal tergum 1.2 times wider than long, coriaceous; (3) terga III–VI finely punctured.

***Variation*:** Some of the specimens labelled as "nest on tree July 3" have the yellow markings on head and metanotum absent or evanescent. Some specimens from both nests have stronger striae on broader propodeal medial furrow than holotype.

Figure 14. *Metapolybia sulamerica* **A** head, frontal view **B** pronotum, lateral view. Scale bars: 0.5 mm.

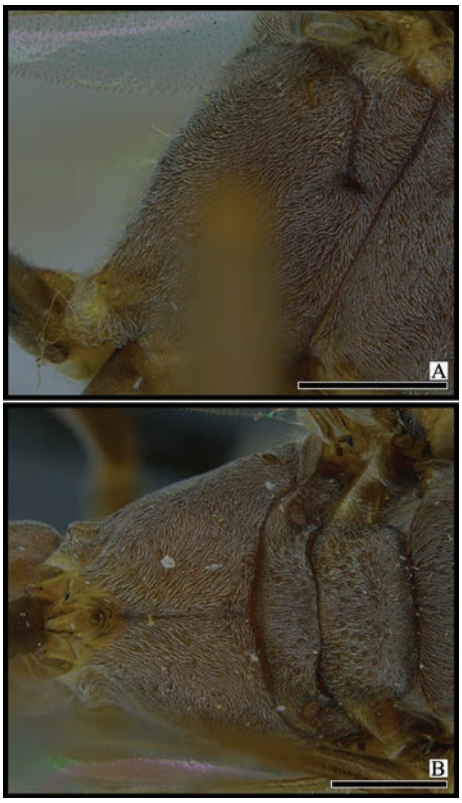

Figure 15. *Metapolybia sulamerica* **A** propodeum, lateral view **B** propodeum, dorsal view. Scale bars: 0.5 mm.

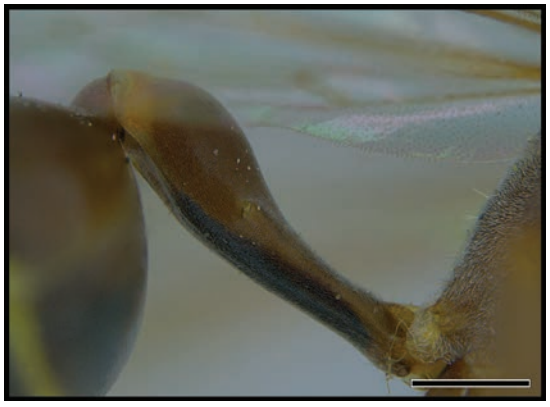

Figure 16. *Metapolybia sulamerica.* Tergo I, lateral view. Scale bar: 0.5 mm.

Male. like female, except for denser and shinier tomentum; narrower clypeus and gena, and more distinct punctures overall, especially the coarser punctures on mesopleura.

***Male genitalia*:** see male genitalia description section below.

Nest. Unknown.

Distribution. Colombia: Boyacá.

Type material. *Holotype*. Colombia • 1 female; Boyacá, Muzo; alt. 900 m.; 2 Jul. 1936; J. Bequaert; "nest in village July 2"; **AMNH**.

***Paratype*.** Colombia • 10 females, 4 males; same data as for holotype; one with extracted genitalia pinned together; **AMNH** • 4 females; same locality as for holotype; "nest on tree July 3"; **AMNH**.

Other material. Colombia • 4 females; same data as for holotype; **AMNH** • 7 females; same locality as for holotype; "nest on tree"; **AMNH** • 3 females; same locality as for holotype; **AMNH**.

Etymology. The specific name is a reference to the geographic distribution of the species.

Metapolybia zucchiana Andena & Carpenter, sp. nov.

https://zoobank.org/F7594BEF-B297-4139-8ADB-6D127A892BB1

Figs 17–20

Diagnosis. The species is easily recognized by its prominent aberrant propodeum, especially bulging laterally which is different of any other species of *Metapolybia* (see description).

Description. Female. *Size*: 6.0 mm. Length of fore wing: 5.0 mm.

***Color*:** Blackish/brownish species. Mandibles, dorsal antennae, tegula, metasoma and legs brownish. Weak yellow markings as follows: apical spot on mandibles; spot on the margin of clypeus and inner orbits; ventral antennae fading yellow apically; small yellow spot along the lateral pronotal carina, spot on lamella behind pretegular carina, and band on posterior margin of pronotum; Tergum I–VI brownish; yellow band present on tergum I–II and sternum II–III; wings hyaline, venation brown.

***Head*:** (1) clypeus 1.3 times wider than longer, punctures shallow, spaced, separated by 2.0 diameters or more; bristles on first third, straight; (2) inter-antennal prominence moderately raised, subacute with weak medial furrow; (3) frons and vertex covered with yellowish pubescence, punctures denser than clypeus, separated by about 1.0–2.0 diameters, becoming sparser on vertex; (4) gena 0.85 wider than width of the eyes, strongly narrowing to mandibular condyle, punctures very small and scattered, pubescence reduced and concentrated on inferior region; (5) tempora narrowing to vertex; (6) posterior region of the head excavated, strongly emarginated.

***Mesosoma*:** (1) lateral pronotal carina raised and acute; (2) humeri moderately produced in front of tegula, gently rounded; (3) pretegular carina acute on upper region, curved, not interrupted; (4) scutum 1.3 times wider than longer with very small and scattered punctures; (5) mesopleura with shallow punctures separated by 2 diameters, like those on clypeus; (6) scutellum with small and distinct punctures, separated by about 1.0–2.0 diameters slightly concave posteriorly, medial line

Figure 17. *Metapolybia zucchiana* **A** lateral view **B** dorsal view. Scale bars: 1.0 mm.

raised anteriorly, vanishing posteriorly (7) metanotum strongly concave, pointed posteriorly; (8) metapleuron with scattered punctures, upper plate 1.3 times longer than wide; (9) propodeum strongly prominent latero-posteriorly, with short and sparse outstanding hairs concentrated on posterior region; (10) propodeal concavity weakly developed anteriorly, broad and deep posteriorly, striation weak, extending laterally; (11) legs brownish; (12) prestigma longer than wide, tip truncate.

***Metasoma*:** (1) first metasomal tergum filiform, widening little after the prominent spiracles, posteriorly convex in lateral view, slightly prominent; (2) second metasomal tergum 1.2 times wider than long, coriaceous finely punctured on posterior fifth; (3) terga three to six densely punctured.

Male. Unknown.

Nest. Unknown.

Distribution. Panama, Barro Colorado Island.

Holotype. Panama • 1 female; Barro Colorado Island; P. Rau; col. #7666; determined as *Metapolybia azteca* by C.K. Starr 1980; **AMNH**.

Etymology. The specific name honors Dr. Ronaldo Zucchi, for his contribution of the knowledge of behavior of Neotropical bees and wasps.

Figure 18. *Metapolybia zucchiana* **A** head, frontal view **B** propodeum, lateral view. Scale bars: 0.5 mm.

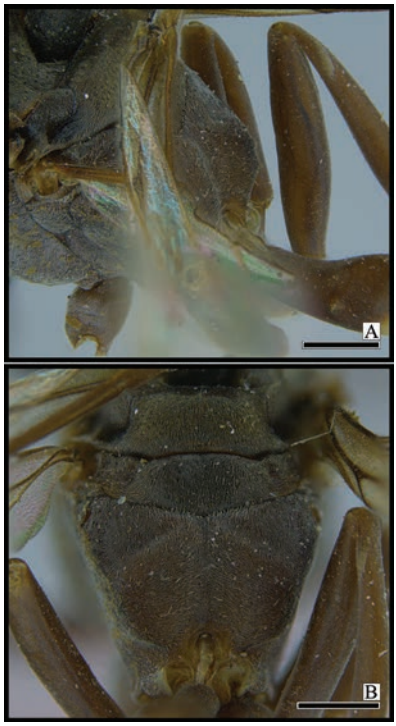

Figure 19. *Metapolybia zucchiana* **A** propodeum, dorso-lateal view **B** propodeum, dorsal view. Scale bars: 0.5 mm.

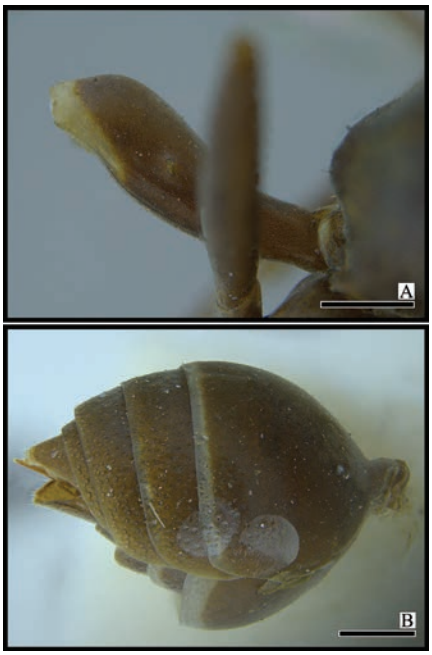

Figure 20. *Metapolybia zucchiana* **A** tergum I, lateral view **B** metasoma, lateral view. Scale bars: 0.5 mm.

Male genitalia descriptions

In this section we describe and depict the male genitalia of the following species: *Metapolybia bromelicola*, *M. carpenteriana*, *M. encantata*, *M. mesoamerica*, *M. rufata*, *M. servilis* and *M. sulamerica*.

Metapolybia bromelicola

Fig. 21A–E

Male genitalia. (1) paramere about 1.7 times longer than wide at middle, basal angle obtuse, apical angle truncate, spine of paramere long, pointed, bare (Fig. 21A); (2) aedeagus slightly curved, lobe rounded weakly produced, lateral margin produced; lateral ridge with a row of short teeth extending laterally; ventral process slightly produced, pointed (Fig. 21B, C); (3) cuspis long and pointed, with short and dense hairs apically, extending laterally (Fig. 21D); (4) digitus long apically, rounded, with short and dense hairs, mesal surface with scattered small punctures (Fig. 21E).

Material examined. Brazil • male; Rio de Janeiro, Itatiaia; **AMNH**.

Metapolybia carpenteriana

Fig. 21F–J

Male genitalia. (1) paramere about 1.5 times longer than wide at middle, basal angle obtuse, apical angle, prominent and truncate, spine of paramere long, pointed, bare

(Fig. 21F); (2) aedeagus curved, lobe rounded and produced, lateral margin produced; lateral ridge with a row of short teeth extending laterally; ventral process produced, pointed (Fig. 21G, H); (3) cuspis long and pointed and slightly curved, with short and dense hairs apically, extending laterally (Fig. 21I); (4) digitus short apically, blunt, with short and dense hairs, mesal surface with scattered small punctures (Fig. 21J).

Material examined. Ecuador • paratype male; Napo, 10 km w Misahualli; 16 Dec. 1990; Carpenter & Wenzel; Nest 901216–4; **AMNH**.

Metapolybia encantata
Fig. 21K–O

Male genitalia. (1) paramere about 1.4 times longer than wide at middle, basal angle obtuse, apical angle truncate, spine of paramere long, pointed, bare (Fig. 21K); (2) aedeagus curved, lobe rounded and produced, lateral margin produced; lateral ridge with a row of short teeth extending laterally; ventral process produced, pointed (Fig. 21L, M); (3) cuspis long and rounded, with short and dense hairs apically, extending laterally (Fig. 21N); (4) digitus long apically, rounded, with short and dense hairs, mesal surface with scattered small punctures (Fig. 21O).

Material examined. Colombia • male; El Encanto; **AMNH**.

Metapolybia mesoamerica
Fig. 22A–E

Male genitalia. (1) paramere about 1.5 times longer than wide at middle, basal angle obtuse, apical angle truncate, spine of paramere long, pointed, bare (Fig. 22A); (2) aedeagus curved, lobe rounded and strongly produced, lateral margin produced; lateral ridge with a row of short teeth extending laterally; ventral process produced, rounded (Fig. 22B, C); (3) cuspis long and pointed, with short and dense hairs apically, extending laterally (Fig. 22D); (4) digitus short apically, blunt, with short and dense hairs, mesal surface with scattered small punctures (Fig. 22E).

Material examined. Costa Rica • male; Limon, Amubri; **AMNH**.

Metapolybia rufata
Fig. 22F–J

Male genitalia. (1) paramere about 1.6 times longer than wide at middle, basal angle obtuse, apical angle truncate, spine of paramere long, pointed, bare (Fig. 22F); (2) aedeagus curved, lobe rounded produced, lateral margin produced; lateral ridge with a row of short teeth extending laterally; ventral process produced, pointed (Fig. 22G, H); (3) cuspis long and pointed, with short and dense hairs apically, extending laterally (Fig. 22I); (4) digitus long apically, rounded, with short and dense hairs, mesal surface with scattered small punctures (Fig. 22J).

Material examined. Brazil • male; Mamiraua; **MPEG**.

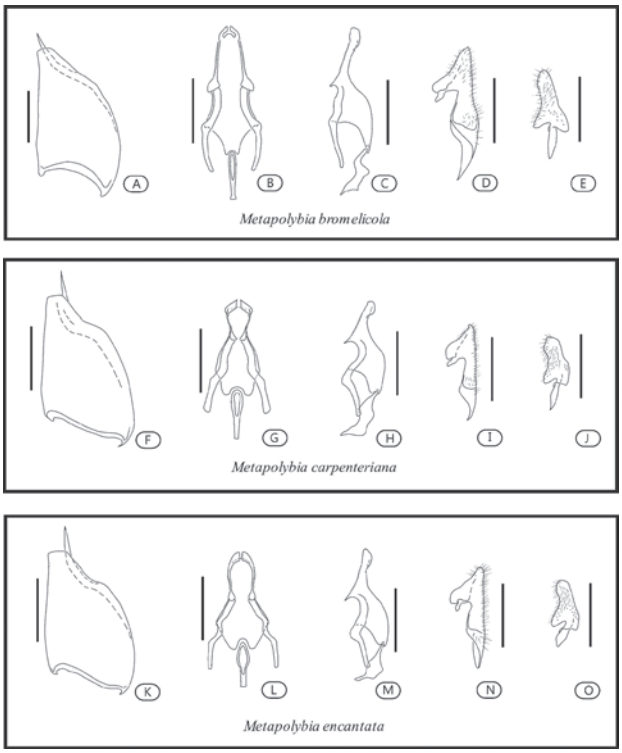

Figure 21. Male genitalia of *Metapolybia bromelicola* (**A–E**), *M. carpentirana* (**F–J**) and *M. encantata* (**K–O**). **A, F, K** paramere **B, G, L** aedeagus, ventral view **C, H, M** aedeagus, lateral view **D, I, N** cuspis, lateral view **E, J, O** digitus, lateral view. Scale bars: 0.5 mm.

Metapolybia servilis

Fig. 22K–O

Male genitalia. (1) paramere about 1.5 times longer than wide at middle, basal angle obtuse, apical angle pointed, spine of paramere long, pointed, bare (Fig. 22K); (2) aedeagus curved, lobe rounded and strongly produced, lateral margin produced; lateral ridge with a row of short teeth extending laterally; ventral process produced, rounded (Fig. 22L, M); (3) cuspis long and pointed, with short and dense hairs apically, extending laterally (Fig. 22N); (4) digitus short apically, blunt, with short and dense hairs, mesal surface with scattered small punctures (Fig. 22O).

Material examined. Paraguay • male, paratype; Pto. Bertoni; **NHM**.

Metapolybia sulamerica

Fig. 23A–E

Male genitalia. (1) paramere about 1.8 times longer than wide at middle, basal angle obtuse, apical angle mostly truncate, spine of paramere long, pointed, bare (Fig. 23A);

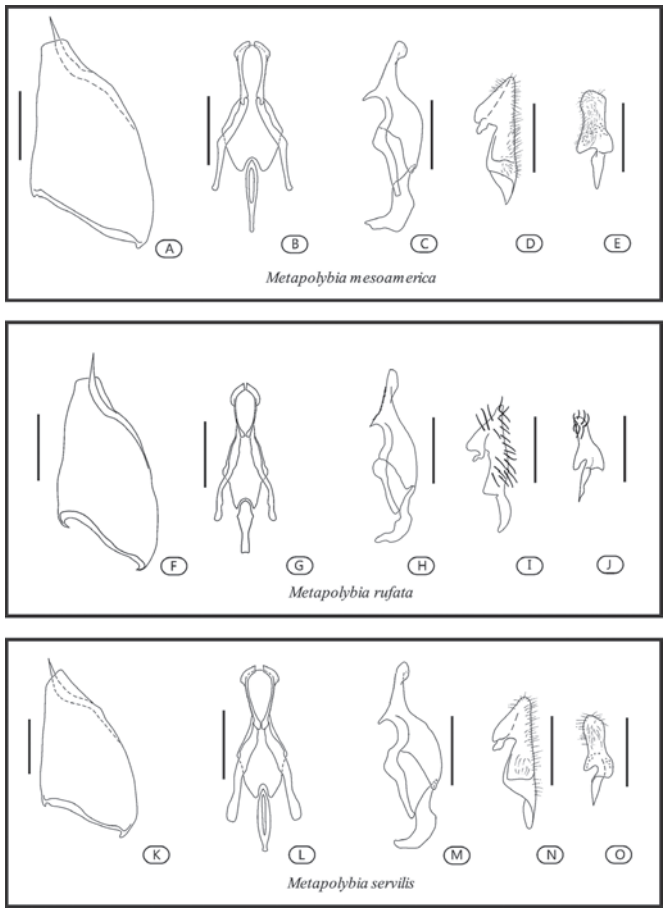

Figure 22. Male genitalia of *Metapolybia mesoamerica* (**A–E**), *M. rufata* (**F–J**) and *M. servilis* (**K–O**) **A, F, K** paramere **B, G, L** aedeagus, ventral view **C, H, M** aedeagus, lateral view **D, I, N** cuspis, lateral view **E, J, O** digitus, lateral view. Scale bars: 0.5 mm.

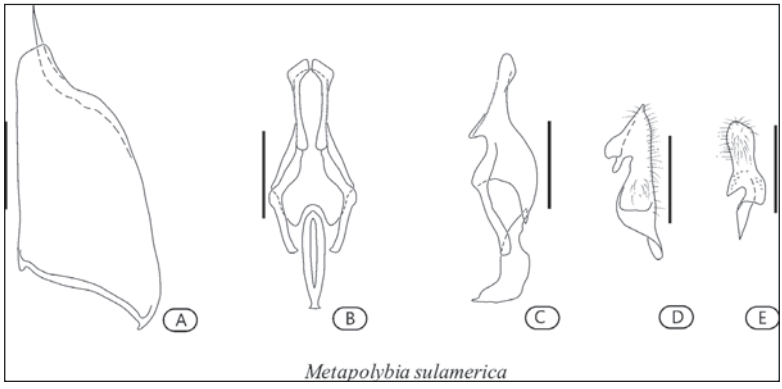

Figure 23. Male genitalia of *Metapolybia sulamerica*. **A** paramere **B** aedeagus, ventral view **C** aedeagus, lateral view **D** cuspis, lateral view **E** digitus, lateral view. Scale bars: 0.5 mm.

(2) aedeagus curved, lobe rounded produced, lateral margin produced; lateral ridge with a row of short teeth extending laterally; ventral process produced, rounded (Fig. 23B, C); (3) cuspis long and pointed and slightly curved, with short and dense hairs apically, extending laterally (Fig. 23D); (4) digitus short apically, blunt, with short and dense hairs, mesal surface with scattered small punctures (Fig. 23E).

Material examined. Colombia • paratype male; Boyacá, Muzo; **AMNH**.

Comparative remarks

Araujo (1945) published a revision of the genus, which, at that time, had only five species, two being described by him. In the revision of Richards (1978), four new species were described (*M. rufata*, *M. aztecoides*, *M. nigra* and *M. docilis*). Richards (1978) recognized the importance of Araujo's revision, but pointed out that the key proposed by Araujo was not very easy to use. He suggested that striation on propodeum, used to separate *M. cingulata* and *M. unilineata*, was less developed than what was described by Araujo (1945). We have seen some variation not only in this feature cited by Richards (1978) but also the punctation, mainly in frons and vertex, which may cause some mistakes during the identification of the species.

The species here described were deposited in the American Museum of Natural History, and were unidentified or misidentified, certainly due to variation. *Metapolybia carpenteriana* was identified as *M. suffusa*, however, as showed above, it has minor differences that place it as a new species. This is the same as the case of *M. miltoni*, which had been misidentified as *M. docilis* and *M. araujoi*, which is very similar to *M. suffusa*. *Metapolybia pseudodocilis* is close to *M. docilis*, however the striation is stronger, a feature cited by Richards that should be better studied. Besides striation the propodeal concavity is broader, a key feature to separate it from *M. docilis*. *Metapolybia sulamerica* is closer to *M. servilis*—three features may help in diagnosis: the pronotal carina less raised and sharp, clypeus wider and propodeal concavity deeper. *Metapolybia zucchiana* is the only new species described that is unique by having an aberrant propodeum that is a very useful diagnostic feature to the species.

In the recent publications about *Metapolybia* (Cooper 1999; Andena and Carpenter (2011); Somavilla and Andena 2018; Andena et al. 2019), as well the revisions of Araujo (1945) and Richards (1978), the characters of the male genitalia did not have special merit. Some authors described the male for some species, but they did not mention the male genitalia, probably because males are seldom collected in nests, and they could have intended to preserve the exemplars.

Concerning male genitalia, the paramere is about 1.8 times longer than wide in *M. bromelicola* and *M. sulamerica.* In the remaining species it ranges from 1.4–1.6 times. The hairs on spine of paramere are absent in *Metapolybia* species. As pointed out by Andena et al (2007) and Andena and Carpenter (2012), the hairs are present only for *Apoica*, *Pseudopolybia* and *Parachartergus*; hence ¨hair absent¨ is general for Epiponini. The apical angle of the paramere is truncate in all species described here, except *M. servilis*, where it is

pointed. *Metapolybia sulamerica* has an apical angle less truncate, little angled, but, here, we considered it also as truncate. In general, the aedeagus is curved (slightly less curved in *M. bromelicola*), with the lobe rounded, however in *M. bromelicola* it is very weak, while in *Metapolybia servilis* and *M. mesoamerica* the lobe is more produced; the remaining species are in between. The ventral process of aedeagus is always produced, however it may separate two forms: 1) long—in *M. bromelicola*, *M. carpenteriana*, *M. encantata* and *M. rufata vs.* 2) rounded—found in *M. mesoamerica*, *M. servilis* and *M. sulamerica.* The cuspis is long and pointed, except *M. encantata*, in which it is rounded. The species of form 1 also share the digitus long apically and rounded, except for *M. carpenteriana* that has the digitus short apically and blunt like those of form 2.

In conclusion, the description of new species, including new information about male genitalia increases the knowledge of the genus and highlights how the diversity of this tribe is still underestimated.

Acknowledgments

The authors thank the curators of the institutions which the study material was studied.

This study was financed in part by the Coordenação de Aperfeiçoamento de Pessoal de Nível Superior - Brasil (CAPES) - Finance Code 001 (proc. # 88887.342340/2019-00), UEFS, grant # CONSEPE 060/2011, FAPESP (grants # 11/06058–5, 19/09215–6) and CNPq (grant # 302952/2022–5).

References

Andena SR, Carpener JM (2011) A new species of *Metapolybia* (Hymenoptera: Vespidae; Polistinae, Epiponini). Entomologica Americana 117 (3/4): 117–120. https://doi.org/10.1664/11-RA-003.1

Andena SR, Carpenter JM (2012) A phylogenetic analysis of the social wasp genus *Brachygastra* Perty, 1833, and description of a new species (Hymenoptera: Vespidae: Epiponini). American Museum Novitates 3753: 1-38. https://doi.org/10.1206/3753.2

Andena SR, Mateus S, Nascimento FS, Carpenter JM (2019) Description of a new species of *Metapolybia*, a Neotropical genus of social wasps, from the Amazon Forest. Sociobiology 66(2): 377–380. https://doi.org/10.13102/sociobiology.v66i2.3731

Andena SR, Noll FB, Carpenter JM, Zucchi R (2007) Phylogenetic analysis of the neotropical Pseudopolybia de Saussure, 1863, with description of the male genitalia of Pseudopolybia vespiceps (Hymenoptera: Vespidae, Epiponini). American Museum Novitates 3586: 1-11. https://doi.org/10.1206/0003-0082(2007)3586[1:PAOTNP]2.0.CO;2

Baio MV, Noll FB, Zucchi R (2003) Shape differences rather than size differences between castes in the Neotropical swarm-founding wasp *Metapolybia docilis* (Hymenoptera, Vespidae, Epiponini). BMC Evolutionary Biology 3: 10. https://doi.org/10.1186/1471-2148-3-10

Barbosa BC, Detoni M, Maciel TT, Prezoto F (2016) Studies of social wasp diversity in Brazil: Over 30 years of research, advancements and priorities. Sociobiology 63: 858–880. https://doi.org/10.13102/sociobiology.v63i3.1031

Carpenter JM, Ross KG (1984) Colony composition in four species of Polistinae from Suriname, with a description of the larva of *Brachygastra scutellaris* (Hymenoptera, Vespidae). Psiche 91: 111–140. https://doi.org/10.1155/1984/73705

Chavarría L, Noll FB (2013) Age polyethism in the swarm-founding wasp *Metapolybia miltoni* (Andena & Carpenter) (Hymenoptera: Vespidae; Polistinae, Epiponini). Sociobiology 60: 214–216. https://doi.org/10.13102/sociobiology.v60i2.214-216

Chavarría-Pizarro L, da Silva M, Ament DC, Almeida EAB, Noll FB (2023) Behavioural evolution of Neotropical social wasps (Vespidae: Polistinae): the queen selection process. Cladistics: the international journal of the Willi Hennig Society 39: 215–228. https://doi.org/10.1111/cla.12529

Cooper M (1999) New species of *Metapolybia* Ducke (Hym., Vespidae, Polistinae). Entomologist's Monthly Magazine 135: 107–110.

Ducke A (1904) Sobre as Vespidas sociaes do Pará. Boletim do Museu Goeldi 4: 317–374. https://doi.org/10.5962/bhl.title.100023

Karsai I, Wenzel JW (2000) Organization and regulation of nest construction behavior in *Metapolybia* wasps. Journal of Insect Behavior 13: 111–140. https://doi.org/10.1023/A:1007771727503

Richards OW (1978) The social wasps of the Americas excluding the Vespinae. British Museum (Natural History), London, 580 pp.

Smethrust ME, Carpenter JM (1998) A new species of *Metapolybia* Ducke from Central America (Hymenoptera: Vespidae; Polistinae). Journal of the New York Entomological Society 105: 180–185.

Somavilla A, Andena SR (2018) *Metapolybia araujoi*, a new species of swarming social wasp from the Brazilian Amazon rainforest (Vespidae: Polistinae). Revista Brasileira de Entomologia 62: 83–86. https://doi.org/10.1016/j.rbe.2018.02.001

Somavilla A, Oliveira ML, Andena SR, Carpenter JM (2018) An illustrated atlas for male genitalia of the New World *Polistes* Latreille, 1802 (Vespidae: Polistinae). Zootaxa. 4504(3): 301–344. https://doi.org/10.11646/zootaxa.4504.3.1

Wenzel JW (1998) A generic key to the nests of hornets, yellow jackets, and paper wasps worldwide (Vepidae: Vepinae, Polistinae). American Museum Novitates 3224: 1–39.

West-Eberhard MJ (1978) Temporary queens in *Metapolybia* wasps: non-reprodutive helpers without altruism? Science 200: 441–443. https://doi.org/10.1126/science.200.4340.441

West-Eberhard MJ (2000) Intragroup selection and evolution of insect societies. In: Alexander RD, Tinkle DW (Orgs.) Natural selection and social behavior. Chiron Press, New York, 3–17.

JHR 97: 807–824 (2024)
doi: 10.3897/jhr.97.126202
https://jhr.pensoft.net

MONOGRAPH

JOURNAL OF Hymenoptera RESEARCH
A peer-reviewed open-access journal
The International Society of Hymenopterists

Three new species of *Conostigmus* from China and redescription of *Conostigmus ampullaceus* Dessart, 1997 (Hymenoptera, Megaspilidae)

Xu Wang[1,2], Shanshan Cui[1], Fang Li[1], Yixin Huang[2,3], Huayan Chen[4]

1 *Anhui Provincial Key Laboratory of the Conservation and Exploitation of Biological Resources, Key Laboratory of Biotic Environment and Ecological Safety in Anhui Province, College of Life Sciences, Anhui Normal University, Wuhu, Anhui 241000, China* **2** *Key Laboratory of Zoological Systematics and Evolution, Institute of Zoology, Chinese Academy of Sciences, Beijing 100000, China* **3** *Collaborative Innovation Center of Recovery and Reconstruction of Degraded Ecosystem in Wanjiang Basin Co-founded by Anhui Province and Ministry of Education, School of Ecology and Environment, Anhui Normal University, Wuhu, Anhui 241000, China* **4** *Guangdong Provincial Key Laboratory of Applied Botany, South China Botanical Garden, Chinese Academy of Sciences, Guangzhou 510650, China*

Corresponding authors: Yixin Huang (huangyx@ahnu.edu.cn); Huayan Chen (huayanc@scbg.ac.cn)

Academic editor: Ankita Gupta | Received 25 April 2024 | Accepted 1 September 2024 | Published 8 October 2024

https://zoobank.org/02DEAD07-723D-4000-90CD-3054B09665F3

Citation: Wang X, Cui S, Li F, Huang Y, Chen H (2024) Three new species of *Conostigmus* from China and redescription of *Conostigmus ampullaceus* Dessart, 1997 (Hymenoptera, Megaspilidae). Journal of Hymenoptera Research 97: 807–824. https://doi.org/10.3897/jhr.97.126202

Abstract

Three new species of *Conostigmus* Dahlbom, 1858 (Hymenoptera: Megaspilidae), *Conostigmus quadripetalus* Wang & Chen, **sp. nov.**, *Conostigmus electrinus* Wang & Chen, **sp. nov.**, *Conostigmus acutus* Wang & Chen, **sp. nov.** are characterized and illustrated from China. *Conostigmus ampullaceus* Dessart, 1997 is redescribed on the basis of 17 specimens and genitalia pictures are provided for the first time.

Keywords

Ceraphronoidea, morphology, parasitoid wasps, taxonomy

Introduction

Conostigmus Dahlbom, 1858 is the richest genus of parasitoid wasps of Megaspilidae, comprises more than 170 species and has a worldwide distribution (Johnson and Musetti 2004; Trietsch et al. 2015; Trietsch et al. 2020). Most species have been recorded from the Palearctic region (Mikó et al. 2016). However, only five species have been recorded from China: *C. abdominalis* Boheman, 1832 from Zhejiang and Shanghai, *C. ampullaceus* Dessart, 1997 and *C. villosus* Dessart, 1997 from Taiwan, *C. xui* Cui & Wang, 2023 from Guangdong (Dessart 1997; Fu et al. 2021; Cui et al. 2023), *Conostigmus nankunensis* Qian & Wang, 2024 from Guangzhou (Qian et al. 2024).

Conostigmus was first described by Dahlbom (1858), who originally proposed it as a subgenus of *Megaspilus* Westwood, 1829. Kieffer (1909) recognized *Conostigmus* as a genus separate from *Megaspilus*. Species of *Conostigmus* can be difficult to distinguish from its sister genus, *Dendrocerus*, due to the numerous exceptions and overlap between these two genera. The combination of characters to distinguish these two genera are as follows: the ocelli of male *Dendrocerus* form an obtuse ocellar triangle whereas the ocelli of male *Conostigmus* usually form an acute or equilateral ocellar triangle; the sternaulus is consistently absent in *Dendrocerus* but may be present or absent in *Conostigmus*. Wings are never absent in *Dendrocerus*, whereas in *Conostigmus*, they may be present or absent. The posterior end of the notauli is always adjacent to the transscutal articulation in *Conostigmus*, whereas in some *Dendrocerus*, it is not. When it comes to male genitalia, the parossiculi are fused with the gonostipes in *Dendrocerus* but never in *Conostigmus*. Additionally, the medioventral conjunctiva of the gonostyle–volsella complex differs: in *Dendrocerus*, the parossiculi are never independent, but in *Conostigmus*, they may be either independent or fused (Dessart 1985, 1995a, 1995b, 1999, 2001; Mikó et al. 2011, 2013; Trietsch et al. 2020).

Conostigmus are known to be associated with Hymenoptera, Coleoptera, Diptera and Mecoptera, but relative to its diversity, little is known about the life history of *Conostigmus* (Graham 1984; Trietsch et al. 2016). Currently, there are only a few breeding records for *Conostigmus* species, i.e., *Conostigmus obscurus* Thomson, 1858 (*C. syrphorum*) reared from a syrphid puparium (Kieffer 1907); *Conostigmus triangularis* (Thomson, 1858) and *Conostigmus timberlakei* Kamal, 1926 reared from pupae of Aphididae (Kamal, 1926); *Conostigmus rufescens* Kieffer, 1907 parasitised eggs and larvae of the pod fly *Dasineura brassicae* (Diptera: Cecidomyiidae) (Laborius 1972; Vidal 2003; Trietsch et al. 2015).

In this paper, we described three new species of *Conostigmus*, *C. quadripetalus* Wang & Chen, sp. nov., *C. electrinus* Wang & Chen, sp. nov., *C. acutus* Wang & Chen, sp. nov. and redescribed one known species, *C. ampullaceus* Dessart, 1997. We also provide a key to males of Chinese *Conostigmus* to aid identification efforts in the future.

Materials and methods

Specimens were collected by using Malaise traps and yellow pan traps. They were mounted on point-cards. Photographs were taken with a Leica M205A stereomicroscope and a Leica DFC-500 digital camera, with extended focusing software. Measurements are given in microns. Plates were created using Adobe photoshop CS3. To prepare male genitalia for study, apical metasomal segments were removed from specimens and placed in 35% NaOH solution, heated in a water bath at 100 °C for 8 min and then transferred to a droplet of glycerin on a concavity slide. Dissections were performed in glycerin using #5 forceps and #2 insect pins. Genitalia were stored in glycerin after dissection.

The types are deposited in AHNU (Auhui Normal University, Anhui, China) and SCBG (South China Botanical Garden, Chinese Academy of Sciences). Morphological terminology and Genitalia terminology follow Mikó and Deans (2009) and Trietsch et al. (2020).

Abbreviations used in the text are as follows: **F1, F2, ..., F9**: Flagellum 1, 2, ..., F9. **LOL**: Lateral ocellar length, shortest distance between inner margins of median and lateral ocelli. **OOL**: Ocular ocellar length, minimum distance between a posterior ocellus to the eye margin. **POL**: Posterior ocellar length, shortest distance between inner margins of posterior ocelli. **HH**: Head height, lateral view. **EHf**: Eye height, anterior view. **HL**: Head length. **HW**: Head width. **IOS**: Interorbital space. **AscW**: Anterior mesoscutal width. **PscW**: Posterior mesoscutal width. **S9**: ninth abdominal sternite.

Taxonomy

Key to species of *Conostigmus* from China (male)

1 Mesosoma 2–2.1 times longer than wide; Preoccipital furrow absent ..... ***C. ampullaceus* Dessart, 1997**

– Mesosoma at most 1.5 times longer than wide; preoccipital furrow present **2**

2 Preoccipital furrow ends posterior to ocellar triangle ..... ***C. quadripetalus* Wang & Chen, sp. nov.**

– Preoccipital furrow ends inside ocellar triangle, but ends posterior to the anterior ocellus **3**

3 Facial sulcus present **4**

– Facial sulcus absent **5**

4 Harpe longer than the gonostipes in lateral view ..... ***C. abdominalis* Boheman, 1832**

– Harpe slightly shorter than gonostipes in lateral view ..... ***C. nankunensis* Qian & Wang, 2024**

5 Basal gastral carinae reaching 1/3 of syntergum length **6**

– Basal gastral carinae reaching 1/4 of syntergum length **7**

6 Head and mesosoma black, scape light-coloured, the rest of antennae black; pterostigma length vs. width: 2.5 ..... ***C. villosus*** **Dessart, 1997**
– Head and mesosoma reddish brown, metasoma and antennae amber; pterostigma length vs. width: 3.7–4.5 ..... ***Conostigmus electrinus*** **Wang & Chen, sp. nov.**
7 Body length less than 2 mm; sternaulus present and equal to mesopleuron length at level of sternaulus ..... ***Conostigmus acutus*** **Wang & Chen, sp. nov.**
– Body length more than 2 mm; sternaulus present and exceeding 2/3 of mesopleuron length at level of sternaulus ..... ***C. xui*** **Cui & Wang, 2023**

Conostigmus ampullaceus Dessart, 1997

Species comments and history. *Conostigmus ampullaceus* were first described by Dessart in 1997, who illustrated the male and female antennae, wings and male head, mesosoma and metasoma for the first time. However, the morphological characteristics were represented by hand drawings, without records of the male genitalia or pictures of the female head, mesosoma, and metasoma. The present paper redescribes male and female, adds descriptions of the male genitalia and color photos of both male and female. Furthermore, this article is the first to describe the syntergal translucent patch.

Material examined. China • 16 males, 1 female. (AHNU) • 4 males: Guangxi, Xingan, Kitten Mountain, 1900 m, yellow pan traps, 26.VI–27.VI.2011, Nasen Wei, SCAU 3045398, SCAU 3045397, SCAU 3045396, SCAU 3045395; (AHNU) • 4 males: Guangxi, Xingan, Kitten Mountain, 1900 m, yellow pan traps, 26.VI–27.VI.2011, Nasen Wei, SCAU 3045394, SCAU 3045393, SCAU 3045392, SCAU 3045392; (AHNU) • 8 males: Guangxi, Xingan, Kitten Mountain, 1900 m, yellow pan traps, 26.VI–27.VI.2011, Nasen Wei, SCAU 3045399, SCAU 3045391, SCAU 3045390, SCAU 3045389, SCAU 3045388, SCAU 3045387, SCAU 3045386, SCAU 3045385; (AHNU) • 1 female: Guangxi, Xingan, Kitten Mountain, 1900 m, yellow pan traps, 26.VI–27.VI.2011, Nasen Wei, SCAU 3045599.

Diagnosis. Head black, mesosoma and metasoma brownish black or reddish brown; body slender; mesosoma very narrow, about 1.8 × longer than wide; metasoma 3.1 × longer than wide (2.5 × in female); facial pit present; preoccipital furrow absent. sternaulus elongate and complete; syntergal translucent patch semi-circular; parossiculi fused with the gonostipes.

Redescription. Male. Body length: 1.6–2.4 mm.

Coloration. Colour hue pattern: head black; pronotum reddish brown; mesosoma and metasoma brownish black (propleuron and petiolus reddish brown); mandibles reddish brown and palps yellow; base of legs dark, rest of legs yellow; scape and pedicel reddish brown, F1–F9 black; pterostigma, costal vein, radial vein and marginal fringes of wings brown; body pubescence yellowish; male genitalia yellow. Color intensity pattern: mesosoma lighter than metasoma; mesosoma anterodorsally lighter than mesometapleuron; scape and pedicel darker than legs.

Head **(Fig. 1D, E).** Head width, dorsal view: slightly wider than mesosoma (about 1.2 × wider than mesosoma). Head width vs. head height: HW: HH = 0.8–1.0. Head

height vs. eye height: HH: EHf = 1.5–1.7. Head height vs. head length: HH: HL = 1.3–1.4. Head width vs. interorbital space: HW: IOS = 1.5–1.8. Lateral ocellar length: ocular ocellar length: LOL: OOL = 0.4–0.5. Lateral ocellar length: posterior ocellar length: LOL: POL = 0.6–0.7. Ocular ocellar length: posterior ocellar length: OOL: POL = 1.5–1.6. Head shape (anterior view): circular. Preoccipital lunula count: absent. Preoccipital carina count: absent. Preoccipital furrow count: absent. Occipital carina count: present. Occipital carina structure: complete and crenulate. Postocellar carina count: absent. Intertorular carina count: present. Intertorular area count: present. Intertorular carina shape: straight. Median process on intertorular carina count: absent. Median region of intertorular area shape: flat. Facial sulcus absent. Facial pit present. Ocellar foveae distinct, and ocellar foveae width equal to ocellus diameter.

Antennae **(Fig. 1A).** Scape length vs. pedicel length: 4.3–4.8. Scape length vs. F1 length: 1.1–1.3. F1 length vs. pedicel length: 3.3–4.1. Longest male flagellomere: F1. F1 length vs. F2 length: 1.2–1.3. Length of pubescence on flagellomere vs. flagellomere width: flagellomeres width about twice pubescence length.

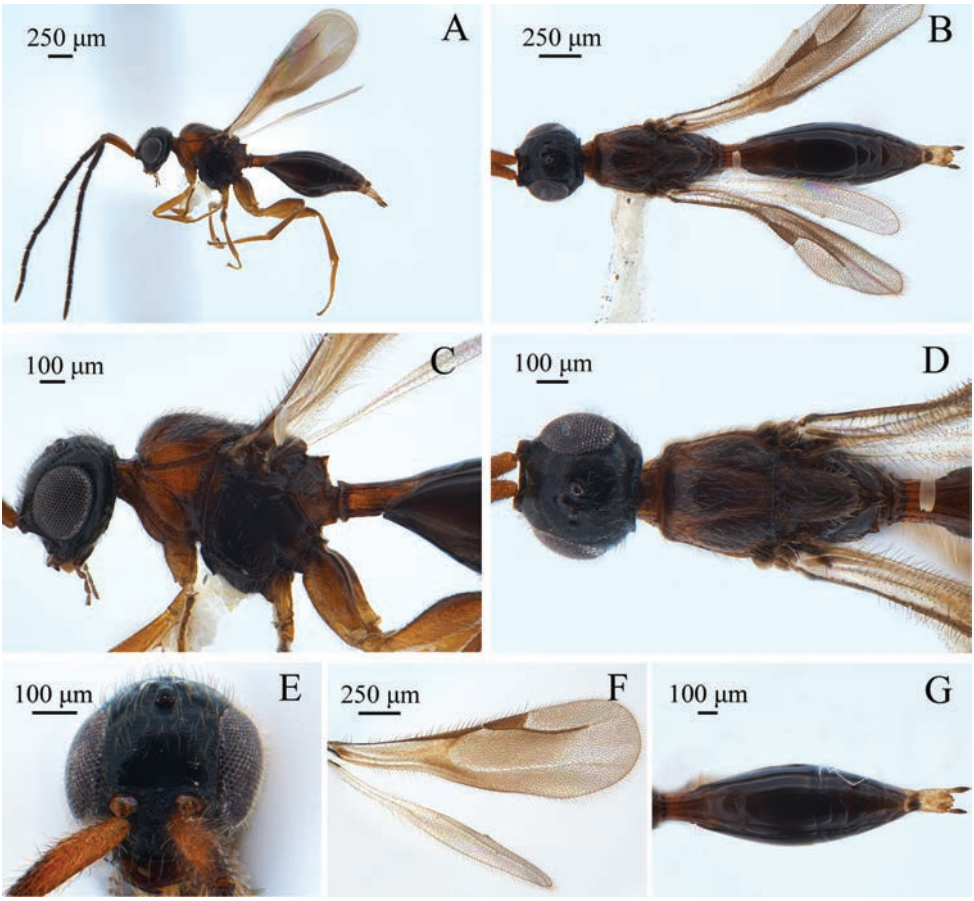

Figure 1. *Conostigmus ampullaceus* Dessart, 1997, male **A** lateral habitus **B** dorsal habitus **C** head and mesosoma, lateral view **D** head and mesosoma, dorsal view **E** head, anterior view **F** wings **G** metasoma, dorsal view.

Mesosoma **(Fig. 1C, D).** Mesosoma very narrow (1.9 × longer than wide) (Length/width/height = 820/408/618 μm). AscW/PscW = 0.7–0.8. Mesoscutum 1.1 × wider than long (Length/width = 352/408 μm). Transscutal articulation evident. Notaulus count: present and complete. Notaulus posterior end: adjacent to transscutal articulation, posterior end of notaulus contracted and adjacent to median mesoscutal sulcus. Median mesoscutal sulcus count: present and complete. Median mesoscutal sulcus posterior end: adjacent to transscutal articulation. Scutoscutellar sulcus count: present. Scutoscutellar sulcus shape: foveolate and adjacent to transscutal articulation. Mesoscutellum 1.6 × longer than wide, and limited by a u-shaped carina. Sternaulus count: present. Sternaulus shape: elongate and complete. Pleural pit present. Mesopleural sulcus shape: straight. Lateral propodeal carina shape: inverted "Y". Anteromedian projection of the metanoto-propodeo-metapecto-mesopectal complex present.

Wings **(Fig. 1F).** Forewing length: 1.5–1.8 mm, infuscate. Forewing macropterous with apex extending past petiole. Forewing with translucent stripes and dense pubescence. Pterostigma triangular, length vs. width: 2.1–2.6. Radius (387 μm), a little curved in the middle, longer (1.5 ×) than pterostigma. Hind wing without vein.

Metasoma **(Fig. 1G).** Metasoma 3.1 × longer than wide (Length/width/height = 1204/386/500 μm). Transverse carina on petiole shape: concave. Syntergum smooth, longer (1.75 ×) than wide. Gastral carinae present and less than 1/3 of syntergum length. Syntergal translucent patch count: present. Syntergal translucent patch shape: semi-circular. Rest of tergites smooth, but with sparse hairs.

Male genitalia **(Fig. 2).** Proximodorsal notch of cupula count: absent. Distodorsal margin of cupula shape: concave. Harpe shape: simple and not bilobed. Distal margin of harpe shape: shrinking to an acute angle. Harpe orientation: dorsomedial. Harpe shorter than gonostipes. Lateral setae of harpe count: present. Lateral setae of harpe orientation: oriented distally. Dense patch of setae on the distoventral edge of the harpe count: present. Parossiculus count or parossiculus and gonostipes fusion: present and parossiculi fused with the gonostipes. Gonossiculus and gonossiculus spine present. Gonossiculus spine length: one spine not more than 2 × as long as the other (s) (spines of similar lengths). Penisvalva curved proximally.

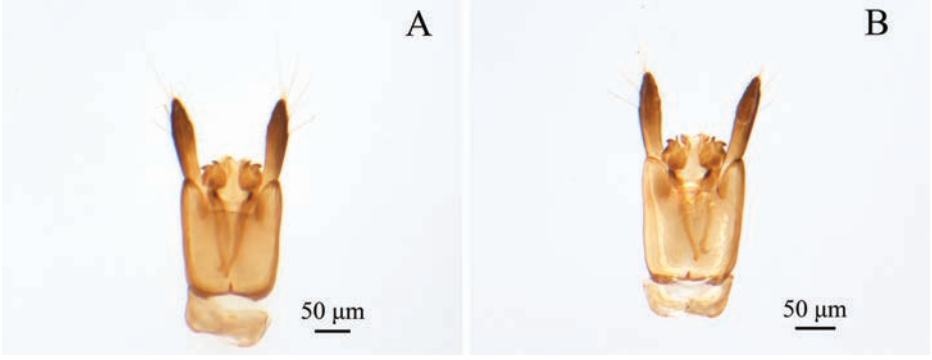

Figure 2. *Conostigmus ampullaceus* Dessart, 1997, male, genitalia **A** ventral view **B** dorsal view.

Female (Fig. 3). Body length: 2.0 mm. Mesosoma and metasoma reddish brown; scape, pedciel yellow; F1–F9 from yellow to black. Lateral ocellar length: ocular ocellar length: LOL: OOL = 0.6. Ocular ocellar length: posterior ocellar length: OOL: POL = 1.1. Scape length longer than the sum of pedicel, F1, F2 and F3. Forewing length: 1.4 mm; Pterostigma length vs. width: 4.6. Radius (270 μm), a little curved in the middle, longer (1.4 ×) than pterostigma. Metasoma 2.5 × longer than wide (Length/width/height = 1150/468/480 μm). The rest of the characteristics are the same as the males.

Distribution. China (Taiwan, Guangxi).

Biology. Unknown.

Differences between Taiwan and Guangxi populations. *Conostigmus ampullaceus* was previously recorded in Taiwan, and this article adds a new distribution record in Guangxi. No differences were found between Taiwan and Guangxi populations.

Differences between males and females. Male and female differences are reflected in sexual dimorphism in the antennae and different genitalia.

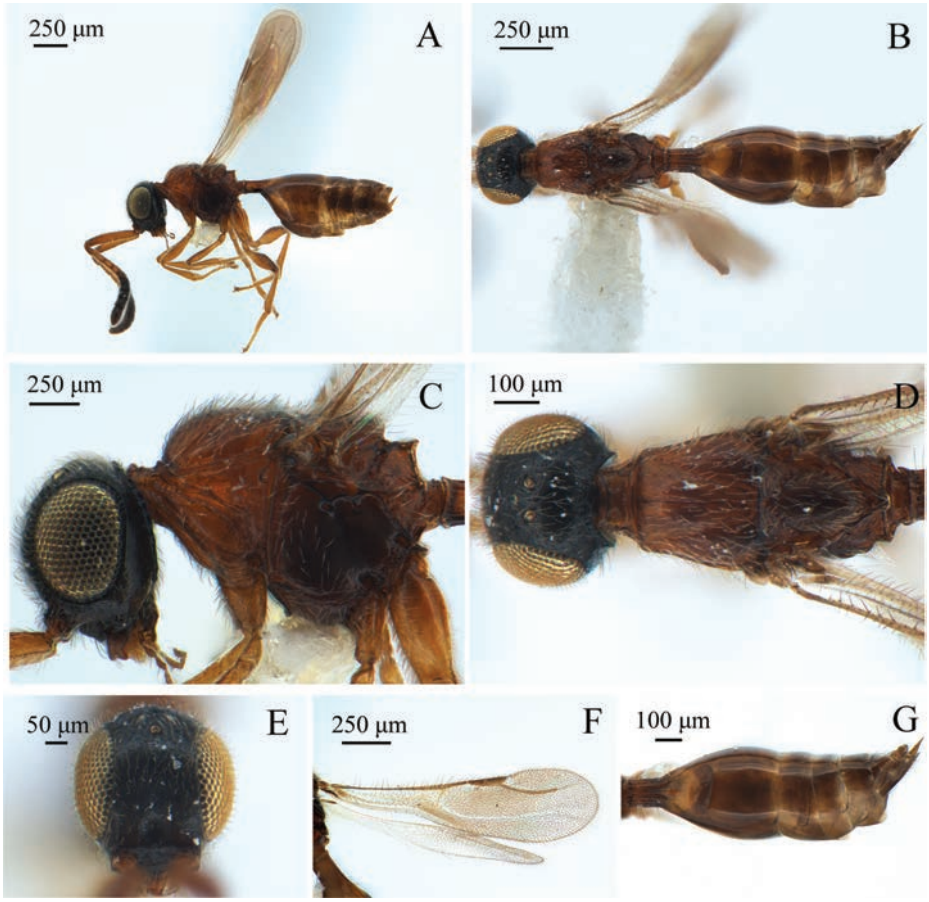

Figure 3. *Conostigmus ampullaceus* Dessart, 1997, female **A** lateral habitus **B** dorsal habitus **C** head and mesosoma, lateral view **D** head and mesosoma, dorsal view **E** head, anterior view **F** wings **G** metasoma, dorsal view.

***Conostigmus acutus* Wang & Chen, sp. nov.**
https://zoobank.org/95EA8A38-BE98-45FA-89C5-6399A20CA735

Material examined. *Holotype*: (AHNU) • male **China:** Shanxi, Lishan National Nature Reserve, Dahe Protection Station, Malaise traps, 22–26.VIII.2012, Yajun You, SCAU 3045598. ***Paratype*:** (SCBG) • 1 male: same collection information as preceding, SCAU 3045597.

Diagnosis. Head and mesosoma coarsely sculptured, metasoma smooth; randomly sized impressions around setal pits present and larger than scutes; median process on intertorular carina present and acute; mesoscutellum length almost equal to width; sternaulus present and complete; anteromedian projection of the metanoto-propodeo-metapecto-mesopectal complex absent; gastral carinae present and reaching 1/4 of syntergum length; male S9 distal setae composing setiferous patches; distal margin of harpe in lateral view acute or straight; Gonossiculus spine count: 2.

Description. Male. Body length: 1.5–1.6 mm.

***Coloration*.** Colour hue pattern: head and mesosoma black (pronotum and propleuron reddish brown); metasoma brownish black (petiolus reddish brown); mandibles reddish brown and palps yellow; legs yellow; scape yellow; pedicel and F1–F9 brown; pterostigma, costal vein, radial vein and marginal fringes of wings brown; body pubescence yellowish; male genitalia yellowish. Color intensity pattern: scape darker than legs.

***Head* (Fig. 4D, E)**. Head width, dorsal view: slightly wider than mesosoma (about 1.05 × wider than mesosoma). Head width vs. head height: HW: HH = 1.1–1.2. Head height vs. eye height: HH: EHf = 1.7–1.8. Head height vs. head length: HH: HL = 1.2–1.4. Head width vs. interorbital space: HW: IOS = 1.6–1.7. Lateral ocellar length: ocular ocellar length: LOL: OOL = 0.4–0.5. Lateral ocellar length: posterior ocellar length: LOL: POL = 0.6–0.7. Ocular ocellar length: posterior ocellar length: OOL: POL = 1.3–1.7. Head coarse; randomly sized impressions around setal pits count: present; the size of impressions around the setal pits on the head: impressions larger than scutes; head shape (anterior view): circular or triangular. Preoccipital lunula count: absent. Preoccipital carina count: absent. Preoccipital furrow count: present. Preoccipital furrow anterior end: preoccipital furrow ends inside ocellar triangle, but ends posterior to the anterior ocellus. Occipital carina count: present. Occipital carina structure: complete and crenulate. Postocellar carina count: present. Intertorular area count: present. Intertorular carina count: present. Median process on intertorular carina count: present. Median process on intertorular carina shape: acute. Median region of intertorular area shape: flat. Facial sulcus absent. Facial pit present. Ocellar foveae distinct, and ocellar foveae width equal to ocellus diameter.

***Antennae* (Fig. 4A).** Scape length vs. pedicel length: 3.8–4.5. Scape length vs. F1 length: 1.2–1.3. F1 length vs. pedicel length: 3.1–3.5. Longest male flagellomere: F1. F1 length vs. F2 length: 1.0–1.2. F3 length almost equal to F4. F7 length almost equal to F8. Length of pubescence on flagellomere vs. flagellomere width: flagellomeres width about twice than pubescence length.

***Mesosoma* (Fig. 4C, D).** Mesosoma roughness and slightly narrow (1.3 × longer than wide) (Length/width/height = 512/393/359 μm). AscW/PscW = 0.8–0.9. Mesoscutum

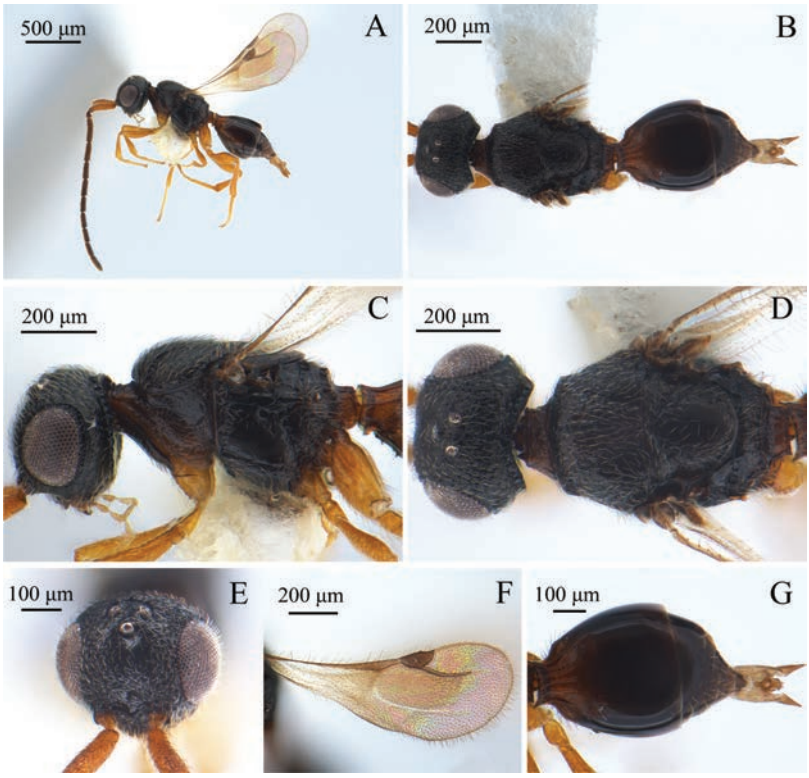

Figure 4. *Conostigmus acutus* Wang & Chen, sp. nov., male, holotype **A** lateral habitus **B** dorsal habitus **C** head and mesosoma, lateral view **D** head and mesosoma, dorsal view **E** head, anterior view **F** wings **G** metasoma, dorsal view.

1.8 × wider than long (Length/width = 222/393 μm). Transscutal articulation evident. Notaulus count: present and complete. Notaulus posterior end: adjacent to transscutal articulation, posterior end of notaulus contracted but not adjacent to median mesoscutal sulcus. Median mesoscutal sulcus count: present and complete. Median mesoscutal sulcus posterior end: adjacent to transscutal articulation. Scutoscutellar sulcus count: present. Scutoscutellar sulcus vs. transscutal articulation location: adjacent. Scutoscutellar sulcus shape: scutoscutellar sulcus angled medially, foveolate. Mesoscutellum length almost equal to width, limited by a u-shaped carina. Sternaulus count: present. Sternaulus shape: elongate and complete. Mesopleural sulcus shape: straight. Pleural pit present. Lateral propodeal carina shape: inverted "Y". Anteromedian projection of the metanoto-propodeo-metapecto-mesopectal complex absent.

***Wings* (Fig. 4F).** Forewing length: 1.1–1.4 mm, translucent. Forewing macropterous with apex extending past petiole. Forewing with translucent stripes and dense pubescence. Pterostigma semi-circular, length vs. width: 2.1–3.2. Radius (200 μm), a little curved in the middle, longer (1.4 ×) than pterostigma. Hind wing without vein.

***Metasoma* (Fig. 4G).** Metasoma 1.6 × longer than wide (Length/width/height = 647/408/357 μm). Transverse carina on petiole shape: concave. Syntergum smooth,

longer (1.1 ×) than wide. Gastral carinae present and reaching 1/4 of syntergum length. Syntergal translucent patch count: present. Syntergal translucent patch shape: long rod-shaped. Rest of tergites smooth, but with sparse hairs.

Male genitalia **(Fig. 5).** Distal margin of male S9 shape: convex. Proximolateral corner of male S9 shape: blunt. Male S9 distal setal line/setal patch count: distal setae composing setiferous patch or patches; distal setae composing transverse setiferous line or lines. Submedial projections on proximal margin of S9 count: absent. Harpe shape: acute triangle. Distal margin of harpe shape: shrinking to an much acute angle. Distal margin of harpe in lateral view: acute or straight. Harpe orientation: dorsomedial. Harpe length: harpe shorter than gonostipes in lateral view. Lateral setae of harpe count: present. Lateral setae of harpe orientation: oriented distally. Dense patch of setae on the distoventral edge of the harpe count: absent. Parossiculus count or parossiculus and gonostipes fusion: present and parossiculi not fused with the gonostipes. Gonossiculus and gonossiculus spine present. Gonossiculus spine count: 2. Gonossiculus spine length: one spine more than 2 × as long as the other (s). Penisvalva curved proximally.

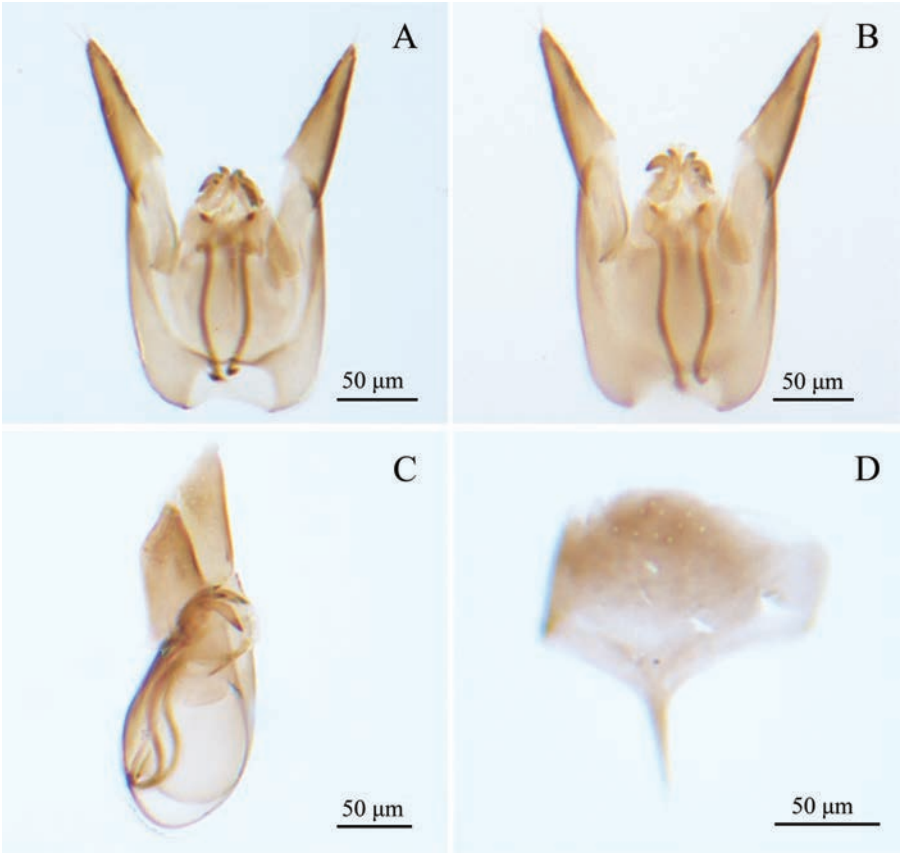

Figure 5. *Conostigmus acutus* Wang & Chen, sp. nov., male, holotype, genitalia **A** ventral view **B** dorsal view **C** lateral view **D** S9.

Distribution. China (Shanxi).

Biology. Unknown.

Etymology. Consistent with the genus name, the species name is a Latin masculine adjective meaning "mucronate", indicating a male mucronate harpe.

***Conostigmus electrinus* Wang & Chen, sp. nov.**

https://zoobank.org/21BD7BA8-1152-4941-ACB5-E5A3686169B5

Material examined. ***Holotype*:** (AHNU) • male **China:** Liaoning, Laotudingzi National Nature Reserve, yellow pan traps, 16–19.VII.2011, Huayan Chen & Kexin Zhao, SCAU 3045596. ***Paratypes*:** (AHNU) • 1 male, Liaoning, Laotudingzi National Nature Reserve, yellow pan traps, 16–19.VII.2011, Huayan Chen, SCAU 3045595; (SCBG) • 2 males: 1 male, same collection information as preceding, Pan Li, SCAU 3045594; 1 male, same collection information as preceding, Huayan Chen & Kexin Zhao, SCAU 3045593.

Diagnosis. This species is distinguished by the following combination of characters: head and mesosoma reddish brown; metasoma and antennae amber; scape length almost equal to F1; facial pit present; preoccipital furrow present; postocellar furrow absent; sternaulus present, elongate and reaching 1/2 of mesopleuron length at the level of the sternaulus; gastral carinae present and reaching 1/3 of syntergum length; syntergal translucent patch bending moon shape; harpe slightly shorter than gonostipes.

Description. Male. Body length: 2–2.2 mm.

***Coloration*.** Colour hue pattern: head and mesosoma reddish brown; metasoma and antennae amber; mandibles reddish brown; palps and legs yellow; pterostigma, costal vein, radial vein and marginal fringes of wings light brown; body pubescence yellowish; male genitalia yellow. Color intensity pattern: head darker than mesosoma; antennae lighter than metasoma; petiole neck and anterior region of syntergite darker in coloration than the posterior region of the syntergite.

Head **(Fig. 6D, E)**. Head width, dorsal view: slightly wider than mesosoma (about 1.3 × wider than mesosoma). Head width vs. head height: HW: HH = 1.1–1.2. Head height vs. eye height: HH: EHf = 2.0–2.2. Head height vs. head length: HH: HL = 1.4–1.6. Head width vs. interorbital space: HW: IOS = 1.6–1.7. Lateral ocellar length: ocular ocellar length: LOL: OOL = 0.2–0.3. Lateral ocellar length: posterior ocellar length: LOL: POL = 0.4–0.45. Ocular ocellar length: posterior ocellar length: OOL: POL = 1.4–1.5. Head shape (anterior view): circular or triangular. Preoccipital lunula count: present. Preoccipital carina count: absent. Preoccipital furrow count: present. Preoccipital furrow anterior end: preoccipital furrow ends inside ocellar triangle, but ends posterior to the anterior ocellus. Preoccipital furrow sculpture: crenulate. Occipital carina count: present. Occipital carina structure: complete and crenulate. Postocellar carina count: absent. Intertorular area count: present. Intertorular carina count: present. Median process on intertorular carina count: absent. Median region of intertorular area shape: flat. Facial sulcus absent. Facial pit present. Ocellar foveae distinct, and ocellar foveae width equal to ocellus diameter.

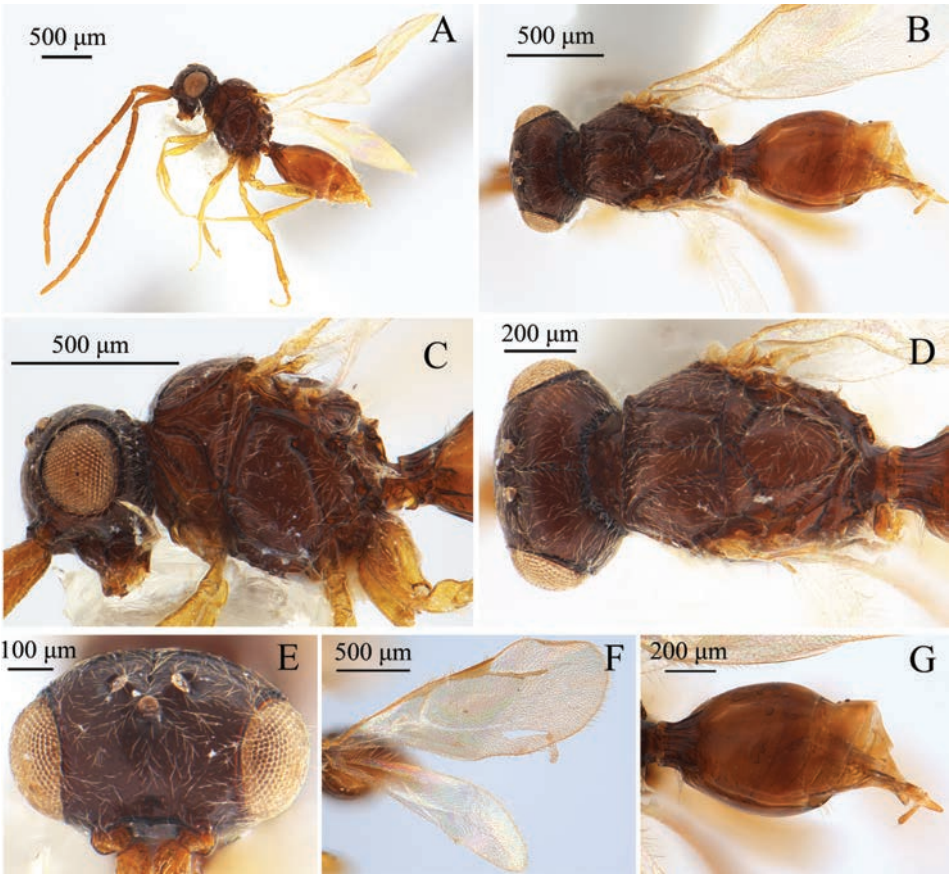

Figure 6. *Conostigmus electrinus* Wang & Chen, sp. nov., male, holotype **A** lateral habitus **B** dorsal habitus **C** head and mesosoma, lateral view **D** head and mesosoma, dorsal view **E** head, anterior view **F** wings **G** metasoma, dorsal view.

Antennae **(Fig. 6A).** Scape length vs. pedicel length: 5.1–5.6. Scape length almost equal to F1. F1 length vs. pedicel length: 5.0–5.3. Longest male flagellomere: F1. F1 length vs. F2 length: 1.2–1.3. Length of pubescence on flagellomere vs. flagellomere width: flagellomeres width about twice than pubescence length.

Mesosoma **(Fig. 6C, D).** Mesosoma slightly narrow (1.4 × longer than wide) (Length/width/height = 686/489/604 µm). AscW/PscW = 0.8–0.9. Mesoscutum 1.75 × wider than long (Length/width = 227/489 µm). Transscutal articulation evident. Notaulus count: present and complete. Notaulus posterior end: adjacent to transscutal articulation, posterior end of notaulus not curved and not adjacent to median mesoscutal sulcus. Median mesoscutal sulcus count: present and complete. Median mesoscutal sulcus posterior end: adjacent to transscutal articulation. Scutoscutellar sulcus count: present. Scutoscutellar sulcus vs. transscutal articulation location: adjacent. Scutoscutellar sulcus shape: scutoscutellar sulcus angled medially, foveolate.

Mesoscutellum 1.3 × longer than wide, limited by a u-shaped carina. Sternaulus count: present. Sternaulus shape: elongate and reaching 1/2 of mesopleuron length at the level of the sternaulus. Mesopleural sulcus shape: straight. Pleural pit present. Lateral propodeal carina shape: inverted " Y ". Anteromedian projection of the metanoto-propodeo-metapecto-mesopectal complex absent.

***Wings* (Fig. 6F).** Forewing length: 1.7–1.8 mm, translucent. Forewing macropterous with apex extending past petiole. Forewing with transparent stripes and dense pubescence (stripes without pubescence). Pterostigma triangular, length vs. width: 3.7–4.5. Radius (383 μm), a little curved, longer (1.2 ×) than pterostigma. Hind wing without vein.

***Metasoma* (Fig. 6G).** Metasoma 2.1 × longer than wide (Length/width/height = 1129/532/462 μm). Transverse carina on petiole shape: straight. Syntergum smooth, longer (1.1 ×) than wide. Gastral carinae present and reaching 1/3 of syntergum length. Syntergal translucent patch count: present. Syntergal translucent patch shape: crescent. Rest of tergites smooth, but with sparse hairs.

***Male genitalia* (Fig. 7).** Harpe shape: simple and not bilobed; finger shape. Distal margin of harpe shape: shrinking to an acute angle. Harpe orientation: dorsomedial. Harpe slightly shorter than gonostipes in lateral view. Lateral setae of harpe count: present. Lateral setae of harpe orientation: oriented distally. Dense patch of setae on the distoventral edge of the harpe count: absent. Parossiculus count or parossiculus and gonostipes fusion: present and parossiculi not fused with the gonostipes. Gonossiculus and gonossiculus spine present. Gonossiculus spine count: 3. Gonossiculus spine length: one spine not more than 2× as long as the other(s). Penisvalva curved and intersecting proximally.

Distribution. China (Liaoning).

Biology. Unknown.

Etymology. Consistent with the genus name, the species name is a Latin masculine adjective meaning "amber", indicating amber antennae and metasoma.

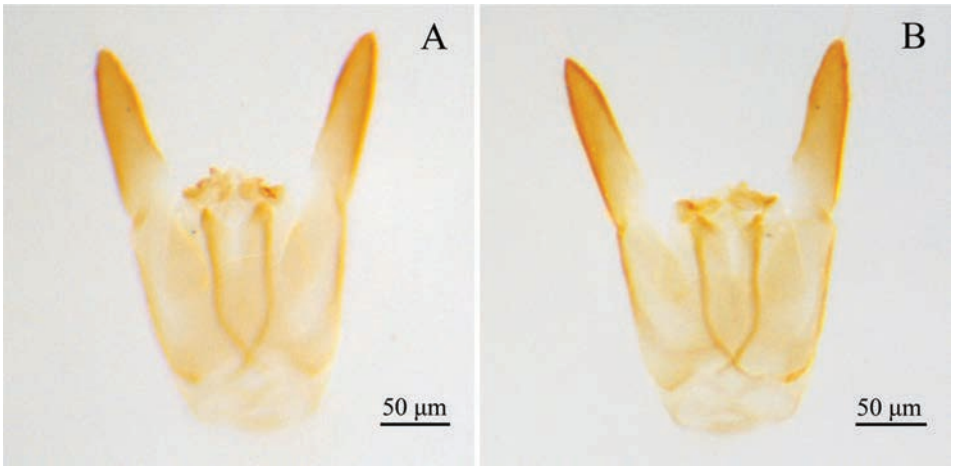

Figure 7. *Conostigmus electrinus* Wang & Chen, sp. nov., male, holotype, genitalia **A** dorsal view **B** ventral view.

***Conostigmus quadripetalus* Wang & Chen, sp. nov.**
https://zoobank.org/F762DB57-97FA-405B-B413-1FED817117C0

Material examined. *Holotype*: (AHNU) • male **China:** Guizhou, Dabanshui National Forest Park, 939 m, 7–10.VI.2011, Dongdong Feng, SCAU 3045592. ***Paratypes*:** (AHNU) • male Guizhou, Dabanshui National Forest Park, 939 m, 7–10.VI.2011, Dongdong Feng, SCAU 3045591. (SCBG) • 2 males: same collection information as preceding, SCAU 3045590, SCAU 3045589.

Diagnosis. This species is distinguished by the following combination of characters: preoccipital lunula present; preoccipital carina present; preoccipital furrow present and preoccipital furrow ends posterior to ocellar triangle; antennal scrobe present; mesoscutellum length almost equal to wide, and not limited by a u-shaped carina; Sternaulus elongate and exceeding 2/3 of mesopleuron length at level of sternaulus; gastral carinae present and reaching 1/3 of syntergum length; distal margin of male S9 shape: convex; proximolateral corner of male S9 shape: blunt; distal margin of harpe blunt or straight; distal margin of harpe in lateral view acute or pointed; harpe shorter than gonostipes in lateral view; 4 gonossiculus spine and one spine more than 2 × as long as the other (s).

Description. Male. Body length: 1.1 mm.

***Coloration*.** Colour hue pattern: head and mesosoma black; metasoma dark brown; mandibles brown; palps yellow; scape yellow to brown, pedicel and flagellum brown; legs yellow; pterostigma, costal vein, radial vein and marginal fringes of wings light brown; body pubescence yellowish; male genitalia yellow. Color intensity pattern: petiole neck and anterior region of syntergite lighter than the posterior region of the syntergite; pedicel and F1 lighter than F2–F9.

***Head* (Fig. 8D, E)**. Head width, dorsal view: slightly wider than mesosoma (about 1.1 × wider than mesosoma). Head width vs. head height: HW: HH = 1.1–1.3. Head height vs. eye height: HH: EHf = 1.5–1.7. Head height vs. head length: HH: HL = 1.2–1.4. Head width vs. interorbital space: HW: IOS = 1.6–1.8. Lateral ocellar length: ocular ocellar length: LOL: OOL = 0.5–0.8. Lateral ocellar length: posterior ocellar length: LOL: POL = 0.4–0.8. Ocular ocellar length: posterior ocellar length: OOL: POL = 1.4–1.9. Head smooth; head shape (anterior view): circular or triangular. Preoccipital lunula count: present. Preoccipital carina count: present. Preoccipital furrow count: present. Preoccipital furrow anterior end: preoccipital furrow ends posterior to ocellar triangle. Occipital carina count: present. Occipital carina structure: complete and crenulate. Intertorular area count: present. Intertorular carina count: present. Median process on intertorular carina count: present. Median process on intertorular carina shape: acute. Median region of intertorular area shape: flat. Antennal scrobe count: present. Facial sulcus absent. Facial pit absent. Ocellar foveae distinct, and ocellar foveae width less than ocellus diameter.

***Antennae* (Fig. 8A).** Scape length vs. pedicel length: 3.0–4.2. Scape length vs. F1 length: 1.2–1.5. F1 length vs. pedicel length: 2.3–2.7. Longest male flagellomere: F1. F1 length vs. F2 length: 1.1–1.2. F4 length almost equal to F6. Length of pubescence on flagellomere vs. flagellomere width: flagellomeres width about twice than pubescence length.

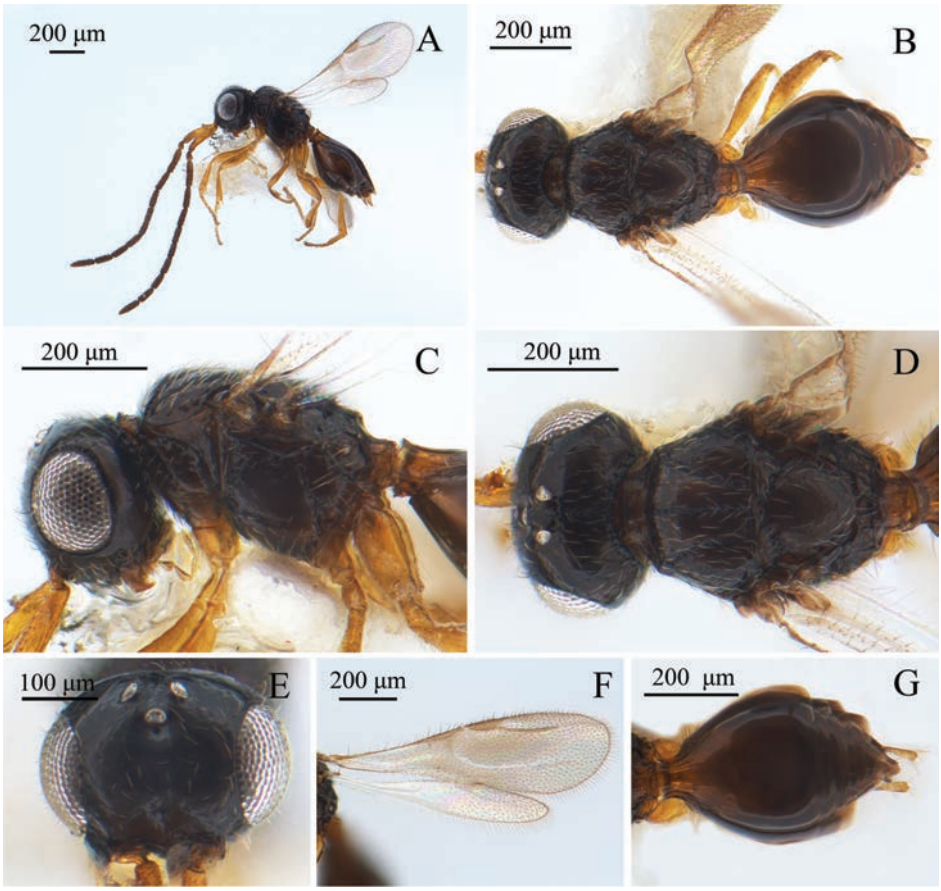

Figure 8. *Conostigmus quadripetalus* Wang & Chen, sp. nov., male, holotype **A** lateral habitus **B** dorsal habitus **C** head and mesosoma, lateral view **D** head and mesosoma, dorsal view **E** head, anterior view **F** wings **G** metasoma, dorsal view.

Mesosoma **(Fig. 8C, D).** Mesosoma slightly narrow (1.4 × longer than wide) (Length/width/height = 403/263/293 μm). AscW/PscW = 0.7–0.9. Mesoscutum 1.85 × wider than long (Length/width = 158/293 μm). Transscutal articulation evident. Notaulus count: present and complete. Notaulus posterior end: adjacent to transscutal articulation, posterior end of notaulus contracted but not adjacent to median mesoscutal sulcus. Median mesoscutal sulcus count: present and complete. Median mesoscutal sulcus posterior end: adjacent to transscutal articulation. Scutoscutellar sulcus count: present. Scutoscutellar sulcus vs. transscutal articulation location: adjacent. Scutoscutellar sulcus shape: scutoscutellar sulcus angled medially, foveolate. Mesoscutellum length almost equal to wide, not limited by a u-shaped carina. Sternaulus count: present. Sternaulus shape: elongate and exceeding 2/3 of mesopleuron length at level of sternaulus. Mesopleural sulcus shape: straight. Pleural pit present. Lateral propodeal carina shape: inverted " Y ". Anteromedian projection of the metanoto-propodeo-metapecto-mesopectal complex absent.

***Wings* (Fig. 8F).** Forewing length: 0.8–1.0 mm, translucent. Forewing macropterous with apex extending past petiole. Forewing with transparent stripes and dense pubescence (stripes without pubescence). Pterostigma semi-circular, length vs. width: 2.7–4.4. Radius (200 μm), a little curved, longer (1.4 ×) than pterostigma. Hind wing without vein.

***Metasoma* (Fig. 8G).** Metasoma 1.6 × longer than wide (Length/width/height = 508/321/252 μm). Transverse carina on petiole shape: concave. Syntergum smooth, longer (1.1 ×) than wide. Gastral carinae present and reaching 1/3 of syntergum length. Syntergal translucent patch count: present. Syntergal translucent patch shape: elliptical. Rest of tergites smooth, but with sparse hairs.

***Male genitalia* (Fig. 9).** Distal margin of male S9 shape: convex. Proximolateral corner of male S9 shape: blunt. Male S9 distal setal line/setal patch count: distal setae composing setiferous patch or patches; distal setae composing transverse setiferous line or lines. Submedial projections on proximal margin of S9 count: absent. Harpe shape: simple and not bilobed. Distal margin of harpe shape: blunt or straight (with a little raised). Distal margin of harpe in lateral view: acute or pointed. Harpe orientation: medial. Harpe length: harpe shorter than gonostipes in lateral view. Lateral setae of harpe count: present. Lateral setae of harpe orientation: oriented distally. Dense patch

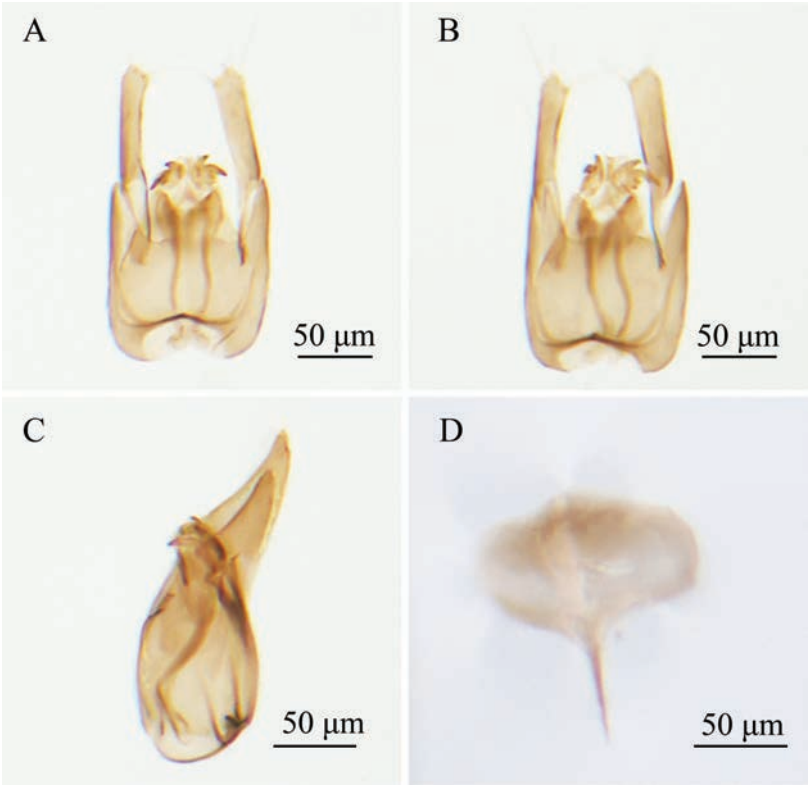

Figure 9. *Conostigmus quadripetalus* Wang & Chen, sp. nov., male, holotype, genitalia **A** dorsal view **B** ventral view **C** lateral view **D** S9.

of setae on the distoventral edge of the harpe count: present. Parossiculus count or parossiculus and gonostipes fusion: present and parossiculi not fused with the gonostipes. Gonossiculus and gonossiculus spine present. Gonossiculus spine count: 4. Gonossiculus spine length: one spine more than 2 × as long as the other (s). Penisvalva curved and intersecting proximally.

Distribution. China (Guangdong).

Biology. Unknown.

Etymology. Consistent with the genus name, the species name is a Latin masculine adjective meaning "quadrifid", indicating 4 gonossiculus spines.

Acknowledgements

This work was supported by the National Natural Science Foundation of China (Grant Nos. 32100352, 32100355), the National Science & Technology Fundamental Resources Investigation Program of China (Grant No. 2019FY101800) and the University Synergy Innovation Program of Anhui Province (GXXT-2022-067).

References

Cui SS, Li F, Huang YX, Huang XZ, Wang X, Zhu CD (2023) Description of a new species of *Conostigmus* Dahlbom, 1858 (Hymenoptera: Megaspilidae) from China. Zootaxa 5315(1): 71–76. https://doi.org/10.11646/zootaxa.5315.1.4

Dessart P (1985) Les *Dendrocerus* a notaulices incompletes (Hymenoptera Ceraphronoidea Megaspilidae). Bulletin et Annales de la Société Royale Belge d'Entomologie 121: 409–458.

Dessart P (1995a) A propos du genre *Dendrocerus* Ratzeburg, 1852. Les espèces du group "penmaricus" (Hymenoptera Ceraphronoidea Megaspilidae). Bulletin et Annales de la Société Royale Belge d'Entomologie 131: 349–382.

Dessart P (1995b) 8.6 Megaspilidae. In: Hanson P, Gauld ID (Eds) Hymenoptera of Costa Rica. Oxford University Press, Oxford, 203–208.

Dessart P (1997) Les Megaspilinae ni européens, ni américains. 1. Le genre *Conostigmus* Dahlbom, 1858 (Hym. Ceraphronoidea; Megaspilidae). Memoires de la Société Royale Belge d'Entomologie 37: 3–144.

Dessart P (1999) Révision des Dendrocerus du groupe «halidayi» (Hym. Ceraphronoidea Megaspilidae). Belgian Journal of Entomology 1: 169–275.

Dessart P (2001) Les Megaspilinae ni européens, ni américains 2. Les *Dendrocerus* Ratzeburg, 1852, à mâles non flabellicornés (Hymenoptera Ceraphronoidea Megaspilidae). Belgian Journal of Entomology 3: 3–124.

Fu Q, He JC, Lu ZX, Alberto TB (2021) Identification and utilization of natural enemies of rice pests in China. Zhejiang Science and Technology Publishing Press, HangZhou, 500–503. [in Chinese]

Graham MDV (1984) A new species of *Conostigmus* (Insecta: Hymenoptera, Ceraphronoidea) from Madeira. Bocagiana 77: 1–5. http://publications.cm-funchal.pt/handle/100/1487

Johnson NF, Musetti L (2004) Catalog of the systematic literature of the superfamily Ceraphronoidea (Hymenoptera). Contributions of the American Entomological Institution 33: 1–149.

Kieffer JJ (1907) Proctotrypidæ (suite). Species Hyménoptères d'Europe & d'Algerie 10: 1–144.

Kamal M (1926) Four new species of parasites from aphidophagous Syrphidae (Hymenoptera). The Canadian Entomologist 58(11): 283–286. https://doi.org/10.4039/Ent58283-11

Laborius A (1972) Untersuchungen über die Parasitierung des Kohlschotenrüßlers (*Ceuthorrhynchus assimilis* Payk.) und der Kohlschotengallmücke (*Dasineura brassicae* Winn.) in Schleswig-Holstein. Zeitschrift für Angewandte Entomologie 72: 14–31. https://doi.org/10.1111/j.1439-0418.1972.tb02213.x

Mikó I, Deans AR (2009) *Masner*, a new genus of Ceraphronidae (Hymenoptera, Ceraphronoidea) described using controlled vocabularies. Zookeys 20: 127–153. https://doi.org/10.3897/zookeys.20.119

Mikó I, Yoder MJ, Deans AR (2011) Order Hymenoptera, Family Megaspilidae, Genus *Dendrocerus*. Arthropod Fauna of the UAE 4: 353–374.

Mikó I, Masner L, Johannes E, Yoder MJ, Deans AR (2013) Male terminalia of Ceraphronoidea: morphological diversity in an otherwise monotonous taxon. Insect Systematics and Evolution 44: 261–347. https://doi.org/10.1163/1876312X-04402002

Mikó I, Trietsch C, Sandall EL, Yoder MJ, Hines H, Deans AR (2016) Malagasy *Conostigmus* (Hymenoptera: Ceraphronoidea) and the secret of scutes. PeerJ 4: e2682. https://doi.org/10.7717/peerj.2682

Qian CZX, Li F, Huang YX, Wang X (2024) *Conostigmus nankunensis* (Hymenoptera: Ceraphronoidea), a new species from China with a long facial sulcus. Zootaxa 5481(1): 141–145. https://doi.org/10.11646/zootaxa.5481.1.9

Trietsch C, Deans AR, Mikó I (2015) Redescription of *Conostigmus albovarius* Dodd, 1915 (Hymenoptera, Megaspilidae), a metallic ceraphronoid, with the first description of males. Journal of Hymenoptera Research 46: 137–150. https://doi.org/10.3897/JHR.46.5534

Trietsch C, Mikó I, Deans AR (2016) The Magnificent Megaspilidae: *Conostigmus* spp. (Hymenoptera: Megaspilidae) of the Nearctic. In 2016 International Congress of Entomology. https://doi.org/10.1603/ICE.2016.112695

Trietsch C, Mikó I, Ezray B, Deans AR (2020) A taxonomic revision of Nearctic *Conostigmus* (Hymenoptera: Ceraphronoidea: Megaspilidae). Zootaxa 4792(1): 1–155. https://doi.org/10.11646/zootaxa.4792.1.1

Vidal S (2003) Identification of Hymenopterous Parasitoids Associated with Oilseed Rape Pests. In: Alford DV (Ed.) Biocontrol of Oilseed Rape Pests, 161–180. https://doi.org/10.1002/9780470750988.ch11

JHR 97: 825–848 (2024)
doi: 10.3897/jhr.97.130713
https://jhr.pensoft.net

RESEARCH ARTICLE

JOURNAL OF Hymenoptera RESEARCH
A peer-reviewed open-access journal
The International Society of Hymenopterists

Diversity and differentiation of the *Chelonus* (*Microchelonus*) species of the Galapagos archipelago (Hymenoptera, Braconidae, Cheloninae)

Ada L. Sandoval-B[1,2], Scott Richard Shaw[3], Henri W. Herrera[2], Carlos E. Sarmiento[1]

1 *Universidad Nacional de Colombia, Instituto de Ciencias Naturales, Laboratorio de Sistemática y Biología Comparada de Insectos, Campus Bogotá, Colombia* **2** *Museo de Entomología, Facultad de Recursos Naturales, Escuela Superior Politécnica de Chimborazo, Riobamba, Ecuador* **3** *Department of Ecosystem Science and Management, University of Wyoming, Laramie, Wyoming, USA*

Corresponding author: Carlos E. Sarmiento (cesarmientom@unal.edu.co)

Academic editor: Jovana M. Jasso-Martínez | Received 10 July 2024 | Accepted 6 September 2024 | Published 8 October 2024

https://zoobank.org/0168976D-0666-4E67-BE64-FBA74CCA7896

Citation: Sandoval-B AL, Shaw SR, Herrera HW, Sarmiento CE (2024) Diversity and differentiation of the *Chelonus* (*Microchelonus*) species of the Galapagos archipelago (Hymenoptera, Braconidae, Cheloninae). Journal of Hymenoptera Research 97: 825–848. https://doi.org/10.3897/jhr.97.130713

Abstract

Despite the significance of the Galapagos archipelago, the richness of diverse groups such as braconid wasps remains poorly studied. Seven species of chelonine Braconidae are recorded for the Galapagos islands for the first time: *Chelonus buscki* Viereck, 1912, *Chelonus carinatus* Provancher, 1881, *Chelonus johni* Marsh, 1979, *Chelonus refluus* (Papp, 2010), *Chelonus sulcifera* (Papp, 2016), *Chelonus topali* (Papp, 1999), and *Chelonus turgoclarus* (Papp, 2010). No endemic species were identified for the islands. We also explore island population differences with respect to island area, age, and distance between islands. The populations of *C. buscki* and *C. carinatus* were statistically differentiated between islands. Morphological differences were associated with island area only for *C. buscki* while no relationship was found between differentiation and age or geographic distance between islands for any species. These results could be a consequence of recent colonization events.

Keywords

Island biogeography, morphological differentiation, parasitoid, proportions spectrum analysis

Introduction

Archipelagos are isolated island systems that can evolve as different environmental units from continental masses (Santamarta 2016). Archipelagos can be blank slates for species colonization and diversification depending on the age, distance from mainland areas, and other characteristics of the islands (Parent et al. 2008; Losos and Ricklefs 2009). The standard colonization process assumes that when the first migratory species arrive, abundant niches are available on the islands (Mayr 1965; Emerson 2008). Then, the number of species increases through speciation and immigration, at a rate dependent on isolation and time (Mayr 1965; Gillespie and Roderick 2002; Emerson 2008). Along with these changes, the phenotypic differentiation between the members of a clade, being either sympatric or allopatric, may occur as species adapt to use different resources (Mayr 1965; MacArthur and Wilson 1967; Rundle and Nosil 2005; Losos and Mahler 2010; Dudaniec et al. 2011).

This process of colonization and differentiation of populations from the oldest to the youngest of islands was described as the rule of progression (Funk and Wagner 1995; Hennig 1966; Poulakakis et al. 2020), and gives an important role to the age of the islands in causing the diversification of the species (Gillespie and Roderick 2002) with numerous examples in archipelagos such as Hawaii (Roderick and Gillespie 1998). However, the expected relationship between differentiation of the founding populations and island age may be altered by events such as the time of arrival of the founding species, its biology, and the geographical complexity of the archipelago (Sequeira et al. 2002; Hormiga et al. 2003; Bonacum et al. 2005; Kvist et al. 2005; Schmitz et al. 2007; Haines et al. 2014). In the case of parasitoid species, such as chelonine wasps, successful colonization depends on prior colonization by suitable host insect species.

For the Galapagos islands, as for practically all the planet, arthropods represent most of the natural terrestrial biodiversity (Peck 1997), indeed, a revision of literature indicates that little more than 2,000 species of insects have been documented for the archipelago, with a high level of endemism (Roque-Albelo L. 2008; Bungartz et al. 2012; Toral et al. 2017; Buchholz et al. 2020). An early inventory of the insects of the archipelago revealed that 47% of the species are endemic (Peck 1997; Peck et al. 1998), suggesting frequent events of early colonization and separation from their continental ancestors (Tye et al. 2002), favoring phenotype differentiation, this being one of the first steps to speciation (Grant et al. 2000; Yamaguchi and Iwasa 2013). However, few detailed studies about the diversification processes of the group in the islands have been conducted (Tye et al. 2002) with most papers focused on survey data.

Cheloninae is one of the largest subfamilies of Braconidae with more than 1,500 valid taxa (Yu et al. 2005; Dong et al. 2019). Despite their great species diversity, chelonines are easily recognized from most other braconids by their rigid, sculptured metasomal carapace, with the other parts of metasoma usually being concealed ventrally (Shaw 1983, 1997, 2006; Dadelahi et al. 2018; Ghahari et al. 2022). Chelonine wasp species are mostly solitary koinobiont egg-larval endoparasitoids of concealed Lepidoptera, especially attacking host species in the Tortricoidea and Pyralidoidea (Shenefelt 1973; Yu et al. 2005; Stireman and Shaw 2021). Chelonines are considered

economically important as biocontrol agents for suppressing plant-feeding caterpillars, especially those in the families Noctuidae, Geometridae, Tortricidae, Pyralidae, and Gelechiidae (Shaw and Huddleston 1991). However, despite their importance to biological control programs only about a quarter of the chelonine wasp species have been described and many are poorly characterized, making their recognition to species level difficult (Aydogdu and Beyarslan 2011).

There is debate regarding the treatment of some genera within Cheloninae. *Microchelonus*, for example, is considered as a subgenus within *Chelonus* by some authors (McComb 1968; Shaw 1991, 1997, 2006; Nascimento and Penteado-Dias 2011; Sharkey et al. 2021; Ghahari et al. 2022; Ranjith and Priyadarsanan 2023). However, some authors have treated *Microchelonus* as a valid genus, close to *Chelonus* (Tobias 1995, 2001, 2008, 2010; Chen and Ji 2002; Papp 2016). Papp (1995) mentions that *Microchelonus* always has 16 antennomeres and a foramen in the apical part of the carapace of males while *Chelonus* is characterized by a variable number of antennomeres and the absence of the apical foramen. The species treated in this paper can all be assigned to the *Chelonus* subgenus *Microchelonus*.

In this study, we explore the morphological differentiation in the populations of the seven known species of *Chelonus* (*Microchelonus*) in the Galapagos Islands. We explore the above-described expectations of evolutionary processes by considering the following hypotheses: 1. Each island of the Galapagos archipelago hosts different species of the genus *Chelonus*, 2. There is a direct relationship between island age and morphologic variation in populations of *Chelonus*, 3. If present, the degree of differentiation between species or populations of *Chelonus* on each island is associated with the age of the islands, 4. If present, the degree of differentiation between species or populations of *Chelonus* on each island is associated with the geographical proximity between the islands.

Methods

Study area and sampling

A total of 114 specimens of *Chelonus* were studied from the following islands of Galapagos archipelago: Floreana, Pinta, San Cristobal, Isabela, Santiago, Fernandina, Española, and Santa Cruz. Voucher specimens from this study are deposited at the Entomology Museum of the Facultad de Recursos Naturales, of the Escuela Superior Politécnica de Chimborazo, Riobamba, Ecuador, and the Terrestrial Invertebrates Collection of the Charles Darwin Research Station, Galapagos, Ecuador (ICCDRS). The specimens were obtained through a standardized survey carried out in the Galapagos Islands from 2017 to 2021. This consisted in the use of three collection methods with standard effort units: four runs of 50 double sweep nets, five pan traps separated by 5 m and left for 72 hours, and finally three Malaise traps separated by 50 m and left for 8 days. These methodologies were carried out in each of the coastal, dry, transition, and wet vegetation covers per island. Thus, the proportional sampling effort was similar between islands.

Specimen analyses

A general description of the specimens found per species is provided. A total of ten linear measurements were taken (Table 1) from standardized photographs through the software ImageJ version 1.53p (Schneider et al. 2012). These measures were suggested in the literature for the separation of species of the genus (Papp 1999; Papp 2016; Mazhar et al. 2018). Specimens were identified to species using revisionary taxonomic keys provided by Papp (2010, 2016). Habitus images were taken with a digital camera Canon EOS 6D with an MPE-65 mm macro lens, attached to a CASTEL-MICRO Novoflex focusing rack stepping motor-controlled; Stacking was reached using the Helicon Focus software 8.2.2. and then edited using the Adobe Photoshop® CS6 v.13.0.

Table 1. Morphometric characters measured for the species of *Chelonus* of the Galapagos archipelago. In parentheses the abbreviations used for each variable.

Measurements	Authors
Stigma width **(SW)**	Papp 2016
Mesosoma length **(ML)**	Papp 1999
Gena height **(GH)**	Mazhar et al. 2018
Face length **(FL)**	Mazhar et al. 2018
Clypeus length **(CL)**	Papp 2016
Metasoma maximum width in lateral view **(MWL)**	Papp 1999
Penultimate flagellomere length **(PFL)**	Papp 2016
Metasoma maximum width in dorsal view **(MWD)**	Papp 2016; Mazhar et al. 2018
Lateral ocellus diameter **(LOD**)	Mazhar et al. 2018
Anterior ocellus diameter **(AOD)**	Mazhar et al. 2018

Morphological differentiation of species between islands

Populations with more than five individuals from each island were included in statistical analyses. Cluster analysis with Euclidean distances and average clustering was used to visualize whether populations are structured, these groups are supported according to an approximately unbiased *P* value, that represents the support to these groups (Efron et al. 1996; Peña 2002). Cluster analysis was performed using the package PVCLUST of R (Suzuki and Shimodaira 2006). PerMANOVA test was used to know whether there are statistical differences between populations PerMANOVA was performed using the package VEGAN of R (Oksanen et al. 2022). Additionally, we applied the shape PCA and the PCA ratio spectrum analyses developed by Baur and Leuenberger (2011) to identify those ratios that discriminate between groups. The ratios came from the linear measurements.

Morphological differentiation, island age, area, and distance between Islands

To study the relationship between morphological differentiation of the populations and area and age of the islands, we used the Mahalanobis distance between the

centroid of each cloud of individuals from each island and the centroid of all samples (Escobedo and Plata 2008). To study the relationship between morphological differentiation of the populations and the linear distances between islands, we used the Euclidean distance between the centroids of each pair of populations as this measure allows to determine how far two vectors are from each other (Shumskaya 2013). For all cases we used simple regression analyses. The ages of the islands were taken from Geist et al. (2014); the area of the islands and the distances between islands from Snell et al. (1996). Statistical analyses were conducted in the environment R 4.1.2 (R Core Team 2021). This protocol is available at DOI: https://dx.doi.org/10.17504/protocols.io.kxygxynmzl8j/v1.

Results

Species records

A total of seven chelonine species were identified from the Galapagos islands (Fig. 1): *Chelonus buscki* Viereck, 1912, *Chelonus carinatus* Provancher, 1881, *Chelonus johni* Marsh, 1979, *Chelonus refluus* (Papp, 2010), *Chelonus sulcifera* (Papp, 2016), *Chelonus topali* (Papp, 1999), and *Chelonus turgoclarus* (Papp, 2010). No endemic species were identified for the islands as in all cases these species have also been reported from other regions of the Neotropics.

Chelonus turgoclarus was found on almost all the islands, except for the Fernandina, Santa Cruz, and San Cristobal islands. *C. carinatus* was collected from Floreana, Santiago, San Cristobal, Santa Cruz, and Isabela islands. *C. topali* was collected from Floreana, Santiago, Santa Cruz, and Isabela islands. *C. buscki* was found on Floreana, Santiago, Pinta and Fernandina islands. *C. johni* was found in Floreana, Isabela and Santa Cruz. *C. sulcifera* and *C. refluus* were found in Floreana only.

The number of species per island was not related to the size of the islands. On Isabela (4588 km^2) four species were reported, on Fernandina (642 km^2) one species, on Santiago (584 km^2) four species, on San Cristobal (558 km^2) one species, on Floreana (172 km^2) seven species, on Española (60 km^2) one species, and on Pinta (59 km^2) two species.

Key to *Chelonus* species known to occur in the Galapagos Islands

1 Frons laterally with a curved carina between lateral ocellus and compound eye **2**

– Frons laterally lacking a curved carina between ocellus and eye **5**

2(1) Apex of metasomal carapace in dorsal view with a pointed tip; (refluus species-group) **3**

– Apex of metasomal carapace in dorsal view rounded or cup-shaped, not pointed **4**

3 (2) Carapace in lateral view, deeply incurved ventrally; in ventral view, aperture of carapace shorter than carapace itself; apex of female carapace lacking a foramen ***Chelonus* (*Microchelonus*) *refluus* (Papp, 2010)**
– Carapace in lateral view apically truncate; in ventral view aperture of carapace nearly as long as carapace itself; apex of female carapace with a small round foramen ..... ***Chelonus* (*Microchelonus*) *sulcifera* (Papp, 2016)**
4(2) Female carapace in lateral view 2.6–2.8× longer than high posteriorly; pterostigma 2.5–2.7× longer than wide..... ***Chelonus* (*Microchelonus*) *buscki* (Viereck, 1912)**
– Female carapace not so high posteriorly, in lateral view 4.4× longer than high posteriorly, 3.0× longer than wide in males; pterostigma 3.3–4.0× longer than wide; carapace either entirely black, or with small yellow spots, widely separated; male carapace with large wide apical foramen 3.0× wider than high laterally, foramen slightly narrowed medially..... ..... ***Chelonus* (*Microchelonus*) *carinatus* Provancher, 1881**
5(1) Face finely punctured but otherwise polished and shiny; female carapace in dorsal view somewhat globose, 1.6× as long as broad..... ..... ***Chelonus* (*Microchelonus*) *turgoclarus* (Papp, 2010)**
– Face finely rugulose and dull; carapace longer and narrower; male carapace with a large oval apical foramen (as in Marsh 1979, Fig. 9).....**7**
6(5) Carapace in dorsal view 2.0× as long as broad, striated with numerous anastomoses.....***Chelonus* (*Microchelonus*) *johni* Marsh, 1979**
– Carapace in dorsal view 1.7× as long as broad; undulate striated, interstriations rugulose ..... ***Chelonus* (*Microchelonus*) *topali* (Papp, 1999)**

Diversity of *Chelonus* in the Galapagos archipelago

***Chelonus buscki* (Viereck, 1912)**
Fig. 1A

Chelonus (*Chelonella*) *buscki* Viereck, 1912: 618. Type locality: Montserrat, Trinidad.
Microchelonus buscki (Viereck): Shenefelt 1973: 878. Papp 2010: 157, 172. Papp 2016: 236–237.

Description. Female. Body length 2.12–2.80 mm. Head black; Mandibles yellow with basal and apical areas brown. Carinae between ocelli and eyes present. Antenna shorter than the body, penultimate flagellomere cuboidal. Scape yellow, pedicel concolorous with the scape. Flagellomeres brownish. Mesosoma black, scutellum rugose. Foreleg entirely yellow. Medial and hind legs as follows: coxa brown-black, trochanter yellow, femur mostly brown to black with proximal and distal apex turning yellow, medial tibia entirely yellow, hind tibia light-yellow with a brown medial macula. Medial and hind leg with tarsi 1–4 yellow, last tarsomere dark brown. Fore wing stigma brown. Metasoma black or brownish, without yellow maculae. In dorsal view basal part of metasoma without longitudinal carinae. Apical foramen of carapace present.

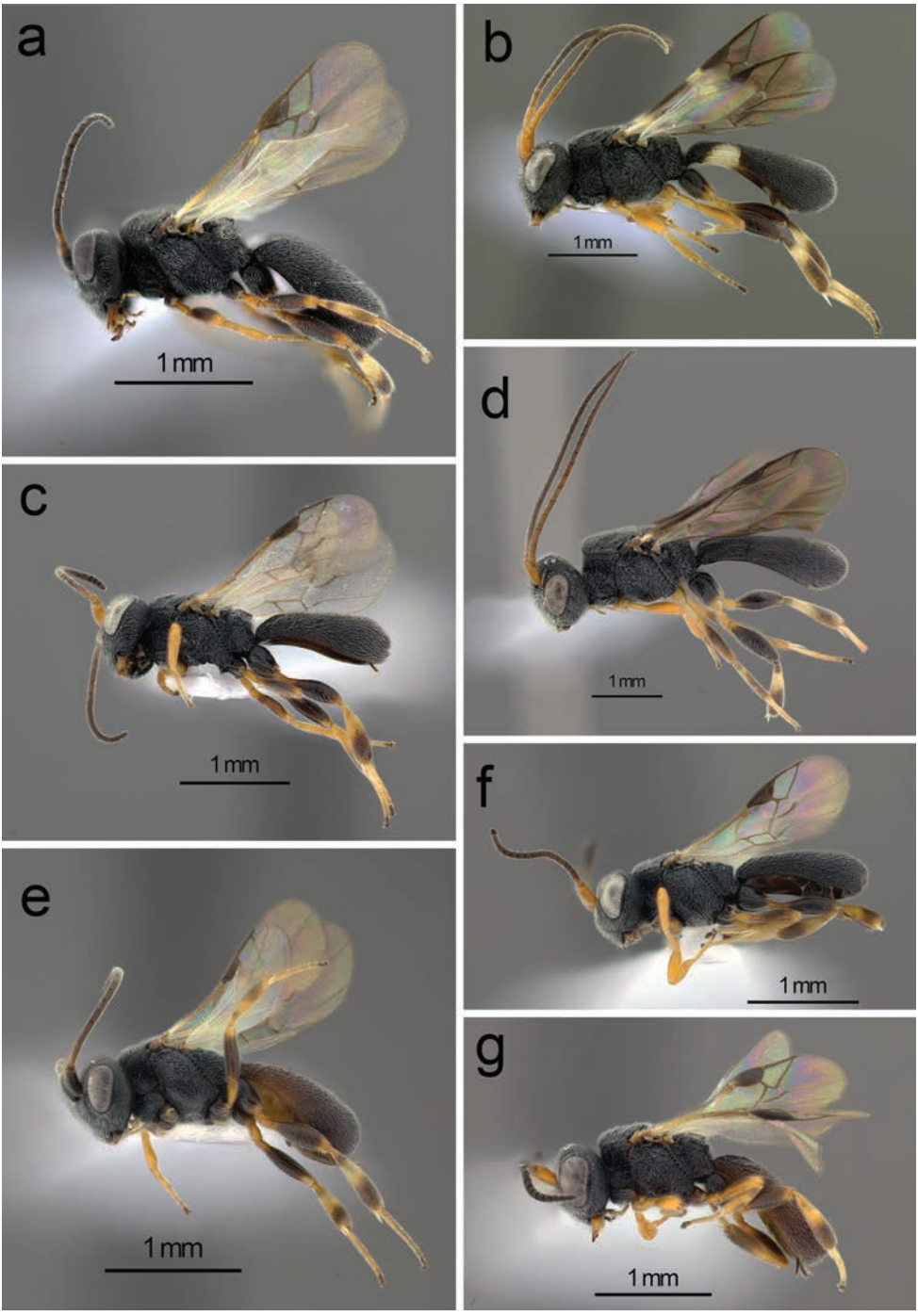

Figure 1. Habitus of the *Chelonus* species found in the Galapagos islands. *Chelonus buscki* **A** *Chelonus carinatus* **B** *Chelonus johni* **C** *Chelonus refluus* **D** *Chelonus sulcifera* **E** *Chelonus topali* **F** *Chelonus turgoclarus* **G**. Scale bars: 1 mm. All are females.

The specimens from Galapagos Archipelago did not show a pair of large yellow spots or a single pale-yellow band on its carapace as indicated in Viereck´s (1912) description. Instead, some specimens have a testaceous or dark brown irregular area as described above.

Comments. *C. buscki* is a very widespread and common neotropical species, having previously been recorded in Costa Rica, Honduras, Panama, Peru, and Trinidad (Papp 2016). This is the first record of the species in the Galapagos.

In Costa Rica, it has been reared from *Omiodes cuniculalis* (Crambidae) feeding on host plants including *Gliricidia sepium*, an introduced species of Fabaceae and other woody host plants (Sharkey et al. 2021). *C. buscki* is a species that is easily identified using Papp's (2016) key and comes out at couplet 42. A full morphological description is on pages 236–237 of Papp's (2016) revision.

Specimens studied. Ecuador, Galápagos – **Floreana** • 7 ♀♀; Cerro Pajas; 1°17'44.592"S, 90°27'29,447"W; 537 m a.s.l; 22–29 May. 2019; J. Avendaño, D. Albuja leg.; Humid zone; malaise trap; ECESPOCH - ICCDRS – **Fernandina** • 2 ♀♀; 0°21'50.076"S, 90°34'22.007"W; 1264 m a.s.l; 04–11 Nov. 2018; H. Herrera, J. Avendaño, P. Picón leg.; Humid zone; malaise trap; ECESPOCH - ICCDRS – **Santiago** • 2 ♀♀; 0°13'3.828"S, 90°43'27.84"W; 334 m a.s.l; 23–26 Jun. 2021;H. Herrera, J. Avendaño, P. Picón leg.; PanTrap; ECESPOCH - ICCDRS – **Pinta** • 5 ♀♀; 0°33'57.744"S, 90°45'14.435"W; 257 m a.s.l; 19–22 Jul. 2021; H. Herrera, J. Avendaño, P. Picón leg.; Humid zone; PanTrap; ECESPOCH - ICCDRS.

Chelonus carinatus Provancher, 1881

Fig. 1B

Chelonus carinatus Provancher, 1881: 199. Type locality: Canada.
Chelonus (*Microchelonus*) *carinatus* (Provancher): McComb 1968: 5, 7, 34.
Microchelonus carinatus (Provancher): Shenefelt 1973: 878. Papp 1999: 189. Papp 2010: 175. Papp 2016: 243.

Description. Female. Body length 3.82–3.88 mm. Head black. Mandibles yellow with basal and apical areas brown. Antenna shorter than the body, penultimate flagellomere longer than wide. Scape yellow to brownish. First half of flagellomeres yellow to brownish. Carinae between ocelli and eyes present. Mesosoma black. Scutellum rugose. Foreleg: Coxa, femur, tibia and basal tarsomere brownish to yellow, trochanter light yellow, last tarsomere brownish to black. Middle leg: Coxa and trochanter brownish yellow, femur and tibia mostly brown to black with proximal and distal apex turning yellow, tarsi 1–4 yellow, last tarsomere black. Hind leg: Coxa black with apex yellow, Trochanter light yellow. Femur brown to black with proximal and distal apex turning yellow, tibia black to brownish with a proximal light-yellow band. Tarsi 1 to 3 mostly yellow, tarsi 4 and 5 brown. Fore wing stigma brown, veins RS, M, RSM and C+SCR light-yellow. Metasoma black with two lateral proximal yellow maculae, apical part also pale colored. Carapace in dorsal view with a pair of basomedially longitudinal carinae. Apical foramen of carapace absent.

Comments. *C. carinatus* has been recorded as occurring widely in Canada, USA (Florida), and Central America (Papp 2016). This is the first record of the species in the Galapagos. *C. carinatus* is distinguished by the carapace being long and narrow (0.4× as wide as long in dorsal view), wings strongly infumated, and mesoscutum with dense confluent punctation. The carapace sculpture dorsally is distinctively longitudinally rugulose. The specimens collected in Galapagos present the apical part of the carapace pale colored while the descriptions provided by McComb (1968) and Papp (2016) indicated this is entirely black.

Specimens studied. Ecuador, Galápagos – **Floreana** • 30 ♀♀; Cerro Pajas; 1°17'38.256"S, 90°27'27.396W; 580 m a.s.l; 22–29 May. 2019; J. Avendaño, D. Albuja leg.; Humid zone; malaise trap; ECESPOCH - ICCDRS – **Isabela** • 1 ♀; 0°50'44.736"S, 91°3'22.355"W; 527 m a.s.l; 05 Jun. 2019; J. Avendaño leg.; Humid zone; swp; ECESPOCH - ICCDRS – **Santiago** • 1 ♀; 0°11'33.396"S, 90°47'43.008"W;42 m a.s.l; 23–26 Jun. 2021; H. Herrera, J. Avendaño, P. Picón leg.; malaise trap; ECESPOCH - ICCDRS – **San Cristobal** • 4 ♀♀; 0°54'55.224"S, 89°26'2.184"W; 149 m a.s.l; 14–17 Jun. 2019; J. Avendaño, D. Albuja leg.; dry zone; PanTrap; ECESPOCH - ICCDRS – **Santa Cruz** • 1 ♀; 0°41'24.9"S, 90°13'18.804"W; 21 m a.s.l; 25 Sep.-02 Oct. 2018; J. Avendaño, Y. Campaña, P. Picón leg.; malaise trap; ECESPOCH - ICCDRS.

Chelonus johni Marsh, 1979

Fig. 1C

Chelonus (*Microchelonus*) *johni* Marsh, 1979: 14. Type locality: Palmira, Colombia.
Microchelonus johni (Marsh): Papp 1999: 185, 191, 194. Papp 2016: 268–270.

Description. Female. Body length 2.10–2.47 mm. Head black. Mandible brownish basally turning yellow distally. Antenna shorter than the body, penultimate flagellomere cuboidal. Scape yellow to brownish, pedicel concolorous with the scape. First two flagellomeres dark yellow, others brownish. Carinae between ocelli absent. Mesosoma black, scutellum rugose. Foreleg yellow with coxa and last tarsomere brownish. Middle leg coxa brownish, trochanter yellow, femur brown to black with proximal and distal apex turning yellow. Tibia and tarsi 1–4 yellow, last tarsomere brown. Hind leg coxa brown, femur and tibia black to brownish with a proximal light-yellow band, tarsi 1–4 yellow, last tarsomere brown. Fore wing stigma brown. Metasoma completely black. Carapace in dorsal view without longitudinal carinae. Opening in ventral part of carapace almost as long as carapace. Apical foramen of carapace present. Marginal cell along wing margin ¾ as long as stigma.

Comments. *Chelonus johni* has previously been recorded as occurring in Colombia, Costa Rica, Mexico, and Honduras (Marsh 1979), where it has been reported as a beneficial species parasitizing the potato tuberworm (*Scrobipalpula* species) and similar pest Gelechiidae. This is the first record of this species occurring in the Galapagos.

Specimens studied. Ecuador, Galápagos – **Floreana** • 3 ♀♀; Cerro Pajas; 1°17'38.292"S, 90°27'27.432"W; 580 m a.s.l; 22–29 May. 2019; J. Avendaño, D. Albuja leg.; humid zone; malaise trap; ECESPOCH - ICCDRS – **Isabela** • 1 ♀; 0°50'19.248"S, 91°4'53.435"W; 762 m a.s.l; 03–10 Jun. 2019; H. Herrera, J. Avendaño, D. Albuja leg.; Humid zone; malaise trap; ECESPOCH - ICCDRS – **Santa Cruz** • 1 ♀; 0°41'25.26"S, 90°13'17.579"W; 20 m a.s.l; 25 Sep.-02 Oct. 2018; J. Avendaño, Y. Campaña, P. Picón leg.; dry zone; malaise trap; ECESPOCH - ICCDRS.

***Chelonus refluus* (Papp, 2010)**
Fig. 1D

Microchelonus refluus Papp, 2010:180. Papp 2016: 296. Type locality: Yoro, Honduras.

Description. Male. Body length 3.82–3.88 mm. Head black. Mandibles yellow with basal and apically area brown. Antenna shorter than the body, penultimate flagellomere longer than wide. Scape yellow to brownish, pedicel concolorous with scape. Flagellomeres 1–3 yellow to brownish, other flagellomeres brownish. Carinae between ocelli and eyes present. Mesosoma black. Scutellum rugose. Foreleg yellow with last tarsomere brown. Middle leg: Coxa and trochanter yellow, femur and tibia brown to black with proximal and distal apex turning yellow, Tarsi 1–4 yellow to brownish, last tarsomere brown. Hind leg: Coxa black with apex yellow, trochanter yellow, femur brown to black with a proximal light-yellow band, tibia black with a light-yellow medial band, Tarsi 1–4 yellow to brownish, last tarsomere brown. Fore wing stigma brown with distal half of submarginal, second submarginal, and marginal cells darker. Metasoma black. Carapace in dorsal view with a pair of basomedially longitudinal carinae. Opening in ventral part of carapace almost as long as carapace. Apical foramen of carapace absent.

The specimens from the Galapagos islands have a completely black carapace differing from the description.

Comments. *C. refluus* has previously been recorded from Honduras (Papp 2016). This is the first record of this species occurring in the Galapagos.

Specimens studied. Ecuador, Galápagos – **Floreana** • 14 ♂♂; Cerro Pajas; 1°17'36.42"S, 90°27'24.767"W; 576 m a.s.l; 22–29 May. 2019; J. Avendaño, D. Albuja leg.; humid zone; malaise trap; ECESPOCH - ICCDRS.

***Chelonus sulcifera* (Papp, 2016)**
Fig. 1E

Microchelonus sulcifera Papp, 2016: 303–305. Type locality: 20 km from Upala, Costa Rica.

Description. Female- Body length 2.00–2.46 mm. Head black. Mandibles yellow with basal and apical areas brown. Antenna shorter than the body, penultimate flagellomere cuboidal. Scape dark yellow. Flagellomeres brownish. Carinae between ocelli and eyes present or

absent. Mesosoma black, scutellum rugose. Foreleg yellow, last tarsomere brown. Middle leg: Coxa brownish, trochanter yellow, both, femur and tibia dark yellow with an extensive medial brown macula, tarsi 1–4 yellow to brownish, last tarsomere brownish. Hind leg: Coxa brown, trochanter dark yellow, femur brown to black with proximal and distal apex yellow, tibia light-yellow with a brown medial macula, tarsi 1–4 yellow to brownish, last tarsomere brownish. Metasoma brownish, without carinae in dorsal basal part. Opening in ventral part of carapace almost as long as carapace. Apical foramen of carapace present.

Comments. *C. sulcifera* was recorded from Costa Rica and Honduras (Papp 2016). This is the first record of the species in the Galapagos.

Specimens studied. Ecuador, Galápagos – **Floreana** • 4 ♀♀; Cerro Pajas; 1°17'36.42"S, 90°27'24.767"W; 576 m a.s.l; 22–29 May. 2019; J. Avendaño, D. Albuja leg.; humid zone; malaise trap; ECESPOCH - ICCDRS.

Chelonus topali (Papp, 1999)

Fig. 1F

Microchelonus topali Papp, 1999: 192. Papp 2016: 305–307. Type locality: Rio Negro, Argentina.

Description. Female. Body length 2.05–2.31 mm. Head black. Mandibles brownish. Antenna shorter than the body, penultimate flagellomere cuboidal. Scape brownish to black. Pedicel concolorous with the scape. Flagellomeres brownish. Carinae between ocelli and eyes absent. Mesosoma black, scutellum punctuate. Leg coloration highly variable, Foreleg: Coxa and trochanter black or brown, femur extensively brown with apex light brown or entirely dark brown. Tibia dark brown, tarsi 1–4 brown last tarsomere black. Middle leg: coxa brownish, femur brown to black, tibia dark yellow with proximal and distal apex turning brown or entirely dark brown, tarsi 1–4 brown last tarsomere black. Hind leg: coxa black, femur brown to black, tibia light-yellow with a brown medial macula, tarsi 1–4 brown or entirely dark brown, last tarsomere brown or entirely dark brown. Fore wing stigma blackish. Metasoma completely black. Opening in ventral part of carapace almost as long as carapace. Carapace in dorsal view without longitudinal carinae. Apical foramen of carapace absent.

Comments. *Chelonus topali* was previously recorded only from Argentina (Papp 1999). This is the first record of this species occurring in the Galapagos.

Specimens studied. Ecuador, Galápagos – **Floreana** • 19 ♀♀; Cerro Pajas; 1°17'38.292"S, 90°27'27.432"W; 580 m a.s.l; 22–29 May. 2019; J. Avendaño, D. Albuja leg.; Humid zone; pantrap; ECESPOCH - ICCDRS – **Isabela** • 3 ♀♀; 0°50'19.248"S, 91°4' 53.435"W; 762 m a.s.l; 03–06 Jun. 2019; J. Avendaño, D. Albuja leg.; Humid zone; pantrap; ECESPOCH - ICCDRS – **Santiago** • 1 ♀; 0°12'1.62"S, 90°42'45.539"W; 98 m a.s.l; 23–26 Jun. 2021; H. Herrera, J. Avendaño, P. Picón leg.;malaise trap; ECESPOCH - ICCDRS – **Santa Cruz** • 1 ♀; 0°41'24.9"S, 90°13'18.804"W; 21 m a.s.l; 25 Sep.-02 Oct. 2018; J. Avendaño, Y. Campaña, P. Picón leg.; malaise trap; ECESPOCH - ICCDRS.

***Chelonus turgoclarus* (Papp, 2010)**
Fig. 1G

Microchelonus turgoclarus Papp, 2010: 186–189. Papp 2016: 309–311. Type locality: Pichin, Rio Pisque, Ecuador.

Description. Female. Body length 2.45–2.60 mm. Head black. Mandibles yellow and apically brown. Antenna shorter than the body, penultimate flagellomere cuboidal. Scape dark yellow. Pedicel and flagellomeres dark yellow to brown apically. Carinae between ocelli and eyes absent. Mesosoma black, scutellum rugose. Foreleg yellow. Last tarsomere brownish. Middle leg coxa brownish, trochanter yellow, femur extensively brown to black with proximal and distal apex turning yellow, tibia dark yellow with proximal and distal apex turning brown. Tarsi 1–4 yellow, last tarsomere 5. Hind leg: Coxa brown to black, trochanter dark yellow, femur mostly brown to black with proximal and distal apex yellow, tibia black with a light-yellow medial band, tarsi 1–4 yellow with the last tarsomere brown. Fore wing stigma brown. Metasoma black or brownish. Opening in ventral part of carapace almost as long as carapace. Carapace in dorsal view without longitudinal carinae. Apical foramen of carapace present.

Comments. *Chelonus turgoclarus* was previously recorded only from continental Ecuador (Papp 2010). This is the first record of this species occurring in the Galapagos.

Specimens studied. Ecuador, Galápagos – **Floreana** • 9 ♀♀; Cerro Pajas; 1°17'38.292"S, 90°27'27.432"W; 580 m a.s.l; 22–29 May. 2019; J. Avendaño, D. Albuja leg.; Humid zone; pantrap; ECESPOCH - ICCDRS – **Isabela** • 2 ♀♀; 0°50'19.248"S, 91°4'53.435"W; 762 m a.s.l; 03–06 Jun. 2019; J. Avendaño, D. Albuja leg.; Humid zone; malaise trap; ECESPOCH - ICCDRS – **Santiago** • 1 ♀; 0°13'43.932"S, 90°44'12.984"W; 543 m a.s.l; 23–26 Jun. 2021; H. Herrera, J. Avendaño, P. Picón leg.; malaise trap; ECESPOCH - ICCDRS – **Pinta** • 1 ♀; 0°34'0.804"N, 90°45'15.947"W; 264 m a.s.l; 19–22 Jun. 2021; H. Herrera, J. Avendaño, P. Picón leg.; malaise trap; ECESPOCH - ICCDRS – **Española** • 1 ♀; 2°0'56.304"S, 98°28'45.084"W; 135 m a.s.l; 03–06 Jul. 2021; J. Avendaño, P. Picón, G. Fiorentino leg.; malaise trap; ECESPOCH - ICCDRS.

Morphological differentiation of populations between islands

Due to sample size, comparisons could only be made for the species *Chelonus buscki* from Floreana and Pinta islands, and for *Chelonus carinatus* from Floreana and San Cristobal islands. For *Chelonus buscki* the PCA showed no evident differentiation by island (Fig. 2A); the cluster analysis formed a single group with a support of 92% that excludes individuals 5, 7, and 9, the first one was collected in Floreana island and the last two from Pinta (Fig. 2B). However, differences for *C. buscki* between the population from Floreana and Pinta islands were identified with the PerMANOVA analysis ($F_{9,1}$ = 83.49, P = 0.002) and these were consistent with the shape PCA (Fig. 3A). The PCA ratio spectrum shows that the two variables that explain most of the variation for

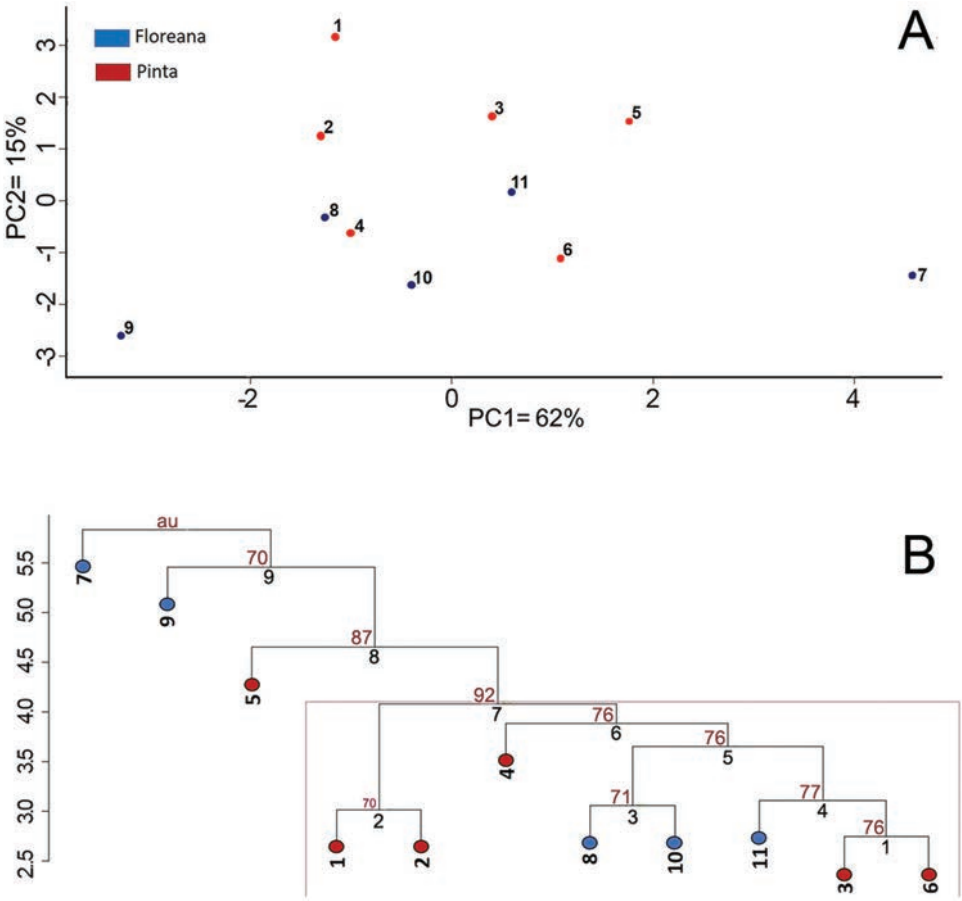

Figure 2. Projection of specimens of *Chelonus buscki* from Floreana and Pinta islands **A** PCA and **B** cluster analysis. Numbers by each circle refer to the individuals. Numbers above a group of individuals show approximate unbiased *P* support. The Frame encloses a group of individuals with 92% support.

the first component are Clypeus Length (CL) and Anterior Ocellus Diameter (AOD); for the second component they are the Penultimate Flagellomere Length (PFL) and the Lateral Ocellus Diameter (LOD) (Fig. 3B).

For *Chelonus carinatus* the PCA showed no evident differentiation by island (Fig. 4A); the cluster analysis yielded individuals 20 and 30 as highly differentiated, and two clusters, the large one contains a single subgroup with 99% support, and the small cluster with 99% support. None of the clusters include individuals of the same islands (Fig. 4B); this differentiation of the two clusters was supported by the PerMANOVA test ($F_{32,1}$ = 47.088, P = 0.001). However, the scatterplot of the shape PCA formed two very clear groups composed of individuals of each island (Fig. 5A). The PCA ratio spectrum shows that the first component is mainly explained by the variables Penultimate Flagellomere Length (PFL) and Clypeus Length (CL) (Fig. 5B, left), while the second

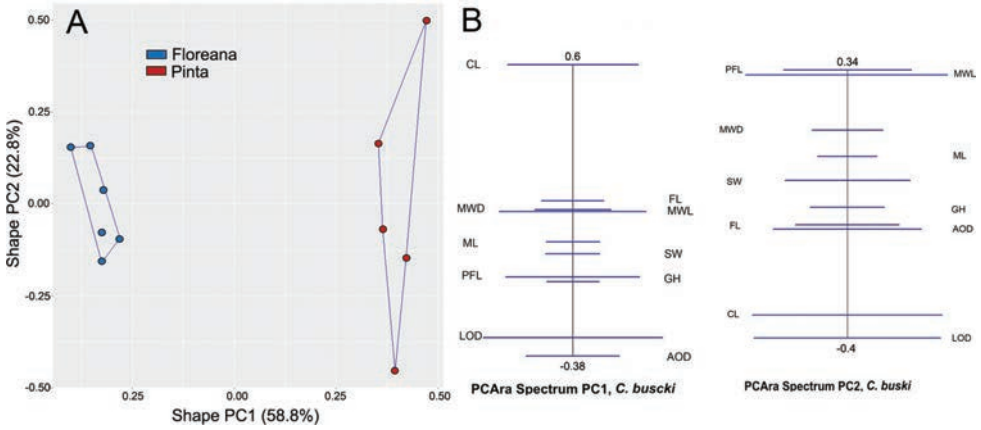

Figure 3. Projection of *Chelonus buscki* from Floreana and Pinta islands based on ratios **A** scatterplot of shape PCA, and **B** PCA ratio spectrum. The first component is displayed on the left, the second component on the right.

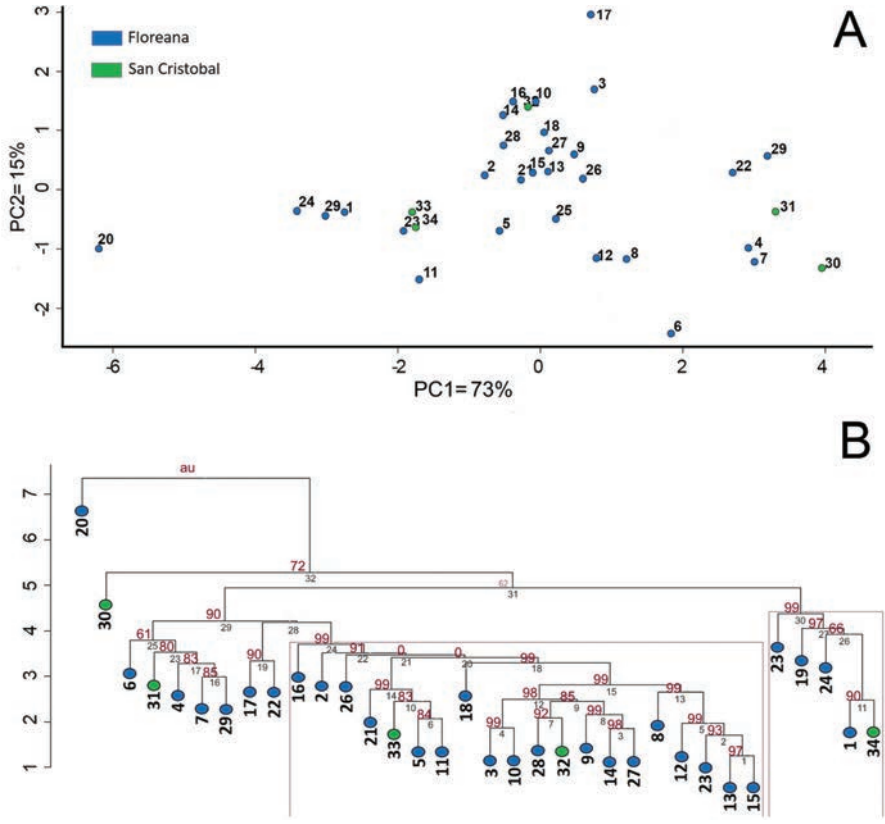

Figure 4. Projection of specimens of *Chelonus carinatus* from Floreana and San Cristobal islands **A** PCA and **B** cluster analysis. Numbers refer to the individuals. Frames enclose groups of individuals with 99% *P* support.

component is due to the combination of Penultimate Flagellomere Length (PFL) and Lateral Ocellus Diameter (LOD) (Fig. 5B, right). These differences between the PCA of the linear measurements and the shape PCA suggest a shape differentiation process.

Linear regression analyses showed a relationship between morphological differentiation and the area of islands for *C. buscki* only (Table 2, Fig. 6); No other variable or species appeared related (Table 2). *C. sulcifera*, *C. refluus*, and *C. johni* were not analyzed since they were present only on one island or were represented by only one or two individuals. For *C. buscki* we found that the larger the islands the smaller the differentiation between wasp populations for this species (Fig. 6).

Discussion

The seven species found in the archipelago are first reports as no previous list of the Hymenoptera of the Galapagos included any reference to the group. *Chelonus* species were found on eight out of ten islands sampled. Larger islands are expected to support higher diversity (Gillespie and Roderick 2002) and this pattern has been reported for

Table 2. Linear regression analyses between morphological differentiation of *Chelonus* species and island traits. Morphological differentiation expressed as Mahalanobis distances. Significant regressions are indicated with an asterisk.

Species	Island age		Island distance		Island area	
	R^2	*p*	R^2	*p*	R^2	*p*
Chelonus buscki	0.36	0.39	0.55	0.08	0.95	0.01*
Chelonus carinatus	0.01	0.84	0.003	0.87	0.33	0.30
Chelonus topali	0.01	0.84	0.57	0.08	0.11	0.66
Chelonus turgoclarus	0.07	0.65	0.11	0.33	0.05	0.76

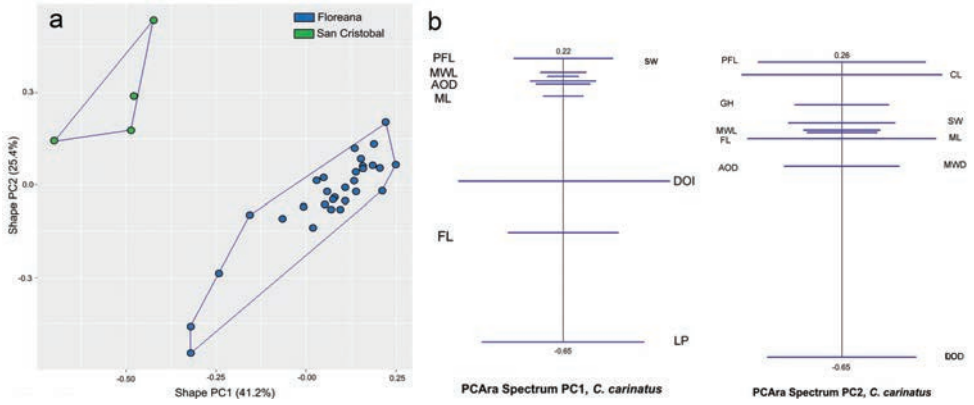

Figure 5. Projection of *Chelonus carinatus* from Floreana and San Cristobal islands based on ratios **A** scatterplot of shape PCA and **B** PCA ratio spectrum. The first component is displayed on the left, the second component on the right.

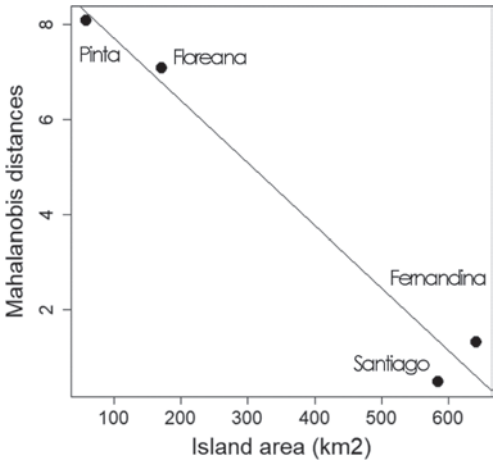

Figure 6. Plot of the relationship between morphologic differentiation of populations of *C. buscki* from each island and island area. This was the only statistically significant regression ($R^2 = 0.95$, $F = 61.78$, $p = 0.01$).

the fauna of the Galapagos archipelago (Tye et al. 2002). However, this seem not the case of the species of *Chelonus*; on Isabela, the largest island, only four species of *Chelonus* were found, while on Floreana, the sixth largest, all seven species are reported. Probably due to the low number of species of the genus in Galapagos, this pattern was not observed, and the pattern is applicable to large number of species.

On the other hand, it is expected that isolation may facilitate modifications in morphology, behavior, and ecology, ranging from population incipient differentiation to a high frequency of endemism in oceanic islands (Roderick and Gillespie 1998), for example in the Galapagos, 47% of insects are endemic (Peck 1997; Peck et al. 1998). In contrast, all the *Chelonus* species are found elsewhere in the Neotropical or Nearctic regions. *C. buscki* is reported from Costa Rica, Honduras, Panama, and Peru. *C. carinatus* from Canada. *C. topali* from Argentina. *C. johni* is found in Colombia, Costa Rica, Honduras, and Mexico. *C. turgoclarus* is reported from continental Ecuador, in the Guayllabamba region, *C. sulcifera* is reported in Costa Rica and Honduras. These species may be part of the numerous entities that recently arrived at Galapagos. As Bulgarella et al. (2022) estimated, more than 500 species of insects have been introduced to the Archipelago.

The distance between islands is proposed as an important factor for differentiation and eventual speciation (Kellie et al. 2019), however, in our study no association was found between this characteristic and the morphological differentiation of the populations; this finding may result from a recent arrival to the archipelago as described above, although multiple studies have found that longer distances not always lead to larger differentiation; such as the case of populations of the lizards *Podarcis bocagei* and *P. hispanica* occurring in the Ria de Arousa archipelago in Spain, where differentiation does not agree with the distance between the islands (Arntezen and Sá-Sousa 2007). In our case, the only significant relationship was negative for *C. buscki* that may be a

consequence of a stronger founder effect of the few wasps in smaller island; further research may clear this preliminary result.

The ages of emergence and colonization time of islands can be related to the differentiation between populations (the progression rule) (Funk and Wagner 1995; Roderick and Gillespie 1998; Juan et al. 2000; Hormiga et al. 2003; Nepokroeff et al. 2003; Holland and Hadfield 2004; Cowie and Holland 2006; Illera et al. 2007). And some groups have shown a general agreement with the progression rule such as the moths of the genus *Galagete* (Schmitz et al. 2007). However, in our case, no association was found between the morphological differentiation of the populations of *Chelonus* species and the ages of the Galapagos islands. An interesting case that could shed light on what happened in *Chelonus* occurs with the subspecies of the bird *Parus caeruleus* from the Canary Islands archipelago; this species initially colonized Tenerife, the fifth oldest island, and later diversified in the archipelago without following a consistent pattern with the ages of the islands (Kvist et al. 2005).

There are other factors of population differentiation that could explain what was observed in *Chelonus* wasps. Selective pressures and local conditions, such as temperature, climate, predators (Chamberland et al. 2020; Mathys and Lockwood 2011), ocean currents and prevailing wind patterns can facilitate the use of islands to promote dispersal (Peake 1981; Ballard and Sytsma 2000; Hoskin 2000; Givnish and Renner 2004; Renner 2004; Cowie and Holland 2006). Several studies (Caccone et al. 2002; Sequeira et al. 2002; Torres-Carvajal et al. 2014) suggest that the colonization of the Galapagos Islands occurred thanks to the Humboldt current, which comes from the South American coast to the archipelago. In the case of the Fortuyniidae mites, they probably arrived due to the Panama Current that transports warm waters from Central America (Lea et al. 2006) and merges with the Peru Current until it reaches the archipelago (Pfingstl and Baumann 2017).

Finally, this work showed that the populations of a few species were morphologically differentiated between islands. Although it would be expected that these differences were associated with age, area, or geographic distance between islands, the results did not show this relationship for most of the species. This result could be a consequence of recent colonization events. As described in detail above, literature shows us that the predictions given by the models are not always fulfilled.

Our assumption about the progression rule has been fulfilled in archipelagos that have undergone geological processes of spatially and temporally ordered appearance of the islands; this is the case of the Hawaiian archipelago (Claridge et al. 2017). By contrast, the Galapagos archipelago has not had this spatial and temporal linearity, its islands have appeared in several island groups with strong variations in geographic distance and direction (Geist et al. 2014). Likewise, it would be unlikely that the progression rule would be fulfilled if the study taxon arrived long after the formation of the islands (Kvist et al. 2005). In our results, the *Chelonus* entities of the Galapagos archipelago are also found in the American continents, so most likely they arrived long after the Galapagos islands were already formed. Our results suggest that the group is recently established in the archipelago and its differentiation processes are very incipient.

Conclusion

This study highlights the need for a more complete exploration of Galapagos fauna. *Chelonus* is a good example as the genus, with its seven new species here reported for the area, was not recorded in previous surveys despite being a common element in survey efforts. The genus appeared as a relatively recent arrival to the archipelago because no endemic species were identified for the islands and morphological differences were not associated with age or geographic distance between islands for any species.

Acknowledgments

Authors thank the following institutions for their support. The Galapagos National Park for their permission to conduct this study granted under codes (DPNG no. 7218, 4219, 4121, PC-65-20 and PC 41-21). We thank Charlotte Causton and Jacqueline Rodriguez, scientists from the Charles Darwin Foundation, who allowed us to use laboratory space, to Patricio Picón Renteria and José Mauricio Avendaño (ESPOCH) for all his support during the field work. We also thank Yessenia Campaña and Fernanda Logroño (ESPOCH) for the project's logistics. This project was supported by Escuela Superior Politécnica de Chimborazo, DDI codes IDIPI-104, IDIPI 334, and the Universidad Nacional de Colombia, Hermes code 55301. Dr. Thomas Defler reviewed the writing. Research support for SRS was provided by McIntire-Stennis Grant Project number WYO-612-20, Studies of Parasitoid Wasps of Forest Ecosystems. This publication is contribution number 2676 of the Charles Darwin Foundation for the Galapagos Islands and number 011 under cooperative agreement ESPOCH-FCD/2017-2022; 2022-2025 and ESPOCH-GNPD/2018-2021. To the referees whom help us to improve the study. This research was supported by Escuela Superior Politécnica de Chimborazo, Ecuador, projects ID: IDIPI-104, 334, and by the Universidad Nacional de Colombia, Hermes code 55301.

References

Arntezen JW, Sá-Sousa P (2007) Morphological and genetical differentiation of lizards (*Podarcis bocagei* and *P. hispanica*) in the Ria de Arosa Archipelago (Galicia, Spain) Resulting from Vicariance and Occasional dispersal. In: Renema W (Ed.) Biogeography, Time and Place: Distributions, Barriers and Islands, Springer, 365–401. https://doi.org/10.1007/978-1-4020-6374-9_12

Aydogdu M, Beyarslan A (2011) Additional notes on *Chelonus* Panzer, 1806 Fauna of Turkey with new records (Hymenoptera, Braconidae, Cheloninae). Journal of the Entomological Research Society 13(2): 75–81. https://www.entomol.org/journal/index.php/JERS/article/view/293/117

Baur H, Leuenberger C (2011) Analysis of ratios in multivariate morphometry. Systematic Biology 60(6): 813-825. https://doi.org/10.1093/sysbio/syr061

Ballard HE, Sytsma KJ (2000) Evolution and biogeography of the woody Hawaiian violets (*Viola*, Violaceae): Artic origins, herbaceous ancestry and bird dispersal. Evolution 54: 1521–1532. https://doi.org/10.1111/j.0014-3820.2000.tb00698.x

Bonacum J, O'Grady PM, Kambysellis M, DeSalle R (2005) Phylogeny and age of diversification of the Planitibia species group of the Hawaiian *Drosophila*. Molecular Phylogenetics and Evolution 37: 73–82. https://doi.org/10.1016/j.ympev.2005.03.008

Buchholz S, Baert L, Rodriguez J, Causton CE, Jager H (2020) Conservation Spiders in Galápagos- diversity, biogeography, and origin. Biological Journal of the Linnean Society 20: 1–8. https://doi.org/10.1093/biolinnean/blaa019

Bulgarella M, Mieles AE, Rodríguez J, Campaña Y, Richardson GM, Keyzers RA, Causton CE, Lester PJ (2022) Integrating biochemical and behavioral approaches to develop a bait to manage the invasive yellow paper wasp *Polistes versicolor* (Hymenoptera, Vespidae) in the Galápagos Islands, Neotropical Biodiversity 8: 271–280. https://doi.org/10.1080/23766808.2022.2098575

Bungartz F, Ziemmeck F, Tirado N, Jaramillo P, Herrera H, Jiménez-Uzcátegui G (2012) The neglected majority: Biodiversity inventories as an integral part of conservation biology. In: Wolff M, Gardener M (Eds) The role of science for conservation, Routledge (London): 119–142.

Caccone A, Gentile G, Gibbs JP, Fritts TH, Snell HL, Betts J, Powell JR (2002) Phylogeography and history of Giant Galápagos Tortoises. Evolution 56: 2052–2056. https://doi.org/10.1111/j.0014-3820.2002.tb00131.x

Chamberland L, Salgado-Roa FC, Basco A, Crastz-Flores A, Binford, GJ, Agnarsson I (2020) Phylogeography of the widespread Caribbean spiny orb weaver *Gasteracantha cancriformis*. PeerJ: e7986. https://doi.org/10.7717/peerj.8976

Chen J, Ji Q (2002) Systematic studies on Cheloninae of China (Hymenoptera, Braconidae, Cheloninae). Fujian Science and Technology Publishing House, 328 pp.

Claridge EM, Gillespie RG, Brewer MS, Roderick GK (2017) Stepping-stones across space and time: repeated radiation of Pacific flightless broad-nosed weevils (Coleoptera: Curculionidae: Entiminae: *Rhyncogonus*). Journal of Biogeography 44(4): 787–796. https://doi.org/10.1111/jbi.12901

Cowie RH, Holland BS (2006) Dispersal is fundamental to biogeography and the evolution of biodiversity on oceanic islands. Journal of Biogeography 33: 193–198. https://doi.org/10.1111/j.1365-2699.2005.01383.x

Dadelahi S, Shaw SR, Aguirre H, de Almeida LF (2018) A taxonomic study of Costa Rican *Leptodrepana* with descriptions of twenty-four new species (Hymenoptera: Braconidae: Cheloninae). Zookeys 750: 59–130. https://doi.org/10.3897/zookeys.750.23536

Dangles O (2009) Los Insectos de Galápagos. Revista Ecuatoriana de Medicina y Ciencias Biológicas 30: 110–111. https://doi.org/10.26807/remcb.v30i1-2.63

Dong Long K, Van Dzuong N, Thi Hoa D (2019) New record of rare genera of the Subfamily Cheloninae (Hymenoptera: Braconidae), with description of two new species from Vietnam. Academia Journal of Biology 41(3): 1–9. https://doi.org/10.15625/0866-7160/v41n3.13884

Dudaniec RY, Schlotfeldt BE, Bertozzi T, Donnellan SC, Kleindorfer S (2011) Genetic and morphological divergence in island and mainland birds: Informing conservation priorities. Biological Conservation 144(12): 2902–2912. https://doi.org/10.1016/j.biocon.2011.08.007

Efron BE, Halloran, S Holmes (1996) Bootstrap confidence levels for phylogenetic trees. Proceedings of the National Academy of Sciences, USA 93: 13429–13434. https://doi.org/10.1073/pnas.93.23.13429

Emerson BC (2008) A century of evolution: Ernst Mayr (1904–2005). Biological Journal of the Linnean Society 95: 47–52. https://doi.org/10.1111/j.1095-8312.2008.01119.x

Escobedo M, Plata A (2008) Mahalanobis y las aplicaciones de su distancia estadística. Cultura Científica y Tecnológica 27: 13–20.

Funk VA, Wagner WL (1995) Biogeographic patterns in the Hawaiian Islands. In: Wagner WL, Funk VA. (Eds). Hawaiian biogeography: Evolution on a hot spot archipelago Smithsonian Institution Press (Washington), 379–419. https://doi.org/10.5962/bhl.title.129909

Geist DJ, Snell H, Snell H, Goddard C, Kurz MD (2014) A Paleogeographic Model of the Galápagos Islands and Biogeographical and Evolutionary Implications. In: Harpp KS, Mittelstaedt E, d'Ozouville N, Graham DW (Eds) The Galápagos: a Natural Laboratory for the Earth Sciences. Wiley (Hoboken), 145–166. https://doi.org/10.1002/9781118852538.ch8

Gillespie RG, Roderick GK (2002) Arthropods on Islands: Colonization, Speciation, and Conservation. Annual Review of Entomology 47: 595–632. https://doi.org/10.1146/annurev.ento.47.091201.145244

Ghahari H, Neveen S, Gadallah, R Kittel N, Shaw SR, Quicke DLJ (2022) Chapter 10. Cheloninae Foerster, 1863. In: Gadallah S, Ghahari H, Shaw SR (Eds) Braconidae of the Middle East (Hymenoptera): Taxonomy, Distribution, Biology, and Biocontrol Benefits of Parasitoid Wasps. Academic Press Amsterdam, 256–288. https://doi.org/10.1016/B978-0-323-96099-1.00001-7

Givnish TJ, Renner SS (2004) Tropical intercontinental disjunctions: Gondwana breakup, immigration from the boreotropics, and transoceanic dispersal. International Journal of Plant Science 165: S1-S6. https://doi.org/10.1086/424022

Grant PR, Grant BR, Petren K (2000) The allopatric phase of speciation: the sharp beaked ground finch (*Geospiza difficilis*) on the Galápagos islands. Biological Journal of the Linnean Society 69: 287–317. https://doi.org/10.1006/bijl.1999.0382

Haines WP, Schmitz P, Rubinoff D (2014) Ancient diversification of *Hyposmocoma* moths in Hawaii. Nature Communications 5(3502): 1–7. https://doi.org/10.1038/ncomms4502

Hennig W (1966) Phylogenetic Systematics. University of Illinois Press (Urbana), 1–280.

Holland BS, Hadfield MG (2004) Origin and diversification of the endemic Hawaiian tree snails (Achatinellinae: Achatinellidae) based on molecular evidence. Molecular Phylogenetics and Evolution 32: 588–600. https://doi.org/10.1016/j.ympev.2004.01.003

Hormiga G, Arnedo M, Gillespie RG (2003) Speciation on a conveyor belt. Sequential Colonization of the Hawaiian Islands by *Orsonwelles* spiders (Araneae, Linyphiidae). Systematic Biology 52: 70–88. https://doi.org/10.1080/10635150390132786

Hoskin MG (2000) Effects of the East Australian Current on the genetic structure of a direct developing muricid snail (*Bedeva hanleyi*, Angas): Variability within and among local populations. Biological Journal of the Linnean Society 69: 245–262. https://doi.org/10.1111/j.1095-8312.2000.tb01201.x

Illera JC, Brent C, Emerson C, Richardson DS (2007) Population history of Berthelot's pipit: Colonization, gene flow and morphological divergence in Macaronesia. Molecular Ecology 16: 4599–4612. https://doi.org/10.1111/j.1365-294X.2007.03543.x

Juan C, Emerson BC, Oromi P, Hewitt GM (2000) Colonization and diversification: towards a phylogeographic synthesis for the Canary Islands. Trends in Ecology and Evolution 15: 104–109. https://doi.org/10.1016/S0169-5347(99)01776-0

Kellie D, Page K, Quiroga D, Salazar R (2019) The origins and Ecology of the Galapagos Islands. In: Kellie D, Page K, Quiroga D, Salazar R (Eds) In the Footsteps of Darwin: Geoheritage, Ecotourism and Conservation in the Galapagos Islands. Geoheritage, Geoparks and Geotourism (Conservation and Management Series), 67–93. https://doi.org/10.1007/978-3-030-05915-6_3

Kvist L, Broggi J, Illera JC, Koivula K (2005) Colonization and diversification of the blue tits (*Parus caeruleus teneriffae* – group) in the Canary Islands. Molecular Phylogenetics and Evolution 34: 501–511. https://doi.org/10.1016/j.ympev.2004.11.017

Lea DW, Pak DW, Belanger CL, Spero HJ, Hall MA, Shackleton NJ (2006) Paleoclimate history of Galápagos surface waters over the last 135,000 yr. Quaterly Science Review 25: 1152–1167. https://doi.org/10.1016/j.quascirev.2005.11.010

Losos JB, Ricklefs RE (2009) Adaptation and diversification on islands. Nature 457: 830–836. https://doi.org/10.1038/nature07893

Losos JB, Mahler DL (2010) Adaptive radiation: the interaction of ecological opportunity, adaptation, and speciation. In: Bell MA, Futuyma DJ, Eanes WF, Levinton JS (Eds) Evolution after Darwin: the first 150 years. Sinauer (Sunderland), 381–420.

MacArthur RH, Wilson EO (1967) The theory of island biogeography. Princeton University Press (Princeton), 1–224.

Mathys BA, Lockwood JL (2011) Contemporary morphological diversification of passerine birds introduced to the Hawaiian archipelago. Proceedings of the Royal Society Biological Sciences 278: 2392–2400. https://doi.org/10.1098/rspb.2010.2302

Mayr E (1965) Avifauna: turnover on islands. Science 150: 1587–1588. https://doi.org/10.1126/science.150.3703.1587

Marsh PM (1979) Descriptions of new Braconidae (Hymenoptera) parasitic on the potato tuberworm and related Lepidoptera from Central and South America. Journal of the Washington Academy of Sciences 69(1): 12–17.

McComb CW (1968) A revision of the *Chelonus* subgenus *Microchelonus* in North America North of Mexico (Hymenoptera: Braconidae). University of Maryland, Agricultural Experimental Station Bulletin, A-149 (1967): 1–148.

Nascimento AR, Penteado-Dias AM (2011) New species of *Chelonus* (*Microchelonus*) Szépligeti, 1908 (Hymenoptera: Braconidae: Cheloninae) from Brazil. Brazilian Journal of Biology 71: 511–515. https://doi.org/10.1590/s1519-69842011000300022

Nepokroeff M, Sytsma KJ, Wagner WL, Zimmer EA (2003) Reconstructing ancestral patterns of colonization and dispersal in the Hawaiian understory tree genus *Psychotria* (Rubiaceae): a comparison of parsimony and likelihood approaches. Systematic Biology 52: 820–838. https://doi.org/10.1093/sysbio/52.6.820

Oksanen J, Kindt R, O'Hara B (2022) Vegan: Community Ecology Package. R package version 2.6-2. https://doi.org/10.32614/CRAN.package.vegan

Parent CE, Caccone A, Petren K (2008) Colonization and diversification of Galápagos terrestrial fauna: a phylogenetic and biogeographical synthesis. Philosophical Transactions of the Royal Society 363: 3347–3361. https://doi.org/10.1098/rstb.2008.0118

Papp J (1995) Revision of C. Wesmael's *Chelonus* species (Hymenoptera Braconidae Cheloninae). Entomologie 65: 115–134.

Papp J (1999) Five new *Mircochelonus* species from the Neotropical Region (Hymenoptera: Braconidae: Cheloninae). Annales Historico-Naturales Musei Nationales Hungarici 91: 177–197.

Papp J (2010) Ten new *Microchelonus* Szépligeti species from the Neotropical Region (Hymenoptera, Braconidae: Cheloninae). Annales Historico-Naturales Musei Nationales Hungarici 102: 155–191.

Papp J (2016) First survey of the Neotropical species of the *Microchelonus* Szepligeti with descriptions of the twenty-five new species (Hymenoptera: Braconidae: Cheloninae). Acta Zoologica Academia Sciences Hungaricae 62(3): 217–344. https://doi.org/10.17109/AZH.62.3.217.2016

Peake JF (1981) The land snails of islands- a dispersalist's view. In: Forey PL (Ed) The evolving biosphere. British Museum (Natural History) (London), 247–263.

Peck SB (1997) The species-scape of Galapagos organisms. Noticias de Galapagos 58: 18–21.

Peck SB, Heraty J, Landry B, Sinclair BJ (1998) Introduced insect fauna of an oceanic archipelago: The Galapagos islands, Ecuador. American Entomologist 44: 219–237. https://doi.org/10.1093/ae/44.4.218

Peña D (2002) Análisis de datos multivariantes. McGraw-Hill (New York), 1–560.

Poulakakis N, Miller JM, Jensen EL, Beheragaray LB, Rusello MA, Glaberman S, Boore J, Caccone A (2020) Colonization history of Galapagos giant tortoises: Insights from mitogenomes support the progression rule. Journal of Zoological Systematics and Evolutionary Research 58: 1262–1275. https://doi.org/10.1111/jzs.12387

Pfingstl T, Baumann J (2017) Morphological diversification among island populations of intertidal mites (Acari, Oribatida, Fortuyniidae) from the Galápagos archipelago. Experimental and Applied Acarology 72: 114–131. https://doi.org/10.1007/s10493-017-0149-3

R Core Team (2021) R: A Language and Environment for Statistical Computing. R Foundation for Statistical Computing (Vienna). https://www.R-project.org

Ranjith AP, Priyadarsanan DR (2023) New subgeneric reports of the genus *Chelonus* (Hymenoptera: Braconidae) from India and Sri Lanka with description of nine species. Zootaxa 5278(3): 461–492. https://doi.org/10.11646/zootaxa.5278.3.3

Renner S (2004) Plant dispersal across the tropical Atlantic by wind and sea currents. International Journal of Plant Sciences 165: S23-S33. https://doi.org/10.1086/383334

Roque-Albelo L (2008) Evaluating land invertebrate species: prioritizing endangered species. In: Parque Nacional Galápagos, Fundación Charles Darwin, Ingala (Eds) Galápagos Report (2006–2007), 111–117.

Roderick GK, Gillespie RG (1998) Speciation and phylogeography of Hawaiian terrestrial arthropods. Molecular Ecology 7: 519–531. https://doi.org/10.1046/j.1365-294x.1998.00309.x

Rundle HD, Nosil P (2005) Ecological Speciation. Ecology letters 8: 336–352. https://doi.org/10.1111/j.1461-0248.2004.00715.x

Santamarta JC (2016) Tratado de Minería de Recursos Hídricos en Islas Volcánicas Oceánicas. Colegio Oficial de Ingenieros de Minas del Sur de España (Sevilla), 19–44.

Schneider CA, Rasband WS, Eliceiri KW (2012) NIH Image to ImageJ: 25 years of image analysis. Nature Methods 9(7): 671–675. https://doi.org/10.1038/nmeth.2089

Schmitz P, Cibois A, Landry B (2007) Molecular phylogeny and dating of an insular endemic moth radiation inferred from mitochondrial and nuclear genes: The genus *Galagete* (Lepidoptera: Autostichidae) of the Galapagos Islands. Molecular Phylogenetics and Evolution 45(1): 180–192. https://doi.org/10.1016/j.ympev.2007.05.010

Sequeira AS, Lanteri AA, Scataglini MA, Confalonieri VA, Farrel BD (2002) Are flightless *Galapaganus* weevils older than the Galápagos Islands they inhabit? Heredity 85: 20–29. https://doi.org/10.1046/j.1365-2540.2000.00690.x

Sharkey MJ, Janzen DH, Hallwachs W, Chapman EG, Smith AS, Dapkey T, Brown A, Ratnasingham S, Naik S, Manjunath R, Perez K, Milton M, Hebert P, Shaw SR, Kittel RN, Solis MA, Metz MA, Goldstein PZ, Brown JW, Quicke DLJ, Achterberg C van, Brown BV, Burns JM (2021) Minimalist revision and description of 403 new species in 11 subfamilies of Costa Rican braconid parasitoid wasps, including host records for 219 species. ZooKeys 1013: 1–665. https://doi.org/10.3897/zookeys.1013.55600

Shaw SR (1983) A taxonomic study of nearctic Ascogaster and a description of a new genus *Leptodrepana* (Hymenoptera: Braconidae). Entomography 2: 1–54.

Shaw SR (1991) An unusual manner of aggregation in the braconid *Chelonus* (*Microchelonus*) *hadrogaster* McComb (Hymenoptera). Journal of Insect Behavior 4: 537–542. https://doi.org/10.1007/BF01049337

Shaw SR (1997) Subfamily Cheloninae. In: Wharton RA, Marsh PM, Sharkey MJ (Eds) Identification Manual of the New World Genera of the Family Braconidae (Hymenoptera), International Society of Hymenopterists Special Publication (Washington), 197–205.

Shaw SR (2006) Chapter 12.2, Familia Braconidae. In: Hanson P, Gauld ID (Eds) Hymenoptera de la Región Neotropical, Memoirs of the American Entomological Institute 77 (Gainesville), 487–585.

Shaw MR, Huddleston T (1991) Classification and biology of braconid wasps (Hymenoptera: Braconidae). Handbooks for the Identification of British Insects 7(11): 1–126.

Shenefelt RD (1973) Braconidae 6.Cheloninae. In:Vecht JV, Shenefelt RD (Eds) Hymenopterorum Catalogus (nova editio) Pars 10: 813–936.

Shumskaya AO (2013) Comparing of Euclidean and Mahalanobis metrics while solving the problem of the text origin identification. American Journal of Control Systems and Information Technology 2: 27–32.

Snell HM, Stone PA, Snell HL (1996) A summary of geographical characteristics of the Galápagos Islands. Journa of Biogeography 23: 619–624. https://doi.org/10.1111/j.1365-2699.1996.tb00022.x

Suzuki R, Shimodaira H (2006) Pvclust: a R package for assessing the uncertainty in hierarchical clustering. Bioinformatics Applications Note 22(12): 1540–1542. https://doi.org/10.1093/bioinformatics/btl117

Torres-Carvajal O, Bornes CW, Pozo-Andrade MJ, Tapia W, Nicholls G (2014) Older than the islands: Origin and diversification of Galápagos leaf-toed geckos (Phyllodactylidae: *Phyllodactylus*) by multiple colonizations. Journal of Biogeography 41: 1883–1894. https://doi.org/10.1111/jbi.12375

Tye A, Snell HL, Peck SB, Adsersen H (2002) Outstanding terrestrial features of the Galapagos archipelago. In: Bensted-Smith R (Ed.) A Biodiversity vision for the Galapagos Islands. Charles Darwin Foundation and World Wildlife Fund (Puerto Ayora), 12–23.

Tobias VI (1995) New subgenus and species of the genus Microchelonus (Hymenoptera, Braconidae) with some comments on synonymy. Entomological Review 75: 158–170. https://doi.org/10.2478/s11756-008-0001-7

Tobias VI (2001) Species of the genus *Microchelonus* Szépl. (Hymenoptera, Braconidae) with yellow abdominal spots and pale coloration of the body from the western Palaearctic region. Entomologicheskoye Obozreniye 80: 137–179.

Tobias VI (2008) Palaearctic species of *Microchelonus retusus* group (Hymenoptera, Braconidae, Cheloninae). Entomological Review 88(9): 1171–1191. https://doi.org/10.1134/S0013873808090157

Tobias VI (2010) Palaearctic species of the genus Microchelonus Szépligeti (Hymenoptera: Braconidae, Cheloninae): key to species. Proceedings of the Russian Entomological Society 81: 1–354. https://doi.org/10.1134/S0013873808090157

Toral-Granda MV, Causton CE, Jaeger H, Trueman M, Izurieta JC, Araujo E, Cruz M, Zander KK, Izurieta A, Garnett ST (2017) Alien species pathways to the Galapagos Islands, Ecuador. PLoS ONE 12(9): e0184379. https://doi.org/10.1371/journal.pone.0184379

Yamaguchi R, Iwasa Y (2013) First passage time to allopatric speciation. Interface Focus 3: 320130026. https://doi.org/10.1098/rsfs.2013.0026

Yu DS, Van Achterberg C, Horstmann K (2005) World Ichneumonoidea 2004. Taxonomy, biology, morphology, and distribution. CD/DVD. Taxapad, Vancouver, Canada.

Supplementary material 1

Dataset *Chelonus* Galapagos

Authors: Ada L. Sandoval-B, Scott Richard Shaw, Carlos E. Sarmiento

Data type: xlsx

Explanation note: The dataset contains a total of ten linear measurements of 114 individuals of the seven species of *Chelonus* reported for the Galapagos.

Link: https://doi.org/10.3897/jhr.97.130713.suppl1

JHR 97: 849–880 (2024)
doi: 10.3897/jhr.97.135381
https://jhr.pensoft.net

RESEARCH ARTICLE

JOURNAL OF Hymenoptera RESEARCH
A peer-reviewed open-access journal
The International Society of Hymenopterists

The genus *Lasioglossum* Curtis, 1833 (Hymenoptera, Halictidae) in Azerbaijan

Yulia V. Astafurova[1], Mahir M. Maharramov[2], Maxim Yu. Proshchalykin[3]

1 *Zoological Institute, Russian Academy of Sciences, Saint Petersburg 199034, Russia* **2** *Nakhchivan State University, Nakhchivan, AZ 7012, Azerbaijan* **3** *Federal Scientific Center of the East Asia Terrestrial Biodiversity, Far East Branch of the Russian Academy of Sciences, Vladivostok 690022, Russia*

Corresponding author: Maxim Yu. Proshchalykin (proshchalikin@biosoil.ru)

Academic editor: Jack Neff | Received 23 August 2024 | Accepted 29 September 2024 | Published 10 October 2024

https://zoobank.org/A2CAD339-15E2-4131-9F41-65FFC4246C97

Citation: Astafurova YuV, Maharramov MM, Proshchalykin MYu (2024) The genus *Lasioglossum* Curtis, 1833 (Hymenoptera, Halictidae) in Azerbaijan. Journal of Hymenoptera Research 97: 849–880. https://doi.org/10.3897/jhr.97.135381

Abstract

Available information about bees of the genus *Lasioglossum* in Azerbaijan is summarised. One hundred and one species are currently known from this country. Twenty-three species are newly recorded from the Caucasus region and additional eighteen species are newly recorded from Azerbaijan. Three species are excluded from the list of Azerbaijani fauna. A new synonymy is proposed for *Lasioglossum euxinicum* Ebmer, 1972 = *L. alievi* Pesenko, 1986, **syn. nov.**, and a lectotype is designated for *Halictus schelkovnikovi* Kokujev, 1913.

Keywords

Anthophila, Apiformes, fauna, new records, new synonym, the Caucasus region

Introduction

The global genus *Lasioglossum* Curtis, 1833 currently includes 1,841 described species (Ascher and Pickering 2024), with the highest known diversity in the Holarctic region (Michener 2007). A total of 450 species are known from the Palaearctic region (Astafurova and Proshchalykin 2017), of which 182 species occur in Europe (Astafurova and Proshchalykin 2023, 2024; Ghisbain et al. 2023), 168 species from Turkey, and 145 species from Iran (Ascher and Pickering 2024).

The Caucasus region is a mountainous area between the Black Sea and the Caspian Sea, considered part of the natural border between Europe and Asia. Geographically, it is usually considered part of western Asia, bordering north-eastern Turkey and north-western Iran. The northern edge of the Caucasus is known as the Ciscaucasus and the southern part as the Transcaucasus. The Ciscaucasus contains most of the Greater Caucasus mountain range, also known as the Great Caucasus. It includes the southern part of European Russia (Krasnodar Territory, Stavropol Territory, Adygea Republic, Karachayevo-Cherkessk Republic, Ingushetia Republic, Kabardino-Balkarsk Republic, Severnaya Osetia Republic, Chechenskaya Republic, and Dagestan Republic) and northern parts of Georgia and Azerbaijan. The Transcaucasus is bordered by Russia to the north, the Black Sea and Turkey to the west, the Caspian Sea to the east and Iran to the south. It includes the Caucasus Mountains and the surrounding lowlands. All of Armenia, Azerbaijan (except the northern parts) and Georgia (except the northern parts) are part of the South Caucasus (Kuhlmann and Proshchalykin 2016; Lelej et al. 2022).

The present paper is a part of the ongoing research of bees of the territory of Azerbaijan (Aliyev et al. 2017; Proshchalykin et al. 2019; Fateryga et al. 2020; Proshchalykin and Maharramov 2020; Maharramov et al. 2021, 2023). Azerbaijan has long been known to have a potentially rich bee fauna. However, there is no modern comprehensive work that summarises all the information on the *Lasioglossum* mentioned in the literature. The present work has been compiled to provide a revised list of the *Lasioglossum* species found in Azerbaijan, to provide a critical assessment of previous literature records, and to analyse the composition of the *Lasioglossum* fauna of Azerbaijan and its similarity with neighbouring countries.

Halictus alpestris [=*Lasioglossum costulatum*] and *H. truncaticollis* [=*L. truncaticolle*] was the first species of the genus described from Azerbaijan (Morawitz 1877), and ten species and one subspecies have been described since from this area (Blüthgen – five species and one subspecies; Pesenko – two species; Friese – one species; Kokujev – one species; Ebmer – one species), with eight of them still valid (Table 1). Sixty *Lasioglossum* species have been recorded from Azerbaijan so far (see "Published data" section below).

In this paper we enumerate 101 species of the genus *Lasioglossum*, including 23 species newly recorded from the Caucasus region, and additional 18 species are newly recorded from Azerbaijan. Three species are excluded from the Azerbaijani fauna.

Materials and methods

The results presented in this paper are based on 2150 specimens collected in Azerbaijan and currently housed in the Zoological Institute, Russian Academy of Sciences (St. Petersburg, Russia, **ZISP**), Federal Scientific Center of the East Asia Terrestrial Biodiversity, Far Eastern Branch of Russian Academy of Sciences (Vladivostok, Russia, **FSCV**) and the collection of the Institute of Zoology of the National Academy of Sciences of Azerbaijan (Baku, Azerbaijan, **IZAB**).

Table 1. Taxa of the genus *Lasioglossum* described from Azerbaijan.

Original spelling	Current status	Source
Halictus acephaloides Blüthgen, 1931	valid, as *Lasioglossum acephaloides* (Blüthgen, 1931)	Astafurova and Proshchalykin 2018
Halictus alpestris Morawitz, 1877	junior synonym of *Lasioglossum costulatum* (Kriechbaumer, 1873)	Astafurova and Proshchalykin 2018
Halictus ciscapus Blüthgen, 1931	valid, as *Lasioglossum ciscapum* (Blüthgen, 1931)	Ebmer 2000
Halictus haesitans Blüthgen, 1931	junior synonym of *Lasioglossum korbi* (Blüthgen, 1929)	Astafurova and Proshchalykin 2018
Halictus kussariensis Blüthgen, 1925	valid, as *Lasioglossum kussariense* (Blüthgen, 1925)	Ebmer 1970
Halictus ordubadensis Friese, 1916	valid, as *Lasioglossum ordubadense* (Friese, 1916)	Ebmer 1995
Halictus schelkovnikovi Kokujev, 1912	junior synonym of *Lasioglossum anellum* (Vachal, 1905)	Ebmer 1981
Halictus talyschensis Blüthgen, 1925	valid, as *Lasioglossum talyschense* (Blüthgen, 1925)	Ebmer 1978
Halictus truncaticollis Morawitz, 1877	valid, as *Lasioglossum truncaticolle* (Morawitz, 1877)	Astafurova and Proshchalykin 2018
Halictus zonulus sinister Blüthgen, 1934	junior synonym of *Lasioglossum zonulum* (Smith, 1848)	Ebmer 1970
Lasioglossum alievi Pesenko, 1986	junior synonym of *Lasioglossum euxinicum* Ebmer, 1972	current paper
Lasioglossum euxanthopus Pesenko, 1986	valid	Astafurova and Proshchalykin 2018
Lasioglossum muganicum Ebmer, 1972	valid	Astafurova and Proshchalykin 2024

The subgeneric classification of *Lasioglossum* is based on the conclusions of Gibbs et al. (2013) and follows Zhang et al. (2022), Ghisbain et al. (2023) and Proshchalykin et al. (2023). Taxonomy, including subspecies status, follows Ebmer (1988, 1995), Pesenko et al. (2000), Pesenko (2006) and Pauly (2016). Distribution of *Lasioglossum* species is mainly based on Pauly (2016), Astafurova and Proshchalykin (2017, 2024), and Boustani et al. (2021) for Lebanon, with some additional references noted in the text. Subgenera and species are given in the text in alphabetical order. Labelling data for all specimens examined can be found in Suppl. material 1.

Specimens were studied with an Olympus SZ51 stereomicroscope, and photographs were taken with a combination of stereomicroscope (Olympus SZX10) and digital camera (Olympus OM-D). Final images are stacked composites generated using Helicon Focus v. 7.7.4 Pro. All images were post-processed for contrast and brightness using Adobe Photoshop. New distributional records are noted with an asterisk (*).

Results

Species list

Genus *Lasioglossum* Curtis, 1833

Lasioglossum Curtis, 1833: pl. 448. Type species: *Lasioglossum tricingulum* Curtis, 1833=*Melitta xanthopus* Kirby, 1802, by original designation.

Subgenus *Biennilaeus* Pesenko, 2007

Lasioglossum marginatum (Brullé, 1832)

Published data. Morawitz 1873: 165, as *Halictus riparius* (Azerbaijan); Aliyev et al. 2007: 255 (Azerbaijan).

Material examined. 180 ♀, 1 ♂.

Distribution. Caucasus: Azerbaijan, Armenia, Georgia, Russia. – Southern and locally Central Europe, North Africa, Turkey, Russia (European part), Syria, Jordan, Israel, Lebanon, Iraq, Iran, Afghanistan, Pakistan, Central Asia, Northwestern India, Nepal.

Remarks. One of the most common of *Lasioglossum* species in Azerbaijan.

Subgenus *Dialictus* Robertson, 1902

Lasioglossum aeratum (Kirby, 1802)

Published data. No records in Azerbaijan.

Material examined. 1 ♀, 3 ♂.

Distribution. Caucasus: *Azerbaijan, Russia. – Europe, Turkey, Russia (European part), Syria, Iran, Central Asia.

Lasioglossum araxanum (Blüthgen, 1923)

Published data. Blüthgen 1923: 244 ("Araxestal" [Aras River valley in Azerbaijan, Armenia and Iran]).

Material examined. –

Distribution. Caucasus: unknown country (Azerbaijan or Armenia). – Iran, Turkey, northern India (Blüthgen 1923; Warncke 1975).

Lasioglossum hethiticum Ebmer, 1970

Published data. No records in Azerbaijan.

Material examined. 1 ♂.

Distribution. *Caucasus: Azerbaijan. – Turkey, Greece, Lebanon (Ghisban et al. 2023).

Lasioglossum leucopus (Kirby, 1802)

Published data. No records in Azerbaijan.

Material examined. 16 ♀, 1 ♂.

Distribution. Caucasus: *Azerbaijan, Russia. – Europe, Turkey, Russia (east to Yakutia), Iran.

Lasioglossum morio (Fabricius, 1793)

Published data. Ebmer 1988: 622 (Caucasus).

Material examined. 5 ♀, 11 ♂.

Distribution. Caucasus: Azerbaijan, Armenia, Georgia, Russia. – Europe, Turkey, Russia (east to Altai), Israel, Lebanon [nominative subspecies]; North Africa, Spain [ssp. *cordialie* (Pérez, 1903)].

Lasioglossum podolicum (Noskiewicz, 1925)

Published data. No records in Azerbaijan.

Material examined. 2 ♀, 1 ♂.

Distribution. *Caucasus: Azerbaijan. – Steppe of Europe east to Russia (Lipetsk Prov.), Turkey [nominative subspecies]; Iran [ssp. *canus* (Warncke, 1982)].

Lasioglossum talyschense (Blüthgen, 1925)

Published data. Blüthgen 1925: 130, as *Halictus talyschensis* (Azerbaijan).

Material examined. –

Distribution. Caucasus: Azerbaijan. – Northeastern Turkey, Iran (Ebmer 1978; Warncke 1982).

Subgenus *Hemihalictus* Cockerell, 1897

Lasioglossum adabaschum (Blüthgen, 1931)

Published data. No records in Azerbaijan.

Material examined. 1 ♀.

Distribution. *Caucasus: Azerbaijan. – Russia (Astrakhan Province, Kalmyk Republic), Turkmenistan.

Lasioglossum brevicorne (Schenck, 1869)

Published data. Aliyev et al. 2007: 255 (Azerbaijan).

Material examined. 9 ♀, 2 ♂.

Distribution. Caucasus: Azerbaijan. – Europe, North Africa, Turkey, Israel, Lebanon, Russia (European part), Iran, Afghanistan [nominative subspecies]; Canary Is. [ssp. *gomerense* Ebmer, 1972].

Lasioglossum bluethgeni Ebmer, 1971

Published data. No records in Azerbaijan.

Material examined. 2 ♀.

Distribution. Caucasus: *Azerbaijan, Georgia, Russia. – Southern and locally middle Europe, Ukraine, Lebanon, Turkey (Ebmer 2000).

Lasioglossum ciscapum (Blüthgen, 1931)

Published data. Blüthgen 1931: 213 (Azerbaijan).

Material examined. 4 ♀.

Distribution. Caucasus: Azerbaijan. – Turkey, Russia (Astrakhan Prov., Kalmyk Rep.), southern Kazakhstan, Turkmenistan, Uzbekistan, Kyrgyzstan (Ebmer 2000).

Lasioglossum clypeare (Schenck, 1853)

Published data. Blüthgen 1935: 120 (Azerbaijan).

Material examined. –

Distribution. Caucasus: Azerbaijan, Georgia, Russia. – Southern and locally central Europe, Lebanon, Turkey, Russia (east to south Ural), Iran, Kyrgyzstan, Kazakhstan.

Lasioglossum clypeiferellum (Strand, 1909)

Published data. No records in Azerbaijan.

Material examined. 50 ♀, 3 ♂.

Distribution. *Caucasus: Azerbaijan. – Egypt, Macedonia, Greece, Crete, Lebanon, Israel, Syria (Hermon Mt.), Cyprus, Turkey, Iran, Afghanistan, Uzbekistan, Kyrgyzstan, Tajikistan, Mongolia (Bytinski-Salz and Ebmer 1974; Ebmer 1980, 1982; Warncke 1982; Murao et al. 2017).

Lasioglossum convexiusculum (Schenck, 1853)

Published data. No records in Azerbaijan.

Material examined. 4 ♀, 1 ♂.

Distribution. *Caucasus: Azerbaijan. – Europe (except north), Lebanon, Turkey, Russia (east to the Urals), Iran.

Remarks. The record of the species from Armenia ("Kasikoporan") by Blüthgen (1935: 117) should be considered as a locality in Turkey.

Lasioglossum corvinum (Morawitz, 1877)

Published data. No records in Azerbaijan.

Material examined. 3 ♀.

Distribution. Caucasus: *Azerbaijan, Armenia, Georgia, Russia. – Southern Europe (north to Germany), North Africa, Lebanon, Caucasus, Turkey, Russia (Crimea, south of the European part), Iran (Morawitz 1877; Skhirtladze 1981; Ebmer 1988; Silló 2024).

Lasioglossum crassepunctatum (Blüthgen, 1923)

Published data. Blüthgen 1923: 280, as *Halictus crassepunctatus* (Azerbaijan); Ebmer 2000: 435 (Azerbaijan).

Material examined. 10 ♀, 1 ♂.

Distribution. Caucasus: Azerbaijan, Russia. – Southern and Central Europe, Israel, Lebanon, Jordan, Turkey, Russia (Crimea, central and south of the European part), Iran.

Lasioglossum croceipes (Morawitz, 1876)

Published data. Blüthgen 1923: 246, as *Halictus longiceps* ("Araxestal" [Aras River valley in Azerbaijan, Armenia and Iran]).

Material examined. –

Distribution. Caucasus: unknown country (Azerbaijan or Armenia). – Turkey, Iran, Afghanistan, Kazakhstan, Turkmenistan, Uzbekistan, Tajikistan, Kyrgyzstan (Ebmer 1997; Murao et al. 2017).

Lasioglossum elegans (Lepeletier, 1841)

Published data. Aliyev et al. 2007: 255 (Azerbaijan).

Material examined. 1 ♀.

Distribution. Caucasus: Azerbaijan, Georgia. – Southern and locally Central Europe, North Africa, Turkey, Russia (south of the European part), Iran, Turkmenistan.

Lasioglossum griseolum (Morawitz, 1872)

Published data. No records in Azerbaijan.

Material examined. 12 ♀.

Distribution. Caucasus: Azerbaijan, Georgia, Russia. – Eastern and South Europe, Turkey, Israel, Lebanon, Russia (south of the European part), Iran, Afghanistan, Kazakhstan, Kyrgyzstan, [nominative subspecies]; North Africa, Saudi Arabia [ssp. *musculum* (Blüthgen, 1924)].

***Lasioglossum hilare* Ebmer, 1972**

Published data. Ebmer 2014: 339 (Azerbaijan).

Material examined. 1 ♀.

Distribution. Caucasus: Azerbaijan. – Macedonia, Greece, Jordan, Turkey, Iran, Afghanistan, Kazakhstan, Uzbekistan, Kyrgyzstan (Ebmer 2014).

***Lasioglossum intermedium* (Schenck, 1869)**

Published data. No records in Azerbaijan.

Material examined. 1 ♀.

Distribution. Caucasus: *Azerbaijan, Russia. – Europe, Turkey, Iran.

***Lasioglossum laevidorsum* (Blüthgen, 1923)**

Published data. Blüthgen 1923: 257 ("Araxestal" [Aras River valley in Azerbaijan, Armenia and Iran]); Aliyev et al. 2007: 255 (Azerbaijan).

Material examined. –

Distribution. Caucasus: Azerbaijan, Armenia. – Southern Europe, Lebanon, eastern Turkey, Iran [nominative subspecies]; Middle Europe [ssp. *priesneriellum* (Warncke, 1981)]; Egypt, Iran [ssp. *katharinae* Ebmer, 1974]; Cyprus [ssp. *troodicum* (Blüthgen, 1938)]. The Balkan (Macedonia, Greece) populations are intermediate ones between ssp. *laevidorsum* and ssp. *priesneriellum* (Ebmer 1988).

***Lasioglossum limbellum* (Morawitz, 1876)**

Published data. No records in Azerbaijan.

Material examined. 15 ♀, 15 ♂.

Distribution. Caucasus: *Azerbaijan, Russia. – Southeastern Europe, Israel, Turkey, Russia (south of the European part), Iran, Afghanistan, Kazakhstan, Uzbekistan, Tajikistan, China (Gansu) [nominative subspecies]; North Africa, southwestern Europe [ssp. *ventrale* (Pérez, 1903)].

***Lasioglossum lucidulum* (Schenck, 1861)**

Published data. Aliyev et al. 2007: 255 (Azerbaijan).

Material examined. 14 ♀, 12 ♂.

Distribution. Caucasus: Azerbaijan, Russia. – Europe, Israel, Lebanon, Turkey, Russia (east to western Siberia), Iran, Afghanistan, Pakistan, Central Asia, Mongolia, Northern China.

***Lasioglossum maculipes* (Morawitz, 1876)**

Published data. No records in Azerbaijan.

Material examined. 2 ♀.

Distribution. *Caucasus: Azerbaijan. – Southeastern Turkmenistan, Tajikistan, Uzbekistan, Iran, Afghanistan (Ebmer 1986).

***Lasioglossum medinai* (Vachal, 1895)**

Published data. No records in Azerbaijan.

Material examined. 45 ♀, 1 ♂.

Distribution. *Caucasus: Azerbaijan. – North Africa, Southern Europe, Russia (south of the European part), Israel.

***Lasioglossum mesosclerum* (Pérez, 1903)**

Published data. Blüthgen 1931: 319 (Azerbaijan); Ebmer 2000: 418 (Azerbaijan).

Material examined. 19 ♀, 3 ♂.

Distribution. Caucasus: Azerbaijan, Armenia, Georgia, Russia. – Southern and Central Europe, North Africa, Syria, Jordan, Israel, Lebanon, Turkey, Russia (south of the European part), Iran, Afghanistan, Central Asia.

***Lasioglossum nitidiusculum* (Kirby, 1802)**

Published data. No records in Azerbaijan.

Material examined. 5 ♀, 3 ♂.

Distribution. Caucasus: *Azerbaijan, Russia. – Europe, North Africa, Lebanon, Turkey, Russia (east to the Altai), Kazakhstan, Turkmenistan, Iran [nominative subspecies]; Sardinia [ssp. *pseudocombinatus* (Blüthgen, 1921)] (Ebmer 2011; Murao et al. 2017).

***Lasioglossum parvulum* (Schenck, 1853)**

Published data. No records in Azerbaijan.

Material examined. 1 ♀, 6 ♂

Distribution. Caucasus: *Azerbaijan, Armenia, Russia. – Europe, Turkey, Russia (east to the Urals), Iran.

***Lasioglossum peregrinum* (Blüthgen, 1923)**

Published data. No records in Azerbaijan.

Material examined. 4 ♀.

Distribution. Caucasus: *Azerbaijan, Armenia, Georgia. – Southern Europe, Israel, Turkey, Iran (Ebmer 1997).

***Lasioglossum popovi* (Blüthgen, 1931)**

Published data. No records in Azerbaijan.

Material examined. 3 ♀.

Distribution. *Caucasus: Azerbaijan. – Southern Kazakhstan, Turkmenistan, Uzbekistan (Blüthgen 1931).

***Lasioglossum punctatissimum* (Schenck, 1853)**

Published data. No records in Azerbaijan.

Material examined. 6 ♀, 1 ♂.

Distribution. Caucasus: *Azerbaijan, ?Armenia, ?Georgia. – Europe, Israel, Lebanon, Turkey, Russia (east to the Urals), Iran [nominative subspecies]; North Africa, Iberian Peninsula, Sicily [ssp. *angustifrons* (Vachal, 1892)].

Remarks. This species was recorded without locality for the Caucasus by Bytinski-Salz and Ebmer (1974: 192).

***Lasioglossum puncticolle* (Morawitz, 1872)**

Published data. No records in Azerbaijan.

Material examined. 12 ♀.

Distribution. Caucasus: *Azerbaijan, Georgia, Russia. – Europe, North Africa, Syria, Lebanon, Turkey, Russia (east to the Urals), Iran.

***Lasioglossum pygmaeum* (Vachal, 1905)**

Published data. Blüthgen 1925: 112, as *Halictus denislucus*; Ebmer 2000: 410 (Azerbaijan).

Material examined. 57 ♀, 5 ♂.

Distribution. Caucasus: Azerbaijan, Armenia, Georgia [ssp. *patulum* (Vachal, 1905)]. – North Africa, southern and locally Central Europe [nominative subspecies]; southeastern Europe, Russia (Crimea, south of the European part), Caucasus, Turkey, Syria, Jordan, Lebanon, Iran, Afghanistan, Pakistan, Central Asia [ssp. *patulum* (Vachal, 1905)].

***Lasioglossum quadrinotatulum* (Schenck, 1861)**

Published data. No records in Azerbaijan.

Material examined. 1 ♀.

Distribution.*Caucasus: Azerbaijan. – Europe, Turkey, Russia (east to eastern Siberia), North China.

***Lasioglossum quadrisignatum* (Schenck, 1853)**

Published data. Ebmer 1997: 954 (Azerbaijan).

Material examined. 1 ♀, 1 ♂.

Distribution. Caucasus: Azerbaijan, Armenia, Georgia. – Europe, Turkey, Russia (central and south of the European part), Iran.

***Lasioglossum rufitarse* (Zetterstedt, 1838)**

Published data. Ebmer and Sakagami 1985: 308 (Azerbaijan).

Material examined. 2 ♀, 17 ♂.

Distribution. Caucasus: Azerbaijan, Russia. – Europe, Russia (east to the Far East), Turkey, Iran, Kazakhstan, Mongolia, China (NE, SE), North Korea, Canada, USA (Ebmer 2011).

***Lasioglossum semilucens* (Alfken, 1914)**

Published data. Ebmer 1988: 663 (Azerbaijan).

Material examined. –

Distribution. Caucasus: Azerbaijan, Russia. – Europe, Russia (European part), Turkey, Afghanistan, Tajikistan, Kyrgyzstan, Kazakhstan (Ebmer 2014).

***Lasioglossum stolidum* (Warncke, 1982)**

Published data. No records in Azerbaijan.

Material examined. 2 ♀.

Distribution. *Caucasus: Azerbaijan. – Israel, Turkey (Warncke 1982, 1984).

***Lasioglossum subaenescens* (Pérez, 1895)**

Published data. Ebmer 1997: 933 (Azerbaijan).

Material examined. 8 ♀, 3 ♂.

Distribution. Caucasus: Azerbaijan [ssp. *asiaticum* (Dalla Torre, 1896)]. – Southern Europe [nominative subspecies, the transgression zone is situated in Macedonia, Bulgaria (Ebmer 1988, 1997)]; Greece, Ukraine, Egypt, Turkey, Near East, Iran, Russia (Crimea, south of the European part), Central Asia, Mongolia, China (Xinijang) [ssp. *asiaticum* (Dalla Torre, 1896)].

Lasioglossum tarsatum (Schenck, 1869)

Published data. No records in Azerbaijan.

Material examined. 1 ♀.

Distribution. *Caucasus: Azerbaijan. – Europe, Russia (European part), Afghanistan.

Lasioglossum transitorium (Schenck, 1869)

Published data. No records in Azerbaijan.

Material examined. 2 ♀.

Distribution. *Caucasus: Azerbaijan [ssp. *uncinum* (Vachal, 1905)]. – Balkans and European part of Turkey [nominative subspecies]; Morocco, Algeria, Tunis, Libya, Portugal, Spain, France, Italy, Sicily, Switzerland [ssp. *planulum* (Pérez, 1903), transgression zone in southern Tirol)]; Egypt, Crete, Syria, Jordan, Lebanon, Israel, Cyprus, Turkey [ssp. *uncinum*].

Lasioglossum truncaticolle (Morawitz, 1877)

Published data. Morawitz 1877: 90 (Azerbaijan).

Material examined. 30 ♀.

Distribution. Caucasus: Azerbaijan, Armenia, Georgia. – Southern and locally central Europe, North Africa, Syria, Israel, Lebanon, Caucasus, Turkey, Russia (Crimea, south of the European part), Iran, Kazakhstan.

Lasioglossum villosulum (Kirby, 1802)

Published data. No records in Azerbaijan.

Material examined. 2 ♂.

Distribution. Caucasus: *Azerbaijan, Russia. – Europe, North Africa, Syria, Israel, Lebanon, Turkey, Russia (east to the Far East), Iran, Afghanistan, Tajikistan, Mongolia, China, Korea, Japan, India, Nepal, Malaysia, Canada, USA.

Remarks. The previous record of the species from the Caucasus (Georgia) by Skhirtladze (1981: 42) may refer to *L. medinai*.

Subgenus *Lasioglossum* s. str.

***Lasioglossum acephaloides* (Blüthgen, 1931)**

Published data. Blüthgen 1925: 100, as *Halictus acephalus*; 1931: 346; Aliyev et al. 2007: 254 (Azerbaijan).

Material examined. –

Distribution. Caucasus: Azerbaijan, Armenia, Georgia, Russia. – Turkey (Blüthgen 1925, 1931; Warncke 1975).

Remarks. This species was described by Blüthgen (1931: 346) from Azerbaijan (Helendorf [Goygol]) and Russia (Prikumsk [Stavropol Terr., Budenovsk]), but was overlooked in the catalogue of Russian bees (Astafurova and Proshchalykin 2017; Proshchalykin et al. 2023).

***Lasioglossum argaeum* (Blüthgen, 1931)**

Published data. No records in Azerbaijan.

Material examined. 1 ♀.

Distribution. *Caucasus: Azerbaijan. – Turkey (Blüthgen 1931; Warncke 1984).

***Lasioglossum bicallosum* (Morawitz, 1873)**

Published data. Pesenko 1986: 124 (Caucasus).

Material examined. 1 ♀.

Distribution. Caucasus: Azerbaijan, Armenia, Georgia, Russia. – Southeastern Europe, Israel, Turkey, Russia (Crimea, south of the European part), Iran.

Remarks. This species was recorded without locality for the Caucasus by Pesenko (1986: 124).

***Lasioglossum caspicum* (Morawitz, 1873)**

Published data. Blüthgen 1923: 266; Aliyev et al. 2007: 254 (Azerbaijan); Pesenko 1986: 124 (Caucasus).

Material examined. 17 ♀.

Distribution. Caucasus: Azerbaijan, Armenia, Georgia, Russia. – Israel, Lebanon, Syria, Turkey, Turkmenistan, Iran, Afghanistan.

***Lasioglossum cristula* (Pérez, 1895)**

Published data. Blüthgen 1925: 87, as *Halictus cristula*; 1929: 55, as *H. korbi* (Azerbaijan); Pesenko 1986: 125 (Caucasus).

Material examined. 3 ♀, 2 ♂.

Distribution. Caucasus: Azerbaijan, Armenia, Georgia, Russia. – Syria, Israel, Lebanon, Turkey, Iran [ssp. *donatum* (Warncke, 1975)]; North Africa, southern Europe [nominative subspecies] (Pesenko 1986).

***Lasioglossum costulatum* (Kriechbaumer, 1873)**

Published data. Pesenko 1986: 137 (Caucasus).

Material examined. 2 ♀, 1 ♂.

Distribution. Caucasus: Azerbaijan, Armenia, Georgia, Russia. – Europe, North Africa, Lebanon, Turkey, Syria, Russia (east to Eastern Siberia), Iran, Central Asia.

Remarks. This species was recorded without locality for the Caucasus by Pesenko (1986: 137).

***Lasioglossum fallax* (Morawitz, 1873)**

Published data. Pesenko 1986: 131 (Caucasus).

Material examined. 2 ♀, 4 ♂.

Distribution. Caucasus: Azerbaijan, Armenia, Georgia, Russia. – South Russia (east to the Urals), Turkey, Iran, Turkmenistan [nominative subspecies]; Kazakhstan, Uzbekistan, Tajikistan, Kyrgyzstan, Afghanistan, Mongolia [ssp. *melanarium* (Morawitz, 1876)]; Pakistan [ssp. *rhadiourgon* Ebmer, 1980] (Ebmer 1998).

Remarks. This species was recorded without locality for the Caucasus by Pesenko (1986: 137).

***Lasioglossum equestre* (Morawitz, 1876)**

Published data. No records in Azerbaijan.

Material examined. 1 ♀.

Distribution. *Caucasus: Azerbaijan. – Turkey, Uzbekistan, Tajikistan, Kyrgyzstan, southeastern Kazakhstan (Pesenko 1986).

***Lasioglossum euxanthopus* Pesenko, 1986**

Published data. Pesenko 1986: 127 (Azerbaijan).

Material examined. –

Distribution. Caucasus: Azerbaijan. – Southwestern Turkmenistan (Pesenko 1986).

Lasioglossum euxinicum Ebmer, 1972

Lasioglossum euxinicum Ebmer, 1972: 233, ♀ (holotype: ♀, Sevastopol, Crimea).
Lasioglossum alievi Pesenko, 1986: 128, fig. 14, ♀ (holotype: ♀, Azerbaijan: Istisu; ZISP), examined, syn. nov.

Published data. Ebmer 1978: 38; 1981: 115 (Ordubad, Azerbaijan); Pesenko 1986, as L. alievi; Aliyev et al. 2007: 254 (Azerbaijan).

Material examined. Holotype of *Lasioglossum alievi* Pesenko.

Distribution. Caucasus: Azerbaijan. – Morocco, Italy, Russia (Crimea), Iran (Pesenko 1986).

Taxonomical note. Pesenko (1986: 128) described *Lasioglossum alievi* from Azerbaijan and noted that this species has a black (without metallic lustre) body. However, the holotype of *L. alievi* has a weak metallic lustre on the head and mesoscutum (see figs 59c, d in Astafurova and Proshchalykin 2018: 54). A.W. Ebmer examined the type in 1988 and labelled the specimen as *Lasioglossum euxinicum* ssp. *euxinicum*, but did not publish the synonymy. Although Pesenko (2007) considered this species to be valid, we have supported Ebmer's opinion and *Lasioglossum alievi* Pesenko, 1986 is established here as a junior synonym for *L. euxinicum* Ebmer, 1972.

Lasioglossum korbi (Blüthgen, 1929)

Published data. Blüthgen 1931: 348, as *Halictus haesitans*; Pesenko 1986: 123 (Azerbaijan).

Material examined. 28 ♀, 5 ♂.

Distribution. Caucasus: Azerbaijan, Russia. – Turkey (Pesenko 1986).

Lasioglossum kussariense (Blüthgen, 1925)

Published data. Blüthgen 1925: 96 (Azerbaijan), Pesenko 1986: 122 (Caucasus).

Material examined. 1 ♀.

Distribution. Caucasus: Azerbaijan, Armenia, Georgia, Russia. – Middle and southeastern Europe, Lebanon, Turkey (Blüthgen 1925, 1931; Ebmer 1988).

Lasioglossum laevigatum (Kirby, 1802)

Published data. Pesenko 1986: 139 (Caucasus).

Material examined. 9 ♀, 5 ♂.

Distribution. Caucasus: Azerbaijan, Armenia, Georgia, Russia. – Europe, Turkey, Russia (east to the Urals), Iran.

Remarks. This species was recorded without locality for the Caucasus by Pesenko (1986: 139).

Lasioglossum lativentre (Schenck, 1853)

Published data. Pesenko 1986: 123 (Caucasus).

Material examined. 17 ♀, 2 ♂.

Distribution. Caucasus: Azerbaijan, Armenia, Georgia, Russia. – Europe, Turkey, Russia (Crimea, European part), Near East, Iran.

Remarks. This species was recorded without locality for the Caucasus by Pesenko (1986: 123).

Lasioglossum prunellum (Warncke, 1975)

Published data. Ebmer 1981: 114 (Azerbaijan).

Material examined. –

Distribution. Caucasus: Azerbaijan. – Greece, Turkey (Ebmer 1981).

Lasioglossum quadrinotatum (Kirby, 1802)

Published data. Pesenko 1986: 124 (Caucasus); Aliyev et al. 2007: 254 (Azerbaijan).

Material examined. 5 ♀.

Distribution. Caucasus: Azerbaijan, Armenia, Georgia, Russia. – Europe, Turkey, Russia (east to the Urals), Iran, Kazakhstan.

Lasioglossum sexnotatum (Kirby, 1802)

Published data. Pesenko 1986: 127 (Caucasus); Aliyev et al. 2007: 254 (Azerbaijan); Ebmer 2014: 316 (Azerbaijan).

Material examined. 4 ♀.

Distribution. Caucasus: Azerbaijan, Armenia, Georgia, Russia. – Europe, Crete, Turkey, Russia (Crimea, European part), Turkmenistan, Iran (Pesenko 1986; Ebmer 2014).

Lasioglossum subfasciatum (Imhoff, 1832)

Published data. Pesenko 1986: 127 (Caucasus).

Material examined. 1 ♀.

Distribution. Caucasus: Azerbaijan, Armenia, Georgia. – Middle and southern Europe, Near East, Turkey, Iran (Warncke 1975; Ebmer 1978).

Remarks. This species was recorded without locality for the Caucasus by Pesenko (1986: 127).

Lasioglossum tungusicum Ebmer, 1978

Published data. Ebmer 1982: 209; Pesenko 1986: 129 (Azerbaijan).

Material examined. 1 ♀.

Distribution. Caucasus: Azerbaijan, Armenia. – Russia (east to Amur Prov.), Turkey, Iran, Kazakhstan, Mongolia, China.

Lasioglossum xanthopus (Kirby, 1802)

Published data. Skhirtladze 1981: 43; Aliyev et al. 2007: 254; Pesenko 1986: 126 (Caucasus).

Material examined. 9 ♀.

Distribution. Caucasus: Azerbaijan, Armenia, Georgia, Russia. – Europe, North Africa, Turkey, Israel, Lebanon, Russia (east to the Urals), Iran, Pakistan, Central Asia, Mongolia, Northwestern China.

Subgenus *Leuchalictus* Warncke, 1975

Lasioglossum aegyptiellum (Strand, 1909)

Published data. Pesenko 1986: 140 (Caucasus).

Material examined. 16 ♀, 2 ♂.

Distribution. Caucasus: Azerbaijan, Armenia, Georgia, Russia. – North Africa, Lebanon, Turkey, Russia (Crimea, Kalmyk Rep.), Near East, Iran, Iraq, Turkmenistan.

Remarks. This species was recorded without locality for the Caucasus by Pesenko (1986: 140).

Lasioglossum discus (Smith, 1853)

Published data. Pesenko 1986: 140 (Caucasus).

Material examined. 1 ♀, 5 ♂.

Distribution. Caucasus: Azerbaijan, Armenia, Georgia, Russia. – Europe (except north), North Africa, Turkey, Israel, Lebanon, Russia (east to Eastern Siberia), Iran, Afghanistan, Central Asia, Northwestern China.

Remarks. This species was recorded without locality for the Caucasus by Pesenko (1986: 140).

***Lasioglossum leucozonium* (Schrank, 1781)**

Published data. Pesenko 1986: 143, as *L. tadschicum*; Aliyev et al. 2007: 254 (Azerbaijan); Pesenko 1986: 143 (Caucasus).

Material examined. 21 ♀, 17 ♂.

Distribution. Caucasus: Azerbaijan, Armenia, Georgia, Russia. – Europe, North Africa, Near East, Turkey, Russia (east to the Far East), Iran, Afghanistan, Pakistan, North India, Central Asia, Mongolia, NW China, North America.

***Lasioglossum picipes* (Morawitz, 1876)**

Published data. No records in Azerbaijan.

Material examined. 1 ♂.

Distribution. *Caucasus: Azerbaijan. – Israel, Turkey, Iraq, Iran, Afghanistan Turkmenistan, Uzbekistan, Tajikistan (Pesenko 1986).

***Lasioglossum zonulus* (Smith, 1848)**

Published data. Pesenko 1986: 142 (Caucasus); Aliyev et al. 2007: 254 (Azerbaijan).

Material examined. 10 ♀, 14 ♂.

Distribution. Caucasus: Azerbaijan, Armenia, Georgia, Russia. – Europe, Turkey, Russia (east to Eastern Siberia), Iran, Central Asia, China, North America.

Subgenus *Pygbalictus* Warncke, 1975

***Lasioglossum glabriusculum* (Morawitz, 1872)**

Published data. No records in Azerbaijan.

Material examined. 96 ♀, 32 ♂.

Distribution. Caucasus: *Azerbaijan, Georgia, Russia. – Europe (except north), Syria, Jordan, Israel, Lebanon, Turkey, Russia (south of the European part), Iran [nominative subspecies]; North Africa [ssp. *ultraparvus* (Cockerell, 1938)].

***Lasioglossum mandibulare* (Morawitz, 1866)**

Published data. Aliyev et al. 2007: 256 (Azerbaijan).

Material examined. 2 ♀.

Distribution. Caucasus: Azerbaijan, Armenia, Russia. – Southern Europe, North Africa, Turkey, Israel, Iraq, Russia (south of the European part), Turkmenistan, Kazakhstan, north-western China (Ebmer 1988, 2014; Murao et al. 2017).

***Lasioglossum politum* (Schenck, 1853)**

Published data. No records in Azerbaijan.

Material examined. 101 ♀, 11 ♂.

Distribution. Caucasus: *Azerbaijan, Georgia, Russia. – Europe (except north), Russia (east to the Urals) [nominative subspecies]; North Africa, Near East, Asia Minor, Uzbekistan, Tajikistan, Kyrgyzstan, Iran [ssp. *atomarium* (Morawitz, 1876)]; Eastern China, Japan [ssp. *pekingense* (Blüthgen, 1925)].

Subgenus *Rostrohalictus* Warncke, 1975

***Lasioglossum longirostre* (Morawitz, 1876)**

Published data. Skhirtladze 1981: 34 (Azerbaijan).

Material examined. 16 ♀, 1 ♂.

Distribution. Caucasus: Azerbaijan, Armenia, Georgia. – Greece, Lebanon, Israel, Turkey, Iran, Kazakhstan, Kyrgyzstan, Uzbekistan, Tajikistan, Afghanistan, China (Morawitz 1876; Blüthgen 1931; Warncke 1982; Nu et al. 2020).

Subgenus *Sphecodogastra* Ashmead, 1899

***Lasioglossum albipes* (Fabricius, 1781)**

Published data. Aliyev et al. 2007: 255 (Azerbaijan).

Material examined. 7 ♀, 8 ♂.

Distribution. Caucasus: Azerbaijan, Georgia, Russia. – Europe, North Africa, Turkey, Russia (European part, Urals, Siberia), Iran, Central Asia, Mongolia, North China, Korea, Japan; Russia (Far East) [ssp. *villosum* Ebmer, 1995].

***Lasioglossum anellum* (Vachal, 1905)**
Fig. 1A–D

Published data. Kokujev 1913: 5, as *Halictus schelkovnikovi* (Azerbaijan); Blüthgen 1923: 295; 1931: 322 (Azerbaijan); Ebmer 1995: 602 (Azerbaijan).

Material examined. Lectotype (**designated here**), 1 ♀, *Halictus schelkovnikovi* Kokujev, 1913 // 2623 Арешск.[ий] у.[езд] [Azerbaijan, Areshsky distr.] А.Б. Шелков.[ников] [A.B. Shelkovnikov leg.] // *H. schelkovnikovi* Kok. <red label> //к.[оллекция] Кокуева [collection of Kokujev] // = *anellus* Vach. ♀, Blüthgen det. 1996 // Lectotypus *Halictus schelkovnikovi* Kokujev, 1913 design. Astafurova et Proshchalykin, 2024 <red label> // Zoological Institute St. Petersburg INS_HYM_0002719.

20 ♀, 1 ♂ of *Lasioglossum anellum*.

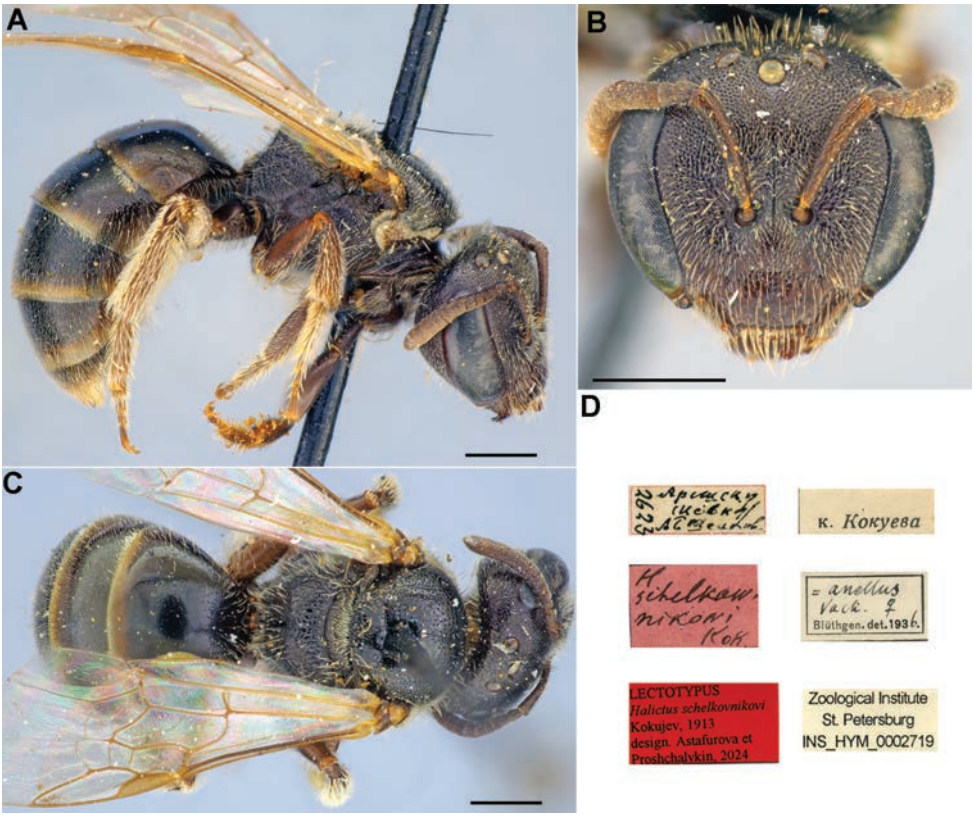

Figure 1. *Halictus schelkovnikovi* Kokujev, 1913, lectotype, female **A, C** habitus, lateral (**A**) and dorsal (**C**) views **B** head, frontal view **D** labels. Scale bar: 1.0 mm.

Distribution. Caucasus: Azerbaijan, Georgia, Russia. – Southeastern Europe, Russia (south of the European part), Turkey, Israel, Lebanon, Syria, Jordan, Iran.

Remarks. *Halictus schelkovnikovi* Kokujev, 1913 was described from Azerbaijan and this name was synonymized with *Lasioglossum anellum* (Vachal, 1905) by Blüthgen (1931: 212). Information on type specimens of *Halictus schelkovnikovi* Kokujev, 1913 was missing from Astafurova and Poshchalykin (2018). This specimen was recently found in the Halictidae collection of the ZISP and is designated here as lectotype (Fig. 1A–D).

Lasioglossum calceatum (Scopoli, 1763)

Published data. Skhirtladze 1981: 29 (Azerbaijan).

Material examined. 21 ♀, 6 ♂.

Distribution. Caucasus: Azerbaijan, Georgia, Russia. – Europe, North Africa, Turkey, Russia (east to Kuril Islands), Iran, Central Asia, Mongolia, North China, Korea, Japan.

***Lasioglossum edessae* Ebmer, 1974**

Published data. No records in Azerbaijan.

Material examined. 24 ♀, 81 ♂.

Distribution. *Caucasus: Azerbaijan. – Turkey, Iran (Ebmer 1995).

***Lasioglossum epipygiale* (Blüthgen, 1924)**

Published data. Blüthgen 1924: 275 ("Araxestal" [Aras River valley in Azerbaijan, Armenia and Iran]).

Material examined. –

Distribution. Caucasus: ?Azerbaijan, Armenia. – Israel, Lebanon, Iran, Turkey, Syria [nominative subspecies]; Southern Iran [?ssp. *bentoni* (Cockerell, 1919)]; Afghanistan, Pakistan [ssp. *quettense* (Blüthgen 1929)]; Pakistan, Northern India, Nepal [ssp. *massuriensis* (Blüthgen 1926)] (Ebmer 1995).

***Lasioglossum euboeense* (Strand, 1909)**

Published data. Blüthgen 1924: 276 (Azerbaijan).

Material examined. 3 ♀, 2 ♂.

Distribution. Caucasus: Azerbaijan, Russia. – Europe (except north), North Africa, Lebanon, Turkey, Russia (south and east of the European part), Iran.

***Lasioglossum fulvicorne* (Kirby, 1802)**

Published data. Aliyev et al. 2007: 255 (Azerbaijan).

Material examined. 17 ♂.

Distribution. Caucasus: Azerbaijan, Armenia, Georgia, Russia. – Europe, Russia (European part), Turkey, Turkmenistan [nominative subspecies]; Armenia, NE Turkey, Iran [ssp. *antelicum* (Warncke, 1975)]; Russia (from Altai to Far East), Mongolia [ssp. *melanocorne* Ebmer, 1988]; Taiwan [ssp. *koshunochare* (Strand, 1914)].

***Lasioglossum fratellum* (Pérez, 1903)**

Published data. No records in Azerbaijan.

Material examined. 22 ♂.

Distribution. Caucasus: *Azerbaijan, Russia. – Europe, Turkey, Russia (east to Eastern Siberia) [nominative subspecies]; Russia (Kamchatka Terr., Yakutia, Primorskii Terr.), North Korea [ssp. *betulae* Ebmer, 1978].

Remarks. Widespread in the Palaearctic region, this species is known only from the Caucasus Mountains, where the southern limit of the species' distribution is probably located.

Lasioglossum hyalinipenne (Morawitz, 1876)

Published data. No records in Azerbaijan.

Material examined. 2 ♀.

Distribution. *Caucasus: Azerbaijan. – Kazakhstan, Kyrgyzstan, Uzbekistan, Tajikistan, Afghanistan, Iran (Morawitz 1876; Blüthgen 1931; Ebmer 1974, 1978; Murao et al. 2017).

Lasioglossum imbecillum Ebmer, 1974

Published data. No records in Azerbaijan.

Material examined. 9 ♀, 11 ♂.

Distribution. *Caucasus: Azerbaijan. – Bulgaria, Macedonia, Greece, Cyprus, Jordan, Turkey, Afghanistan (Ebmer 1995, 2014).

Lasioglossum interruptum (Panzer, 1798)

Published data. No records in Azerbaijan.

Material examined. 13 ♀, 3 ♂.

Distribution. Caucasus: *Azerbaijan [nominative subspecies], Armenia [ssp. *trispinosus* (Alfken, 1907)]. – Europe, North Africa, Lebanon, Russia (Crimea, European part) [nominative subspecies]; Romania, Syria, Turkey, Iran [ssp. *trispinosus*] (Ebmer 1988, 1995).

Lasioglossum laticeps (Schenck, 1869)

Published data. Blüthgen 1924: 280; Warncke 1982: 124, as *L. debilior*; Ebmer 1995: 562, as *L. debilior* (Kussary, Azerbaijan).

Material examined. 9 ♀, 39 ♂.

Distribution. Caucasus: Azerbaijan, Georgia Armenia, [ssp. *debilior* (Pérez, 1910)], Russia. – Europe, Russia (east to Ural) [nominative subspecies]; Crete, Israel, Syria, Lebanon, Greece, Cyprus, Turkey, Iran [ssp. *debilior*, transgression zone is situated in Greece, Turkey, Armenia and Georgia (Ebmer 1995)].

Remarks. According to Ebmer (2014: 323) *Lasioglossum debilior* (Pérez, 1910) is probably a senior synonym of *L. laticeps* ssp. *hellenicus* (Blüthgen, 1938). A. Pauly (2016), who re-examined the type, noted that the type specimens appears to be suitable. We support this opinion and consider *L. debilior* as a synonym of *L. laticeps* ssp. *hellenicus*.

***Lasioglossum laeve* (Kirby, 1802)**

Published data. No records in Azerbaijan.

Material examined. 1 ♀, 5 ♂.

Distribution. Caucasus: *Azerbaijan, Armenia, Georgia. – Europe, Russia (east to Altai), Lebanon, Israel, Syria, Turkey, Iran.

***Lasioglossum lineare* (Schenck, 1869)**

Published data. Blüthgen 1924: 278 (Azerbaijan).

Material examined. 8 ♀.

Distribution. Caucasus: Azerbaijan, Armenia, Georgia. – Europe, Turkey, Syria, Israel, Lebanon, Russia (Crimea, European part), Iran, Turkmenistan.

***Lasioglossum leucopymatum* (Dalla Torre, 1896)**

Published data. No records in Azerbaijan.

Material examined. 11 ♀, 1 ♂.

Distribution. *Caucasus: Azerbaijan. – Afghanistan, Kazakhstan, Turkmenistan, Uzbekistan (Ebmer 1995).

***Lasioglossum malachurum* (Kirby, 1802)**

Published data. Aliyev et al. 2007: 255 (Azerbaijan).

Material examined. 389 ♀, 65 ♂.

Distribution. Caucasus: Azerbaijan, Georgia, Russia. – Europe, North Africa, Turkey, Israel, Lebanon, Russia (Crimea, European part), Iran, Turkmenistan.

Remarks. This is one of the most common *Lasioglossum* species with a long flight period from late March to November.

***Lasioglossum mediterraneum* (Blüthgen, 1926)**

Published data. No records in Azerbaijan.

Material examined. 6 ♀, 3 ♂.

Distribution. *Caucasus: Azerbaijan. – North Africa, southern Europe (Ebmer 1976, 1985).

Remarks. The records from Israel, Turkey and Iran (Bytinski-Salz and Ebmer 1974; Warncke 1975) are based on misidentifications of *Lasioglossum laticeps* ssp. *hellenicum*.

***Lasioglossum muganicum* Ebmer, 1972**

Published data. Ebmer 1972: 239 (Azerbaijan).

Material examined. 39 ♀, 8 ♂.

Distribution. Caucasus: Azerbaijan. – Greece, Turkey, Russia (Astrakhan Prov., Kalmyk Rep.), Iran.

Remarks. The status of the species was restored by Astafurova and Proshchalykin (2024: 238).

***Lasioglossum nigripes* (Lepeletier, 1841)**

Published data. Blüthgen 1924: 275 (Azerbaijan).

Material examined. 11 ♀, 4 ♂.

Distribution. Caucasus: Azerbaijan, Armenia, Georgia, Russia. – Europe, North Africa, Turkey, Jordan, Syria, Lebanon, Israel, Russia (Crimea, south of the European part), Iran, Turkmenistan, Kazakhstan.

***Lasioglossum obscuratum* (Morawitz, 1876)**

Published data. Ebmer 1995: 547; Aliyev et al. 2007: 255 (Azerbaijan).

Material examined. 7 ♀, 16 ♂.

Distribution. Caucasus: Azerbaijan, Russia. –, Turkey, Syria, Jordan Israel, Iran, Afghanistan, Central Asia [nominative subspecies]; Southeastern Europe, Russia (Crimea, south of the European part) [ssp. *acerbus* (Warncke, 1975)].

***Lasioglossum ordubadense* (Friese, 1916)**

Published data. Friese 1916: 33; Aliyev et al. 2007: 255 (Azerbaijan).

Material examined. 6 ♀.

Distribution. Caucasus: Azerbaijan, Armenia. – Israel, Syria, Turkey, Iraq, Iran (Bytinski-Salz and Ebmer 1974; Ebmer 1995).

***Lasioglossum pauxillum* (Schenck, 1853)**

Published data. Ebmer 1995: 582 (Azerbaijan).

Material examined. 79 ♀, 69 ♂.

Distribution. Caucasus: Azerbaijan, Armenia, Georgia, Russia. – Europe, North Africa, Israel, Turkey, Russia (east to Western Siberia), Iran, Turkmenistan.

***Lasioglossum pistorium* (Vachal, 1902)**

Published data. No records in Azerbaijan.
Material examined. 9 ♂.
Distribution. *Caucasus: Azerbaijan. – Southern Turkmenistan, southern Uzbekistan, western Iran, northeastern Afghanistan (Blüthgen 1923; Ebmer 1995).

***Lasioglossum reinigi* Ebmer, 1978**

Published data. No records in Azerbaijan.
Material examined. 1 ♀, 13 ♂.
Distribution. *Caucasus: Azerbaijan. – Iran (Ebmer 1978, 1995).

***Lasioglossum skorikovi* (Blüthgen, 1929)**

Published data. Blüthgen 1931: 354, as *Halictus samarkandinus* (Julfa, Azerbaijan).
Material examined. –
Distribution. Caucasus: Azerbaijan. – Turkey, Iran, Afghanistan, Turkmenistan, Uzbekistan (Blüthgen 1931; Ebmer 1995).

***Lasioglossum setulosum* (Strand, 1909)**

Published data. No records in Azerbaijan.
Material examined. 1 ♀.
Distribution. *Caucasus: Azerbaijan. – Central and Eastern Europe.

***Lasioglossum sociorum* (Blüthgen, 1924)**

Published data. Blüthgen 1924: 263 ("Araxestal" [Aras River valley in Azerbaijan, Armenia and Iran]).
Material examined. 2 ♀, 3 ♂.
Distribution. Caucasus: *Azerbaijan, Armenia. – Cyprus, Turkey, Iran (Ebmer 1995).

Species to be excluded from the Azerbaijani *Lasioglossum* checklist

***Lasioglossum* (*Lasioglossum*) *lebedevi* Ebmer, 1972**

Published data. Aliyev et al. 2007: 254 (Azerbaijan).
Distribution. Southern Kazakhstan.

Remarks. We do not confirm the record of this species from Azerbaijan, the record of this species by Aliyev et al. (2007) is a possible misidentification.

***Lasioglossum* (*Lasioglossum*) *sexmaculatum* (Schenck, 1853)**

Published data. Aliyev et al. 2007: 254 (Azerbaijan).

Distribution. Europe (to Poland and Lithuania), Iran.

Remarks. We not confirm the record of this species from Azerbaijan, the record of this species by Aliyev et al. (2007) is a possible misidentification.

***Lasioglossum* (*Leuchalictus*) *niveocinctum* (Blüthgen, 1923)**

Published data. Aliyev et al. 2007: 255 (Azerbaijan).

Distribution. Russia (North Caucasus, South of the European part), Turkmenistan, Tajikistan, Uzbekistan, Kazakhstan, Mongolia, North China.

Remarks. We not confirm the record of this species from Azerbaijan, the record of this species by Aliyev et al. (2007) is a possible misidentification.

Discussion

In total, 101 *Lasioglossum* species are recorded from Azerbaijan. For comparison, 120 species are known from the whole of the Caucasus (Suppl. material 2). To date, the *Lasioglossum* fauna of Azerbaijan is the most studied in the Caucasus region.

Only 14 species recorded in Azerbaijan are widespread in the whole Palaearctic region: *L. albipes*, *L. calceatum*, *L. fulvicorne*, *L. fratellum*, *L. leucozonium*, *L. leucopus*, *L. lucidulum*, *L. marginatum*, *L. politum*, *L. quadrinotatulum*, *L. rufitarse*, *L. tungusicum*, *L. villosulum*, *L. zonulum.* Twenty-five species are widespread in West Palaearctic: *L. ageratum*, *L. brevicorne*, *L. clypeare*, *L. convexiusculum*, *L. costulatum*, *L. elegans*, *L. euboeense*, *L. fallax*, *L. interruptum*, *L. laeve*, *L. laticeps*, *L. lineare*, *L. malachurum*, *L. morio*, *L. nigripes*, *L. nitidiusculum*, *L. obscuratum*, *L. quadrinotatum*, *L. parvulum*, *L. pauxillum*, *L. punctatissimum*, *L. puncticolle*, *L. semilucens*, *L. sexnotatum*, and *L. xanthopus*. Six species are distributed in Europe to Caucasus: *L. intermedium*, *L. laevigatum*, *L. lativentre*, *L. quadrisignatum*, *L. setulosum*, and *L. tarsatum.* Fourteen species occur from Mediterranean region or South Europe to Central Asia (or some species to Mongolia and North China): *L. aegyptiellum*, *L. caspicum*, *L. clypeiferellum*, *L. discus*, *L. fallax*, *L. hilare*, *L. limbellum*, *L. longirostre*, *L. mandibulare*, *L. mesosclerum*, *L. pygmaeum*, *L. picipes*, *L. subaenescens*, and *L. truncaticolle.*

More than half of the *Lasioglossum* fauna of Azerbaijan is formed by species with smaller areal or endemic distributions. Twenty-four species are distributed from southern Europe to the Caucasus, or from the Mediterranean to the Middle East and

the Caucasus (some species also occur in Iran, Afghanistan and India): *L. anellum*, *L. bicallosum*, *L. bluethgeni*, *L. corvinum*, *L. crassepunctatum*, *L. cristula*, *L. epipygiale*, *L. euxinicum*, *L. glabriusculum*, *L. griseolum*, *L. hethiticum*, *L. imbecillum*, *L. kussariense*, *L. laevidorsum*, *L. medinai*, *L. mediterraneum*, *L. muganicum*, *L. ordubadense*, *L. peregrinum*, *L. podolicum*, *L. prunellum*, *L. stolidum*, *L. subfasciatum*, and *L. transitorium.*

Eleven species have the Caucasus-Central Asian distribution: *L. adabaschum*, *L. ciscapum*, *L. croceipes*, *L. equestre*, *L. euxanthopus*, *L. hyalinipenne*, *L. leucopymatum*, *L. maculipes*, *L. popovi*, *L. pastorium*, *L. skorikovi.*

Eight species are endemic to Turkey and the Caucasus (some species found in Iran or northern India): *L. araxanum*, *L. acephaloides*, *L. argaeum*, *L. edessae*, *L. korbi*, *L. reinigi*, *L. sociorum*, and *L. talyschense.*

Thus, the fauna of Azerbaijan is very diverse and consists of species with wide Palaearctic or Western Palaearctic ranges, as well as elements of Mediterranean, European, Central Asian faunas and a small number of endemics.

Most species are confined to the steppe zone, polyzonal species are common, but forest and desert species are also found. According to the studied material, *Lasioglossum malachurum*, *L. marginatum*, *L. politum*, and *L. glabriusculum* are the most common species of *Lasioglossum* in Azerbaijan.

Acknowledgements

We are grateful to Jack Neff (Austin, USA), Simone Flaminio (Mons, Belgium), Alain Pauly (Brussels, Belgium) and an anonymous reviewer for valuable comments, which helped to improve the quality of this paper.

The research was carried out within the state assignment of Ministry of Science and Higher Education of the Russian Federation (themes No. 122031100272-3 and No. 124012400285-7).

References

Aliyev KhA, Huseinzade GA, Maharramov MM (2007) Towards the knowledge of the bee fauna of the family Halictidae (Hymenoptera: Apoidea) of Nakhichevan Autonomous Republic of Azerbaijan. Caucasian Entomological Bulletin 3(2): 251–256. [in Russian] https://doi.org/10.23885/1814-3326-2007-3-2-251-256

Aliyev KhA, Proshchalykin MYu, Maharramov MM, Huseinzade GA (2017) To the knowledge of the genus *Andrena* Fabricius, 1775 (Hymenoptera: Apoidea: Andrenidae) of Azerbaijan. Caucasian Entomological Bulletin 13(1): 99–109. [in Russian] https://doi.org/10.23885/1814-3326-2017-13-1-99-109

Ascher JS, Pickering J (2024) Discover Life bee species guide and world checklist (Hymenoptera: Apoidea: Anthophila). http://www.discoverlife.org/mp/20q?guide=Apoidea_species [accessed 15 July 2024]

Astafurova YuV, Proshchalykin MYu (2017) Family Halictidae In: Lelej AS, Proshchalykin MYu, Loktionov VM (Eds) Annotated Catalogue of the Hymenoptera of Russia. Volume I. Symphyta and Apocrita: Aculeata. Proceedings of the Zoological Institute RAS, Supplement 6: 277–292.

Astafurova YuV, Proshchalykin MYu (2018) The type specimens of bees (Hymenoptera, Apoidea) deposited in the Zoological Institute of the Russian Academy of Sciences, St. Petersburg. Contribution I. Family Halictidae, genus *Lasioglossum* Curtis, 1833. Zootaxa 4408(1): 1–66. https://doi.org/10.11646/zootaxa.4408.1.1

Astafurova YuV, Proshchalykin MYu (2023) First record of *Lasioglossum adabaschum* (Blüthgen, 1931) (Hymenoptera: Halictidae) from Europe with description of hitherto unknown male. Far Eastern Entomologist 479: 1–6. https://doi.org/10.25221/fee.479.1

Astafurova YuV, Proshchalykin MYu (2024) Review of the bee genus *Lasioglossum* Curtis, 1833 (Hymenoptera: Halictidae) fauna of the European South of Russia. Russian Entomological Journal 33(2): 230–242.

Blüthgen P (1923) Beiträge zur Kenntnis der Bienengattung *Halictus* Latr. Archiv fur Naturgeschichte, Abt. A 1923(89/5): 232–332.

Blüthgen P (1924) Beiträge zur Systematik der Bienengattung *Halictus* Latr. (Hym.) [Anm.: Schluss]. – Konowia 3: 253–284. https://doi.org/10.1002/mmnd.192419240601

Blüthgen P (1925) Beiträge zur Kenntnis der Bienengattung *Halictus* Latr. II. Archiv Naturgeschihte (A), 90(10): 86–136.

Blüthgen P (1929) Neue turkestanische *Halictus*-Arten (Hym., Apidae). Konowia 8(1): 51–86. https://doi.org/10.1002/mmnd.48019290303

Blüthgen P (1931) Beiträge zur Kenntnis der Bienengattung *Halictus* Latr. III. Mitteilungen aus dem Zoologischen Museum in Berlin 17(3): 319–398.

Blüthgen P (1935) Neue paläarktische *Halictus*-Arten (Hym., Apidae). [II]. Deutsche Entomologische Zeitschrift 1935(1/2): 111–120. https://doi.org/10.1002/mmnd.193519350106

Boustani M, Rasmont P, Dathe HH, Ghisbain G, Kasparek M, Michez D, Müller A, Pauly A, Risch S, Straka J, Terzo M, Van Achter X, Wood TJ, Nemer N (2021) The bees of Lebanon (Hymenoptera: Apoidea: Anthophila). Zootaxa 4976(1): 1–146. https://doi.org/10.11646/zootaxa.4976.1.1

Bytinski-Salz H, Ebmer AW (1974) The Halictidae of Israel (Hymenoptera, Apoidea) II. Genus *Lasioglossum*. Israel Journal of Entomology 9: 174–217. https://digitalcommons.usu.edu/bee_lab_du/44

Curtis J (1833) British Entomology: Being illustrations and descriptions of the genera of Insects found in Great Britain and Ireland. Vol. 10. Printed for the author, London, 47 pp. [pp. 434–481]

Ebmer AW (1970) Die Bienen des Genus *Halictus* Latr. s.l. im Großraum von Linz (Hymenoptera, Apidae) Teil 2. Naturkundliches Jahrbuch der Stadt Linz 16: 19–82.

Ebmer AW (1972) Neue westpaläarktische Halictidae (Halictidae, Apoidea). Mitteilungen aus dem Zoologischen Museum in Berlin 48(2): 225–263. https://doi.org/10.1002/mmnz.19720480202

Ebmer AW (1974) Die Halictidae Makedoniens. Acta Musei Macedonici Scientiarum Naturalium 14: 45–66.

Ebmer AW (1976) *Halictus* und *Lasioglossum* aus Marokko. Linzer biologische Beiträge 8(1): 205–266.

Ebmer AW (1978) *Halictus*, *Lasioglossum*, *Rophites* und *Systropha* aus dem Iran (Halictidae, Apoidea) sowie neue Arten aus der Paläarktis. Linzer Biologische Beiträge 10(1): 1–109.

Ebmer AW (1980) Asiatische Halictidae (Apoidea, Hymenoptera). Linzer biologische Beiträge 12(2): 469–506.

Ebmer AW (1981) *Halictus* und *Lasioglossum* aus Kreta (Halictidae, Apoidea). Linzer Biologische Beitrage 13(1): 101–127.

Ebmer AW (1982) Zur Bienenfaund der Mongolei die Arten der Gattungen *Halictus* Latr. und *Lasioglossum* Curt. (Hymenoptera: Halictidae) ergebnisse der mongolisch-deutschen biologischen Expedition set 1962, nr. 108. Mitteilungen aus dem Zoologischen Museum in Berlin 58(2): 199–227. https://doi.org/10.1002/mmnz.4830580202

Ebmer AW (1985) *Halictus* und *Lasioglossum* aus Marokko (Hymenoptera, Apoidea, Halctidae) Erster Nachtrag. Linzer biologische Beiträge 17(2): 271–293.

Ebmer AW (1986) Die Artgruppe des *Lasioglossum strictifrons* (Vachal 1895) mit einer Bestimmungstabelle der Weibchen (Hymenoptera, Apoidea, Halictidae). Linzer biologische Beiträge 18(2): 417–443.

Ebmer AW (1988) Kritische Liste der nicht-parasitischen Halictidae Österreichs mit Berücksichtigung aller mitteleuropäischen Arten (Insecta: Hymenoptera: Apoidea: Halictidae). Linzer biologische Beiträge 20(2): 527–711.

Ebmer AW (1995) Asiatische Halictidae, 3. Die Artengruppe de *Lasioglossum* carinate-*Evylaeus*. Linzer biologische Beiträge 27(2): 525–652.

Ebmer AW (1997) Asiatische Halictidae, 6. *Lasioglossum* carinaless-*Evylaeus*: Erganzungen zu den Artengruppen von *L. nitidiusculum* and *L. punctatissimum* s. l., sowie die Artengruppe des *L. marginellum* (Insecta: Hymenoptera: Apoidea: Halictidae: Halictinae). Linzer biologische Beitrage 29(2): 921–982.

Ebmer AW (1998) Asiatische Halictidae - 7. Neue *Lasioglossum*-Arten mit einer Übersicht der *Lasioglossum* s. str.-Arten der nepalischen und yunnanischen Subregion, sowie des nördlichen Zentral-China (Insecta: Hymenoptera: Apoidea: Halictidae: Halictinae). Linzer biologische Beiträge 30(1): 365–430.

Ebmer AW (2000) Asiatische Halictidae, 9. Die Artengruppe des *Lasioglossum pauperatum* (Insecta: Hymenoptera: Apoidea: Halictidae: Halictinae). Linzer biologische Beitrage 32(2): 399–453.

Ebmer AW (2011) Holarktische Bienenarten – autochthon, eingeführt, eingeschleppt. Linzer biologische Beitrage 43(1): 5–83.

Ebmer AW (2014) Die nicht-parasitischen Halictidae der Insel Zypern im Vergleich zu Kreta mit einer Monographie der *Lasioglossum bimaculatum*-Artengruppe und einer Übersicht der *Halictus nicosiae*-Untergruppe (Insecta: Hymenoptera: Apoidea: Halictidae). Linzer biologische Beiträge 46(1): 291–413.

Ebmer AW, Sakagami SF (1985) Taxonomic notes on the palearctic species of the *Lasioglossum nitidiusculum* group, with description of *Lasioglossum allodalum*, new species (Hymenoptera, Halictidae). Kontyû 53(2): 297–310.

Fateryga AV, Proshchalykin MYu, Maharramov MM (2020) Bees of the tribe Anthidiini (Hymenoptera, Megachilidae) of Nakhchivan Autonomous Republic of Azerbaijan. Entomological Review 100(3): 323–336. https://doi.org/10.1134/S0013873820030069

Friese H (1916) Die Formen des *Halictus quadricinctus* F., sowie einige neue *Halictus*-Arten der paläarktischen Region (Hym.). Deutsche Entomologische Zeitschrift 1916: 25–34. https://doi.org/10.1002/mmnd.48019160105

Ghisbain G, Rosa P, Bogusch P, Flaminio S, Le Divelec R, Dorchin A, Kasparek M, Kuhlmann M, Litman J, Mignot M, Müller A, Praz C, Radchenko VG, Rasmont P, Risch S, Roberts SPM, Smit J, Wood TJ, Michez D, Reverté S (2023) The new annotated checklist of the wild bees of Europe (Hymenoptera: Anthophila). Zootaxa 5327(1): 1–147. https://doi.org/10.11646/zootaxa.5327.1.1

Gibbs J, Packer L, Dumesh S, Danforth BN (2013) Revision and reclassification of *Lasioglossum* (*Evylaeus*), *L.* (*Hemihalictus*) and *L.* (*Sphecodogastra*) in eastern North America (Hymenoptera: Apoidea: Halictidae). Zootaxa 3672(1): 1–117. https://doi.org/10.11646/zootaxa.3672.1.1

Kokujev NR (1913) New species of Hymenoptera from Caucasus, collected by A.B. Schelkovnikov. Izvestiya Kavkazskogo Muzeya (Tiflis) 7: 1–6. [in Russian]

Kuhlmann M, Proshchalykin MYu (2016) The bees of the genus *Colletes* Latreille (Hymenoptera: Colletidae) of the Caucasus region. Zootaxa 4161(3): 367–385. https://doi.org/10.11646/zootaxa.4161.3.5

Lelej AS, Proshchalykin MYu, Maharramov MM (2022) A review of the Mutillidae (Hymenoptera) of Azerbaijan. Zootaxa 5155(1): 61–86. https://doi.org/10.11646/zootaxa.5155.1.3

Maharramov MM, Fateryga AV, Proshchalykin MYu (2021) Megachilid bees (Hymenoptera: Megachilidae) of the Nakhchivan Autonomous Republic of Azerbaijan: tribes Lithurgini, Dioxyini, and Megachilini. Far Eastern Entomologist 428: 12–24. https://doi.org/10.25221/fee.428.3

Maharramov MM, Fateryga AV, Proshchalykin MYu (2023) New records of megachilid bees (Hymenoptera: Megachilidae) from the Nakhchivan Autonomous Republic of Azerbaijan. Far Eastern Entomologist 472: 18–24. https://doi.org/10.25221/fee.472.2

Michener CD (2007) The Bees of the World (2nd edn). Johns Hopkins University Press, Baltimore, 953 pp. [+ 20 pls]

Morawitz F (1873) Die Bienen Daghestans. Horae Societatis Entomologicae Rossicae 10(2/4): 129–189.

Morawitz F (1876) A Travel to Turkestan by the Member-Founder of the Society A. P. Fedtschenko, accomplished from the Imperial Society of Naturalists, Anthropologists, and Ethnographists on a Commission from the General-Governor of Turkestan K. P. von Kaufmann (Issue 9). Vol. II. Zoogeographical Investigations. Pt. V. (Division 7). Bees (Mellifera). Pt. 2 [Andrenidae]. Izvestiya Imperatorskogo Obshchestva Lyubiteley Estestvoznaniya. Anthropologii i Ethnografii 21(3): 161–303. [in Russian]

Morawitz F (1877) Nachtrag zur Bienenfauna Caucasiens. Horae Societatis Entomologicae Rossicae 14(1): 3–112.

Murao R, Tadauchi O, Miyanaga R (2017) The bee family Halictidae (Hymenoptera, Apoidea) from Central Asia collected by the Kyushu and Shimane Universities expeditions. Biodiversity Data Journal 5: 1–43.

Niu Z-Q, Zhang D, Zhu C-D (2020) Extraordinary bees of the genus *Lasioglossum* Curtis, 1833 (Hymenoptera: Apoidea: Halictidae) from China. Zoological Systematics 45(1): 50–58. https://doi.org/10.11865/zs.202005

Pauly A (2016) Le genre *Lasioglossum*, sous-genre *Evylaeus* Robertson, 1902, de la Region Paléarctique. Atlas Hymenoptera. http://www.atlashymenoptera.net/page.aspx??ID=95 [accessed 15 July 2024]

Pesenko YuA (1986) An annotated key to the Palaearctic species of bees of the genus *Lasioglossum* sensu stricto (Hymenoptera, Halictidae) for females, with descriptions of new subgenera and species. Trudy Zoologicheskogo Instituta Akademii Nauk SSSR 159: 113–151. [in Russian]

Pesenko YuA (2006) Contributions to the halictid fauna of the Eastern Palaearctic Region: genus *Lasioglossum* Curtis (Hymenoptera: Halictidae, Halictinae). Zoosystematica Rossica 15(1): 133–166. https://doi.org/10.31610/zsr/2006.15.1.133

Pesenko YuA (2007) Subgeneric classification of the Palaearctic bees of the genus *Evylaeus* Robertson (Hymenoptera: Halictidae). Zootaxa 1500(1): 1–54. https://doi.org/10.11646/ZOOTAXA.1500.1.1

Pesenko YuA, Banaszak J, Radchenko VG, Cierzniak T (2000) Bees of the family Halictidae (excluding *Sphecodes*) of Poland: taxonomy, ecology, bionomics. Pedagogical University, Bydgoszcz, 348 pp.

Proshchalykin MYu, Maharramov MM (2020) Additional records of osmiine bees (Hymenoptera: Megachilidae: Osmiini) from Azerbaijan. Acta Biologica Sibirica 6: 33–42. https://doi.org/10.3897/abs.6.e53095

Proshchalykin MYu, Maharramov MM, Aliyev KhA (2019) New data on the tribe Osmiini (Hymenoptera: Megachilidae) from Azerbaijan. Far Eastern Entomologist 383: 12–20. https://doi.org/10.25221/fee.383.3

Proshchalykin MYu, Fateryga AV, Astafurova YuV (2023) Corrections and additions to the catalogue of the bees (Hymenoptera, Anthophila) of Russia. ZooKeys 1187: 301–339. https://doi.org/10.3897/zookeys.1187.113240

Silló N (2024) Wiederfund der Schmalbiene *Lasioglossum corvinum* (Morawitz, 1877) in Deutschland und Erstfund für Südwest-deutschland (Hymenoptera: Halictidae). Anthophila 1: 1–9.

Skhirtladze IA (1981) The Bees of the Transcaucasus (Hymenoptera, Apoidea). Metsniereba, Tbilisi, 148 pp. [in Russian]

Warncke K (1975) Beiträge zur systematik und Verbreitung der Furchenbienen in der Türkei (Hymenoptera, Apoidea, *Halictus*). Polskie Pismo Entomologiczne 45: 81–123.

Warncke K (1982) Beitrag zur Bienenfauna des Iran. – 14. Die Gattung *Halictus* Latr., mit Bemerkungen über unbekannte und neue *Halictus*-Arten in der Westpaläarktis und Zentralasien. Bollettino del Museo Civico di Storia Naturale di Venezia 32: 67–166.

Warncke K (1984) Ergänzungen zur Verbreitung der Bienengattung *Halictus* Latr. in der Türkei (Hymenoptera, Apidae). Linzer biologische Beiträge 16(2): 277–318.

Zhang D, Niu Z-Q, Luo A-R, Orr MC, Ferrari RR, Jin J-F, Wu Q-T, Zhang F, Zhu C-D (2022) Testing the systematic status of *Homalictus* and *Rostrohalictus* with weakened cross-vein groups within Halictini (Hymenoptera: Halictidae) using low-coverage whole-genome sequencing. Insect Science 29: 1819–1833. https://doi.org/10.1111/1744-7917.13034

Supplementary material 1

List of Azerbaijani *Lasioglossum* species with labeling data

Authors: Yulia V. Astafurova, Mahir M. Maharramov, Maxim Yu. Proshchalykin

Data type: docx

Explanation note: List of all 2150 examined specimens of the *Lasioglossum* bees from Azerbaijan.

Link: https://doi.org/10.3897/jhr.97.135381.suppl1

Supplementary material 2

List of *Lasioglossum* bees recorded from the Caucasus region

Authors: Yulia V. Astafurova, Mahir M. Maharramov, Maxim Yu. Proshchalykin

Data type: docx

Explanation note: List of 120 species of bees of the genus *Lasioglossum* recorded in the Caucasus region, with distribution by countries and subregions.

Link: https://doi.org/10.3897/jhr.97.135381.suppl2

JHR 97: 881–893 (2024)
doi: 10.3897/jhr.97.134513
https://jhr.pensoft.net

RESEARCH ARTICLE

JOURNAL OF Hymenoptera RESEARCH
A peer-reviewed open-access journal
The International Society of Hymenopterists

An update on the wild bee fauna (Hymenoptera, Apoidea, Anthophila) of Serbia

Sonja Mudri-Stojnić[1], Andrijana Andrić[2], Laura Likov[1], Ana Grković[1], Tamara Tot[1], Ivana Kavgić[1], Ante Vujić[1]

1 *Department of Biology and Ecology, Faculty of Sciences, University of Novi Sad, Department of Biology and Ecology, Trg Dositeja Obradovića 2, 21000 Novi Sad, Serbia* **2** *BioSense Institute, University of Novi Sad, Dr Zorana Đinđića 1, 21000 Novi Sad, Serbia*

Corresponding author: Sonja Mudri-Stojnić (sonja.mudri-stojnic@dbe.uns.ac.rs)

Academic editor: Christopher K. Starr | Received 12 August 2024 | Accepted 17 September 2024 | Published 15 October 2024

https://zoobank.org/136F6129-8247-4DD0-9131-90A6DC063503

Citation: Mudri-Stojnić S, Andrić A, Likov L, Grković A, Tot T, Kavgić I, Vujić A (2024) An update on the wild bee fauna (Hymenoptera, Apoidea, Anthophila) of Serbia. Journal of Hymenoptera Research 97: 881–893. https://doi.org/10.3897/jhr.97.134513

Abstract

Numerous wild bee (Hymenoptera, Apoidea, Anthophila) species show negative population trends, while the knowledge gaps on their occurrences and distributions prevent adequate conservation actions. The need for continuous updating of species records and reconfirmation of their presence has been recognized, especially in understudied areas. The present study presents the results of bee monitoring at 30 Serbian localities, each surveyed three times during 2023. Two sampling methods were used, the transect walks and the pan traps, resulting in a detection of 232 wild bee species. Among them, 13 species found at 13 localities, represent the first published records from Serbia: *Andrena ferox* Smith, 1847, *A. nana* (Kirby, 1802), *A. praecox* (Scopoli, 1763), *A. pusilla* Pérez, 1903, *A. susterai* Alfken, 1914, *A. angustior* (Kirby,1802), *A. curvungula* Thomson,1870, *A. falsifica* Perkins, 1915, *Hoplitis mitis* (Nylander, 1852), *Hylaeus friesei* (Alfken, 1904), *Melitta melanura* (Nylander, 1852), *Nomada trapeziformis* Schmiedeknecht, 1882, and *Osmia uncinata* Gerstaecker, 1869. This study contributes to an update of the list of bee species in Serbia, that now counts 744 species, and also provides additional data on European distributions. The new information on *Melitta melanura* is especially noteworthy, since this species has been assessed as Endangered by the European Red List of Bees due to its small area of occupancy and a severely fragmented distribution. Other important findings include the confirmation of the presence of some wild bee species in Serbia, i.e., 10 species reported as new records within the previous update, and 19 species that were without previously available records from the 21st century. Additionally, the present study indicates the effectiveness of both conducted monitoring techniques, in terms of different recorded species and numbers of specimens. These results lead to the conclusion that corroborates the application of complementary sampling methods as an adequate way to survey bee diversity and abundance.

Keywords
Diversity, *Melitta melanura*, monitoring, new records, sampling methods, wild bee species

Introduction

The crucial role of bees (Hymenoptera, Apoidea, Anthophila), as the most important pollinator group in ecosystems worldwide, is unquestionable nowadays. At the same time, many wild bees show negative population trends, while the knowledge on their spatial distribution is incomplete, with data gaps preventing adequate conservation actions in Europe (Nieto et al. 2014; Potts et al. 2021). Thus, an effort has recently been made to update the information on present species, including their occurrences (Ghisbain et al. 2023; Reverté et al. 2023). However, this is an ongoing issue, especially in the data deficient areas such as Southeastern Europe (Potts et al. 2021), where several scientific projects are being implemented in terms of the systematic monitoring and the gathering of information on bees and other wild pollinating insects, e.g., in Serbia (Mudri-Stojnić et al. 2023).

Serbia is situated at the crossroads of Southeast and Central Europe, within the central Balkan Peninsula and the southern Pannonian Plain. Such a geographical position leads to a mixture of elements of various habitat types, i.e., Pannonian, continental, sub-Mediterranean and mountain. Agricultural landscapes occupy the majority of its territory (63.7%), while protected areas cover 7.6%, and the ecological network of nationally and internationally significant areas cover 21% of the total area of Serbia (Spatial Plan RS 2021–2035 in Official Gazette RS 2020). The diversity of habitat types and the presence of quite well-preserved habitats have affected the relatively high diversity of wild bees. Namely, according to the latest data, Serbia hosts as many as 731 bee species (Mudri-Stojnić et al. 2021, 2023). The neighboring countries, with somewhat similar habitat types, have comparable numbers, i.e., 704 bee species in Hungary (Józan 2011), and 760 in Romania (Tomozii 2010). A number of rich ecosystems, with high species diversity of numerous groups of organisms, has led to enacting several national laws and by-laws regulating the field of nature conservation in Serbia, including the "Rulebook on declaration and protection of strictly protected and protected wild species of plants, animals and fungi" (Official Gazette RS 2016). According to this Rulebook (Appendix 2), the only species of the superfamily Apoidea listed as protected at the national level is *Bombus confusus* Schenck, 1861. However, there are a number of bee species recorded in Serbia which are of conservation concern at the European level (Mudri-Stojnić et al. 2021, 2023). Namely, according to the current European Red List (Nieto et al. 2014), one species (*Bombus cullumanus* Kirby, 1802) is listed as Critically Endangered, 18 as Endangered, 10 as Vulnerable, and 64 as Near Threatened. Nevertheless, almost one third of bee species known in Serbia are classified as Data Deficient in Europe, while many of the listed species have not been recently recorded in Serbia.

Therefore, the need for reconfirmation of the current presence and re-evaluation of the conservation status of species has been noted, especially since there is still no national Red List of bees for Serbia. In recent years, steps have been taken in that direction, firstly

by summarizing the available data and preparing the preliminary list of species (Mudri-Stojnić et al. 2021), and then by conducting additional surveys in order to confirm and update this list (Mudri-Stojnić et al. 2023). An important contribution to obtaining the data regarding the status of bees, and other key groups of wild insect pollinators in Serbia, is the recent establishment of the scientific project "Serbian Pollinator Advice Strategy - for the next normal" (SPAS 2022–2024), as a preparatory phase for the EU Pollinator Monitoring Scheme (EU-PoMS, Potts et al. 2021). The goal of the SPAS project is to build a long-term national monitoring strategy compatible with the European one.

Considering that the updating of species records is a continuous issue, the main aim of the present study is to proceed to amend the information on wild bees occurring in Serbia. Thus, the specific goals are: (1) to present the first published records from Serbia for 13 species; (2) to confirm the presence of 19 species for which 21st century records have been lacking; and (3) to confirm the presence of 10 species reported as new records during the previous update of Serbian bee fauna.

Materials and methods

The data for the present study were obtained within the implementation of the national scientific project SPAS (2022–2024). The project encompasses monitoring insect pollinators at 30 localities across Serbia (Fig. 1), including various habitat types: forest steppe, forest meadow, mountain meadow, wet meadow, sub-Mediterranean grassland, rocky grassland, and steppe grassland. The information introduced in the present study was gathered during 2023. The surveys were conducted on three occasions per locality, from the end of March to September, a period which coincides with the blooming of most flowering plant species in Serbia.

Specimens of wild bees were collected using two methods, following the protocol applied within the SPAS project (Mudri-Stojnić et al. 2023). Transect walks included a collection with a sweep net, lasting ~ 30 min per site, and covering ~ 500 m length and 2 m width. Placed along each transect was a set of ten pan trap stations, with three colored bowls per group (white, yellow and blue), filled with water and some soap. The species were identified in the laboratory of the Department of Biology and Ecology, Faculty of Sciences, University of Novi Sad, Serbia (**FSUNS**), and by expert Józan Zsolt (Mernye, Hungary).

The list of previously unpublished records for bee species in Serbia is provided in full, whereas the list of all recorded species can be found in Suppl. material 1, with additional information provided for each species: IUCN (The International Union for Conservation of Nature) categories (Nieto et al. 2014), collection methodology types, data on species with previous records based solely on literature data. Detailed information on collected specimens (i.e., locality, date, sex, identification code, collection methodology type, legator) has been provided within Suppl. material 2 for species with occurrences previously available only from sources prior to the year 2000, and within Suppl. material 3 for species reported as new records during the previous update of Serbian bee fauna (Mudri-Stojnić et al. 2023).

Figure 1. Map of Serbia showing collection localities. Stars indicate localities where new species records were detected.

Results

During the survey of all 30 localities conducted throughout the 2023 season, 2,950 specimens from 232 bee species were recorded (Suppl. material 1). The method of transect walks resulted in the detection of 92 species, 55 species were caught in pan traps and 85 species were found using both methods. With respect to the so far published information (Mudri-Stojnić et al. 2021, 2023), 13 species recorded in the present study have not been previously recorded in Serbia. These 13 species were detected at 13 localities (Fig. 1), eight species (16 specimens) during transect walks (*Andrena angustior* (Kirby,1802), *A. ferox* Smith, 1847, *A. nana* (Kirby, 1802), *A. susterai* Alfken, 1914, *Nomada trapeziformis* Schmiedeknecht, 1882, *Hylaeus friesei* (Alfken, 1904), *Osmia uncinata* Gerstaecker, 1869, and *Melitta melanura* (Nylander, 1852)), and four species (six specimens) were found in pan traps (*Andrena curvungula* Thomson, 1870, *A. praecox* (Scopoli, 1763), *A. pusilla* Pérez, 1903, and *Hoplitis mitis* (Nylander, 1852)), while only one species (*Andrena falsifica* Perkins, 1915) was recorded using both collection methods (five specimens with sweep net and two specimens in pan traps). According to the IUCN Red List Categories (Europe) (Nieto et al. 2014), these 13 species have been accessed as: EN - Endangered (one species, i.e., *Melitta melanura*), NT - Near Threatened (two species), LC - Least Concern (four species), and DD - Data Deficient (six species).

Nineteen bee species recorded in the present study (46 specimens, see Suppl. material 2) were without confirmed records from the 21st century, i.e., they were known to be present in Serbia only according to older literature data, some of them dating ~ 100 years back, i.e.: *Nomada striata* Fabricius, 1793 (Apfelbeck 1896), *Protosmia longiceps* Friese, 1899 (Vorgin 1918), *Andrena denticulata* (Kirby, 1802), *A. ventralis* Imhoff,

1832, and *Eucera dalmatica* Lepeletier, 1841 (Lebedev 1931). According to sampling methodologies, out of these 19 species, 10 species (33 specimens) were detected only by the use of pan traps, eight species (10 specimens) were recorded solely on transect walks, and one species (*Andrena combinata* (Christ, 1791)) was found by both methods (two specimens with sweep net and one specimen in pan trap).

Another noteworthy finding of the present study is the recording of 10 bee species (out of 25) introduced by Mudri-Stojnić et al. (2023) as new records for Serbia (Suppl. material 3). Thus, their presence has now been confirmed and furthermore, eight of these species have been found at different localities than previously, i.e., four solely at new localities and four at both new and some previously recorded localities. One of the 10 species was detected using a different method than previously, six using the same method, and three species found using both sampling methods in the 2022 survey were recorded by only one of the methods in the 2023 survey (see Suppl. material 1). Out of the 232 bee species recorded in the present study (survey of 2023), 180 species were also recorded during the previous survey (2022) (Mudri-Stojnić et al. 2023). The majority, i.e., 109 species were detected using the same sampling method in both years, 16 species were found by different methods, and 55 species were recorded using one method during one year and both methods during the second year (see Suppl. material 1).

New records of wild bee species in Serbia

Family Andrenidae

***Andrena* Fabricius, 1775**

***Andrena angustior* (Kirby, 1802) [DD]**

- 1 ♀; Suva planina, Bojanine vode; 43.2260°N, 22.1068°E; 23 Apr. 2023; Laura Likov leg.; FSUNS SPAS10842.

***Andrena curvungula* Thomson, 1870 [DD]**

- 1 ♀; Fruška gora, Glavica; 45.1851°N, 19.8562°E; 12 Jun. 2023; white pan trap; FSUNS SPAS31681.

***Andrena falsifica* Perkins, 1915 [DD]**

- 1 ♀; Kopaonik, Kadijevac; 43.3203°N, 20.7621°E; 20 May 2023; yellow pan trap; FSUNS SPAS31396 • 1 ♀; Vlasina, mahala Damnjaničovi; 42.6947°N, 22.3580°E; 24 May 2023; yellow pan trap; FSUNS SPAS11175 • 1 ♀; Deliblato Sands, Čardak; 44.8626°N, 21.0569°E; 23 Apr. 2023; Sonja Mudri-Stojnić leg.; FSUNS SPAS01610 • 3 ♀♀; Zlatibor, Obudovica; 43.7227°N, 19.6881°E; 17 May 2023; Ana Grković leg.; FSUNS SPAS31164, SPAS31175, SPAS31176 • 1 ♀; Zlatibor, Semegnjevo; 43.7514°N, 19.6037°E; 14 Jun. 2023; Ana Grković leg.; FSUNS SPAS31432.

***Andrena ferox* Smith, 1847 [DD]**

• 1 ♂; Deliblato Sands, Šušara; 44.9261°N, 21.1353°E; 23 Apr. 2023; Sonja Mudri-Stojnić leg.; FSUNS SPAS01582.

***Andrena nana* (Kirby, 1802) [LC]**

• 1 ♂; Zlatibor, Obudovica; 43.7227°N, 19.6881°E; 17 May 2023; Ana Grković leg.; FSUNS SPAS31172.

***Andrena praecox* (Scopoli, 1763) [LC]**

• 1 ♀; Fruška gora, Neradin; 45.1061°N, 19.9156°E; 30 Mar. 2023; yellow pan trap; FSUNS SPAS01169 • 2 ♀♀; Vlasina, mahala Damnjaničovi; 42.6947°N, 22.3580°E; 24 May 2023; yellow pan trap; FSUNS SPAS11173; white pan trap; FSUNS SPAS11177.

***Andrena pusilla* Pérez, 1903 [DD]**

• 1 ♀; Fruška gora, Neradin; 45.1061°N, 19.9156°E; 30 Mar. 2023; blue pan trap; FSUNS SPAS01452.

***Andrena susterai* Alfken, 1914 [DD]**

• 2 ♀♀; Rajac, Gornji Banjani; 44.1200°N, 20.2643°E; 16 May 2023; Ana Grković leg.; FSUNS SPAS 31129; FSUNS SPAS31130 • 1 ♀; Rajac, Slavkovica; 44.1404°N, 20.2471°E; 16 May 2023; Ana Grković leg.; FSUNS SPAS31071.

Family Apidae

***Nomada* Scopoli, 1770**

***Nomada trapeziformis* Schmiedeknecht, 1882 [NT]**

• 2 ♀♀; Vlasina, mahala Damnjaničovi; 42.6947°N, 22.3580°E; 24 May 2023; Laura Likov leg.; FSUNS SPAS11132, SPAS11133.

Family Colletidae

***Hylaeus* Fabricius, 1793**

***Hylaeus friesei* (Alfken, 1904) [NT]**

• 1 ♀; Lazar's canyon, Lazar's cave; 44.0286°N, 21.9587°E; 9 Jun. 2023; Tamara Tot leg.; FSUNS SPAS20912.

Family Megachilidae

***Hoplitis* Klug, 1807**

***Hoplitis mitis* (Nylander, 1852)**

• 1 ♂; Kopaonik, Mali Karaman; 43.2910°N, 20.8235°E; 23 Jun. 2023; blue pan trap; FSUNS SPAS31655.

Osmia Panzer, 1806

***Osmia uncinata* Gerstaecker, 1869 [LC]**
• 1 ♀; Kopaonik, Kadijavac; 43.3203°N, 20.7621°E; 23 Jun. 2023; Ana Grković leg.; FSUNS SPAS31641.

Family Melittidae

***Melitta* Kirby, 1802**

Melitta melanura (Nylander, 1852) [EN]

• 4 ♀♀; Deliblato Sands, Šušara; 44.9261°N, 21.1353°E; 29 Aug. 2023; Ante Vujić leg.; FSUNS SPAS02277, SPAS02282, SPAS02283, SPAS02284 • 2 ♂♂; Deliblato Sands, Šušara; 44.9261°N, 21.1353°E; 29 Aug. 2023; Ante Vujić leg.; FSUNS SPAS02287, SPAS02279.

Discussion

The present study has resulted in the introduction of 13 wild bee species (from five different families) previously unrecorded in Serbia. Most of them belong to the family Andrenidae with eight species from the genus *Andrena*. They are followed by Megachilidae (one *Hoplitis* and one *Osmia* species) and one species each from Apidae (*Nomada*), Colletidae (*Hylaeus*), and Melittidae (*Melitta*). The previous update of Serbian wild bee fauna (Mudri-Stojnić et al. 2023) also presented the majority (10 out of 25 newly-recorded) species from the genus *Andrena*, and the recently published preliminary list of bee species in Serbia (Mudri-Stojnić et al. 2021) mentions *Andrena* as the genus most rich in species. According to the results of the present study, *Andrena* remains as the genus with the highest number of species in Serbia, namely 122. Considering all recorded species, including the newly-presented records, the bee fauna of Serbia numbers 744 species.

One of the valuable findings of the present study is the detection of six specimens of *Melitta melanura*, a species assessed as Endangered according to the latest European regional assessment (Michez and Nieto 2012). Up to date, it has not been recorded in

Serbia (Mudri-Stojnić et al. 2021, 2023). However, there are records from the neighboring countries (Reverté et al. 2023), i.e., Romania (Tomozii 2010) and Hungary (as synonym *Melitta wankowiczi* (Radoszkowski, 1891)) (Józan 2011). Although widely distributed in Palaearctic, from Siberia to Austria to Turkey (Michez and Eardley 2007; Michez and Nieto 2012; Özbek 2014), the species records are rare and the populations are isolated, and it has been assessed as Endangered due to its small area of occupancy and a severely fragmented distribution (Michez and Nieto 2012). Therefore, the new information could represent a valuable asset to the knowledge on the presence of this species in areas where it has not been previously recorded. Although considered threatened at national levels in some countries, no direct conservation measures are in place; however, it has been suggested that natural reserves should be created to protect the host-plants in locations of isolated populations of *M. melanura* (Radchenko 2009; Michez and Nieto 2012). These oligolectic bees live in temperate grassland vegetation with Campanulaceae, mostly *Campanula* sp. as host-plants (Michez and Eardley 2007; Michez et al. 2008). The locality where *M. melanura* was found in the present study is situated within the Deliblato Sands Special Nature Reserve, whose diverse flora includes ten species of *Campanula* L. (Ćuk 2019).

With respect to the two applied collection methodologies, most of the species recorded in the present study (40%) were detected only during transect walks, 24% of species were caught only in pan traps, and 36% were found using both methods. The similar pattern was found by Mudri-Stojnić et al. (2023) with 41%, 27%, and 32% of the total number of found species, respectively. Regarding the 13 new species records for Serbia, 61% were detected only during transect walks, 31% only in pan traps, and 8% by both methods, while these percentages for the number of specimens were 57%, 21.5%, and 21.5%, respectively. Regarding the 19 species previously known only from old literature, this ratio was 42%, 53%, and 5% for the number of species, and 22%, 72%, and 6% for the number of specimens. Taking into account all these percentages, a conclusion imposes itself that the use of both collection methods is the best way to assess bee diversity and abundance, since many species were detected by only one of the used sampling techniques, with the number of specimens between them varying. Furthermore, it may be noted that for some species the method used to sample them was not the same during both survey years. Comparing the results of the present survey with the previous one (Mudri-Stojnić et al. 2023), 61% of species recorded in both surveys were found using the same sampling method, 9% were detected by a different method, and 30% of species were recorded using one method during one year and both methods during the second year. Both the transect walks, designed to survey flying insects, and the pan traps, intended for nectar-searching insects, have been recognized as methods suitable for the monitoring of bees. However, both approaches have some limitations and a combination has been suggested as the most effective (Nielsen et al. 2011; Potts et al. 2021; Leclercq et al. 2022). The validity of transect walks depends on the experience of collectors (Nielsen et al. 2011), whereas pan traps provide data without observer bias, but they are not always representative of the local community and their effectiveness might be influenced by the surrounding floral resources (Cane et al. 2000; Roulston et al. 2007; Westphal et al. 2008). Furthermore, there is a need for further research in terms of standardization,

and a regular review of sampling designs for future long-term bee monitoring programs (Krahner et al. 2024). The conservation management efforts and decisions depend on the understanding of bees' ecological communities, and are thus influenced by the choice of sampling methods (Kuhlman et al. 2021), thus determining the most suitable monitoring techniques is a prerequisite for assessing the status and trends of bee populations.

Acknowledgements

We are especially grateful to Zsolt Józan for assistance in species identification. Thanks also to to Igor Ivkov for his English proofreading. We also thank the reviewer Sara Reverté. The data for this study were obtained as part of the implementation of project SPAS - Serbian Pollinator Advice Strategy - for the next normal (Science Fund of the Republic of Serbia, Program IDEAS, GA ID: 7737504). The authors also acknowledge the financial support of the Ministry of Science, Technological Development and Innovation of the Republic of Serbia (Grants No. 451-03-66/2024-03/200125 and 451-03-65/2024-03/200125, and Grant No. 451-03-66/2024-03/200358).

References

Apfelbeck V (1896) Balkanske Apide (pčele). Glasnik zemaljskog muzeja u Bosni i Hercegovini 8: 329–342.

Cane JH, Minckley RL, Kervin LJ (2000) Sampling bees (Hymenoptera: Apiformes) for pollinator community studies: pitfalls of pan-trapping. Journal of the Kansas Entomological Society 73: 225–231. https://www.jstor.org/stable/25085973

Ćuk M (2019) Status and temporal dynamics of the flora and vegetation of the Deliblato Sands. PHD Thesis. Faculty of Sciences, University of Novi Sad (Serbia).

Ghisbain G, Rosa P, Bogusch P, Flaminio S, Le Divelec R, Dorchin A, Kasparek M, Kuhlmann M, Litman J, Mignot M, Müller A, Praz C, Radchenko VG, Rasmont P, Risch S, Roberts SPM, Smit J, Wood TJ, Michez D, Reverté S (2023) The new annotated checklist of the wild bees of Europe (Hymenoptera: Anthophila). Zootaxa 5327(1): 1–147. https://doi.org/10.11646/zootaxa.5327.1.1

Józan Z (2011) Checklist of Hungarian Sphecidae and Apidae species (Hymenoptera, Sphecidae and Apidae). Natura Somogyiensis 19: 177–199. https://doi.org/10.24394/NatSom.2011.19.177

Krahner A, Dietzsch AC, Jütte T, Pistorius J, Everaars J (2024) Standardising bee sampling: A systematic review of pan trapping and associated floral surveys. Ecology and Evolution 14(3): e11157. https://doi.org/10.1002/ece3.11157

Kuhlman MP, Burrows S, Mummey DL, Ramsey PW, Hahn PG (2021) Relative bee abundance varies by collection method and flowering richness: Implications for understanding patterns in bee community data. Ecological Solutions and Evidence 2(2): e12071. https://doi.org/10.1002/2688-8319.12071

Lebedev A (1931) Prilog poznavanju jugoslovenskih pčela. Glasnik Jugoslovenskog entomološkog društva, Beograd, Jugoslavija 5–6(1–2): 39–48.

Leclercq N, Marshall L, Weekers T, Anselmo A, Benda D, Bevk D, Bogusch P, Cejas D, Drepper B, Galloni M, Gérard M, Ghisbain G, Hutchinson L, Martinet B, Michez D, Molenberg J-M, Nikolic P, Smagghe G, Straka J, Vandamme P, Wood T, Vereecken N (2022) A comparative analysis of crop pollinator survey methods along a climatic gradient. Agriculture, Ecosystems and Environment 329: e107871. https://doi.org/10.1016/j.agee.2022.107871

Michez D, Eardley CD (2007) Monographic revision of the bee genus *Melitta* Kirby, 1802 (Hymenoptera: Apoidea: Melittidae). Annales de la Société Entomologique de France (n. s.) 43(4): 379–440. https://doi.org/10.1080/00379271.2007.10697535

Michez D, Nieto A (2012) *Melitta melanura* (Europe assessment). The IUCN Red List of Threatened Species 2012: e.T13324607A13324761. https://www.iucnredlist.org/species/13324607/13324761#assessment-information [Accessed on 18.06.2024]

Michez D, Patiny S, Rasmont P, Timmermann K, Vereecken NJ (2008) Phylogeny and host-plant evolution in Melittidae s.l. (Hymenoptera: Apoidea). Apidologie 39: 146–162. https://doi.org/10.1051/apido:2007048

Mudri-Stojnić S, Andrić A, Markov-Ristić Z, Đukić A, Vujić A (2021) Contribution to the knowledge of the bee fauna (Hymenoptera, Apoidea, Anthophila) in Serbia. ZooKeys 1053: 43–105. https://doi.org/10.3897/zookeys.1053.67288

Mudri-Stojnić S, Andrić A, Józan Z, Likov L, Tot T, Grković A, Vujić A (2023) New records for the wild bee fauna (Hymenoptera, Anthophila) of Serbia. Journal of Hymenoptera Research 96: 761–781. https://doi.org/10.3897/jhr.96.107595

Nielsen A, Steffan-Dewenter I, Westphal C, Messinger O, Potts SG, Roberts SPM, Settele J, Szentgyörgyi H, Vaissière BE, Vaitis M, Woyciechowski M, Bazos I, Biesmeijer JC, Bommarco R, Kunin WE, Tscheulin T, Lamborn E, Petanidou T (2011) Assessing bee species richness in two Mediterranean communities: importance of habitat type and sampling techniques. Ecological Research 26(5): 969–983. https://doi.org/10.1007/s11284-011-0852-1

Nieto A, Roberts SPM, Kemp J, Rasmont P, Kuhlmann M, García Criado M, Biesmeijer JC, Bogusch P, Dathe HH, De la Rúa P, De Meulemeester T, Dehon M, Dewulf A, Ortiz-Sánchez FJ, Lhomme P, Pauly A, Potts SG, Praz C, Quaranta M, Radchenko VG, Scheuchl E, Smit J, Straka J, Terzo M, Tomozii B, Window J, Michez D (2014) European Red List of Bees. Publications Office of the European Union (Luxembourg): 1–84. https://doi.org/10.2779/77003

Official Gazette RS (2016) Rulebook on declaration and protection of strictly protected and protected wild species of plants, animals and fungi. Official Gazette of Republic of Serbia No. 05/10, 47/11, 32/16 and 98/16. https://www.pravno-informacioni-sistem.rs/SlGlasnikPortal/eli/rep/sgrs/ministarstva/pravilnik/2010/5/3/reg [Accessed on 20.06.2024]

Official Gazette RS (2020) Spatial Plan Republic of Serbia 2021–2035. Official Gazette of Republic of Serbia No. 48/19. https://media1.opstinamalocrnice.rs/2020/03/PROSTORNI-PLAN-REPUBLIKE-SRBIJE-OD-2021.-DO-2035.GODINE.pdf [Accessed on 20.06.2024]

Özbek H (2014) Distribution data on the family Melittidae (Hymenoptera) of Turkey with considerations about their importance as pollinators. Turkish Journal of Zoology 38(4): 444–459. https://doi.org/10.3906/zoo-1309-5

Potts S, Dauber J, Hochkirch A, Oteman B, Roy D, Ahnre K, Biesmeijer JC, Breeze T, Carvell C, Ferreira C, Fitzpatrick Ú, Isaac N, Kuussaari M, Ljubomirov T, Maes J, Ngo H, Pardo A, Polce C, Quaranta M, Settele J, Sorg M, Stefancesu C, Vujić A (2021) Proposal for an EU pollinator monitoring scheme. Publications Office of the European Union (Ispra), 1–310. https://doi.org/10.2760/881843

Radchenko V (2009) *Melitta* (*Cilissa*) *wankowiczi* (Radoszkowski, 1891). In: Akimov IA (Ed.) Red Data Book of Ukraine - Animal Kingdom. Global consulting (Kiev), 252–252.

Reverté S, Miličić M, Ačanski J, Andrić A, Aracil A, Aubert M, Balzan MV, Bartomeus I, Bogusch P, Bosch J, Budrys E, Cantú-Salazar L, Castro S, Cornalba M, Demeter I, Devalez J, Dorchin A, Dufrêne E, Đorđević A, Fisler L, Fitzpatrick Ú, Flaminio S, Földesi R, Gaspar H, Genoud D, Geslin B, Ghisbain G, Gilbert F, Gogala A, Grković A, Heimburg H, Herrera-Mesías F, Jacobs M, Milosavljević MJ, Janssen K, Jensen J-K, Ješovnik A, Józan Z, Karlis G, Kasparek M, Kovács-Hostyánszki A, Kuhlmann M, Le Divelec R, Leclercq N, Likov L, Litman J, Ljubomirov T, Madsen HB, Marshall L, Mazánek L, Milić D, Mignot M, Mudri-Stojnić S, Müller A, Nedeljković Z, Nikolić P, Ødegaard F, Patiny S, Paukkunen J, Pennards G, Pérez-Bañón C, Perrard A, Petanidou T, Pettersson LB, Popov G, Popov S, Praz C, Prokhorov A, Quaranta M, Radchenko VG, Radenković S, Rasmont P, Rasmussen C, Reemer M, Ricarte A, Risch S, Roberts SPM, Rojo S, Ropars L, Rosa P, Ruiz C, Sentil A, Shparyk V, Smit J, Sommaggio D, Soon V, Ssymank A, Ståhls G, Stavrinides M, Straka J, Tarlap P, Terzo M, Tomozii B, Tot T, van der Ent L-J, van Steenis J, van Steenis W, Varnava AI, Vereecken NJ, Veselić S, Vesnić A, Weigand A, Wisniowski B, Wood TJ, Zimmermann D, Michez D, Vujić A (2023) National records of 3000 European bee and hoverfly species: A contribution to pollinator conservation. Insect Conservation and Diversity 16: 758–775. https://doi.org/10.1111/icad.12680

Roulston TH, Smith SA, Brewster AL (2007) A comparison of pan trap and intensive net sampling techniques for documenting a bee (Hymenoptera: Apiformes) fauna. Journal of the Kansas Entomological Society 80(2): 179–181. https://doi.org/10.2317/0022-8567(2007)80[179:ACOPTA]2.0.CO;2

SPAS (2022–2024) Serbian Pollinator Advice Strategy - for the next normal. Science Fund of the Republic of Serbia, Program IDEAS, GA ID: 7737504. https://spas.pmf.uns.ac.rs/en/ [Accessed on 01.07.2024]

Tomozii B (2010) Bees of Romania. https://www.beesofromania.ro/home [Accessed on 01.07.2024]

Vorgin V (1918) Pregled Apidae hrvatske Slavonije i hrvatskog Primorja s obzirom na faunu Apida Dalmacije. Glasnik Hrvatskoga prirodoslovnoga društva, Zagreb 30: 1–4.

Westphal C, Bommarco R, Carré G, Lamborn E, Morison N, Petanidou T, Potts SG, Roberts SPM, Szentgyörgyi H, Tscheulin T, Vaissière BE, Woyciechowski M, Biesmeijer JC, Kunin WE, Settele J, Steffan-Dewenter I (2008) Measuring bee diversity in different European habitats and biogeographical regions. Ecological Monographs 78(4): 653–671. https://doi.org/10.1890/07-1292.1

Supplementary material 1

The list of all bee species recorded during the surveys of selected sites in 2023

Authors: Sonja Mudri-Stojnić, Andrijana Andrić, Laura Likov, Ana Grković, Tamara Tot, Ivana Kavgić, Ante Vujić

Data type: xlsx

Explanation note: The list of all recorded bee species with additional information: IUCN categories; collection methodology types; records new for Serbia; records previously based only on literature data.

Link: https://doi.org/10.3897/jhr.97.134513.suppl1

Supplementary material 2

The list of specimens of bee species with data previously available only from sources prior to year 2000

Authors: Sonja Mudri-Stojnić, Andrijana Andrić, Laura Likov, Ana Grković, Tamara Tot, Ivana Kavgić, Ante Vujić

Data type: xlsx

Explanation note: Detailed information on collected specimens of bee species with data previously available only from sources prior to year 2000: locality, date, sex, identification code, collection methodology, legator.

Link: https://doi.org/10.3897/jhr.97.134513.suppl2

Supplementary material 3

The list of specimens of bee species reported as new records in the previous update of Serbian bee fauna

Authors: Sonja Mudri-Stojnić, Andrijana Andrić, Laura Likov, Ana Grković, Tamara Tot, Ivana Kavgić, Ante Vujić

Data type: xlsx

Explanation note: Detailed information on collected specimens of bee species reported as new records in the previous update of Serbian bee fauna: locality, date, sex, identification code, collection methodology, legator.

Link: https://doi.org/10.3897/jhr.97.134513.suppl3

JHR 97: 895–914 (2024)
doi: 10.3897/jhr.97.132937
https://jhr.pensoft.net

RESEARCH ARTICLE

JOURNAL OF Hymenoptera RESEARCH
A peer-reviewed open-access journal
The International Society of Hymenopterists

Molecular data support *Bombus sonorus* and *Bombus pensylvanicus* (Hymenoptera, Apidae) as distinct species

Jessica L. Beckham[1], Jeff A. Johnson[2,3], Russell S. Pfau[4]

1 *Department of Integrative Biology, University of Texas at San Antonio, One UTSA Circle, San Antonio TX, 78249, USA* **2** *Department of Biological Sciences, University of North Texas, 1155 Union Circle #305220, Denton, TX 76203, USA* **3** *The Peregrine Fund, The World Center for Birds of Prey, 5668 West Flying Hawk Lane, Boise, ID 83709, USA* **4** *Department of Biological Sciences, Tarleton State University, Stephenville, TX, 76402, USA*

Corresponding author: Russell S. Pfau (rspfau@proton.me)

Academic editor: Jack Neff | Received 4 August 2024 | Accepted 3 October 2024 | Published 17 October 2024

https://zoobank.org/43B15D10-9964-4997-94AC-513D15A21E09

Citation: Beckham JL, Johnson JA, Pfau RS (2024) Molecular data support *Bombus sonorus* and *Bombus pensylvanicus* (Hymenoptera, Apidae) as distinct species. Journal of Hymenoptera Research 97: 895–914. https://doi.org/10.3897/jhr.97.132937

Abstract

Despite their distinctive banding patterns, setal coloration, and geographic ranges, the Sonoran bumble bee (*Bombus sonorus* Say, 1837) and the American bumble bee (*Bombus pensylvanicus* De Geer, 1773) are often treated as conspecific, with some authorities ranking *B. sonorus* as a subspecies of *B. pensylvanicus*. This lack of taxonomic clarity creates challenges, particularly for population monitoring and conservation initiatives. In this study, we used genetic analyses to assess the potential for clinal variation, ongoing hybridization, and historical introgression between *B. pensylvanicus* and *B. sonorus* within a broad area of sympatry across the state of Texas. Double digest restriction associated DNA sequencing (ddRADseq) was performed on 166 specimens (58 *B. sonorus* and 108 *B. pensylvanicus*), and a portion of the mitochondrial COI gene was sequenced for a subset of the specimens from Texas (46 *B. sonorus* and 32 *B. pensylvanicus*) and eight specimens of *B. sonorus* from California. An additional five sequences of *B. pensylvanicus* from Georgia and Florida were obtained from Genbank and BOLD along with one each of *B. transversalis* (Olivier, 1789), *B. mexicanus* Cresson, 1879, *B. medius* Cresson, 1863 and *B. fervidus* (Fabricius, 1798), and *B. mesomelas* Gerstäcker, 1869. For both genetic datasets (nuclear ddRADseq and mtDNA COI), individuals formed two distinct groups concordant with species identification based on setal coloration. We found no evidence supporting a clinal pattern of variation, ongoing hybridization, or historical introgression within the study area and conclude that *B. sonorus* should be recognized as a species under the Biological Species Concept.

Keywords

Bombus pensylvanicus, *Bombus sonorus*, bumble bee, COI, RADseq, sympatry

Introduction

Bombus sonorus Say, 1837, commonly referred to as the Sonoran bumble bee, has a contentious taxonomic history. First described from Mexico (Say 1837), *B. sonorus* continued to be recognized as a species by Franklin (1913), Thorp (1983) but often with some hesitation. Others have considered *B. sonorus* as conspecific with *Bombus pensylvanicus* (De Geer 1773; Williams 1998) and often as a subspecies (*B. p. sonorus*; Handlirsch 1888; Peters 1968; Milliron 1973; Labougle 1990; Williams et al. 2014). The range of *B. sonorus* extends from California to central Texas and south to southern Mexico, overlapping with *B. pensylvanicus* within Texas and Mexico where the two are broadly sympatric. Within this region of sympatry, there have been anecdotal reports of chromatically intermediate individuals in Mexico and southwestern Texas (Labougle 1990; Williams et al. 2014). However, we are aware of only one description that has been provided as to what constitutes an intermediate phenotype for these two taxa: Labougle (1990) simply stated that setal coloration of the scutellum and punctation of the clypeus was intermediate. In a study of the hymenopteran fauna of Mexico, Peters (1968) did not mention specimens with an intermediate phenotype, but noted that both color forms occurred together; he reported collecting both on the same shrub and observed an individual of *B. sonorus* at the entrance of a nest along with 10 *B. pensylvanicus*. Because of this, he considered them to be conspecific and stated that he found it difficult to give them even subspecies designations. Based on these accounts, some authorities have been hesitant to recognize these as distinct species. More recently, Cameron et al. (2007) used four nuclear loci and one mitochondrial (mtDNA) locus (16S) to analyze a nearly complete sampling of *Bombus* (218 of 250 species). Their data showed that *B. sonorus* and *B. pensylvanicus* were polyphyletic, suggesting either introgression between the two taxa or the existence of shared ancestral variation (i.e., incomplete lineage sorting).

Some populations of *B. pensylvanicus* and *B. sonorus* are in decline (Committee on the Status of Pollinators 2007; Colla and Packer 2008; Grixti et al. 2009; Cameron et al. 2011; Colla et al. 2011, 2012; Bartomeus et al. 2013; Hatfield et al. 2015). As such, *B. pensylvanicus sensu lato* is under review for federal protection under the Endangered Species Act (USFS 2021) and is listed as Vulnerable on the IUCN Red List (Hatfield et al. 2015). Additionally, though commonly observed in Texas, both *B. sonorus* and *B. pensylvanicus* have been designated as Species of Greatest Conservation Need (SGCN) in the Texas Conservation Action Plan generated by the Texas Parks and Wildlife Department (TPWD 2012). Further study is warranted to provide additional evidence to resolve the taxonomic uncertainty of *B. sonorus* in order to help inform monitoring practices and conservation measures.

Genetic data can provide evidence to help resolve taxonomic uncertainty when morphological differences are ambiguous. Mitochondrial DNA sequences have been used to identify and delineate species among many taxonomic groups. However, the value of mtDNA sequence analysis is limited because it represents a single locus; moreover, mtDNA sequences may have a different evolutionary history relative to nuclear loci because of their maternal inheritance pattern (Moritz and Cicero 2004; Galtier et al. 2009; Taylor and Harris 2012). Other potential complications are specific to arthro-

pods, such as indirect selection on mtDNA arising from linkage disequilibrium with maternally inherited symbionts (Hurst and Jiggins 2005). An increasing number of studies, including those of *Bombus* (Duennes et al. 2012; Lozier et al. 2016; McKendrick et al. 2017), are using mtDNA sequences in combination with multi-locus nuclear genetic data. Next-generation sequencing techniques can generate large numbers of nuclear loci for the analysis of species delineation. Peterson et al. (2012) described a cost-effective reduced representation genomic sequencing approach called double digest restriction associated DNA sequencing (ddRADseq) that can produce thousands of loci from hundreds of specimens. Taken together, analyses of mtDNA sequences and ddRADseq data can provide compelling genetic insight into taxonomic relationships.

To clarify whether *B. sonorus* should be considered a distinct species, we generated ddRADseq and mtDNA cytochrome c oxidase subunit I (COI) gene sequence datasets for *B. sonorus* and *B. pensylvanicus* individuals collected across a broad area of sympatry in Texas. We sought to determine if the genetic data were concordant with species identification based on setal coloration and assessed the evidence for clinal variation, hybridization, and historical introgression.

Materials and methods

Specimen identification

For purposes of this study, we visually identified *B. sonorus* and *B. pensylvanicus* based on setal coloration (banding pattern and shade of yellow) following the descriptions of Franklin (1913), Milliron (1973), and Labougle (1990), and as depicted in Fig. 1. Specifically, the thoracic setal pile of female *B. sonorus* is black with yellow pile on the pronotum, anterior portion of scutum, and scutellum resulting in a black interalar band. In contrast, *B. pensylvanicus* usually (but not always) has a black scutellum – though some specimens bear, on the scutellum, yellow and black pile mixed, or rarely all yellow. Additionally, while T2–T3 of both taxa are yellow, T1 of *B. sonorus* is described as entirely yellow, while T1 of *B. pensylvanicus* is black with the posterior portion yellow. Lastly, *B. sonorus* exhibits a much deeper (golden) yellow than *B. pensylvanicus* (which has been described as being canary or lemon yellow).

Geographic distribution

To determine the extent of geographic overlap of *B. pensylvanicus* and *B. sonorus* within the study area (Texas), we examined photographic documentation of occurrence data on the iNaturalist platform (www.inaturalist.org). We filtered iNaturalist observations by species and location (i.e., filtered for *B. sonorus* in Texas and *B. pensylvanicus* in Texas) and then verified species identifications for all observations using the identification criteria described above. Observations were only included in our dataset if the photograph quality allowed for species identification. We then downloaded these verified observations from the Global Biodiversity Information Facility

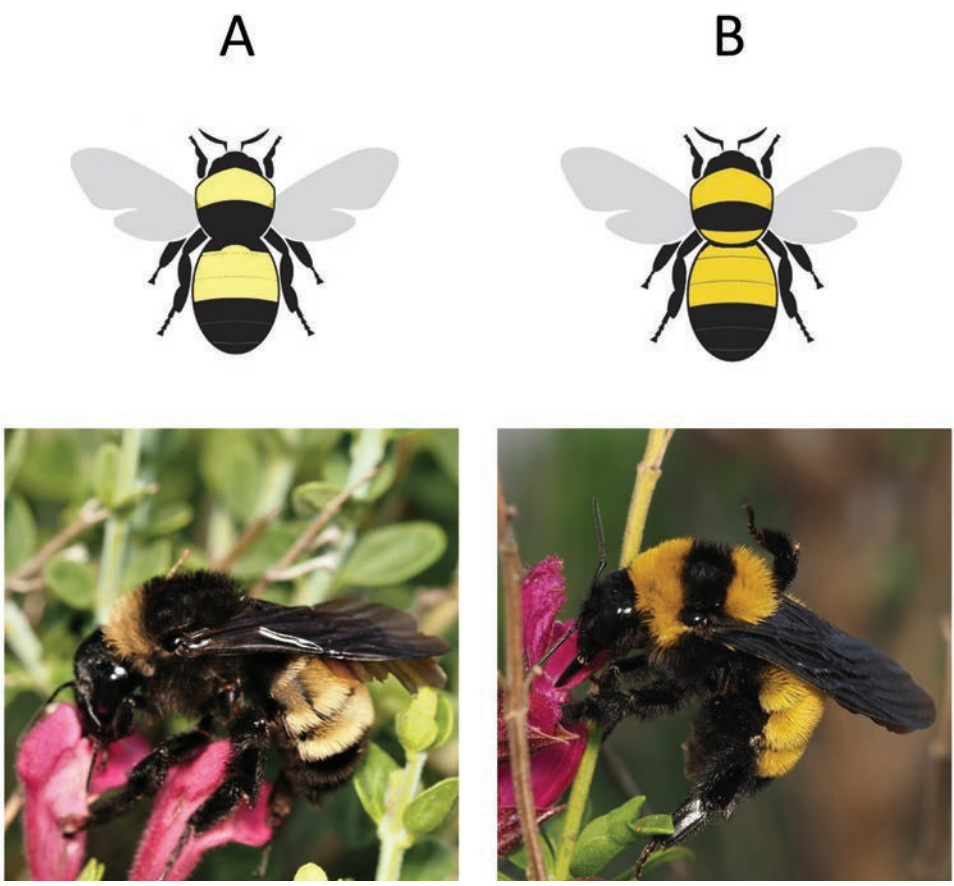

Figure 1. Coloration (banding pattern and shade of yellow) characteristic of female *B. pensylvanicus* (**A**) and *B. sonorus* (**B**) Diagram (top) modified from image provided by Texas Parks & Wildlife.

(https://www.gbif.org) and mapped each locality using QGIS (QGIS Development Team 2021). Additionally, we compared these records with the distributional map of Texas *Bombus* compiled by Warriner (2012) based on museum collections, as well as documented and projected distributions from Beckham and Atkinson (2017).

Survey area and specimen collection

To gather specimens for genetic analyses, we surveyed for bumble bees during July – September, 2016 to coincide with times of peak bumble bee activity. We identified target areas for surveys within the projected area of sympatry in Texas; these target areas were prioritized for collection trips, but we also acquired bees opportunistically from other areas of the state. Most collection events took place along public roadsides, and survey locations were chosen based on accessibility and the presence of flowering plants. Bees were collected using an aerial net and placed in a mobile cooler for transport to the lab where they were maintained at -80 °C.

We collected 166 bumble bees from 113 sites in 66 Texas counties (Fig. 2; Suppl. material 1: appendix S1); of these, all but one were female. We collected *B. sonorus* from 39 sites in 25 counties and *B. pensylvanicus* from 83 sites in 51 counties. In 11 of the 66 counties, we collected both species. Based on the distributional data (Fig. 2), 53 of the 66 counties sampled are likely within the area of sympatry in Texas (the exceptions being those counties east and south of the documented occurrence of *B. sonorus*; these include Atascosa, Bastrop, Brazos, Burleson, Caldwell, Fayette, Frio, Grayson, Lee, Milam, Montgomery, Robertson, and Wilson). None of the individuals that we collected displayed setal coloration (banding pattern and shade of yellow) intermediate between typical *B. sonorus* and *B. pensylvanicus*. Because specimens were heavily damaged during the DNA extraction process, we did not retain museum vouchers. However, photographic vouchers of most specimens can be accessed from the Dryad Digital Repository https://doi.org/10.5061/dryad.08kprr5b2. See Suppl. material 1: appendix S1 for a list of specimens examined, including locality data and mitochondrial haplotype for each.

DNA Extraction

DNA was extracted from either the head and thorax or all legs of each specimen in sterile conditions with QIAGEN® DNeasy Blood and Tissue kits using the manufacturer's protocol for DNA extraction from insect tissue, with minor adjustments. Specifically, body parts were removed from each individual bee using a sterile razor blade, and then chopped into smaller pieces. Tissue was placed in a 1.7 µl microcentrifuge tube and homogenized with a disposable micropestle prior to adding the tissue lysis buffer. Two final elutions, the first of which (Q1) was 200 µl and the second (Q2) 100 µl, were performed for each sample. DNA concentrations were determined using a Qubit™ Fluorometer. In the case of samples whose Q1 DNA concentrations were lower than 10 ng/ul, Q1 and Q2 were combined and concentrated using a Thermo Savant SpeedVac Concentrator. Samples (Q1 or concentrated Q1 + Q2) were then prepared for sequencing in volumes that yielded approximately 2 ng of DNA.

Genomic ddRAD-sequencing

Genomic sequence data were generated using a reduced-representation genomic sequencing approach (ddRADseq) following methods described in Peterson et al. (2012). All libraries were prepared and sequenced at the Texas A&M AgriLife Genomics Facility. Briefly, genomic DNA was digested using restriction enzymes EcoRI and MspI. Barcode adaptors (110bp) were ligated to each fragment, and DNA libraries were amplified using PCR. Fragments ranging from 225–500 bases in length were size selected using a Pippen Prep instrument (Sage Science). Amplified size-selected fragment libraries were quantified and pooled in equimolar amounts, and then sequenced on two lanes of an Illumina HiSeq 4000 (150 bp paired-end reads). Two sequencing runs were performed in order to generate sufficient read depth, and raw reads of the two runs were combined after verifying that the restriction enzyme cut-sites and sample-specific barcodes were removed. The initial ddRADseq dataset (n = 166 samples) consisted of 694,934,628

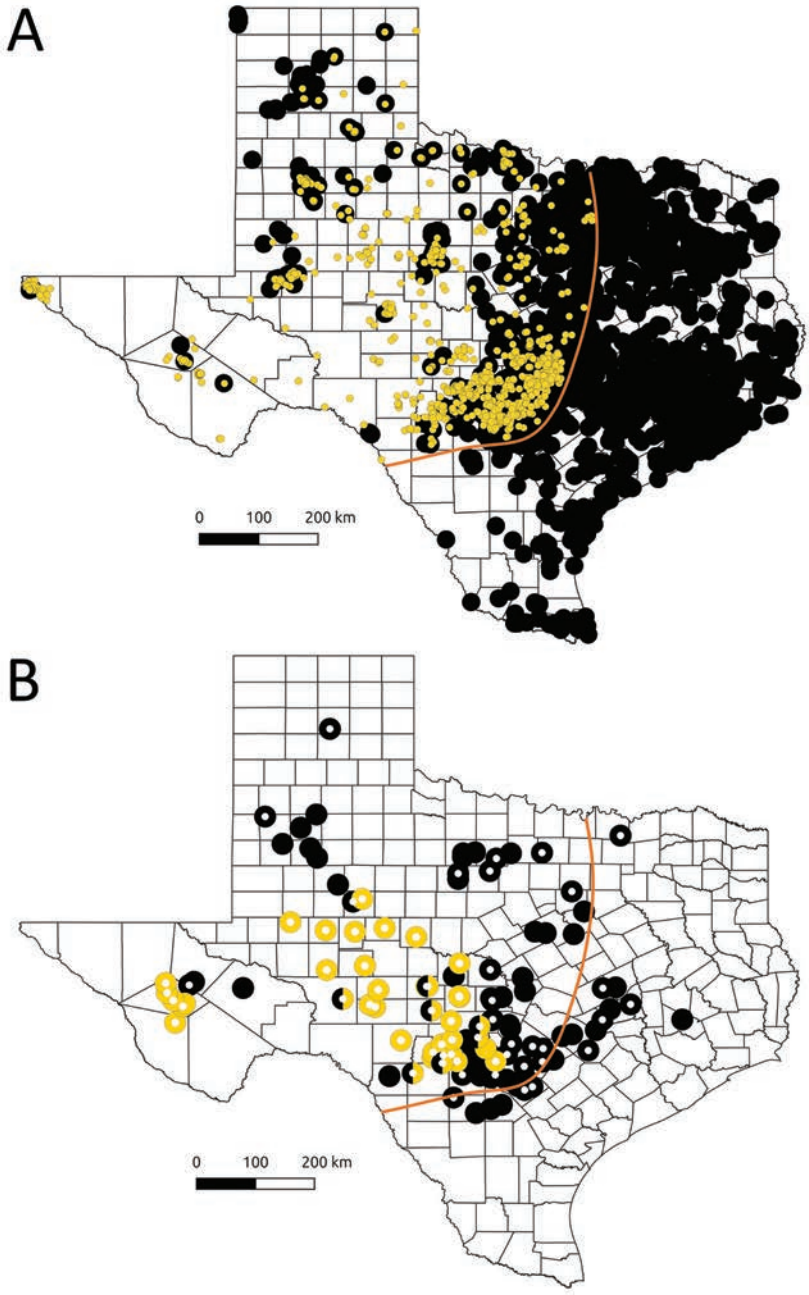

Figure 2. Occurrence of *B. pensylvanicus* (larger black circles) and *B. sonorus* (smaller yellow circles) within Texas based on iNaturalist observations (**A**) locations sampled for this study (**B**) showing locations with *B. pensylvanicus* (black circles), *B. sonorus* (yellow circles), and both species (half black and half yellow circles) as identified by ddRADseq. White dots over colored circles are locations from which mtDNA sequences were also obtained. Orange line indicates the apparent eastern- and southern-most extent of *B. sonorus* (based on iNaturalist data) for ease of comparison between the two figures.

paired demultiplexed raw sequence reads. Using Fastx Toolkit v. 0.0.13 (http://hannonlab.cshl.edu/fastx_toolkit/), we trimmed the first five and four bases from the forward and reverse reads, respectively, to remove low quality sites based on visualization of the fastq files. We employed the ipyrad v.0.7.15 pipeline (http://github.com/dereneaton/ipyrad; Eaton 2020) for assembly, variant calling, and quality filtering.

For ipyrad, default parameters were specified unless otherwise noted for each of the seven steps used in the pipeline. Individual reads were filtered based on a minimum Phred quality score of 20 and a maximum number of Ns in a read set to 5. Reads were then de-replicated, followed by within sample de novo clustering using VSEARCH (Rognes et al. 2016). Reads were matched with a minimum sequence similarity threshold of 0.85. Clustered sequences were then aligned using MUSCLE (Edgar 2004), and rates of heterozygosity and sequencing error were then estimated across sites for subsequent consensus base calling and filtering. We assumed a maximum of 2 consensus alleles per individual and removed consensus sequences with >5 Ns per end of paired-end reads. After clustering and aligning reads for each sample to consensus sequences, the dataset was filtered based on maximum number of single nucleotide polymorphisms (SNPs) per locus (20), maximum number of indels allowed per read (8), maximum proportion of shared heterozygous sites per locus (0.5), and minimum number of samples per locus (97 for *B. pensylvanicus*, 52 for *B. sonorus*; or 90% for each group). We performed final filtering using VCFtools as follows: max-missing 0.8 (to remove loci with genotypes having ≥ 20% missing data), min-alleles 2 and max-alleles 2 (to include only biallelic sites), mac 2 (to include only sites with minor allele count ≥ 2), and thinned to retain only 1 SNP per locus.

In order to assign individuals to clusters and identify potential admixture between *B. pensylvanicus* and *B. sonorus*, we performed a principal components analysis (PCA), conducted STRUCTURE analyses (a Bayesian clustering method), and created a NeighborNet network. PCA was performed using R (R Core Team 2021) and the package adegenet 2.1.10 (Jombart 2008). The software STRUCTURE 2.3.4 (Pritchard et al. 2000; Falush et al. 2003), given a specified number of clusters (K), estimates population membership for each individual by assuming Hardy-Weinberg and linkage equilibrium within clusters. Therefore, we limited our dataset to a single SNP per RADseq locus to reduce bias due to linkage among SNPs. Each run consisted of a burn-in length of 50,000 iterations and a run length of 500,000 iterations. Each run for K = 1 to 4 was replicated ten times using an ancestry model assuming admixture, a model of correlated allele frequencies that did not include prior information on population origin, and an individual alpha for each population (Wang 2017). StrAuto (Chhatre and Emerson 2017) which implements GNU parallel (Tange 2023) was used to automate STRUCTURE runs across multiple cores of a Jetstream virtual machine (Stewart et al. 2015; Towns et al. 2014). Structure Harvester (Earl and vonHoldt 2012) was used to assess likelihood values across multiple values of K. Results of multiple STRUCTURE runs at each value of K were visualized using CLUMPAK (Kopelman et al. 2015), which implements CLUMPP (Jakobsson and Rossenberg 2007) and DISTRUCT (Rosenberg 2004) to align runs across K values and identify major and

minor modalities among runs (Jakobsson and Rosenberg 2007). We constructed the NeighborNet network using SplitsTree4 v.4.13.1 (Huson and Bryant 2006) using p-distance and 1000 bootstrap replicates.

Mitochondrial sequencing (COI)

For a subset of the Texas specimens (and eight *B. sonorus* from California), we amplified a portion of the mitochondrial cytochrome c oxidase subunit I (COI) gene using polymerase chain reaction (PCR) and sequenced (forward and reverse) the resulting PCR products using automated Sanger dideoxy chain termination sequencing. This dataset included 77 of the 166 Texas specimens (45 *B. sonorus* and 32 *B. pensylvanicus*) because COI failed to amplify or sequence in all 166 specimens, and the eight *B. sonorus* from California (Genbank accession numbers PP840056–PP840059). We carried out PCRs and sequencing reactions using the primers LCO1490 and HCO2198 (Folmer et al. 1994), targeting a region of 658 bp (excluding primers). PCR reactions occurred in a final volume of 25 µL consisting of 1X buffer, 0.16 mM deoxynucleotide triphosphates, 2.5 mM of $MgCl_2$, 0.1 µM of each primer, and 0.05 units of Taq DNA polymerase. The thermal profile consisted of a step-down procedure with the initial denaturation cycle consisting of 120 seconds at 95 °C, then 20 cycles of 30 seconds at 95 °C, 30 seconds at an initial temperature of 56 °C stepping down 0.5 °C per cycle to a 20th cycle temperature of 46 °C, then 90 seconds at 72 °C, 20 cycles of 30 seconds at 95 °C, 30 seconds at 46 °C, and 90 seconds at 72 °C followed by a final extension of 72 °C for 10 minutes.

In addition to sequences that we generated, we obtained five sequences of *B. pensylvanicus* from BOLD (http://www.barcodinglife.org; Georgia: BBBEE941-11 and BBBEE939-11; Florida: BBHYA070-12, BBHYA087-12, and BBHYA069-12) and one each of *B. transversalis* (Olivier, 1789), *B. mexicanus* Cresson, 1879, *B. medius* Cresson, 1863 and *B. fervidus* (Fabricius, 1798) from Genbank (www.ncbi.nlm.nih.gov/Genbank; KJ848950, MG279409, KC853364, and MG448456).

We aligned sequences using ClustalW within the program MEGA-X (Kumar et al. 2018) and trimmed the alignment to omit missing sites at each end resulting in 520 bp. We constructed a phylogenetic tree using MrBayes with *B. mesomelas* Gerstäcker, 1869 as an outgroup (Genbank HQ563805) based on its relationship to the other species included (Cameron et al. 2007). The best-fit substitution model was determined to be HKY in jModelTest v.2.1.10 (Guindon and Gascuel 2003; Darriba et al. 2012) using BIC. Within MrBayes, the sample and print frequency was set to 500, the diagnostic frequency was 5,000, and the run length was 1,000,000. Trees were summarized to produce posterior probabilities of each split and branch lengths. We visualized the resulting tree using FigTree 1.4.4 (http://tree.bio.ed.ac.uk/software/figtree/). Uncorrected mean genetic distances (p-distances) between haplotypes were generated using the program MEGA-X (Kumar et al. 2018). We created a median-joining haplotype network using POPART 1.7 (Bandelt et al. 1999; Leigh and Bryant 2015) using uncorrected p-distance.

Results

Geographic distribution

The iNaturalist occurrence data included 2,008 *B. sonorus* (GBIF.org 2024a; retrieved on 20 April 2024 and included observations spanning the years 2005–2024) and 11,984 *B. pensylvanicus* (GBIF.org 2024b; retrieved on 20 April 2024 and included observations spanning the years 1972–2024 [only two observations predated 2004]). iNaturalist records documented the occurrence of *B. pensylvanicus* state-wide and were largely consistent with Warriner (2012), which was based on vouchered museum specimens, and Beckham and Atkinson (2017), which included both vouchered museum specimens and citizen science data. For *B. sonorus*, however, iNaturalist records showed a broader distribution than reported by both Warriner (2012) and Beckham and Atkinson (2017), extending further north and northwest than reported in either publication. Also, two records reported by Warriner (2012) appeared extralimital relative to iNaturalist records. We confirmed one of these records as being in error (the locality was misinterpreted; see Discussion).

ddRADseq analyses

We obtained an average of 4.2 million paired-end reads per sample after *q*-score and adapter filtering. Sequencing reads are available on the NCBI Short Reads Archive (BioProject ID PRJNA1115193). After de novo assembly and subsequent filtering using ipyrad, 17,352 loci were identified. The final dataset consisted of 3,371 loci after further filtering using VCFtools. We conducted all subsequent analyses using this final dataset.

The PCA showed two well-separated clusters of individuals (Fig. 3). STRUCTURE assigned individuals to two groups for K = 2, 3, and 4 (Fig. 4A; Suppl. material 2), with consistency across all 10 runs (no multimodality). At K = 2, membership coefficients were >0.842 for *B. pensylvanicus* ($\bar{x}$ = 0.989, SD = 0.026) and >0.942 for *B. sonorus* ($\bar{x}$ = 0.995, SD = 0.013). The NeighborNet network clearly separated samples into two groups (Fig. 4B). All three analyses were concordant with species identification of each individual based on coloration.

Mitochondrial (COI) analyses

Of the 90 COI sequences analyzed, we identified five COI haplotypes: one from *B. sonorus* and 4 from *B. pensylvanicus* (Fig. 5; Suppl. material 1: appendix S1; Genbank accession numbers PP840056–PP840059; BOLD accession number BBHYA069-12). Within the Bayesian phylogenetic tree and haplotype network, all specimens clustered according to species (as defined by coloration; Fig. 5). Within the haplotype network, haplotypes of the two species were separated by five mutational steps. The mean intraspecific genetic distance (p-distance) was 0.10% for *B. pensylvanicus* and 0% for *B. sonorus*. The mean interspecific genetic distance (p-distance between the two species) was 1.03%.

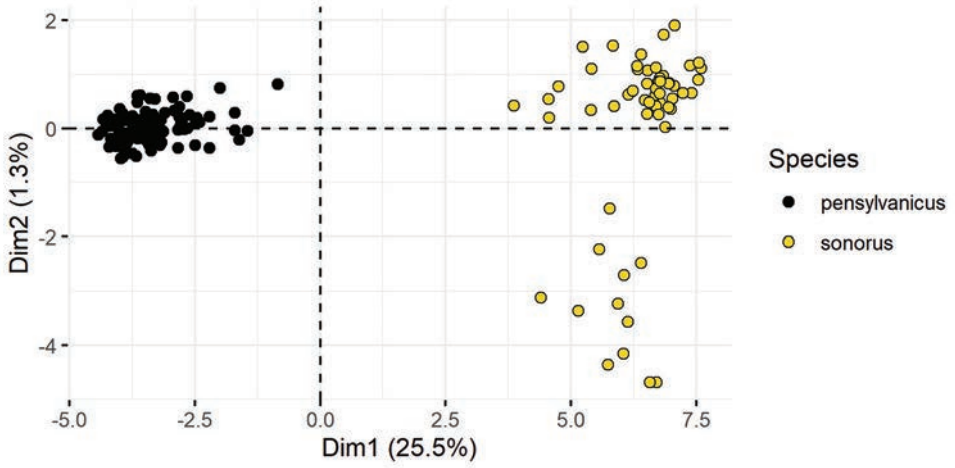

Figure 3. Principal components analysis based on ddRADseq of Texas *B. pensylvanicus* and *B. sonorus*.

Discussion

We evaluated species boundaries of the taxonomically controversial bumble bees *B. sonorus* and *B. pensylvanicus* within a broad area of sympatry using two genetic datasets (nuclear ddRADseq and mitochondrial COI) combined with examination of setal coloration (banding pattern and shade of yellow). To aid in interpreting our genetic data, we documented the extent of geographic overlap of *B. sonorus* and *B. pensylvanicus* using occurrence data from the iNaturalist platform. While the iNaturalist dataset is limited to presence data, we relied on these data because there are numerous records documented within the past two decades, each of which can be assessed visually to verify correct species identification. We found the range of *B. sonorus* documented in iNaturalist to be broader than that reported by either Warriner (2012) or Beckham and Atkinson (2017); this could be due to the different datasets used for each study or might suggest a *B. sonorus* range expansion. Warriner (2012) documented Texas bumble bee distributions primarily using historical data from vouchered museum specimens. In Warriner (2012), two county records of *B. sonorus* in eastern Texas (Hunt and Grimes counties) appeared to be extralimital. We reached out to the collection curators to verify locality data and species identification of these two records. The record reported to be *B. sonorus* from Hunt Co. had actually been collected in Hunt, TX which is in Kerr Co., Texas (well within the known distribution of *B. sonorus*). The Grimes Co. specimen of *B. sonorus* appears to be valid and was collected in 1961; however, the absence of any other specimens of *B. sonorus* this far east casts doubt on this record. Beckham and Atkinson (2017) also relied heavily on museum specimens, incorporating the data gathered by Warriner (2012) and additional museum records; a small amount of citizen science data available at the time was also included. Many museums identify *B. sonorus* as *B. pensylvanicus*, and so it is possible that both papers

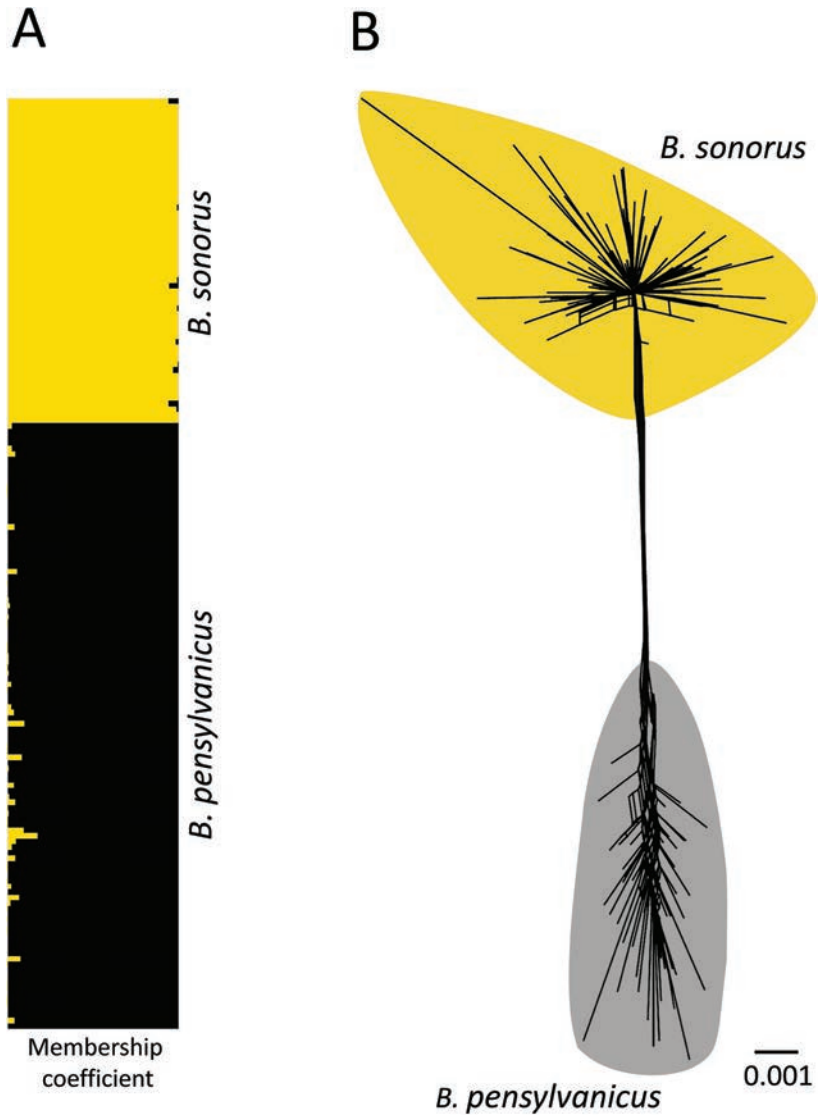

Figure 4. Results of STRUCTURE analysis (bars indicate membership coefficients) (**A**) and Neighbor-Net network (**B**) of Texas *B. pensylvanicus* and *B. sonorus* based on ddRADseq.

underreported the presence of *B. sonorus* and may have also overreported the presence of *B. pensylvanicus*. Additionally, the range of *B. sonorus* may be expanding north and east. Since the study by Beckham and Atkinson (2017), many more iNaturalist records of Texas bumble bees have been uploaded. Based on the totality of evidence, *B. sonorus* occurs in the western two-thirds of Texas (Fig. 2). In contrast, *B. pensylvanicus* occurs throughout Texas, including as far west as the vicinity of El Paso (Fig. 2). Thus, the area of sympatry includes the entirety of the distribution of *B. sonorus* in the state of Texas.

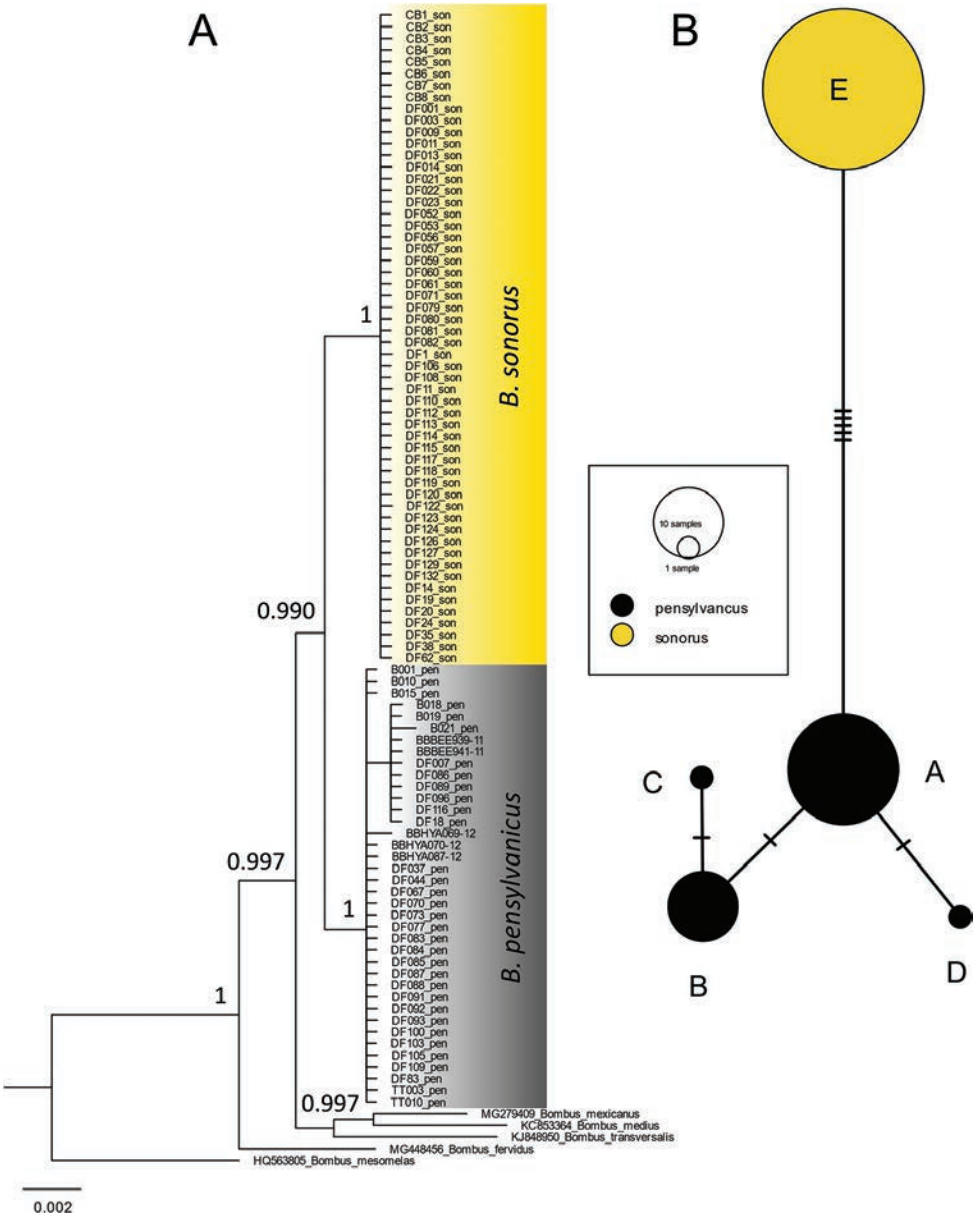

Figure 5. Bayesian phylogenetic tree of individuals (**A**) and median-joining haplotype network (**B**) of *Bombus* based on COI mtDNA sequences. The tree was rooted with *B. mesomelas*. Numbers along branches in the phylogenetic tree indicate support (posterior probability; provided only for major clades). Within the network, sizes of circles are proportional to haplotype frequency and lines across branches represent mutational steps between haplotypes. The color of circles in the network indicates species in which the haplotype was found.

All of our analyses were consistent in providing evidence that *B. sonorus* and *B. pensylvanicus* are genetically distinct across the documented area of sympatry in Texas. We found no evidence of a pattern of clinal variation, hybridization, or historical

introgression within the broad area of sympatry sampled for this project (Texas). If these color forms represent a single species, or if extensive interbreeding occurred, we would have expected one of three patterns: (1) a single genetic group, (2) individuals not grouping concordant with coloration, or (3) individuals having mixed membership to more than one cluster (for example, an F1 hybrid between two divergent lineages would have approximately 50% membership to each of two clusters in STRUCTURE). Instead, all analyses showed two distinct genetic groups. The mitochondrial COI dataset showed all individuals forming reciprocally monophyletic clades in concordance with their identification as *B. sonorus* or *B. pensylvanicus* according to coloration. Additionally, we found no instances of individuals identified as one species by ddRADseq possessing a mtDNA haplotype of the other species. If the two forms hybridize extensively and produce fertile offspring within the area of sympatry, historical introgression of mitochondria (due to backcrossing) would be expected, resulting in a lack of concordance between datasets. The lowest STRUCTURE membership coefficient was 0.842, which could represent a hybrid backcross individual; however, incomplete lineage sorting (the presence of shared variation predating speciation) results in patterns such as this which can be attributed falsely to hybridization (Hey 2006). Furthermore, perfect assignment of all individuals is never seen in this type of analysis. Given the low COI sequence divergence between *B. sonorus* and *B. pensylvanicus*, combined with no evidence of mtDNA introgression, incomplete sorting of nuclear alleles is to be expected.

Our results showed the two taxa as reciprocally monophyletic. This contrasts with Cameron et al. (2007) which showed a polyphyletic relationship between *B. sonorus* and *B. pensylvanicus*. Their study addressed the entire *Bombus* genus (thus included only two specimens each of *B. sonorus* and *B. pensylvanicus*) and used a concatenation of four nuclear genes and the mitochondrial 16S rRNA gene. Given the lower overall substitution rate of these genes, combined with the close relationship between these two species (as shown by the 1.04% COI divergence from our study), the polyphyletic pattern in Cameron et al. (2007) could be explained by incomplete lineage sorting, a well-known phenomenon among recently diverged species (Ferrer Obiol et al. 2021; DeRaad et al 2023; Nabholz 2024). We do not interpret a particular threshold of COI divergence as indicative of species status. There are numerous examples that show lack of mtDNA divergence among species that can be delineated by other means (Wiemers and Fiedler 2007; Ammerman et al. 2016; Nabholz 2024). For purposes of our study, the presence of reciprocal monophyly (regardless of degree of divergence) which is concordant with coloration and RADseq data provides evidence that hybridization (either ongoing or historical) is minimal. We interpret the low degree of divergence as evidence that these taxa are sister species that evolved from a common ancestor relatively recently.

All specimens that we collected for this study were clearly identifiable to species based on coloration, and we observed no phenotypically intermediate specimens among our samples. Milliron (1973) mentioned that the difference in shade of yellow was less in areas of sympatry. However, among the specimens we collected the shade of yellow was consistent across all individuals. Labougle (1990) reported that chromatically intermediate specimens occur, mainly in northeastern Mexico and southwestern Texas, referring to Mexican specimens as being difficult to place in either taxon because of

color of the scutellum and punctation of the clypeus intermediate between them. However, within their key, Labougle (1990) stated "scutellum and T-1 sometimes with an even mixture of black and yellow hairs". What constituted "chromatically intermediate" was not described. Among our samples, we did not observe specimens that we would describe as chromatically intermediate; the color of the scutellum was always distinct, as was the shade of yellow. Given that our sampling efforts did not extend into Mexico, we cannot be certain that the intermediates described by Labougle (1990) do not exist. There is a great need for future work in Mexico to verify the existence of intermediates.

Upon examining photographic records on iNaturalist, we did find several instances of female *B. pensylvanicus* in the U.S. with numerous yellow hairs on the scutellum (GBIF.org 2004c), as mentioned by Milliron (1973) and Labougle (1990) in their description of *B. pensylvanicus*. Importantly, these specimens were documented far from areas of sympatry between the two species (Florida, Georgia, Mississippi, and Arkansas) and, therefore, this coloration could not have been acquired by interbreeding with *B. sonorus*. We urge caution in using chromatic intermediates as evidence of hybridization given that female specimens with numerous yellow hairs on the scutellum occur far from areas of sympatry.

The observation by Peters (1968) of an individual of *B. sonorus* at the entrance of a nest along with 10 *B. pensylvanicus* was interpreted as evidence that these are color variants of the same species. However, such an interaction should not be used to determine species status. Plath (1927) found *B. terricola* Kirby, 1837 workers in 6 of 36 nests of *B. affinis* Cresson, 1863 which he explained by "natural requeening." Additionally, several instances of attempted mating involving a species of *Bombus* and another species have been photo-documented on iNaturalist (GBIF 2004d). These include *B. impatiens* Cresson 1863 with *Xylocopa virginica* (Linnaeus, 1771), *Andrena* Fabricius, 1775 with *B. griseocollis* (DeGeer, 1773), *B. fervidus* with *B. bimaculatus* Cresson, 1863, *B. impatiens* with *B. fraternus* (Smith, 1854), and *B. flavifrons* Cresson, 1863 with *B. melanopygus* Nylander, 1848. Based on these observations, it is not surprising to also see photo-documentation of a *B. sonorus* male attempting to mate with a *B. pensylvanicus* female (GBIF.org 2024e). Lastly, successful hybridization between recognized species of *Bombus* has been documented but has not been used as evidence that the species were morphological variants of the same species (Kanbe et al. 2008; Kondo et al. 2009; Yoon et al. 2009; Yoon et al. 2011; Kubo et al. 2023). In fact, natural hybridization between recognized species of animals and plants has been well documented (Arnold 1997; Mallet 2005; Taylor and Larson 2019). A critical factor in species delimitation is not whether hybridization occurs, but to what extent.

Conclusion

Our data demonstrate that hybridization events between *B. pensylvanicus* and *B. sonorus* are absent or very rare, despite ample opportunity for mating in sympatry, justifying the status of *B. sonorus* as a distinct species under the Biological Species Concept (Mayr 1963). Nuclear ddRADseq, mitochondrial COI, and coloration were concordant in distinguishing *B. sonorus* from *B. pensylvanicus*. Given the lack of evidence supporting

clinal variation, hybridization, or historical introgression between these species across the broad area of sympatry in Texas, it seems unlikely that these phenomena would be occurring in Mexico where the two species are also reportedly sympatric. However, future research should focus on the assessment of populations of *B. sonorus and B. pensylvanicus* in Mexico, to include documentation of areas in which the two species are sympatric and confirmation of the anecdotal reports of individuals displaying intermediate coloration. Until evidence of clinal variation or extensive hybridization between *B. sonorus* and *B. pensylvanicus* is documented using multilocus genetic datasets, we recommend that *B. sonorus* be recognized as a distinct species and that conservation efforts designate them as such.

Data accessibility

Raw sequencing reads (ddRADseq) are available on the NCBI Short Reads Archive (BioProject ID PRJNA1115193). COI mtDNA sequences are available at NCBI (Genbank accession numbers: PP840056–PP840059). The ddRADseq VCF, COI sequence alignment, and photographic vouchers of specimens are available from the Dryad Digital Repository https://doi.org/10.5061/dryad.08kprr5b2.

Acknowledgments

This research was supported by the Texas Parks and Wildlife Department (State Wildlife Grant, 2016), the Advanced Environmental Research Institute at the University of North Texas, and Tarleton State University. We thank the following individuals who assisted with collection efforts: Tom Barnes, David Beckham, Deborah Douglas, Tom Fisher, Danny Kern, Michael Eckenfels, and Scott Longing. We thank John Ascher, Jack Neff, Leif Richardson, Robbin Thorp, Michael Warriner, and Paul Williams for providing insight via personal communications. We thank Joel Neylon for providing a list of iNaturalist observations of attempted interspecific mating and examples in the literature of interspecific behaviors. We thank the >5000 observers and >1000 identifiers on the iNaturalist platform for their contributions to documenting and identifying, respectively, *Bombus* within the state of Texas and beyond. Special thanks to Joel Neylon and John Ascher who confirmed and contributed identifications for over >13,000 and >8000 specimens, respectively, of Texas *Bombus* on iNaturalist. We also thank the four reviewers for helpful comments.

References

Ammerman LK, Lee DN, Pfau RS (2016) Patterns of genetic divergence among *Myotis californicus*, *M. ciliolabrum*, and *M. leibii* based on amplified fragment length polymorphism. Acta Chiropterologica 18: 336–346. https://doi.org/10.3161/15081109ACC2016.18.2.003

Arnold ML (1997) Natural hybridization and evolution. Oxford University Press on Demand (Oxford, UK): 1–232. https://doi.org/10.1093/oso/9780195099744.001.0001

Bandelt HJ, Forster P, Röhl A (1999) Median-joining networks for inferring intraspecific phylogenies. Molecular Biology and Evolution 16: 37–48. https://doi.org/10.1093/oxfordjournals.molbev.a026036

Bartomeus I, Ascher JS, Gibbs J, Danforth BN, Wagner DL, Hedtke SM, Winfree R (2013) Historical changes in northeastern US bee pollinators related to shared ecological traits. Proceedings of the National Academy of Sciences 110: 4656–4660. https://doi.org/10.1073/pnas.1218503110

Beckham JL, Atkinson S (2017) An updated understanding of Texas bumble bee (Hymenoptera: Apidae) species presence and potential distributions in Texas, USA. PeerJ 5: e3612. https://doi.org/10.7717/peerj.3612

Cameron SA, Hines HM, Williams PH (2007) A comprehensive phylogeny of the bumble bees (*Bombus*). Biological Journal of the Linnean Society 91: 161–188. https://doi.org/10.1111/j.1095-8312.2007.00784.x

Cameron SA, Lozier JD, Strange JP, Koch JB, Cordes N, Solter LF, Griswold TL (2011) Patterns of widespread decline in North American bumble bees. Proceedings of the National Academy of Sciences of the United States of America 108: 662–667. https://doi.org/10.1073/pnas.1014743108

Chhatre VE, Emerson KJ (2017) StrAuto: automation and parallelization of STRUCTURE analysis. BMC Bioinformatics 18: 1–5. https://doi.org/10.1186/s12859-017-1593-0

Colla SR, Gadallah F, Richardson L, Wagner D, Gall L (2012) Assessing declines of North American bumble bees (*Bombus* spp.) using museum specimens. Biodiversity & Conservation 21: 3585–3595. https://doi.org/10.1007/s10531-012-0383-2

Colla SR, Packer L (2008) Evidence for decline in eastern North American bumblebees (Hymenoptera: Apidae), with special focus on *Bombus affinis* Cresson. Biodiversity & Conservation 17: 1379–1391. https://doi.org/10.1007/s10531-008-9340-5

Colla S, Richardson L, Williams P (2011) Bumble bees of the eastern United States. US Department of Agriculture Pollinator Partnership (Washington, D.C.): 1–103.

Committee on the Status of Pollinators in North America, National Research Council (2007) Status of Pollinators in North America. National Academy Press (Washington, DC): 1–326. https://doi.org/10.17226/11761

Darriba D, Taboada GL, Doallo R, Posada D (2012) jModelTest 2: More models, new heuristics and parallel computing. Nature Methods 9: 772. https://doi.org/10.1038/nmeth.2109

DeRaad DA, McCullough JM, DeCicco LH, Hime PM, Joseph L, Andersen MJ, Moyle RG (2023) Mitonuclear discordance results from incomplete lineage sorting, with no detectable evidence for gene flow, in a rapid radiation of *Todiramphus* kingfishers. Molecular Ecology 32: 4844–4862. https://doi.org/10.1111/mec.17080

Duennes MA, Lozier JD, Hines HM, Cameron SA (2012) Geographical patterns of genetic divergence in the widespread Mesoamerican bumble bee *Bombus ephippiatus* (Hymenoptera: Apidae). Molecular Phylogenetics and Evolution 64: 219–231. https://doi.org/10.1016/j.ympev.2012.03.018

Earl DA, vonHoldt BM (2012) STRUCTURE HARVESTER: A website and program for visualizing STRUCTURE output and implementing the Evanno method. Conservation Genetics Resources 4: 359–361. https://doi.org/10.1007/s12686-011-9548-7

Eaton DA, Overcast I (2020) ipyrad: Interactive assembly and analysis of RADseq datasets. Bioinformatics 36: 2592–2594. https://doi.org/10.1093/bioinformatics/btz966

Edgar RC (2004) MUSCLE: multiple sequence alignment with high accuracy and high throughput. Nucleic Acids Research 32: 1792–1797. https://doi.org/10.1093/nar/gkh340

Falush D, Stephens M, Pritchard JK (2003) Inference of population structure using multilocus genotype data: linked loci and correlated allele frequencies. Genetics 164: 1567–1587. https://doi.org/10.1093/genetics/164.4.1567

Ferrer Obiol J, James HF, Chesser RT, Bretagnolle V, González-Solís J, Rozas J, Riutort M, Welch AJ (2021) Integrating sequence capture and restriction site-associated DNA sequencing to resolve recent radiations of pelagic seabirds. Systematic Biology 70: 976–996. https://doi.org/10.1093/sysbio/syaa101

Folmer O, Black M, Hoeh W, Lutz R, Vrijenhoek R (1994) DNA primers for amplification of mitochondrial cytochrome c oxidase subunit I from diverse metazoan invertebrates. Molecular Marine Biology Biotech: 294–299.

Franklin HJ (1913) The Bombidae of the new world. Transactions of the American Entomological Society 38: 177–486. https://doi.org/10.5962/bhl.title.122585

Galtier N, Nabholz B, Glémin S, Hurst GDD (2009) Mitochondrial DNA as a marker of molecular diversity: a reappraisal. Molecular Ecology 18: 4541–4550. https://doi.org/10.1111/j.1365-294x.2009.04380.x

GBIF.org (2024a) GBIF Occurrence Download. https://doi.org/10.15468/dl.g3k63f

GBIF.org (2024b) GBIF Occurrence Download. https://doi.org/10.15468/dl.gmfudu

GBIF.org (2024c) GBIF Occurrence Download. https://doi.org/10.15468/dl.fwppxw

GBIF.org (2024d) GBIF Occurrence Download. https://doi.org/10.15468/dl.sng27x

GBIF.org (2024e) GBIF Occurrence Download. https://doi.org/10.15468/dl.u8u39w

Grixti JC, Wong LT, Cameron SA, Favret C (2009) Decline of bumble bees (*Bombus*) in the North American Midwest. Biological Conservation 142: 75–84. https://doi.org/10.1016/j.biocon.2008.09.027

Guindon S, Gascuel O (2003) A simple, fast and accurate method to estimate large phylogenies by maximum-likelihood. Systematic Biology 52: 696–704. https://doi.org/10.1080/10635150390235520

Handlirsch A (1888) Die Hummelsammlung des k. k. naturhistorischen Hofmuseums. Annalen des Naturhistorischen Museums in Wien 3: 209–250.

Hatfield R, Jepsen S, Thorp R, Richardson L, Colla S, Foltz Jordan S (2015) *Bombus pensylvanicus*. The IUCN Red List of Threatened Species 2015: e.T21215172A21215281.

Hurst GDD, Jiggins FM (2005) Problems with mitochondrial DNA as a marker in population, phylogeographic and phylogenetic studies: the effects of inherited symbionts. Proceedings of the Royal Society B: Biological Sciences 272: 1525–1534. https://doi.org/10.1098/rspb.2005.3056

Huson DH, Bryant D (2006) Application of phylogenetic networks in evolutionary studies. Molecular Biology and Evolution 23: 254–267. https://doi.org/10.1093/molbev/msj030

Jakobsson M, Rosenberg NA (2007) CLUMPP: A cluster matching and permutation program for dealing with label switching and multimodality in analysis of population structure. Bioinformatics 23: 1801–1806. https://doi.org/10.1093/bioinformatics/btm233

Jombart T (2008) adegenet: a R package for the multivariate analysis of genetic markers. Bioinformatics 24: 1403–1405. https://doi.org/10.1093/bioinformatics/btn129

Kanbe Y, Okada I, Yoneda M, Goka K, Tsuchida K (2008) Interspecific mating of the introduced bumblebee *Bombus terrestris* and the native Japanese bumblebee *Bombus hypocrita sapporoensis* results in inviable hybrids. Naturwissenschaften 95: 1003–1008. https://doi.org/10.1007/s00114-008-0415-7

Kondo NI, Yamanaka D, Kanbe Y, Kunitake YK, Yoneda M, Tsuchida K, Goka K (2009) Reproductive disturbance of Japanese bumblebees by the introduced European bumblebee *Bombus terrestris*. Naturwissenschaften 96: 467–475. https://doi.org/10.1007/s00114-008-0495-4

Kopelman NM, Mayzel J, Jakobsson M, Rosenberg NA, Mayrose I (2015) CLUMPAK: A program for identifying clustering modes and packaging population structure inferences across K. Molecular Ecology Resources 15: 1179–1191. https://doi.org/10.1111/1755-0998.12387

Kubo R, Asanuma Y, Fujimoto E, Okuyama H, Ono M, Takahashi J-I (2023) Cross-mating between the alien bumblebee *Bombus terrestris* and two native Japanese bumblebees, *B. hypocrita sapporoensis* and *B. cryptarum florilegus*, in the Nemuro Peninsula, Japan. Scientific Reports 13: 11506. https://doi.org/10.1038/s41598-023-38631-7

Kumar S, Stecher G, Li M, Khyaz C, Tamura K (2018) MEGA X: Molecular evolutionary genetics analysis across computing platforms. Molecular Biology and Evolution 35: 1547–1549. https://doi.org/10.1093/molbev/msy096

Labougle JM (1990) *Bombus* of Mexico and Central America (Hymenoptera, Apidae). University of Kansas Science Bulletin 54: 35–73.

Leigh WL, Bryant D (2015) POPART: Full-feature software for haplotype network construction. Methods in Ecology and Evolution 6: 1110–1116. https://doi.org/10.1111/2041-210X.12410

Lozier JD, Jackson JM, Dillon ME, Strange JP (2016) Population genomics of divergence among extreme and intermediate color forms in a polymorphic insect. Ecology and Evolution 6: 1075–1091. https://doi.org/10.1002/ece3.1928

Mallet J (2005) Hybridization as an invasion of the genome. Trends in Ecology & Evolution 20: 229–237. https://doi.org/10.1016/j.tree.2005.02.010

McKendrick L, Provan J, Fitzpatrick Ú, Brown MJF, Murray TE, Stolle E, Paxton RJ (2017) Microsatellite analysis supports the existence of three cryptic species within the bumble bee *Bombus lucorum sensu lato*. Conservation Genetics 18: 573–584. https://doi.org/10.1007/s10592-017-0965-3

Milliron HE (1973) A monograph of the Western Hemisphere bumblebees (Hymenoptera: Apidae; Bombinae). II. The genus *Megabombus* subgenus *Megabombus*. Memoirs of the Entomological Society of Canada 89: 81–237. https://doi.org/10.4039/entm10589fv

Moritz C, Cicero C (2004) DNA Barcoding: Promise and Pitfalls. PLoS Biology 2: e354. https://doi.org/10.1371/journal.pbio.0020354

Nabholz B (2024) Incomplete lineage sorting explains the low performance of DNA barcoding in a radiation of four species of Western European grasshoppers (Orthoptera: Acrididae: Chorthippus). Biological Journal of the Linnean Society 141: 33–50. https://doi.org/10.1093/biolinnean/blad106

Peters DS (1968) Beitrage zur Kenntnis aculeater Hymenopteren von Mexiko. I. Apinae (Apidae, Apoidea). Senckenbergiana Biologica 49: 237–248.

Peterson BK, Weber JN, Kay EH, Fisher HS, Hoekstra HE (2012) Double Digest RADseq: An inexpensive method for de dovo SNP discovery and genotyping in model and non-model species. PLoS ONE 7: e37135. https://doi.org/10.1371/journal.pone.0037135

Plath OE (1927) Notes on the nesting habits of some of the less common new England bumblebees. Psyche: A Journal of Entomology 34: 122–128. https://doi.org/10.1155/1927/43469

Pritchard JK, Stephens M, Donnelly P (2000) Inference of population structure using multilocus genotype data. Genetics 155: 945–959. https://doi.org/10.1093/genetics/155.2.945

QGIS Development Team (2021) QGIS Geographic Information System. Open Source Geospatial Foundation. http://qgis.org

R Core Team (2021) R: A language and environment for statistical computing. R Foundation for Statistical Computing, Vienna, Austria. https://www.R-project.org/

Rognes T, Flouri T, Nichols B, Quince C, Mahé F (2016) VSEARCH: a versatile open source tool for metagenomics. PeerJ 4: e2584. https://doi.org/10.7717/peerj.2584

Stewart CA, Cockerill TM, Foster I, Hancock D, Merchant N, Skidmore E, Stanzione D, Taylor J, Tuecke S, Turner G, Vaughn M, Gaffney NI (2015) Jetstream: a self-provisioned, scalable science and engineering cloud environment. In Proceedings of the 2015 XSEDE Conference Scientific Advancements Enabled by Enhanced Cyberinfrastructure, St. Louis, Missouri (USA), July 2015. Association for Computing Machinery: 1–8. https://doi.org/10.1145/2792745.2792774

Tange O (2023) GNU Parallel 20230122 ('Bolsonaristas'). https://doi.org/10.5281/zenodo.7558957

Taylor HR, Harris WE (2012) An emergent science on the brink of irrelevance: a review of the past 8 years of DNA barcoding. Molecular Ecology Resources 12: 377–388. https://doi.org/10.1111/j.1755-0998.2012.03119.x

Taylor SA, Larson EL (2019) Insights from genomes into the evolutionary importance and prevalence of hybridization in nature. Nature Ecology & Evolution 3: 170–177. https://doi.org/10.1038/s41559-018-0777-y

TPWD [Texas Parks and Wildlife Department] (2012) Texas Conservation Action Plan 2012–2016: Statewide/Multi-region Handbook. In: Connaly W (Ed.) TPWD (Austin, TX, USA): 1–78.

Thorp RW, Horning Jr. DS, Dunning LL (1983) Bumble bees and cuckoo bumble bees of California (Hymenoptera, Apidae). University of California Press (Los Angeles): 1–79.

Towns J, Cockerill T, Dahan M, Foster I, Gaither K, Grimshaw A, Hazlewood V, Lathrop S, Lifka D, Peterson GD, Roskies R, Scott JR, Wilkins-Diehr N (2014) XSEDE: Accelerating scientific discovery. Computing in Science & Engineering 16: 62–74. https://doi.org/10.1109/MCSE.2014.80

Wang J (2017) The computer program STRUCTURE for assigning individuals to populations: easy to use but easier to misuse. Molecular Ecology Resources 17: 981–990. https://doi.org/10.1111/1755-0998.12650

Warriner MD (2012) Bumble bees (Hymenoptera: Apidae) of Texas: historical distributions. The Southwestern Naturalist 57: 442–445. https://doi.org/10.1894/0038-4909-57.4.442

Wiemers M, Fiedler K (2007) Does the DNA barcoding gap exist? – a case study in blue butterflies (Lepidoptera: Lycaenidae). Frontiers in Zoology: 1–16. https://doi.org/10.1186/1742-9994-4-8

Williams PH (1998) An annotated checklist of bumble bees with an analysis of patterns of description (Hymenoptera: Apidae, Bombini). Bulletin-Natural History Museum Entomology Series 67: 79–152.

Williams P, Thorp RW, Richardson L, Colla SR (2014) Bumble bees of North America: an identification guide. Princeton University Press (Princeton, NJ): 1–208.

Yoon HJ, Kim SY, Lee KY, Lee SB, Park IG, Kim IS (2009) Interspecific hybridization of the bumblebees *Bombus ignitus* and *B. terrestris*. International Journal of Industrial Entomology 18: 41–48.

Yoon H-J, Park I-G, Lee K-Y, Kim M-A, Jin B-R (2011) Interspecific hybridization of the Korean native bumblebee *Bombus hypocrita sapporoensis* and the European bumblebee *B. terrestris*. International Journal of Industrial Entomology 23: 167–174. https://doi.org/10.7852/ijie.2011.23.1.167

Supplementary material 1

Specimens of *Bombus* examined for this study including locality data, species, sex, whether RADseq data was collected, and mtDNA haplotype

Authors: Jessica L. Beckham, Jeff A. Johnson, Russell S. Pfau

Data type: xlsx

Link: https://doi.org/10.3897/jhr.97.132937.suppl1

Supplementary material 2

Clumpak output from STRUCTURE run files of RADseq data

Authors: Jessica L. Beckham, Jeff A. Johnson, Russell S. Pfau

Data type: pdf

Link: https://doi.org/10.3897/jhr.97.132937.suppl2

JHR 97: 915–936 (2024)
doi: 10.3897/jhr.97.135728
https://jhr.pensoft.net

RESEARCH ARTICLE

JOURNAL OF Hymenoptera RESEARCH
A peer-reviewed open-access journal
The International Society of Hymenopterists

A new species of *Braunsia* (Hymenoptera, Braconidae, Agathidinae), a natural enemy of *Cydalima perspectalis* (Lepidoptera, Crambidae) from South Korea: species description and notes on its biology

Soohyun Kim[1,2,3], Jong Bong Choi[3], Hwal-Su Hwang[1], Marc Kenis[4], M. Lukas Seehausen[4], Ikju Park[5], Jin-Kyung Choi[6], Kyeong-Yeoll Lee[1,2,7], Michael J. Sharkey[8], Ilgoo Kang[3,9]

1 *Department of Applied Biology, Kyungpook National University, Daegu, Republic of Korea* **2** *Department of Plant Protection and Quarantine, Kyungpook National University, Daegu, Republic of Korea* **3** *Department of Ecological Science, Kyungpook National University, Sangju-si, Republic of Korea* **4** *CABI, Delémont, Switzerland* **5** *Department of Entomology, University of California, Riverside, CA, USA* **6** *Department of Science Education, Daegu National University of Education, Daegu, Republic of Korea* **7** *Department of Plant Medicine, Kyungpook National University, Daegu, Republic of Korea* **8** *The Hymenoptera Institute, Redlands, CA, USA* **9** *Department of Entomology, Kyungpook National University, Sangju-si, Republic of Korea*

Corresponding author: Ilgoo Kang (ikang@knu.ac.kr)

Academic editor: Jovana M. Jasso-Martínez | Received 28 August 2024 | Accepted 2 October 2024 | Published 24 October 2024

https://zoobank.org/3AEC7296-DCE5-4750-99EE-757D9ED4AEC1

Citation: Kim S, Choi JB, Hwang H-S, Kenis M, Seehausen ML, Park I, Choi J-K, Lee K-Y, Sharkey MJ, Kang I (2024) A new species of *Braunsia* (Hymenoptera, Braconidae, Agathidinae), a natural enemy of *Cydalima perspectalis* (Lepidoptera, Crambidae) from South Korea: species description and notes on its biology. Journal of Hymenoptera Research 97: 915–936. https://doi.org/10.3897/jhr.97.135728

Abstract

The invasion of *Cydalima perspectalis* (Walker, 1859) (Lepidoptera, Crambidae) poses a significant threat to European ecosystems and North American ornamentals. In an effort to identify potential biological control agents from the native habitats of *C. perspectalis*, a field survey was conducted from 2022 to 2024 in South Korea. During the survey, a new braconid agathidine species of *Braunsia* Kriechbaumer, 1894 was discovered: *Braunsia hodorii* Kang, **sp. nov.** The new species is delimited and described based on morphological, molecular, and phylogenetic data. Additionally, information on the behavior of *B. hodorii* **sp. nov.** is presented regarding the larval external feeding phase. A key to species of *Braunsia* in Korea is included accompanied by detailed images. This research contributes to the evaluation of natural enemies as biological control agents against *C. perspectalis* in its invasive range.

Keywords
Box tree moth, braconid taxonomy, classical biological control, hymenopteran parasitoid, invasive species

Introduction

The expansion of global trade has played a significant role in the introduction of non-indigenous species, particularly through commerce of live plants (Meyerson and Mooney 2007; Roques et al. 2016). Along with the trade of ornamental box trees (also called boxwood, *Buxus* spp., Buxaceae) from Asia to Europe, a lepidopteran insect pest, the box tree moth, *Cydalima perspectalis* (Walker, 1859) (Lepidoptera, Crambidae), was accidentally introduced to European countries (Kenis et al. 2013). Since its first record in southwestern Germany in 2007 (Krüger 2008), the moth has been expanding its range across Europe and into West Asia (Kenis 2015; Bras et al. 2019) and North Africa (Haddad et al. 2020). The widespread expansion of the box tree moth has had devastating effects on the common box tree (*Buxus sempervirens* L., 1753) (Wan et al. 2014; Mitchell et al. 2018), which has been valued for ornamental purposes in Europe since the Roman period (van der Veen et al. 2009). In North America, *C. perspectalis* was reported the first time in Ontario, Canada, in 2018 (NAPPO 2019; Wiesner et al. 2021) and also detected in Connecticut, Michigan, Ohio, and South Carolina, USA, in 2021 (USDA APHIS 2021). In 2014, boxwood comprised 15 percent of broadleaf evergreen sales in the United States, with an estimated value of 126 million US dollars (USDA-NASS 2015), so the potential impact is considerable.

For the development of classical biological control strategies to mitigate the spread and impact of *C. perspectalis*, the foreign exploration of potential biological control agents was initiated in the native ranges of *C. perspectalis* in Asia (Wan et al. 2014). The native distributions of *C. perspectalis* spans across the east palearctic and oriental regions, including China (Walker 1859), Far East Russia (Kirpichnikova 2005), India (Hampson 1896), Japan (Inoue 1982), and South Korea (Gu 1970). A total of 11 species of arthropod predators and parasitoids have been recorded from China, Japan, and Switzerland (Wan et al. 2014). These natural enemies are in need of more detailed study due to identification errors and incomplete or erroneous biological data of the parasitoids of *C. perspectalis.* Discovering host-specific parasitoids on *C. perspectalis* is crucial to identify potential classical biological control agents. Thus, enhancing our understanding of the interactions between parasitoids and their hosts is imperative for developing more targeted and efficient pest management strategies.

CABI and a research team of the Kyungpook National University collaborated and searched for natural enemies of *C. perspectalis* in South Korea. Among the hymenopteran parasitoids that were found during the surveys, a new species of *Braunsia* Kriechbaumer, 1894 (Agathidinae Haliday, 1833) was discovered. Most members of Agathidinae are known to be solitary koinobiont endoparasitoids of leaf- rolling or stem-boring lepidopteran larvae (Sharkey 1996). *Braunsia* is an Old World genus, and members are recorded as parasitoids of Erebidae, Lasiocampidae, Noctuidae, and Pyralidae (Yu et al. 2016). Seventy-three species of *Braunsia* were recorded worldwide

prior to the current project (Yu et al. 2016; Tang et al. 2017), and only two species were recorded from Korea (Park and Lee 2022).

During a three-year survey period (2022 to 2024), members of the new species of *Braunsia*, *Braunsia hodorii* sp. nov., were reared from larvae of *C. perspectalis* and its biology was recorded with detailed images and videos. A description of *Braunsia hodorii*, host and biological information, DNA data, a phylogenetic tree based on molecular data, and a key to species of *Braunsia* of Korea are included here.

Material and methods

Collecting and rearing

Larvae of *C. perspectalis* were collected from wild *Buxus* sp. at two sites: Munsan-ri, Yeongwol-eup, Yeongwol-gun, Gangwon-do, South Korea (37°15'48.4"N, 128°31'13.8"E) in May 2022 and 2023 and Bangjeol-ri, Yeongwol-eup, Yeongwol-gun, Gangwon-do, South Korea (37°12'20.9"N, 128°26'1.2"E) in May 2022 and 2024. The collected larvae of *C. perspectalis* were reared in groups of approximately 20 larvae with similar body length and weight on commercial *Buxus* spp. plants (Keewoom farm, Okcheon-gun, Chungcheongbuk-do, South Korea). This rearing was conducted during May–June 2022, utilizing plastic pots (28.0 cm diameter × 28.0 cm height, 10 L; IKEA) with 4 L of potting soil mix (Baroker bed soil, Seoul Bio., Eumseong-gun, Chungcheongbuk-do, South Korea) and 1 L pumice stone (Hwabun world, Chilgok-gun, Gyeongsangbuk-do, South Korea). In May–June 2023, collected larvae were reared in plastic cages (7.2 cm wide × 7.2 cm length × 10.0 cm height, Insect breeding box, SPL Life Science, Pocheon-si, Gyeonggi-do, South Korea). Each cage contained commercial *Buxus* spp. branches with leaves with 5 larvae per cage. Both the pots and plastic cages were kept in a laboratory at Kyungpook National University in Daegu, South Korea under controlled conditions of 25 ± 1 °C and 56 ± 12% relative humidity during May–June 2022 and May–June 2023.

When parasitoid larvae emerged from the *C. perspectalis* larvae, the behavior of the parasitoids were observed until they became adults. Images and videos were taken and recorded. Adult parasitoids were transferred to a rearing cage (10.0 cm diameter × 4.0 cm height; Insect Breeding Dish & Jar, SPL Life Science, Pocheon-si, Gyeonggi-do, South Korea). A 10% honey water solution (Australia Eucalyptus Honey, Capilano Honey Limited, Queensland, Australia) was provided as often as needed. Dead specimens were preserved in a 1.5 mL microcentrifuge tube with 99% ethanol.

Specimen information

Type specimens are deposited in the insect collection in the Department of Entomology of Kyungpook National University (**KNUS**; Sangju-si, Gyeongsangbuk-do, South Korea) and will be deposited in the National Institute of Biological Resources (**NIBR**; Incheon, South Korea). Non-type specimens are deposited at **CABI** (Delémont, Switzerland).

Morphological analysis

Using stereo microscopes (Leica M165 C & Leica S9E, Leica Microsystems, Wetzlar, Germany), braconid specimens were examined. Identification keys, diagnostic characters, species descriptions, checklists, and phylogenetic data by Sharkey (1996), Sharkey and Bennett (2004), Sharkey and Clutts (2011), Tang et al. (2017), and Park and Lee (2022) were used for morphological identifications. Images were captured with a Sony A7R4 camera (Sony, Japan), equipped with a Canon Macro Photo Lens MP-E 65 mm f/2.8 1–5 × (Canon, Japan). Images were stacked using Zerene Stacker (Zerene System, USA) and were then edited using Adobe Photoshop 2024 (Adobe, USA). The same Adobe software was used to measure morphometric characters. The external morphological terminology is based on Shakey and Wharton (1997), and a modified Comstock-Needham system for wing veins by Sharkey and Wharton (1997) was used. Terms for external body sculpture are based on Harris (1979). The following are acronyms used throughout the article: POL: distance between posterior ocelli, T1: first metasomal tergite, T2: second metasomal tergite, T3: third metasomal tergite, T4: fourth metasomal tergite, T5: fifth metasomal tergite, T6: sixth metasomal tergite.

Molecular analysis

Following manufacturer's instructions, genomic DNA was extracted using a PureLink Genomic DNA Mini Kit (Invitrogen, Carlsbad, CA, USA). Legs or whole-body samples were macerated using a pestle in 180 µL of genomic digestion buffer and 20 µL of proteinase K (50 µg/mL). All extracted DNA samples were stored at -20 °C until further analysis. PCR amplification was performed using Veriti™ 96-Well Fast Thermal Cycler (Thermo Fisher Scientific, Boston, Massachusetts, USA). PCR reaction volumes were 30 µL comprising of 15 µL of SolgTM 2 × Taq Pre-Mix (Solgent, Daejeon, South Korea), 2 µL of each primer (10 pmol/µL), 2 µL of DNA template and 9 µL of double-distilled H_2O in a total reaction. Approximately 650 bp of the mitochondrial cytochrome *c* oxidase subunit I (COI) DNA region was targeted and amplified using the following primer sets:

LCO1490 (5′ - GGTCAACAAATCATAAAGATATTGG - 3′) and
HCO2198 (5′- TAAACTTCAGGGTGACCAAAAAATCA- 3′) (Folmer et al. 1994),
or LepF1 (5′-ATTCAACCAATCATAAAGATATTGG-3′) and
LepR1 (5′-TAAACTTCTGGATGTCCAAAAAATC A-3′) (Hebert et al. 2004).

The PCR conditions for COI included an initial denaturation at 94 °C for 1 min, followed by 40 cycles of denaturation at 94 °C for 30 secs, annealing at 50 °C for 40 secs, extension at 72 °C for 1 min, and a final extension step at 72 °C for 5 mins. The D2 region of nuclear 28S rRNA (28S) genes was amplified using the primer set:

28SD2hymF (5′ - AGAGAGAGTTCAAGAGTACGTG - 3′) (Belshaw and Quicke 1997) and 28SD3hymR (5′ - TAGTTCACCATCTTTCGGGTC - 3′) (Belshaw et al. 2001).

The 28S PCR conditions followed Smith et al. (2008) but the number of cycles reduced from 35 to 30; consisted of initial denaturation at 94 °C for 2 mins, 30 cycles of denaturation at 94 °C for 30 secs, annealing at 56 °C for 30 secs, extension at 72 °C for 2 mins, and a final extension at 72 °C for 2 mins. The PCR products were separated by 1% agarose gel electrophoresis, stained with ethidium bromide solution, and bands were visualized under ultraviolet light. Crude PCR products were cleaned up using Solg™ Gel & PCR Purification Kit (Solgent, Daejeon, South Korea) and sequenced at the Solgent Sequencing Facility (Solgent, Daejeon, South Korea).

DNA assembly and phylogenetic analyses

Both COI and 28S DNA sequences produced by Sanger sequencing were edited and assembled in Geneious Prime 2024.0.2 (https://www.geneious.com). To construct reliable phylogenetic trees, COI sequences from *Aerophilus* Szépligeti, 1902 and *Braunsia* species deposited in the Barcode of Life Datasystem (BOLD) (Hebert et al. 2003), along with 28S DNA sequences from GenBank of the National Center for Biotechnology Information (NCBI) were downloaded and included into the current project (Table 1). All obtained sequences were aligned using MUltiple Sequence Comparison (MUSCLE) (Edgar 2004) in GENEIOUS PRIME. For the genetic distance estimation, MEGA11 was used, and the Kimura-2-parameter model (K2P) was selected (Kimura 1980). A concatenated 28S+COI dataset was produced using MEGA11 (Tamura et al. 2021). The concatenated 28S+COI dataset was partitioned by codon position for COI (1st, 2nd, and 3rd codon positions; 3 partitions) and codon position and gene region for 28S+COI (gene region, 1st, 2nd, and 3rd codon; 4 partitions). Neighbor joining (NJ) analyses was conducted using PAUP* (v. 4.0; Swofford 2003) with the p-distance setting. For Maximum Likelihood (ML) analyses, RAxML version 8.2.11 (Stamatakis 2014) was utilized with a bootstrapping strategy involving 1,000 Rapid replicates to gauge the reliability of the ML tree. Model selection was facilitated by the FindModel tool (http://hiv.lanl.gov/content/sequence/findmodel/findmodel.html), resulting in the adoption of the GTR+G rate model—General Time Reversible with gamma-distributed rate variation among sites. The choice of this model is informed by the principles outlined in the MODELTEST paper (Posada and Crandall 1998), which is the basis for the FindModel approach in ML analyses. Bayesian inference analyses (BI) for the concatenated dataset was conducted using MrBayes (v.3.2.6; Ronquist et al. 2012) with the GTR+G rate model. The analysis involved conducting Markov Chain Monte Carlo (MCMC) searches, including two independent runs of 50,000,000 generations, with four chains and sampling every 1000 generations. The first 50% of the generations were discarded as burn-in. To enable individual partitions to possess their unique collection of parameter approximations, the following parameters were unlinked: statefreq, revmat, shape, tratio, and pinvar. *Aerophilus jdherndoni* and *A. minys* were selected as outgroups because it was shown to be the sister-group to *Braunsia* (Sharkey and Chapman 2017, 2018).

Table 1. Metadata of specimens used for phylogenetic analyses.

Metadata Species	NCBI		BOLD		Locality	Voucher Number
	COI	28S	COI	28S		
Aerophilus jdherndoni	–	KU059013	AAU4708	–	USA	H1307
Aerophilus minys	–	KU059031	AAP1178	–	USA	H1263
Braunsia fumipennis	MF098378	HQ667946	AAV0736	–	Thailand	H915
Braunsia smithii	–	HQ667949	AAV0735	–	Thailand	H906
***Braunsia* sp.**	–	KU058998	AAP3216	–	Republic Congo	H1876
***Braunsia* sp.**	–	KU058999	AAV0730	–	Uganda	H1893
***Braunsia* sp.**	–	KU058996	AAV0732	–	Kenya	H1884
***Braunsia* sp.**	–	KP943695	AAV0733	–	Republic Congo	H1891
***Braunsia* sp.**	–	KU058992	AAV0734	–	Kenya	H1892
***Braunsia hodorii* sp. nov.**	PP437200	PP464023	–	–	Korea	P7_2
***Braunsia hodorii* sp. nov.**	PP441967	PP464024	–	–	Korea	P7_6

Results

Species delimitation

Based on morphological characteristics, we hypothesize that *Braunsia antefurcalis*, *B. matsumurai*, and *B. hodorii* sp. nov. are distinct species. COI genetic distances among *Braunsia* taxa ranged from ~4.7% to ~12.7% (Table 2). *Braunsia hodorii* sp. nov. sequences were ~7.7% different from the nearest neighbor. *Braunsia hodorii* sp. nov. was also clearly recovered as distinct in phylogenetic data based on 28S+COI (Fig. 1) data.

Phylogenetic relationships

Both BI and ML phylogenetic trees recovered identical topologies. In contrast, the NJ trees based on 28S + COI and COI only data showed differences in the main clusters (Suppl. materials 1, 3). Most clades exhibited robust nodal support values in ML and BI trees based on 28S + COI data, but relatively not in clusters in the NJ trees (Suppl. materials 1, 3), and a clade consisting of *Braunsia* sp. Republic Congo H1876, *Braunsia* sp. Uganda H1893,

Table 2. Estimates of genetic distances between COI sequences (rounded up to 3 digits).

	***Braunsia* sp. H1891**	***Braunsia* sp. H1892**	***Braunsia* sp. H1876**	***Braunsia* sp. H1884**	***Braunsia* sp. H1893**	***Braunsia fumipennis* H915**	***Braunsia smithii* H906**	***Braunsia hodorii* sp. nov. P7_2**	***Braunsia hodorii* sp. nov. P7_6**
***Braunsia* sp. H1891**									
***Braunsia* sp. H1892**	0.047								
***Braunsia* sp. H1876**	0.088	0.077							
***Braunsia* sp. H1884**	0.081	0.064	0.062						
***Braunsia* sp. H1893**	0.079	0.080	0.055	0.071					
***Braunsia fumipennis* H915**	0.110	0.093	0.102	0.104	0.089				
***Braunsia smithii* H906**	0.125	0.114	0.101	0.101	0.113	0.097			
***Braunsia hodorii* sp. nov. P7_2**	0.127	0.103	0.100	0.096	0.091	0.079	0.077		
***Braunsia hodorii* sp. nov. P7_6**	0.127	0.103	0.100	0.096	0.091	0.079	0.077	0.000	

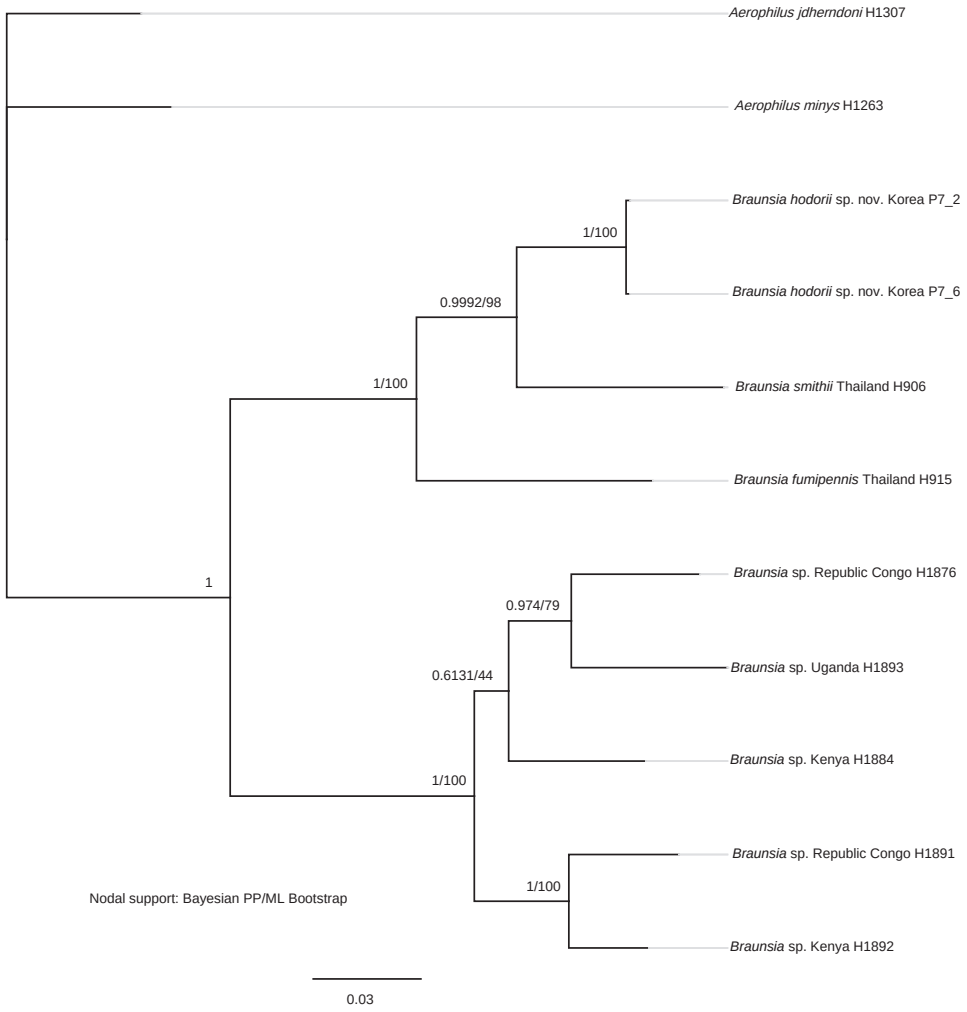

Figure 1. The BI tree based on concatenated 28S and COI data for *Braunsia* species. Bayesian posterior probabilities and Maximum Likelihood bootstrap values are plotted.

and *Braunsia* sp. Kenya H1884 in the ML and BI trees (Fig. 1 and Suppl. material 2). For *Braunsia*, two main clades were recovered in the ML and BI trees. One clade consists of three species occurring in the Palearctic and Oriental regions: *B. hodorii* sp. nov., *B. smithii* (Dalla Torre, 1898), and *B. fumipennis* (Cameron, 1899). The remaining five undescribed species occur in the Afrotropical region, forming the second clade. Within the Palearctic and Oriental clade, *B. fumipennis* was recovered as the sister taxon to *B. hodorii* sp. nov.

Systematics

Braunsia Kriechbaumer, 1894

Type species. *Braunsia bicolor* Kriechbaumer, 1894, designated by Viereck (1914).

Key to species of *Braunsia* of Korea

1 **A.** Forewing with entirely dark brown pterostigma .....
.....***B. antefurcalis*** **Watanabe, 1937**

– **B.** Forewing with partially or completely pale pterostigma.....**2**

2 **A.** Mesopleuron entirely pale; precoxal sulcus less crenulate; **AA.** T1 uniformly colored, entirely melanic or pale, 1.7 × longer than apical width; T2–T4 1.4 × longer than apical width .....***B. matsumurai*** **Watanabe, 1937**

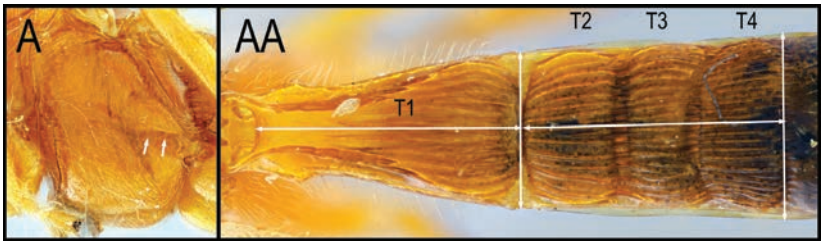

– **B.** Mesopleuron mostly black; precoxal sulcus more crenulate; **BB.** T1 bicolored, melanic at posterior half, 1.4 × longer than apical width; T2–T4 1.6 × longer than apical width ..... ***B. hodorii*** **Kang, sp. nov.**

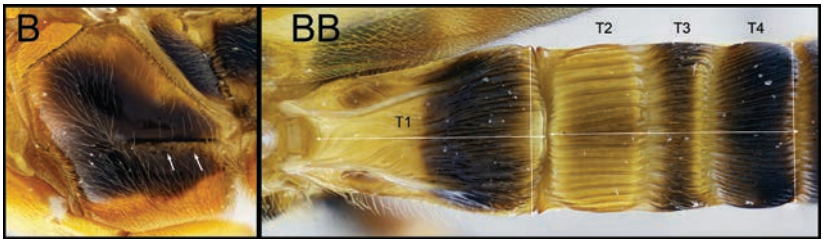

***Braunsia hodorii* Kang, sp. nov.**
https://zoobank.org/3F31B9BB-546B-4AE0-B50C-2D8C0D192829

Material examined. *Holotype*: Korea • ♀; Gangwon-do, Yeongwol-gun, Munsan-ri, near Jatbong (peak); 37°15.81'N, 128°31.23'E, 229 m a.s.l.; 6 May. 2022 (host caterpillar collection date); S. Kim, I. Park, S. Hong leg.; reared from *C. perspectalis*; host plant: *Buxus* sp.; det. Ilgoo Kang. ***Paratypes*:** • 1♀, 2♂, same as holotype. • 1♂, same as holotype except the host caterpillar collection date, collector and parasitoid eclosion date: 26 May. 2023; S. Kim leg., 1 June. 2023 • 2♂, Gangwon-do, Yeongwol-gun, Bangjeol-ri, near Seondol; 37°12.35'N, 128°26.02'E, 296 m a.s.l.; 10 May 2024 (host caterpillar collection date); I. Kang & S. Kim leg.; reared from *C. perspectalis*; host plant: *Buxus* sp.; det. Ilgoo Kang. Holotype and paratypes will be deposited at NIBR, two paratypes will be deposited at KNUS.

Diagnosis. Members of *Braunsia hodorii* sp. nov. are most similar to those of *B. matsumurai* (Fig. 6) and can be distinguished from them by the characters in the key and from all other members of *Braunsia* by the combination of the following characters: Forewing yellow with two melanic bands (Fig. 2B). Hind wing Cub vein partially present, neither reaching cu-a nor posterior margin; distance between cu-a to Cub closer than the space of *B. matsumurai* (Fig. 2B). Hind coxa and femur mostly melanic. Hind tibia with 7−8 spines apically (Fig. 3B). Median areola of propodeum mostly black, open posteriorly (Fig. 2E). T1 1.4 × longer than apical width, bi-colored, anteriorly pale posteriorly black, with longitudinal carinae in posterior 2/3 (Fig. 2F). T2−T4 1.6 × longer than apical width. T5 striate on anterior third. T6 to remaining tergites yellowish-orange (Fig. 2F).

Description. Holotype. Body 12.6 mm. Forewing length: 11.3 mm. Hind wing length: 8.6 mm.

***Head*.** Antenna with 44 flagellomeres. Interantennal space with weak median carina. POL 1.3 × longer than diameter of anterior ocellus (0.18:0.14). Eye without setae; length of eye 2.3 × longer than median width of gena in lateral view (0.60:0.26). Frontoclypeal suture absent. Malar space 2.8 × longer than basal width of mandible (0.36:0.13). Mandible bidentate; lower tooth acute; upper tooth obtuse. Maxillary palpus five-segmented; apical maxillary palpomere 1.2 × longer than penultimate maxillary palpomere (0.28:0.23). Labial palpus four-segmented. Posterolateral corner of gena sharp.

***Mesosoma*.** Pronotum mostly smooth, anteriorly carinate with crenulate posterior margin. Notauli present, deep and smooth. Scutellar sulcus with round anterior margin, weekly crenulate. Postscutellar depression absent. Propodeum mostly smooth; median areola of propodeum present, closed anteriorly, opened posteriorly; anterior transverse carina of the propodeum reaching lateral margin. Mesopleuron mostly smooth, 1.6 × longer than median width (2.15:1.31), dorsally and posteriorly with crenulate margin; precoxal sulcus present at posterior 3/4. Metapleuron dorsally smooth and posteroventrally strongly sculptured.

***Legs*.** Combined length of foretrochanter and trochantellus 0.5 × longer than foretibia (0.58:1.15). Combined length of mid trochanter and trochantellus 0.3 × longer than basitarsus (0.56:1.86). Mid tibia with 1−2 spines medially and 1−2 spines apically

(variation among females). Hind tibia 1.6 × longer than hind femur (3.63:2.29), with 7–8 spines apically (variation among females); basal spur on hind tibia 0.3 × longer than basitarsus (0.64:1.88). Claws simple and with a basal lobe.

***Wings*.** Forewing second submarginal cell trapezoidal, 1.1 × longer than width (0.40:0.36); RS+M vein of forewing absent; pterostigma 3.5 × longer than medial

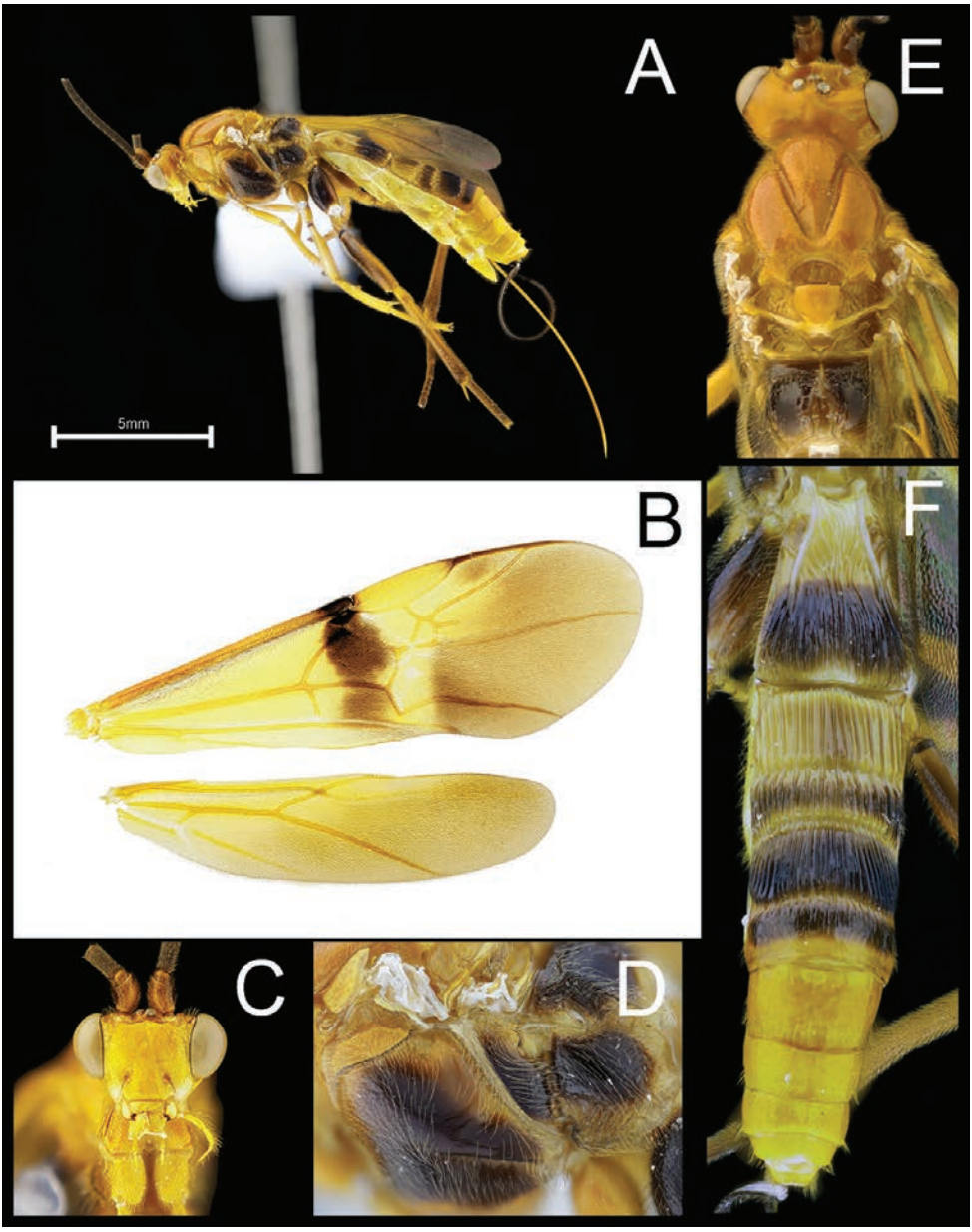

Figure 2. *Braunsia hodorii* sp. nov., holotype, ♀: **A** lateral habitus **B** wings **C** anterior head **D** mesopleuron and metapleuron **E** head and mesosoma, and **F** metasoma. Scale bar: 5 mm (**A**).

width (2.14:0.62); spurious vein, RS2b present, as long as 2RS; 2cu-a absent. Hind wing Cub vein partially present, neither reaching cu-a nor posterior margin; subbasal cell not angled distally.

***Metasoma*.** Metasoma length: 7.4 mm. T1 entirely striate, with horizontal striae at anterior third and longitudinal striae at posterior 2/3; pair of carinae strong, reaching posterior margin; median length of T1 1.4 × longer than apical width (2.22:1.60). T2 1.6 × longer than T3 (0.90:0.58). T2–T4 entirely striate, with longitudinal striae. T5 mostly smooth, with weak longitudinal striae anteriorly. Remaining tergites entirely smooth. Protruded ovipositor as long as metasoma (7.4:7.6), 2.1 × longer than hind tibia (7.6:3.63). Ovipositor length: 7.6 mm.

Male. Similar to female except the following: Body slightly shorter than female, 11.5 mm. Antenna with 42 flagellomeres. Mid tibia with 3 spines medially and 3 spines apically (Fig. 4).

Color. Mostly pale orange and yellow except the following which are brown to black: antenna, mesopleuron, metapleuron, mid coxa, hind coxa, hind femur, hind tibia posteriorly, hind tarsus, hind claw, propodeum, T1 posteriorly, T2 medially, T3 posteriorly, T4, T5 anteriorly. Forewing yellow with two melanic bands. Hind wing yellow basally brown apically.

Distribution. Yeongwol-gun, Gangwon-do, South Korea.

Etymology. The species is named after "Hodori", the male tiger mascot of the Seoul Olympic games in 1988 due to similarity in the color patterns (orange and with black stripes) (Fig. 5). Additionally, the long antennae resemble Hodori's distinctive hat streamer.

Figure 3. Mid tibia and hind tibia of *B. hodorii* sp. nov., holotype, ♀): **A** spines on mid tibia, and **B** spines on hind tibia.

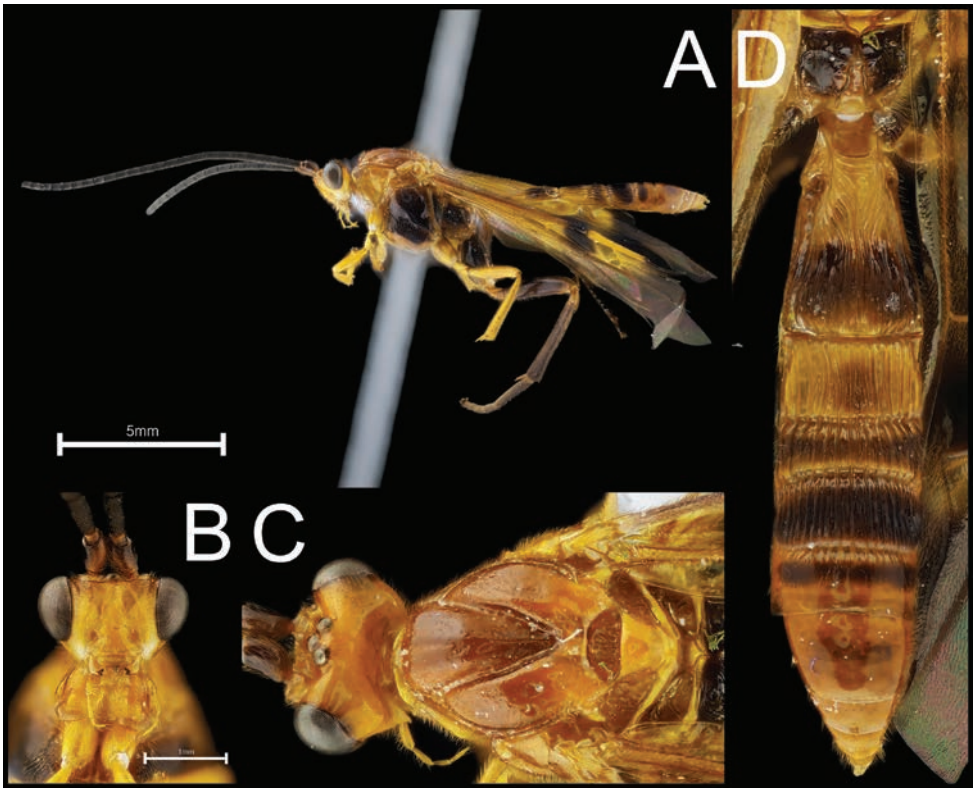

Figure 4. *Braunsia hodorii* sp. nov., paratype, ♂: **A** lateral habitus **B** anterior head **C** head and mesoscutum, and **D** propodeum and metasoma.

Figure 5. Lateral view *B. hodorii* sp. nov. female that was preserved in ethanol.

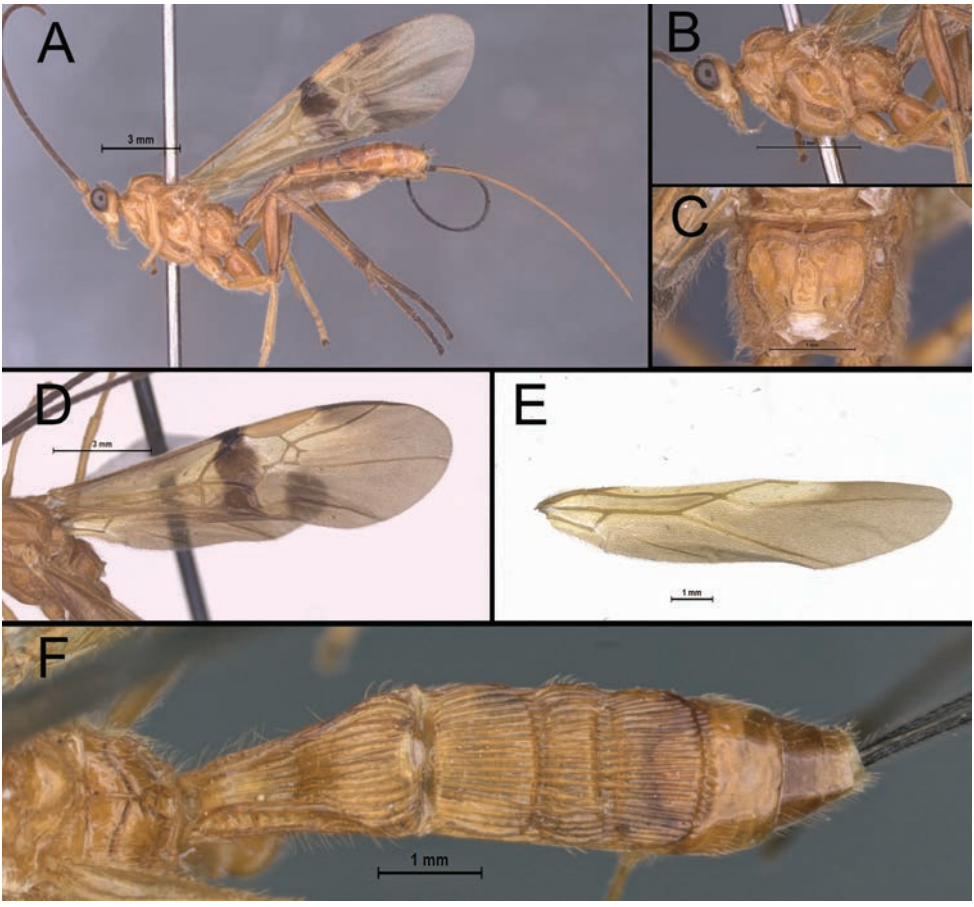

Figure 6. *Braunsia matsumurai* female: **A** lateral habitus **B** lateral head to mesosoma **C** propodeum **D** forewing **E** hind wing, and **F** metasoma.

Notes. Korean common name: 호돌이구멍줄고치벌 (신칭). "호돌이" means the male tiger mascot of the Seoul Olympic Games in Korean and "구멍줄고치벌" is the Korean common name of *Braunsia* spp.

Molecular data. NCBI Accession Numbers: PP437200, PP441967 (COI); PP464023, PP464024(28S).

Host. *Cydalima perspectalis* (Walker, 1859) (Lepidoptera, Crambidae).

Biology. Larvae of *Cydalima perspectalis* are leaf-webbers, loosely weaving leaves together with silken threads (Fig. 7). Unparasitized, last-instar larvae (6th or 7th instar) typically build a dense shelter with their silk, in which they pupate. Parasitized *C. perspectalis* larvae build highly similar shelters, although somewhat less dense, prematurely, in their 5th instar. They cease movement, and their bodies gradually become shorter and fatter within the shelter before the egression of the parasitoid larva.

Like most other Agathidinae, members of *Braunsia hodorii* sp. nov. are solitary koinobiont endoparasitoids. Upon the egression of parasitoid larvae from the host

Figure 7. A Woven leaves with silken threads spun by *Cydalima perspectalis* larvae **B** parasitoid cocoon within the web of *C. perspectalis*.

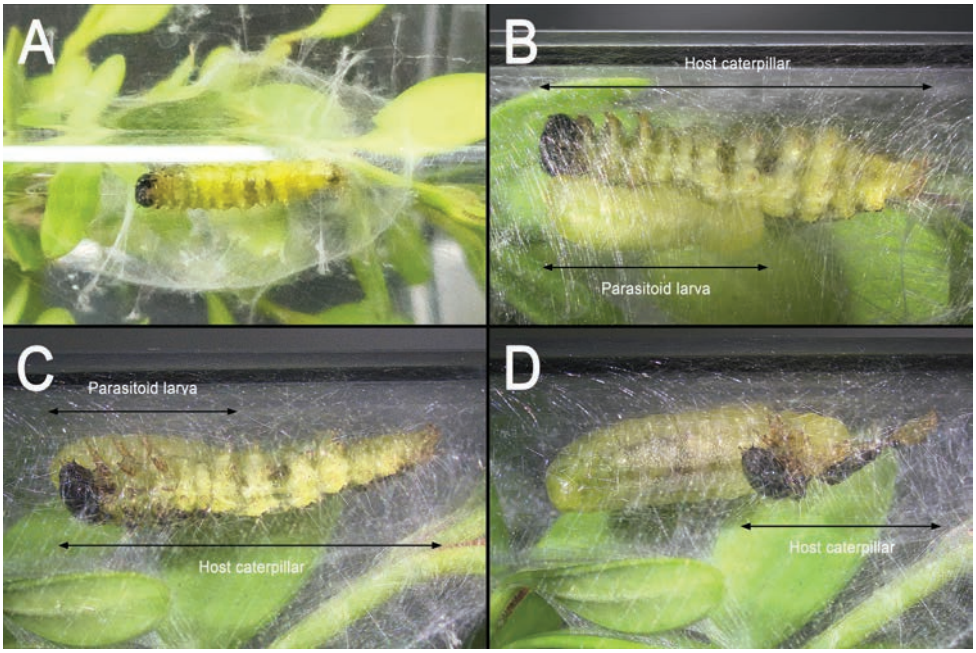

Figure 8. A Parasitized host caterpillar in an inner space made of silk **B, C, D** *B. hodorii* sp. nov. larva consumes the host caterpillar during an external feeding phase.

caterpillars, the parasitoid larvae are greenish-yellow, while the host caterpillars retain their original color. The parasitoid larvae then enter an external feeding phase (Suppl. material 4). The host caterpillars gradually shrink, leaving only their skin and head capsule. Among agathidine braconids, this external feeding phase was only reported for *Therophilus dimidiator* (Nees, 1834) (as *Agathis laticinctus*) (Dondale 1954) before the present study. The external feeding phase takes a little more than 8 hours, with the parasitoid larvae completing their feeding during this period (Fig. 8). Parasitoid larvae then spin a semi-translucent cocoon in the silk web of *C. perspectalis*, where they pupate (Figs 7, 9 and Suppl. material 5). Pupal development lasts about ten days at 25 ± 1 °C.

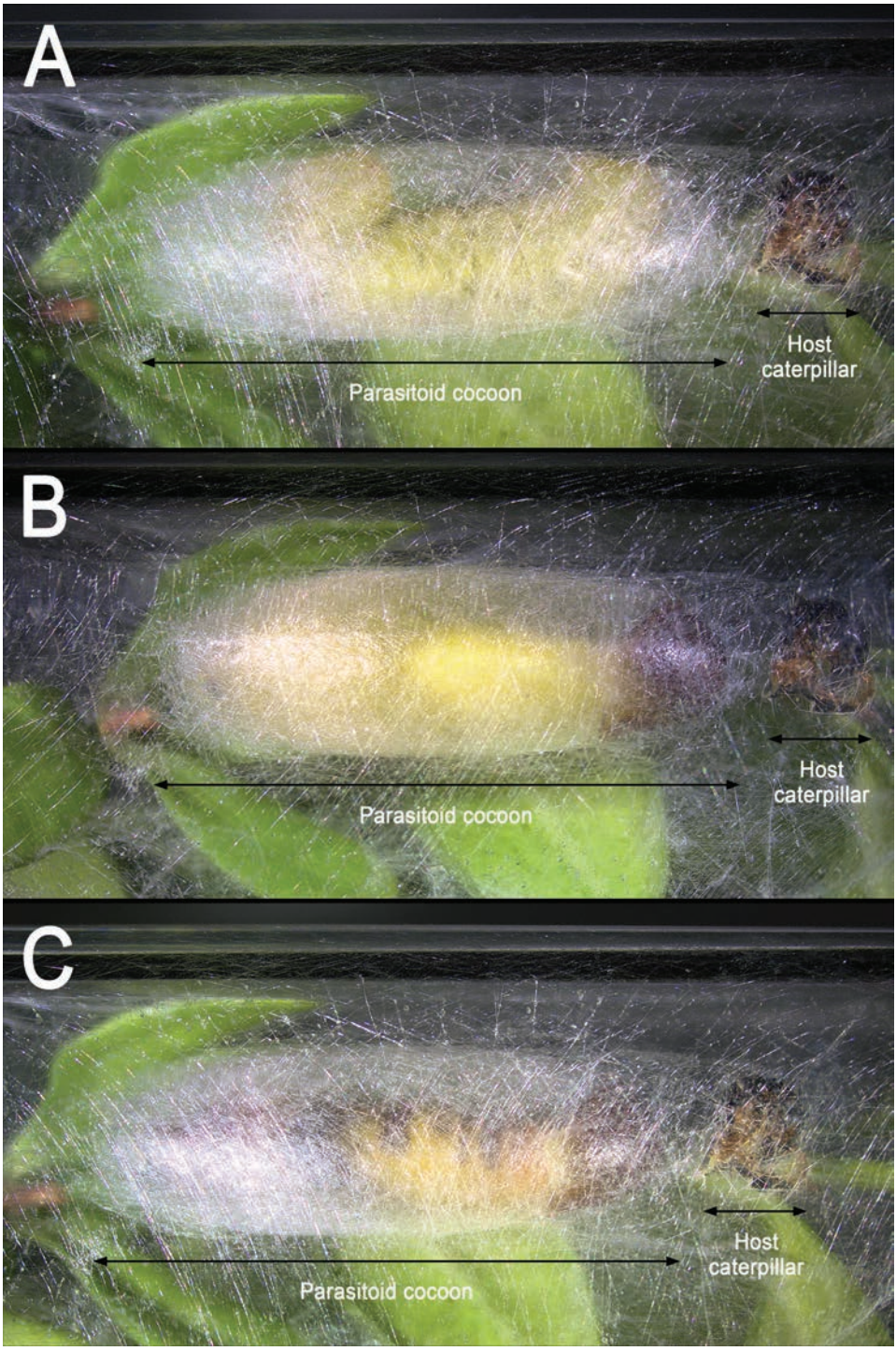

Figure 9. Semi-translucent cocoon of *B. hodorii* sp. nov.: **A** parasitoid larva spinning the cocoon during the first day of cocoon formation **B** parasitoid pupa in the cocoon after six days, and **C** melanizing parasitoid pupa in the cocoon after eight days.

Discussion

Species delimitation and phylogenetic analyses

Initially, the primary goal of the project was to enhance our species concepts based on integrative taxonomic data, morphological data and molecular data, an approach that has been demonstrated in many studies (Jasso-Martínez et al. 2019, 2024; Quicke et al. 2021, 2024; Slater-Baker et al. 2022; van Achterberg et al. 2024; Žikić et al. 2024). We successfully established morphospecies concepts. Unfortunately, due to the age and fungal contamination of the specimens in our possession, we were unable to obtain DNA from exemplars of *B. antefurcalis* and *B. matsumurai*. Given the limited molecular data, we added sequence data of *Braunsia* available in public databases, NCBI GenBank and BOLD, to our data to support our hypotheses. These data allowed estimates of genetic distances based on COI barcodes and we were able to construct phylogenetic trees using 28S and COI sequences.

Based on the genetic distance estimations (Table 2), we confirmed that COI barcoding for *Braunsia* species is a useful tool for delimiting species, given distances among species are relatively high compared to typical COI barcode-based species boundaries, 2.0%, which is also utilized by the BIN algorithm (Ratnasingham and Hebert 2013).

For multigene analyses, we selected taxa represented by both 28S and COI sequence data available in GenBank and BOLD. When either 28S or COI sequence was unavailable, the taxa were excluded. The phylogenetic trees clearly indicate that *B. hodorii* sp. nov. is not conspecific with any other *Braunsia* species included in the study. In addition, two main clades separated by geographic regions suggest that geographic isolation affected diversification of *Braunsia* members (Fig. 1 and Suppl. material 2).

Despite these limitations, this work serves as a starting point for understanding the species boundaries and evolutionary relationships within *Braunsia* based on integrative data. Future research for Korean *Braunsia* should prioritize obtaining fresh specimens and generating complete molecular data for all relevant taxa. Sharkey and Clutts (2011) has been the only published taxonomic research on *Braunsia* based on molecular data prior to the current study. Collaborative projects among braconid taxonomists worldwide are essential to enhance our understanding of poorly understood taxa such as *Braunsia* with broad global distributions.

Acknowledgements

We extend our gratitude to Dr Jong-Kyun Park from the Department of Entomology at the Kyungpook National University for allowing us to use the imaging system. We would like to express our appreciation to Dr Sun-Hee Hong from the School of Plant Science and Landscape Architecture at the Hankyong National University, South Korea for providing valuable assistance in site search and sample collection. Special thanks are also extended to Ms Eunji Lim at Dreaming Mariposas Workshop, Suwon, South Korea for her guidance in insect rearing. This work was supported by a grant from the Nation-

al Institute of Biological Resources (NIBR), funded by the Ministry of Environment (MOE) of the South Korea. In addition, this research was funded by the Korea Institute of Planning and Evaluation for Technology in Food, Agriculture, and Forestry (IPET) through the Agriculture, Food, and Rural Affairs Convergence Technologies Program for Educating Creative Global Leader Project funded by the Ministry of Agriculture, Food, and Rural Affairs (MAFRA) (No. 321001-03). Funding for the surveys was provided by the Horticultural Research Institute, the Canadian nursery and landscape association, the Animal and Plant Health Inspection Service (APHIS), Plant Protection and Quarantine (PPQ), the European Union through the Horizon 2020 Programme for Research & Innovation under grant agreement no.771271 and from Landscape Ontario, Ontario Ministry of Food, Agriculture & Rural Affairs (OMAFRA). CABI as an international intergovernmental not-for-profit organization gratefully acknowledges the generous support received from many donors, sponsors, and partners. In particular, CABI thanks its Member Countries for their vital financial and strategic contributions.

References

Belshaw R, Quicke DL (1997) A molecular phylogeny of the Aphidiinae (Hymenoptera: Braconidae). Molecular Phylogenetics Evolution 7(3): 281–293. https://doi.org/10.1006/mpev.1996.0400

Belshaw R, Lopez-Vaamonde C, Degerli N, Quicke DL (2001) Paraphyletic taxa and taxonomic chaining: evaluating the classification of braconine wasps (Hymenoptera: Braconidae) using 28S D2–3 rDNA sequences and morphological characters. Biological Journal of the Linnean Society 73: 411–424. https://doi.org/10.1111/j.1095-8312.2001.tb01370.x

Bras A, Avtzis DN, Kenis M, Li H, Vétek G, Bernard A, Courtin C, Rousselet J, Roques A, Auger-Rozenberg MA (2019) A complex invasion story underlies the fast spread of the invasive box tree moth (*Cydalima perspectalis*) across Europe. Journal of Pest Science 92: 1187–1202. https://doi.org/10.1007/s10340-019-01111-x

Dondale CD (1954) Biology of *Agathis laticinctus* (Cress.) (Hymenoptera: Braconidae) a parasite of the eye-spotted bud moth in Nova Scotia. The Canadian Entomologist 86: 40–44. https://doi.org/10.4039/Ent8640-1

Edgar RC (2004) MUSCLE: multiple sequence alignment with high accuracy and high throughput. Nucleic Acids Research 32(5): 1792–1797. https://doi.org/10.1093/nar/gkh340

Folmer O, Black M, Hoeh W, Lutz R, Vrijenhoek R (1994) DNA primers for amplification of mitochondrial cytochrome c oxidase subunit I from diverse metazoan invertebrates. Molecular Marine Biology and Biotechnology 3(5): 294–299.

Gu G (1970) On the Box Tree Pyralid, *Glyphodes perspectalis* Waker (Lepidoptera; Pyralidae) from Korea. The Korean Journal of Zoology 13(2): 57–60. https://koreascience.kr/article/JAKO197011919884615.page

Haddad K, Kalaentzis K, Demetriou J (2020) On track to becoming a cosmopolitan invasive species: First record of the box tree moth *Cydalima perspectalis* (Lepidoptera: Crambidae) in the African continent. Entomologia Hellenica 29(2): 27–32. https://doi.org/10.12681/eh.23483

Hampson GF (1896) Moths 4. The Fauna of British India, including Ceylon and Burma. Taylor & Francis, London, 1–594. https://doi.org/10.5962/bhl.title.58657

Harris RA (1979) Glossary of surface sculpturing. Occasional Papers in Entomology 28: 1–31. https://doi.org/10.5281/zenodo.26215

Hebert PD, Cywinska A, Ball SL (2003) Biological identifications through DNA barcodes. Proceedings of the Royal Society of London B: Biological Sciences 270(1512): 313–321. https://doi.org/10.1098/rspb.2002.2218

Hebert PD, Stoeckle MY, Zemlak TS, Francis CM (2004) Identification of birds through DNA barcodes. PLoS Biology 2(10): e312. https://doi.org/10.1371/journal.pbio.0020312

Inoue H (1982) Pyralidae. In: Inoue H, Sugi S, Kuroko H, Moriuti S, Kawabe A (Eds) Moths of Japan 1, 2. Kodansha (Tokyo) 1: 307–404, 223–254; 2: 36–48, 228, 296–314.

Jasso-Martínez JM, Belokobylskij SA, Zaldívar-Riverón A (2019) Molecular phylogenetics and evolution of generic diagnostic morphological features in the doryctine wasp tribe Rhaconotini (Hymenoptera: Braconidae). Zoologischer Anzeiger 279: 164–171. https://doi.org/10.1016/j.jcz.2019.02.002

Jasso-Martínez JM, Martínez JJ, Aguilar-Velasco RG, Zaldívar-Riverón (2024) A Four new species of *Triraphis* Ruthe, 1855 (Braconidae, Rogadinae) from a Mexican tropical dry forest and morphological descriptions of *T. bradzlotnicki* Sharkey, 2021 and *T. davidwahli* Sharkey, 2021. European Journal of Taxonomy 917: 50–73. https://doi.org/10.5852/ejt.2024.917.2387

Kenis M, Nacambo S, Leuthardt FL, Domenico FD, Haye T (2013) The box tree moth, *Cydalima perspectalis*, in Europe: horticultural pest or environmental disaster? Aliens: The Invasive Species Bulletin 33: 38–41. http://www.issg.org/pdf/aliens_newsletters/A33.pdf

Kenis M (2015) *Cydalima perspectalis* (box tree moth). CABI Compendium. https://doi.org/10.1079/cabicompendium.118433

Kimura M (1980) A simple method for estimating evolutionary rates of base substitutions through comparative studies of nucleotide sequences. Journal of Molecular Evolution 16(2): 111–120. https://doi.org/10.1007/BF01731581

Kirpichnikova VA (2005) Pyralidae. In: Ler PA (Ed.) Key to the insects of Russian Far East 5 (2). Dalnauka,Vladivostok, 526–539. [in Russian]

Krüger EO (2008) *Glyphodes perspectalis* (Walker, 1859)-new for the European fauna (Lepidoptera: Crambidae). Entomologische Zeitschrift mit Insekten-Börse 118(2): 81−83.

Meyerson LA, Mooney HA (2007) Invasive alien species in an era of globalization. Frontiers in Ecology and the Environment 5(4): 199–208. https://doi.org/10.1890/1540-9295(2007)5[199:IASIAE]2.0.CO;2

Mitchell R, Chitanava S, Dbar R, Kramarets V, Lehtijärvi A, Matchutadze I, Mamadashvili G, Matsiakh I, Nacambo S, Papazova-Anakieva I, Sathyapala S (2018) Identifying the ecological and societal consequences of a decline in *Buxus* forests in Europe and the Caucasus. Biological Invasions 20: 3605−3620. https://doi.org/10.1007/s10530-018-1799-8

NAPPO (2019) Detection of *Cydalima perspectalis* (box tree moth) in Ontario. 2019 Feb 21. In: Official Pest Report. https://www.pestalerts.org/nappo/official-pest-reports/29/ [accessed 2024 March 26]

Park J, Lee J (2022) Check list of insects from Korea. Korean Society of Applied Entomology (Suwon) & The Entomological Society of Korea (Daegu), 1−1055.

Posada D, Crandall KA (1998) MODELTEST: testing the model of DNA substitution. Bioinformatics (Oxford) 14: 817–818. https://doi.org/10.1093/bioinformatics/14.9.817

Quicke DLJ, Fagan-Jeffries EP, Jasso-Martínez JM, Zaldivar-Riverón A, Shaw MR, Janzen DH, Hallwachs W, Smith MA, Hebert PDN, Hrcek J, Miller S, Sharkey MJ, Shaw SR, Butcher BA (2021) A molecular phylogeny of the parasitoid wasp subfamily Rogadinae (Ichneumonoidea: Braconidae) with descriptions of three new genera. Systematic Entomology 46(4): 1019–1044. https://doi.org/10.1111/syen.12507

Quicke DLJ, Jasso-Martínez JM, Ranjith AP, Sharkey MJ, Manjunath R, Naik S, Hebert PDN, Priyadarsanan DR, Thurman J, Butcher BA (2024) Phylogeny of the Braconinae (Hymenoptera: Braconidae): a new tribal order! Systematic Entomology 49(1): 84–109. https://doi.org/10.1111/syen.12608

Rakotoarison A, Scherz MD, Glaw F, Köhler J, Andreone F, Franzen M, Glos J, Hawlitschek O, Jono T, Mori A, Ndriantsoa SH, Raminosoa NR, Riemann JC, Rödel M-O, Rosa GM, Vieites DR, Crottini A, Vences M (2017) Describing the smaller majority: integrative taxonomy reveals twenty-six new species of tiny microhylid frogs (genus *Stumpffia*) from Madagascar. Vertebrate Zoology 67: 271–398. https://doi.org/10.3897/vz.67.e31595

Ratnasingham S, Hebert PDN (2013) A DNA-based registry for all animal species: the Barcode Index Number (BIN) system. PLOS ONE 8: e66213. https://doi.org/10.1371/journal.pone.0066213

Ronquist F, Teslenko M, van der Mark P, Ayres DL, Darling A, Höhna S, Larget B, Liu L, Suchard MA, Huelsenbeck JP (2012) MrBayes 3.2: Efficient Bayesian phylogenetic inference and model choice across a large model space. Systematic Biology 61: 539–542. https://doi.org/10.1093/sysbio/sys029

Roques A, Auger-Rozenberg MA, Blackburn TM, Garnas J, Pyšek P, Rabitsch W, Richardson DM, Wingfield MJ, Liebhold AM, Duncan RP (2016) Temporal and interspecific variation in rates of spread for insect species invading Europe during the last 200 years. Biological invasions 18: 907–920. https://doi.org/10.1007/s10530-016-1080-y

Sharkey MJ (1996) The Agathidinae (Hymenoptera: Braconidae) of Japan. Bulletin of the National Institute of Agro-Environmental Sciences 13: 1−100. http://agriknowledge.affrc.go.jp/RN/2010542363

Sharkey MJ, Bennett DJ (2004) The Agathidinae (Insecta: Hymenoptera: Braconidae) of Sakhalin and the Kuril Islands. Species Diversity 9(2): 151−164. https://doi.org/10.12782/specdiv.9.151

Sharkey MJ, Chapman E (2017) Ten new genera of Agathidini (Hymenoptera, Braconidae, Agathidinae) from Southeast Asia. ZooKeys 660: 107–150. https://doi.org/10.3897/zookeys.660.12390

Sharkey MJ, Chapman EG (2018) Revision of *Zosteragathis* Sharkey of Thailand (Hymenoptera, Braconidae, Agathidinae, Agathidini). Deutsche Entomologische Zeitschrift 65(2): 225–253. https://doi.org/10.3897/dez.65.25772

Sharkey MJ, Clutts SA (2011) A revision of Thai Agathidinae (Hymenoptera, Braconidae), with descriptions of six new species. Journal of Hymenoptera Research 22: 69–132. https://doi.org/10.3897/jhr.22.1299

Sharkey MJ,Wharton RA (1997) Morphology and terminology. In: Wharton RA, Marsh PM, Sharkey MJ (Eds) Manual of the New World genera of the family Braconidae (Hymenoptera). Special Publication of the International Society of Hymenopterists, 19−37.

Slater-Baker MR, Austin AD, Whitfield JB, Fagan-Jeffries EP (2022) First record of miracine parasitoid wasps (Hymenoptera: Braconidae) from Australia: molecular phylogenetics and morphology reveal multiple new species. Austral Entomology 61(1): 49–67. https://doi.org/10.1111/aen.12582

Stamatakis A (2014) RAxML Version 8: a tool for phylogenetic analysis and post-analysis of large phylogenies. Bioinformatics 30: 1312–1313. https://doi.org/10.1093/bioinformatics/btu033

Swofford DL (2003) PAUP*. Phylogenetic Analysis Using Parsimony (*and Other Methods). Version 4. Sinauer Associates, Sunderland, Massachusetts.

Tamura K, Stecher G, Kumar S (2021) MEGA11: Molecular Evolutionary Genetics Analysis Version 11. Molecular Biology and Evolution 38(7): 3022–3027. https://doi.org/10.1093/molbev/msab120

Tang P, van Achterberg C, Chen X-X (2017) The genus *Braunsia* Kriechbaumer, 1894 from China with description of two new species (Hymenoptera, Braconidae, Agathidinae). ZooKeys 705: 95–114. https://doi.org/10.3897/zookeys.705.14717

The FindModel (2016) The FindModel web implementation. http://hiv.lanl.gov/content/sequence/findmodel/findmodel.html

USDA APHIS (2021) *Cydalima perspectalis*: APHIS confirms box tree moth and takes action to contain and eradicate the pest. 2021 July 13. In: Official Pest Report. https://www.pestalerts.org/nappo/official-pest-reports/987/ [accessed 2024 March 26]

van Achterberg C, Shaw MR, Fernandez-Triana J, Quicke DLJ (2024) Resolution of the *Aleiodes seriatus* (Herrich-Schäffer, 1838)-aggregate in the western Palaearctic (Hymenoptera, Braconidae, Rogadinae), with description of a new species. ZooKeys 1208: 241–258. https://doi.org/10.3897/zookeys.1208.127135

van der Veen M, Livarda A, Hill A (2008) New Plant Foods in Roman Britain — Dispersal and Social Access. Environmental Archaeology 13(1): 11–36. https://doi.org/10.1179/174963108X279193

Walker F (1859) List of the Specimens of Lepidopterous Insects in the Collection of the British Museum: 18: Pyralides. Edward Newman, London, 1−798.

Wan H, Haye T, Kenis M, Nacambo S, Xu H, Zhang F, Li H (2014) Biology and natural enemies of *Cydalima perspectalis* in Asia: Is there biological control potential in Europe? Journal of Applied Entomology 138(10): 715−722. https://doi.org/10.1111/jen.12132

Wiesner A, Llewellyn J, Smith SM, Scott-Dupree C (2021) Biology and distribution of box tree moth (*Cydalima perspectalis*) (Walker, 1859) in southern Ontario. In: Proceedings of the 1st International Electronic Conference on Entomology 2021, 1–15. https://doi.org/10.3390/IECE-10514

Yu DSK, van Achterberg C, Horstmann K (2016) Taxapad 2016, Ichneumonoidea 2015. Database on flash-drive. Nepean, Ontario.

Žikić V, Mitrović M, Stanković SS, Fernández-Triana JL, Lazarević M, van Achterberg K, Marczak D, Milošević MI, Shaw MR (2024) An integrative taxonomic study of north temperate *Cotesia* Cameron (Hymenoptera, Braconidae, Microgastrinae) that form silken cocoon balls, with the description of a new species. Journal of Hymenoptera Research 97: 255–276. https://doi.org/10.3897/jhr.97.116378

Supplementary material 1

The NJ tree based on the concatenated 28S and COI data for *Braunsia* species
Authors: Soohyun Kim, Jong Bong Choi, Hwal-Su Hwang, Marc Kenis, M. Lukas Seehausen, Ikju Park, Jin-Kyung Choi, Kyeong-Yeoll Lee, Michael J. Sharkey, Ilgoo Kang
Data type: png
Explanation note: The bootstrap values are shown along the branches.

Link: https://doi.org/10.3897/jhr.97.135728.suppl1

Supplementary material 2

The ML tree based on the concatenated 28S and COI data for *Braunsia* species
Authors: Soohyun Kim, Jong Bong Choi, Hwal-Su Hwang, Marc Kenis, M. Lukas Seehausen, Ikju Park, Jin-Kyung Choi, Kyeong-Yeoll Lee, Michael J. Sharkey, Ilgoo Kang
Data type: png
Explanation note: The bootstrap values are shown along the branches.

Link: https://doi.org/10.3897/jhr.97.135728.suppl2

Supplementary material 3

The NJ tree based on only COI data for *Braunsia* species
Authors: Soohyun Kim, Jong Bong Choi, Hwal-Su Hwang, Marc Kenis, M. Lukas Seehausen, Ikju Park, Jin-Kyung Choi, Kyeong-Yeoll Lee, Michael J. Sharkey, Ilgoo Kang
Data type: png
Explanation note: The bootstrap values are shown along the branches.

Link: https://doi.org/10.3897/jhr.97.135728.suppl3

Supplementary material 4

Video: feeding behavior of *Braunsia hodorii* sp. nov.

Authors: Soohyun Kim, Jong Bong Choi, Hwal-Su Hwang, Marc Kenis, M. Lukas Seehausen, Ikju Park, Jin-Kyung Choi, Kyeong-Yeoll Lee, Michael J. Sharkey, Ilgoo Kang

Data type: mp4

Link: https://doi.org/10.3897/jhr.97.135728.suppl4

Supplementary material 5

Video: cocoon spinning by *Braunsia hodorii* sp. nov.

Authors: Soohyun Kim, Jong Bong Choi, Hwal-Su Hwang, Marc Kenis, M. Lukas Seehausen, Ikju Park, Jin-Kyung Choi, Kyeong-Yeoll Lee, Michael J. Sharkey, Ilgoo Kang

Data type: mp4

Link: https://doi.org/10.3897/jhr.97.135728.suppl5

JHR 97: 937–944 (2024)
doi: 10.3897/jhr.97.135648
https://jhr.pensoft.net

RESEARCH ARTICLE

JOURNAL OF Hymenoptera RESEARCH
A peer-reviewed open-access journal
The International Society of Hymenopterists

A new species of *Merismomorpha* Girault, 1913 (Chalcidoidea, Pteromalidae) from the Palaearctic region

Ekaterina V. Tselikh[1], Jean-Yves Rasplus[2], Jaehyeon Lee[3], Natalie Dale-Skey[4], Ankita Gupta[5], Deok-Seo Ku[6]

1 *Zoological Institute, Russian Academy of Sciences, St. Petersburg, Russia* **2** *CBGP, INRAE, CIRAD, IRD, Montpellier SupAgro, University of Montpellier, Montpellier, France* **3** *Department of Plant Medicine, Gyeongsang National University, Jinju 52828, Republic of Korea* **4** *Natural History Museum, London, UK* **5** *ICAR-National Bureau of Agricultural Insect Resources, Bangalore, India* **6** *The Science Museum of Natural Enemies, Geochang 50147, Republic of Korea*

Corresponding author: Ekaterina V. Tselikh (tselikhk@gmail.com)

Academic editor: Petr Janšta | Received 27 August 2024 | Accepted 30 September 2024 | Published 25 October 2024

https://zoobank.org/D3473710-0E18-413F-BBFD-4BC62CB66C7C

Citation: Tselikh EV, Rasplus J-Y, Lee J, Dale-Skey N, Gupta A, Ku D-S (2024) A new species of *Merismomorpha* Girault, 1913 (Chalcidoidea, Pteromalidae) from the Palaearctic region. Journal of Hymenoptera Research 97: 937–944. https://doi.org/10.3897/jhr.97.135648

Abstract

A new species of *Merismomorpha* Girault, 1913, *M. ulleungensis* Tselikh, Rasplus & Ku, **sp. nov.**, is described and illustrated from the Palaearctic region (Russian Far East and South Korea). An updated diagnosis of the genus is given, as well as a comparison to the closely related genus *Pterosemopsis* Girault, 1917.

Keywords

New records, new species, Pteromalinae, taxonomy

Introduction

The pteromalid genus *Merismomorpha* Girault, 1913 (type species *Merismomorpha acutiventris* Girault, 1913) belongs to the family Pteromalidae, subfamily Pteromalinae, tribe Pteromalini (Burks et al. 2022).

Until now, the genus comprised fourteen species and appears widely distributed in the Old World. Indeed, five species (*Merismomorpha elongata* Sureshan, 2000; *M. minuta* Sureshan, 2000; *M. tamilnadensis* Sureshan, Manickavasagam & Dhanya,

2013; *M. truncata* Sureshan, 2000; *M. yousufi* Ahmad & Agarwal, 1994) occur in the Oriental region (Ahmad and Agarwal 1994; Sureshan 2000; Narendran et al. 2006; Sureshan et al. 2006). Eight species (*Merismomorpha acutiventris* Girault, 1913; *M. asilus* (Girault, 1915); *M. faunus* Girault, 1933; *M. flavipetiole* (Girault, 1933); *M. fulvicoxa* Girault, 1913; *M. nigra* Girault, 1913; *M. petiolata* (Girault & Dodd, 1915); *M. sicarius* (Girault, 1915)) are distributed in the Australasian region (Bouček 1988; UCD Community 2023). *Merismomorpha gatra* Narendran, 2006 is reported from the mountains of South-Western Yemen, an area that formally belongs to the Afrotropical region (Narendran et al. 2006). While the generic assignation of this species requires to be confirmed, undescribed species are known from the Afrotropical region (Mitroiu et al. 2024). Finally, Koponen and Askew (2002) reported specimens tentatively identified as *Merismomorpha* from the Canary Islands (La Palma and Tenerife) (as "?*Merismorpha* sp.", sic). This archipelago is part of the Macaronesian subregion (Western Palaearctic).

The biology of species of *Merismomorpha* is poorly known. Bouček (1988), based on the biology of closely related genera, suggested the genus as a possible parasitoid of Agromyzidae and other Diptera. However, the only reared *Merismomorpha* species (*M. tamilnadensis*) has been obtained from *Cerococcus* sp. (Hemiptera: Coccoidea: Cerococcidae) on *Hibiscus* sp. (Sureshan et al. 2006). Cerococcidae is a small family of scale insects that comprises several pests of cultivated trees and is distributed worldwide (Hodgson and Williams 2016).

During our study of Pteromalidae of the Eastern Palaearctic region, several specimens of a new species of *Merismomorpha* were collected in forested areas of Eastern Part of Russia and South Korea. These samples represent the first confirmed occurrence of the genus in the Palaearctic region. Hereafter, we describe this new Palaearctic species of *Merismomorpha*. A comparative diagnosis of *Merismomorpha* Girault is also given.

Material and methods

The material used in this study is deposited in the Hymenoptera collections of the Natural History Museum, London, United Kingdom (**NHMUK**), National Institute of Biological Resources, Incheon, Republic of Korea (**NIBR**), Zoological Institute of the Russian Academy of Sciences, St. Petersburg, Russia (**ZISP**) and Zoological Survey of India, Western Ghats Field Research Station, Kerala, India (**ZSIK**).

Morphological terminology, including sculpture and wing venation nomenclature, follows Bouček and Rasplus (1991); Gibson (1997) and Burks et al. (2022). The following abbreviations are used: **POL** – posterior ocellar line, the minimum distance between the posterior ocelli; **OOL** – ocello–ocular line, the minimum distance between a posterior ocellus and compound eye; $\mathbf{clv_1}$–$\mathbf{clv_4}$ – clavomeres 1–4; **mv** – marginal vein; **stv** – stigmal vein; **pmv** – postmarginal vein; $\mathbf{fu_1}$–$\mathbf{fu_5}$ – funicular segments 1 to 5; $\mathbf{Mt_1}$ – petiole; $\mathbf{Mt_2}$–$\mathbf{Mt_8}$ – metasomal terga posterior to petiole. The scape is measured without the radicle; the pedicel is measured in lateral view. The distance between the clypeal lower margin and the toruli is measured from the lower margins of the toruli. Eye height is measured as maximum diameter, eye length as minimum diameter. Eye, mesosoma and metasoma are measured in lateral view, the latter including the ovipositor sheaths.

Taxonomy

Merismomorpha Girault, 1913

Epipolycystus Girault, 1915: 336. Type species: *Epipolycystus asilus* Girault, 1915, by original designation. Synonymy by Bouček (1988: 461).

Giorgionia Girault, 1933. Type species: *Giorgionia flavipetiole* Girault, 1933, by monotypy. Synonymy by Bouček (1988: 461).

Neopolycystella Girault, 1915: 336. Type species: *Neopolycystella sicarius* Girault, 1915, by original designation. Synonymy by Bouček (1988: 461).

Type species. *Merismomorpha acutiventris* Girault, 1913, by original designation Girault (1913: 82–83).

Diagnosis. Head without occipital carina (Fig. 7). Gena with a shallow malar depression; genal lamina absent. Clypeal margin medially produced, subconical (Figs 5, 17). Antennal formula 11354 (Fig. 5); flagellum slightly or obviously clavate; clava symmetric, area of micropilosity large, extending from distal clv_1 to clv_4 (Fig. 5). Antenna inserted above lower ocular line; antennal protuberance absent; scrobes shallow (Figs 5, 17). Pronotum short with collar not carinate (Figs 1, 7, 14); notauli complete (Figs 7, 15) or incomplete. Mesoscutellum arched, frenal area not raised (Figs 1, 14). Propodeum reticulate with conspicuous,long and posteriorly converging plical furrows; costula and median carina absent, nucha distinct; propodeal spiracle inserted close to anterior propodeal margin (Fig. 7). Fore wing hyaline, with distinct speculum; mv not widened and longer than stv and pmv (Figs 3, 16). Hind coxa dorsally bare (Fig. 4, 14). Petiole in dorsal view smooth and fusiform (Fig. 2); in lateral view appears as bipartite and curved (Fig. 4). Mt_2 large with tapered base (Fig. 2), cerci with setae subequal in length, ovipositor shortly protruding.

Remarks. *Merismomorpha* Girault belongs to a small group of pteromaline genera with elongated petiole (Bouček 1988); it looks similar to *Pterosemopsis* Girault, 1917, with which it could be confused. Indeed, the two genera exhibit shared characters: a lower clypeal margin medially produced and subconical (Figs 5, 10, 17); antennal formula 11354 (Figs 5, 8); antennal toruli situated above level of lower ocular line (Figs 5, 10, 17); propodeum with converging plical furrows (Figs 7, 9, 11); long and smooth petiole (Figs 2, 11). However, *Merismomorpha* differs from *Pterosemopsis* by the petiole in lateral view appears as bipartite and curved (Fig. 4) *vs* petiole in lateral view appears as single and not curved in lateral view (Fig. 8); frenal area of mesoscutellum not raised (Fig. 1) *vs* raised (Figs. 8, 12); collar margin of pronotum not carinate (Fig. 1) *vs* carinate (Fig. 8).

Accurate circumscription and diagnoses of these genera have not been published yet and only the key to Australasian genera of Pteromalidae (Bouček 1988) can be used to separate them, which could be troublesome for Oriental species. Indeed, some of the species of *Pterosemopsis* have erroneously been identified as belonging to *Merismomorpha*. Likewise, some species of *Merismomorpha* may not belong here (e.g. *M. gatra*) (Sureshan et al. 2006) and the two genera are in need of revision.

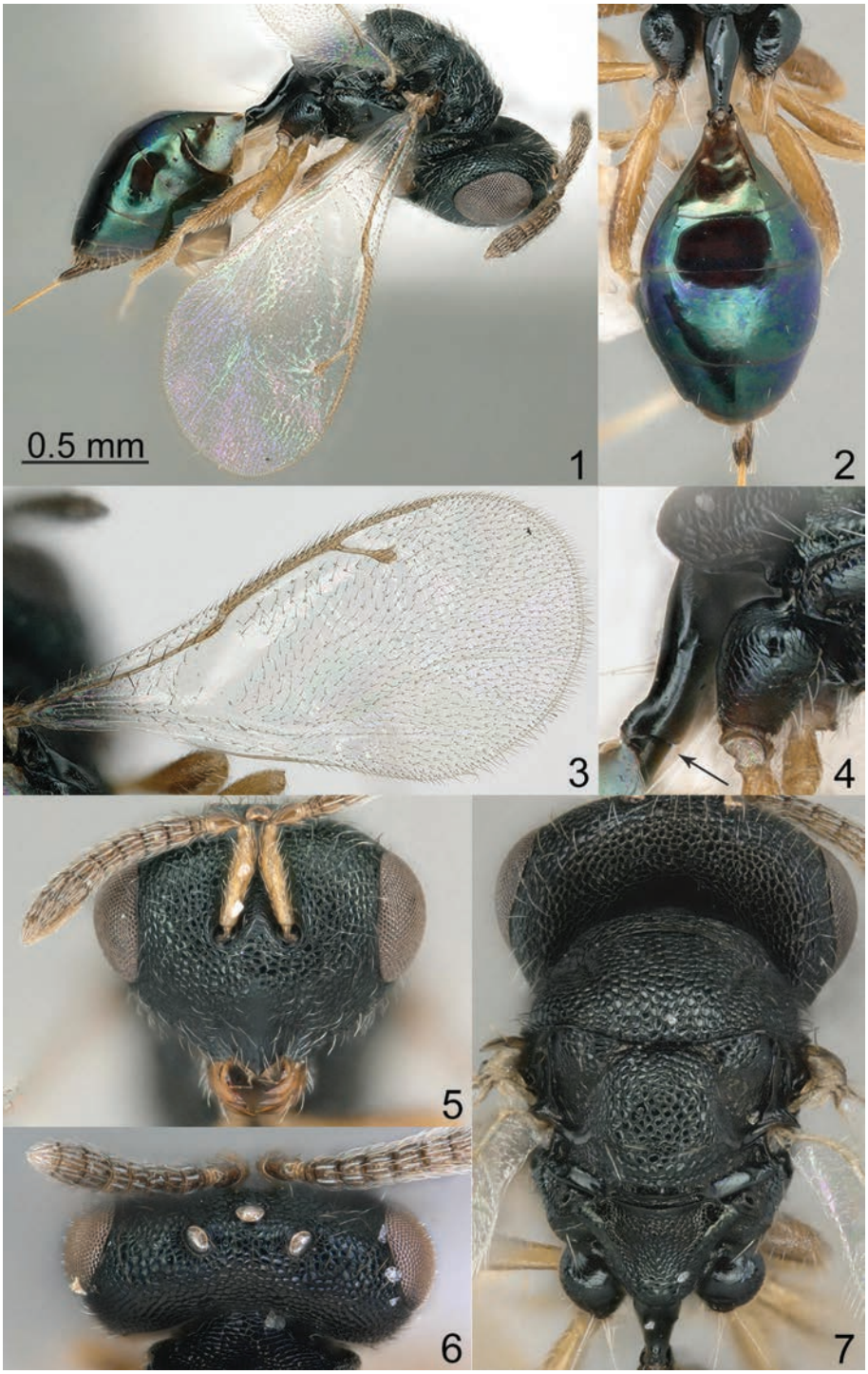

Figures 1–7. *Merismomorpha ulleungensis* Tselikh, Rasplus & Ku, sp. nov., holotype female **1** body, lateral view **2** metasoma, dorsal view **3** fore wing **4** petiole and hind coxa, lateral view **5** head and antenna, frontal view **6** head, dorsal view **7** mesosoma and propodeum, dorsal view.

***Merismomorpha ulleungensis* Tselikh, Rasplus & Ku, sp. nov.**
https://zoobank.org/BDD0E889-00E9-4757-AB8B-4795A5295593
Figs 1–7

Description. Female. Body length 1.50–1.90 mm. Fore wing length 1.20–1.40 mm.

Head black; antenna with scape yellowish-brown, pedicel and flagellum brown. Mesosoma and all coxae black; all femora brown; all tibiae and tarsi yellowish-brown. Fore wing hyaline, venation brown. Metasoma dark metallic bluish-green with diffuse violet iridescence; ovipositor sheath dark brown.

Head reticulate; clypeus and area above clypeus shallowly alutaceous. Mesosoma reticulate; lateral part of propodeum finely reticulate, nucha shallowly alutaceous. Petiole and gaster smooth and shiny.

Head in dorsal view 2.24–2.30 times as broad as long and 1.28–1.32 times as broad as mesoscutum; in frontal view 1.21–1.23 times as broad as high. Lower margin of clypeus angulate. POL 0.96–1.05 times OOL. Eye height 1.30 times eye length and 1.70–1.76 times as long as malar space. Distance between antennal toruli and lower margin of clypeus 1.45–1.57 times distance between antennal toruli and median ocellus. Antenna with scape 0.73–0.80 times as long as eye height and 0.95–1.07 times as long as eye length; pedicel 1.62–1.70 times as long as broad and 1.63–1.65 times as long as fu_1; combined length of pedicel and flagellum 0.82–0.84 times breadth of head; fu_1–fu_5 wider than long; clava 2.20–2.40 times as long as broad.

Mesosoma 1.45–1.55 times as long as broad. Mesoscutellum 0.88–0.90 times as long as broad. Propodeum 0.87–0.93 times as long as mesoscutellum. Fore wing 2.15–2.20 times as long as maximum width; basal cell partly pilose; basal vein pilose; speculum closed; mv 1.32–1.40 times as long as pmv and 2.09–2.22 times as long as stv.

Gaster 1.65–2.20 times as long as broad, 0.95–0.96 times as long as mesosoma and 0.72–0.74 times as long as mesosoma and head. Petiole fusiform, 2.55–2.63 times as long as broad and longer than hind coxa. Mt_2 and Mt_3 posteriorly not emarginate. Ovipositor sheath projecting beyond apex of metasoma.

Comparative diagnosis. The new species shares similarities with *Merismomorpha minuta* Sureshan, 2000: clypeus with angulate lower margin (Figs 5, 17), scape not reaching lower edge of median ocellus (Figs 5, 17), fore wing with mv longer than pmv (Figs 3, 16). However, *M. ulleungensis* has POL 0.96–1.05 times OOL (Fig. 6); the basal cell of fore wing is partly pilose; basal vein pilose, mv 1.32–1.40 times as long as pmv (Fig. 3), petiole longer than hind coxa (Fig. 4); whereas *M. minuta* has POL 1.30–1.40 times OOL (Fig. 15), basal cell and basal vein bare, mv 2.20–2.32 times as long as pmv (Fig. 16); petiole shorter than hind coxae (Fig. 14).

Etymology. The species is named in honour of the type locality, Ulleung-do Island (adjective).

Material examined. ***Holotype*:** South Korea • ♀; **Ulleung-do**, Ulleung-gun, Seo-myeon, Hakpo-ri, Malaise Trap, 37.5021918734491, 130.804925476545, 01–15.VIII.2017, coll. D.S Ku; deposited in NIBR. ***Paratype***: Russia • 1 ♀; **Amur Prov.**, Chingan Reserve, 24 km W Archara Vill., Kleshinskoe Lake, 10–11.VIII.2022, coll. O. Kosheleva; deposited in ZISP.

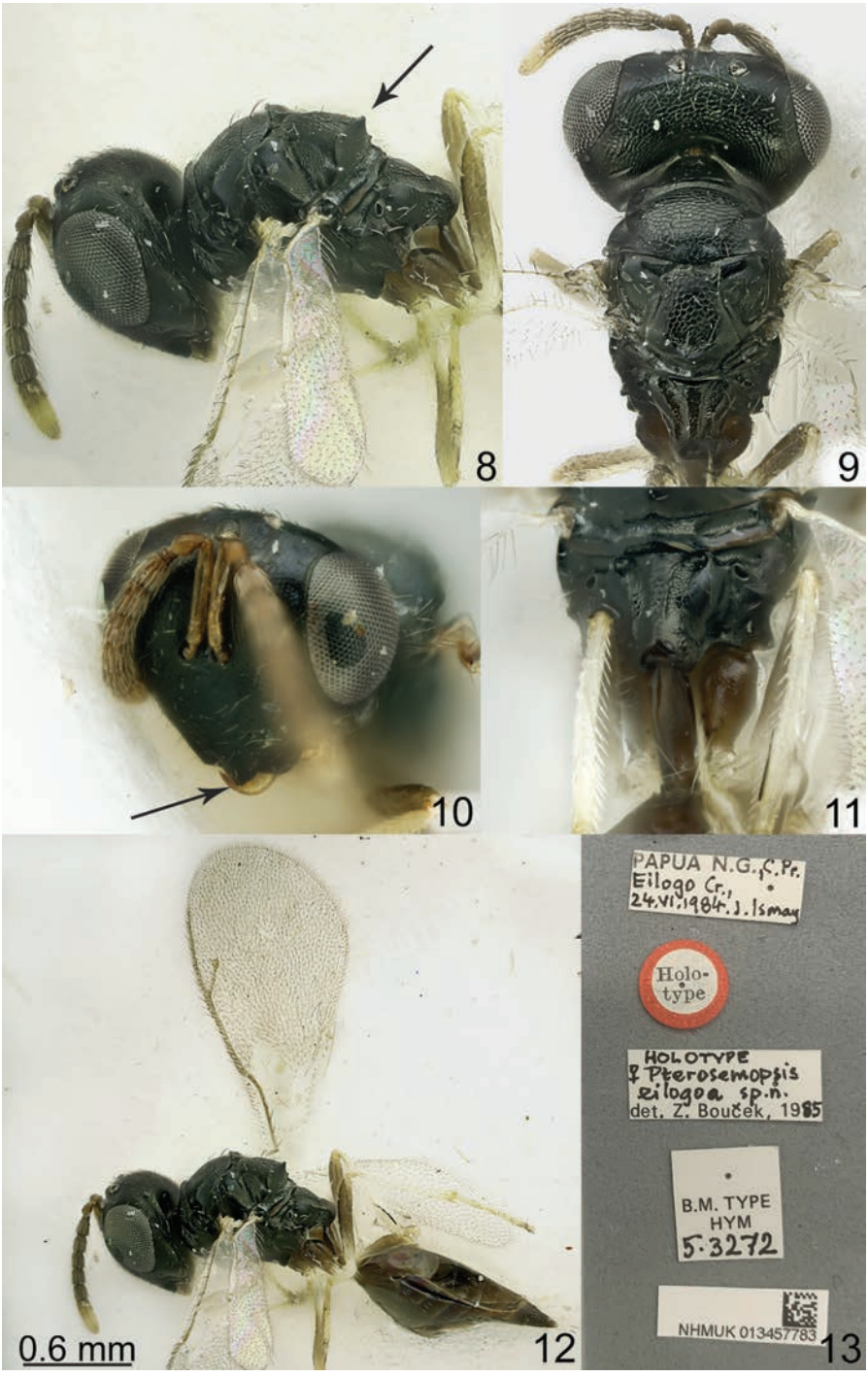

Figures 8–13. *Pterosemopsis eilogoa* Bouček, 1988, holotype female (NHMUK) **8** head and mesosoma, lateral view **9** head and mesosoma, dorsal view **10** head and antenna, frontal view **11** propodeum and petiole, dorsal view **12** body, lateral view **13** labels.

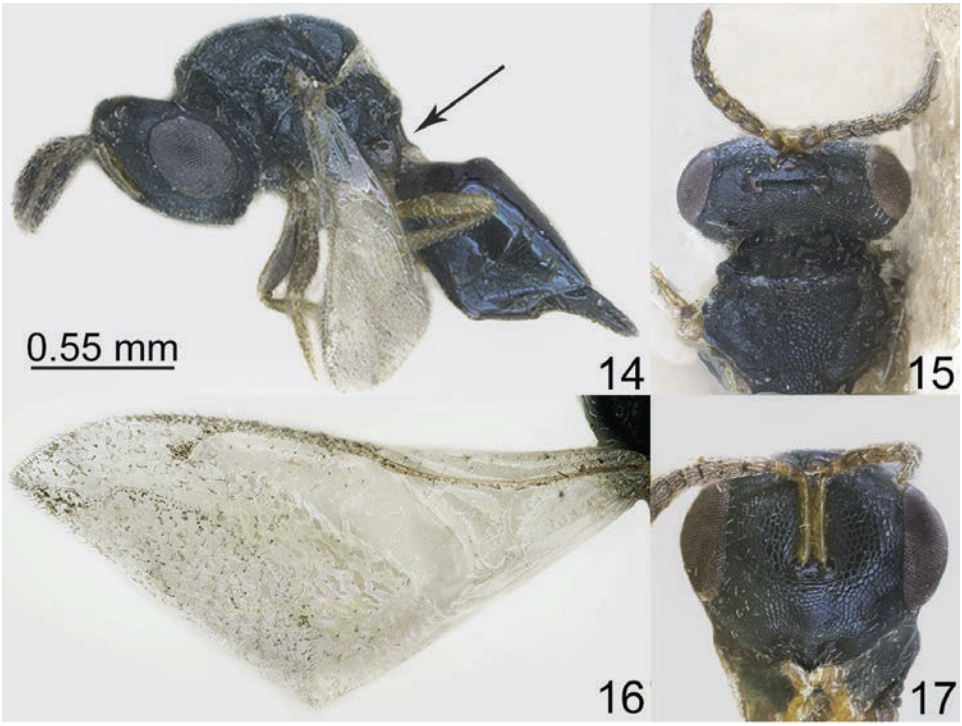

Figures 14–17. *Merismomorpha minuta* Sureshan, 2000, holotype female (ZSIK) **14** body, lateral view **15** head and mesosoma, dorsal view **16** fore wing **17** head, frontal view.

Male. Unknown.
Distribution. Russian Far East, South Korea.

Acknowledgements

This work was supported by a grant from the National Institute of Biological Resources (NIBR), funded by the Ministry of Environment (MOE) of the Republic of Korea (NIBR201801201, NIBR202402202). And it was partially funded by Russian State Research (project No. 122031100272-3). AG is grateful to Director ICAR-NBAIR for research support and to Dr P. M. Sureshan, ex Officer-Incharge, WGRC, ZSI, Kozhikode for sharing the images of *Merismomorpha minuta*.

References

Ahmad MJ, Agarwal MM (1994) A new species of *Merismomorpha* Girault (Chalcidoidea: Pteromalidae) from north India. Journal of Entomological Research 18(3): 229–232.

Bouček Z (1988) Australasian Chalcidoidea (Hymenoptera). A biosystematic revision of genera of fourteen families, with a reclassification of species. CAB International, Wallingford, Oxon, U.K., Cambrian News Ltd; Aberystwyth, Wales, 832 pp.

Bouček Z, Rasplus J-Y (1991) Illustrated key to West-Palaearctic genera of Pteromalidae (Hymenoptera: Chalcidoidea). Institut National de la Recherche Agronomique, Paris, 140 pp.

Burks R, Mitroiu M-D, Fusu L, Heraty JM, Janšta P, Heydon S, Papilloud ND-S, Peters RS, Tselikh EV, Woolley JB, van Noort S, Baur H, Cruaud A, Darling C, Haas M, Hanson P, Krogmann L, Rasplus J-Y (2022) From hell's heart I stab at thee! A determined approach towards a monophyletic Pteromalidae and reclassification of Chalcidoidea (Hymenoptera). Journal of Hymenoptera Research 94: 13–88. https://doi.org/10.3897/jhr.94.94263

Gibson G (1997) Morphology and Terminology. In: Gibson GAP, Huber JT, Woolley JB (Eds) Annotated Keys to the Genera of Nearctic Chalcidoidea (Hymenoptera). NRC Research Press, Ottawa, 16–44.

Girault AA (1913) Some chalcidoid Hymenoptera from north Queensland. Archiv für Naturgeschichte (A) 79(6): 70–90.

Girault AA (1915) Australian Hymenoptera Chalcidoidea IV. Supplement. Memoirs of the Queensland Museum 3: 180–299.

Girault AA (1933) Some beauties inhabitant not of commercial boudoirs but of nature's bosom, notably new insects. Brisbane, private publication, 5 pp.

Hodgson CJ, Williams DJ (2016) A revision of the family Cerococcidae Balachowsky (Hemiptera: Sternorrhyncha, Coccomorpha) with particular reference to species from the Afrotropical, western Palaearctic and western Oriental Regions, with the revival of *Antecerococcus* Green and description of a new genus and fifteen new species, and with ten new synonomies. Zootaxa 4091(1): 1–175. https://doi.org/10.11646/zootaxa.4091.1.1

Koponen M, Askew RR (2002) Chalcids from Madeira, Canary Islands and Azores (Hymenoptera, Chalcidoidea). Vieraea (Folia Scientarum Biologicarum Canariensum) 30, 115–145.

Mitroiu MD, Rasplus J-Y, van Noort S (2024) New genera of Afrotropical Chalcidoidea (Hymenoptera: Cerocephalidae, Epichrysomallidae, Pirenidae and Pteromalidae). PeerJ 12, e16798. https://doi.org/10.7717/peerj.16798.

Narendran TC, Girish Kumar P, Sheeba M, Kishore L (2006) Three new species of Pteromalidae (Hymenoptera: Chalcidoidea) from middle-east. Uttar Pradesh Journal of Zoology 26(1): 29–34.

Sureshan PM (2000) Taxonomic studies on *Merismomorpha* with the description of three new species from India (Hymenoptera: Chalcidoidea: Pteromalidae). Records of the Zoological Survey of India 98: 103–110. https://doi.org/10.26515/rzsi/v98/i3/2000/159665

Sureshan PM, Manickavasagam S, Dhanya B (2006) A review of the Oriental species of *Merismomorpha* Girault (Hymenoptera: Pteromalidae) with description of a new species parasitising *Cerococcus* sp. (Hemiptera: Sternorrhyncha: Cerococcidae) from Tamil Nadu, India. Hexapoda (Insecta indica) 19(1): 15–21.

UCD Community (2023) Universal Chalcidoidea Database (UCD) curated in TaxonWorks, 1143. https://sfg.taxonworks.org/api/v1/ [Accessed on 04 August 2024]